

EL-ELIMAT, TAMAM M., Ph.D. Discovering New Structural Diversity from Unexplored Fungi. (2014)
Directed by Dr. Nicholas H. Oberlies. 375 pp.

Discovery of anticancer drugs with high efficacy coupled with action at novel target sites is necessary to combat cancer. As part of a multidisciplinary project to identify anticancer leads from diverse natural product resources, our group has been studying fungi from different ecological habitats, including filamentous Ascomycota from terrestrial, freshwater, and symbiotic fungi (fungal endophytes), as a source of novel scaffolds for drug design and development. During the course of my research work, 56 bioactive compounds have been isolated and identified, with 30 of the isolated leads representing new chemical entities. Our lab relies on bioactivity-directed fractionation methodology for the isolation and purification of cytotoxic lead compounds from fungi, in which the bioassay results guide the purification processes. However, one of the inefficient outputs of utilizing this methodology is the re-isolation of previously known compounds, particularly mycotoxins. It is hypothesized that discovery of cytotoxic bioactive compounds with novel structures will be expedited by development and application of a dereplication methodology that has the capability to identify known compounds at the level of the crude extract. A dereplication methodology has been developed and implemented successfully for the identification of fungal secondary metabolites in crude culture extracts using a UPLC-PDA-HRMS-MS/MS method. Finally, the chemical diversity of the isolated compounds was analyzed through principal component analysis.

DISCOVERING NEW STRUCTURAL DIVERSITY FROM UNEXPLORED FUNGI

by

Tamam M. El-Elimat

A Dissertation Submitted to
the Faculty of the Graduate School at
The University of North Carolina at Greensboro
in Partial Fulfillment
of the Requirements for the Degree
Doctor of Philosophy

Greensboro
2014

Approved by

Committee Chair

To Dr. Feras Alali

APPROVAL PAGE

This dissertation, written by Tamam M. El-Elimat, has been approved by the following committee of the Faculty of The Graduate School at the University of North Carolina at Greensboro

Committee Chair _____

Nicholas Oberlies

Committee Members _____

Alice Haddy

Nadja Cech

Mitchell Croatt

Date of Acceptance by Committee

Date of Final Oral Examination

ACKNOWLEDGEMENTS

First and foremost I want to thank my advisor, Dr. Nicholas Oberlies, for being such a great teacher and mentor. I highly appreciate his efforts to make my Ph.D. experience enjoyable and productive. In addition to our research work, I greatly value his true friendship. I could not imagine having a better advisor.

I am thankful and indebted to my former master thesis research advisor at Jordan University of Science and Technology, Dr. Feras Alali, for recommending me to work with Dr. Oberlies and for his continuous help, support, and advice.

I am grateful to Dr. Mansukh C. Wani, RTI International, the co-discoverer of taxol, for the honor he bestowed on me by attending my dissertation seminar.

I would like to thank my dissertation committee members, Dr. Alice Haddy, Dr. Nadja Cech, and Dr. Mitchell Croatt, for their valuable comments and discussions.

Special thanks to the friendly and cheerful members of the Oberlies group who contributed immensely to my personal and research experiences at UNCG. I am especially grateful to Dr. Mario Figueroa. I have had the pleasure to work with him for two enjoyable and fruitful years. I would like to thank Dr. Huzefa Raja and Tyler Graf for their continuous help and unlimited support. Past and present members of the Oberlies group that I have had the pleasure to work with also include Dr. Arlene Sy-Cordero, Dr. Sloan Ayers, Dr. Amninder Kaur, Danielle Hayes, Karen VanderMolen, Noemi Paguigan, Vincent Sica, Sarah Winters, and Diana Kao, and Edem Tchegnon.

Great appreciation to my parents, brothers, and sisters, as well as my friend Lara, for their sincere love, kindness, and support.

I would like to acknowledge the financial support of the Department of Chemistry and Biochemistry at UNCG through awarding me a teaching assistantship.

This research was supported in part by program project grant P01 CA125066 from the National Cancer Institute, National Institutes of Health, Bethesda, MD. Partial support was also provided by a Collaborative Funding Grant (2011-CFG-8008) from the North Carolina Biotechnology Center and the Kenan Institute for Engineering, Technology & Science.

TABLE OF CONTENTS

CHAPTER	Page
I. INTRODUCTION	1
II. BENZOQUINONES AND TERPHENYL COMPOUNDS AS PHOSPHODIESTERASE-4B INHIBITORS FROM A FUNGUS OF THE ORDER CHAETOTHYRIALES (MSX47445)	6
III. WAOL A, <i>TRANS</i> -DIHYDROWAOL A, AND <i>CIS</i> -DIHYDROWAOL A: POLYKETIDE-DERIVED γ -LACTONES FROM A <i>VOLUTELLA</i> SPECIES	31
IV. SORBICILLINOID ANALOGUES WITH CYTOTOXIC AND SELECTIVE ANTI- <i>ASPERGILLUS</i> ACTIVITIES FROM <i>SCYTALIDIUM ALBUM</i>	49
V. CYTOTOXIC POLYKETIDES FROM FUNGAL CO-CULTURE OF <i>ASPERGILLUS VERSICOLOR</i> AND <i>SETOPHOMA TERRESTRIS</i>	84
VI. ISOCHROMENONES, ISOBENZOFURANONE, AND TETRAHYDRONAPHTHALENES PRODUCED BY <i>PARAPHOMA RADICINA</i> , A FUNGUS ISOLATED FROM A FRESHWATER HABITAT	142
VII. RESORCYLIC ACID LACTONES FROM A FRESHWATER <i>HALENOSPORA</i> SP.	172
VIII. FLAVONOLIGNANS FROM <i>ASPERGILLUS IIZUKAE</i> , A FUNGAL ENDOPHYTE OF MILK THISTLE (<i>SILYBUM MARIANUM</i>)	227
IX. HIGH-RESOLUTION MS, MS/MS, AND UV DATABASE OF FUNGAL SECONDARY METABOLITES AS A DEREPLICATION PROTOCOL FOR BIOACTIVE NATURAL PRODUCTS	247
X. CHEMICAL DIVERSITY OF METABOLITES FROM FUNGI, CYANOBACTERIA, AND PLANTS RELATIVE TO FDA-APPROVED ANTICANCER AGENTS	322

REFERENCES 339

CHAPTER I

INTRODUCTION

Cancer is defined as a class of diseases characterized by uncontrolled growth of abnormal cells that have the capability to metastasize to other tissues.¹ More than 100 types of cancer are known so far.¹ The global impact of cancer is enormous; it is the leading cause of death in developed countries and the second leading cause of death in developing countries, exceeded only by cardiovascular diseases.² Global cancer statistics revealed that of the 12.7 million cancer cases that have been diagnosed in 2011, breast cancer ranked number one with 23%, followed by lung cancer with 17%. Of the diagnosed cases, 7.6 million deaths were reported, or the death of about 21,000 people per day. Globally of these, lung cancer was the leading cause of death, followed by breast cancer, with 23% and 14% of the mortality, respectively.³ In the US, the estimated number of new cases of cancer for 2013 was 1,660,290 (excluding non-invasive cancer), while the estimated number of deaths was 580,350.² While these are staggering statistics, the number of deaths can be reduced by early diagnosis and treatment, and most importantly, by implementing preventive measures, for certain types of cancer, including changing the style of life. Cancer treatment depends primarily on the type and stage of cancer. Four standard methods of treatment are available: surgery, radiation therapy, chemotherapy, and biological therapy. For chemotherapeutic agents, there is no single cure for all types of cancer. A combination of several drugs for varying lengths of time is

usually used. A critical problem in cancer chemotherapy is the development of drug resistance.⁴ Consequently, there is always a necessity for discovering new anticancer agents with novel mechanisms of action.

Historically, natural products have been a key player in drug discovery programs, particularly in the field of cancer, by providing novel drugs and drug leads for synthetic modifications. For example, of the 175 small molecules that were introduced as anticancer drugs over the time period between the 1940s and 2010, 74.8% were other than synthetic, and 48.6% were either natural products or directly derived therefrom.⁵ Moreover, one-third of the global annual \$9-billion market for chemotherapeutic agents as calculated in 2003, could be attributed to camptothecin, taxol and their structural analogues, first-in-class natural chemotherapeutic agents.⁶ Of the thirteen natural product-derived drugs that were approved in the US between 2005 and 2007, five were the first members of new classes.⁷

Nature's supply of secondary metabolites comes through the six kingdoms of life: Plantae, Eubacteria, Fungi, Archaea, Animalia, and Protocista, with the first three being the most prominent.⁸ The impact of fungi on the drug discovery process is immense and cannot be overlooked. It has been the source of many life-saving drugs. Penicillin G, the first natural antibiotic, was isolated from *Penicillium chrysogenum*.⁹ Moreover, the top selling cholesterol-lowering class of drugs, statins, represented by lovastatin, was discovered from fungi.¹⁰ In the area of cancer, there are a number of promising fungal-derived compounds that are currently under development in different phases of clinical trials. Interestingly, two compounds, polysaccharide K (PKS) and lentinan were approved

in Japan for the adjuvant treatment of cancer patients. On the other hand, one of the most promising compounds in the field of cancer chemotherapy is the fungus-derived compound, irifulven, which showed potent anticancer properties, and currently is in phase III clinical development against several types of solid tumors.¹¹ Although several breakthrough drugs were discovered from fungi, it is still considered a highly underexplored source of bioactive secondary metabolites.

Fungi are one of the most extremely diverse groups of organisms that live on earth. They exist everywhere and have the ability to grow in a wide range of habitats.¹² This dissertation presents part of the findings of my research, which studied the chemical mycology of fungi from different ecological habitats, including filamentous Ascomycota from terrestrial, freshwater, and symbiotic fungi (fungal endophytes), as a source of novel scaffolds for drug design and development, particularly in the field of cancer.

The dissertation includes chapters devoted to the isolation and characterization of fungal secondary metabolites from terrestrial filamentous fungi using bioactivity-guided fractionation methodology, as part of a multi-disciplinary project to identify anticancer agents from diverse natural sources. So far, more than 100 compounds representing diverse chemical classes of bioactive cytotoxic fungal agents were isolated and elucidated. Chapters 2-5 present selected examples of such studies. Two benzoquinones, of which one was new, and a terphenyl compound were isolated and identified as phosphodiesterase-4B inhibitors from a fungus of the order Chaetothyriales (MSX47445) (Chapter 2). Two known and one new polyketide-derived γ -lactones were identified from a *Volutella* species (MSX58801) (Chapter 3). Eight sorbicillinoid analogues, of which

four were new, with cytotoxic and selective anti-*Aspergillus* activities along with two phthalides and one naphthalenone were isolated and identified from an organic extract of the fungus *Scytalidium album* (MSX51631) (Chapter 4). Sixteen polyketides, six of which were new, belonging to diverse structural classes, including monomeric/dimeric tetrahydroxanones and resorcylic acid lactones, were isolated from an organic extract of the fungus (MSX45109) (Chapter 5). These are followed by chapters focused on the chemical mycology of freshwater fungi (Chapters 6 and 7), in which new compounds belonging to diverse structural classes are presented along with their antimicrobial evaluation. Six isochromenones, of which two were new, one isobenzofuranone, and two tetrahydronaphthalene derivatives, with one being new, were identified from a culture of the fungus *Paraphoma radicina* (G104), which was isolated from submerged wood sampled in October of 2011 from a freshwater lake in Greensboro, North Carolina, USA (Chapter 6). Thirteen new resorcylic acid lactones, along with the known cryptosporiopsin A, were isolated from an organic extract of a culture of the freshwater aquatic fungus *Zalerion varium Anastasiou* (G87) (Chapter 7). *Z. varium Anastasiou* (G87) was isolated from a sample of submerged wood collected in October of 2011 from a freshwater stream on the campus of the University of North Carolina at Greensboro. Chapter 8 presents details of an interesting finding during the course of my work in endophytic fungi, in which three of the seven flavonolignans that constitute silymarin, an extract of the fruits of milk thistle (*Silybum marianum*), were detected for the first time from a fungal endophyte, *Aspergillus iizukae*, isolated from the surface-sterilized leaves of *S. marianum*.

A major challenge of working with fungi as a source of bioactive lead compounds is re-isolation of previously known compounds, particularly mycotoxins, which can be observed across different fungal species. Examples of these include aflatoxins, ochratoxins, trichothecenes, citreoviridin, fumonisins, and various indole-derived tremorgenics.¹³ Such re-isolations waste time and resources, distracting chemists from focusing on more promising leads. To address this problem, a dereplication methodology was developed and implemented successfully in our lab for the identification of fungal secondary metabolites in crude culture extracts using a UPLC-PDA-HRMS-MS/MS method. Chapter 9 is devoted to description of the details of this dereplication methodology, with examples presented to show the applicability of the method. So far, more than 350 fungal extracts have been dereplicated, with approximately more than 30% of these eliminated from further study after the confident identification of known compounds. Moreover, knowing that certain fungi make known compounds of interest is helpful for the re-isolation of compounds that are undergoing further development.

A multidisciplinary project has been undertaken to identify anticancer leads from diverse natural product sources, including filamentous fungi, cyanobacteria, and tropical plants. The structural variety of the resulting leads was broad, ranging from peptides to polyketides to terpenoids and myriad combinations thereof. Through principal component analysis, the chemical space covered by compounds isolated and characterized from these three sources was compared to each other and to the chemical space of selected FDA-approved anticancer drugs. Chapter 10 is devoted to this chemical diversity study, including visual representations of the data through plots of the principal components.

CHAPTER II
BENZOQUINONES AND TERPHENYL COMPOUNDS AS
PHOSPHODIESTERASE-4B INHIBITORS FROM A FUNGUS OF THE ORDER
CHAETOTHYRIALES (MSX47445)

Tamam El-Elimat, Mario Figueroa, Huzefa A. Raja, Tyler N. Graf, Audrey F. Adcock, David J. Kroll, Cynthia S. Day, Mansukh C. Wani, Cedric J. Pearce, and Nicholas H. Oberlies. *Journal of Natural Products* 2013, 76, 382-387.

Three bioactive compounds were isolated from an organic extract of an ascomycete fungus of the order Chaetothyriales (MSX47445) using bioactivity-directed fractionation as part of a search for anticancer leads from filamentous fungi. Of these, two were benzoquinones [betulinan A (**1**) and betulinan C (**3**)] and the third was a terphenyl compound BTH-II0204-207:A (**2**). The structures were elucidated using a set of spectroscopic and spectrometric techniques; the structure of the new compound (**3**) was confirmed via single crystal X-ray diffraction. Compounds (**1-3**) were evaluated for cytotoxicity against a human cancer cell panel, for antimicrobial activity against *Staphylococcus aureus* and *Candida albicans*, and for phosphodiesterase (PDE4B2) inhibitory activities. The putative binding mode of **1-3** with PDE4B2 was examined using a validated docking protocol, and the binding and enzyme inhibitory activities correlated.

Historically, natural products have played an important role in drug discovery. Of the 1355 newly approved drugs worldwide during the time period of 1981–2010, ~50% can be traced to, or were inspired by, natural products.⁵ Moreover, of the thirteen natural product–derived drugs that were approved in the US between 2005 and 2007, five were the first members of new classes,⁷ and in 2010, fingolimod, an analogue of the fungal metabolite myriocin, was approved as the first oral drug to reduce multiple sclerosis relapses.¹⁴ In July of 2012, carfilzomib, an analogue of the natural product epoxomicin, which was isolated originally from an Actinomycete,¹⁵ was approved to treat patients with multiple myeloma.¹⁶ In short, natural products remain an invaluable source for novel bioactive leads.

As part of a multidisciplinary project to identify structurally diverse anticancer leads,^{11,17} the Mycosynthetix library, representing over 55,000 accessions of filamentous fungi, is being examined systematically.^{18–22} Fungi represent an under explored source for bioactive secondary metabolites. In 1991, the number of fungi was estimated as 1.5 million species,²³ while current estimates suggest more than 5.1 million species.⁸ Regardless, less than 100,000 species have been characterized taxonomically,⁸ with likely a smaller percentage studied for bioactive secondary metabolites, and only a portion of these have been evaluated for anticancer activity.

An organic fraction of the filamentous fungus MSX47445⁹, which was isolated from highly decomposed woody debris from a tropical forest in 1990, displayed modest but equipotent cytotoxic activity against a panel of three cancer cell lines: MCF-7, H460, and SF268 (~75% inhibition of cell growth when tested at 20 $\mu\text{g}/\text{mL}$). Hence, this fungus was

selected for further study, and three compounds, two benzoquinones (**1** and **3**) and one terphenyl compound (**2**), were isolated and characterized. All three compounds were evaluated for cytotoxicity against a human cancer cell panel, for antimicrobial activity against *Staphylococcus aureus* and *Candida albicans*, and for their phosphodiesterase (PDE4B2) inhibitory activities; the results with the latter were the most encouraging and led to docking studies.

Results and Discussion

A solid-phase culture of MSX47445 was extracted with 1:1 CHCl₃-MeOH and partitioned with organic solvents to yield an orange-red extract, which was purified using flash chromatography to yield seven fractions. Of these, fraction 2 was the most cytotoxic against three cancer cell lines, and it was subjected to further purifications using preparative and semipreparative HPLC to yield three compounds (**1-3**) with > 97% purity as measured by UPLC (Supporting Information Figure 4).

Compound **1** (30.2 mg) was obtained as an orange powder. The molecular formula was determined as C₂₀H₁₆O₄ by HRESIMS. The NMR data, in conjunction with HRMS data and UV maxima of 194, 238, and 320 nm, identified **1** as the known compound betulinan A, first described by Lee et al.²⁴ in 1996 from the fungus *Lenzites betulina*.

Compound **2** (12.1 mg) was obtained as a pale yellow powder. HRESIMS data suggested a molecular formula of C₁₉H₁₆O₃. The compound showed distinctive UV maxima at 202, 259, and 315 nm. The NMR data were in agreement with those reported for BTH-II0204-207:A, a terphenyl compound first reported in 2011 by Beggins et al.²⁵ from the pathogenic bacterium *Burkholderia pseudomallei*.

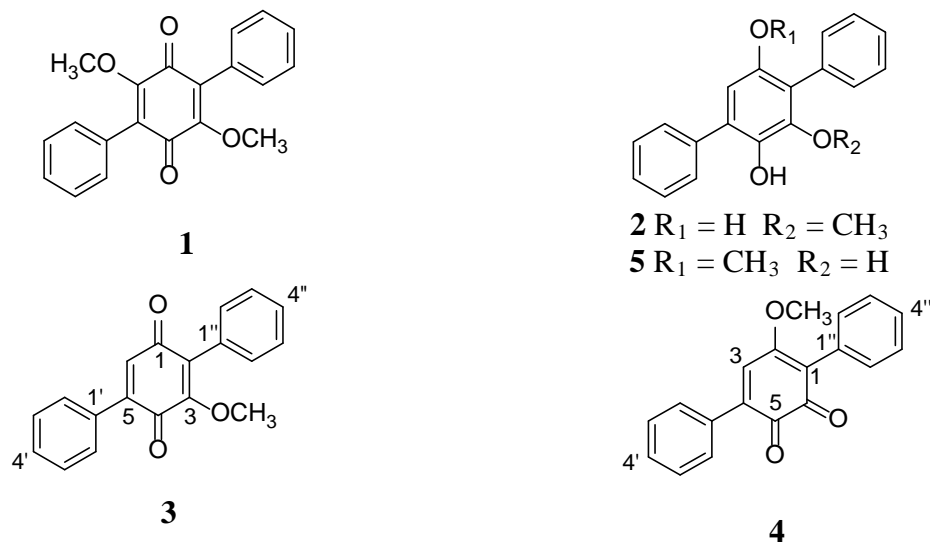


Figure 1. Structures of compound **1-4**.

Compound **3** (6.2 mg) was obtained as an orange powder. The molecular formula was determined as $C_{19}H_{14}O_3$ via HRESIMS, establishing an index of hydrogen deficiency of 13. The UV maxima (198, 235, and 331 nm) and NMR data suggested structural similarity with compound **1**, although a key difference was the loss of structural symmetry. Relative to **1**, compound **3** also lacked one methoxy moiety, as supported by a 30 amu difference in the HRMS data. 1H NMR data (Table 1) revealed the presence of 10 aromatic protons (δ_H 7.45-7.52 for H-2' to H-6' and δ_H 7.33-7.42 for H-2'' to H-6''), suggesting two mono substituted benzene rings, one olefinic proton (δ_H 6.88, H-6), and one methoxy group (δ_H 3.80, 3-OCH₃). The ^{13}C NMR data revealed the presence of 19 carbons, consistent with the molecular formula and indicative of two carbonyls, which were assigned as quinone carbons (δ_C 187.4 and 183.3, for C-1 and C-4, respectively), four olefinic carbons (δ_C 132.7, 155.4, 144.5, and 133.0, for C-2, C-3, C-5, and C-6, respectively), and 10 aromatic carbons (δ_C 130.7, 128.2, 129.0, 128.2, 130.7, 129.4,

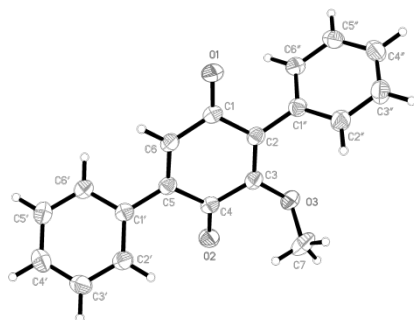
128.8, 130.3, 128.8, and 129.4, for C-2', C-3', C-4', C-5', C-6', C-2'', C-3'', C4'', C-5'', and C-6'', respectively). Thus far, the spectroscopic data accounted for 12 of the 13 degrees of unsaturation, and hence, the 13th degree completed the quinone ring. COSY data identified two spin systems, which corresponded to the aromatic protons of the two phenyl rings. An HMBC correlation was observed from 3-OCH₃ to C-3, indicating the connectivity of the methoxy group. HMBC correlations from H-6 to C-4, C-2, and C-1' were observed. NOESY correlations were observed from the olefinic proton H-6 to the equivalent C-2'/C-6' and from the 3-OCH₃ to the equivalent C-2''/C-6'' (Figure 2b). The last structure elucidation hurdle was to verify whether the central ring was an ortho or para quinone, but the spectroscopic data were inconclusive, since the observed HMBC and NOESY correlations for the H-3 and the 3-OCH₃ were equally valid for either substitution pattern. What increased the dilemma of the substitution pattern were contradictory NMR data that were published by two different research groups for a synthetic²⁶ and a natural²⁷ compound with the same molecular formula (compound **4**). Our NMR data were in agreement with those reported by Singh and co-workers, except for one carbon where the ¹³C NMR data differed by about 12 ppm.²⁷ Sawayama et al.²⁶ reported the synthesis of **4**, where clear differences were observed between the NMR data of synthetic and natural **4**, and they stated that reexamination of the structure of natural **4** was “underway by Dr. S. B. Singh.” However, since this reexamination has not been reported yet, compound **3** was crystallized from ethyl acetate at room temperature to give monoclinic crystals, and single crystal X-ray diffraction established the structure of **3**

with the carbonyl carbons para to each other (Figure 2a). To be consistent with the literature, the trivial name betulinan C was ascribed to **3**.

Table 1. ^1H (500 MHz) and ^{13}C (125 MHz) NMR Data for Betulinan C (**3**) in CDCl_3

position	δ_{C} , type	δ_{H} (J in Hz)
1	187.4, C	--
2	132.7, C	--
3	155.4, C	--
4	183.3, C	--
5	144.5, C	--
6	133.0, CH	6.88, s
1'	128.8, C	--
2', 6'	129.4, CH	7.52, dd (8.0, 1.7)
3', 5'	128.8, CH	7.45, m
4'	130.3, CH	7.45, m
1''	130.0, C	--
2'', 6''	130.7, CH	7.33, dd (8.0, 1.7)
3'', 5''	128.2, CH	7.42, m
4''	129.0, CH	7.40, m
3-OCH ₃	61.67, CH ₃	3.80, s

(a)



(b)

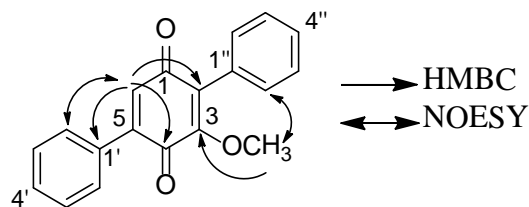


Figure 2. (a) X-ray crystallographic structure with 50% probability ellipsoids. (b) key HMBC and NOESY correlations of **3**.

Compounds structurally related to **1-3** have been identified as phosphodiesterase (PDE) inhibitors. Terferol (**5**), which was isolated from *Streptomyces showdoensis* SANK 65080, possessed inhibitory activity against cyclic adenosine 3',5'-monophosphate phosphodiesterase (cAMP-PDE) and cyclic guanosine 3',5'-monophosphate phosphodiesterase (cGMP-PDE).²⁸ The concentrations of **5** required for 50% inhibition of cAMP-PDE and cGMP-PDE were 0.82 and 0.96 μM , respectively.²⁸ Moreover, Biggins et al.²⁵ evaluated two terferol related compounds, BTH-II0204-207:A (**2**) and BTH-II0204-207:C, for PDE inhibition activity against 11 PDE families. The latter was inactive, while **2** showed activity against PDE11 as well as four out of the five PDE4s that were examined. PDE4 is an essential regulator of the secondary messenger cAMP in numerous cell types, and the reduction in cAMP degradation by several inhibitors, such as rolipram, piclamilast, roflumilast, cilomilast, and tetomilast, has suggested a broad range of clinical applications for the treatment of asthma and chronic obstructive pulmonary disease (COPD),^{29,30} some types of brain tumors,^{31,32} and other inflammatory diseases.³³ In 2011, roflumilast (Daliresp) was approved by the U.S. FDA as the first selective PDE4 inhibitor to reduce COPD exacerbations.³⁴ Moreover, abnormal regulation of cAMP and/or cGMP metabolism upon altered expression and activity of PDE isoforms has been implicated in the pathogenesis of various types of cancer, including prostate cancer, colon cancer, hematological malignancies, melanoma, and brain tumors.^{35,36} Based on these reports, the effect of **1-3** on the activity of recombinant human PDE4B2³⁷ were evaluated; PDE4B is the predominant isoform present in human monocytes and neutrophils and is involved mainly in inflammation.³⁸ Of these, **3** was the

most potent with an IC_{50} value of $17 \mu\text{M}$, followed by compounds **2** and **1** with IC_{50} values of 31 and $44 \mu\text{M}$, respectively (Figure 3; Table 2).

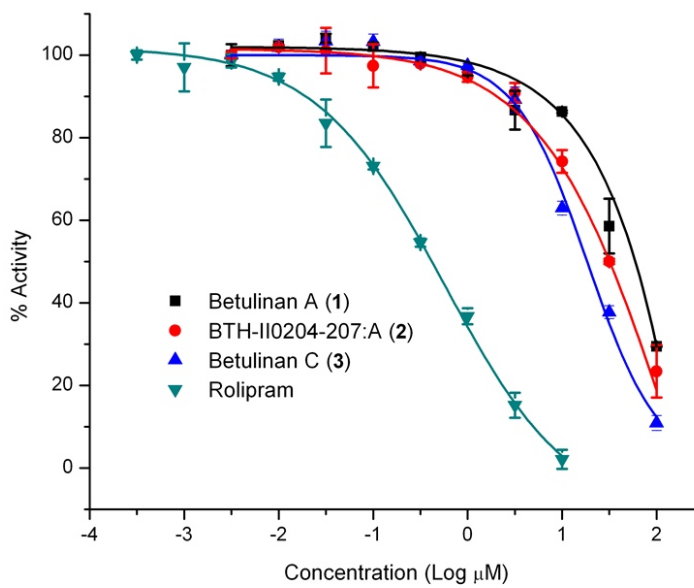


Figure 3. Plots of the effect of compounds **1-3** and rolipram (positive control) on PDE4B2 activity. Substrate Conc. = 100 nM (cAMP).

Table 2. PDE4B2 Inhibition Activity and Docking Results of Compounds 1-3

compound	PDE4B2 inhibition IC_{50} (μM)	Docking score (kcal/mol)	Docking score rank
betulinan A (1)	44	-8.071	4
BTH-II0204-207:A (2)	31	-8.277	3
betulinan C (3)	17	-8.732	2
rolipram ^a	0.4	-11.396	1
^a postive control			

Molecular docking and other computational approaches are being used increasingly to explore the ligand-binding interactions of PDE4 inhibitors.³⁹⁻⁴² As such, compounds **1-**

3 were docked into the crystal structure of human PDE4B using Glide Extra Precision.^{43,44} The docking protocol was verified by testing its ability to reproduce the experimental binding mode of co-crystallized rolipram (Supporting Information Figure 8). To this end, rolipram bound to the crystal structure was removed from the binding pocket and docked back into the cofactor binding site; the root-mean-square deviation between the predicted conformation and the observed X-ray crystallographic data was 1.1 Å, indicating the capability of the docking protocol to reproduce the binding mode of rolipram (Supporting Information Figure 8). Compounds **1-3** were docked into the cAMP binding site of PDE4B. The docking scores calculated with Glide correlated with the biological activity (Table 2); compound **3** displayed the highest activity (IC₅₀ value of 17 μM) and also the top-ranked docking score (-8.732 kcal/mol). In contrast, compound **1** had the lowest activity (IC₅₀ value of 44 μM) and showed the lowest docking score (-8.071 kcal/mol). Finally, the pyrrolidinone rolipram was included, not only for the docking protocol validation, but also as a positive control in the enzymatic assay; rolipram was top ranked in both docking score and in vitro activity.

Compounds **1-3** and rolipram displayed a similar binding mode (Figures 4 and 9). The two predicted hydrogen bonds between the free amino group of Gln443 and the cyclopentyloxy and methoxyphenyl groups of rolipram were in agreement with the observations derived from the crystallographic structure of PDE4B in complex with rolipram. As shown, Glide found a similar hydrogen bond with Gln443 and the carboxyl group for the most active compound **3** (Figures 4c and 4d); favorable π interactions with Phe446 in the binding pocket were also observed. Compounds **1** and **2** did not show

hydrogen bonds with Gln433, but similar π interactions were predicted (Figures 4a, 4b and 9). Taken together, these observations suggested that the binding modes predicted with Glide for compounds **1-3** were reasonable.

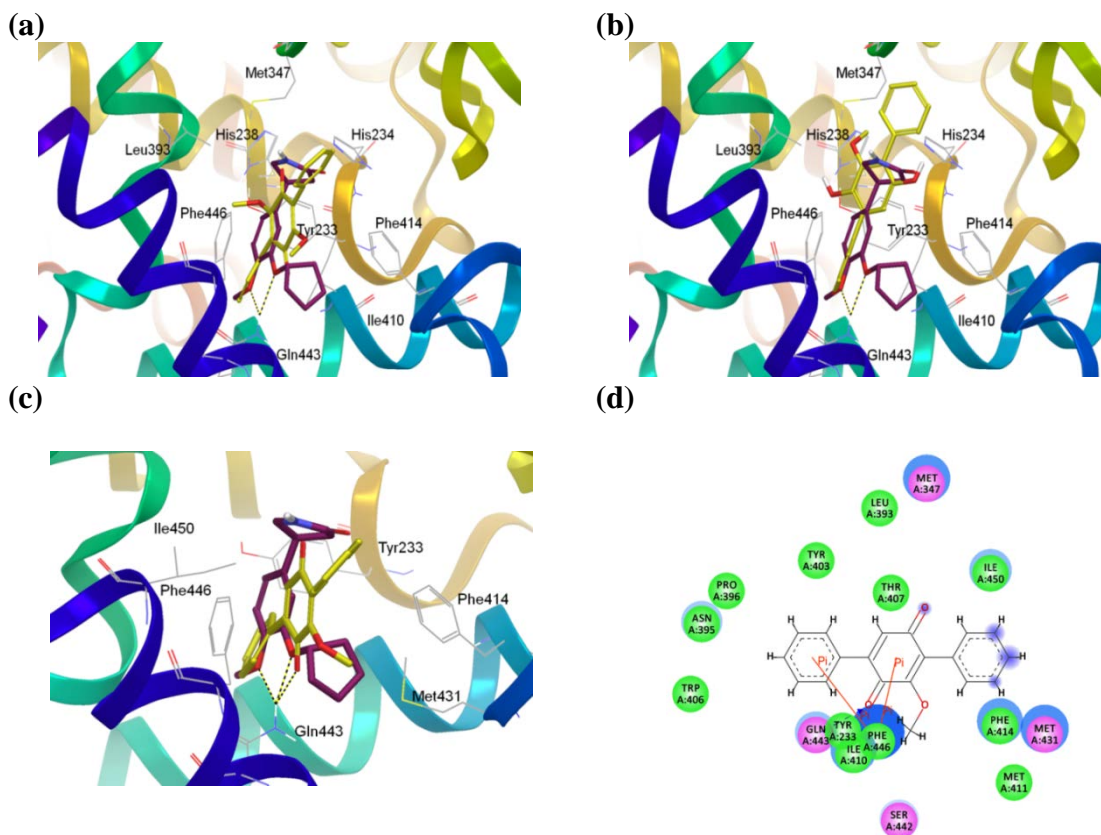


Figure 4. Binding conformation of **1** (a), **2** (b) and **3** (c) predicted by Glide. Crystallographic rolipram (maroon) is shown as a reference with hydrogen bonds displayed as yellow/black dashes. Nonpolar hydrogen atoms are omitted. (d) Two-dimensional interaction map of the optimized docking model of compound **3** in the cAMP binding pocket of PDE4B. Amino acid residues within 4.5 Å of the ligand are displayed. Blue arrows indicate hydrogen bonding to amino acid side chain atoms.

Compounds **1-3** were assayed for cytotoxicity and antimicrobial activity. When tested against the three cancer cell lines MCF-7, H460, and SF268 (Supporting

Information Table 4), compounds **2** and **3** showed moderate cytotoxicity while **1** was inactive. Compounds **2** and **3** were equipotent against *S. aureus* with MIC values of 25 $\mu\text{g/mL}$, while none of the compounds showed activity against *C. albicans*.

In conclusion, three compounds (**1-3**) were isolated and characterized from the fungus MSX47445. The structure of the new paraquinone, **3**, was assigned unequivocally by NMR and single crystal X-ray diffraction. The effect of compounds **1-3** on the activity of PDE4B was assessed both in vitro and in silico; compound **3** was the most potent, being approximately a half order of magnitude less potent than the positive control, rolipram. Further studies are ongoing to expand the knowledge base of this class of compounds, particularly given their compact structures.

Experimental Section

General Experimental Procedures. UV and IR spectra were acquired on a Varian Cary 100 Bio UV-Vis spectrophotometer and a Perkin-Elmer Spectrum One with Universal ATR attachment, respectively. NMR experiments were conducted in either CDCl_3 , acetone- d_6 or $\text{DMSO-}d_6$ with TMS as a reference via a JEOL ECA-500, operating at 500 MHz for ^1H and 125 MHz for ^{13}C . HRESIMS was performed on a Thermo LTQ Orbitrap XL mass spectrometer equipped with an electrospray ionization source. UPLC was carried out on a Waters Acquity system with data collected and analyzed using Empower software. HPLC was carried out using a Varian Prostar HPLC system equipped with ProStar 210 pumps and a Prostar 335 photodiode array detector (PDA), with data collected and analyzed using Galaxie Chromatography Workstation software (version 1.9.3.2). For preparative HPLC, a Phenomenex Synergi Max-RP 80 (4

μm ; 250×21.2 mm) column was used at a 21 mL/min flow rate, while for the semi-preparative HPLC, a Phenomenex Gemini-NX C₁₈ ($4 \mu\text{m}$; 250×10 mm) column was used at a 4.7 mL/min flow rate. For UPLC, a Waters BEH C₁₈ column ($1.7 \mu\text{m}$; 50×2.1 mm) was used with a 0.6 mL/min flow rate. Flash chromatography was performed on a Teledyne ISCO CombiFlash Rf using a 40 g Silica Gold column and monitored by UV and evaporative light-scattering detectors. X-ray crystallography data were acquired using a Bruker APEX CCD diffractometer (MoK α radiation, graphite monochromator). All other reagents and solvents were obtained from Fisher Scientific and were used without further purification.

Producing Organism and Fermentation. Mycosynthetix fungal strain 47445 was isolated from highly decomposed woody debris in 1990. The growth conditions were as described previously^{19,22} and outlined in the supplementary materials. For molecular identification, the internal transcribed spacer regions 1 & 2 and 5.8S nrDNA (ITS) were sequenced, since this region of the ribosomal RNA operon has been proposed as a barcode marker for fungi.⁴⁵ Detailed methodology for DNA extraction, PCR amplification, sequencing, and phylogenetic analyses are outlined in the supplementary materials. The combined ITS and LSU sequence was deposited in the GenBank (accession no JX310275). The analyses of both the rRNA regions (ITS and D1/D2 of the LSU) suggested that MSX47445 was a member of the Chaetothyriales, Ascomycota and shares phylogenetic affinities with the mitosporic fungus *Cyphellophora* sp.

Extraction and Isolation. To the large-scale solid fermentation culture of MSX47445, 500 mL of 1:1 MeOH-CHCl₃ were added. The culture was chopped with a

spatula and shaken overnight (~16 h) at ~100 rpm at rt. The sample was filtered with vacuum, and the remaining residues were washed with 100 mL of 1:1 MeOH-CHCl₃. To the filtrate, 900 mL CHCl₃ and 1500 mL H₂O were added; the mixture was stirred for 2 h and then transferred into a separatory funnel. The bottom layer was drawn off and evaporated to dryness. The dried organic extract was re-constituted in 300 mL of 1:1 MeOH-CH₃CN and 200 mL of hexanes. The biphasic solution was stirred for an hour and then transferred to a separatory funnel. The MeOH-CH₃CN layer was drawn off and evaporated to dryness under vacuum. The defatted material (1.2 g, orange red) was dissolved in a mixture of CHCl₃-MeOH, adsorbed onto Celite 545, and fractionated via flash chromatography using a gradient solvent system of hexane-CHCl₃-MeOH at a 40 mL/min flow rate and 53.3 column volumes over 63.9 min to afford seven fractions. Fraction 2 eluted with 100% CHCl₃ (~247 mg) was subjected to preparative HPLC using an isocratic system of 55:45 CH₃CN-H₂O over 30 min at a flow rate of 4.7 mL/min to yield seven sub-fractions. Sub-fraction 5 yielded compound **1** (30.2 mg), which eluted at ~22.5 min. Sub-fraction 2 was subjected to semipreparative HPLC and yielded compounds **2** (12.1 mg) and **3** (6.2 mg), which eluted at 9.5 and 19.0 min, respectively. UPLC was used to evaluate the purity of **1-3** using a gradient solvent system that initiated with 20:80 CH₃CN-H₂O to 100% CH₃CN over 4.5 min; all compounds were >97% pure (Supporting Information Figure 5).

Betulinan C (3): orange powder; UV (MeOH) λ_{\max} (log ϵ) 330 (3.62), 235 (4.14), 203 (4.32) nm; IR (diamond) ν_{\max} 1661, 1640, 1593, 1330, 1267, 1090, 1072, 935, 889,

849, 809, 776, 766 cm^{-1} ; ^1H NMR (CDCl_3 , 500 MHz) and ^{13}C NMR (CDCl_3 , 125 MHz), see Table 1; HRESIMS m/z 291.1017 $[\text{M} + \text{H}]^+$ (calcd for $\text{C}_{19}\text{H}_{14}\text{O}_3$ 291.1016).

X-ray Crystallography. Crystallographic data for compound **3** has been deposited with the Cambridge Crystallographic Data Centre, deposition number 904704.

Compound's **3** crystals were grown in ethyl acetate at rt. X-ray crystal structure analysis of **3** were as follows: formula $\text{C}_{19}\text{H}_{13}\text{O}_3$, MW = 290.31, block-shaped yellow crystal, $a = 14.6693$ (18) Å, $b = 7.3806$ (9) Å, $c = 14.3582$ (18) Å, $\beta = 115.259$ (1)°, $T = 193$ (2) K, $Z = 4$, monoclinic, space group $P2(1)/c$, $GOF = S = 1.043$, $V = 1405.9$ (3) Å³, RI (3088 reflections, $I > 2\sigma(I)$) = 0.0521, $wR2$ (all 3719 reflections) = 0.1476, $\lambda = 0.71073$ Å.

Cytotoxicity Assay. The cytotoxicity measurements against the MCF-7⁴⁶ human breast carcinoma (Barbara A. Karmanos Cancer Center), NCI-H460⁴⁷ human large cell lung carcinoma (HTB-177, American Type Culture Collection (ATCC), and SF-268⁴⁸ human astrocytoma (NCI Developmental Therapeutics Program) cell lines were performed as described previously.^{49,50}

Antimicrobial Assay. The compounds were screened for antimicrobial activity using an agar plate diffusion assay as described previously.¹⁸

Phosphodiesterase Inhibitor Assay. The PDE inhibitor assay was performed at BPS Bioscience Inc. as described previously.¹³ Detailed experimental procedures are provided in the Supporting Information.

Molecular Modeling. Compounds **1-3** were prepared using the LigPrep 2.4 module of Maestro 9.1 (Schrödinger, LLC). The crystal structure of human PDE4B in complex to the inhibitor rolipram was retrieved from the Protein Data Bank (PDB entry 1RO6).⁵¹

Docking was performed with the cAMP catalytic domain using Glide (Grid-Based Ligand Docking with Energetics; Schrödinger, LLC) program, version 5.6.⁴⁴ The Protein Preparation Wizard module of Maestro was used to prepare the protein.⁵² During protein preparation, H₂O molecules were deleted. For docking, the scoring grids were centered on the crystal structure of rolipram using the default bounding sizes. All structures were docked and scored using Glide.⁴⁴ The best docked poses were selected as the ones with the lowest Glide Score; the more negative the Glide Score, the more favorable the binding. 2D interactions maps were generated with Discovery Studio 3.1 from Accelrys Software Inc.

Supporting Information

Producing Organism and Fermentation. The culture was stored on a malt extract slant and was transferred periodically. A fresh culture was grown on a similar slant, and a piece was transferred to a medium containing 2% soy peptone, 2% dextrose, and 1% yeast extract (YESD media). Following incubation (7 d) at 22 °C with agitation, the culture was used to inoculate 50 mL of a rice medium, prepared using rice to which was added a vitamin solution and twice the volume of rice with H₂O, in a 250 mL Erlenmeyer flask. This was incubated at 22 °C until the culture showed good growth (approximately 14 d). The scale-up culture was grown in a 2.8 L Fernbach flask containing 150 g of rice and 300 mL of H₂O and was inoculated using a seed culture grown in YESD medium. This was incubated at 22 °C for 14 d.

For extraction of genomic DNA of fungal strain MSX47445, mycelium from axenic cultures grown in YESD broth was scraped with a sterile scalpel and ground to a fine powder in liquid N₂ using a mortar and pestle. Approximately 400 μL of AP1 buffer from the DNAeasy Plant Mini Kit (QIAGEN Inc.) was added to the mycelial powder, and DNA was extracted following the manufacturer's instructions. The DNA was eluted in approximately 25–30 μL distilled H₂O. The complete ITS region, along with the partial region of divergent domains D1/D2 of the large subunit of the 28S nuclear ribosomal DNA (LSU), were amplified with ITS1F and LR3 by PCR using puReTaq™ Ready-To-Go PCR beads (Amersham Biosciences Corp.). The PCR products were sequenced subsequently in a 11 μL sequencing reaction with BigDye® Terminators v3.1 (Applied Biosystems) using ITS primers ITS1F and ITS4^{53,54} and LSU primers LROR and LR3.^{55,56} For PCR, the following protocol was used: initial denaturation at 95 °C for 5 min, followed by 35 or 40 cycles of 95 °C for 30 s, 41 or 50 °C for 15 s, and 72 °C for 1 min with a final extension step of 72 °C for 10 min. To enhance the PCR reactions, 2.5 μL of BSA (bovine serum albumin, New England Biolabs) and/or 2.5 μL of DMSO were added. The PCR products were purified to remove excess primers, dNTPs, and nonspecific amplification products with the QIAquick PCR Purification Kit (QIAGEN Inc.). Sequences were generated on an Applied Biosystems 3730XL high-throughput capillary sequencer at the University of Illinois Urbana-Champaign Biotech facility.

The complete ITS sequence, including both spacers and the 5.8S region of MSX47445 (~644 base pairs), was compared with GenBank's database⁵⁷ using the Blastn search.⁵⁸ The Blast search revealed *Cyphellophora eucalypti* Cheew & Crous

(GQ303274) as the closest match (query coverage of 100%, and a sequence similarity of 89%). To be considered conspecific based on ITS data, studies of Ascomycota fungi have used a ≥ 97 –98% or 99% cut off as a proxy for species level identification.^{59,60} Since, *C. eucalypti*, a member of Chaetothyriales, (Chaetothyriomycetidae, Eurotiomycetes, Ascomycota) was the closest match in the GenBank and shared 89% sequence similarity with the ITS sequence, MSX47445 had affinities only to the level of the order Chaetothyriales. The variable D1/D2 regions of LSU of MSX47445 (~ 600 bp) were subjected to a Blast search in GenBank. Blast search with the D1/D2 region also revealed *C. eucalypti* (GQ303305) as the closest match with MSX47445 (query coverage of 96% and a sequence similarity of 99%). These sequences were downloaded and a Maximum Likelihood (ML) analysis was performed to determine the phylogenetic affinities of MSX47445 with members of the Chaetothyriales. Multiple sequence alignment and phylogenetic analysis was performed following programs reviewed previously.⁶¹ Results of the ML phylogenetic analysis indicated that MSX47445 shared phylogenetic affinities with *C. eucalypti* but without significant bootstrap support values (See Supplementary Figure 10).

Experimental Protocol for the Phosphodiesterase Inhibitor Assay. The PDE inhibitor assay was performed at BPS Bioscience Inc. A series of dilutions of the test compounds were prepared with 10% DMSO in assay buffer, and 5 μ L of the dilution were added to a 50 μ L reaction so that the final concentration of DMSO was 1% in all of the reactions. The enzymatic reactions were conducted at rt for 60 min in a 50 μ L mixture containing PDE assay buffer, 100 nM FAM-cAMP, PDEB2 enzyme and the test

compound. After the enzymatic reaction, 100 μ L of a binding solution (1:100 dilution of the binding agent with the binding agent diluent) were added to each reaction, and the reaction was performed at rt for 60 min. Fluorescence intensity was measured at an excitation of 485 nm and an emission of 528 nm using a Tecan Infinite M1000 microplate reader.

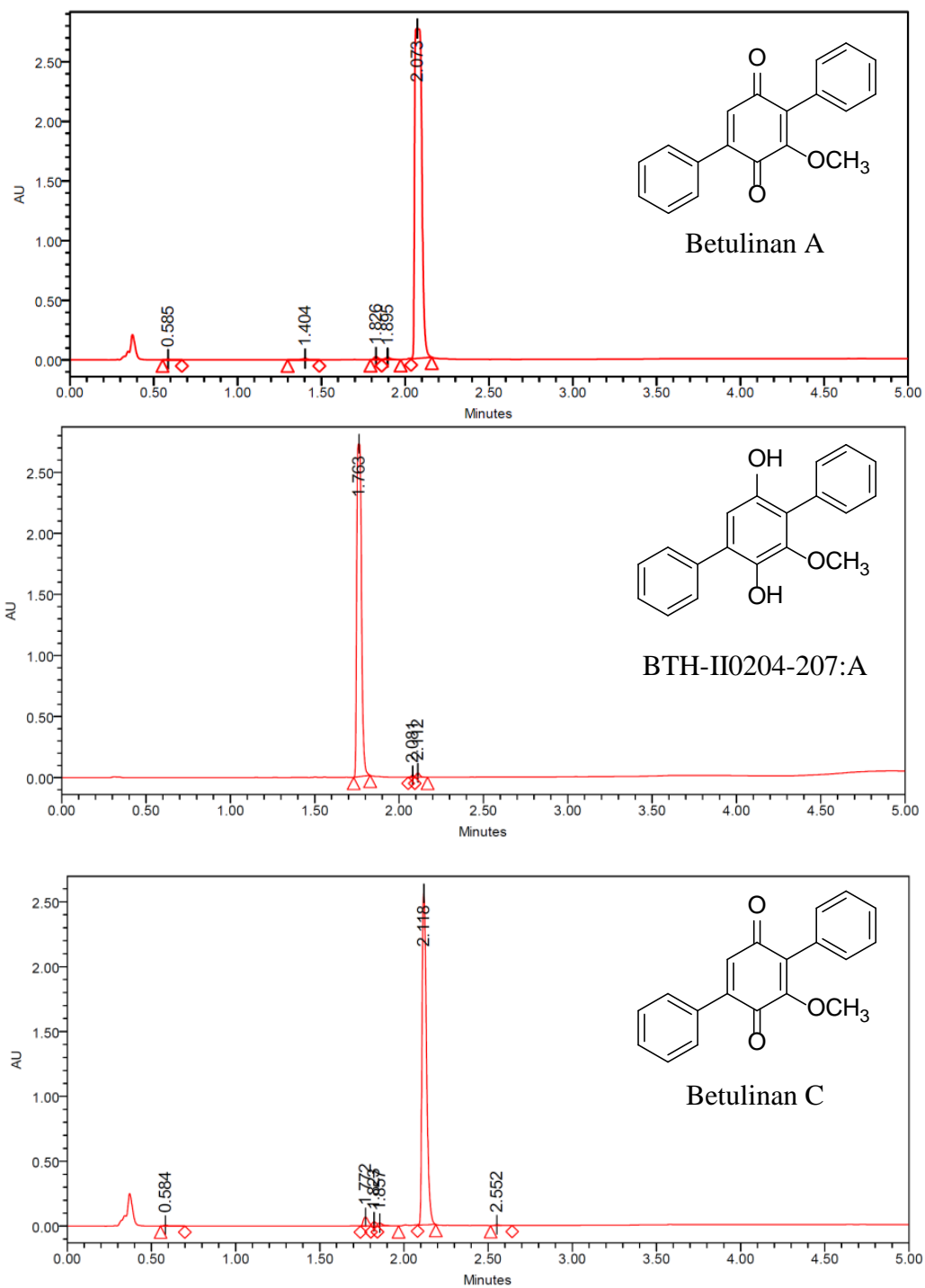


Figure 5. UPLC chromatograms of compounds **1-3** (λ 210 nm).

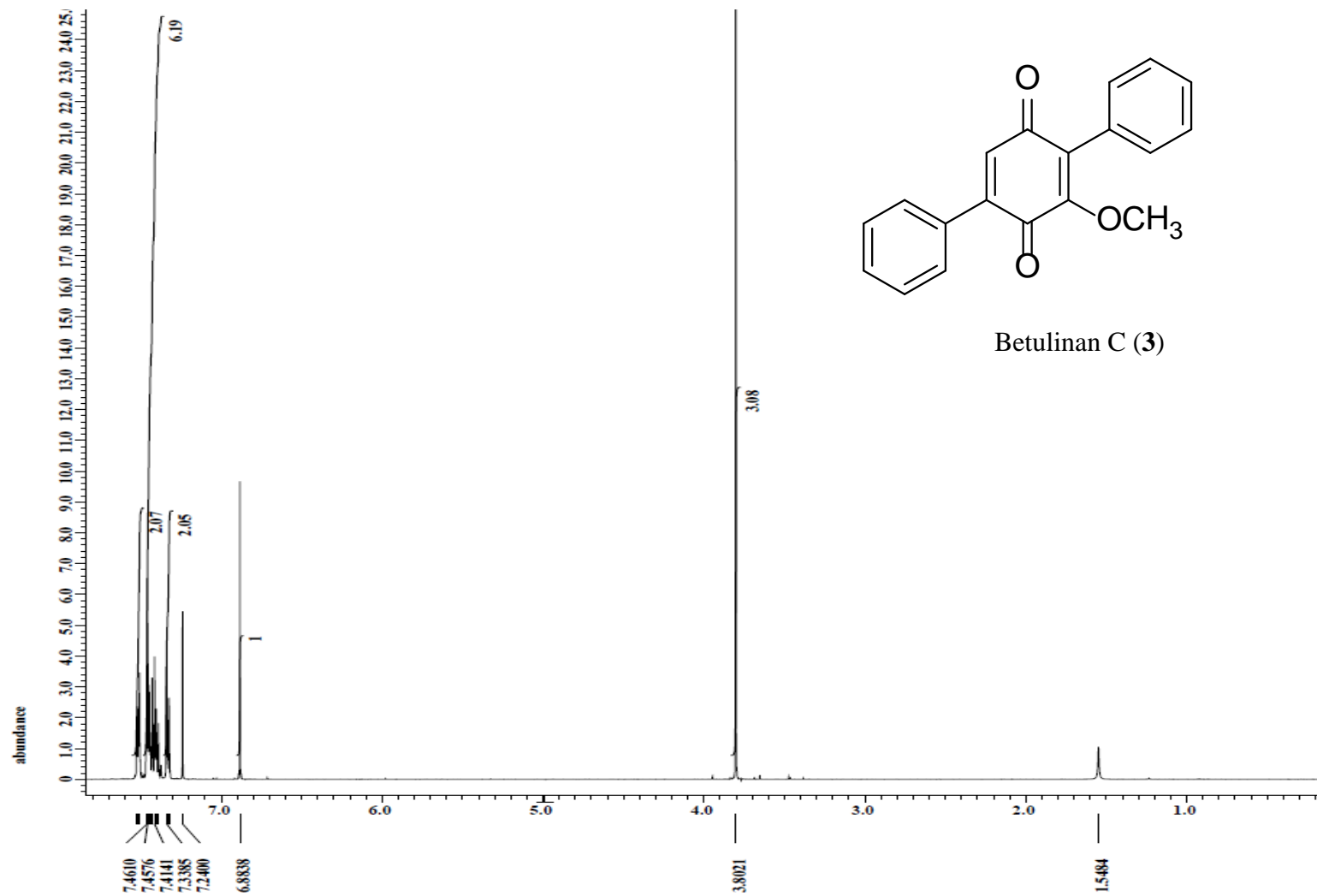


Figure 6. ^1H NMR (500 MHz, CDCl_3) of betulinan C (3).

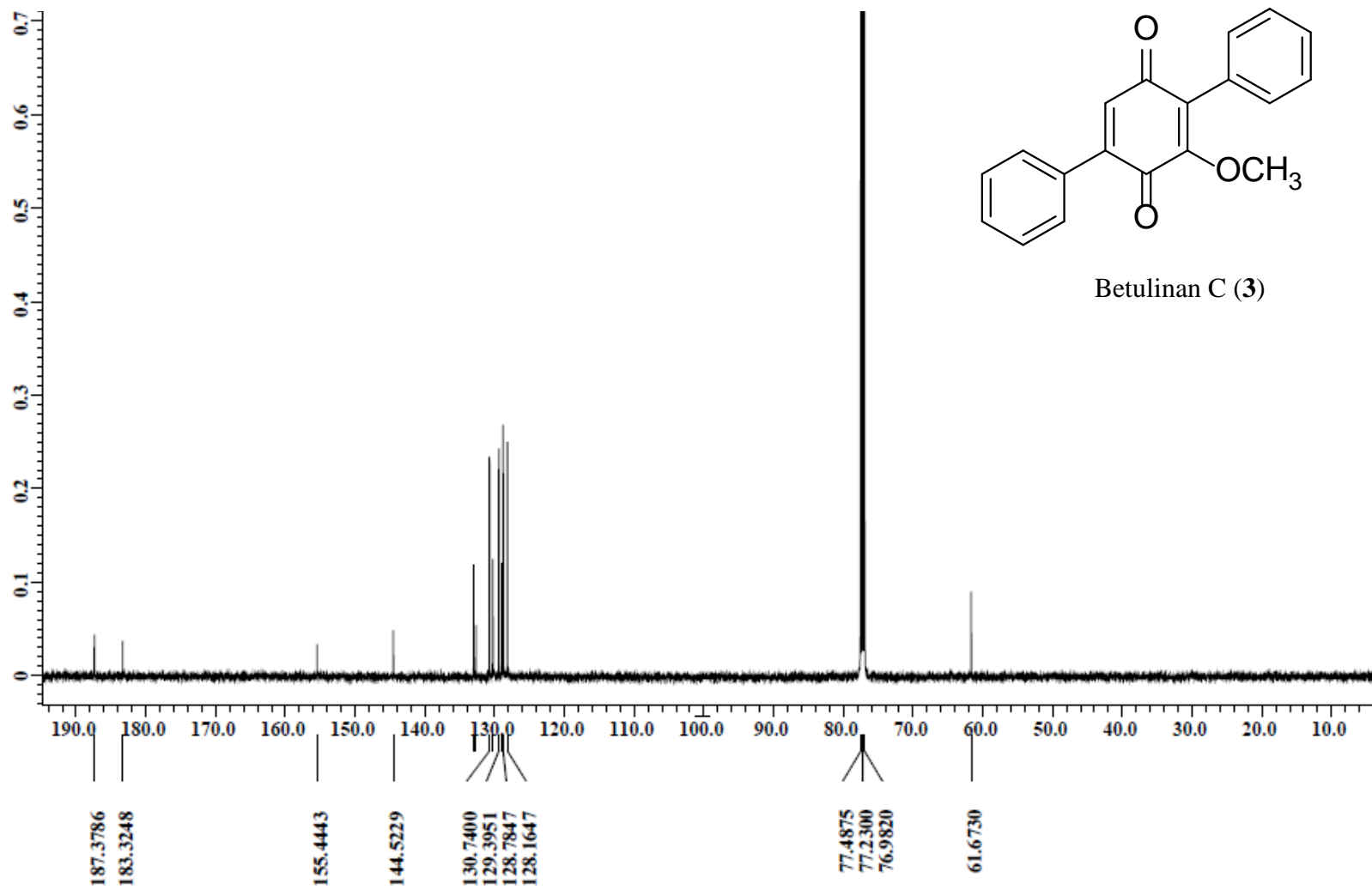


Figure 7. ^{13}C NMR (125 MHz, CDCl_3) of betulinan C (3).

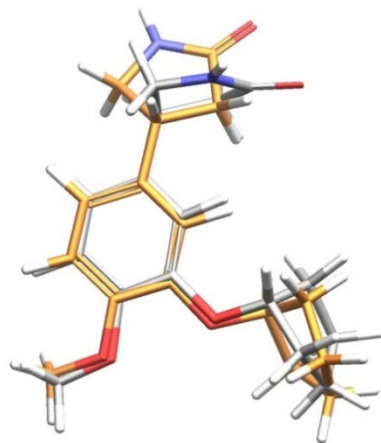


Figure 8. Comparison between the binding position of rolipram within the crystal structure (grey) and the binding mode predicted by Glide (orange).

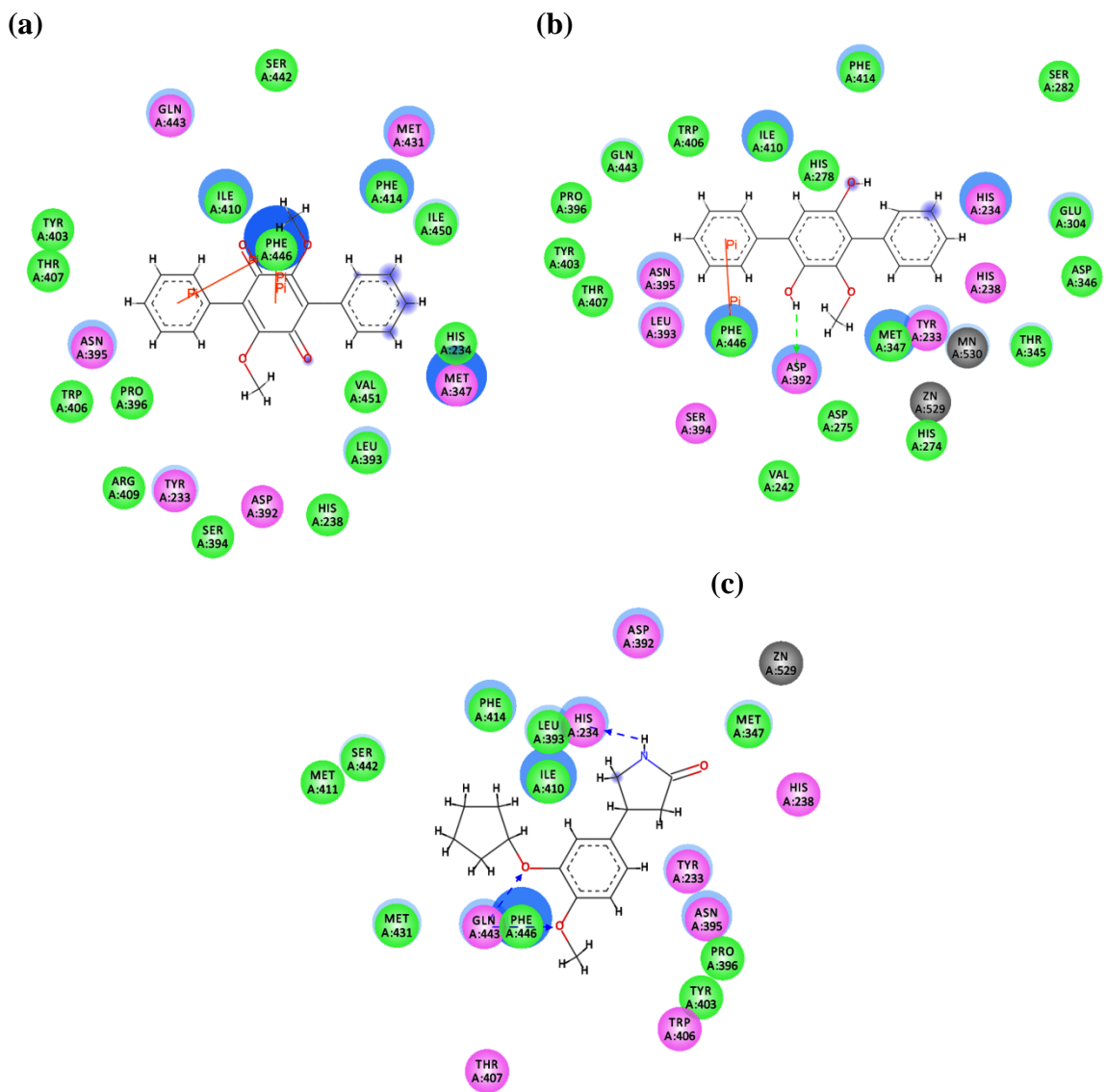


Figure 9. Two-dimensional interaction map of the optimized docking model of compound **1** (a), **2** (b), and rolipram (c) in the cAMP binding pocket of PDE4B. Amino acid residues within 4.5 Å of the ligand are displayed. Blue and green arrows indicate hydrogen bonding to amino acid side chain and main chain atoms, respectively.

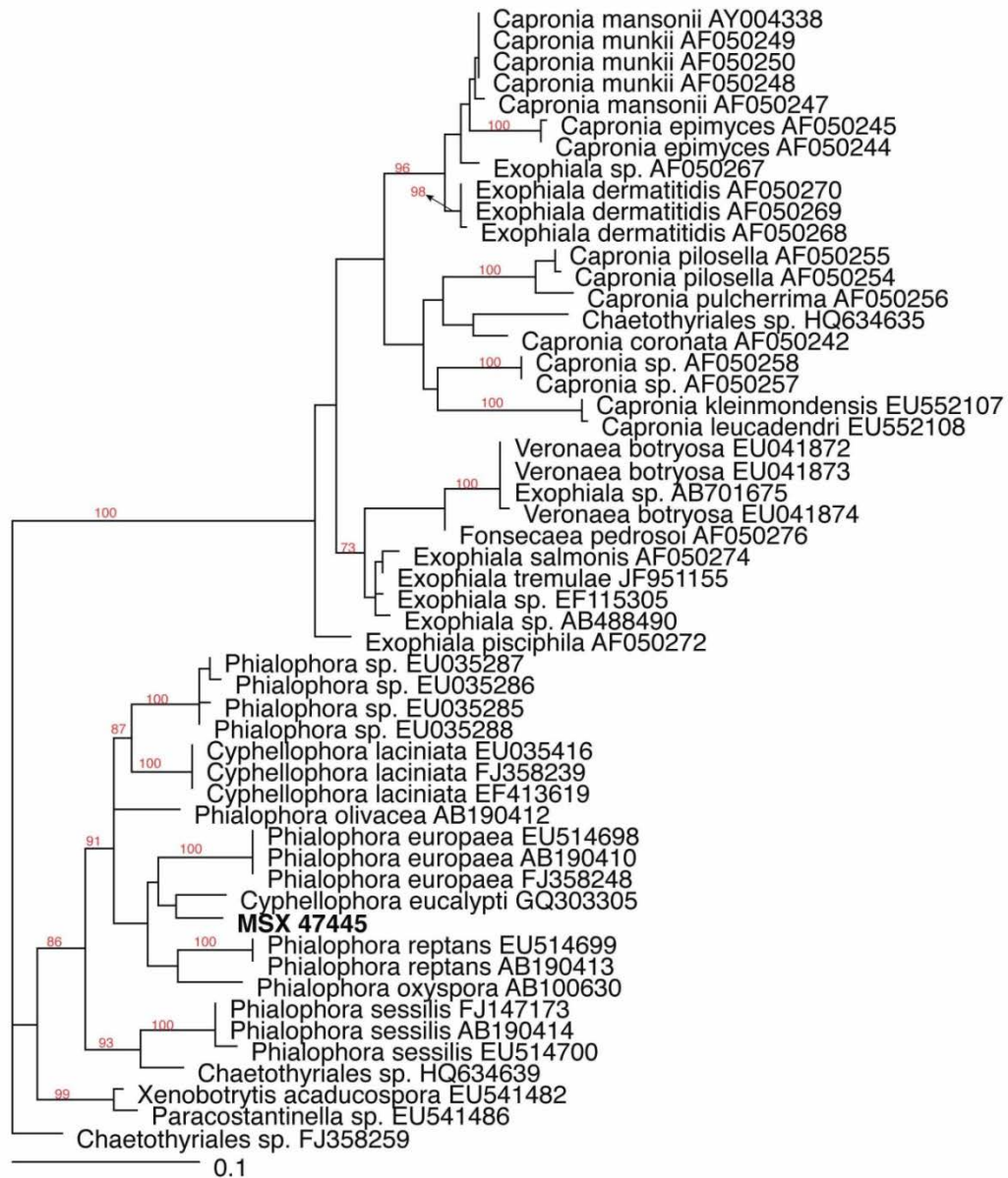


Figure 10. Phylogram of the most likely tree ($-\ln L = 4401.180$) from a RAxML analysis of 53 taxa based on partial region of the 28S large subunit nrDNA (1296 bp). Numbers refer to RAxML bootstrap support values $\geq 70\%$ based on 1000 replicates. MSX47445 is shown in bold.

Note: MSX47445 shows phylogenetic affinities to *Cyphellophora eucalypti* (GQ303305) but without significant bootstrap support.

Table 3. Cytotoxicity and Antimicrobial Activities of Compounds (1-3)

Compound	Cytotoxicity IC ₅₀ (μM)			MIC (μg/mL)	
	MCF-7	H460	SF268	<i>C. albicans</i>	<i>S. aureus</i>
betulinan A (1)	100.0	101.2	79.7	>150	>150
BTH-II0204-207:A (2)	39.0	21.8	38.8	>150	25
betulinan C (3)	26.1	19.5	32.8	100	25
camptothecin ^a	0.1	0.0	0.0	---	---
amphotericin B ^a	---	---	---	<0.025	---
novobiocin ^a	---	---	---	---	<0.025
^a positive controls					

CHAPTER III

WAOL A, *TRANS*-DIHYDROWAOL A, AND *CIS*-DIHYDROWAOL A: POLYKETIDE-DERIVED γ -LACTONES FROM A *VOLUTELLA* SPECIES

Tamam El-Elimat, Mario Figueroa, Huzefa A. Raja, Audrey F. Adcock, David J. Kroll, Steven M. Swanson, Mansukh C. Wani, Cedric J. Pearce, Nicholas H. Oberlies. *Tetrahedron Letters* 2013, 54, 4300-4302.

An organic extract of a filamentous fungus (MSX58801), identified as a *Volutella* sp. (Hypocreales, Ascomycota), displayed moderate cytotoxic activity against NCI-H460 human large cell lung carcinoma. Bioactivity-directed fractionation led to the isolation of three γ -lactones having the furo[3,4-*b*]pyran-5-one bicyclic ring system [waol A (**1**), *trans*-dihydrowaol A (**2**), and *cis*-dihydrowaol A (**3**)]. The structures were elucidated using a set of spectroscopic and spectrometric techniques; the absolute configuration of **2** was established via a modified Mosher's ester method. Compounds **1** and **2** were evaluated for cytotoxicity against a human cancer cell panel.

In pursuit of structurally diverse anticancer leads from nature,^{11,17} our group has been investigating filamentous fungi, particularly the Mycosynthetix library, representing over 55,000 accessions.^{18-22,62,63} Fungi represent an exciting reservoir of bioactive natural products, as they are an underexplored and renewable resource.^{8,13,23}

An organic extract of the filamentous fungus MSX58801, which was isolated from leaf litter in 1991, displayed moderate cytotoxic activity against NCI-H460 human large cell lung carcinoma (~86% inhibition of cell growth when tested at 20 $\mu\text{g/mL}$).¹⁹ Bioactivity-directed fractionation using flash chromatography followed by preparative RP-HPLC resulted in the isolation of three γ -lactones (**1-3**) containing a furo[3,4-*b*]pyran-5-one bicyclic ring system, with >95% purity for compounds **1** and **2** according to UPLC (Figure 14, Supplementary data). Compounds **1** and **2** were evaluated for cytotoxicity against a human cancer cell panel.

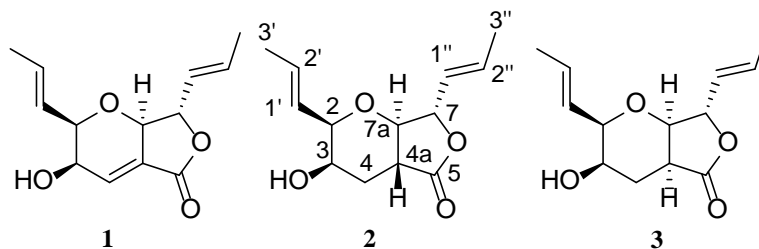


Figure 11. Structures of compounds **1-3**.

Compound **1** (2.46 mg), which was obtained as a colorless oil, had a molecular formula of $\text{C}_{13}\text{H}_{16}\text{O}_4$ as determined by HRESIMS. The NMR (Figure 15, Supplementary data), HRMS, and optical rotation data identified **1** as the known compound, waol A (FD-211; Figure 11). First isolated in 1995 from a fermentation of *Myceliophthora lutea* TF-0409,⁶⁴ the structure of **1** was revised in 2003.^{65,66}

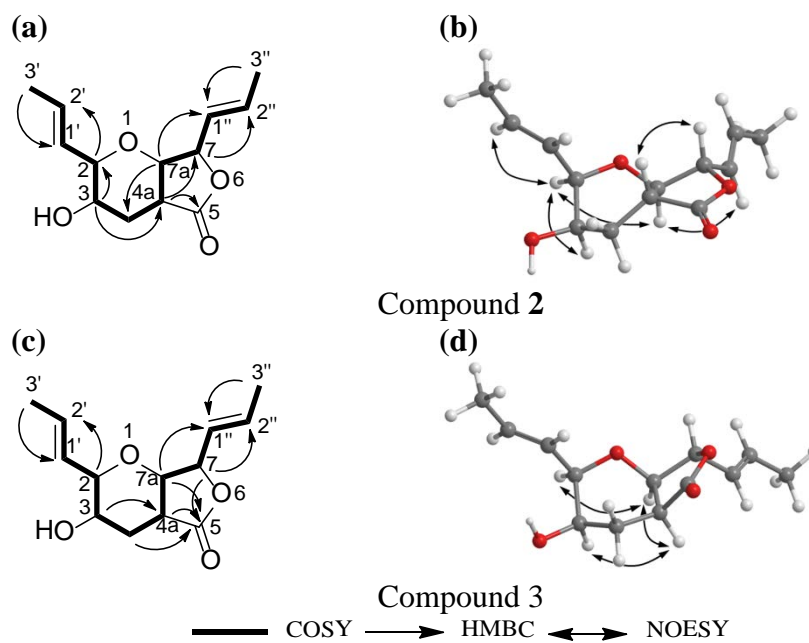


Figure 12. Key HMBC, COSY, and NOESY correlations of **2** and **3**.

Compound **2** (9.67 mg) was also obtained as a colorless oil.⁶⁷ The molecular formula was determined as C₁₃H₁₈O₄ via HRESIMS, establishing an index of hydrogen deficiency of 5. The NMR data suggested structural similarity with compound **1**. However, compound **2** lacked the olefinic proton at δ_{H} 6.90, which was replaced by three aliphatic protons (δ_{H} 1.79, 2.43, and 2.91). These data suggested a difference between **1** and **2** of a double bond, as supported by a 2 amu difference in the HRMS data. The ¹H NMR data of **2** revealed the presence of four olefinic protons, corresponding to two *trans*-disubstituted olefins (δ_{H} 5.52, ddq, $J = 15.5, 8.0, 1.7$; 5.55, ddq, $J = 15.5, 5.2, 1.7$; 5.91, dqd, $J = 15.5, 6.9, 1.7$; and 5.99, dq, $J = 15.5, 6.9$, for H-1'', H-1', H-2', and H-2'', respectively), four oxymethines (δ_{H} 3.48, dd, $J = 12.0, 8.6$; 3.84, bq, $J = 2.9$; 4.03, ddd, $J = 5.2, 2.9, 1.7$; and 4.67, dd, $J = 8.6, 8.0$, for H-7a, H-3, H-2, and H-7, respectively), one

methine (δ_{H} 2.91, ddd, $J = 12.6, 12.0, 3.4$, for H-4a), one methylene (δ_{H} 1.79, ddd, $J = 13.2, 12.6, 2.9$; and 2.43, ddd, $J = 13.2, 3.4, 2.9$, for H-4 α and H-4 β , respectively), two equivalent methyls (δ_{H} 1.77, dd, $J = 6.9, 1.7$, for H-3' and H-3''), and one exchangeable proton (δ_{H} 1.84, for 3-OH). The ^{13}C NMR data revealed 13 carbons, consistent with the HRMS data and indicative of one carbonyl (δ_{C} 173.5 for C-5), four olefinic carbons (δ_{C} 125.7, 126.4, 130.6, and 134.3, for C-1'', C-1', C-2', and C-2'', respectively), five methines (δ_{C} 39.0, 66.3, 81.2, 82.1, and 82.4 for C-4a, C-3, C-2, C-7a, and C-7, respectively), one methylene (δ_{C} 30.0 for C-4), and two methyls (δ_{C} 18.1 and 18.2 for C-3' and C-3'', respectively) (see Supplementary Figures 16 and 17 for the ^1H and ^{13}C NMR spectra and Table 4). The two double bonds and the carbonyl group accounted for three degrees of unsaturations, leaving the remaining two accommodated by the bicyclic ring system. COSY data identified one spin system as H₃-3'/H-2'/H-1'/H-2/H-3/H₂-4/H-4a/H-7a/H-7/H-1''/H-2''/H₃-3'' (Figure 12a). The following key HMBC correlations were observed: H₃-3'→C-1', H₃-3''→C-1'', H-2→C-2', H-7→C-2'', H-3→C-4a, H-7a→C-4, H-4a→C-7, and H-4a→C-5 (Figure 12a). NOESY correlations from H-1'' to H-7a, from H-7a to H-2, and from H-2 to H-3 and H-2' indicated that H-1'', H-7a, H-2, H-3, and H-2' were all on the same face. Alternatively, NOESY correlations observed from H-4a to H-7 indicated that these two protons were on the same side of the molecule but opposite to the previous set (Figure 12b). Comparing all of these data with those for **1** yielded the structure of **2** (Figure 11), which was ascribed the trivial name *trans*-dihydrowaol A. The absolute configuration of **2** was assigned via a modified Mosher's ester method,⁶⁸ establishing the configuration as 2*R*, 3*R*, 4*aR*, 7*S*, and 7*aR* (Figure 13).⁶⁹

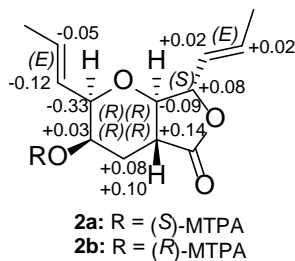


Figure 13. $\Delta\delta_{\text{H}}$ values [$\Delta\delta$ (in ppm) = $\delta_{\text{S}} - \delta_{\text{R}}$] obtained for (S)- and (R)-MTPA esters (**2a** and **2b**, respectively) of *trans*-dihydrowaol A (**2**) in pyridine- d_5 .

Compound **3** (1.45 mg) was obtained as a colorless oil.⁷⁰ The molecular formula was determined as $\text{C}_{13}\text{H}_{18}\text{O}_4$ via HRESIMS, and was the same as compound **2**. The NMR data (Table 5 and Figures 18 and 19) suggested structural similarity with **2**. Key differences were a coupling constant of 0.6 Hz between H-4a (δ_{H} 2.58, ddd, $J = 7.5, 2.3, 0.6$) and H-7a (δ_{H} 4.17, dd, $J = 4.6, 0.6$) in **3** vs 12 Hz in **2**, and a NOESY correlation from H-4a to H-7a in **3** vs H-4a to H-7 in **2** (Figure 12d). These data implied a pseudoaxial/pseudoequatorial *cis* orientation of H-4a/H-7a. NOESY correlations were also observed from H-2 to H-7a and H-4a, and from H-4a to H-3, indicating that those protons were on the same face (Figure 12d). These data suggested an inversion in the configuration at C-4a in **3** relative to **2**, establishing the structure of **3** as an epimer of **2** (Figure 11). The trivial name, *cis*-dihydrowaol A (**3**), was ascribed to this compound. The relative configuration of **3** was assigned by comparison with **2** as 2*R*, 3*R*, 4a*S*, 7*S*, and 7a*R*. An attempt to establish the absolute configuration via a modified Mosher's ester method⁶⁸ was unsuccessful.

Table 4. Cytotoxicity of Compounds 1 and 2 Against Two Human Tumor Cell Lines^a

compound	IC ₅₀ values in μM	
	MDA-MB-435 ^b	SW-620 ^c
waol A (1)	39.6	13.8
<i>trans</i> -dihydrowaol A (2)	>40	>40

^aPositive controls were vinblastine and bortezomib. Vinblastine was tested at concentrations of 3 ng/mL and 1 ng/mL: MDA-MB-435 cells had 37% and 99% viable cells; SW620 cells had 76% and 90% viable cells; respectively. Bortezomib was tested at concentrations of 5 nM and 2.5 nM: MDA-MB-435 cells had 90% and 91% viable cells; SW620 cells had 79% and 71% viable cells; respectively.

^bmelanoma and ^ccolon tumor cell lines were tested using published protocols.^{19,71}

Compounds **1** and **2** were tested against two cancer cell lines, MDA-MB-435 (human melanoma) and SW-620 (human colon cancer), using methods described previously;^{19,71} due to paucity of sample, compound **3** was not tested. While compound **1** showed moderate cytotoxic activity against the SW-620 cancer cell line, compound **2** was inactive against both cancer cell lines (Table 4), suggesting the importance of the double bond for cytotoxicity. Compound **1** was reported by Nozawa et al⁶⁴ to have broad spectrum activity against cultured tumor cell lines, including adriamycin-resistant HL-60 cells. Several compounds having the furo[3,4-*b*]pyran-5-one bicyclic ring system have been reported from fungi with diverse biological activities, including antibacterial and cytotoxic activities.⁷²⁻⁷⁷

Supplementary Data

General Experimental Procedures. Optical rotation data were acquired on a Rudolph Research Autopol III polarimeter. NMR experiments were conducted in CDCl_3 with TMS as a reference via a JEOL ECA-500, operating at 500 MHz for ^1H and 125 MHz for ^{13}C . HRESIMS was performed on a Thermo LTQ Orbitrap XL mass spectrometer equipped with an electrospray ionization source. UPLC was carried out on a Waters Acquity system with data collected and analyzed using Empower software. HPLC was carried out using a Varian Prostar HPLC system equipped with ProStar 210 pumps and a Prostar 335 photodiode array detector (PDA), with data collected and analyzed using Galaxie Chromatography Workstation software (version 1.9.3.2). For preparative HPLC, a Phenomenex Gemini-NX C_{18} ($5\ \mu\text{m}$; $250 \times 21.2\ \text{mm}$) column was used at a 21.24 mL/min flow rate. For UPLC, a Waters BEH C_{18} column ($1.7\ \mu\text{m}$; $50 \times 2.1\ \text{mm}$) was used with a 0.5 mL/min flow rate. Flash chromatography was performed on a Teledyne ISCO CombiFlash Rf using a 12 g Silica Gold column and monitored by UV and evaporative light-scattering detectors. All other reagents and solvents were obtained from Fisher Scientific and were used without further purification.

Producing Organism and Fermentation. Mycosynthetix fungal strain 58801 was isolated from leaf litter in 1991. The culture was stored on a malt extract slant and was transferred periodically. A fresh culture was grown on a similar slant, and a piece was transferred to a medium containing 2% soy peptone, 2% dextrose, and 1% yeast extract (YESD media). Following incubation (7 d) at 22 °C with agitation, the culture was used to inoculate 50 mL of a rice medium, prepared using rice to which was added a vitamin

solution and twice the volume of rice with H₂O, in a 250 mL Erlenmeyer flask. This was incubated at 22 °C until the culture showed good growth (approximately 14 d). The scale-up culture was grown in a 2.8 L Fernbach flask containing 150 g of rice and 300 mL of H₂O and was inoculated using a seed culture grown in YESD medium. This was incubated at 22 °C for 14 d.

Fungal strain MSX58801 was characterized using molecular data from the internal transcribed spacer region of the rRNA gene (ITS). The ITS region has been proposed as a barcode marker for fungal species identification.⁴⁵ The ITS region (ITS1-5.8S-ITS2) was amplified using illustra Ready-To-Go™ PCR Beads (GE Healthcare, Waukesha, WI) with a combination of ITS1F/ITS1 and ITS4 primers,^{53,54} using the following thermocycler conditions: initial denaturing at 94 °C for 5 min; 39 cycles of denaturing at 94 °C for 30 s, annealing at 50 °C for 15 s; extension at 72 °C for 1 min; and a final extension step of 72 °C for 10 min. Purified PCR products were sequenced in 11 μL sequencing reactions with BigDye Terminators v. 3.1 (Applied Biosystems, Foster City, CA) in combination with the following ITS primers: ITS1F/ITS5 and ITS4 at the University of Illinois Biotech facility. The ITS sequence was then subjected to a BLAST search using NCBI GenBank database. Based on this, the closest hits were members of the genus *Volutella*, Ascomycota [*Volutella consors* (Ellis & Everh.) Seifert, Gräfenhan & Schroers., GenBank FN598959; Identities = 432/443 (98%); Gaps = 4/443 (0%), *Volutella* sp., GenBank EF029211.1; Identities = 538/556 (97%); Gaps = 7/556 (1%)]. *Volutella* is a mitosporic fungus that has been poorly studied in the light of molecular phylogenetic analyses and includes about 120 described species.⁷⁸ The top BLAST

matches were subsequently downloaded, including the type species *V. ciliata* (Alb. & Schw.: Fr.) Fr., and a maximum likelihood (ML) analysis⁶¹ was performed using methods outlined earlier.⁷⁹ The ML analysis placed MSX58801 within a well-supported clade (based on 1000 ML bootstrap replicates) consisting of *Volutella* sp., and it was sister to a clade containing species of *V. ciliata* (Figure 20). Therefore, based on results of the BLAST search and ML phylogenetic analysis, the strain MSX58801 was identified as a *Volutella* sp. (Ascomycota; Pezizomycotina; Sordariomycetes; Hypocreomycetidae; Hypocreales; Nectriaceae). The sequence data for MSX58801 was deposited in GenBank (accession no KC963031).

Extraction and Isolation. Six large scale fermentation cultures (LS-1 to LS-6) of the fungus MSX58801 were processed during the course of this project due to the challenges associated with getting the fungus to reliably produce the target compounds. Compound **2** was detected in LS-1, LS-3, and LS-4, compound **3** was detected only in LS-1, while compound **1** was detected in LS-3 and LS-4. None of the target compounds were detected in LS-2, LS-5, and LS-6. To each large-scale solid fermentation culture of MSX58801, 500 mL of 1:1 MeOH-CHCl₃ were added. The culture was chopped with a spatula and shaken overnight (~16 h) at ~100 rpm at rt. The sample was filtered with vacuum, and the remaining residues were washed with 100 mL of 1:1 MeOH-CHCl₃. To the filtrate, 900 mL CHCl₃ and 1500 mL H₂O were added; the mixture was stirred for 2 h and then transferred into a separatory funnel. The bottom layer was drawn off and evaporated to dryness. The dried organic extract was re-constituted in 300 mL of 1:1 MeOH-CH₃CN and 200 mL of hexanes. The biphasic solution was stirred for an hour

and then transferred to a separatory funnel. The MeOH-CH₃CN layer was drawn off and evaporated to dryness under vacuum. Each defatted material (860, 620, and 1000 mg, for LS-1, 3, and 4, respectively, which were found to produce the target compounds) was dissolved in a mixture of CHCl₃-MeOH, adsorbed onto Celite 545, and fractionated via flash chromatography using a gradient solvent system of hexane-CHCl₃-MeOH at a 40 mL/min flow rate and 53.3 column volumes over 63.9 min to afford 5 fractions. Fraction 3, which eluted with 100% CHCl₃, was subjected to preparative HPLC using a gradient solvent system that initiated with 30:70 of CH₃CN-H₂O to 50:50 over 30 min at a flow rate of 21.24 mL/min to yield three sub-fractions. Sub-fractions 1, 2, and 3 which eluted at 13.0, 14.0 and 15.3 min, yielded compounds **3** (1.45 mg), **2** (9.67 mg) and **1** (2.46 mg), respectively. UPLC was used to evaluate the purity of the isolated compounds using a gradient solvent system that initiated with 20:80 CH₃CN-H₂O to 100% CH₃CN over 4.5 min; compounds **1** and **2** were >95% pure.

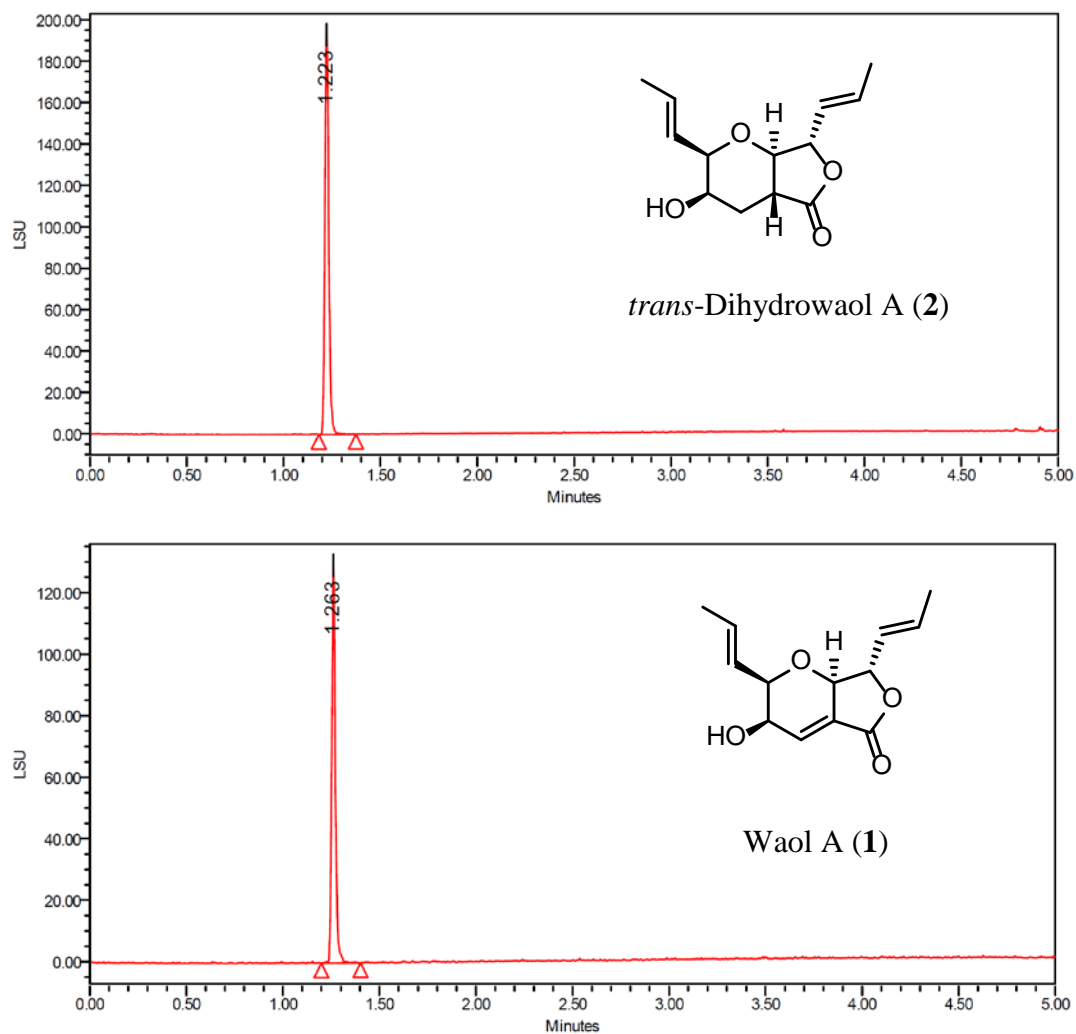


Figure 14. UPLC chromatograms of compounds **1** and **2** (ELSD detection) demonstrating >95% purity.

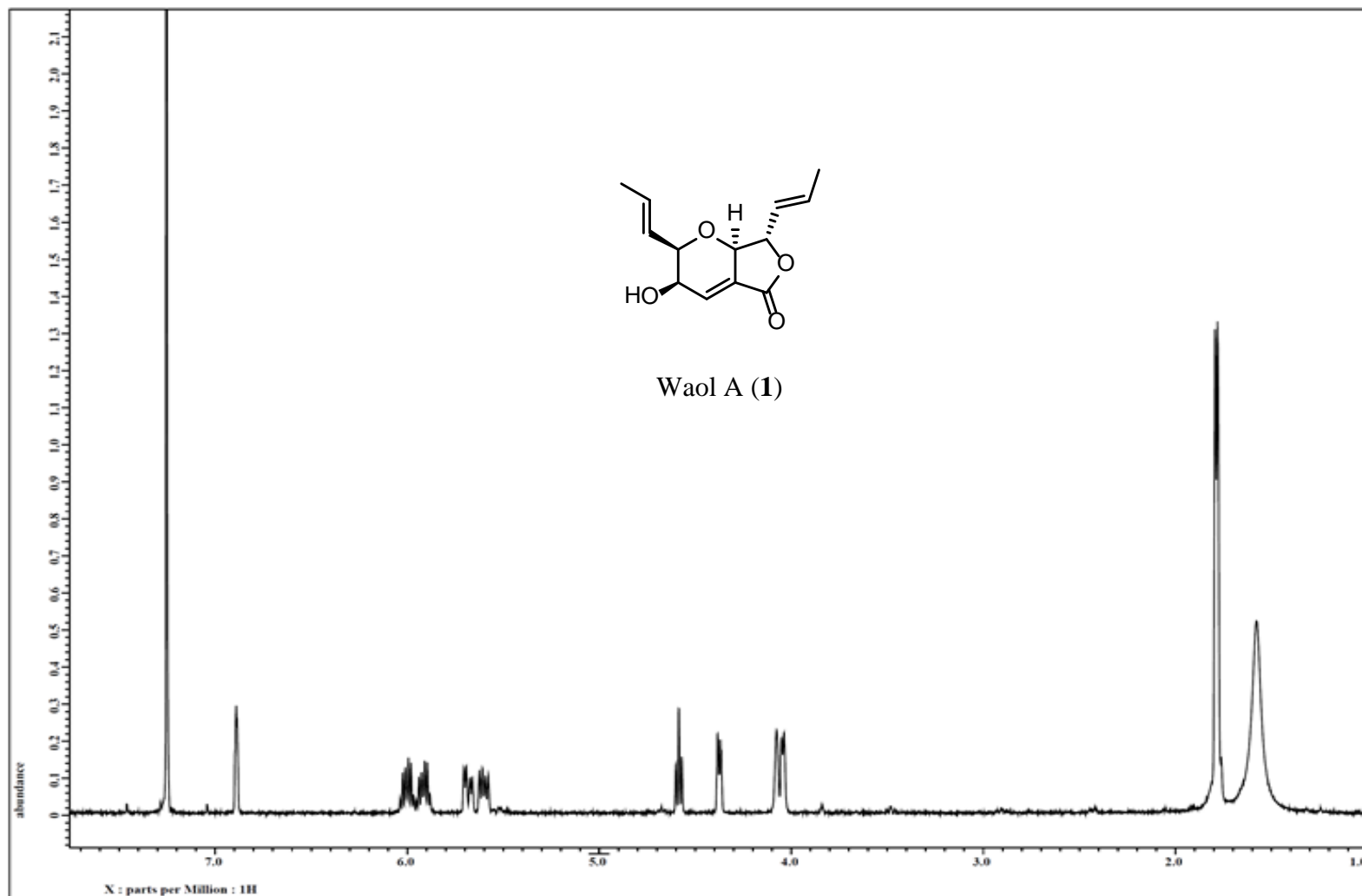


Figure 15. ¹H NMR spectrum of waol A (1) [500 MHz, CDCl₃].

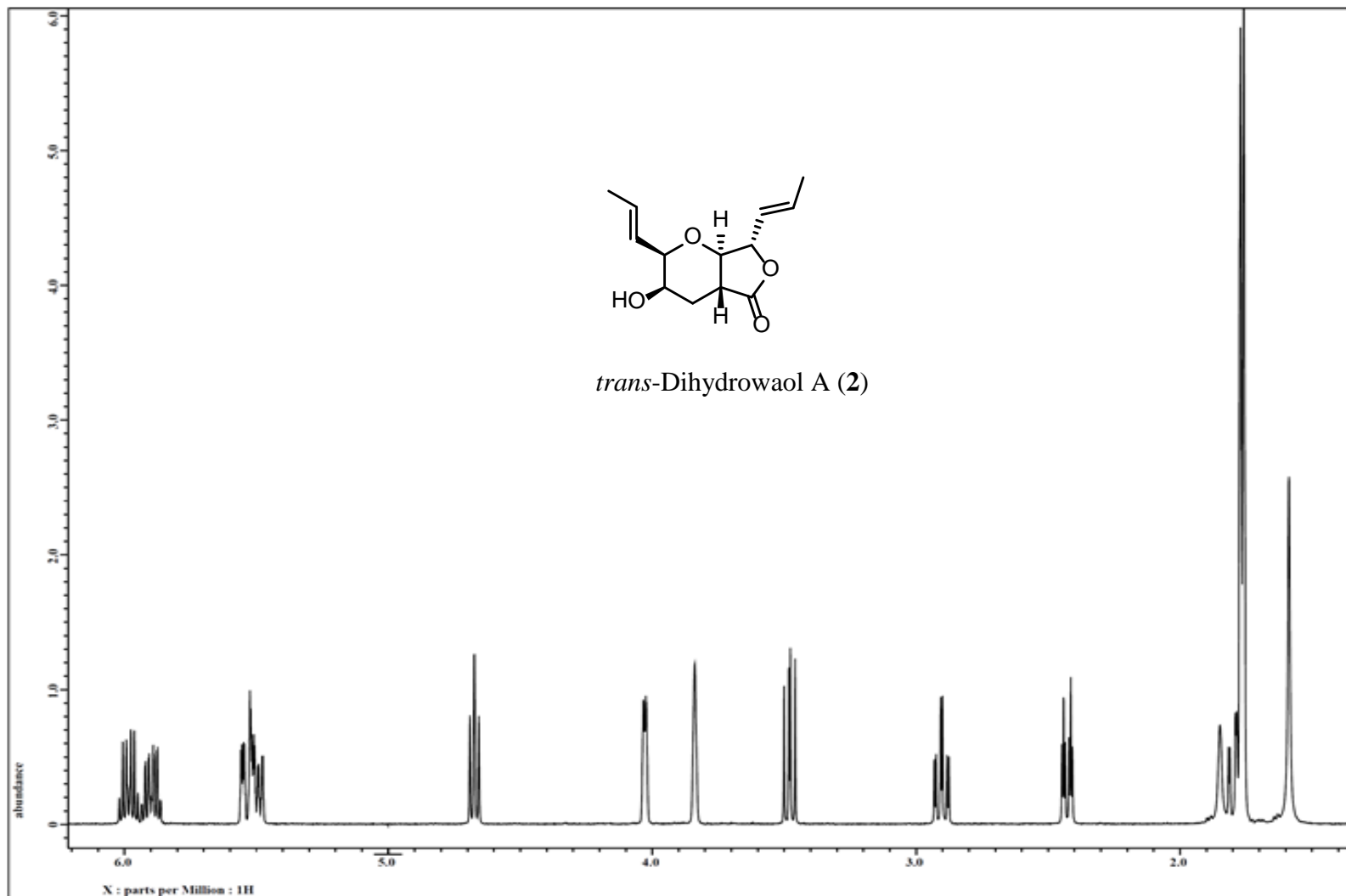


Figure 16. ¹H NMR spectrum of *trans*-dihydrowaol A (2) [500 MHz, CDCl₃].

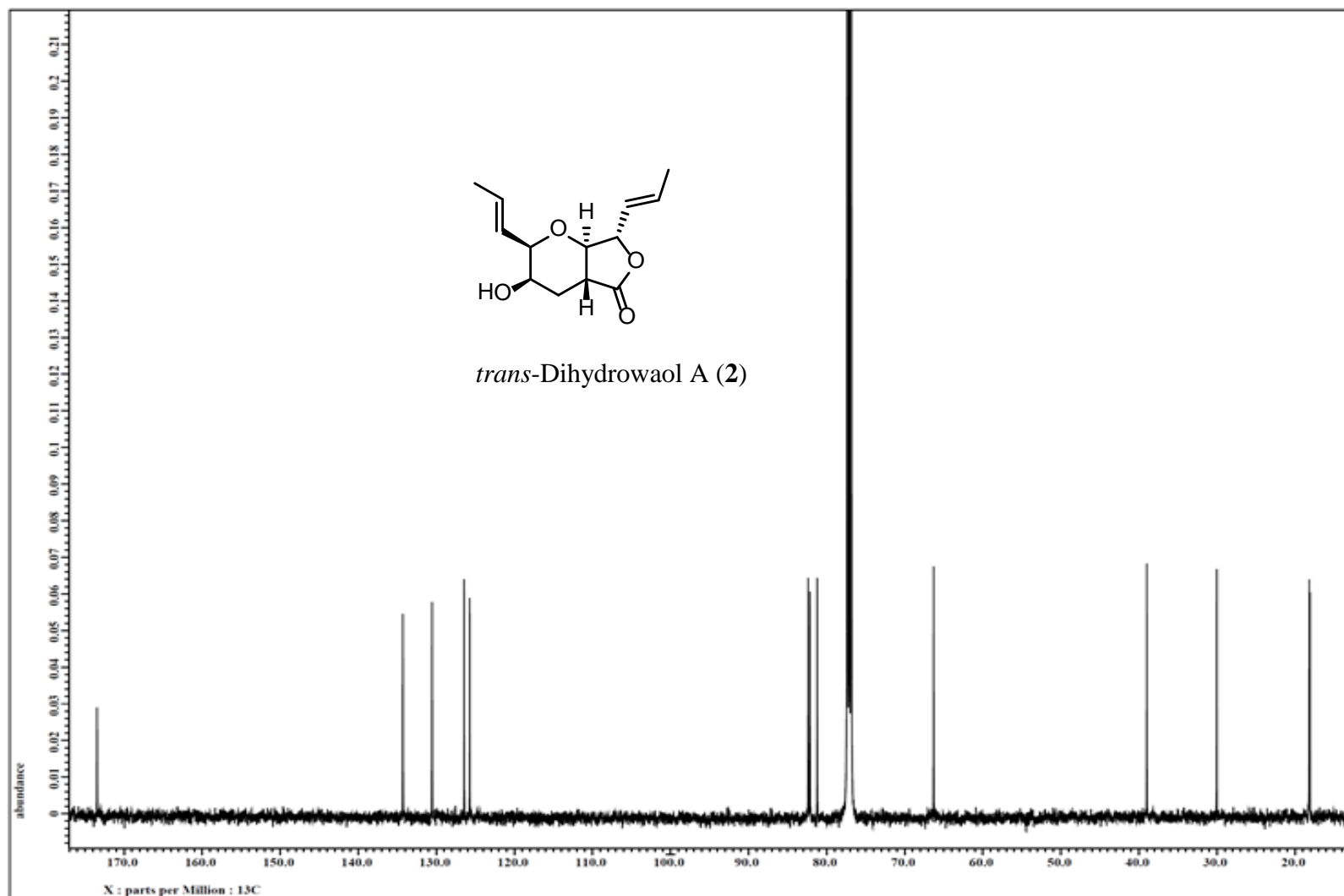


Figure 17. ^{13}C NMR spectrum of *trans*-dihydrowaol A (2) [125 MHz, CDCl_3].

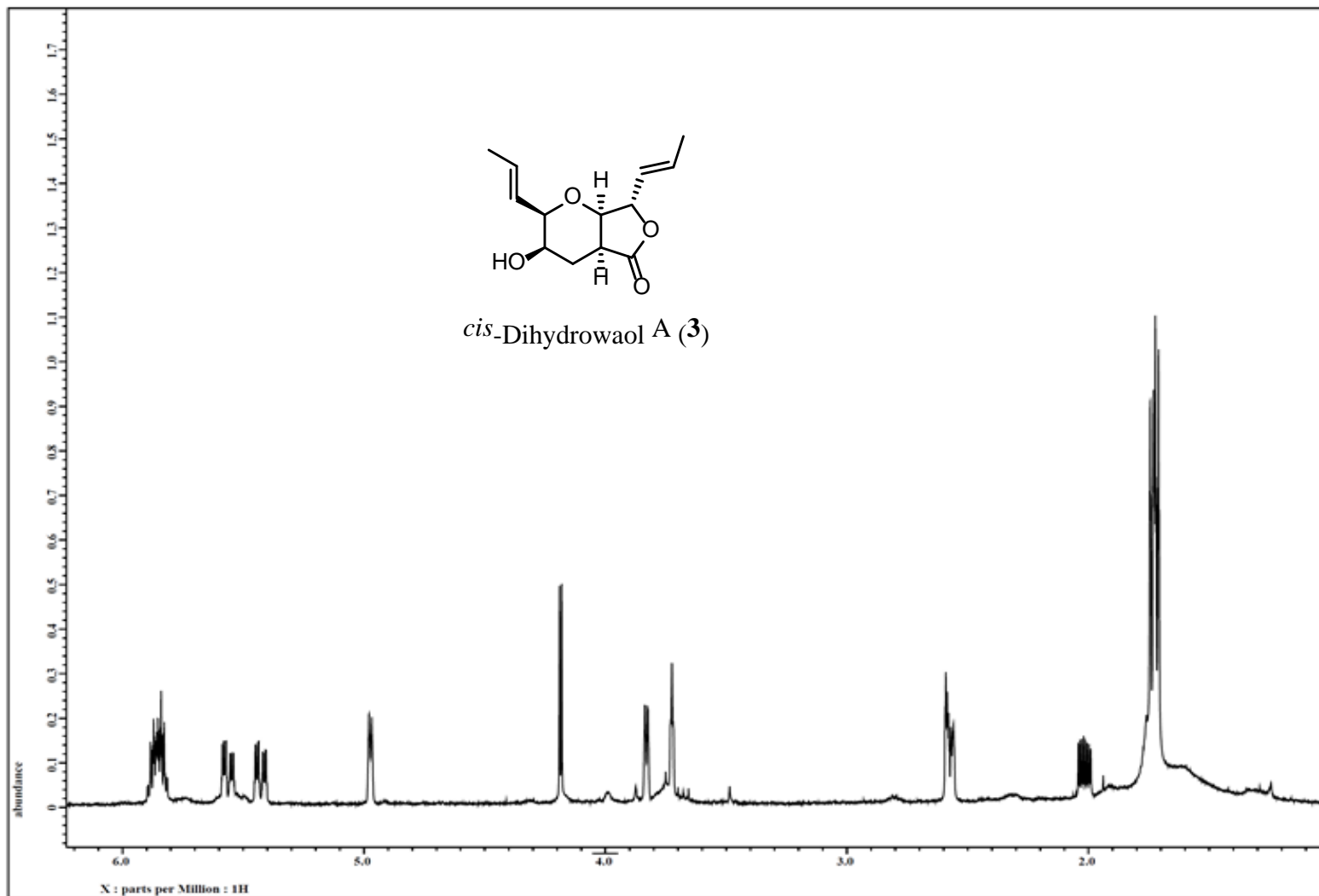


Figure 18. ¹H NMR spectrum of *cis*-dihydrowaol A (**3**) [500 MHz, CDCl₃].

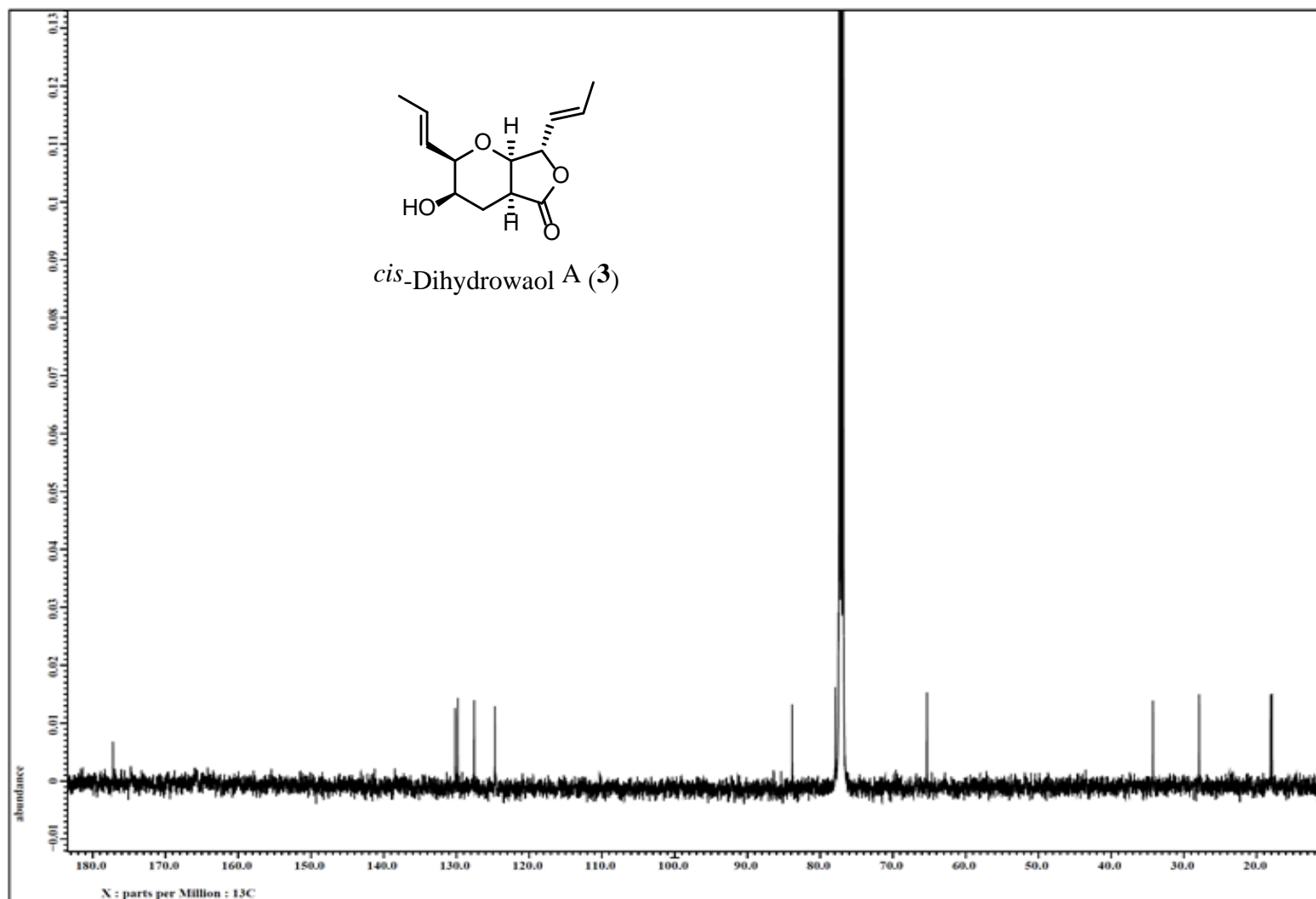


Figure 19. ^{13}C NMR spectrum of *cis*-dihydrowaol A (3) [125 MHz, CDCl_3].

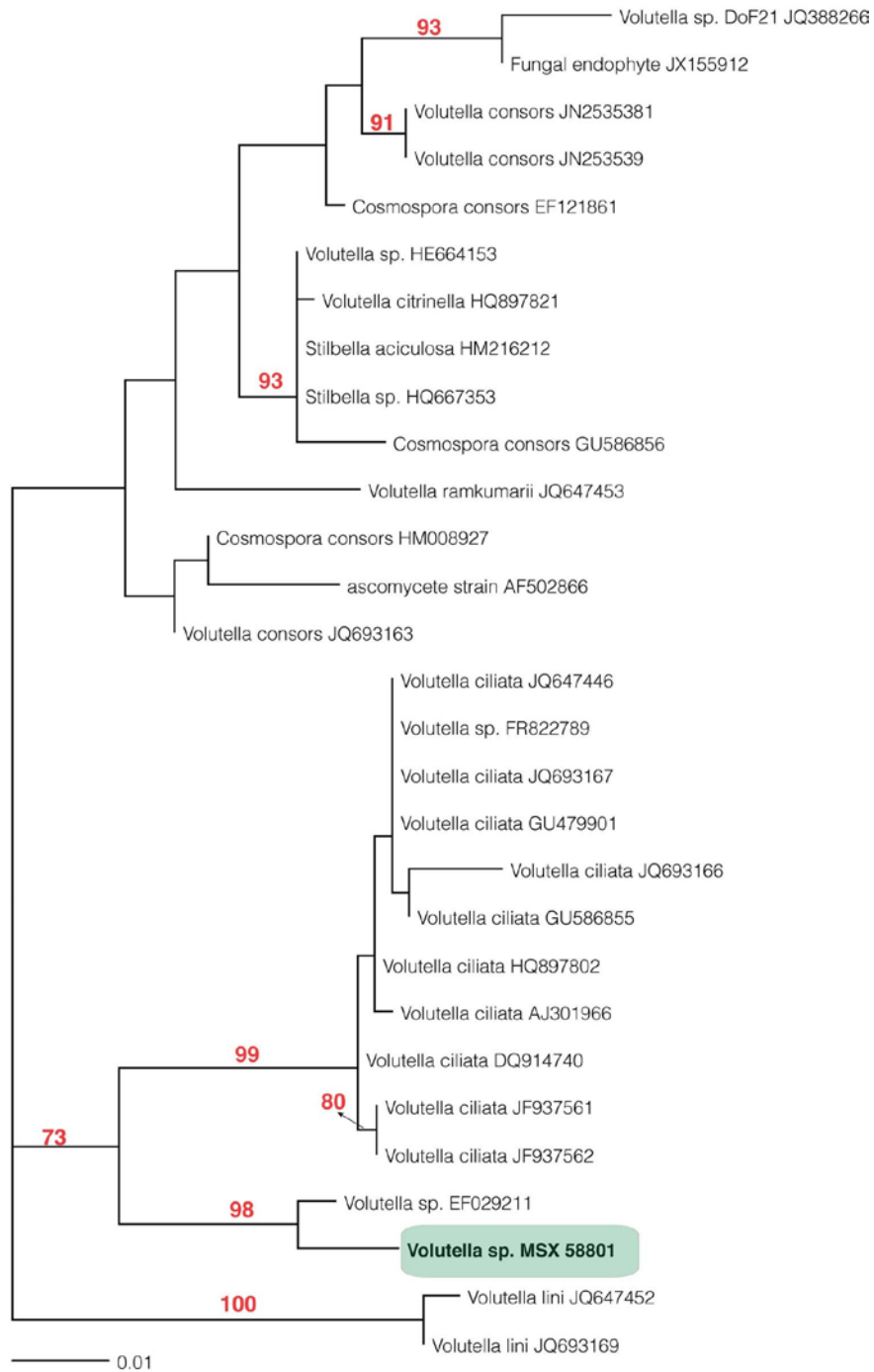


Figure 20. Phylogram of the most likely tree ($-\ln L = 1561.75$) from a PHYML analysis of 29 taxa based on ITS nrDNA sequence data (556 bp). Numbers refer to PHYML bootstrap support values $\geq 70\%$ based on 1000 replicates. MSX58801 identified as *Volutella* sp. (highlighted in green). Bar indicates nucleotide substitution per site.

Table 5. NMR Data for *trans*-Dihydrowaol A (2) and *cis*-Dihydrowaol A (3) [500 MHz for ¹H, 125 MHz for ¹³C; Chemical Shifts in δ , Coupling Constants in Hz, CDCl₃]

position	2		3	
	δ_C , type	δ_H , mult (<i>J</i> in Hz)	δ_C , type	δ_H , mult (<i>J</i> in Hz)
2	81.2, CH	4.03, ddd (5.2, 2.9, 1.7)	77.5, CH	3.82, ddd (5.7, 2.3, 1.2)
3	66.3, CH	3.84, bq (2.9)	65.3, CH	3.71, ddd (3.4, 2.3, 1.2)
4 α	30.0, CH ₂	1.79, ddd (13.2, 12.6, 2.9)	27.9, CH ₂	2.02, ddd (14.9, 7.5, 3.4)
4 β		2.43, ddd (13.2, 3.4, 2.9)		2.57, ddd (14.9, 2.3, 1.2)
4a	39.0, CH	2.91, ddd (12.6, 12.0, 3.4)	34.3, CH	2.58, ddd (7.5, 2.3, 0.6)
5	173.5, C	--	177.2, C	--
7	82.4, CH	4.67, dd (8.6, 8.0)	83.8, CH	4.97, ddd (5.7, 4.6, 1.7)
7a	82.1, CH	3.48, dd (12.0, 8.6)	77.9, CH	4.17, dd (4.6, 0.6)
1'	126.4, CH	5.55, ddq (15.5, 5.2, 1.7)	127.6, CH	5.54, ddq (15.5, 5.7, 1.7)
2'	130.6, CH	5.91, dqd (15.5, 6.9, 1.7)	129.8, CH	5.85, dqd (15.5, 6.9, 1.2)
3'	18.1, CH ₃	1.77, dd (6.9, 1.7)	18.1, CH ₃	1.74, dd (6.9, 1.7)
1''	125.7, CH	5.52, ddq (15.5, 8.0, 1.7)	124.7, CH	5.43, ddq (15.5, 5.7, 1.7)
2''	134.3, CH	5.99, dq (15.5, 6.9)	130.2, CH	5.85, dqd (15.5, 6.9, 1.7)
3''	18.2, CH ₃	1.77, dd (6.9, 1.7)	17.9, CH ₃	1.72, dd (6.9, 1.7)
3-OH	–	1.84, br s	–	1.76, br s

CHAPTER IV

SORBICILLINOID ANALOGUES WITH CYTOTOXIC AND SELECTIVE ANTI- *ASPERGILLUS* ACTIVITIES FROM *SCYTALIDIUM ALBUM*

Tamam El-Elimat, Mario Figueroa, Huzefa A. Raja, Steven M. Swanson, Joseph O. Falkinham III, David M. Lucas, Mansukh C. Wani, Cedric J. Pearce, and Nicholas H. Oberlies. This chapter is intended for submission to *Journal of Antibiotics* (2014).

As part of an ongoing project to explore filamentous fungi for anticancer and antibiotic leads, eleven bioactive compounds were isolated and identified from an organic extract of the fungus *Scytalidium album* (MSX51631) using bioactivity-directed fractionation against a human cancer cell panel. Of these, eight were a series of sorbicillinoid analogues (**1-8**), of which four were new [scalbucillin A (**2**), scalbucillin B (**3**), scalbucillin C (**6**) and scalbucillin D (**8**)], two were phthalides (**9-10**), and one was naphthalenone (**11**). Compounds (**1-11**) were tested in the MDA-MB-435 (melanoma) and SW-620 (colon) cancer cell lines. Compound **1** was the most potent with IC₅₀ values of 1.5 μM, respectively, followed by compound **5**, with IC₅₀ values of 2.3 and 2.5 μM at 72 h. Compound **1** showed a 48-h IC₅₀ value of 3.1 μM when tested against the lymphocytic leukemia cell line OSU-CLL. Compounds **1** and **5** showed selective and equipotent activity against *Aspergillus niger* with minimum inhibitory concentration values of 0.05 and 0.04 μg/ml (0.20 and 0.16 μM), respectively. The *in vitro* hemolytic

activity against sheep erythrocytes of compounds **1** and **5** was investigated and were found to provoke 10% hemolysis at 45 and 37.5 µg/ml, respectively.

Introduction

Bioactivity-directed purification studies of filamentous fungi from the Mycosynthetix library, representing over 55,000 accessions, have yielded structurally diverse cytotoxic secondary metabolites.^{17,62,63,80-82} As part of these, the organic extract of a solid phase culture of a fungus identified as *Scytalidium album* (MSX51631), which was isolated in 1990 from Cobb county, Georgia, USA, showed promising cytotoxic activities against the SW-620 (colon) and MDA-MB-435 (melanoma) cancer cell lines. Bioactivity-directed fractionation resulted in the isolation and identification of eight sorbicillinoid analogues (**1-8**), of which four were new [scalbucillin A (**2**), scalbucillin B (**3**), scalbucillin C (**6**) and scalbucillin D (**8**)] and four were known [5'-formyl-2'-hydroxyl-4'-methoxy-(*E,E*)-sorbophenone (**1**), 1-(2'-hydroxy-4'-methoxy-5'-methylphenyl)-2,4-*E,E*-hexadien-1-one (**4**), 5'-formyl-2'-hydroxy-4'-methoxy-(*E*)-4-hexenophenone (**5**), and 1-(2'-hydroxy-4'-methoxy-5'-hydroxymethylphenyl)-*E*-4-hexen-1-one (**7**)]. Also isolated were two phthalides [5,7-dimethoxyphthalide (**9**) and 4,6-dimethoxyphthalide (**10**)] and one naphthalenone [isosclerone (**11**)]. Compounds **1-11** were evaluated for cytotoxicity against a human cancer cell panel and for antimicrobial activity in an array of bacteria and fungi. The hemolytic activity of compounds **1**, **3**, and **5** was measured against sheep red blood cells. Compounds **1** and **5** were further evaluated for growth inhibitory activity against a B-lymphocytic leukemia cell line, OSU-CLL.⁸³

Overall, the growth inhibitory activity of the primary organic extract was attributed to compounds **1** and **5**.

Results and Discussion

Two solid-substrate large-scale cultures of the fungus *Scytalidium album* were extracted with 1:1 CHCl₃-MeOH and partitioned with water. The vacuum-dried organic extract was then defatted with 1:1 CH₃CN/MeOH-hexane. The resulting CH₃CN/MeOH-soluble extract showed cytotoxic activity against the SW-620 and MDA-MB-435 cancer cell lines (~83% and 71% inhibition of cell growth when tested at 20 µg/ml, respectively) and was subjected to fractionation using flash chromatography. Active fractions on the two cancer cell lines were purified using reversed-phase preparative and semi-preparative HPLC to yield compounds **1-11** with >95% purity as evidenced by UPLC (Supplementary Figure 23).

A series of eight sorbicillinoid analogues (**1-8**), of which four were new, all possessing the carbon skeleton of the known antibiotic, sorbicillin,⁸⁴ were isolated and identified in this study. The NMR, HRMS, and UV data identified **1** (13.87 mg) and **5** (3.25 mg) as the known 5'-formyl-2'-hydroxyl-4'-methoxy-(*E,E*)-sorbophenone and 5'-formyl-2'-hydroxy-4'-methoxy-(*E*)-4-hexenophenone, respectively. Both of these were isolated in 1973 from the fungus *Scytalidium* sp. FY strain.⁸⁵ In an analogous manner, compounds **4** (5.89 mg) and **7** (8.21 mg) were identified as the known 1-(2'-hydroxy-4'-methoxy-5'-methylphenyl)-*E,E*-2,4-hexadien-1-one, and 1-(2'-hydroxy-4'-methoxy-5'-hydroxymethylphenyl)-*E*-4-hexen-1-one, respectively. Both **4** and **7** were isolated in 2006 from a fungicolous isolate of the genus *Phaeoacremonium*.⁸⁶ Characterization data

for all isolates compared favorably with the literature (See Supplementary Figures 24, 27, 28, and 30 for ^1H and ^{13}C NMR spectra of compounds **1**, **4**, **5**, and **7**, respectively).

Four new sorbicillinoid analogues (**2**, **3**, **6**, and **8**) were isolated as well, and their structures were identified by comparison of HRMS and NMR data with each other and with structurally related known compounds. Compound **2** (1.77 mg) was obtained as a yellow powder. The molecular formula was determined as $\text{C}_{14}\text{H}_{14}\text{O}_5$ via HRESIMS along with ^1H , ^{13}C , and edited-HSQC data (Tables 6 and 8, Supplementary Figure 25), establishing an index of hydrogen deficiency of 8. Inspection of the HRMS and NMR data suggested **2** as a sorbicillinoid analogue with structural similarity with **1**. For example, compound **2** showed the characteristic C1'-C6' sorbyl side chain, as noted by two conjugated double bonds with coupling constants consistent with an *E, E* configuration ($J_{\text{H-2/H-3}}$ and $J_{\text{H-4/H-5}} = 14.6$ Hz) that were conjugated with a ketone carbonyl ($\delta_{\text{C}} 192.8$) that was further conjugated with an aryl group. Additional similarities included NMR signals characteristic of six aromatic carbons and two singlet aromatic protons, suggesting a 1,2,4,5-tetrasubstituted benzene ring with two aromatic protons *para* to each other, a methoxy group, and a hydrogen-bonded phenolic proton. All of the benzene ring substituents were confirmed by HMBC correlations (Figure 22). Key differences between compounds **1** and **2** were the replacement of the singlet aldehyde proton and the carbonyl carbon in **1** ($\delta_{\text{H}}/\delta_{\text{C}} 10.27/187.7$) by a broad exchangeable proton and a carboxylic acid carbon in **2** ($\delta_{\text{H}}/\delta_{\text{C}} 10.05/164.3$). These data, along with an extra oxygen atom in **2** relative to **1**, as supported by a 16 amu difference in the HRMS data, suggested that the aldehyde substituent at C-5' of the benzene ring in **1**

was replaced by a carboxylic acid group in **2**. The trivial name scabucillin A was ascribed to **2**.

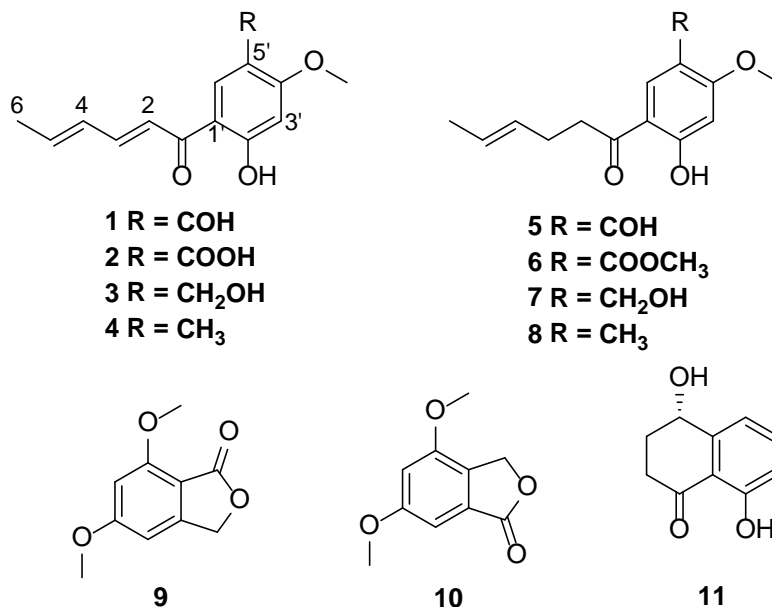


Figure 21. Structure of compounds (**1-11**) isolated from *S. album*.

Compound **3** (1.10 mg) was obtained as a yellow powder with a molecular formula of C₁₄H₁₆O₄ as determined by HRESIMS and analysis of ¹H NMR, ¹³C NMR, and edited-HSQC data (Tables 6 and 8, Supplementary Figure 26). Inspection of the NMR data suggested compound **3** as a sorbicillinoid analogue with structural similarity to **7**. However, compound **3** lacked the four aliphatic protons H₂-2 and H₂-3 (δ_H 2.98 and 2.41), which were replaced by two olefinic protons (δ_H 6.95 and 7.49) with a coupling constant consistent with an *E* configuration (*J*_{H-2/H-3} = 15.0 Hz). Conjugation of the C2-C3 double bond with the ketone carbonyl resulted in an upfield shift of the chemical shift of C1 in **3** relative to **7**. Further examination of the NMR data, including COSY and

HMBC spectra (Figure 22), yielded the structure of **3**, which was ascribed the trivial name scabucillin B.

Compound **6** (9.97 mg) was obtained as a white powder. The chemical formula was determined as C₁₅H₁₈O₅ by HRESIMS and analysis of ¹H NMR, ¹³C NMR, and edited-HSQC data (Tables 7 and 8, Supplementary Figure 29). Examining the NMR data suggested a sorbicillinoid analogue with structural similarity to **5** (Table 7). As in **5**, compound **6** showed NMR signals consistent with a side chain containing two-coupled olefinic protons with a coupling constant that supported an *E* configuration ($J_{\text{H-4/H-5}} = 15.5$ Hz). A chemical shift of the ketone carbonyl of 204.7 ppm indicated the lack of conjugation with the double bond. Furthermore, the presence of a three proton doublet of doublets ($\delta_{\text{H-6}} 1.65$, dd, $J = 6.3, 1.2$ Hz) with a chemical shift and coupling constants consistent with an allylic position established the side chain of compound **6** (Figure 21). Additional similarities included NMR data characteristic of a 1,2,4,5-tetrasubstituted benzene ring with two sharp singlet aromatic protons, indicating positions *para* to each other. A sharp singlet proton ($\delta_{\text{H}} 13.05$), which did not show single bond coupling to a carbon as evidenced from the edited HSQC experiment, indicated a phenolic proton *ortho* to the side chain and hydrogen-bonded with the carbonyl carbon. Key differences between compounds **5** and **6** include replacement of the aldehyde proton in **5** ($\delta_{\text{H}} 10.26$) by a methoxy functionality in **6** ($\delta_{\text{H}}/\delta_{\text{C}} 3.88/52.2$) and replacement of the aldehyde carbon ($\delta_{\text{C}} 187.5$) by an ester functionality ($\delta_{\text{C}} 165.4$). These data, along with a 30 amu difference in the HRMS data of compounds **5** and **6**, indicated replacement of the

aldehyde in **5** by a methyl ester in **6**. The trivial name scalbucillin C was ascribed to compound **6**.

Compound **8** (2.47 mg), which was obtained as a white powder, had a molecular formula of C₁₄H₁₈O₃ as determined by HRESIMS and analysis of ¹H NMR, ¹³C NMR and edited-HSQC data (Tables 7 and 8, Supplementary Figure 31). The NMR data of **8** indicated a sorbicillinoid analogue with structural similarity to **4**. However, **8** lacked the H-2 and H-3 olefinic protons, which were replaced by four aliphatic protons (δ_{H} 2.95 and 2.40 for H₂-2 and H₂-3, respectively). This resulted in a downfield shift of C1 in **8** (δ_{C} 204.2), relative to that in **4** (δ_{C} 192.3), since the latter conjugates with the C2-C3 double bond. Further analysis of the NMR data including COSY and HMBC experiments (Figure 22), yielded the structure of **8**, which was ascribed the trivial name scalbucillin D.

In addition to compounds **1-8**, two known phthalides [5,7-dimethoxyphthalide (**9**)^{87,88} and 4,6-dimethoxyphthalide (**10**)^{89,90}], and one known naphthalenone [isosclerone (**11**)]⁹¹ were isolated and identified by comparison of NMR, HRMS, and optical rotation data (for compound **11**) to the literature. This is the first report of **10** from a fungal source.

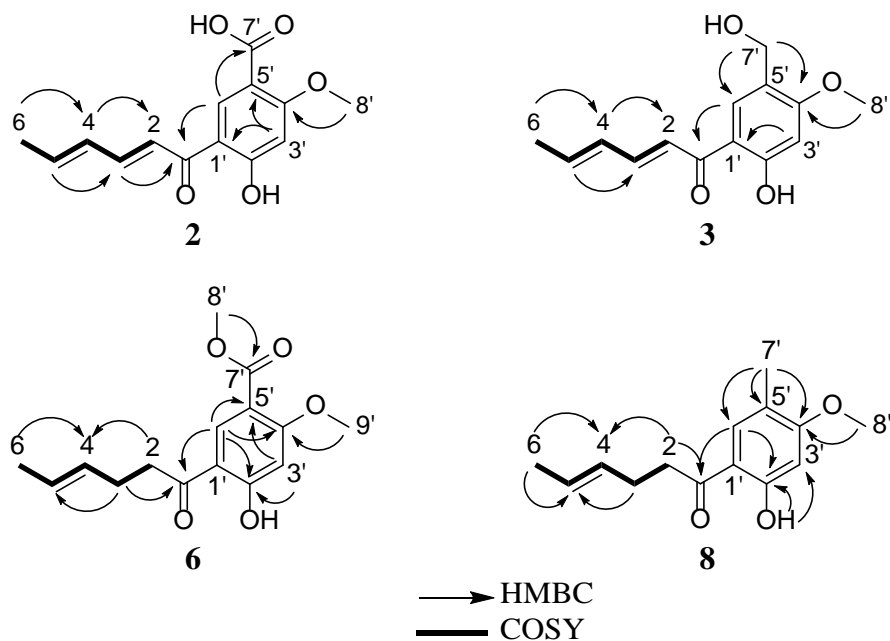


Figure 22. Key HMBC and COSY correlations of compounds **2**, **3**, **6**, and **8**.

Table 6. ^1H NMR Data for Compounds **2** and **3** (in CDCl_3 , 700 MHz, Chemical Shifts in δ , Coupling Constants in Hz)

position	2	3
	δ_{H} , Mult. (<i>J</i> in Hz)	δ_{H} , Mult. (<i>J</i> in Hz)
2	7.05, d (14.6)	6.95, d (15.0)
3	7.54, dd (14.6, 9.9)	7.49, dd (15.0, 10.6)
4	6.39, m	6.34, m
5	6.38, dq (14.6, 5.1)	6.31, dq (15.0, 6.4)
6	1.94, d (5.1)	1.92, dd (6.4, 0.6)
3'	6.58, s	6.46, s
6'	8.74, s	7.71, s
7'	—	4.64, d (6.1)
8'	4.12, s	3.90, s
9'	—	—
2'-OH	13.87, s	13.58, s
7'-OH	10.05, bs	2.02, t (6.1)

Table 7. ¹H NMR Data for Compounds 6 and 8 (in CDCl₃, 500 MHz, Chemical Shifts in δ , Coupling Constants in Hz)

position	6	8
	δ_H , Mult. (J in Hz)	δ_H , Mult. (J in Hz)
2	3.02, dd (7.5, 6.9)	2.95, dd (8.0, 7.5)
3	2.41, ddd (7.5, 6.9, 6.3)	2.40, ddd (8.0, 7.5, 5.2)
4	5.49, dtq (15.5, 6.3, 1.2)	5.49, dtq (15.5, 5.2, 0.6)
5	5.50, dq (15.5, 6.3)	5.50, dq (15.5, 5.2)
6	1.65, dd (6.3, 1.2)	1.65, dd (5.2, 0.6)
3'	6.47, s	6.37, s
6'	8.37, s	7.44, s
8'	3.88, s	3.84, s
9'	3.93, s	—
2'-OH	13.05	12.79, s

Table 8. ¹³C NMR Data for Compounds 2, 3, 6 and 8 (in CDCl₃, 175 MHz for 2 and 3 and 125 MHz for 6 and 8, Chemical Shifts in δ)

position	2	3	6	8
1	192.8	192.4	204.7	204.2
2	120.6	121.4	38.0	38.0
3	146.9	145.1	27.2	27.5
4	130.4	130.4	129.2	129.6
5	143.5	141.8	126.6	126.2
6	19.1	19.0	18.0	18.0
1'	115.1	113.3	112.9	112.7
2'	169.6	166.5	167.9	164.0
3'	100.5	99.7	100.5	99.0
4'	163.1	163.8	165.5	164.3
5'	109.2	120.7	111.6	118.1
6'	137.2	129.9	135.9	131.1
7'	164.3	61.2	165.4	15.8
8'	57.2	55.8	52.2	55.8
9'	—	—	56.5	—

The cytotoxicity of compounds (**1-11**) were measured against MDA-MB-435 and SW-620 cancer cell lines. Compound **1** was the most potent with IC₅₀ values (concentrations that inhibit growth by 50% relative to untreated cells) of 1.5 and 0.5 μM, respectively, followed by compound **5**, with IC₅₀ values of 2.3 and 2.5 μM, respectively (Table 9). Testing of closely related analogues permitted preliminary conclusions regarding structure-activity relationships, particularly the importance of the aldehyde group at 5'. Replacing the aldehyde with a carboxylic acid rendered the compounds inactive, as in **2**. A second important structural feature was the requirement of the intact sorbyl side chain for biological activity. Compound **5**, with a reduced C2-C3 double bond, was less active by 1.5 and 5 fold in comparison with **1** when measured against the MDA-MB-435 and SW-620 cancer cell lines, respectively. This latter observation was supported by moderate growth inhibitory activity with compounds **3** and **4** that was not present in compounds **7** and **8**, which differ only by reduction of the same double bond. Interestingly, compound **1** was similarly active against the B-lymphocytic leukemia cell line OSU-CLL as compared to the solid tumor cell lines (48-hr IC₅₀ of 3.1 μM), but compound **5** lacked significant activity in this context. Compound **1**, which was isolated previously from the fungus *Scytalidium album*,^{85,92} displayed cytotoxic activity when tested against 9KB as reported by the National Cancer Institute (NSC 174259), with ED₅₀ (dose that inhibits growth to 50% of the control growth by 3 days after addition of the drug) value of 0.3 μg/mL.⁹² Neither the researchers' own activity data of compound **1** nor the NCI data were published (Personal communication with Dr. David Newman, National Cancer Institute).

Table 9. Activity of Compounds 1-11 Against Two Human Tumor Cell Lines

compound ^a	IC ₅₀ values in μM ^b	
	MDA-MB-435 ^c	SW-620 ^c
1	1.5	0.5
3	67.9	16.0
4	65.2	15.1
5	2.3	2.5

^aCompounds **2** and **6-11** were inactive.

^bIC₅₀ values were determined as the concentration required to inhibit growth to 50% of control with a 72 h incubation.

^cPositive control was vinblastine tested at concentration of 1 nM in MDA-MB-435 cells and 10 nM in SW620 cells, which had 48% and 30% viable cells, respectively.

The antimicrobial activity of the isolated compounds (**1-11**) was evaluated against a panel of bacteria and fungi (Table 10). Compounds **1** and **5** showed selective and equipotent activity against the filamentous fungus *Aspergillus niger* with MIC values of 0.05 and 0.04 $\mu\text{g/ml}$, respectively, followed by compound **3** with an MIC value of 0.60 $\mu\text{g/ml}$. Relative to amphotericin B, a clinically used agent that was used as a positive control, compounds **1** and **5** were more potent by more than two orders of magnitude. A hemolytic assay was used to assess the toxicity of compounds **1**, **3**, and **5** towards sheep red blood cells *in vitro*. Compounds **1**, **3**, and **5** resulted in 10% hemolysis of sheep red blood cells at 45.0, 52.5, and 37.5 $\mu\text{g/ml}$, respectively, with safety factors (calculated as the 10% hemolysis concentration over MIC) of 900.0, 87.5, and 937.5, respectively (Table 10). Antifungal activities in disk assays against *A. flavus* and *F. verticillioides* of compounds **1** and **7** were reported previously by Reátegui et al.⁸⁶ In the current study, compound **7** showed no activity in the tested fungal strains.

Table 10. Antifungal and Hemolytic Activity of Compounds 1, 3, and 5

compound	Minimal inhibitory concentration ($\mu\text{g/ml}$)			10% Hemolysis ($\mu\text{g/ml}$) ^a	Safety factor ^b
	<i>C. albicans</i>	<i>C. neoformans</i>	<i>A. niger</i>		
1	>53	>53	0.05	52.5	1050
3	>38	>38	0.60	37.5	62.5
5	>45	>45	0.04	45.0	1125
Amphotericin B ^c	16	8	31	NT	NA
Triton X-100 ^c	NT	NT	NT	0.40	NA

^aHemolytic activity is the concentration required to provoke 10% hemolysis.
^bSafety factor was calculated as the concentration inducing 10% hemolysis over MIC against *A. niger*.
^cPositive controls.
Abbreviations: NT, not tested. NA, not available.

Conclusions

A series of eight sorbicillinoid analogues (**1-8**), of which four were new, along with two phthalides (**9-10**), and one naphthalenone (**11**), were isolated from the fungus *Scytalidium album* (MSX51631). Although the sorbicillinoid family encompasses over 50 members, only 4 sorbicillin-type phenolics, as described by Harned et al.,⁸⁴ have been isolated previously from natural sources. This study served to double that to eight related analogues; it is not clear, however, if these compounds are produced by the same biosynthetic route that leads to sorbicillin.⁸⁴ This report expands significantly upon the structure-activity relationship of these compounds in cytotoxicity assays, establishing the importance of the aldehyde moiety at the 5' position and the conjugated sorbyl side chain. Whether the aldehyde was oxidized to the carboxylic acid (such as compound **2**), or reduced to the primary alcohol (such as compound **3**), the growth inhibitory was

diminished, suggesting the reaction of the aldehyde-containing compounds with DNA or proteins to form Schiff base adducts.^{93,94}

Similarly, when the aldehyde was retained but the sorbyl side chain was reduced, as in compound **5** versus **1**, the growth inhibitory activity was reduced by 1.5-5 fold in solid tumor cell lines, and at least ten-fold in a B-lymphocytic cell line (IC₅₀ of **5** not reached in these cells). This is in clear contrast to the activities of compounds **1** and **5** against *A. niger*, in which they are effectively equipotent. This difference suggests that the saturated sorbyl side chain is important for the biologic activity of compound **1** only in mammalian cells. This interesting observation may not only provide clues as to mechanism of action of this class of agents, it also suggests that compound **5** may be a potential candidate for drug development as an antifungal, as it may not elicit substantial negative effects in normal cells. This hypothesis is supported by the relatively high safety factor of compound **5** (as well as **1**) with regards to hemolysis of sheep red blood cells. In addition to compounds **1** and **5**, compound **3** also showed selective potency against *A. niger*, with a similarly low toxicity toward sheep red blood cells *in vitro* but a lower safety factor (*i.e.*, higher MIC).

The discovery of strong, narrow-spectrum anti-*A. niger* activity underscores the utility of subjecting natural products to as wide a screen as possible to detect biological activity. *Aspergillus* species are highly invasive to human beings and continue to present safety challenges for agricultural products and food, the exploration of novel structures for potential application in these settings is a high priority. The exceptional potency and

apparent selectivity of several of the compounds isolated here strongly supports further exploration of this class of secondary metabolites.

Methods

General. UV spectra were obtained using a Varian Cary 100 Bio UV-Vis spectrophotometer (Varian Inc., Walnut Creek, CA, USA). NMR data were collected using either a JEOL ECA-500 NMR spectrometer operating at 500 MHz for ^1H and 125 MHz for ^{13}C , or a JEOL ECS-400 NMR spectrometer equipped with a high sensitivity JEOL Royal probe and a 24-slot autosampler operating at 400 MHz for ^1H and 100 MHz for ^{13}C (both from JEOL Ltd., Tokyo, Japan), or an Agilent 700 MHz NMR spectrometer (Agilent Technologies, Inc., Santa Clara, CA, USA), equipped with a cryoprobe, operating at 700 MHz for ^1H and 175 MHz for ^{13}C . Residual solvent signals were utilized for referencing. High resolution mass spectra (HRMS) were obtained using a Thermo LTQ Orbitrap XL mass spectrometer equipped with an electrospray ionization source (Thermo Fisher Scientific, San Jose, CA, USA). A Waters Acquity UPLC system (Waters Corp., Milford, MA, USA) utilizing a Waters BEH C_{18} column (1.7 μm ; 50 \times 2.1 mm) was used to check the purity of the isolated compounds with data collected and analyzed using Empower software. Phenomenex Gemini-NX C_{18} analytical (5 μm ; 250 \times 4.6 mm), preparative (5 μm ; 250 \times 21.2 mm), and semipreparative (5 μm ; 250 \times 10.0 mm) columns (all from Phenomenex, Torrance, CA, USA) and a YMC ODS-A analytical (5 μm ; 150 \times 4.6 mm), preparative (5 μm ; 250 \times 20 mm), and semipreparative (5 μm ; 250 \times 10.0 mm) columns (all from YMC America, Inc., Allentown, PA, USA) were used on a Varian Prostar HPLC system equipped with ProStar 210 pumps and a Prostar 335

photodiode array detector (PDA), with data collected and analyzed using Galaxie Chromatography Workstation software (version 1.9.3.2, Varian Inc.). Flash chromatography was conducted on a Teledyne ISCO CombiFlash Rf using Silica Gold columns and monitored by UV and evaporative light-scattering detectors (both from Teledyne Isco, Lincoln, NE, USA).

Fungal Strain Isolation and Identification. Mycosynthetix fungal strain MSX51631 was collected in 1990 from Cobb County, Georgia, USA. Molecular techniques were used to identify the strain by sequencing the nuclear internal transcribed spacers and intervening 5.8S gene⁴⁵ along with the D1/D2 regions of the adjacent nuclear ribosomal large subunit.^{95,96} DNA extraction, PCR amplification, sequencing, and phylogenetic analyses were conducted as described previously.^{63,81,97-99} The ITS region was used for species-level identification using the pairwise sequence alignment option on the Fungal Barcoding webpage (<http://www.fungalbarcoding.org/>).⁹⁶ This function allows performing online alignment between an input (query) sequence and the available sequences in the database, which comprise different curated global fungal databases, including, Q-bank Fungi database (<http://www.q-bank.edu/Fungi>); CBS-KNAW Fungal Biodiversity Centre (<http://www.cbs.knaw.nl/Collections>); Molecular Mycology Research Laboratory (<http://www.mycologylab.org/>); Portuguese Yeast Culture Collection (<http://pycc.bio-aware.com/>); and NCBI GenBank. The search returns the best-matching piecewise (local) or global alignments of two query sequences. Identifications were performed in a monophasic way; in which sequences were compared to produce a global similarity or probability coefficient between the unknown sequence

and the reference sequence database (<http://www.fungalbarcoding.org/>). Based on the results of the pairwise sequence alignment, the closest genus and species that matched the ITS sequence of the strain MSX51631 were representatives of *Scytalidium album* (isotype sequence; CBS 372.65) (identities = 482/485 (99.3%), gaps = 0), the other closest matches included those of *Ascomycota* sp. olrim237 (AY787735; identities = 470/470 (100%), gaps = 0), *Ascomycota* sp. olrim349 (HM036638; identities = 454/454 (100%), gaps = 0). Pairwise sequence alignment was also performed with combined ITS-LSU region, which suggested that the closest match of the query sequence was *Scytalidium album* (isotype sequence; CBS 372.65) (identities = 927/942 (98%), gaps = 6 (0.7%).

A combined ITS-LSU rDNA complete linkage tree was generated using pairwise sequence alignment search on the Fungal Barcoding webpage (Supplementary Figure 35). Therefore, the strain MSX51631 was identified as having affinities to *Scytalidium album* L. Beyer & Klingström. (Helotiales, Leotiomycetidae, Leotiomycetes, Pezizomycotina, Ascomycota). The combined ITS-LSU sequence will be deposited in the GenBank (accession no XXXX).

Fermentation, Extraction and Isolation. Storage conditions, fermentation, and extraction procedure of the fungal strain MSX51631 were as described previously.^{19,62,63} Briefly, cultures of strain MSX51631 were grown in 2.8-l Fernbach flasks (Corning, Inc., Corning, NY, USA) containing 150 g rice and 300 ml H₂O. A seed culture grown in YESD medium was used as an inoculum. Following incubation at 22 °C for 14 d, the solid culture was extracted by adding a 500 ml mixture of 1:1 MeOH-CHCl₃. The culture

was cut into small pieces using a spatula and shaken for about 16 h at ~125 rpm at rt, followed by vacuum filtration. The remaining residues were washed with 100 ml of 1:1 MeOH-CHCl₃. To the filtrate, 900 ml CHCl₃ and 1500 ml H₂O were added; the mixture was stirred for ½ h and then transferred into a separatory funnel. The bottom layer was drawn off and evaporated to dryness. The dried organic extract was re-constituted in 100 ml of 1:1 MeOH-CH₃CN and 100 ml of hexanes. The biphasic solution was shaken vigorously and then transferred to a separatory funnel. The MeOH-CH₃CN layer was drawn off and evaporated to dryness under vacuum. The defatted material (~750 mg) was dissolved in a mixture of CHCl₃-MeOH, adsorbed onto Celite 545, and fractionated via flash chromatography using a gradient solvent system of hexane-CHCl₃-MeOH at a 30 ml/min flow rate and 61.0 column volumes over 34.1 min to afford five fractions. Fraction 2 (~315.97 mg) was subjected to preparative reversed phase HPLC over a Phenomenex Gemini-NX C₁₈ preparative column using a gradient system of 50:50 to 70:30 over 50 min to 100:00 of CH₃CN-H₂O (acidified with 0.1% formic acid) at a flow rate of 21 ml/min to yield thirteenth sub-fractions. Sub-fractions 2 and 7 yielded compounds **11** (0.46 mg) and **3** (0.55 mg), which eluted at ~6.5 and ~27.5 min, respectively. Sub-fractions 8-11 were subjected to further purifications. Sub-fraction 8 (3.23 mg) was subjected to semi-preparative HPLC purification over a Phenomenex Gemini-NX C₁₈ column using a gradient system of 50:50 to 60:40 of CH₃CN-H₂O (acidified with 0.1% formic acid) over 15 min at a flow rate of 4.72 ml/min to yield compounds **2** (0.75 mg) and **7** (1.65 mg), which eluted at ~8.2 and ~10.5 min, respectively. Sub-fraction 9 (9.14 mg) was subjected to semi-preparative HPLC

purification using a Phenomenex Gemini-NX C₁₈ and a gradient system of 70:30 to 80:20 of CH₃OH-H₂O (acidified with 0.1% formic acid) over 20 min at a flow rate of 4.72 ml/min to yield compound **1** (3.10 mg) that eluted at ~12.5 min. Sub-fraction 10 (14.2 mg) was subjected to preparative HPLC purification using a YMC ODS-A column and an isocratic solvent system of 60:40 of CH₃OH-H₂O (acidified with 0.1% formic acid) at a flow rate of 15 ml/min to yield compounds **1** (5.21 mg), **5** (4.16 mg), and **6** (1.83 mg), which eluted at ~80.2, ~91.5, and ~106.3 min, respectively. Sub-fraction 11 (146.52 mg) was subjected to preparative HPLC purification using a Phenomenex Gemini-NX C₁₈ and a gradient system of 60:40 to 100:00 of CH₃CN-H₂O (acidified with 0.1% formic acid) over 30 min at a flow rate of 21.24 ml/min to yield compounds **1** (3.33 mg) and **4** (3.10 mg), which eluted at ~11.0 and ~16.3 min, respectively. To obtain purity over 95% as measured by UPLC, compounds **5-6** were further purified using semipreparative reversed phase HPLC.

Another two large scale cultures of MSX51631 were extracted, combined, and fractionated as described above. The MeOH-CH₃CN fraction (1.77 g) was subjected to fractionation using flash chromatography and a gradient solvent system of hexane-CHCl₃-MeOH at a 40 ml/min flow rate and 53.3 column volumes over 63.9 min to afford four fractions. Fraction 2 (~868.95 mg) was subjected to extensive purifications using preparative and semipreparative reversed phase HPLC and yielded additional amounts of compounds **1-7**, which were isolated from the first processed large scale of MSX51631, along with compounds **8** (2.47 mg), **9** (5.54 mg), and **10** (7.91 mg).

Scalbuicillin A (2): Compound **2** was isolated as a yellow solid (1.77 mg); UV (MeOH) λ_{\max} (log ϵ) 349 (3.57), 309 (3.64), 247 (3.51), 222 (3.47) nm; ^1H NMR (CDCl_3 , 700 MHz) and ^{13}C NMR (CDCl_3 , 175 MHz), see Tables 6 and 8 and Supplementary Figure 25; HRESIMS m/z 263.0910 $[\text{M} + \text{H}]^+$ (calcd for $\text{C}_{14}\text{H}_{15}\text{O}_5$ 263.0914).

Scalbuicillin B (3): Compound **3** was isolated as a yellow solid (1.10 mg); UV (MeOH) λ_{\max} (log ϵ) 349 (3.22), 310 (3.31), 231 (3.22) nm; ^1H NMR (CDCl_3 , 700 MHz) and ^{13}C NMR (CDCl_3 , 175 MHz), see Tables 6 and 8 and Supplementary Figure 26; HRESIMS m/z 249.1115 $[\text{M} + \text{H}]^+$ (calcd for $\text{C}_{14}\text{H}_{17}\text{O}_4$ 249.1121).

Scalbuicillin C (6): Compound **6** was isolated as a white solid (9.97 mg); UV (MeOH) λ_{\max} (log ϵ) 312 (3.56), 275 (3.71), 246 (3.71) nm; ^1H NMR (CDCl_3 , 500 MHz) and ^{13}C NMR (CDCl_3 , 125 MHz), see Tables 7 and 8 and Supplementary Figure 29; HRESIMS m/z 279.1221 $[\text{M} + \text{H}]^+$ (calcd for $\text{C}_{15}\text{H}_{19}\text{O}_5$ 279.1227).

Scalbuicillin D (8): Compound **8** was isolated as a white solid (2.47 mg); UV (MeOH) λ_{\max} (log ϵ) 324 (3.61), 275 (3.65), 237 (3.62) nm; ^1H NMR (CDCl_3 , 500 MHz) and ^{13}C NMR (CDCl_3 , 125 MHz), see Tables 7 and 8 and Supplementary Figure 31; HRESIMS m/z 235.1323 $[\text{M} + \text{H}]^+$ (calcd for $\text{C}_{14}\text{H}_{18}\text{O}_3$ 235.1329).

Cytotoxicity Assays. Compounds (**1-11**) were tested against the MDA-MB-435¹⁰⁰ human melanoma (HTB-129, ATCC) and the SW-620¹⁰¹ human colorectal adenocarcinoma (CCL-227, ATCC) cell lines as described previously.¹⁹ Compounds **1** and **5** were also tested against the B-lymphocytic cell line OSU-CLL⁸³ using CellTiter 96

reagents according to the manufacturer's instructions (Promega, Madison WI). The 48-hr IC_{50} of compound **1** was calculated using Prism software (GraphPad, La Jolla, CA).

Antimicrobial Assay. Minimal inhibitory concentrations (MICs) of compounds (**1-11**) against a panel of bacteria and fungi were measured as described previously.^{18,102,103}

All measurements were made in duplicate.

Hemolytic Assay. Hemolytic activity of compounds **1**, **3**, and **5** was measured against sheep red blood cells as described elsewhere.¹⁰⁴

Supporting Information

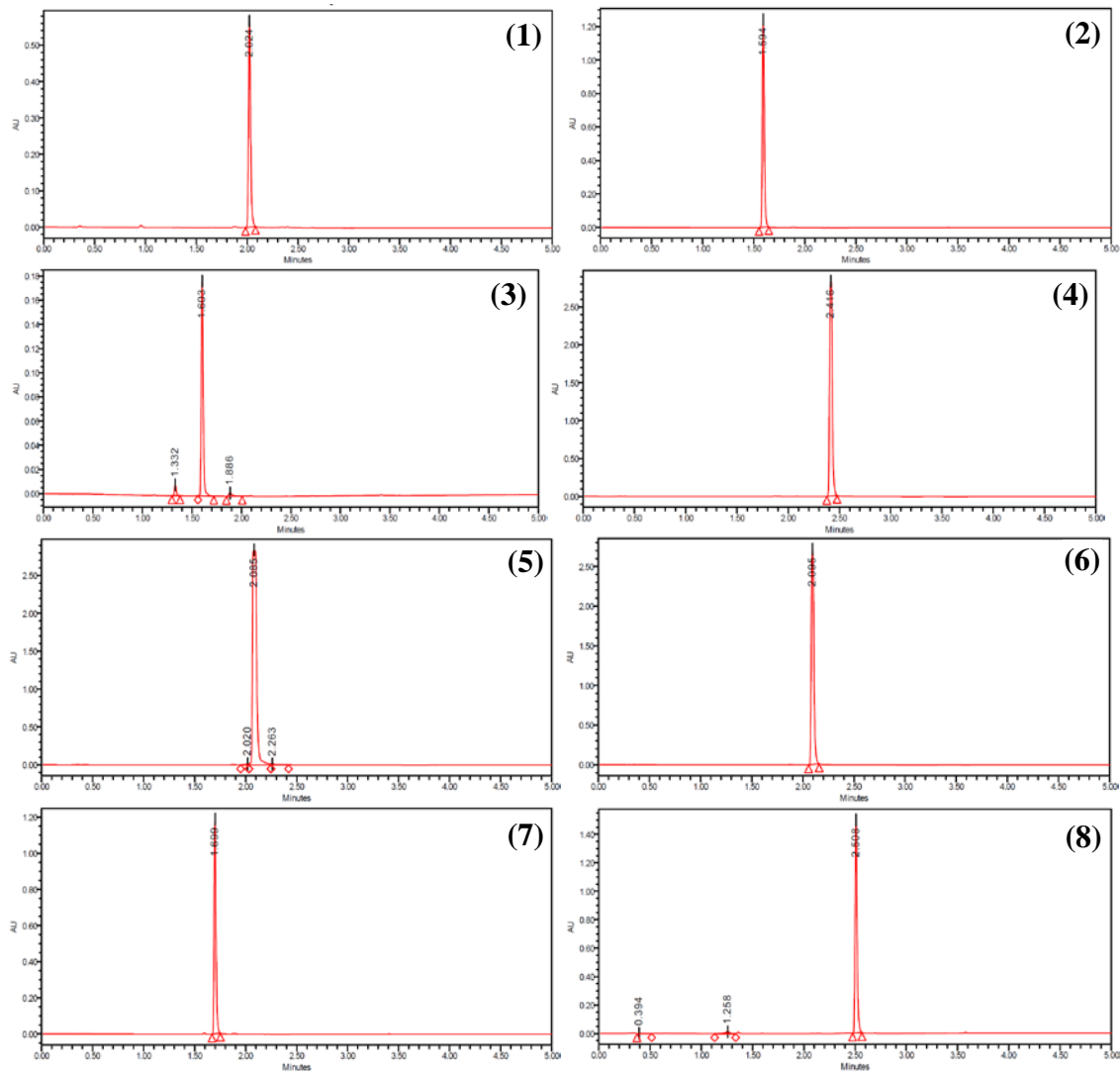


Figure 23. UPLC chromatograms of compounds **1-11** (λ 254 nm) demonstrating >95% purity. Acquity UPLC system; ACQUITY UPLC BEH C₁₈ 1.7 μ m 2.1 \times 50 mm column; gradient CH₃CN/H₂O 20 to 100% over 4.5 min; Injection volume 3 μ l.

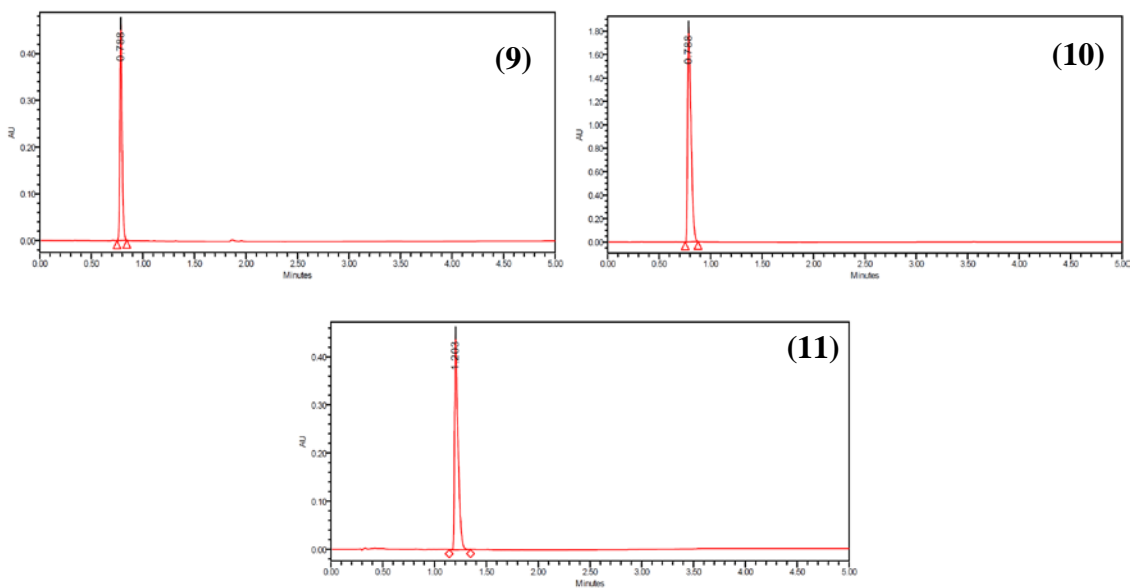


Figure 23 (continued). UPLC chromatograms of compounds **1-11** (λ 254 nm) demonstrating >95% purity. Acquity UPLC system; ACQUITY UPLC BEH C_{18} 1.7 μ m 2.1 \times 50 mm column; gradient CH_3CN/H_2O 20 to 100% over 4.5 min; Injection volume 3 μ l.

Table 11. Antimicrobial Activities of Compounds (1-11)

compound	Minimal inhibitory activity ($\mu\text{g/mL}$)							
	<i>M. luteus</i>	<i>S. aureus</i>	<i>E. coli</i>	<i>M. smegmatis</i>	<i>S. cerevisiae</i>	<i>C. albicans</i>	<i>C. neoformans</i>	<i>A. niger</i>
1	>53	>53	>53	>53	>53	>53	>53	0.05
2	>108	>108	>108	>108	>108	>108	>108	>108
3	>38	>38	>38	>38	>38	>38	>38	0.60
4	>118	>118	>118	>118	>118	>118	>118	>118
5	>45	>45	>45	>45	>45	>45	>45	0.04
6	>105	>105	>105	>105	>105	>105	>105	>105
7	>105	>105	>105	>105	>105	>105	>105	>105
8	>85	>85	>143	>143	>143	>143	>143	>143
9	>85	>85	>145	>145	>145	>145	>145	>145
10	>85	>85	>85	>85	>85	>85	>85	>85
11	>105	>105	>105	>105	>105	>105	>105	>105
Ampicillin ^a	4	0.2	>250	>250	>250	>250	>250	>250
Rifamycin ^a	0.06	0.2	31	4	>250	>250	>250	>250
Amphotericin B ^a	>250	0.2	>250	>250	3.9	16	8	31
^a Positive controls								

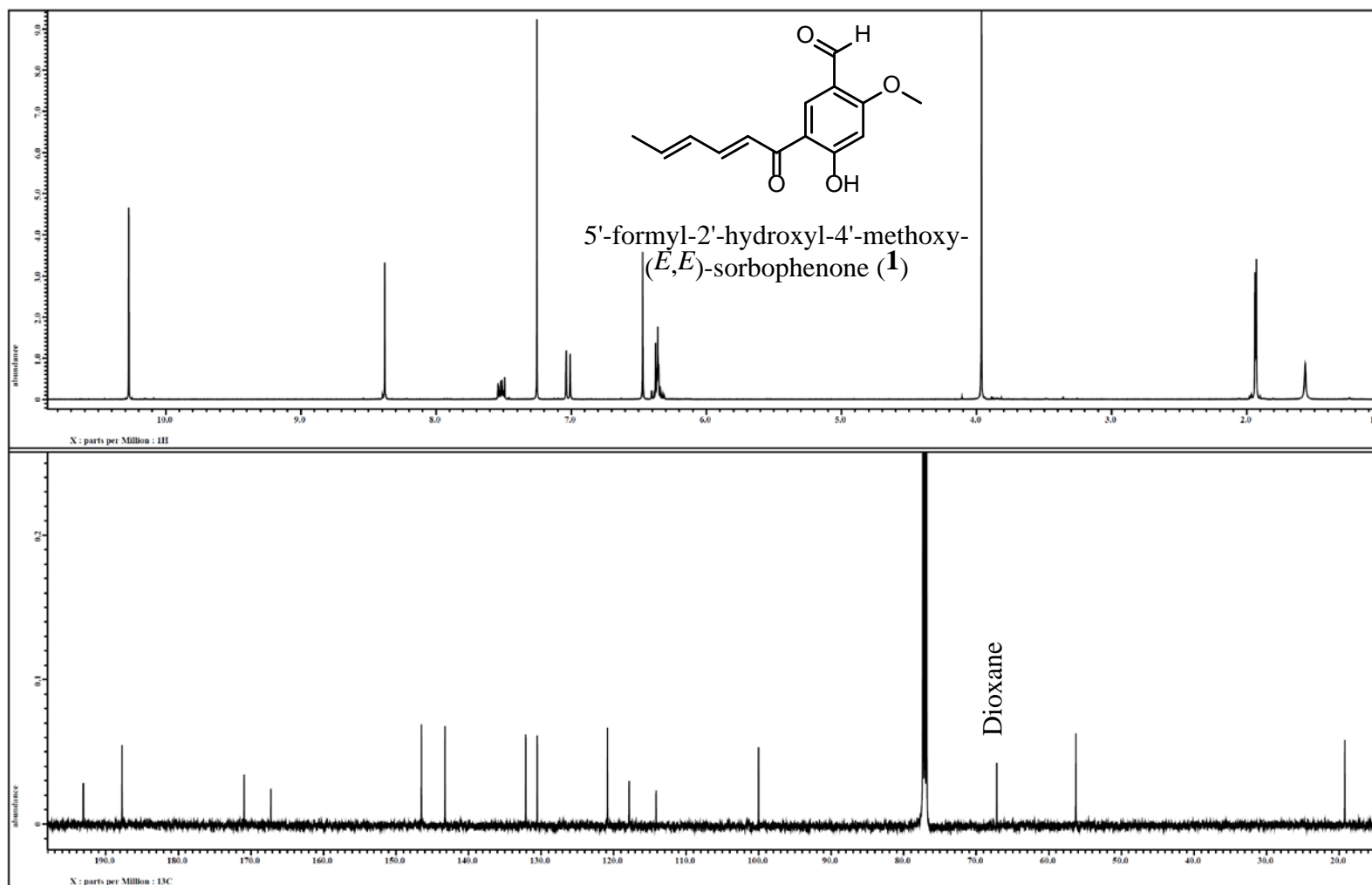


Figure 24. ^1H and ^{13}C NMR spectra of compound **1** [500 MHz for ^1H and 125 MHz for ^{13}C , CDCl_3].

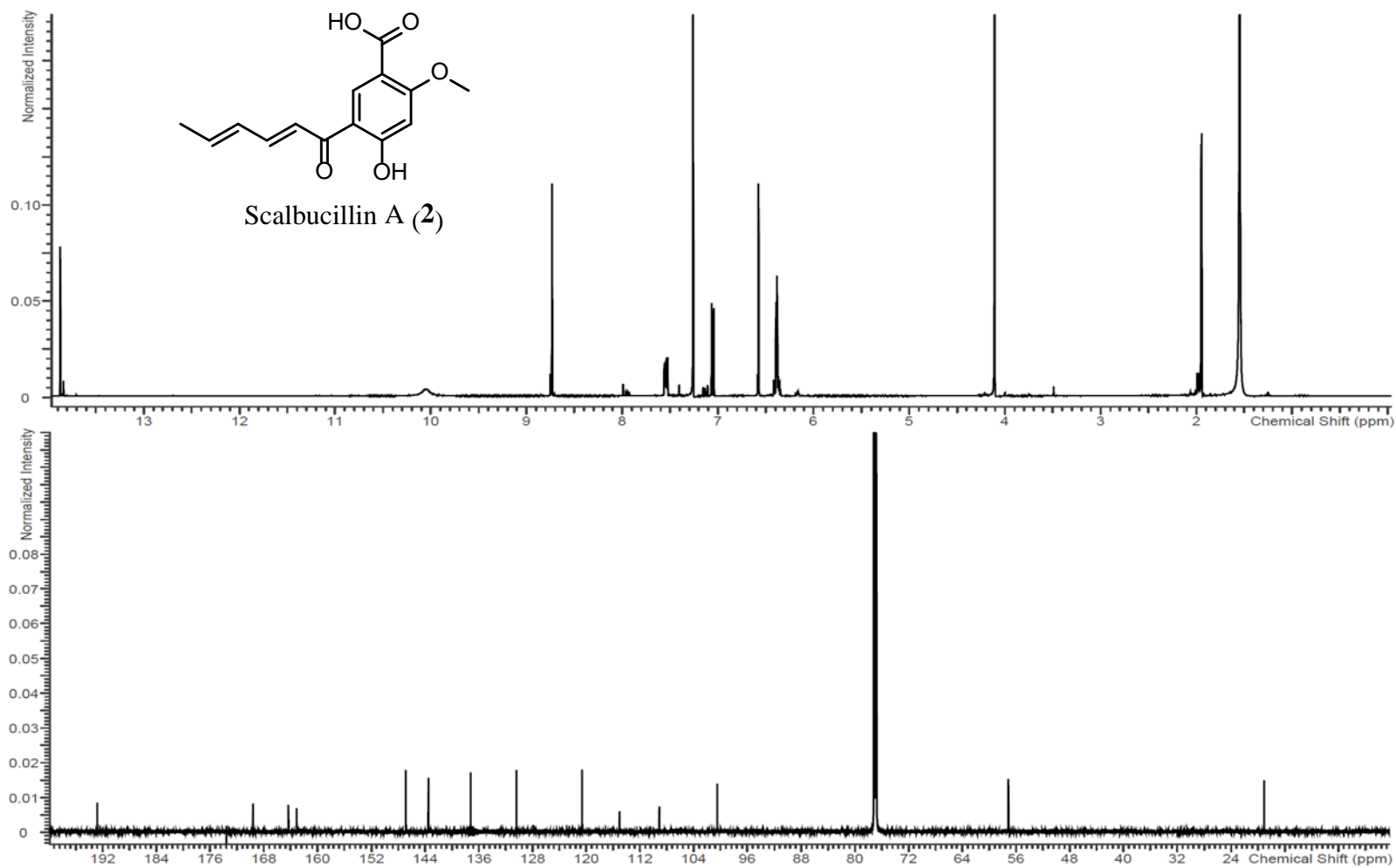


Figure 25. ^1H and ^{13}C NMR spectra of compound 2 [700 MHz for ^1H and 175 MHz for ^{13}C , CDCl_3].

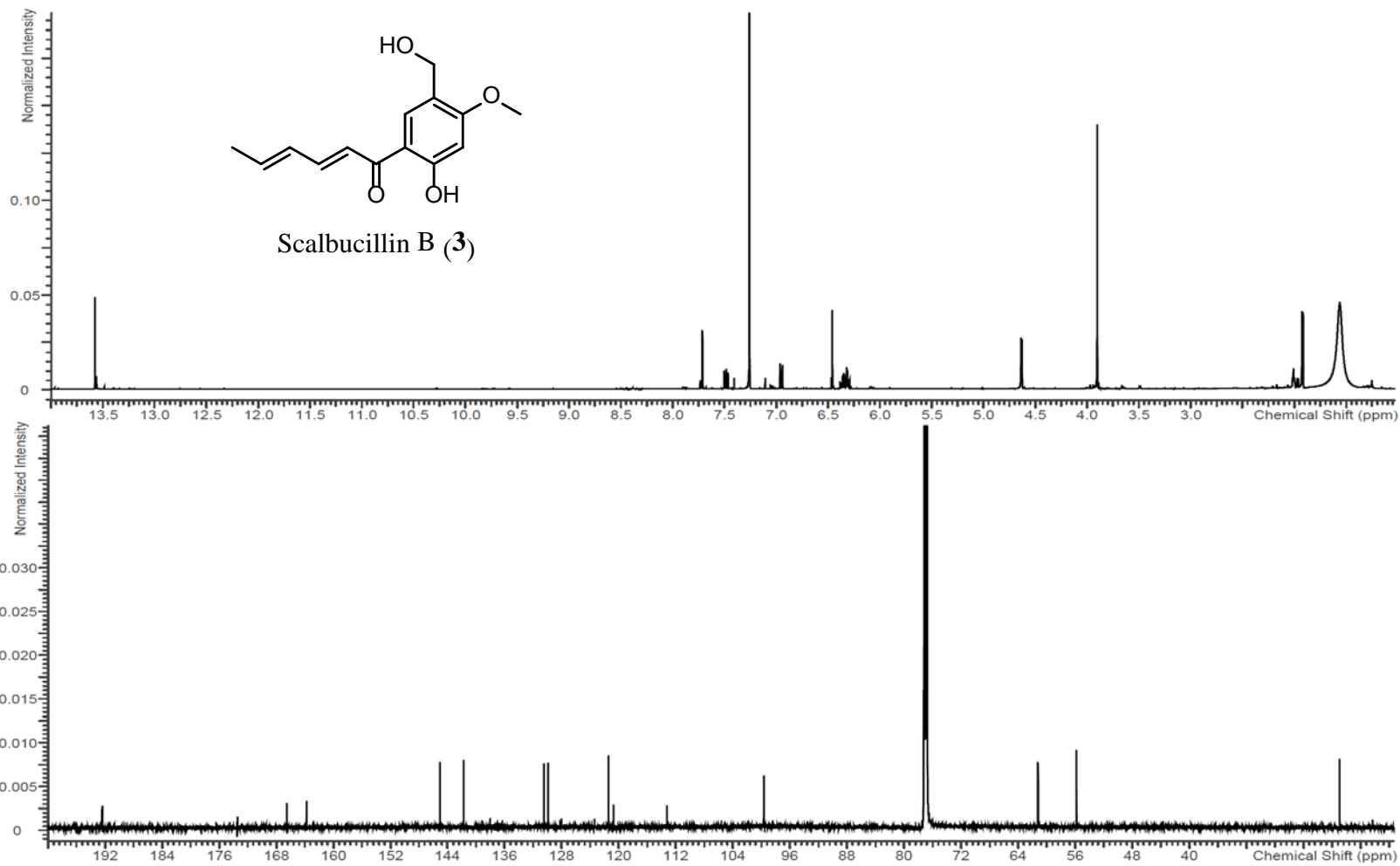


Figure 26. ^1H and ^{13}C NMR spectra of compound **3** [700 MHz for ^1H and 175 MHz for ^{13}C , CDCl_3].

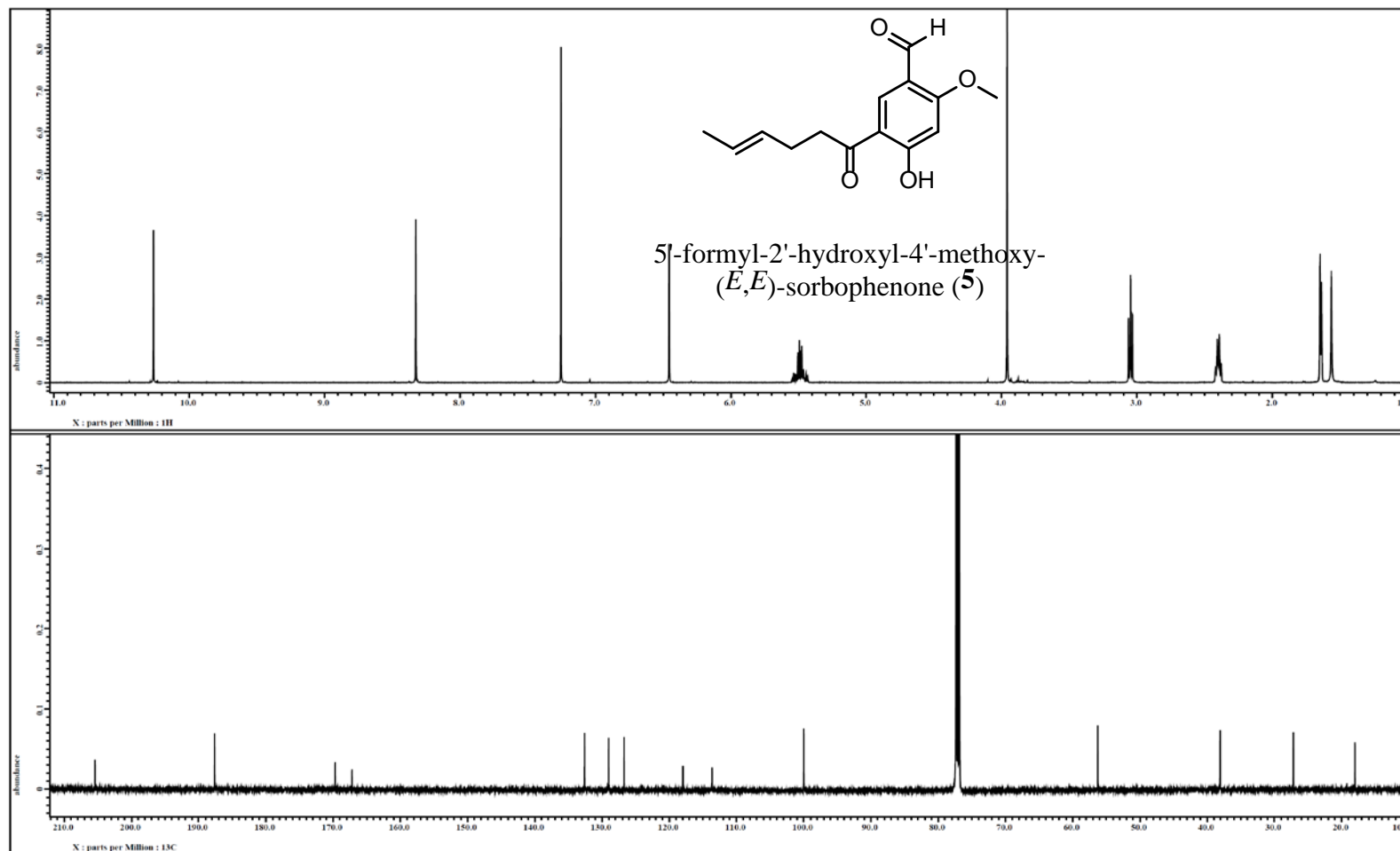


Figure 28. ^1H and ^{13}C NMR spectra of compound **5** [500 MHz for ^1H and 125 MHz for ^{13}C , CDCl_3].

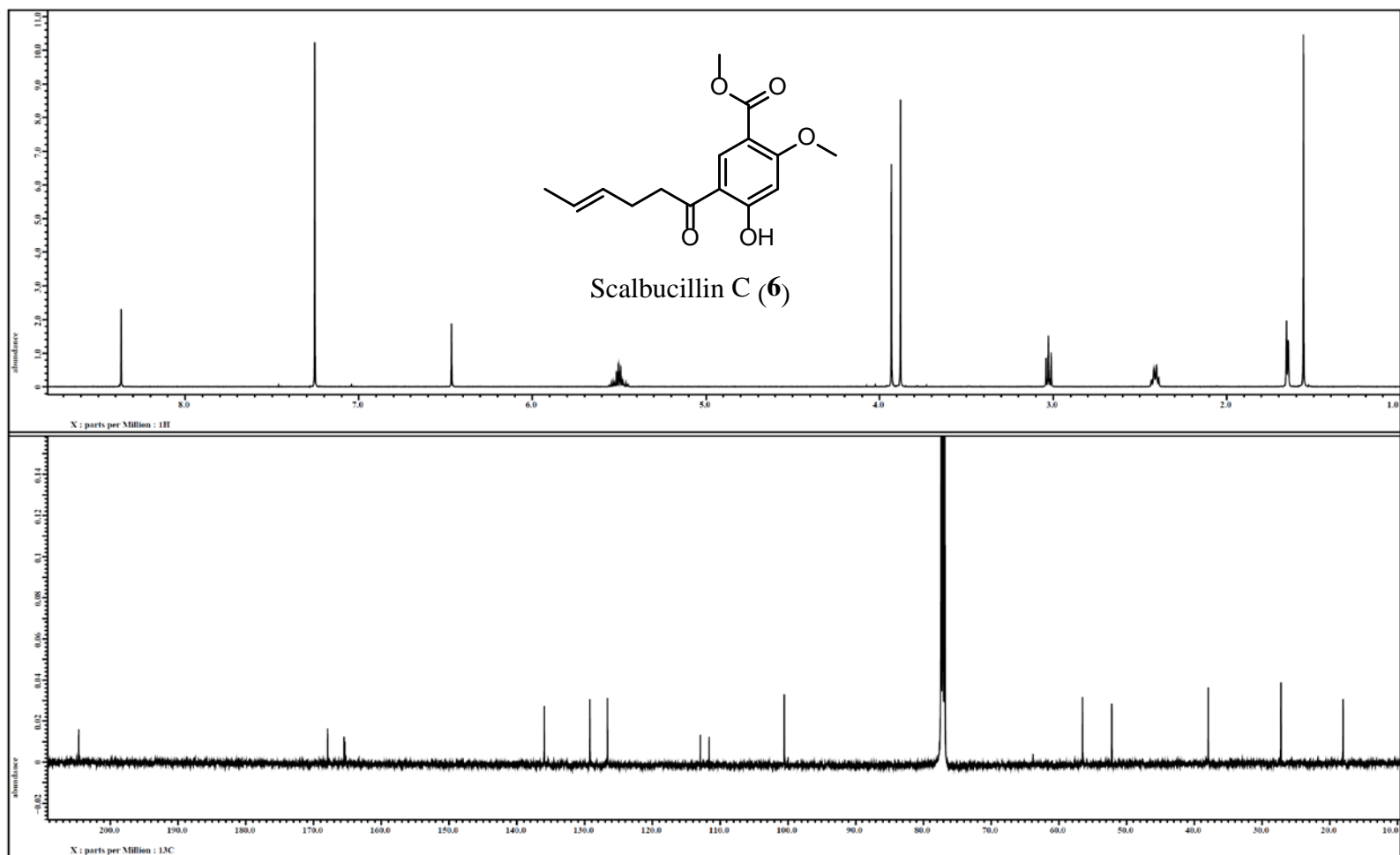


Figure 29. ^1H and ^{13}C NMR spectra of compound 6 [500 MHz for ^1H and 125 MHz for ^{13}C , CDCl_3].

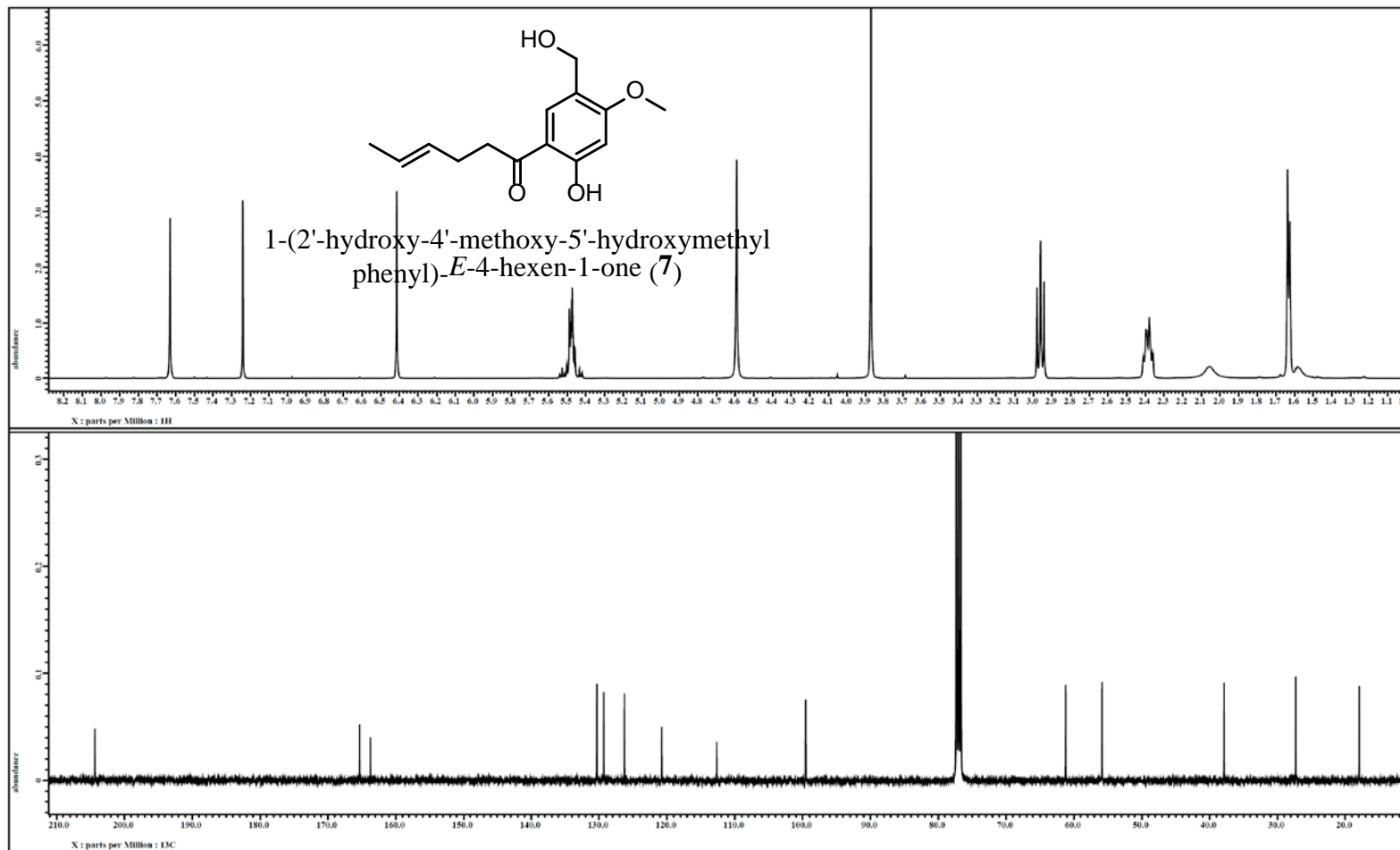


Figure 30. ^1H and ^{13}C NMR spectra of compound **7** [400 MHz for ^1H and 100 MHz for ^{13}C , CDCl_3].

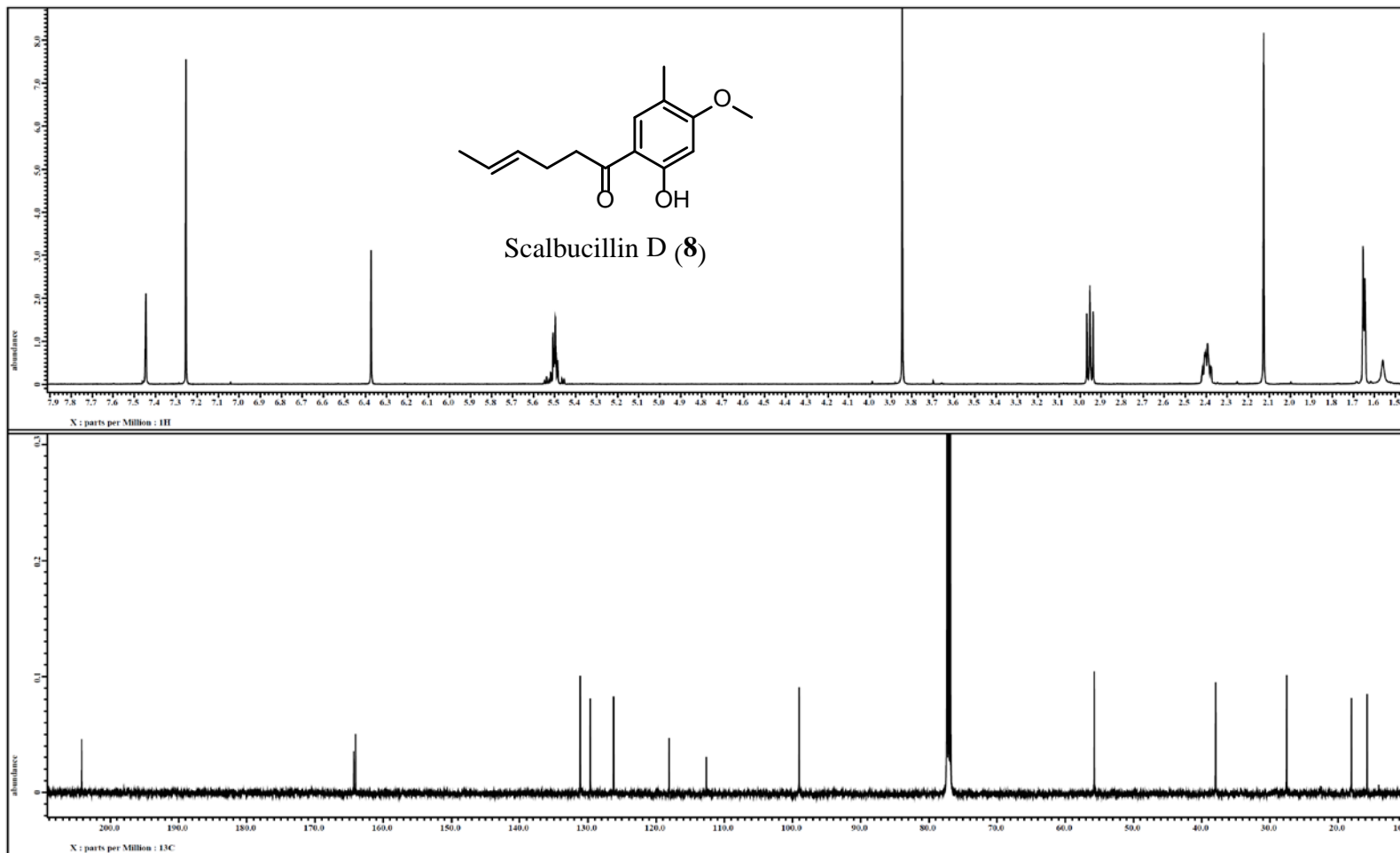


Figure 31. ^1H and ^{13}C NMR spectra of compound **8** [500 MHz for ^1H and 125 MHz for ^{13}C , CDCl_3].

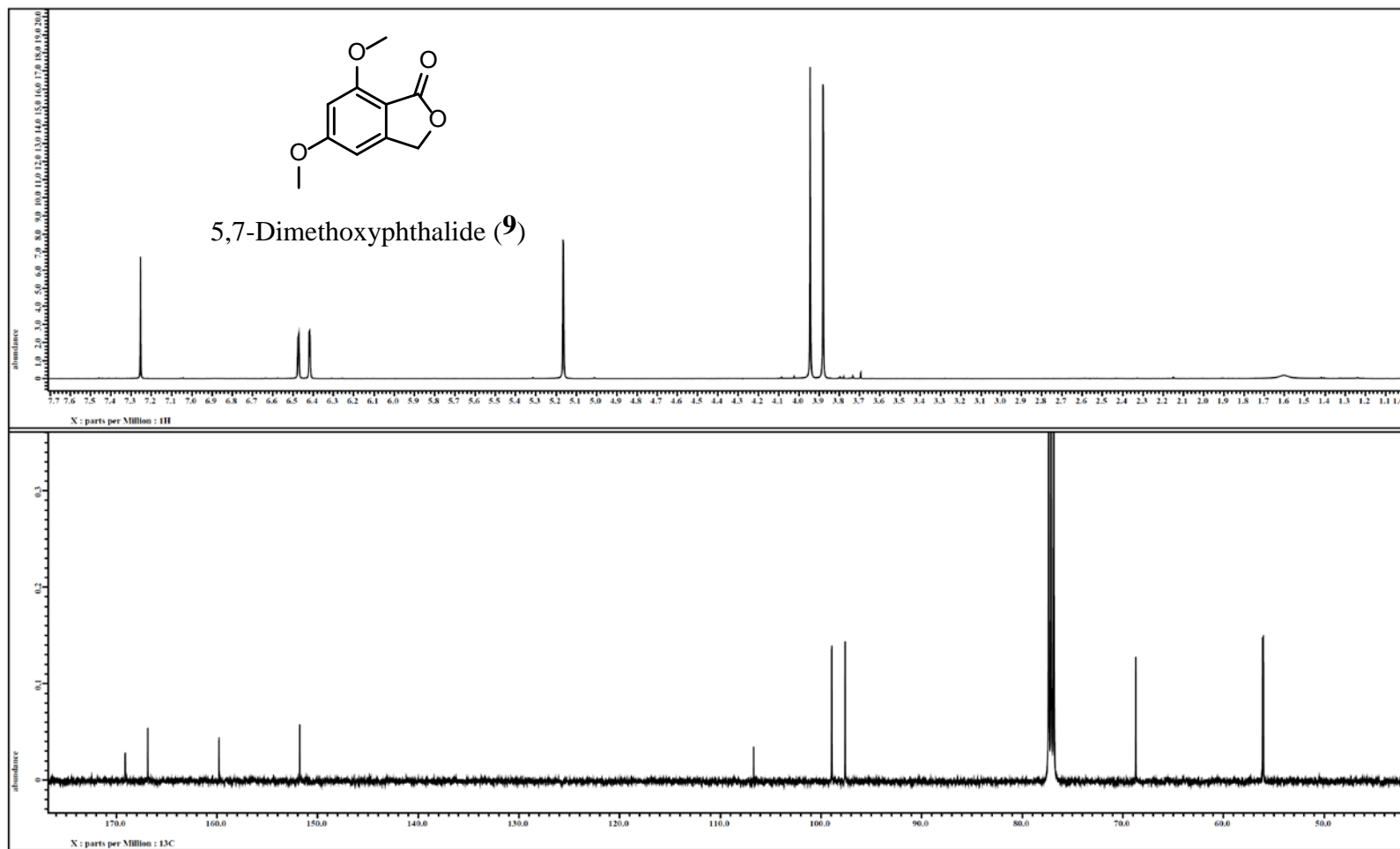


Figure 32. ^1H and ^{13}C NMR spectra of compound 9 [500 MHz for ^1H and 125 MHz for ^{13}C , CDCl_3].

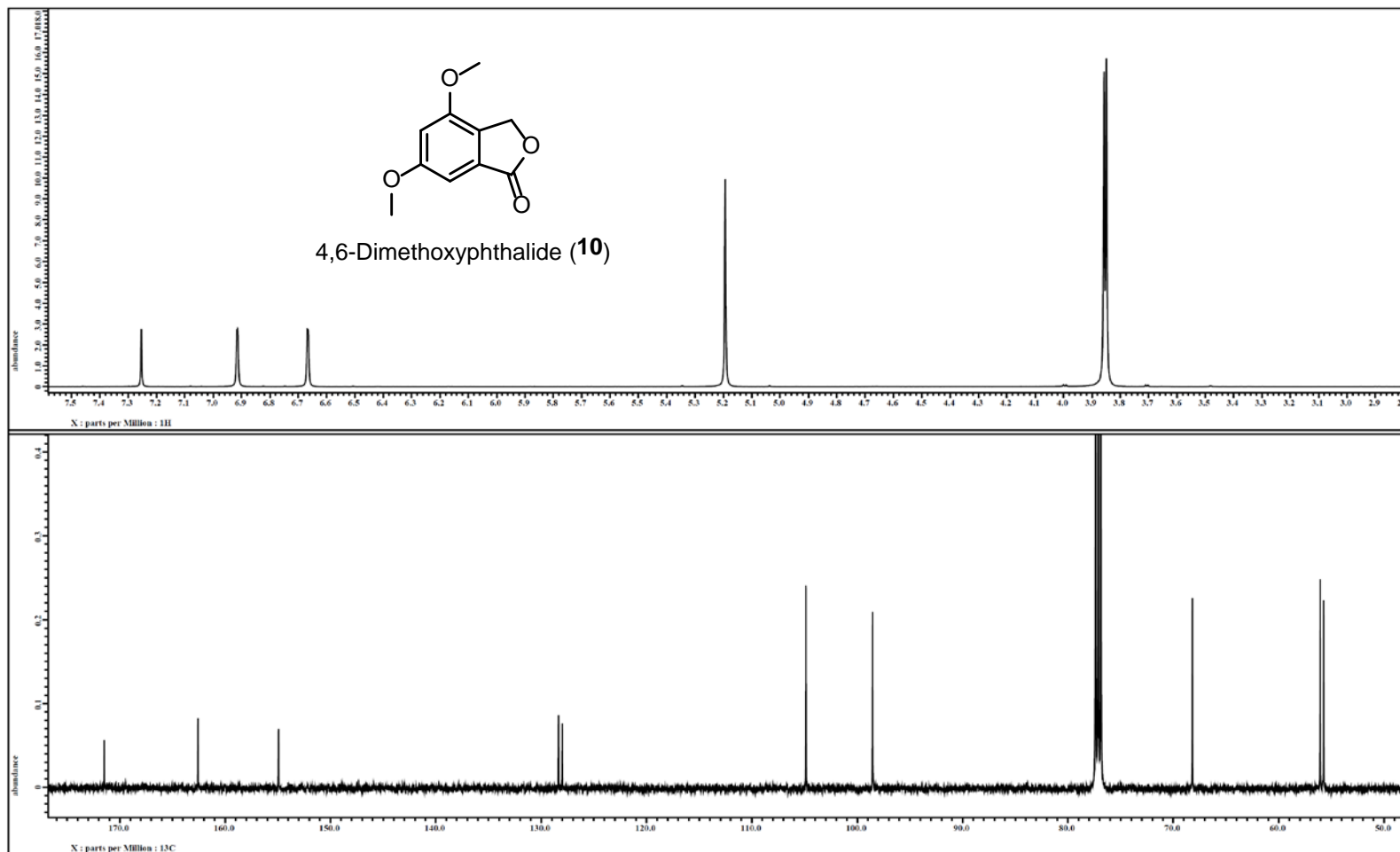


Figure 33. ^1H and ^{13}C NMR spectra of compound **10** [500 MHz for ^1H and 125 MHz for ^{13}C , CDCl_3].

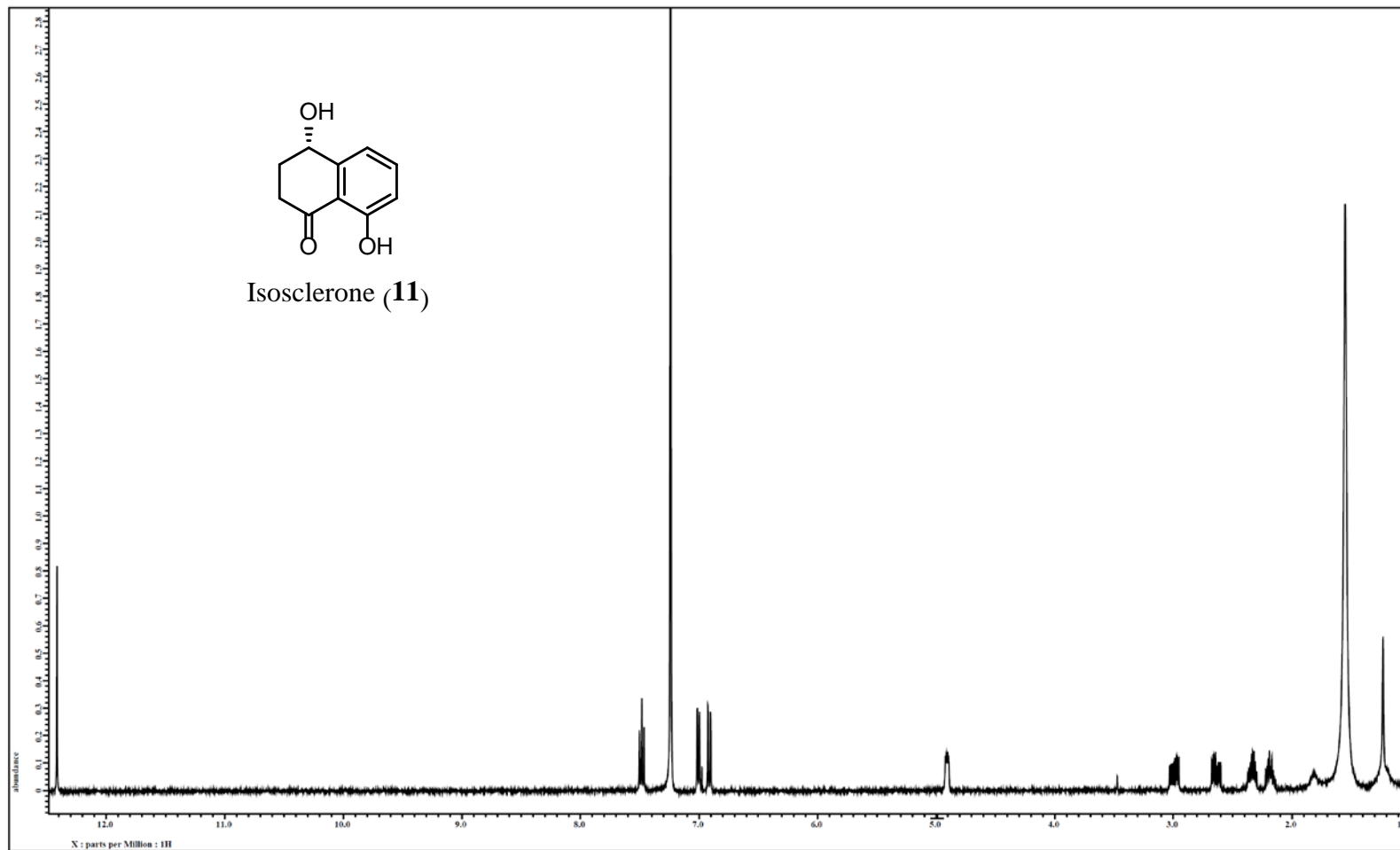


Figure 34. ¹H NMR spectrum of compound **11** [400 MHz, CDCl₃].

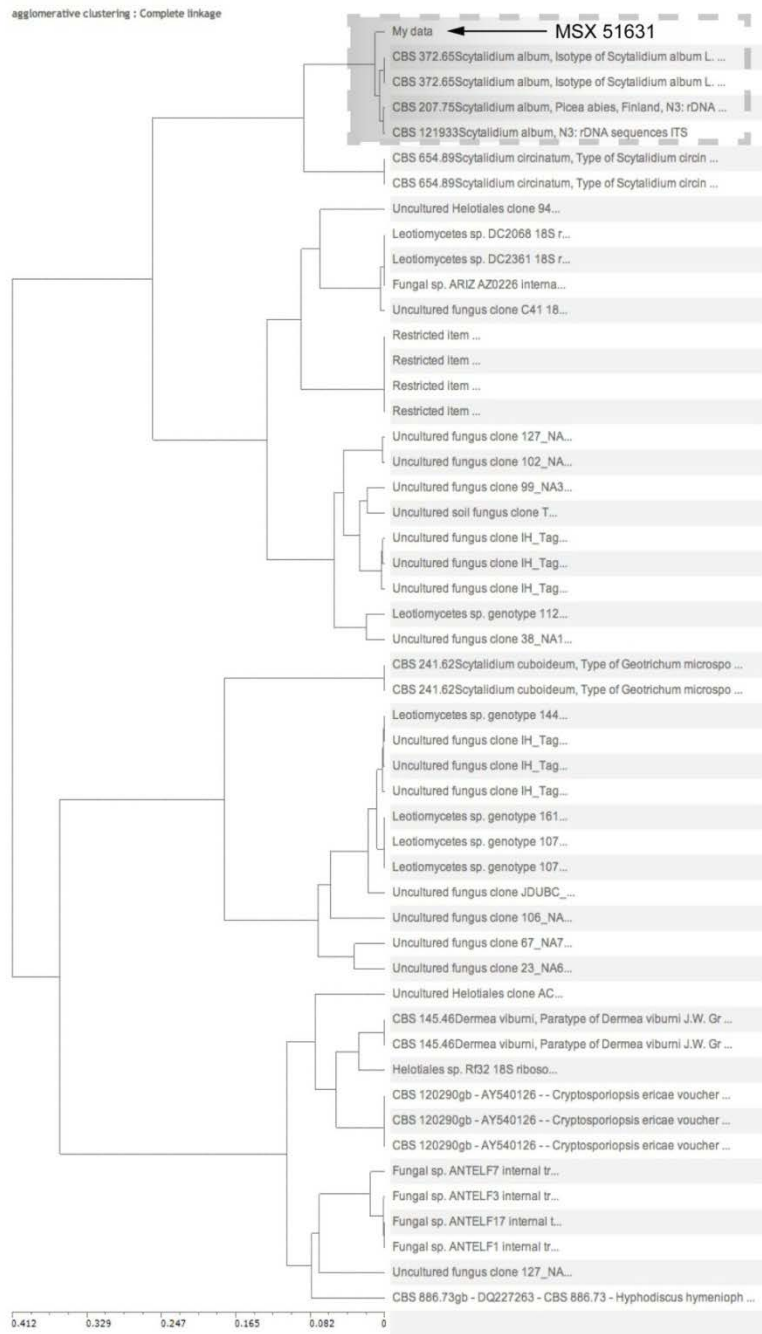


Figure 35. Complete linkage tree generated using complete ITS and partial region of the 28S large subunit nrDNA (954 bp) using pairwise sequence alignment option using Fungal Barcoding website (<http://www.fungalbarcoding.org>). MSX51631 clusters in a clade (highlighted with dashed lines) with *Scytalidium album* as sister species.

CHAPTER V

CYTOTOXIC POLYKETIDES FROM FUNGAL CO-CULTURE OF *ASPERGILLUS* *VERSICOLOR* AND *SETOPHOMA TERRESTRIS*

Tamam El-Elimat, Mario Figueroa, Huzefa A. Raja, Tyler N. Graf, Audrey F. Adcock, David J. Kroll, Steven M. Swanson, Joseph O. Falkinham III, Mansukh C. Wani, Cedric J. Pearce, and Nicholas H. Oberlies. This chapter is intended for submission to *Chemistry - A European Journal* (2014).

Sixteen polyketides belonging to diverse structural classes including monomeric/dimeric tetrahydroxanones and resorcylic acid lactones were isolated from an organic extract of a fungal co-culture of *Aspergillus versicolor* and *Setophoma terrestris* (MSX45109) using bioactivity-directed fractionation as part of a search for anticancer leads from filamentous fungi. Of these, six were new: penicillixanthone B (**5**), blennolide H (**6**), 11-deoxy blennolide D (**7**), blennolide I (**9**), blennolide J (**10**), and pyrenomycin (**16**). The known compounds were: secalonic acid A (**1**), secalonic acid E (**2**), secalonic acid G (**3**), penicillixanthone A (**4**), paecilin B (**8**), aigialomycin A (**11**), hypothemycin (**12**), dihydrohypothemycin (**13**), pyrenochaetic acid C (**14**), and nidulalin B (**15**). The structures were elucidated using a set of spectroscopic and spectrometric techniques; the absolute configurations of compounds **1-10** were determined using CD spectroscopy combined with time-dependent density functional theory (TDDFT) calculations, while a modified Mosher's ester method was used for compound **16**. The

cytotoxic activities of compounds (**1-15**) were evaluated using the MDA-MB-435 (melanoma) and SW-620 (colon) cancer cell lines. Compounds **1**, **4**, and **12** were the most potent with IC₅₀ values ranging from 0.16 to 2.14 μM. When tested against a panel of bacteria and fungi, compounds **3** and **5** showed promising activity against the Gram-positive bacterium *Micrococcus luteus* with MIC values of 5 and 15 μg/mL, respectively.

Structurally diverse cytotoxic secondary metabolites have been isolated and identified from filamentous fungi of the Mycosynthetix library, representing over 55,000 accessions, as part of ongoing bioactivity-directed studies for discovery of anticancer drug leads.^{17,19-22,62,63,80,82,105} As a continuation of such studies, the organic extract of a solid culture medium of a fungal co-culture of *Aspergillus versicolor* and *Setophoma terrestris* (MSX45109), which was isolated from plant material collected in a mangrove habitat in 1989, showed potent cytotoxic activities against the SW-620 (colon) and MDA-MB-435 (melanoma) cancer cell lines (~91% and 100% inhibition of cell growth when tested at 20 μg/mL, respectively). Bioactivity-directed fractionation resulted in the isolation and structural identification of sixteen polyketides belonging to diverse structural classes, of which six were new: penicillixanthone B (**5**), blennolide H (**6**), 11-deoxy blennolide D (**7**), blennolide I (**9**), blennolide J (**10**), and pyrenomycin (**16**). The known compounds were: secalonic acid A (**1**), secalonic acid E (**2**), secalonic acid G (**3**), penicillixanthone A (**4**), paecilin B (**8**), aigialomycin (**11**), hypothemycin (**12**), dihydrohypothemycin (**13**), pyrenochaetic acid C (**14**), and nidulalin B (**15**). Compounds **1-10** were identified as a series of monomeric/dimeric tetrahydroxanthones, an important

class of mycotoxins that are produced by a variety of microorganisms with remarkable biological activities.^{106,107} Ergochromes is a joint name for a group of structurally related compounds, including secalonic acids, ergoflavins, ergochrysin, and chrysergonic acid.^{107,108} They were isolated as homo/heterodimers of six monotetrahydroxanthones (hemisecalonic acids A-F).¹⁰⁸ This class of biologically active mycotoxins, which have displayed antitumor, antibacterial, and anti-HIV activities,¹⁰⁹⁻¹¹² was first isolated from ergot, *Claviceps purpurea*, in 1958.¹¹³ Of the six postulated monomeric tetrahydroxanthones (hemisecalonic acids A-F), only blennolide A and B, which are the monomer units of secalonic acids B and D, respectively, were isolated fairly recently.¹¹⁴ In the current study, a series of new monomeric and homo/hetero dimeric tetrahydroxanthones were identified, which expanded the diversity of this class of natural products and updated the literature on structural elucidation and absolute configuration determination of structurally related compounds, and hence important for dereplication considerations.⁸⁰ Interestingly, a recent and comprehensive study reported a similar series of compounds though with opposite absolute configuration.¹¹⁴ On the other hand, compounds **11-13** were characterized as a series of structurally related resorcylic acid lactones (RALs), a family of benzannulated macrolides that are produced by a variety of fungi with a wide range of biological activities, including antitumor, antifungal, antibiotic, and antiviral properties.¹¹⁵ The absolute configurations of compounds **1-10** were determined using time-dependent density functional theory (TDDFT) calculations of CD spectra, while for **16** a modified Mosher's ester method was used. The dimeric tetrahydroxanthone derivatives **1** and **4** and the RAL **12** showed potent inhibition of the

melanoma (MDA-MB-435) and colon (SW-620) cancer cell lines. Alternatively, compounds **3** and **5** showed promising activity against the Gram-positive bacterium *Micrococcus luteus*.

Results and Discussion

The organic extracts of a large-scale solid-substrate fungal co-culture of *A. versicolor* and *S. terrestris* (MSX45109) showed potent cytotoxic activity against the SW-620 and MDA-MB-435 cancer cell lines and was fractionated by silica gel flash chromatography to yield 5 fractions. The third fraction, which eluted with 10% MeOH-CHCl₃, showed potent cytotoxic activity on the two cancer cell lines, and as such, it was purified using reversed-phase preparative and semipreparative HPLC to yield compounds **1-16**. The purity of the isolated compounds was verified using UPLC (Figure 49).

A total of sixteen polyketides were isolated and identified in this study. Compounds **1-10** were identified as a series of monomeric (**6-8**), homodimeric (**1-5**), and heterodimeric (**9** and **10**) tetrahydroxanthones by comparison of HRMS, NMR, and CD data with each other and with structurally related compounds. Stereoisomeric compounds **1** (35.10 mg), **2** (51.25 mg), and **3** (9.49 mg) were obtained as yellow powders with a molecular formula of C₃₂H₃₀O₁₄ as determined by HRESIMS. The ¹H and ¹³C NMR spectra of compounds **1** and **2** showed the presence of only 15 protons and 16 carbons, indicating that these compounds were symmetric, whereas **3** was asymmetric. A search of the Dictionary of Natural Products for the molecular formula and a UV range of 325-345 nm resulted in 12 hits, 5 of which were excluded based on NMR data. The remaining 7 hits were the secalonic acids A-G containing a 2,2'-linkage. The fact that compounds **1**

and **2** were symmetric cut down the number of possibilities for compounds **1** and **2** into secalonic acids A, B, D, or E, while compound **3** could be either secalonic acid C, F, or G. Key differences between compounds **1** and **2** were the chemical shift values and splitting patterns of H-5, H-6, and H₂-7. A proton doublet corresponding to H-5/H-5' (δ_{H} 3.92, d, $J = 11.2$) in **1** was downfield shifted in **2** (δ_{H} 4.12, d, $J = 1.2$). These J values implied a pseudodiaxial *trans* orientation of H-5/H-6 in **1** and a pseudoaxial/pseudoequatorial *cis* orientation in **2** (Figures 51 and 52, Table 19). On the other hand, the ¹H NMR spectrum of **3** showed similarity with the combined ¹H NMR spectra of **1** and **2** by revealing two sets of protons that corresponded to two asymmetric monomers (Figure 41, Table 19). The 2,2'-linkage in **1-3** was confirmed by diagnostic HMBC cross correlations of H-3 and H-3' with C-2' and C-2, respectively. The absolute configurations of the 2,2'-secalonic acids have been determined by CD spectroscopy.^{116,117} The Cotton effect around 330 nm has been correlated with the configurations of C-10a and C-10a'. Negative Cotton effects at 332 nm in the CD spectra of compounds **1**, **2**, and **3**, $\Delta\epsilon = -38.8, -24.6, -31.2$, respectively, indicated an *S*-configuration at both C-10a and C-10a' (Figure 37). This allowed the assignment of the *R*-configuration at C-6 and C-6' based on the *trans* orientation of C-6/6' and C-10a/10a' substituents deduced from the biosynthetic route for the formation of stereoisomeric tetrahydroxanthone precursors of secalonic acids, with no exception so far in literature.¹¹⁸ Combining all the data together suggested the absolute configuration as (5*S*,6*R*,10a*S*,5'*S*,6'*R*,10a'*S*), (5*R*,6*R*,10a*S*,5'*R*,6'*R*,10a'*S*), and (5*R*,6*R*,10a*S*,5'*S*,6'*R*,10a'*S*) for compounds **1-3**, respectively. Consequently, compounds **1-3** were identified as

secalonic acid A,¹¹⁹ secalonic acid E,¹²⁰ and secalonic acid G,¹²¹ respectively, in accordance with published data (Table 20). Most literature pertaining to these compounds dates back to the 1960s and 1970s, therefore to update the literature, the ¹H and ¹³C NMR data for **1-3** were provided in the Supporting Information (Table 19, Figures 51-53).

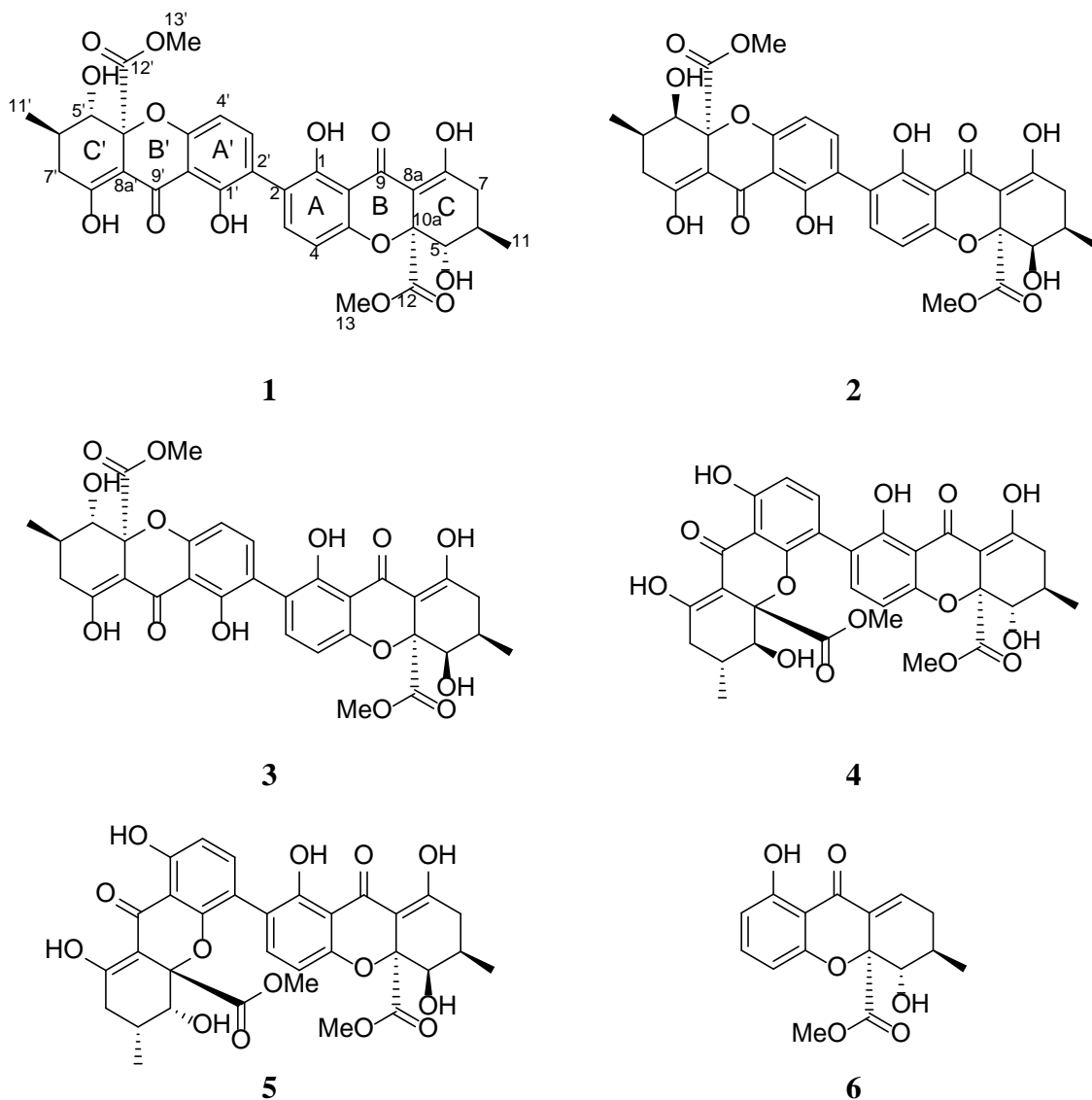


Figure 36. Structures of compounds **1-16**

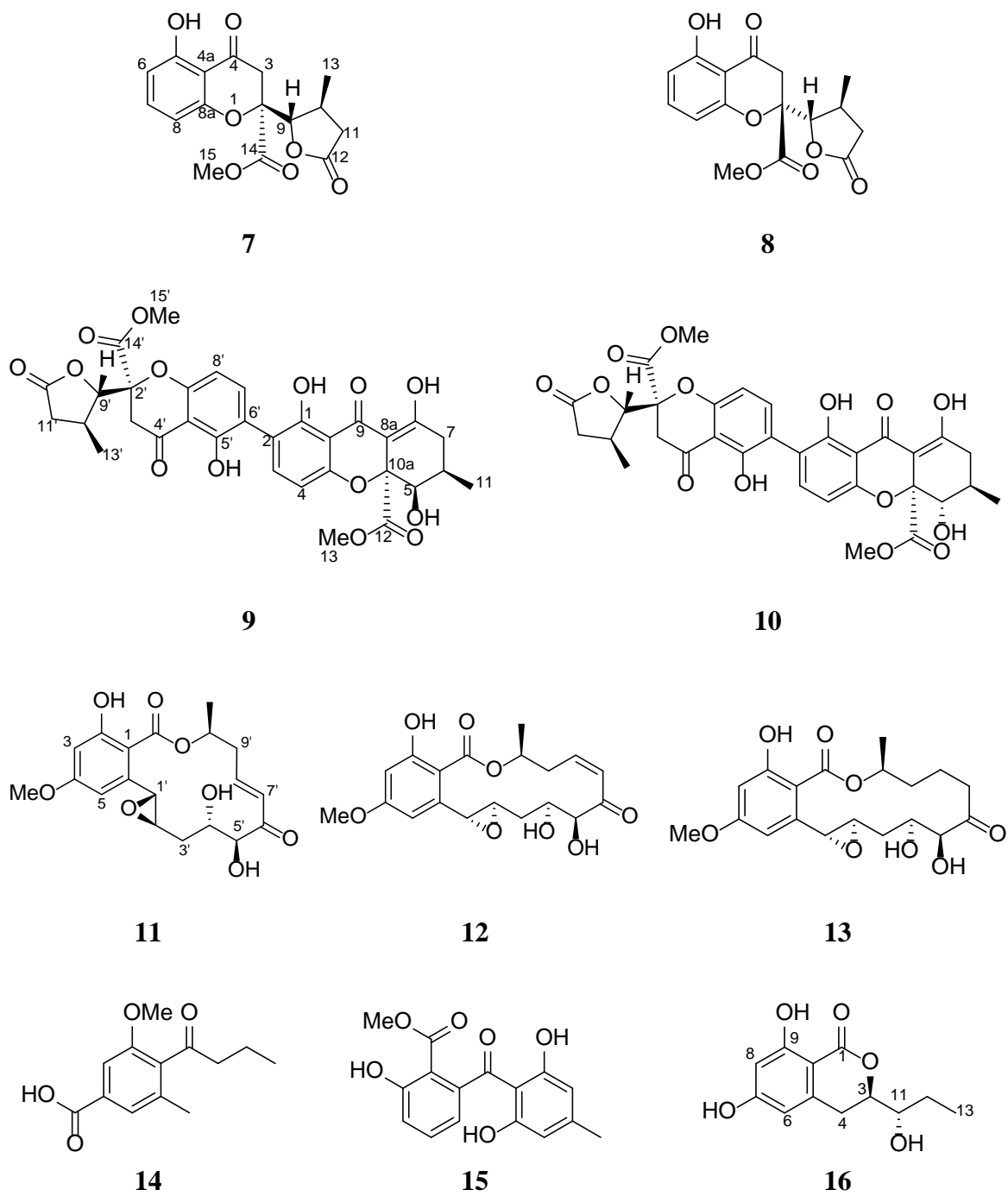


Figure 36 (continued). Structures of compounds 1-16

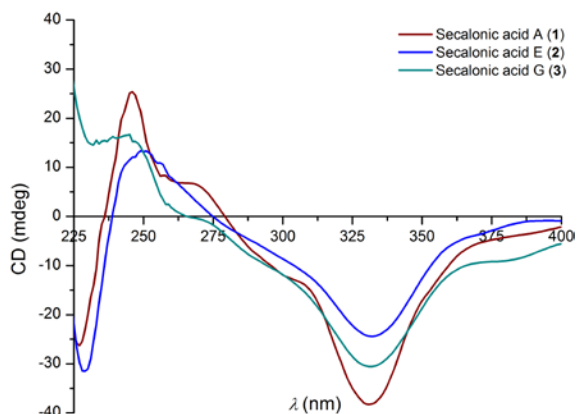


Figure 37. ECD spectra of secalonic acids **1**, **2**, and **3** in chloroform at 0.03 mM concentration, cell length 2 cm.

Compound **4** (5.39 mg) was obtained as a yellow powder. The chemical formula was determined as $C_{32}H_{30}O_{14}$ by HRESIMS and analysis of 1H NMR, ^{13}C NMR and edited-HSQC data (Figure 54). The NMR data suggested an asymmetric secalonic acid analogue with structural similarity to **1** (Figure 54, Table 21). However, a key difference between **4** and **1** was the linkage point of the monomeric units, being a 2,2' in **1** vs. 2,4' in **4**, which rendered **4** asymmetric, as evidenced by diagnostic HMBC cross correlations of H-3 and H-3' with C-4' and C-4, respectively (Figure 50). The two monomeric moieties in **4** were assigned the same configuration as **1**, as evidenced by a negative Cotton effect at 331 nm in the CD spectrum of **4**, $\Delta\epsilon = -24.8$, and negative values of optical rotation for both **1** and **4** (Figure 38, Table 20). The absolute configuration of **4** was established as (5*S*,6*R*,10*aS*,5'*S*,6'*R*,10*a*'*S*) by comparing experimental and calculated ECD spectra predicted by the time-dependent density functional theory (TDDFT) method (Figure 39).¹²²⁻¹²⁵ The NMR and optical rotation data were in agreement with those reported for

penicillixanthone A.¹²⁶ Interestingly, compound **4** was reported by Kurobane et al.¹²⁷ as a chemically rearranged analogue of **1** by dissolving the latter into polar organic solvents, such as pyridine, acetone, and acetonitrile, either at room or higher temperatures for hours to days, depending on the solvent used. This suggests that **4** may have occurred as an artifact of the purification scheme. The NMR data of compound **4** were given in the Supporting Information (Table 21, Figure 54).

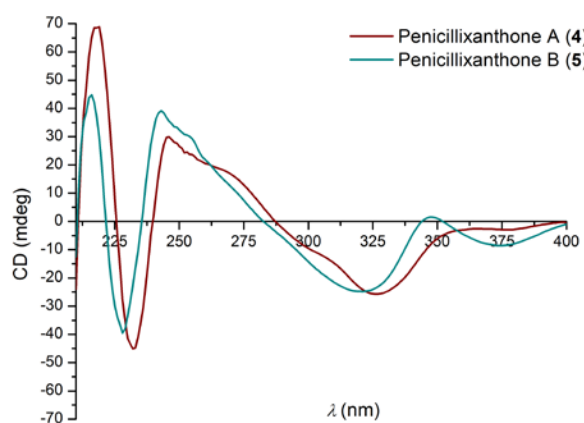


Figure 38. ECD spectra of penicillixanthone A (**4**) [0.05 mM] and penicillixanthone B (**5**) [0.06 mM] in CHCl_3 , cell length 2 cm.

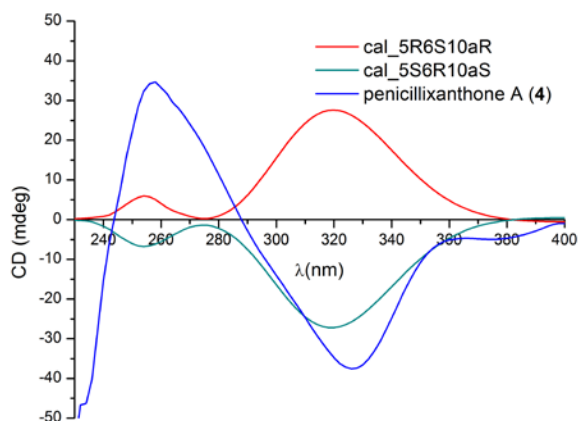


Figure 39. Experimental and calculated CD spectra for penicillixanthone A (**4**) in chloroform.

Compound **5** (2.05 mg), which was obtained as a yellow powder, had a chemical formula of $C_{32}H_{30}O_{14}$ as determined by HRESIMS and analysis of 1H NMR, ^{13}C NMR and edited-HSQC data (Figure 55), establishing an index of hydrogen deficiency of 18. The NMR data suggested an asymmetric secalononic acid analogue with structural similarity to **2** (Figure 41, Table 12). However, as was observed in **1** vs. **4**, the 2,2'-linkage in **2** was supplanted by a 2,4'-linkage in **5**, as evidenced by diagnostic HMBC cross correlations of H-3 and H-3' with C-4' and C-4, respectively (Figure 41). Two proton singlets, corresponding to H-5/H-5' (δ_H 4.14/3.99) in **5** implied a pseudoaxial/pseudoequatorial *cis* orientation of H-5/H-6 and H-5'/H-6', similar to that in **2**, which were further supported by NOESY correlations between H-5/H-6 and H-5'/H-6' (Figure 41). The two monomeric moieties in **5** were assigned the same configuration as **2**, as evidenced by a negative Cotton effect at 332 nm in the CD spectrum of **5**, $\Delta\epsilon = -18.9$, and negative values of optical rotation for both compounds (Table 20). The absolute

configuration of **5** was established as (5*R*,6*R*,10*aS*,5'*R*,6'*R*,10*a'S*) by comparing experimental and calculated ECD spectra predicted by TDDFT (Figure 40).¹²²⁻¹²⁵ These data suggested the structure of **5**, which was ascribed the trivial name penicillixanthone B. As noted for **4**,¹¹⁹ compound **5** was likely an artifact produced by rearrangement of **2** in polar organic solvents.

Table 12. NMR Data for 5 (500 MHz for ¹H, 125 MHz for ¹³C; Chemical Shifts in δ , Coupling Constants in Hz, CDCl₃)

position	δ_C	δ_H mult (<i>J</i> in Hz)	Position	δ_C	δ_H mult (<i>J</i> in Hz)
1	159.39		1'	161.90	
2	119.37		2'	110.79	6.60, d (8.6)
3	139.57	7.47, d (8.6)	3'	140.09	7.33, d (8.6)
4	107.90	6.58, d (8.6)	4'	115.87	
4a	157.22		4a'	154.51	
5	71.46	4.14, s	5'	70.89	3.99, s
6	28.56	2.12, m	6'	28.54	2.12, m
7	32.73	2.38, m	7'	32.58	2.38, m
		2.49, m			2.49, m
8	180.23		8'	179.43	
8a	99.94		8'a	99.73	
9	187.64		9'	187.89	
9a	107.03		9'a	106.88	
10a	84.89		10'a	84.40	
11	17.62	1.17, dd (6.9, 0.6)	11'	17.60	1.13, dd (6.9, 0.6)
12	171.38		12'	170.89	
13	53.69	3.75, s	13'	53.41	3.64, s
1-OH		11.91	1'-OH		11.56
5-OH		2.55, brs	5'-OH		2.77, brs

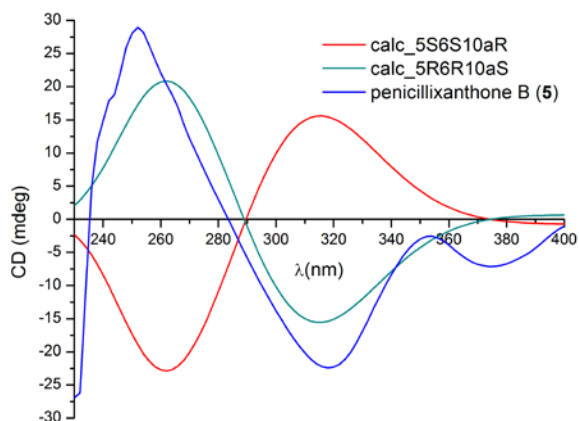


Figure 40. Experimental and calculated CD spectra for penicillixanthone B (**5**) in chloroform.

Compound **6** (0.75 mg) was obtained as a yellow gum. The molecular formula was deduced as $C_{16}H_{16}O_6$ by HRESIMS and analysis of 1H NMR, ^{13}C NMR and edited-HSQC data (Figure 56), indicating an index of hydrogen deficiency of 9. Inspection of the HRMS and NMR data suggested **6** as a tetrahydroxanthone derivative with structural similarity to the monomeric unit of **1**. However, key differences were the replacement of the C-2 quaternary carbon in **1** (δ_C 118.3) by an aromatic methine in **6** (δ_H/δ_C 110.5/6.54), and the replacement of the hydrogen-bonded phenolic proton in **1** (δ_H 13.78) by an olefinic proton in **6** (δ_H 7.23) (Tables 13 and 19). COSY data identified two spin systems as H-5/H-6/H₂-7/H-8 and H-2/H-3/H-4 (Figure 41). Further examination of the NMR spectra, including HMBC data (Figure 41), yielded the planar structure of **6**, which was ascribed the trivial name blennolide H. The relative configuration of **6** was found to be (5*S*,6*R*,10*aS*), the same as that of the monomeric units of **1**, deduced from NOESY

correlations, coupling constants, and negative optical rotation values for both compounds (Figure 41, Table 20).

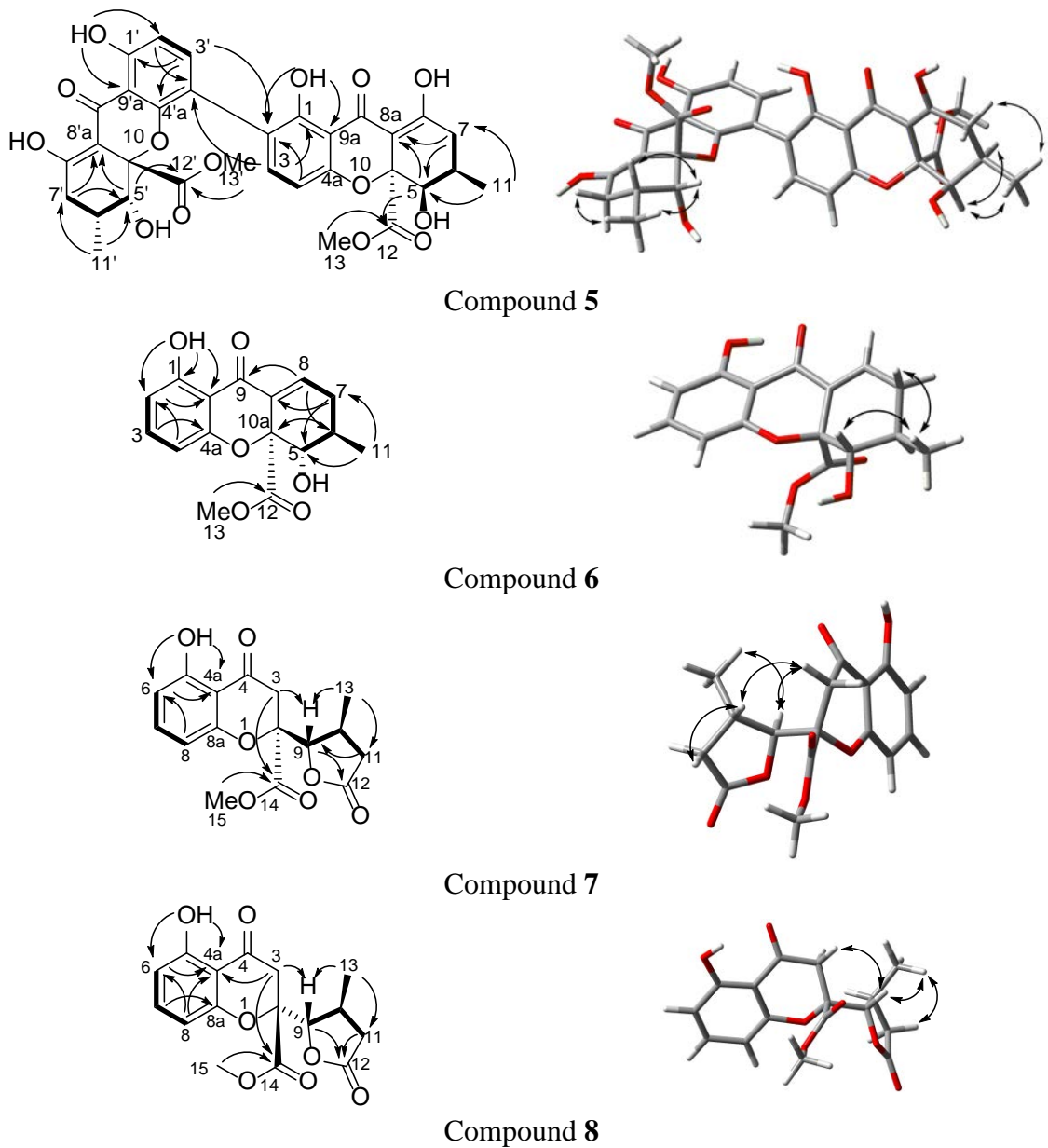
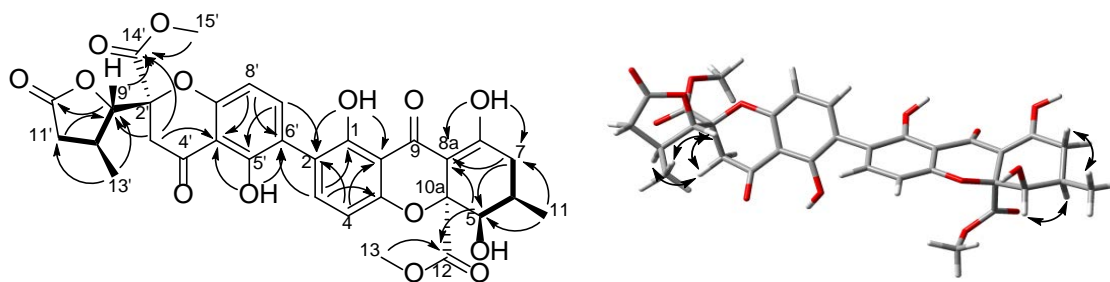
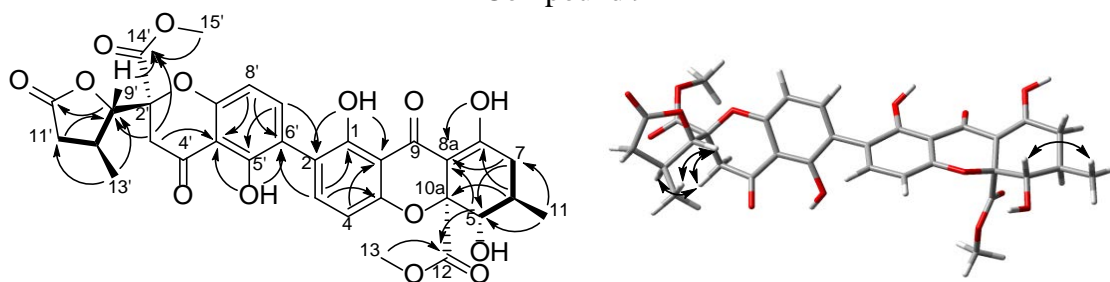


Figure 41. Key HMBC, COSY, and NOESY correlations of **5-10** and **16**.



Compound 9



Compound 10



Compound 16

COSY HMBC NOESY

Figure 41 (continued). Key HMBC, COSY, and NOESY correlations of 5-10 and 16.

Table 13. NMR data for 6 (500 MHz for ^1H , 175 MHz for ^{13}C ; chemical shifts in δ , coupling constants in Hz, Methnol- d_4)

position	δ_{C}	δ_{H} mult (J in Hz)
1	163.0	
2	110.5	6.54, dd (8.6, 0.6)
3	138.5	7.39, dd (8.6, 8.0)
4	107.7	6.56, dd (8.0, 0.6)
4a	159.5	
5	77.5	3.92, dd (11.5, 2.9)
6	30.0	2.36, m
7	33.8	2.16, ddd (20.6, 10.3, 2.9) 2.72, dt (20.6, 5.2)
8	141.9	7.23, dd (5.2, 2.9)
8a	129.9	
9	184.7	
9a	107.7	
10a	85.8	
11	17.7	1.15, d (6.3)
12	169.1	
13	53.3	3.69, s
1-OH		12.00, s
5-OH		2.74, s

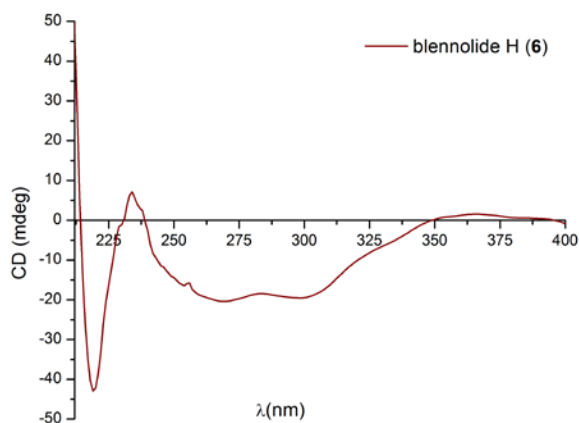


Figure 42. ECD spectrum of blennolide H (6) [0.43 mM] in MeOH, cell length 2 cm.

Diastereoisomers **7** (5.36 mg) and **8** (1.02 mg) were obtained as colorless oils with a molecular formula of C₁₆H₁₆O₇, as determined by HRESIMS and analysis of ¹H NMR, ¹³C NMR and edited-HSQC data (Figures 57 and 58), establishing an index of hydrogen deficiency of 9. Compounds **7** and **8** showed similar ¹H and ¹³C NMR spectra (Figures 57 and 58, Table 14) with small differences in four chemical shift values. Interestingly, compounds **7** and **8** displayed opposite signs for optical rotation data; while compound **7** was levorotatory (-26.14°), compound **8** was dextrorotary (+42.05°). Moreover, the CD spectra of **7** and **8** were mirror images of each other (Figure 43). Analysis of the HRMS and NMR data indicated **7** and **8** as monomers and structurally related to the monomeric units of compounds **1-5**. In comparison to the chromanone moiety in compounds **1-5**, the chromanone moiety, rings A and B, were reserved in **7** and **8**, as evidenced from comparable ¹³C NMR data and the hydrogen-bonded phenolic proton (δ_{H} 11.43), except for a quaternary aromatic carbon that was replaced by an aromatic methine in **7** and **8**. In contrast, however, ring C experienced significant changes, as evidenced from 1D and 2D-NMR data. The ¹³C NMR spectra displayed signals characteristic of ester functionality (δ_{C} 175.3 and 175.7 for **7** and **8**, respectively; Table 14). Thus, ring C was established as a γ -lactone moiety, as evidenced from the ¹H-¹H COSY spin system of H-9/H-10/(H₃-13)/H-11 and HMBC correlations from H₃-13 to C-11 and C-9, H-9 to C-12, and H-11 to C-9 (Figure 41). On the other hand, HMBC correlations from H₂-3 to C-9 and C-14 and from H-9 to C-14 indicated a 2,9-linkage between the chromanone and the γ -lactone moieties, establishing the planar structures of **7** and **8** (Figure 41). The relative configuration of ring C in compounds **7** and **8** was similar based on NOESY correlations

between H₃-13 and H-9 and coupling constant values of 4.0 and 3.4 ppm for H-9 in compounds **7** and **8**, respectively, implying a pseudodiaxial *trans* orientation of H-9/H-10 (Figure 41). The spatial arrangement of **7** and **8** were different, as observed via NOESY data, particularly between H-10 to H-11 α and H-3 α , H-9 to H₂-3 in **7** and from H-9 to H-3 α in **8** (Figure 41). Putting these data together, and taking into consideration the fact that compounds **7** and **8** could not be enantiomers, since they were separated using non-enantioselective methods, compounds **7** and **8** could either be epimers in C-2 or have the same configuration at C-2 but the opposite configuration of ring C. Eventually, the absolute configuration of **7** and **8** was established by comparing the experimental ECD data with those obtained through molecular modeling calculations. The agreement between the observed and calculated ECD (Figure 44) established the absolute configuration of **7** as (2*S*,9*S*,10*S*) and for **8** as (2*R*,9*S*,10*S*), supporting epimerization at C-2. The NMR and optical rotation data of **8** indicated similarity with paecilin B, which was isolated from the mangrove endophytic fungus, *Paecilomyces* sp., and its planar structure was published on 2007.¹²⁸ However, significant differences in the ¹H and ¹³C NMR data of compound **8** and paecilin B were observed (See supplementary Table 22 for comparison). Recently, paecilin B was reported as a monomer and as a subunit of a dimer from the seagrass-derived fungus *Bipolaris* sp. with the same absolute configuration determined for **8**.¹²⁹ Two structurally related compounds, blennolide D and blennolide E, where C-11 is hydroxylated, were reported previously from *Blennoria* sp.¹¹⁴ Hence, the trivial name 11-deoxyblennolide D was ascribed to compound **7**. The planar structure of

compounds **7** and **8** was reported previously by synthesis but without the reporting of NMR data.¹³⁰

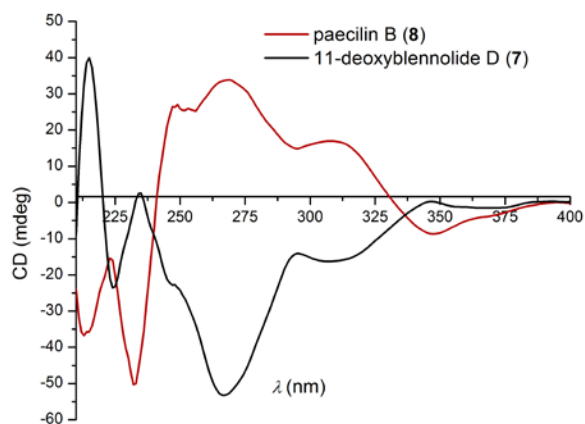


Figure 43. ECD spectra of 11-deoxyblennolide D (**7**) [0.16 mM] and paecilin B (**8**) [0.56 mM] in chloroform, cell length 2 cm.

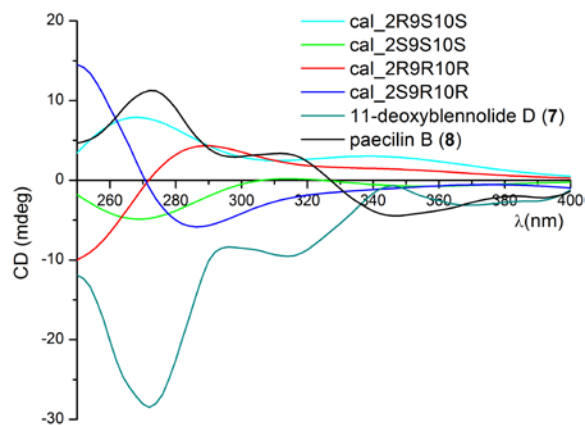


Figure 44. Experimental and calculated CD spectra for 11-deoxyblennolide D (**7**) paecilin B (**8**) in chloroform.

Table 14. NMR Data for 7 and 8 (500 MHz for ^1H , 125 MHz for ^{13}C ; Chemical Shifts in δ , Coupling Constants in Hz, CDCl_3)

position	7		8	
	δ_{C} , type	δ_{H} mult (J in Hz)	δ_{C} , type	δ_{H} mult (J in Hz)
2	84.3		84.3	
3	39.8	3.04, dd (17.2, 0.6) 3.17, d (17.2)	40.7	3.07, d (17.2) 3.48, d (17.2)
4	194.1		194.9	
4a	107.7		107.5	
5	162.0		161.9	
6	110.7	6.55, dd (8.6, 0.6)	110.6	6.54, dd (8.6, 0.6)
7	139.2	7.42, t (8.6)	139.0	7.40, t (8.6)
8	107.7	6.54, dd (8.6, 0.6)	107.5	6.49, dd (8.6, 0.6)
8a	159.2		159.3	
9	87.6	4.43, dd (4.0, 0.6)	86.5	4.36, dd (3.4, 0.6)
10	30.1	2.83, m	29.7	2.85, m
11	36.2	2.21, dd (17.8, 4.6) 2.89, dd (17.8, 9.2)	36.4	2.21, dd (17.8, 4.6) 3.01, dd (17.8, 9.2)
12	175.3		175.7	
13	20.9	1.28, d (6.9)	20.7	1.18, d (6.9)
14	168.9		169.2	
15	53.8,	3.72, s	53.7	3.74, s
5-OH		11.43, s		11.45, s

Compound **9** (1.07 mg) was isolated as a yellow gum with a molecular formula of $\text{C}_{16}\text{H}_{16}\text{O}_6$ as deduced by HRESIMS, ^1H NMR, ^{13}C NMR and edited-HSQC data (Figure 47), indicating an index of hydrogen deficiency of 18. Analysis of the NMR data, including HMBC and NOESY spectra, suggested **9** as a heterodimer, with one monomeric moiety similar to the monomeric units of **2** and the other similar to **7** (Table 15 and Figure 41). A key difference between the monomeric moiety in **9** that was related to **7** was replacement of the C-6 aromatic methine ($\delta_{\text{H}}/\delta_{\text{C}}$ 110.7/6.55) in **7** by a quaternary carbon in **9** (δ_{C} 118.1). A 2,6'-linkage in **9** was evident by diagnostic HMBC correlations of H-3 to C-6' and H-7' to C-2, respectively, establishing the planar structure

of **9** (Figure 41). The absolute configuration was deduced based on the monomeric constituents. The secalonic acid moiety was assigned the same configuration as **2**, evidenced from similar NOESY correlations and coupling constant values of H-5 and preservation of the configuration at C-10a through the series. As well, the moiety similar to **7** was assigned the same configuration as **7** based on consistencies in the ^1H , ^{13}C , and NOESY NMR data (Tables 14 and 15, and Figure 41). Hence the absolute structure of **9** was assigned as (5*R*,6*R*,10a*S*,2'*S*,9'*S*,10'*S*) and was confirmed by ECD calculations (Figure 46). The NMR data of **9** were found to be in agreement with those for blennolide G, which was reported previously from *Blennoria* sp.¹¹⁴ However, compound **9** and blennolide G showed opposite CD and optical rotation data, and opposite absolute configuration at four chiral centers, indicating **9** as a diastereoisomer of blennolide G (Table 20, Figure 45). The trivial name blennolide I was ascribed to **9**.

Table 15. NMR Data for 9 and 10 (700 MHz for ^1H , 175 MHz for ^{13}C ; Chemical Shifts in δ , Coupling Constants in Hz, CDCl_3)

position	9		10	
	δ_{C}	δ_{H} mult (J in Hz)	δ_{C}	δ_{H} mult (J in Hz)
1	159.4		159.3	
2	118.3		117.8	
3	139.6	7.42, d (8.3)	140.1	7.45, d (8.5)
4	107.5	6.57, d (8.3)	107.5	6.62, d (8.5)
4a	157.2		158.4	
5	71.3	4.12, s	78.0	3.93, dd (11.2, 2.7)
6	28.5	2.11, m	29.2	2.41, m
7	32.6	2.40, dd (18.9, 6.1) 2.52, dd (18.9, 11.2)	36.2	2.32, dd (19.4, 10.6) 2.73, dd (19.4, 6.5)
8	179.9		177.6	
8a	99.9		101.5	
9	187.5		187.1	
9a	107.0		106.9	
10a	84.8		84.8	
11	17.5	1.17, d, (7.1)	18.0	1.17, d, (6.5)
12	171.2		170.2	
13	53.5	3.71, s	53.3	3.71, s
1-OH		11.85		11.72
5-OH		2.52		2.77, d (2.7)
8-OH		13.95		13.76
2'	84.2		84.2	
3'	39.7	3.05, d (17), 3.21, d (17)	39.7	3.05, d (17), 3.21, d (17)
4'	194.0		194.0	
4'a	107.6		107.6	
5'	159.2		159.2	
6'	118.1		118.1	
7'	141.3	7.52, d (8.3)	141.3	7.51, d (8.5)
8'	107.3	6.61, d (8.3)	107.3	6.62, d (8.5)
8'a	158.6		158.6	
9'	87.5	4.45, d (3.8)	87.5	4.46, d (4.1)
10'	30	2.84, m	30	2.84, m
11'	36.0	2.91, dd (18.0, 9.3) 2.23, dd (18.0, 4.8)	36.0	2.92, dd (17.9, 9.4) 2.22, dd (17.9, 4.6)
12'	175.1		175.1	
13'	20.9	1.28, d (7.1)	20.9	1.28, d (6.8)
14'	168.8		168.8	
15'	53.7	3.76, s	53.7	3.75, s
5'-OH		11.88		11.89

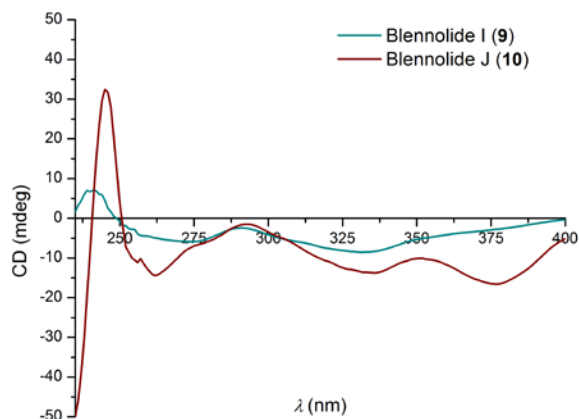


Figure 45. ECD spectra of blennolide I (**9**) [0.06 mM] and blennolide J (**10**) [0.17 mM] in chloroform, cell length 2 cm.

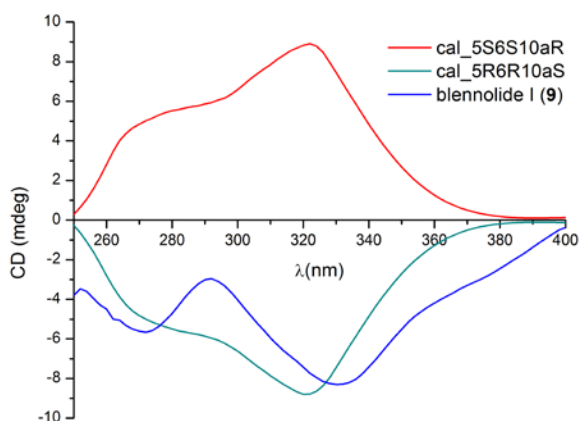


Figure 46. Experimental and calculated CD spectra for blennolide I (**9**) in chloroform.

Compound **10** (0.63 mg), which was isolated as a yellow gum, had a molecular formula of $C_{16}H_{16}O_6$ as deduced by HRESIMS, 1H NMR, ^{13}C NMR and edited-HSQC data (Figure 60), indicating an index of hydrogen deficiency of 18. Analysis of the NMR data indicated **10** as an asymmetric heterodimer with structural similarity to **9**. Key differences between **9** and **10** were chemical shift values and splitting patterns of H-5, H-6, and H₂-7 (Table 15, Figures 59 and 60). A proton singlet in **9** (δ_H 4.12), corresponding

to H-5, was replaced by a doublet (δ_{H} 3.93, d, $J = 11.2$) in **10**, suggesting a pseudodiaxial *trans* orientation of H-5/H-6 in **10**. These data indicated that the secalonic acid moiety in **10** was similar to the monomeric units of **1**, while the 11-deoxyblennolide D moiety was preserved, as in **9**. A 2,6'-linkage in **10**, also similar to **9**, was confirmed by diagnostic HMBC correlations of H-3 with C-6' and H-7' with C-2, respectively, establishing the planar structure of **10** (Figure 41). As for **9**, the absolute configuration of **10** was deduced based on the monomeric constituents and ECD calculations as (5*S*,6*R*,10*aS*,2'*S*,9'*S*,10'*S*) (Figure 47). The trivial name blennolide J was ascribed to compound **10**.

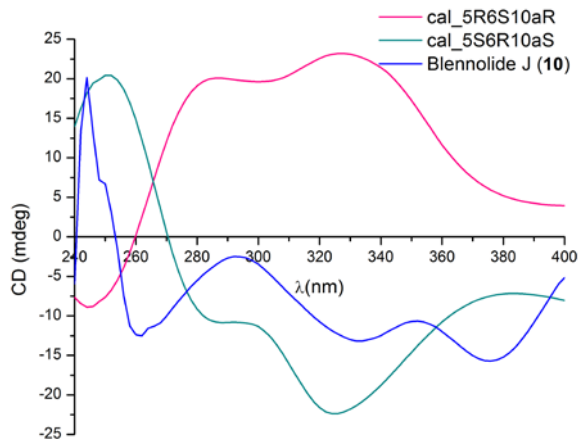


Figure 47. Experimental and calculated CD spectra for blennolide J (**10**) in chloroform.

Compounds **11-13** were identified as the resorcylic acid lactones, aigialomycin (4.24 mg),¹³¹ hypothemycin (19.58 mg),¹³² and dihydrohypothemycin (3.68 mg),¹³¹ respectively, while compounds **14** and **15** were pyrenochaetic acid C (2.71 mg)¹³³ and nidulalin B (1.68 mg),¹³⁴ respectively. In all cases, the spectroscopic and spectrometric data were in agreement with those reported in the literature.

Compound **16** (0.79 mg) was isolated as a colorless oil with a molecular formula of $C_{12}H_{14}O_5$ as revealed by HRESIMS, 1H NMR, ^{13}C NMR and edited-HSQC data (Figure 66), indicating an index of hydrogen deficiency of 6. UV absorption maxima of 301, 270, and 233 nm were indicative of an aromatic carbonyl compound.¹³⁵ Inspection of the NMR data showed signals characteristic of six aromatic carbons, two of which were oxygenated, and two doublet aromatic protons with coupling constant values of 2.3 Hz, and two phenolic protons. These data suggested a 1,2,3,5-tetrasubstituted benzene ring with two aromatic protons *meta* to each other (Figure 66, Table 16). Benzene ring substituents were confirmed by HMBC correlations (Figure 41). COSY data identified a 1,2,3-tetrasubstituted pentane moiety ($H_2-4/H-3/H-11/H-12/H-13$) with C-3 and C-11 being oxygenated and the terminal methylene attached to the benzene ring (Figure 41). HMBC correlations from H_2-4 to C-6 and C-10 confirmed C-5 as the attachment point of the aliphatic side chain with the aromatic ring. Chemical shift values (δ_H/δ_C 4.43/81.1) for H-3/C-3 indicated esterification of C-3 to form a six membered ring with the ester carbonyl (δ_C 170.2) that was attached to the benzene ring at C-2. Further examination of the NMR data yielded the planar dihydroisocoumarin structure of **16**, which was ascribed the trivial name pyrenomycin. The absolute configuration of **16** was assigned via a modified Mosher's ester method,⁶⁸ establishing the configuration as 3*R* and 11*S* (Figure 48). Similar dihydroisocoumarin compounds were isolated previously from marine sponges, plants, fungi, and insects, including hiburipyrone,¹³⁶ 3-(2-hydroxypropyl)-8-hydroxy-3,4-dihydroisocoumarin,¹³⁷ and (3*S*,1'*R*)-3-(1-hydroxyethyl)-6,8-dihydroxy-7-methyl-3,4-dihydroisocoumarin.¹³⁸

Table 16. NMR Data for 16 (700 MHz for ^1H , 175 MHz for ^{13}C ; Chemical Shifts in δ , Coupling Constants in Hz, Methnol- d_4)

position	δ_{C}	δ_{H} mult (J in Hz)
1	170.2	
3	81.1	4.43, dt (12.7, 3.3)
4	29.0	2.75, dd (16.4, 3.3) 3.11, dd (16.4, 12.7)
5	142.2	
6	107.2	6.21, brd (2.3)
7	164.2	
8	100.9	6.15, d (2.3)
9	168.8	
10	99.6	
11	73.1	3.58, dt (8.6, 3.3)
12	25.1	1.67, m
13	9.2	1.03, t (7.5)
9-OH		8.55, s
11-OH		1.28, brs
7-OH		4.57, brs

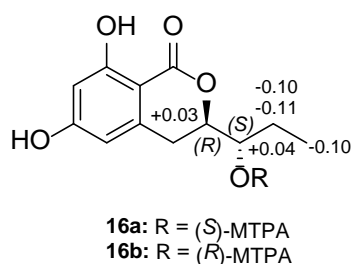


Figure 48. $\Delta\delta_{\text{H}}$ values [$\Delta\delta$ (in ppm) = $\delta_{\text{S}} - \delta_{\text{R}}$] obtained for (*S*)- and (*R*)-MTPA esters (**16a** and **16b**, respectively) of pyrenomycin (**16**) in pyridine- d_5 .

Compounds (**1-15**) were tested for cytotoxicity in the MDA-MB-435 and SW-620 cancer cell lines. Of the tetrahydroxanthone derivatives, **1** and **4** were the most potent with IC_{50} values less than $0.50 \mu\text{M}$ in both cell lines (Table 17). Based on the cytotoxicity data of related analogues, the configuration of C-5/C-5' became evident

(Table 17). Compounds **1** and **4**, with *5S,5'S* configuration, were the most potent, with a 2,2'-linkage for **1** and a 2,4'-linkage for **4**. A *5S,5'R* configuration, as in **3**, was approximately 20 times less active than **1**, while a *5R,5'R* configuration rendered **2** inactive; all of these had a 2,2'-linkage of the monomeric units. For those with a 2,4'-linkage, compound **5** with *5R,5'R* was approximately 30 times less active than **4**. Heterodimeric **10**, which was composed of the monomeric units of **1** and compound **7**, was approximately 25 times less active than **1**. Conversely, compound **9**, which was composed of the monomeric units of **2** and compound **7** was inactive. On the other hand, all three monomeric compounds (**6-8**) were inactive. Consistent with the cytotoxicity data obtained in this study, **1** and its chemically rearranged 2,4'-dimer **4**, were reported to have equipotent activity against cultured mouse leukemia L1210 cells.¹¹⁰ Moreover, **1** was reported to have a protecting effect of the dopaminergic neurons from 1-methyl-4-phenylpyridinium (MPP⁺)-induced cell death,¹³⁹ and attenuation of colchicine-induced apoptosis of the cortical neurons.¹⁴⁰

In agreement with the literature,¹¹⁵ cytotoxicity data of the structurally related RALs (**11-13**) indicated the importance of the (*Z*)-enone for activity, as in hypothemycin (IC₅₀ value of 0.58 μM, MDA-MB-435). Alternatively, dihydrohypothemycin, with an (*E*)-enone, and aigialomycin A, with a reduced enone, were both inactive (IC₅₀ value > 10 μM). RALs containing a (*Z*)-enone have been reported as potent inhibitors of several ATPases and kinases, including TAK1.^{141,142}

Table 17. Cytotoxicity of Compounds 1-15 Against Two Human Tumor Cell Lines

compound ^a	IC ₅₀ values in μM ^b	
	MDA-MB-435 ^c	SW-620 ^c
1	0.16	0.41
2	NA	19.12
3	3.27	3.67
4	0.18	0.21
5	5.20	5.55
10	4.06	6.14
12	0.58	2.14

^aCompounds **6-9**, **11**, and **13-15** were inactive with IC₅₀ >20 μM .

^bIC₅₀ values were determined as the concentration required to inhibit growth to 50% of control with 72 h incubation.

^cPositive control was vinblastine tested at concentration of 1 nM in MDA-MB-435 cells and 10 nM in SW620 cells, which had 23% and 76% viable cells, respectively.

The antimicrobial activity of the isolated compounds (**1-15**) was evaluated against a panel of bacteria and fungi (Table 18 and 23). Compounds **3** and **5** showed promising activity against the Gram-positive bacterium *Micrococcus luteus* with MIC values of 5 and 15 $\mu\text{g/mL}$, respectively. Secalonic acid A (**1**) was reported to have activity against *Bacillus subtilis* and *Piriculaia oryzae*¹⁰⁷ and a phlogistic activity,¹⁴³ while penicillixanthone A (**4**) was reported to have medium antibacterial activity against *M. luteus*, *Pseudoalteromonas nigrifaciens*, and *B. subtilis*.¹⁴⁴

Table 18. Antimicrobial Activities of Compounds 1-15

compound ^a	Antimicrobial activity MIC ($\mu\text{g/mL}$)	
	<i>M. luteus</i>	<i>S. aureus</i>
1	38	75
2	36	NA ^[b]
3	5	39
4	46	93
5	15	59
10	43	43
Ampicillin ^b	4	
Vancomycin ^b	--	0.25

^aSee table 23 for compounds **6-9**, **11**, and **12-15**.
^bPositive control.
^cNA: not active with MIC > 145 $\mu\text{g/mL}$.

In summary, a total of 18 polyketides (**1-16**), of which six were new, were isolated from a fungal co-culture of *A. versicolor* and *S. terrestris* (MSX45109). Cytotoxicity assays suggested compounds **1**, **4**, and **12** as the most potent. When evaluated for antimicrobial activity, compounds **3** and **5** showed promising *M. luteus* activity. In addition of updating the literature with spectroscopic and spectrometric data for some the known isolated compounds, this study also updated the literature with bioassay and SAR data of structurally related analogues.

Methods

General. UV and CD spectra were obtained using a Varian Cary 100 Bio UV-Vis spectrophotometer (Varian Inc., Walnut Creek, CA, USA) and an Olis DSM 17 CD spectrophotometer (Olis, Inc. Bogart, GA, USA), respectively. NMR data were collected using either a JEOL ECA-500 NMR spectrometer operating at 500 MHz for ¹H and 125

MHz for ^{13}C , or a JEOL ECS-400 NMR spectrometer equipped with a high sensitivity JEOL Royal probe operating at 400 MHz for ^1H and 100 MHz for ^{13}C (both from JEOL Ltd., Tokyo, Japan), or an Agilent 700 MHz NMR spectrometer (Agilent Technologies, Inc., Santa Clara, CA, USA), equipped with a cryoprobe, operating at 700 MHz for ^1H and 175 MHz for ^{13}C . Residual solvent signals were utilized for referencing. High resolution mass spectra (HRMS) were obtained using a Thermo LTQ Orbitrap XL mass spectrometer equipped with an electrospray ionization source (Thermo Fisher Scientific, San Jose, CA, USA). A Waters Acquity UPLC system (Waters Corp., Milford, MA, USA) utilizing a Waters BEH C_{18} column (1.7 μm ; 50 \times 2.1 mm) was used to check the purity of the isolated compounds with data collected and analyzed using Empower software. Phenomenex Gemini-NX C_{18} analytical (5 μm ; 250 \times 4.6 mm), preparative (5 μm ; 250 \times 21.2 mm), and semipreparative (5 μm ; 250 \times 10.0 mm) columns (all from Phenomenex, Torrance, CA, USA) were used on a Varian Prostar HPLC system equipped with ProStar 210 pumps and a Prostar 335 photodiode array detector (PDA), with data collected and analyzed using Galaxie Chromatography Workstation software (version 1.9.3.2, Varian Inc.). Flash chromatography was performed on a Teledyne ISCO CombiFlash Rf 200 using Silica Gold columns (both from Teledyne Isco, Lincoln, NE, USA) and monitored by UV and evaporative light-scattering detectors.

Fungal Strain Isolation and Identification. Mycosynthetix fungal strain MSX45109 was isolated from plant material collected in a mangrove habitat in 1989. Morphological examination of cultures suggested that MSX45109 was not a pure culture, but a mixture of two morphologically different strains. Molecular techniques were used

to identify these strains by sequencing the internal transcribed spacer regions 1 & 2 and 5.8S nrDNA (ITS).⁴⁵ DNA extraction, PCR amplification, sequencing, and phylogenetic analyses were performed as described previously.^{63,81,97-99} BLAST search in GenBank and (http://www.boldsystems.org/index.php/IDS_OpenIdEngine) database, the curated BOLD systems, using ITS rDNA sequences suggested that one strain belonged to the *Aspergillus versicolor* (Eurotiales, Ascomycota), while the other strain belonged to *Setophoma terrestris* (Pleosporales, Ascomycota). Morphological examinations of the culture characteristics corroborated the ITS data. The ITS sequences of the two strains will be deposited in the GenBank (accession no XXX). A voucher culture of two strains of MSX45109 is maintained in the Mycosynthetix Inc., Hillsborough, NC, USA.

Fermentation, Extraction and Isolation. Storage conditions, fermentation, and extraction procedure of the fungal strain MSX45109 were as described previously.^{19,62,63} In brief, a seed culture of strain MSX45109 grown in YESD medium was used to inoculate a 2.8-L Fernbach flask (Corning, Inc., Corning, NY, USA) containing 150 g rice and 300 mL H₂O. The solid culture was incubated at room temperature for 14 days and then extracted by addition of a 500 mL mixture of 1:1 MeOH-CHCl₃. The culture was chopped into small pieces and left to shake at ~125 rpm at room temperature. followed by vacuum filtration. The solid phase was washed with 100 mL of 1:1 MeOH-CHCl₃. To the filtrate, 900 mL CHCl₃ and 1500 mL H₂O were added so that the final ratio of CHCl₃-MeOH-H₂O was 4:1:5. The mixture was mixed by stirring for ½ h and then transferred into a separatory funnel. The organic bottom layer was drawn off and evaporated to dryness and then re-constituted in 100 mL of 1:1 MeOH-CH₃CN and 100

mL of hexanes. The biphasic solution was stirred for 15 min and then transferred to a separatory funnel. The MeOH-CH₃CN layer was drawn off and evaporated to dryness under vacuum. The defatted material (~1.5 g) was dissolved in a mixture of CHCl₃-MeOH, adsorbed onto Celite 545, and fractionated via flash chromatography using a gradient solvent system of hexane-CHCl₃-MeOH at a 40 mL/min flow rate and 53.3 column volumes over 63.9 min to afford five fractions. Fraction 3 (~627 mg) was subjected to preparative reversed phase HPLC over a Phenomenex Gemini-NX C₁₈ preparative column using a gradient system of 40:60 to 60:40 over 30 min of CH₃CN-H₂O (acidified with 0.1% formic acid) at a flow rate of 21.24 mL/min to yield thirteenth sub-fractions. Sub-fractions 4, 5, 10, and 12 yielded compounds **11** (4.24 mg), **12** (19.58 mg), **1** (35.10), and **2** (48.40 mg), which eluted at 7.8, 8.7, 25.1, and 29.0 min, respectively. The other sub-fractions were subjected to further purifications as follows: sub-fraction 1 (2.34 mg) was subjected to semi-preparative HPLC purification over a Phenomenex Gemini-NX C₁₈ column using a gradient system of 50:50 to 70:30 of MeOH-H₂O (acidified with 0.1% formic acid) over 15 min at a flow rate of 4.72 mL/min to yield compound **16** (0.79 mg), which eluted at ~13.1 min. Sub-fraction 6 (8.54 mg) was subjected to preparative HPLC purification using a Phenomenex Gemini-NX C₁₈ and a gradient system of 50:50 to 70:30 of MeOH-H₂O (acidified with 0.1% formic acid) over 15 min at a flow rate of 21.24 mL/min to yield compounds **15** (1.68 mg) and **13** (3.68 mg), which eluted at ~8.0 and ~18.9 min, respectively. Sub-fraction 7 (1.49 mg) was subjected to semipreparative HPLC purification using a Phenomenex Gemini-NX C₁₈ column and a gradient system of 50:50 to 70:30 of MeOH-H₂O (acidified with 0.1%

formic acid) over 15 min at a flow rate of 4.72 mL/min to yield compound **6** (0.75 mg), which eluted at ~17.5 min. Sub-fraction 9 (18.23 mg) was subjected to preparative HPLC purification using a Phenomenex Gemini-NX C₁₈ and a gradient system of 50:50 to 70:30 of MeOH-H₂O (acidified with 0.1% formic acid) over 15 min at a flow rate of 21.24 mL/min to yield compounds **7** (5.36 mg), **8** (1.02), and **14** (2.71 mg), which eluted at ~11.6, ~13.5 and ~19.5 min, respectively. An aliquot of sub-fraction 10 (~20 mg) was further purified using preparative HPLC over a Phenomenex Gemini-NX C₁₈ utilizing a gradient solvent system of 70:30 to 90:10 of MeOH-H₂O (acidified with 0.1% formic acid) over 15 min at a flow rate of 21.24 mL/min to yield compounds **10** (0.63 mg) and **1** (3.11 mg), which eluted at ~9.5 and ~14.8 min, respectively. An aliquot of sub-fraction 11 (~20 mg) was subjected to semi-preparative HPLC purification over a Phenomenex Gemini-NX C₁₈ column using a gradient system of 70:30 to 90:10 of MeOH-H₂O (acidified with 0.1% formic acid) over 15 min at a flow rate of 4.72 mL/min to yield compound **3** (9.49 mg), which eluted at ~12.3 min and compound **9** (1.07 mg) that was obtained by further purification of sub-fraction 1. Sub-fraction 13 (21.49 mg) was subjected to preparative HPLC purification using a Phenomenex Gemini-NX C₁₈ and a gradient system of 70:30 to 90:10 of MeOH-H₂O (acidified with 0.1% formic acid) over 15 min at a flow rate of 21.24 mL/min to yield compounds **2** (2.85 mg) and **4** (5.39 mg), which eluted at ~10.5 and ~19.9 min, respectively, and compound **5** (2.05 mg), which obtained by further purification of sub-fraction 2.

Penicillixanthone B (5): Yellow powder; $[\alpha]_D^{20} = -112^\circ$ ($c = 0.03$ in acetone); UV (MeOH) λ_{\max} (log ϵ) 349 (3.64), 336 (3.63), 250 (3.58) nm; CD ($c 6.26 \times 10^{-5}$ M,

CHCl₃) λ ($\Delta\epsilon$) 225 (-55.3) nm, 243 (+48.4) nm, 332 (-18.9) nm; 347 (+2.6) nm, 376 (-8.8) nm; ¹H NMR (CDCl₃, 500 MHz) and ¹³C NMR (CDCl₃, 125 MHz), see Table 12 and Supplementary Figure 55; HRESIMS m/z 639.1691 [M + H]⁺ (calcd for C₃₂H₃₁O₁₄ 639.1708).

Blennolide H (6): Yellow gum; $[\alpha]_D^{20} = -25.3^\circ$ ($c = 0.01$ in chloroform); UV (MeOH) λ_{\max} (log ϵ) 283 (3.48), 193 (3.68) nm; CD ($c 4.27 \times 10^{-4}$ M, CHCl₃) λ ($\Delta\epsilon$) 231 (+11.9) nm, 269 (-20.9) nm, 298 (-19.8) nm; ¹H NMR (CDCl₃, 500 MHz) and ¹³C NMR (CDCl₃, 175 MHz), see Table 13 and Supplementary Figure 56; HRESIMS m/z 305.1012 [M + H]⁺ (calcd for C₁₆H₁₇O₆ 305.1020).

11-Deoxyblennolide D (7): Colorless oil; $[\alpha]_D^{20} = -26.14^\circ$ ($c = 0.03$ in chloroform); UV (MeOH) λ_{\max} (log ϵ) 349 (3.21), 270 (3.45), 224 (3.37) nm; CD ($c 1.56 \times 10^{-4}$ M, CHCl₃) λ ($\Delta\epsilon$) 235 (+6.2) nm, 267 (-53.8) nm, 307 (-16.4) nm; 346 (+0.5) nm; ¹H NMR (CDCl₃, 500 MHz) and ¹³C NMR (CDCl₃, 125 MHz), see Table 14 and Supplementary Figure 57; HRESIMS m/z 321.0963 [M + H]⁺ (calcd for C₁₆H₁₇O₇ 321.0969).

Paecilin B (8): Colorless oil; $[\alpha]_D^{20} = +42.05^\circ$ ($c = 0.09$ in chloroform); UV (MeOH) λ_{\max} (log ϵ) 346 (3.20), 271 (3.49), 193 (3.70) nm; CD ($c 5.62 \times 10^{-4}$ M, CHCl₃) λ ($\Delta\epsilon$) 235 (-44.7) nm, 267 (+35.2) nm, 307 (+17.0) nm; 346 (-8.7) nm; ¹H NMR (CDCl₃, 500 MHz) and ¹³C NMR (CDCl₃, 125 MHz), see Table 14 and Supplementary Figure 58; HRESIMS m/z 321.0961 [M + H]⁺ (calcd for C₁₆H₁₇O₇ 321.0969).

Blennolide I (9): Yellow powder; $[\alpha]_{\text{D}}^{20} = -102.30^\circ$ ($c = 0.09$ in chloroform); UV (MeOH) λ_{max} ($\log \epsilon$) 349 (2.81), 258 (3.69), 224 (3.69) nm; CD ($c 6.26 \times 10^{-5}$ M, CHCl_3) λ ($\Delta\epsilon$) 241 (+13.9), 275 (-6.3) nm, 334 (-8.7) nm; ^1H NMR (CDCl_3 , 700 MHz) and ^{13}C NMR (CDCl_3 , 175 MHz), see Table 15 and Supplementary Figure 59; HRESIMS m/z 639.1682 $[\text{M} + \text{H}]^+$ (calcd for $\text{C}_{32}\text{H}_{31}\text{O}_{14}$ 639.1708).

Blennolide J (10): Yellow powder; $[\alpha]_{\text{D}}^{20} = -93.5^\circ$ ($c = 0.08$ in chloroform); UV (MeOH) λ_{max} ($\log \epsilon$) 349 (3.37), 336 (3.37), 237 (3.4) nm; CD ($c 1.72 \times 10^{-4}$ M, CHCl_3) λ ($\Delta\epsilon$) 245 (38.9), 262 (-14.9) nm, 337 (-13.9) nm, 377 (-16.7) nm; ^1H NMR (CDCl_3 , 700 MHz) and ^{13}C NMR (CDCl_3 , 175 MHz), see Table 15 and Supplementary Figure 60; HRESIMS m/z 639.1683 $[\text{M} + \text{H}]^+$ (calcd for $\text{C}_{32}\text{H}_{31}\text{O}_{14}$ 639.1708).

Pyrenomycin (16): Coloreless oil; $[\alpha]_{\text{D}}^{20} = -5.7^\circ$ ($c = 0.05$ in chloroform); UV (MeOH) λ_{max} ($\log \epsilon$) 301 (3.09), 270 (3.12), 233 (3.07) nm; ^1H NMR (Methnol- d_4 , 700 MHz) and ^{13}C NMR (CDCl_3 , 175 MHz), see Table 16 and Supplementary Figure 66; HRESIMS m/z 239.0909 $[\text{M} + \text{H}]^+$ (calcd for $\text{C}_{12}\text{H}_{16}\text{O}_5$ 239.0914).

Preparation of the (R)- and (S)-MTPA ester derivatives of Pyrenomycin (16):

To 0.10 mg of compound **16** was added 400 μL of pyridine- d_5 and transferred into an NMR tube. To initiate the reaction, 20 μL of *S*-(+)- α -methoxy- α -(trifluoromethyl)phenylacetyl (MTPA) chloride was added into the NMR tube with careful shaking and then monitored immediately by ^1H NMR at the following time points: 0, 5, 10, 15, 30, 60, and 120 min. The reaction was found to be complete in 2 h, yielding the mono (*R*)-MTPA ester derivative (**16b**) of **16**. ^1H NMR data of **16b** (500

MHz, pyridine-*d*₅): δ_H 1.85 (3H, d, $J = 7.5$, H₃-13), 1.81 (1H, m, H-12a), 1.90 (1H, m, H-12b), 4.81 (1H, m, H-11), 5.61 (1H, m, H-3). In an analogous manner, 0.10 mg of compound **16** dissolved in 400 μ L pyridine-*d*₅ was reacted in a second NMR tube with 20 μ L (*R*)-(-)- α -MTPA chloride for 1 h, to afford the mono (*S*)-MTPA ester (**6a**). ¹H NMR data of **6a** (500 MHz, pyridine-*d*₅): δ_H 1.75 (3H, d, $J = 6.9$, H₃-13), 1.70 (1H, m, H-12a), 1.80 (1H, m, H-12b), 4.85 (1H, m, H-11), 5.65 (1H, m, H-3).

Cytotoxicity Assay. The cytotoxicity of compounds (**1-15**) were tested against the MDA-MB-435¹⁰⁰ human melanoma (HTB-129, ATCC) and the SW-620¹⁰¹ human colorectal adenocarcinoma (CCL-227, ATCC) cell lines as described previously.¹⁹

Antimicrobial Assay. Minimal inhibitory concentrations (MICs) of compounds (**1-15**) were measured against a panel of bacteria and fungi as described previously.^{18,102,103} All measurements were made in duplicate.

Supporting Information

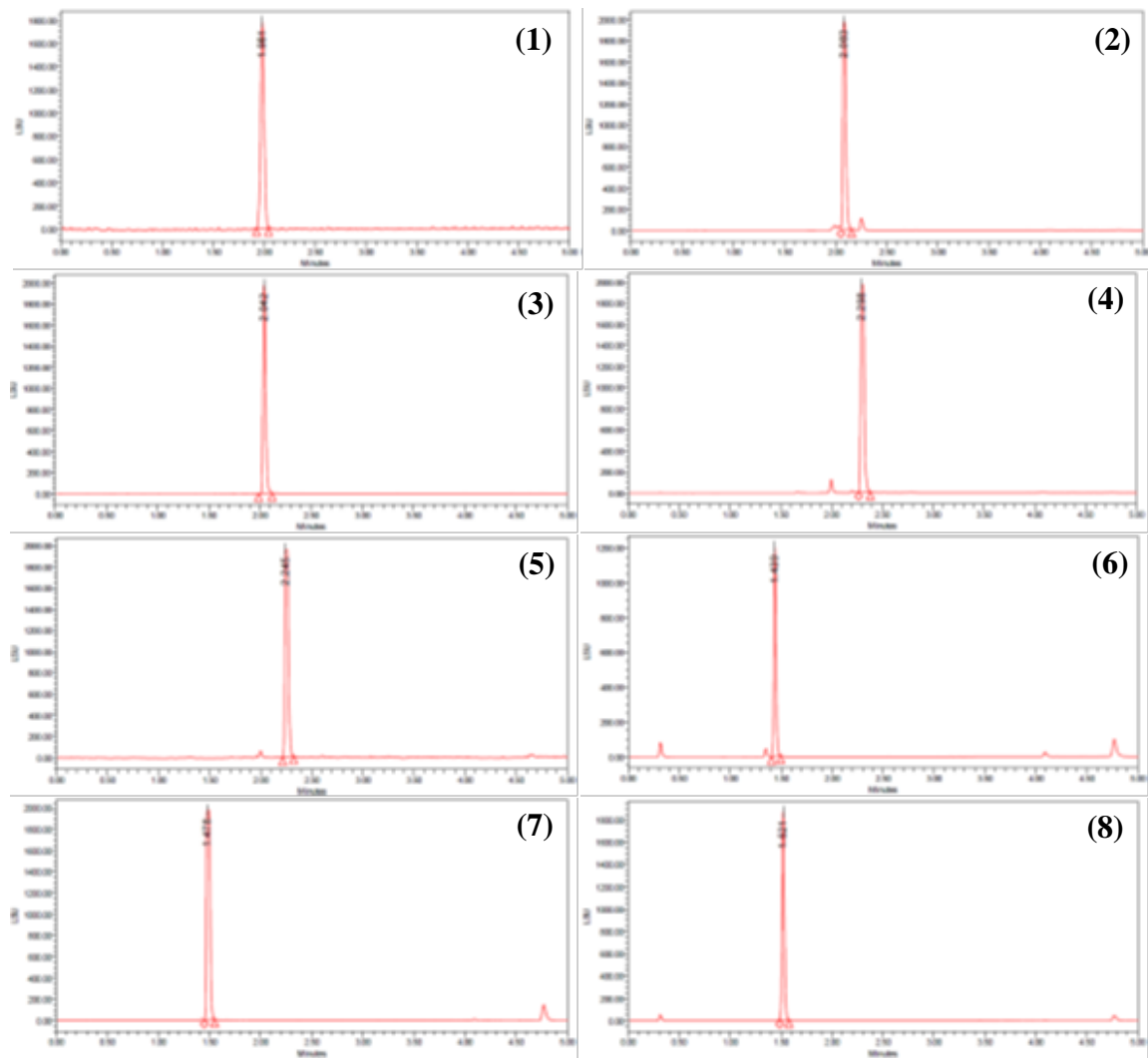


Figure 49. UPLC chromatograms of compounds **1-16** (ELSD detection), demonstrating >90% purity. All data were acquired via an Acquity UPLC system with a BEH C₁₈ (1.7 μ m 2.1 \times 50 mm) column and a CH₃CN-H₂O gradient that increased linearly from 20 to 100% CH₃CN over 4.5 min.

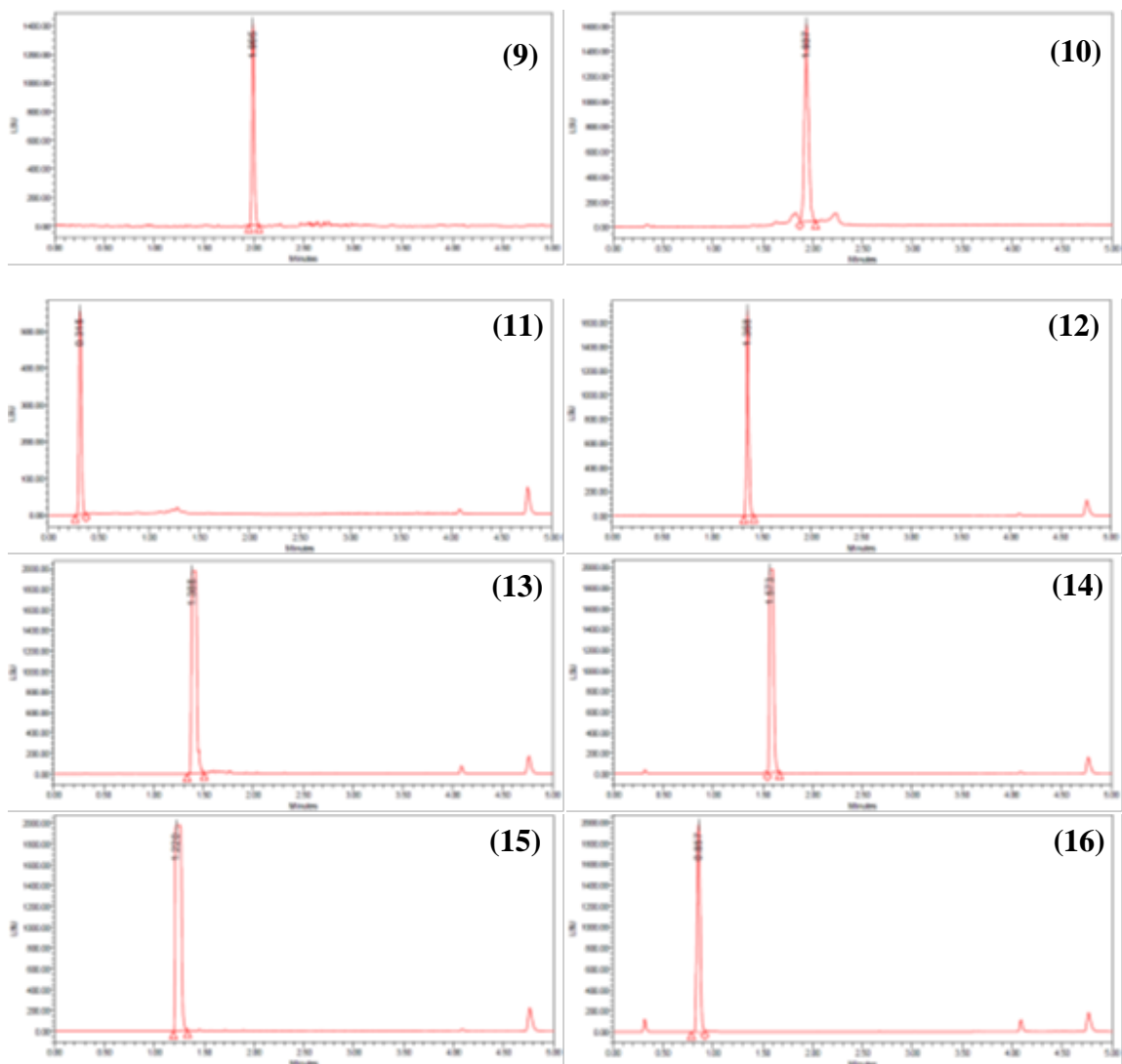


Figure 49 (continued). UPLC chromatograms of compounds **1-16** (ELSD detection), demonstrating >90% purity. All data were acquired via an Acquity UPLC system with a BEH C₁₈ (1.7 μm 2.1 × 50 mm) column and a CH₃CN-H₂O gradient that increased linearly from 20 to 100% CH₃CN over 4.5 min.

Table 19. ^1H NMR Data for 1-3 (500 MHz; Chemical Shifts in δ , Coupling Constants in Hz, CDCl_3)

position	δ_{H} mult (J in Hz)		
	1	2	3
3	7.45, d (8.6)	7.42, d (8.6)	7.42, d (8.6)
4	6.63, d (8.6)	6.57, d (8.6)	6.57, d (8.6)
5	3.92, dd (11.2, 0.5)	4.11, d (1.2)	4.11, s
6	2.41, m	2.10, m	2.10, m
7	2.31, dd (19.2, 10.7)	2.40, dd (18.9, 6.3)	2.40, dd (18.9, 6.3)
	2.73, dd (19.2, 6.4)	2.52, dd (18.9, 11.4)	2.52, dd (18.9, 11.5)
11	1.17, d, (6.4)	1.17, d, (6.9)	1.17, d, (6.9)
13	3.72, s	3.72, s	3.72, s
1-OH	11.76	11.87	11.88
5-OH	2.81, d (2.7)	2.60, brs	2.57, s
8-OH	13.78		
3'	7.45, d (8.6)	7.42, d (8.6)	7.45, d (8.6)
4'	6.63, d (8.6)	6.57, d (8.6)	6.62, d (8.6)
5'	3.92, dd (11.2, 0.5)	4.11, d (1.2)	3.92, dd (11.5, 0.5)
6'	2.41, m	2.10, m	2.41, m
7'	2.31, dd (19.2, 10.7)	2.40, dd (18.9, 6.3)	2.31, dd (18.9, 10.9)
	2.73, dd (19.2, 6.4)	2.52, dd (18.9, 11.4)	2.73, dd (18.9, 6.3)
11'	1.17, d, (6.4)	1.17, d, (6.9)	1.17, d, (6.3)
13'	3.72, s	3.72, s	3.72, s
1'-OH	11.76	11.87	11.74
5'-OH	2.81, d (2.7)	2.60, brs	2.84, s
8'-OH	13.78	---	---

Table 20. CD and Optical Rotation Data, Experimental vs. Literature, of Compounds 1-4, 8-9, and Blennolide G

compound	CD: Conc. Solvent; λ_{\max} ($\Delta\epsilon$) nm		Optical rotation	
	Experimental	Literature	Experimental	Literature
Secalonic acid A (1)	0.03×10^{-3} M, CHCl ₃ 332 (-38.8)	CHCl ₃ 334 (~ -8) ¹⁴⁵	$[\alpha]_D^{25} = -61^\circ$ (c = 0.38, Chloroform)	$[\alpha]_D^{20} = -76^\circ$ (chloroform). ¹⁴⁶ $[\alpha]_D^{20} = -177^\circ$ (pyridine). ¹⁴⁶
Secalonic acid E (2)	0.03×10^{-3} M, CHCl ₃ 332 (-24.6)	----	$[\alpha]_D^{25} = -108^\circ$ (c = 0.04, Chloroform)	$[\alpha]_D^{22} = -212^\circ$ (c = 0.41, pyridine). ¹²⁰ $[\alpha]_D^{25} = -106.9^\circ$ (c = 1.055, Chloroform). ¹²¹
Secalonic acid G (3)	0.03×10^{-3} M, CHCl ₃ 332 (-31.2)	----	$[\alpha]_D^{25} = -73^\circ$ (c = 0.6, Chloroform)	$[\alpha]_D = -201.6^\circ$ (c = 1.105, pyridine). ¹³⁰ $[\alpha]_D^{25} = -2.201^\circ$ (c = 0.25, Acetone). ¹²⁶ $[\alpha]_D^{20} = -110.9^\circ$ (c = 0.289, pyridine). ¹²⁷
Penicillixanthone A (4)	0.05×10^{-3} M, CHCl ₃ 331 (-24.7), 322 (-24.9)	dioxane 330 (~ -15) ¹²⁷	$[\alpha]_D^{26} = -16^\circ$ (c = 0.4, Acetone)	
Paecilin B (8)	0.56×10^{-4} M, CHCl ₃ 235 (-44.7), 267 (+35.2), 307 (+17.0); 346 (-8.7)	----	$[\alpha]_D^{20} = +42^\circ$ (c = 0.09, Chloroform)	$[\alpha]_D^{25} = +40.6^\circ$ (c = 0.1, chloroform). ¹²⁸
Blennolide I (9)	6.26×10^{-5} M 334 (-8.7), 275 (-6.3) 241 (+13.9)	---	$[\alpha]_D^{20} = -102^\circ$ (c = 0.09, Chloroform)	----
Blennolide G	----	6.2×10^{-3} M 379 (+2.4), 361 (+3.4), 333 (+4.4), 279 (+2.3), 274 (+2.3), 224 (-19.4) ¹¹⁴	----	$[\alpha]_D^{25} = +81.1^\circ$ (c = 0.29, Chloroform). ¹¹⁴

Table 21. NMR Data for 4 (500 MHz for ^1H , 125 MHz for ^{13}C ; Chemical Shifts in δ , Coupling Constants in Hz, CDCl_3)

position	δ_{C}	δ_{H} mult (J in Hz)	position	δ_{C}	δ_{H} mult (J in Hz)
1	159.5		1'	161.9	
2	118.2		2'	110.6	6.60, d (8.6)
3	140.7	7.80, d (8.6)	3'	140.9	7.48, d (8.6)
4	107.6	6.61, d (8.6)	4'	115.6	
4a	158.5		4a'	155.5	
5	77.1	3.93, dd (11.5, 0.6)	5'	76.8	3.82, d (11.5, 0.6)
6	29.5	2.40, m	6'	29.3	2.40, m
7	36.4	2.29, m	7'	36.4	2.29, m
		2.72, m			2.72, m
8	177.5		8'	177.9	
8a	101.9		8'a	101.7	
9	187.3		9'	187.4	
9a	107.3		9'a	107.2	
10a	85.2		10'a	85.1	
11	18.3	1.17, d (6.3)	11'	18.2	1.10, d (6.3)
12	170.5		12'	170.3	
13	53.5	3.72, s	13'	53.4	3.68, s
1-OH		11.64, s	1'-OH		11.39, s
5-OH		2.85, brs	5'-OH		2.61, brs

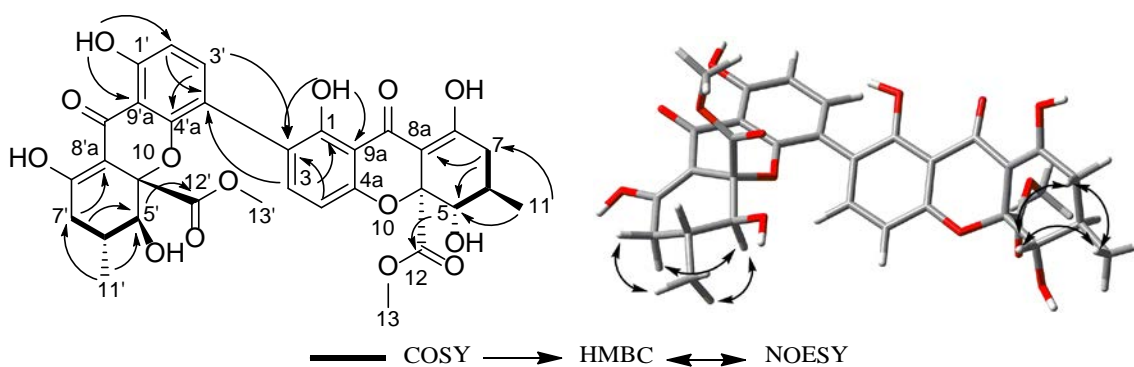


Figure 50. Key HMBC, COSY, and NOESY correlations of 4.

Table 22. NMR Data for 8 and Paecilin B (500 MHz for ^1H , 125 MHz for ^{13}C ; Chemical Shifts in δ , Coupling Constants in Hz, CDCl_3)

Position	8		paecilin B ^a	
	δ_{C} , type	δ_{H} mult (<i>J</i> in Hz)	δ_{C} , type	δ_{H} mult (<i>J</i> in Hz)
2	84.3		84.87	
3	40.7	3.07, d (17.2) 3.48, d (17.2)	39.98	3.53, d (17.4) 3.16, d (17.4)
4	194.9		195.00	
4a	107.5		130.42	
5	161.9		161.89	
6	110.6	6.54, dd (8.6, 0.6)	109.77	6.61, d (8.1)
7	139.0	7.40, t (8.6)	138.97	7.46, t (8.4, 8.3)
8	107.5	6.49, dd (8.6, 0.6)	107.80	6.51, d (7.8)
8a	159.3		155.38	
9	86.5	4.36, dd (3.4, 0.6)	82.63	4.97, d (6.6)
10	29.7	2.85, m	33.58	2.87, m
11	36.4	2.21, dd (17.8, 4.6) 3.01, dd (17.8, 9.2)	36.8	2.73, dd (17, 7) 2.41, dd (17, 7)
12	175.7		174.66	
13	20.7	1.18, d (6.9)	14.63	1.34, d (6.9)
14	169.2		169.30	
15	53.7	3.74, s	53.10	3.72, s
5-OH		11.45, s		11.49, br s

^aZ. Y. Guo, Z. G. She, C. L. Shao, L. Wen, F. Liu, Z. H. Zheng and Y. C. Lin, *Magn. Reson. Chem.* **2007**, *45*, 777-780.

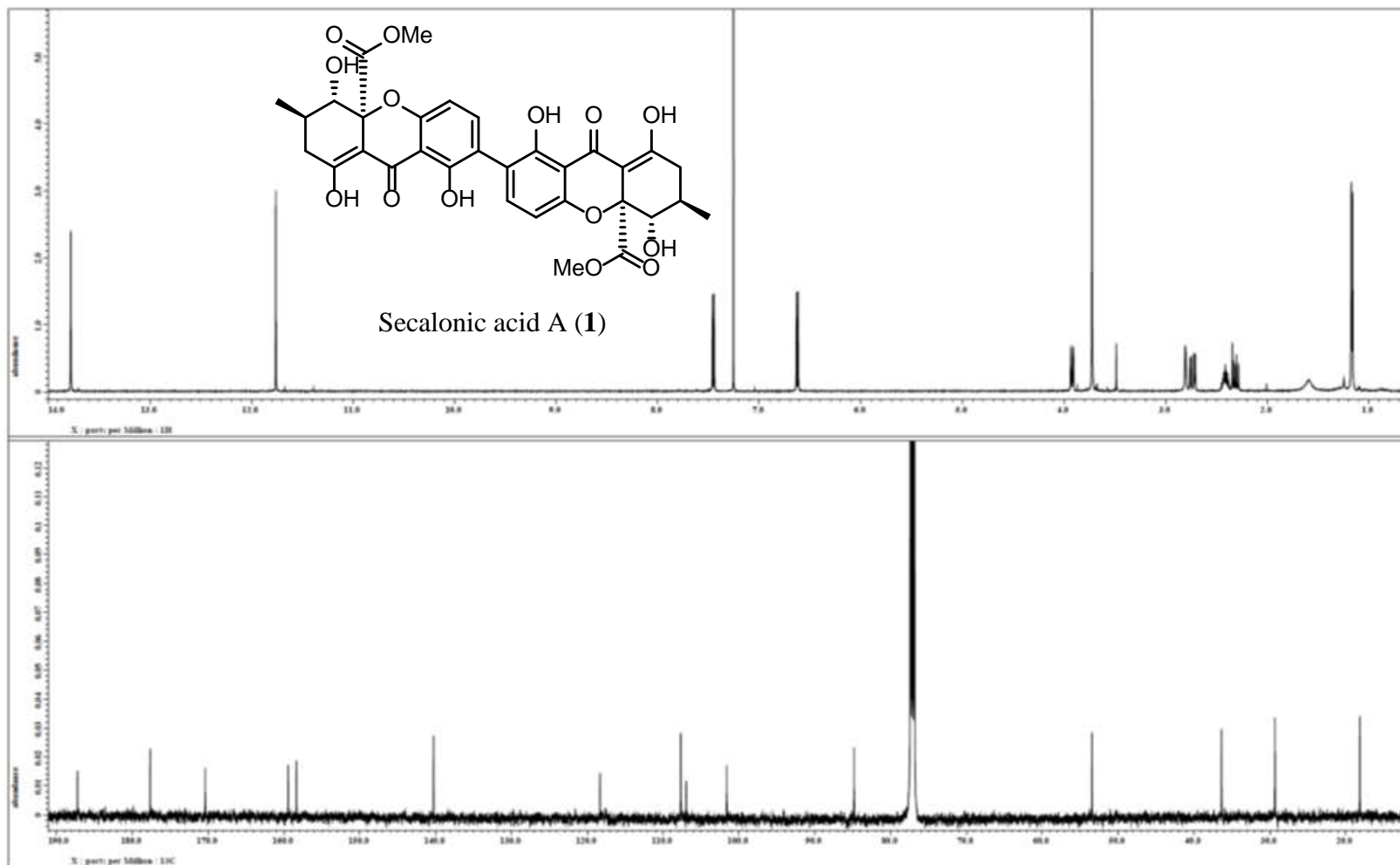


Figure 51. ^1H and ^{13}C NMR spectra of compound 1 [500 MHz for ^1H and 125 MHz for ^{13}C , CDCl_3].

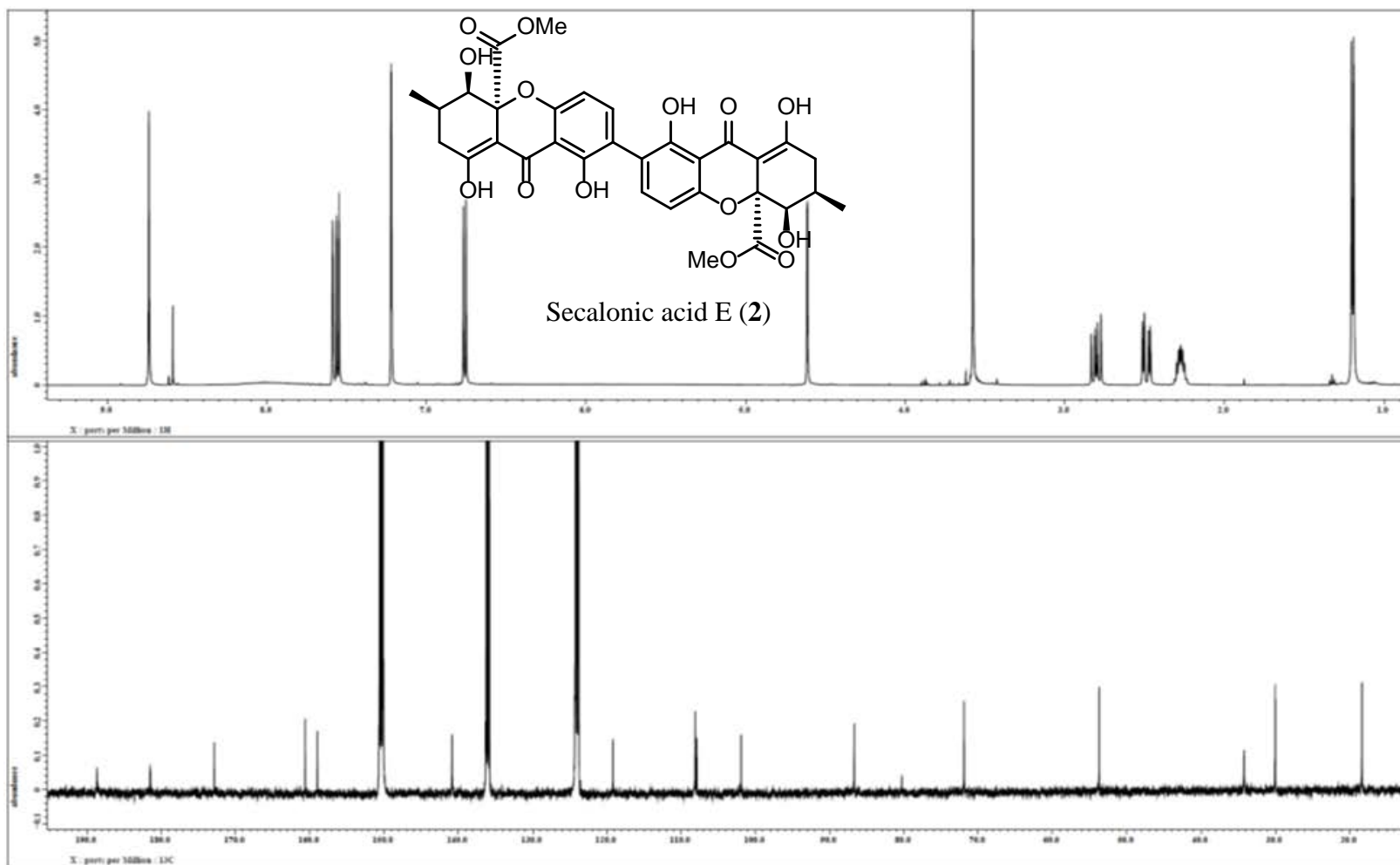


Figure 52. ^1H and ^{13}C NMR spectra of compound 2 [500 MHz for ^1H and 125 MHz for ^{13}C , pyridine- d_5].

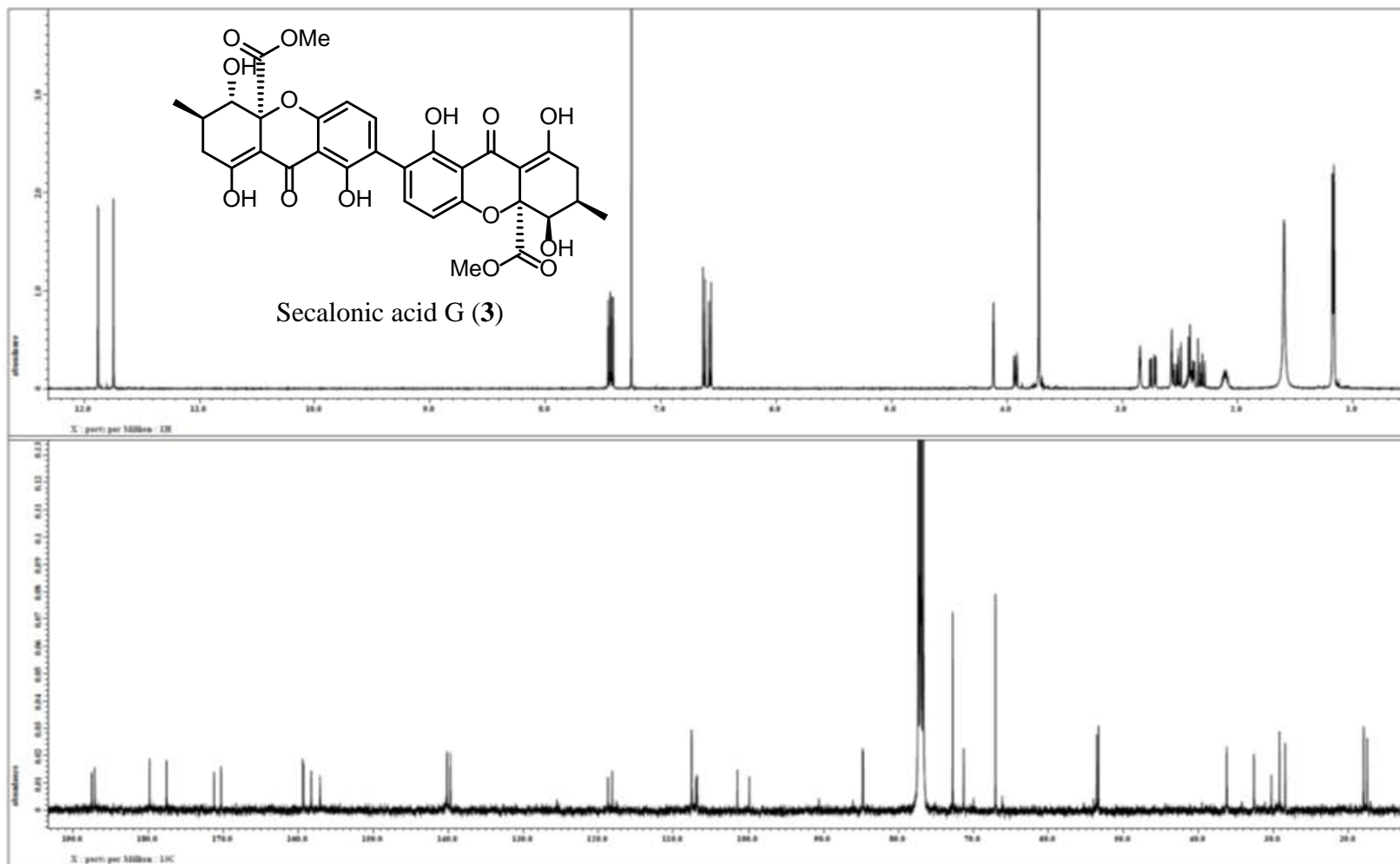


Figure 53. ^1H and ^{13}C NMR spectra of compound 3 [500 MHz for ^1H and 100 MHz for ^{13}C , CDCl_3].

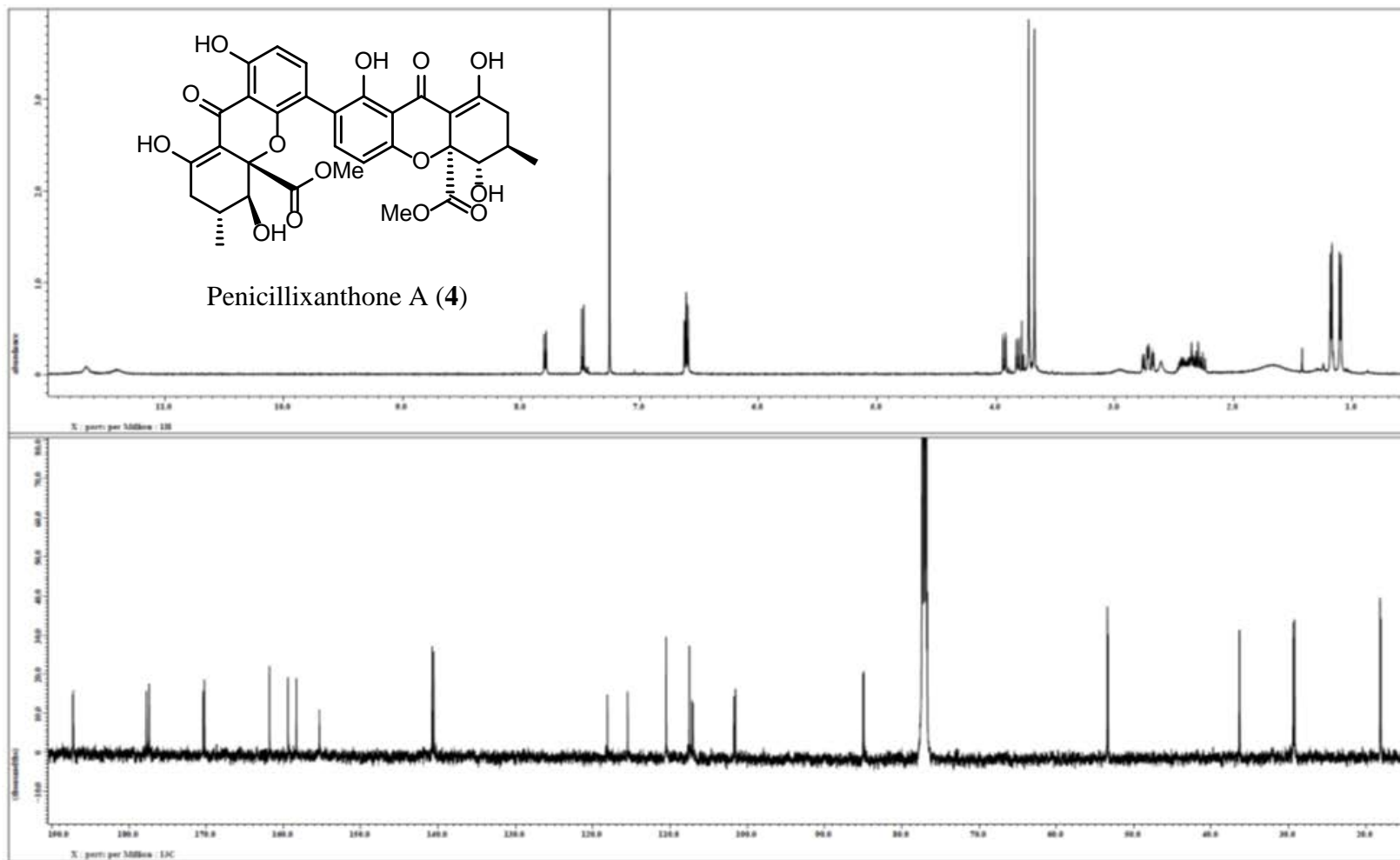


Figure 54. ^1H and ^{13}C NMR spectra of compound 4 [500 MHz for ^1H and 100 MHz for ^{13}C , CDCl_3].

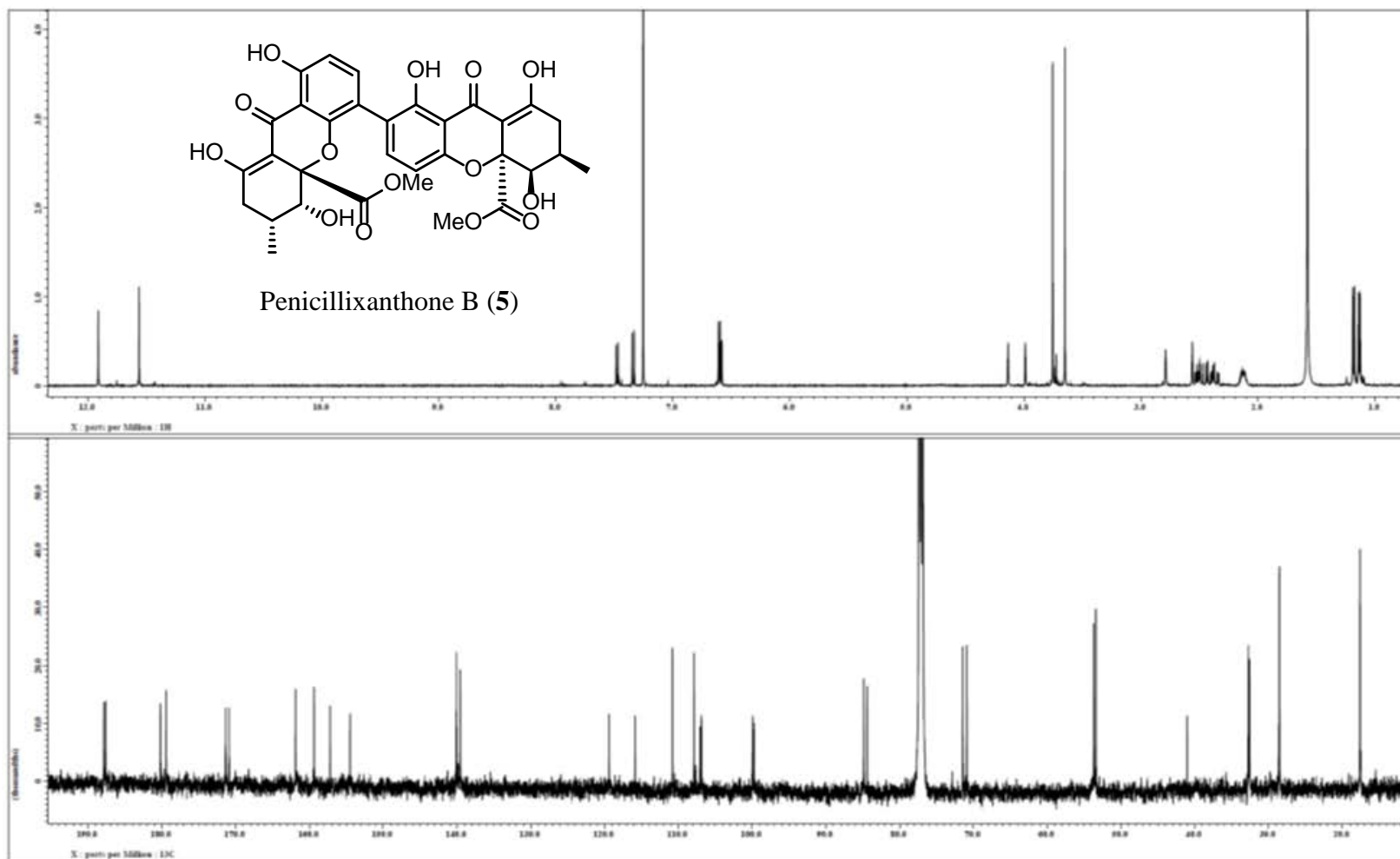


Figure 55. ^1H and ^{13}C NMR spectra of compound 5 [500 MHz for ^1H and 100 MHz for ^{13}C , CDCl_3].

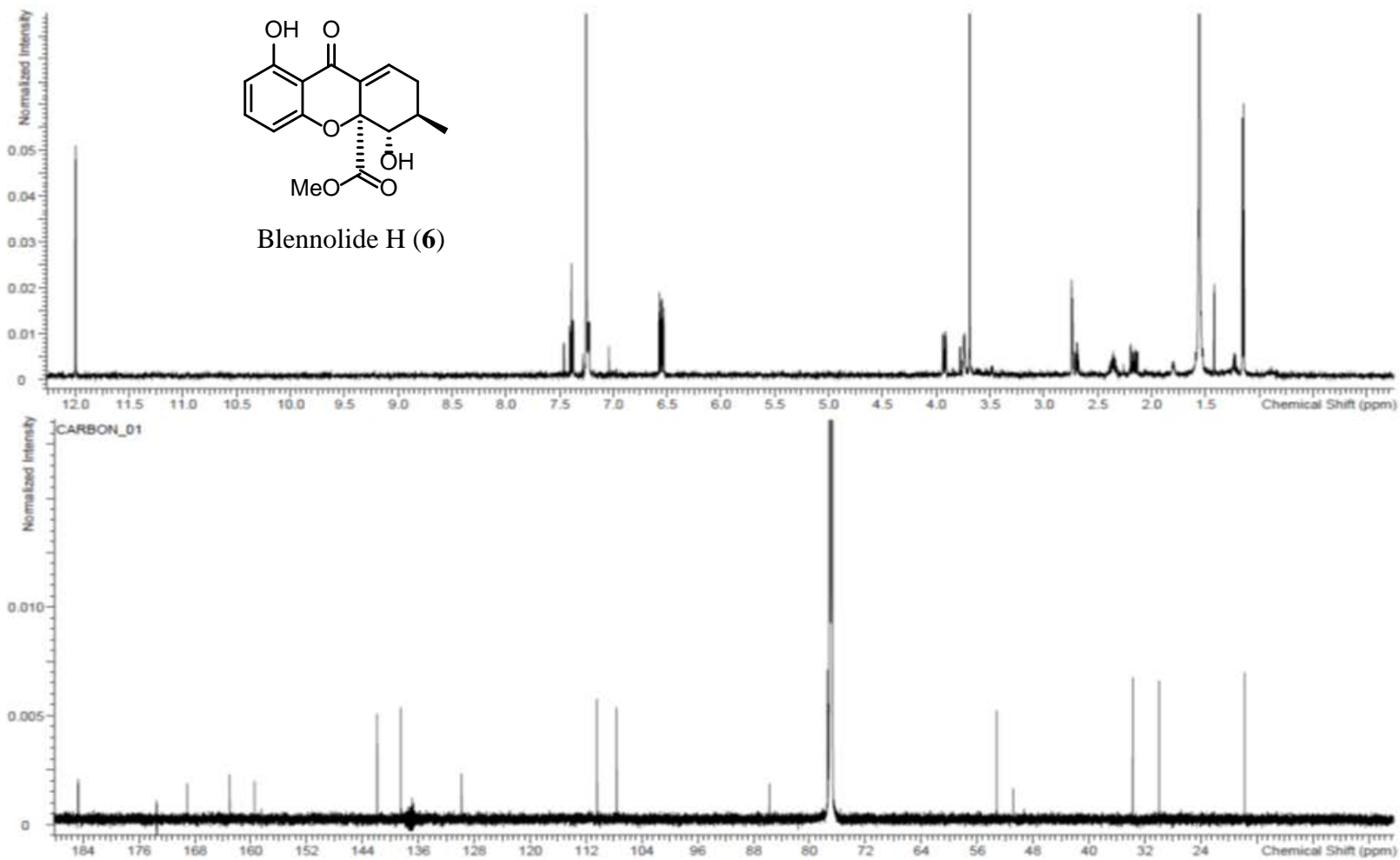


Figure 56. ¹H and ¹³C NMR spectra of compound 6 [500 MHz for ¹H and 175 MHz for ¹³C, CDCl₃].

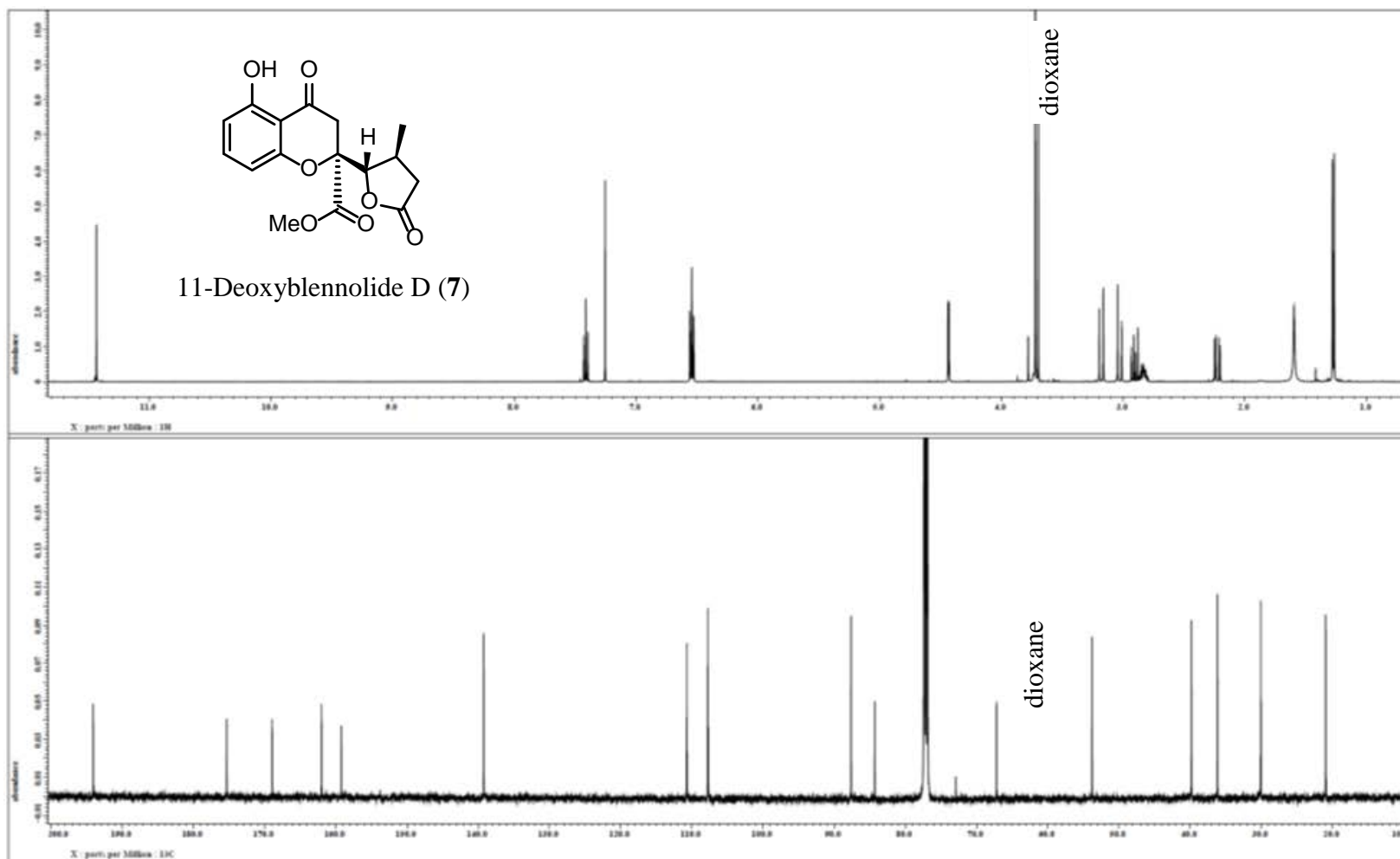


Figure 57. ^1H and ^{13}C NMR spectra of compound 7 [500 MHz for ^1H and 125 MHz for ^{13}C , CDCl_3].

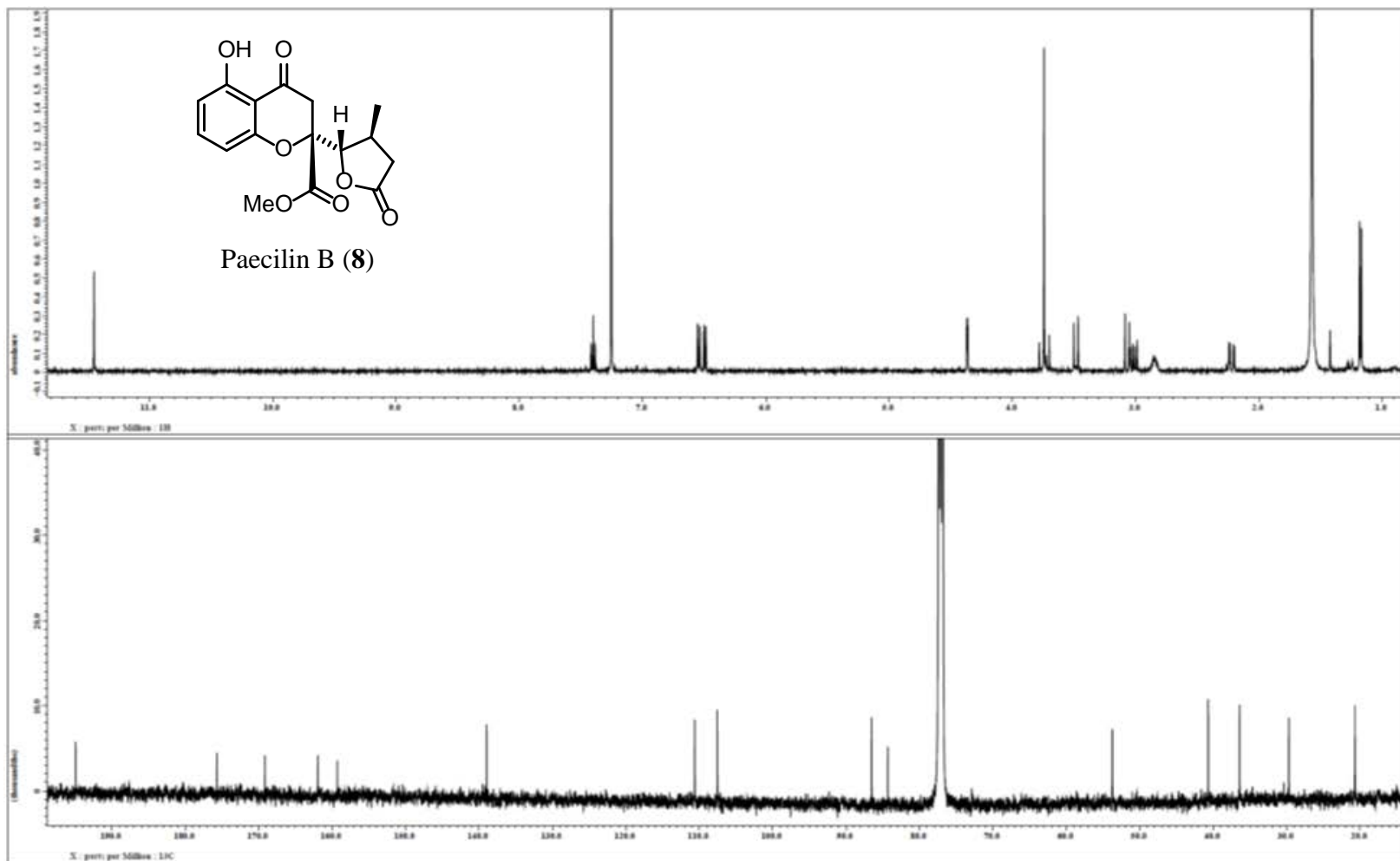


Figure 58. ^1H and ^{13}C NMR spectra of compound **8** [500 MHz for ^1H and 125 MHz for ^{13}C , CDCl_3].

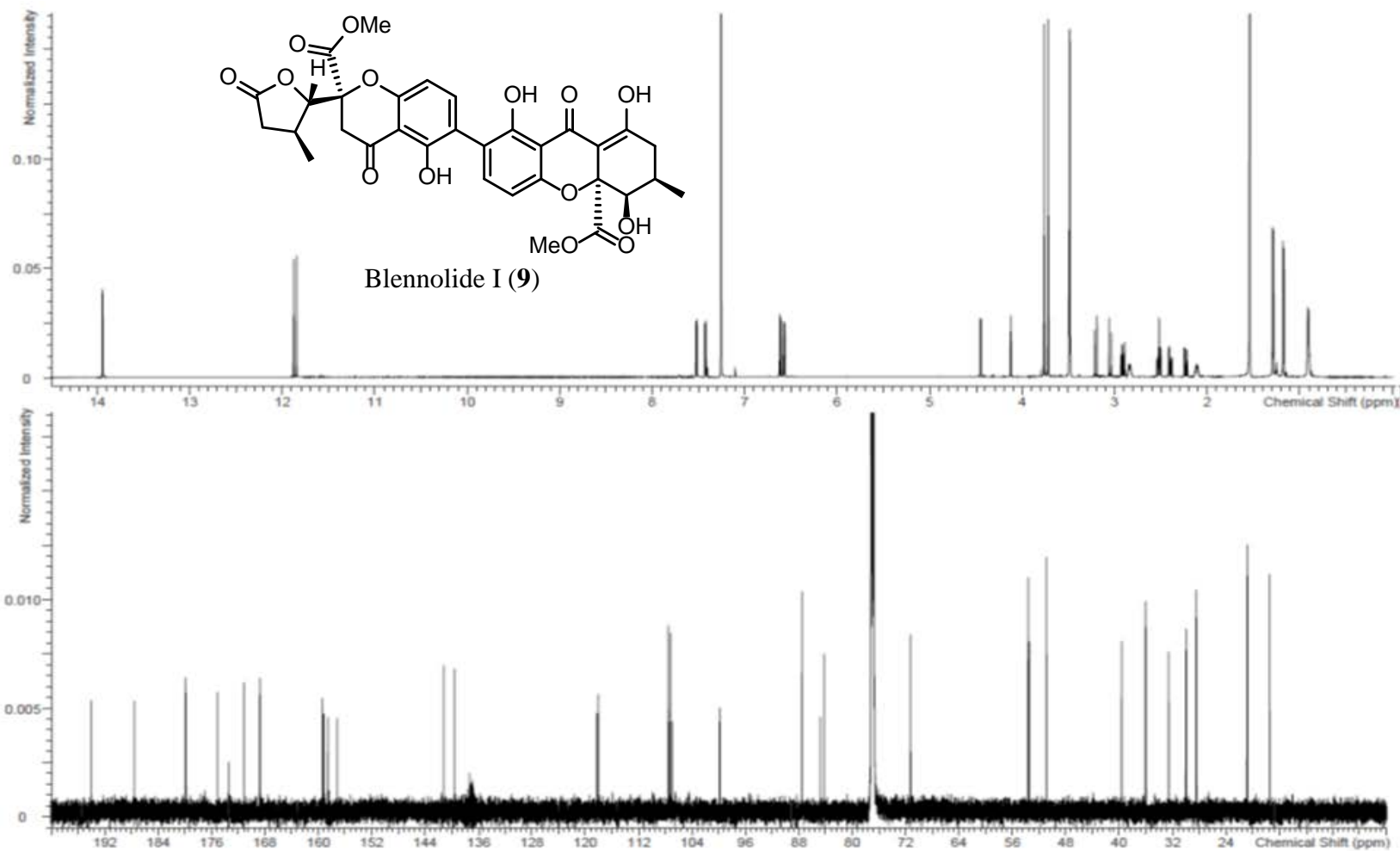


Figure 59. ^1H and ^{13}C NMR spectra of compound **9** [700 MHz for ^1H and 175 MHz for ^{13}C , CDCl₃].

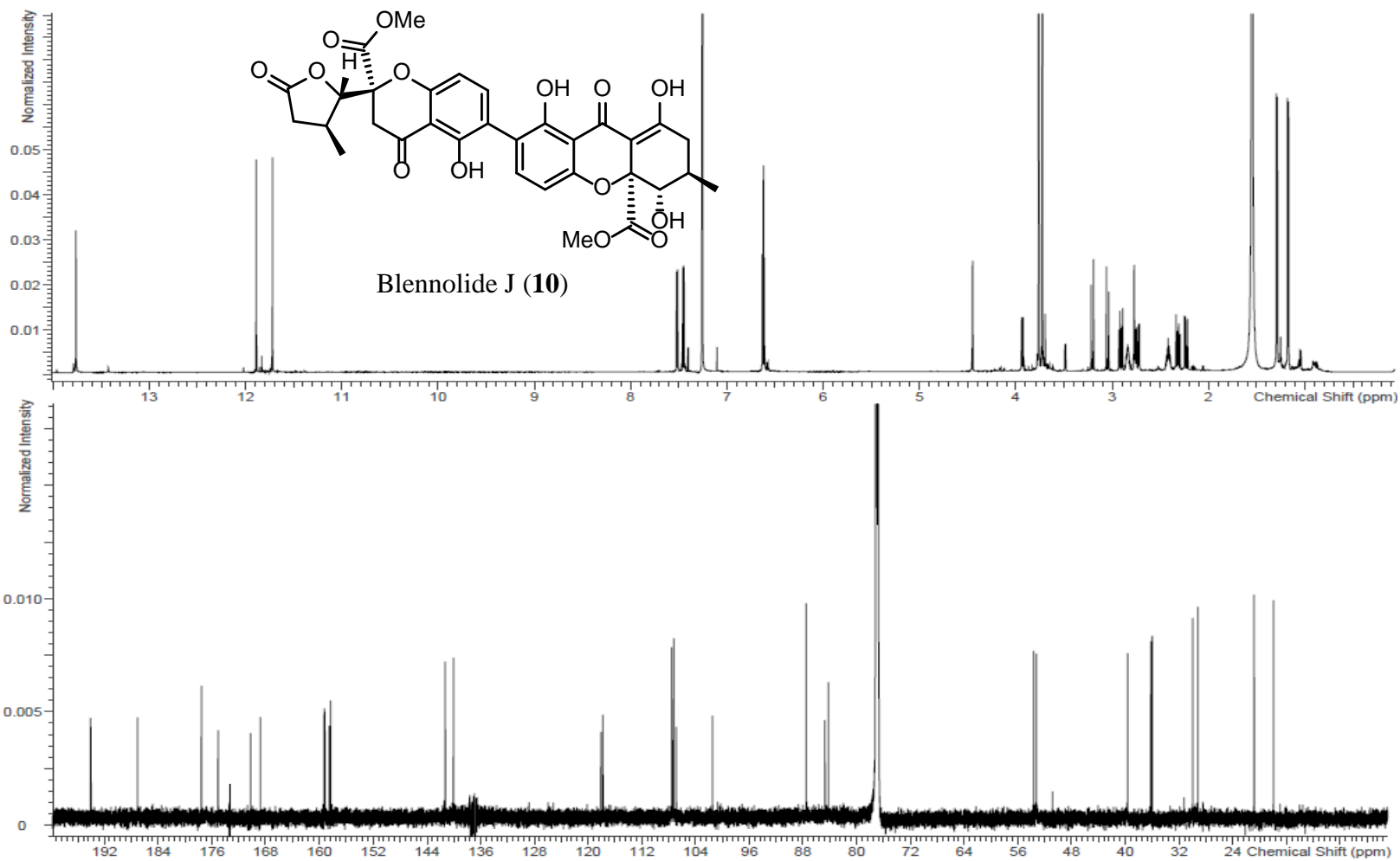


Figure 60. ¹H and ¹³C NMR spectra of compound **10** [700 MHz for ¹H and 175 MHz for ¹³C, CDCl₃].

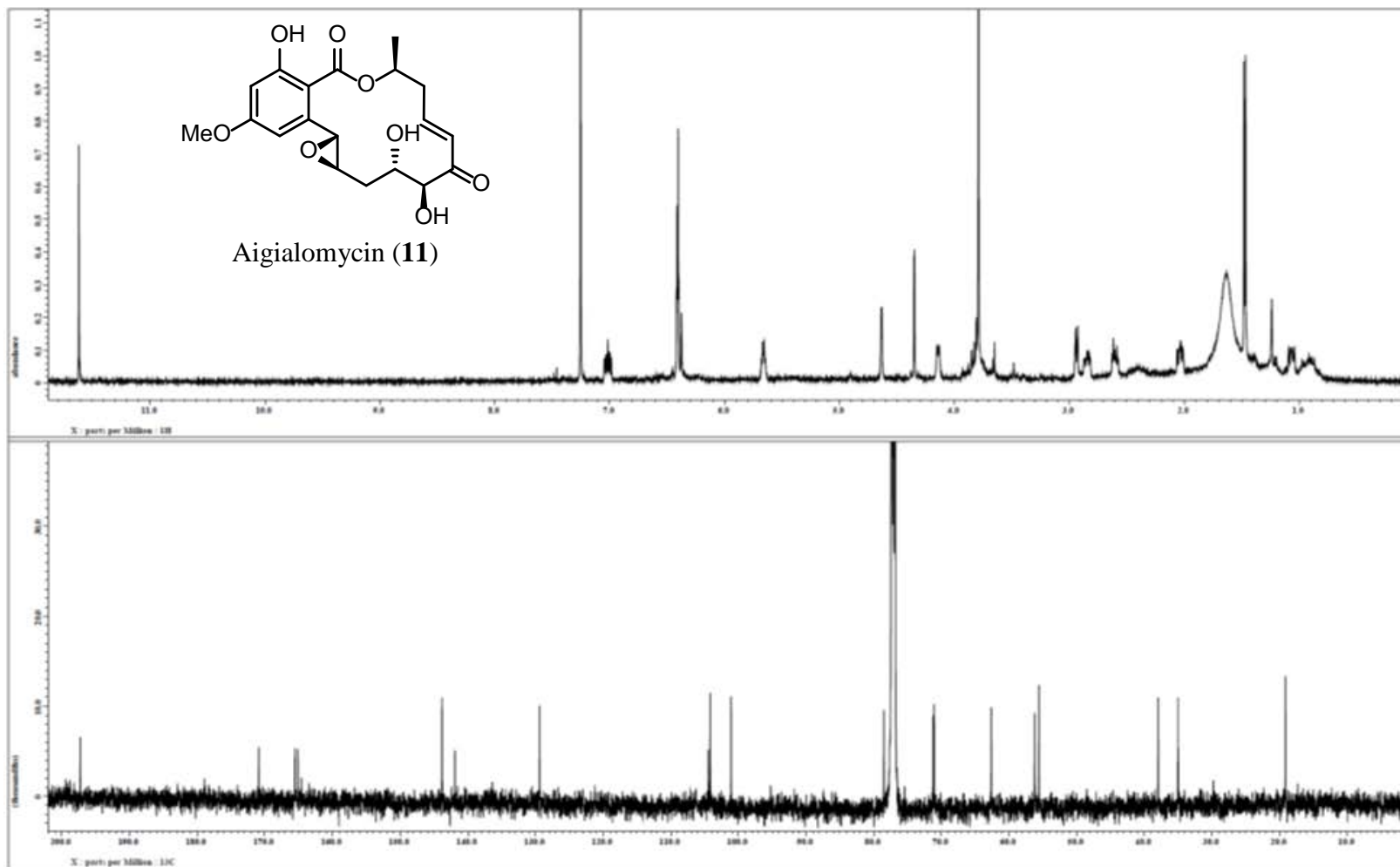


Figure 61. ^1H and ^{13}C NMR spectra of compound **11** [500 MHz for ^1H and 125 MHz for ^{13}C , CDCl_3].

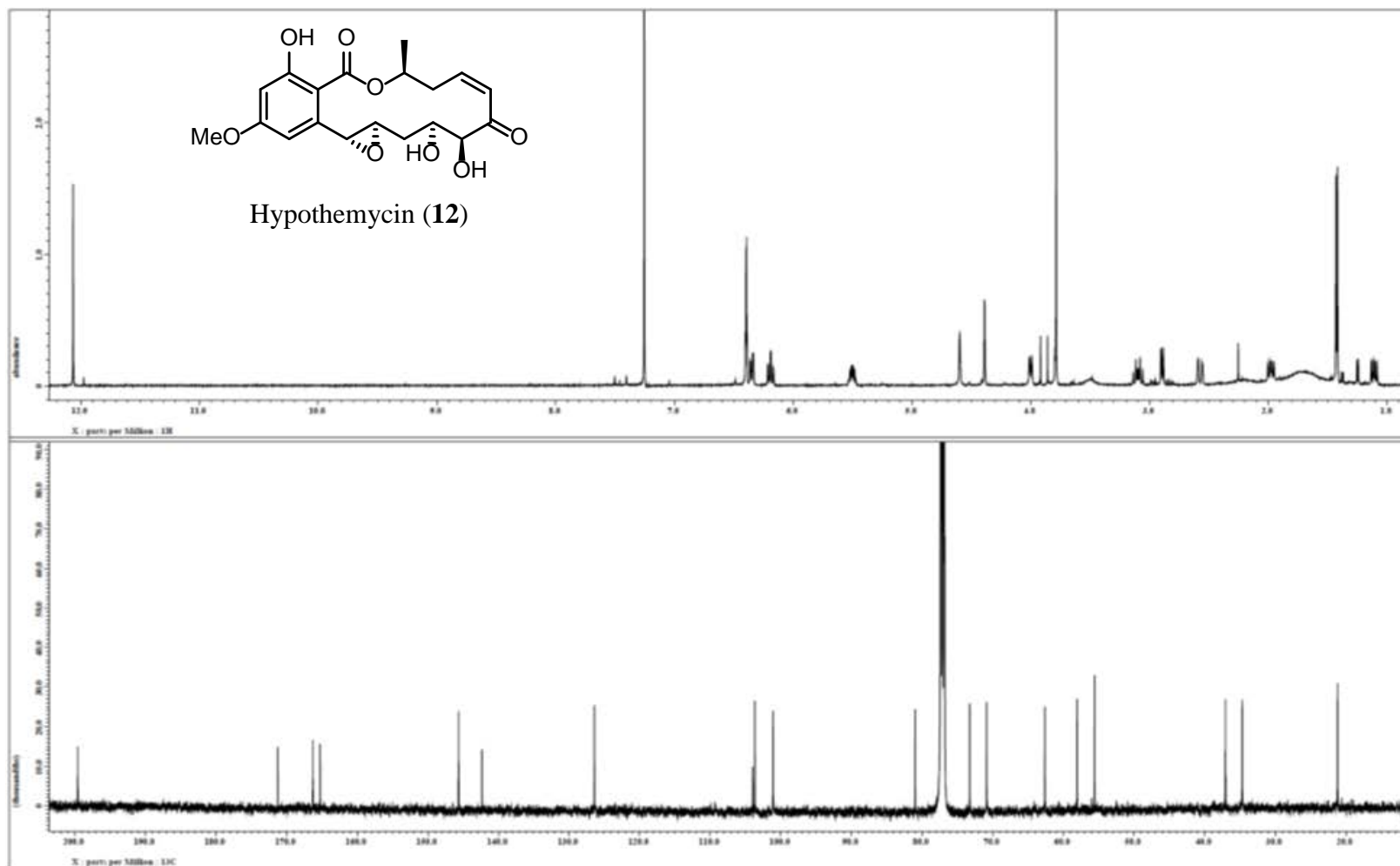


Figure 62. ^1H and ^{13}C NMR spectra of compound **12** [500 MHz for ^1H and 125 MHz for ^{13}C , CDCl_3].

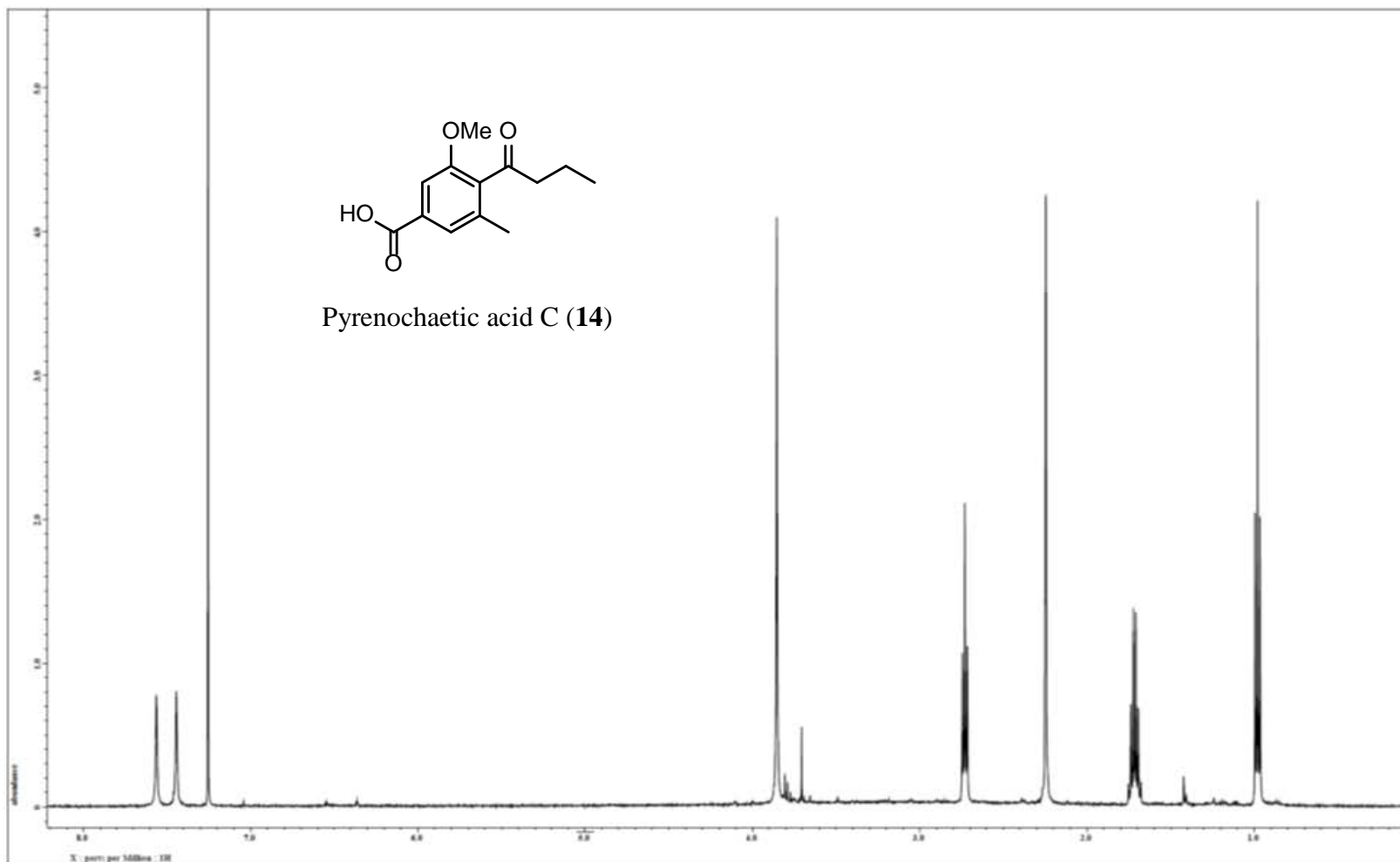


Figure 64. ¹H NMR spectrum of compound **14** [500 MHz, CDCl₃].

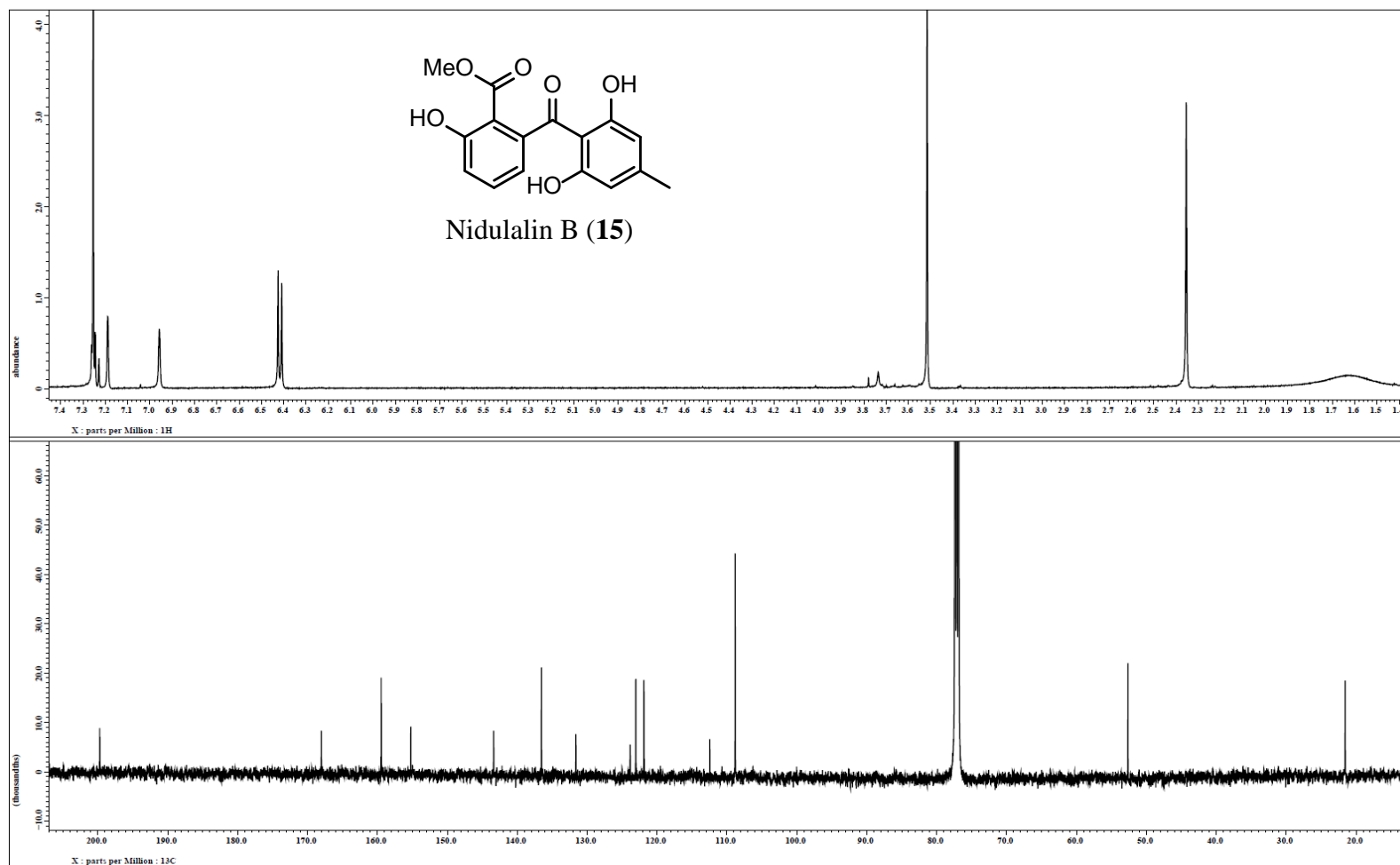


Figure 65. ^1H and ^{13}C NMR spectra of compound **15** [500 MHz for ^1H and 125 MHz for ^{13}C , CDCl_3].

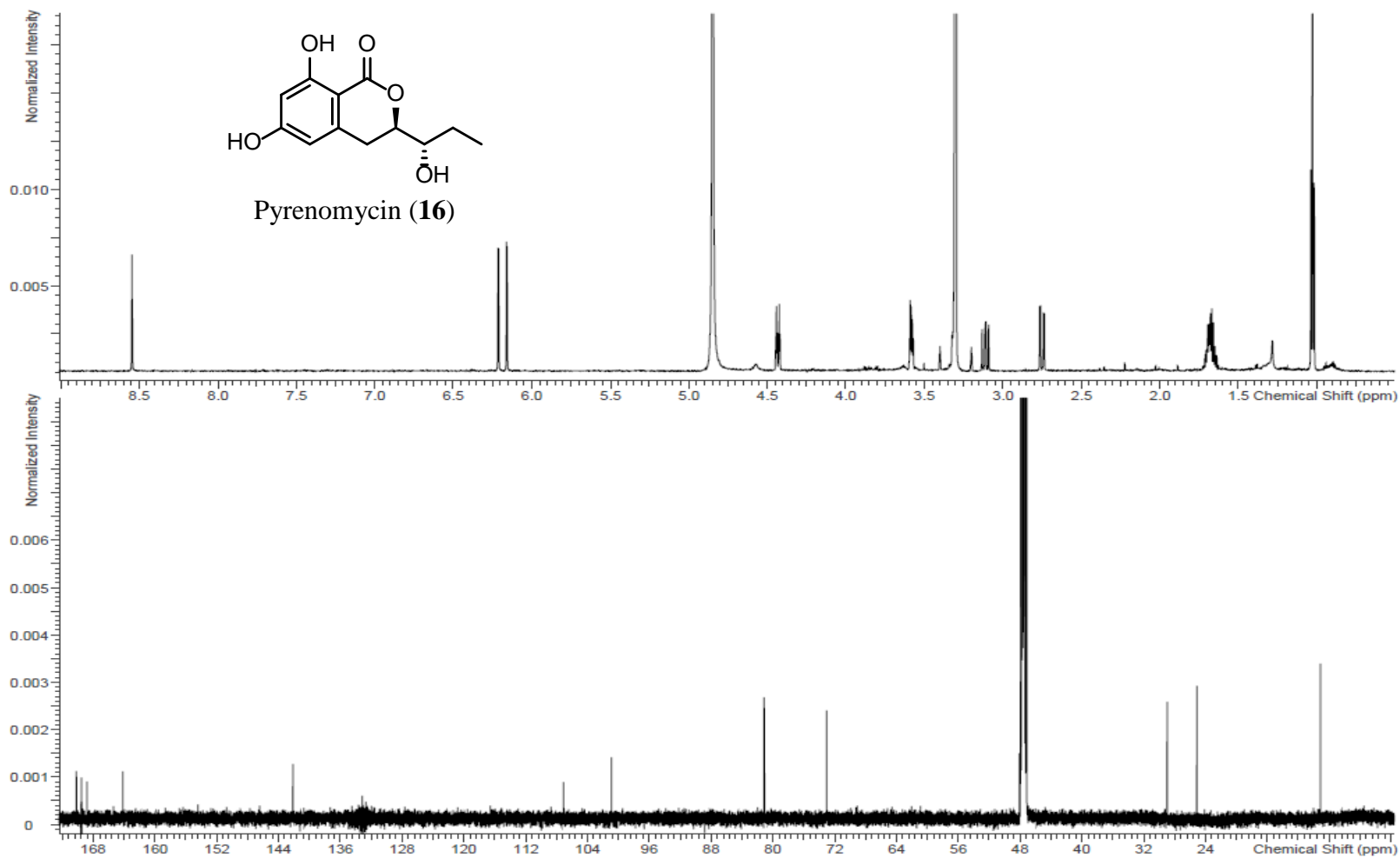


Figure 66. ^1H and ^{13}C NMR spectra of compound **16** [700 MHz for ^1H and 175 MHz for ^{13}C , Methanol- d_4].

Table 23. Antimicrobial Activities of Compounds 1-15

compound	Antimicrobial Activity MIC ($\mu\text{g/mL}$)							
	<i>M. luteus</i>	<i>S. aureus</i>	<i>E. coli</i>	<i>M. smegmatis</i>	<i>S. cerevisiae</i>	<i>C. albicans</i>	<i>C. neoformans</i>	<i>A. niger</i>
1	38	75	75	>75	75	75	75	75
2	36	>145	>145	>145	>145	>145	>145	>145
3	5	39	>78	>78	>78	>78	>78	>78
4	46	93	>93	>93	>93	>93	>93	>93
5	15	59	>118	>118	>118	>118	>118	>118
6	>43	>43	>43	>43	>43	>43	>43	>43
7	>58	>58	>58	>58	>58	>58	>58	>58
8	>40	>40	>40	>40	>40	>40	>40	>40
9	>70	>70	>70	>70	>70	>70	>70	>70
10	43	43	>85	>85	>85	>85	>85	>85
11	>88	>88	>88	>88	>88	>88	>88	>88
12	>133	>133	>133	>133	>133	>133	>133	>133
13	>120	>120	>120	>120	>120	>120	>120	>120
14	>70	>70	>70	>70	>70	>70	>70	>70
15	>83	>83	>83	>83	>83	>83	>83	>83
Vancomycin ^a	--	0.25	--	--	--	--	--	--
Ampicillin ^a	4	--	8	--	--	--	--	--
Ciprofloxacin ^a	--	--	--	2	--	--	--	--
Amphotericin B ^a	--	--	--	--	3.9	25	25	100
^a Positive controls								

CHAPTER VI
ISOCHROMENONES, ISOBENZOFURANONE, AND
TETRAHYDRONAPHTHALENES PRODUCED BY *PARAPHOMA RADICINA*, A
FUNGUS ISOLATED FROM A FRESHWATER HABITAT

Tamam El-Elimat, Huzefa A. Raja, Mario Figueroa, Joseph O. Falkinham III,
Nicholas H. Oberlies. This chapter has been submitted to *Phytochemistry* (2014).

Six isochromenones (**1-6**), of which two were new [clearanols F (**5**) and G (**6**)], one isobenzofuranone (**7**), and two tetrahydronaphthalene derivatives (**8** and **9**), the latter of which was new [radinaphthalenone (**9**)], were isolated and identified from a culture of the fungus *Paraphoma radicina*, which was isolated from submerged wood in a freshwater lake. The structures were elucidated using a set of spectroscopic and spectrometric techniques; the absolute configurations of compounds **5** and **6** were determined by comparison of their experimental ECD measurements with values predicted by TDDFT calculations. Compounds **1-9** were evaluated for antimicrobial activity against an array of bacteria and fungi. The inhibitory activity of compound **4** against *Staphylococcus aureus* biofilm formation was evaluated.

Introduction

In search of structurally diverse scaffolds from ecologically unique fungi, our group has initiated investigations of freshwater fungi,^{98,99} specifically ascomycetes that inhabit submerged woody and herbaceous organic matter in lakes and streams.¹⁴⁷ Freshwater fungi represent an ecologically important though poorly studied class of fungi in terms of chemistry^{148,149} and mycology.¹⁴⁷ Only fragmentary knowledge, at best, exists regarding habitat and substrate distribution patterns, species identities, and role(s) that these fungi play in freshwater ecosystems. Of the 1.5 M to 5.1 M estimated fungi in the world,^{8,23} only about 3,000 species have been characterized from freshwater habitats. This is somewhat surprising given that less than 2% of the planet is covered by freshwater.^{147,150} Similarly, of the 14,000 secondary metabolites that have been isolated from fungi,¹⁵¹ only about 125 compounds, i.e. less than 1%, have been from freshwater fungi.^{148,149}

A fungus, which was accessioned as G104, was isolated from submerged wood in a freshwater lake and was identified as *Paraphoma radicina*. This fungus produced six isochromenones (**1-6**), of which two were new [clearanol F (**5**), and clearanol G (**6**)], and four were known [(*R*)-3,4-dihydro-4,6,8-trihydroxy-4,5-dimethyl-3-methyleneisochromen-1-one (**1**), (*R*)-3,4-dihydro-4,8-dihydroxy-6-methoxy-4,5-dimethyl-3-methyleneisochromen-1-one (**2**), 3,8-dihydroxy-3-hydroxymethyl-6-methoxy-4,5-dimethyl-isochroman-1-one (**3**), and clearanol C (**4**)]. Also isolated were one known isobenzofuranone (*R*)-7-hydroxy-3-((*S*)-1-hydroxyethyl)-5-methoxy-3,4-dimethylisobenzofuran-1(3H)-one (**7**) and two tetrahydronaphthalene derivatives [isosclerone (**8**) and radinaphthalenone (**9**)], the latter having not been reported

previously. Herein, details of the isolation, structural elucidation, and determination of the absolute configuration of these compounds are presented. Structurally related compounds have been reported to have various degrees of antifungal activity¹⁵²⁻¹⁵⁴ and mild antimycobacterial activity.¹⁵⁵ As such, compounds **1-9** were evaluated against a panel of microorganisms; the most promising (**4**) was also tested in a *Staphylococcus aureus* biofilm assay.

Results and Discussion

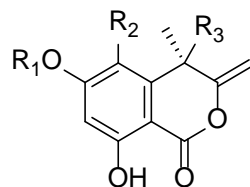
Two large-scale solid-phase cultures (LS1 and LS2) of the fungus (G104) were extracted with 1:1 CHCl₃-MeOH and partitioned with organic solvents. The organic extracts were purified using flash chromatography to yield 3 and 4 fractions, respectively, which were then subjected to further purifications using preparative and semipreparative HPLC to yield nine compounds (**1-9**). The purity of the isolated compounds was evaluated via UPLC (Figure 72). Compounds **1-6** and **7** belong to isochromenone and isobenzofuranone classes of natural products, respectively, while compounds **8** and **9** were tetrahydronaphthalene derivatives.

Compounds **1** (5.53 mg), **2** (34.16 mg), and **4** (9.19 mg) had molecular formulas of C₁₂H₁₂O₅, C₁₃H₁₄O₅, and C₁₃H₁₄O₄, respectively, as determined by HRESIMS. The NMR and HRMS data of these were similar, indicative of analogous structures, with key differences being a methoxy moiety in **2** relative to **1** and an OH moiety in **2** relative to **4**. The NMR, HRMS, CD and optical rotation data identified **1**, **2**, and **4** as the known compounds, (*R*)-3,4-dihydro-4,6,8-trihydroxy-4,5-dimethyl-3-methyleneisochromen-1-one, (*R*)-3,4-dihydro-4,8-dihydroxy-6-methoxy-4,5-dimethyl-3-methyleneisochromen-1-

one, and (*S*)-8-hydroxy-6-methoxy-4,5-dimethyl-3-methyleneisochromen-1-one (clearanol C), respectively (Figure 67 and Table 26). Compound **2** was first isolated in 2002 from the EtOAc extract of a broth of the marine fungus *Halorosellinia oceanica*,¹⁵⁵ and compounds **1**, **2** and **4** were isolated in 2011 from the culture broth of *Leptosphaeria* sp., which was collected from woody debris.^{152,154} Compound **4** was re-isolated in 2012 from a complex microbial mat that occupied an iron-rich freshwater spring and was ascribed the trivial name clearanol C.¹⁵³

Compound **3** (7.5 mg) was obtained as a colorless oil with a molecular formula of C₁₃H₁₆O₆ as determined by HRESIMS. The NMR data revealed the presence of an inseparable pair of compounds existing in 7:1 ratio, with the major one identified as the known compound 3,8-dihydroxy-3-hydroxymethyl-6-methoxy-4,5-dimethyl-isochroman-1-one (See Table 26 for CD and optical rotation data).¹⁵⁴ Tayone et al. suggested the minor compound as a stereogenic tautomer of the major compound around the hemiacetal moiety at C3 (Figure 67).¹⁵⁴ These were first isolated in 2011 from an *Allantophomopsis* sp.¹⁵⁶ and later in the same year from a *Leptosphaeria* sp.¹⁵⁴

Compound **7** (3.5 mg), which was obtained as a colorless oil, had a molecular formula of C₁₃H₁₆O₅ as determined by HRESIMS. The NMR, HRMS, and optical rotation data identified **7** as the known compound (*R*)-7-hydroxy-3-((*S*)-1-hydroxyethyl)-5-methoxy-3,4-dimethylisobenzofuran-1(3H)-one (Figure 67 and Table 26),¹⁵² which was first isolated in 2011 from the culture broth of *Leptosphaeria* sp.¹⁵²



- 1:** R₁ = H R₂ = CH₃ R₃ = OH
2: R₁ = CH₃ R₂ = CH₃ R₃ = OH
4: R₁ = CH₃ R₂ = CH₃ R₃ = H
6: R₁ = CH₃ R₂ = CH₂OH R₃ = OH

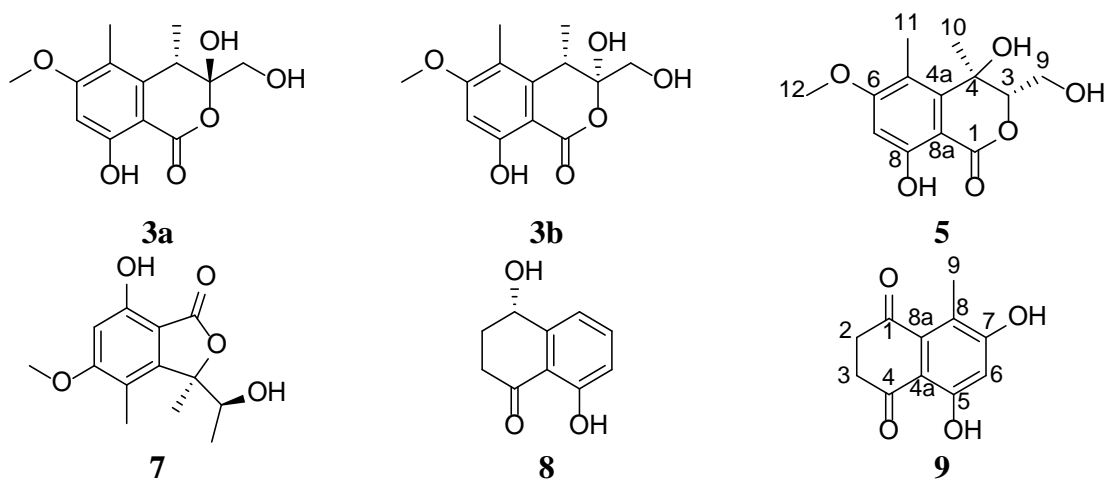


Figure 67. Structures of compounds **1-9**.

Compound **5** (0.85 mg) was also obtained as a colorless oil. The molecular formula was determined as C₁₃H₁₆O₆ via HRESIMS, establishing an index of hydrogen deficiency of 6. The NMR data suggested structural similarity with **3a**, both having the same molecular formula. Key differences were noticed in the chemical shift and splitting of the C-10 methyl group. It changed from a doublet that resonated at 1.14 ppm in **3a** into a singlet resonating at 1.53 ppm in **5**. Moreover, C-3 changed from a quaternary carbon (δ_C 103.3) in **3a** into a methine (δ_H/δ_C 4.36/82.4) in **5**. Additionally, C-4 changed from a methine in **3a** (δ_H/δ_C 3.27/36.1) into an oxygenated quaternary carbon (δ_C 72.4) in **5**.

These data suggested a switch in the hydroxyl group position from C-3 in **3a** to C-4 in **5** (Table 24 and Figures 73 and 74 for the ^1H and ^{13}C NMR data). An HMBC correlation was observed from 12-OCH₃ to C-6, indicating the connectivity of the methoxy group. HMBC correlations from H-11 to C-6 and C-4a, from H-7 to C-5 and C-8a, from 8-OH to C-7 and C-8, from 10-CH₃ to C-4a and C-3, from 4-OH to 10-CH₃, from H-3 to C-4a, and from 9-CH₂ to C-4 were observed (Figure 68). These data suggested the planar structure of **5** (Figure 67), which was ascribed the trivial name clearanol F. The absolute configuration of **5** was determined by comparing experimental and calculated ECD spectra predicted by the time-dependent density functional theory (TDDFT) method.¹²²⁻

¹²⁵ Similar studies have used calculated ECD values for determination of the absolute configuration of a series of chromone derivatives from *Penicillium* species¹⁵⁷ and isochromenones from *Leptosphaeria* species.^{152,154} Theoretical ECD spectra calculated for the four possible diastereomers **5a–5d** were compared with the experimental spectra (Figure 79). A detailed conformational search was performed for each diastereomer using molecular mechanics followed by geometry optimization with DFT at the B3LYP/DGDZVP2 level for the most stable conformers.^{125,158} The relative free energies and the Boltzmann distribution for the most relevant conformers of each diastereomer (4, 7, 4, and 5 conformers for **5a–5d**, respectively), each with a ΔG^0 range of between 0.0 and 3.0 kcal mol⁻¹, were taken into account to obtain population-weighted averaged calculated ECD spectra (Figures 69 and 79, and Table 27). The results for **5c** (3*S*,4*R*) were in excellent agreement with the experimental ECD spectrum where two negative low amplitude Cotton effects were observed at approximately 225 and 255 nm, along

with two positive effects at approximately 235 and 275 nm (Figure 70), confirming the *S* and *R* configurations at C-3 and C-4, respectively.

Table 24. NMR Data for 5 and 6 [700 MHz for ^1H , 175 MHz for ^{13}C ; Chemical Shifts in δ , Coupling Constants in Hz, CDCl_3]

position	5		6	
	δ_{C} , type	δ_{H} , mult, <i>J</i> in Hz	δ_{C} , type	δ_{H} , mult, <i>J</i> in Hz
1	169.5, C	---	166.5, C	---
3	82.4, CH	4.36, dd, 6.3, 5.7	159.6, C	---
4	72.4, C	---	72.3, C	---
4a	144.6, C	---	146.1, C	---
5	116.2, C	---	117.6, C	---
6	165.8, C	---	165.4, C	---
7	98.8, CH	6.42, s	99.2, CH	6.46, s
8	163.7, C	---	164.8, C	---
8a	98.9, C	---	99.2, C	---
9	61.2, CH_2	4.06, dd, 11.5, 6.3 4.12, dd, 11.5, 5.7	95.9, CH_2	4.94, d, 1.7 5.12, d, 1.7
10	21.1, CH_3	1.53, s	31.3, CH_3	1.72, s
11	12.2, CH_3	2.33, s	55.3, CH_2	4.98, d, 9.2
12	56.2, CH_3	3.85, s	56.4, CH_3	3.88, s
4-OH	---	2.51, s	---	---
8-OH	---	11.45, s	---	11.40, s
9-OH	---	2.17, br s	---	2.28, br

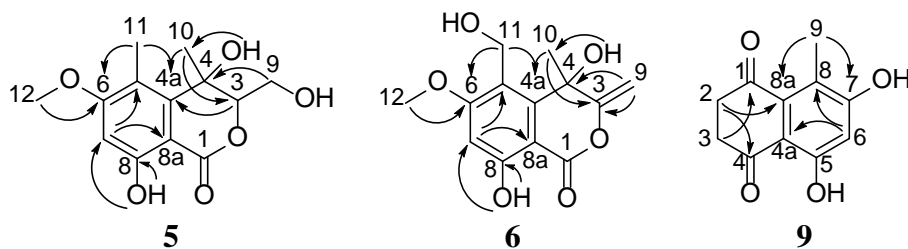


Figure 68. Key HMBC correlations of compounds 5, 6, and 9.

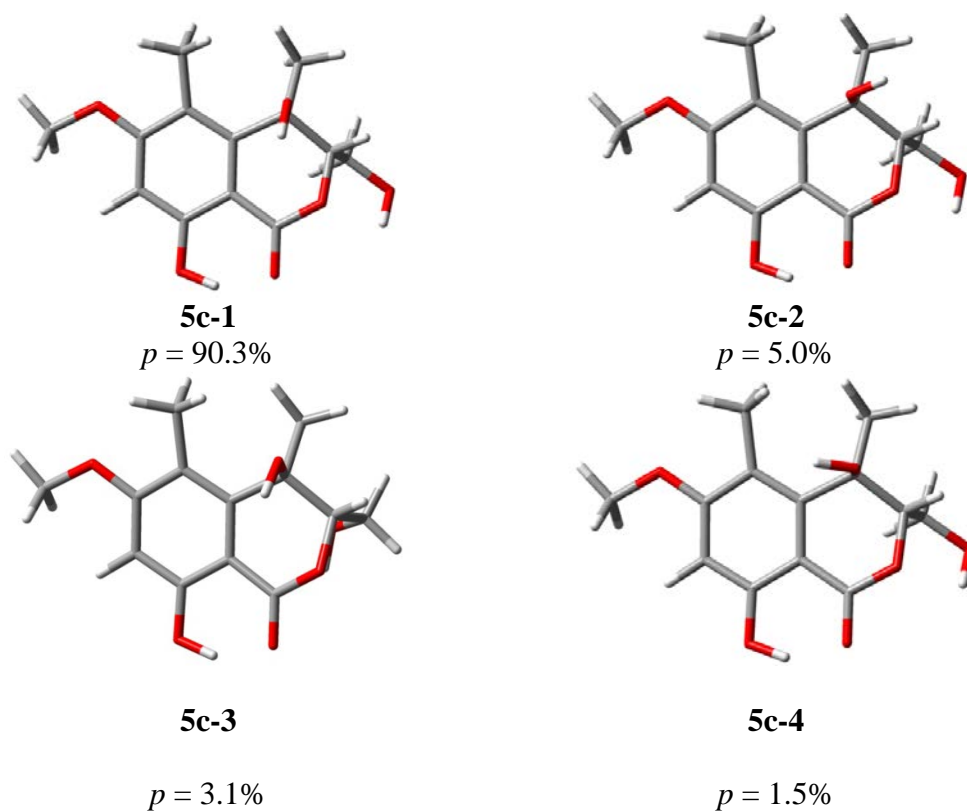


Figure 69. DFT B3LYP/DGDZVP2 geometry optimized conformers of **5c** [(3*S*,4*R*)-**5**] at 298 K and 1 atm, accounting for ca. 99% of the conformational population.

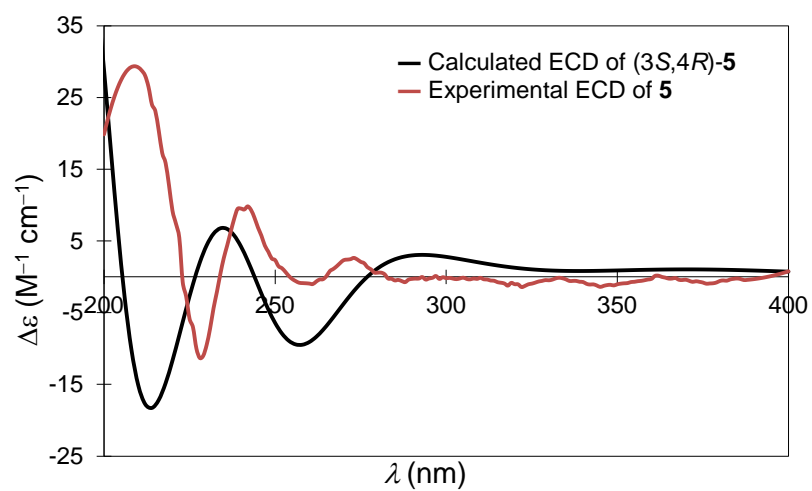


Figure 70. Experimental and calculated CD spectra for **5** in CH_3CN .

Compound **6** (0.65 mg) was obtained as a colorless oil. The molecular formula was determined as $C_{13}H_{14}O_6$ via HRESIMS. The NMR data suggested an isochromenone with structural similarity to **2**. However, compound **6** had an extra oxygen atom as evidenced by a 16 amu difference in the HRMS between **2** and **6**. Examination of the 1- and 2-D NMR data indicated that the C-11 methyl group in **2** (δ_H/δ_C 2.36/29.0) was hydroxylated in **6** (δ_H/δ_C 4.98/55.3). Key HMBC correlations were observed from H₂-11 to C-6 and C-4a, confirming the connectivity of the methylene hydroxyl group to C-4 and establishing the structure of **6** (Figures 67, 68, 75, and 76). The trivial name, clearanol G, was ascribed to this compound. The absolute configuration at C-4 was established by comparing the ECD data with those obtained through molecular modeling calculations following the same protocol described for compound **5** (Table 28). The agreement between the observed and calculated ECD (Figure 71) confirmed the *R* configuration at C-4.

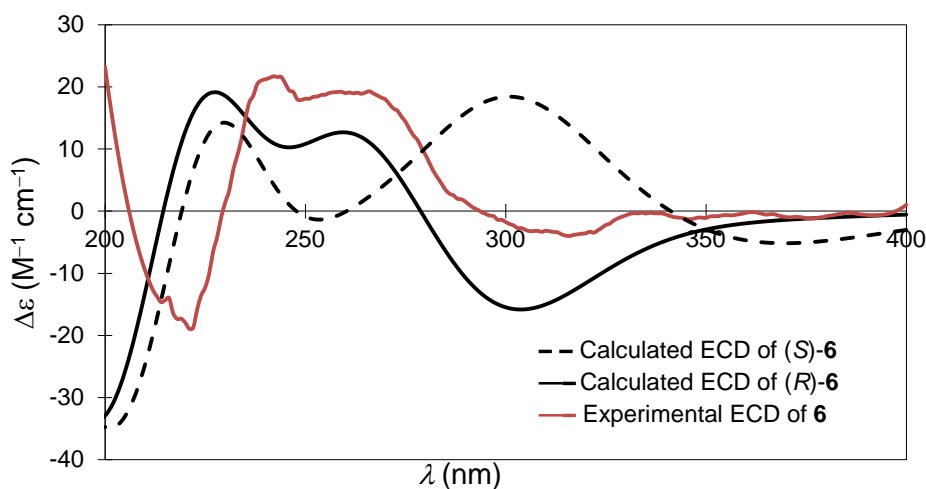


Figure 71. Experimental and calculated CD spectra for **6** in CH_3CN .

In addition to compounds **1-7**, two tetrahydronaphthalene derivatives, one known (**8**) and one new (**9**), were isolated and identified as well. The known compound **8** was identified as isosclerone by means of NMR, HRMS, and optical rotation data, which all compared favorably to the literature.⁹¹ Compound **9** (0.81 mg) was isolated as an off-white powder. The molecular formula was determined as C₁₁H₁₀O₄ by HRESIMS, indicative of an index of hydrogen deficiency of 7. The ¹H NMR data revealed the presence of one aromatic proton (δ_{H} 6.57, s), two methylenes (δ_{H} 2.98, m, and 3.02 m), one methyl (δ_{H} 2.38, s), and two hydroxyl protons (δ_{H} 11.36, s, and 5.91, broad peak, for 5-OH and 7-OH, respectively) (Table 25 and Figure 77). The ¹³C NMR data revealed 11 carbons, consistent with the HRMS data and indicative of two carbonyls (δ_{C} 198.8 and 201.5 for C-1 and C-4, respectively), six aromatic carbons (δ_{C} 113.4, 162.1, 107.3, 163.0, 118.5, and 135.7 for C-4a, C-5, C-6, C-7, C-8, and C-8a, respectively), suggesting a penta substituted benzene ring, two methylenes (δ_{C} 40.0 and 37.2 for C-2 and C-3, respectively), and one methyl (δ_{C} 11.9 for C-9) (Table 25 and Figure 78). The benzene ring and the two carbonyl groups accounted for six degrees of unsaturation, leaving the remaining one accommodated by a ring. HMBC correlations were observed from CH₃-9 to C-7 and C-8a from H-6 to C-8 and C-4a, from CH₂-2 to C-8a, and C-4, and from CH₂-3 to C-1 (Figure 68). These spectroscopic and spectrometric data suggested the structure of **9** (Figure 67), which was ascribed the trivial name radinaphthalenone.

Table 25. NMR Data for 9 (500 MHz for 1H, 100 MHz for 13C; Chemical Shifts in δ , Coupling Constants in Hz, CDCl₃)

position	δ_C , type	δ_H , mult
1	198.8, C	---
2	40.0, CH ₂	2.98, m
3	37.2, CH ₂	3.02, m
4	201.5, C	---
4a	113.4, C	---
5	162.1, C	---
6	107.3, CH	6.57, s
7	163.0, C	---
8	118.5, C	---
8a	135.7, C	---
9	11.9, CH ₃	2.38, s
5-OH	---	11.36, s
7-OH	---	5.91, broad

Compounds **1-9** were tested for antimicrobial activity against an array of bacteria and fungi (Table 29). Compound **4** showed promising activity against *S. aureus* with an MIC value of 33 $\mu\text{g/mL}$. Compound **4** was reported by Gereá et al.¹⁵³ to have weak inhibitory activity against *Candida albicans* biofilm formation and modest inhibition against polyene-resistant *C. albicans*. As such, **4** was evaluated for inhibitory activity against *S. aureus* biofilm formation and was found inactive. Compound **7** was reported to have strong antifungal activity against *Cochliobolus miyabeanus* at 0.5 $\mu\text{g/mL}$.¹⁵² When tested against *A. niger*, compound **7** was inactive (Table 29).

Conclusions

From a fungus that was isolated from a freshwater niche, nine compounds (**1-9**) belonging to three structural classes, isochromenones, isobenzofuranones, and tetrahydronaphthalenes, were isolated and identified. The absolute configuration of the

new isochromenones, **5** and **6**, was elucidated by means of TDDFT ECD spectra calculations. While most of the compounds were inactive, compound **4** had activity against *S. aureus*. Coupled with literature data on **4** and **7** regarding activity against biofilm formation in *C. albicans* and antifungal activity against *C. miyabeanus*, these compounds may confer a competitive advantage for this fungus, which was collected from a freshwater habitat. The current study demonstrated how structurally diverse compounds can be revealed from ecologically unique environments such as freshwater habitat, a highly underexplored source of bioactive natural products.

Paraphoma radicina is a plurivorous species, and it was originally reported from young cysts of nematodes from root surfaces of soybean in different counties in North Carolina, USA.¹⁵⁹ It was interesting to isolate the same species of fungus from the same state but a different environment. Its occurrence in both terrestrial and freshwater habitats suggested that it may be an immigrant species sensu Park.¹⁶⁰

Experimental

General Experimental Procedures. UV and CD spectra were acquired on a Varian Cary 100 Bio UV-Vis spectrophotometer and an Olis DSM 17 CD spectrophotometer (Olis), respectively. NMR experiments were conducted using either a JEOL ECA-500 NMR spectrometer operating at 500 MHz for ¹H and 125 MHz for ¹³C, or a JEOL ECS-400 NMR spectrometer equipped with a high sensitivity JEOL Royal probe operating at 400 MHz for ¹H and 100 MHz for ¹³C, or an Agilent 700 MHz NMR spectrometer, equipped with a cryoprobe, operating at 700 MHz for ¹H and 175 MHz for ¹³C. Residual solvent signals were utilized for referencing. HRESIMS was performed on a Thermo

LTQ Orbitrap XL mass spectrometer equipped with an electrospray ionization source. UPLC was carried out on a Waters Acquity system with data collected and analyzed using Empower 3 software. HPLC was carried out using a Varian Prostar HPLC system equipped with ProStar 210 pumps and a Prostar 335 photodiode array detector (PDA), with data collected and analyzed using Galaxie Chromatography Workstation software (version 1.9.3.2). For preparative HPLC, a Phenomenex Gemini-NX C₁₈ (5 μ m; 250 \times 21.2 mm) column was used at a 21 mL/min flow rate. For UPLC, a Waters BEH C₁₈ column (1.7 μ m; 50 \times 2.1 mm) was used with a 0.6 mL/min flow rate. Flash chromatography was performed on a Teledyne ISCO CombiFlash Rf 200 using a 4 g Silica Gold column and monitored by UV and evaporative light-scattering detectors. All other reagents and solvents were obtained from Fisher Scientific and were used without further purification. The HTP MBEC Assay Biofilm Incubator (Innovotech Inc., Edmonton, Alberta, Canada) was used for the *S. aurous* biofilm assay.

Fungal Strain Isolation and Identification. The fungal strain, G104, was isolated from submerged wood sampled in October of 2011 from a freshwater lake in Greensboro, North Carolina, USA (Lake Brandt; 36°10' 1"N, 79°50' 18"W). Collection methods and culturing conditions were based on earlier work by Shearer et al.^{161,162} Strain G104 was identified using molecular techniques by sequencing the internal transcribed spacer regions 1 & 2 and 5.8S nrDNA (ITS)⁴⁵ along with the D1 and D2 regions of the 28S nuclear ribosomal large subunit rRNA gene (LSU).⁹⁵ Methodology for DNA extraction, PCR amplification, sequencing, and phylogenetic analyses were performed as described previously.^{63,81,97-99} BLAST search in GenBank using ITS rDNA sequences and

phylogenetic analysis using partial LSU sequence data suggested that strain G104 had phylogenetic affinities to *Paraphoma radicina* (McAlpine) Morgan-Jones & J.F. White belonging to the section *Phoma* (Figure 80).^{159,163} Therefore, strain G104 was identified as *Paraphoma radicina* (Ascomycota). The combined ITS and LSU sequence was deposited in the GenBank (accession no. KF938577). A voucher culture of strain G104 is maintained in the Department of Chemistry and Biochemistry culture collection at the University of North Carolina at Greensboro.

Fermentation and Isolation. The culture of strain G104 was stored on a malt extract slant and was transferred periodically. A fresh culture was prepared in a similar slant and subsequently grown on 2% MEA, potato dextrose agar (PDA, Difco), and YESD media. After 14–21 d, agar plugs of the fungus were used to inoculate 30 mL of autoclaved rice medium, prepared using 10 g of rice and twice the volume of rice with H₂O in a 250 mL Erlenmeyer flask. Large scale cultures were prepared by the parallel processing of four such cultures in quadruplicates, which were incubated at 22 °C until showing good growth (approximately 14 d).

To a large scale culture, 500 mL of 1:1 MeOH-CHCl₃ were added. The culture was chopped with a spatula and shaken overnight (~16 h) at ~100 rpm at rt. The sample was filtered with vacuum, and the remaining residues were washed with 100 mL of 1:1 MeOH-CHCl₃. To the filtrate, 900 mL CHCl₃ and 1500 mL H₂O were added; the mixture was stirred for 30 min and then transferred into a separatory funnel. The bottom layer was drawn off and evaporated to dryness. The dried organic extract was reconstituted in 100 mL of 1:1 MeOH-CH₃CN and 100 mL of hexanes. The biphasic

solution was shaken vigorously and then transferred to a separatory funnel. The MeOH-CH₃CN layer was drawn off and evaporated to dryness under vacuum. The defatted material (231 mg) was dissolved in a mixture of CHCl₃-MeOH, adsorbed onto Celite 545, and fractionated via flash chromatography using a gradient solvent system of hexane-CHCl₃-MeOH at a 18 mL/min flow rate and 68.1 column volumes over 18.2 min to afford three fractions. Fraction 1 (78.87 mg) was subjected to preparative HPLC using a gradient system of 20:80 to 80:20 of CH₃CN-H₂O (acidified with 0.1% formic acid) over 20 min at a flow rate of 21 mL/min to yield six sub-fractions. Sub-fractions 1, 3, 4, and 6 yielded compounds **8** (0.71 mg), **7** (1.61 mg), **2** (16.05 mg), and **4** (9.19 mg), which eluted at ~11.3, 12.0, 17.6, and 21.2 min, respectively. Fraction 2 (26.11 mg) was subjected to preparative HPLC using a gradient system of 30:70 to 40:60 of CH₃CN-H₂O (acidified with 0.1% formic acid) over 20 min at a flow rate of 21 mL/min to yield four sub-fractions. Sub-fractions 1 and 2 yielded compounds **6** (0.65 mg) and **3** (5.64 mg), which eluted at 10.7 and 12.6 min, respectively. Fraction 3 (~84.99 mg) was subjected to preparative HPLC using a gradient system of 20:80 to 40:60 of CH₃CN-H₂O (acidified with 0.1% formic acid) over 20 min at a flow rate of 21 mL/min to yield four sub-fractions. Sub-fractions 3 and 4 yielded compounds **5** (0.85 mg) and **3** (1.88 mg), which eluted at ~17.1 and 19.6 min, respectively.

To generate more material for biological evaluation, another large scale culture of strain G104 was extracted and fractionated as described above. The MeOH-CH₃CN fraction (242 mg) was subjected to fractionation using flash chromatography using a gradient solvent system of hexane-CHCl₃-MeOH at a 30 mL/min flow rate and 61.0

column volumes over 34.1 min to afford four fractions. Fraction 2 (145.95 mg) was subjected to preparative HPLC using a gradient system of 40:60 to 80:20 of CH₃CN-H₂O (acidified with 0.1% formic acid) over 15 min at a flow rate of 21 mL/min to yield six sub-fractions. Sub-fractions 1, 2, and 3 yielded compounds **7** (1.89 mg), **8** (0.82 mg), and **2** (18.11 mg), which eluted at 4.5, 7.6, and 13.1 min, respectively. Fraction 3 (35.69 mg) was subjected to preparative HPLC using a gradient system of 20:80 to 60:40 of CH₃CN-H₂O (acidified with 0.1% formic acid) over 15 min at a flow rate of 21 mL/min to yield four sub-fractions. Sub-fraction 3 yielded compound **1** (5.53 mg), which eluted at ~16.0 min.

Clearanol F (5): Colorless oil; $[\alpha]_D^{25} = +18^\circ$ ($c = 0.05$, Chloroform); UV (MeOH) λ_{\max} (log ϵ) 313 (3.20), 269 (3.36), 228 (3.36), 217 (3.75) nm; CD ($c 7.46 \times 10^{-5}$ M, CH₃CN) λ ($\Delta\epsilon$) 209 (+29.4) nm, 228 (-11.3) nm, 242 (+9.8) nm; 261 (-1.0) nm, 273 (+2.6) nm; ¹H NMR (CDCl₃, 700 MHz) and ¹³C NMR (CDCl₃, 175 MHz), see Table 24; HRESIMS m/z 269.1013 [M + H]⁺ (calcd for C₁₃H₁₇O₆ 269.1020).

Clearanol G (6): Colorless oil; $[\alpha]_D^{25} = +43^\circ$ ($c = 0.03$, Chloroform); UV (MeOH) λ_{\max} (log ϵ) 308 (3.18), 268 (3.36), 228 (3.41) nm; CD ($c 7.51 \times 10^{-5}$ M, CH₃CN) λ ($\Delta\epsilon$) 221 (-18.9) nm, 242 (+21.7) nm, 266 (+19.3) nm, 316 (-4.0) nm; ¹H NMR (CDCl₃, 700 MHz) and ¹³C NMR (CDCl₃, 175 MHz), see Table 24; HRESIMS m/z 267.0861 [M + H]⁺ (calcd for C₁₃H₁₅O₆ 267.0863).

Radinaphthalenone (9): Off-white powder; UV (MeOH) λ_{\max} (log ϵ) 352 (3.28), 293 (3.24), 244 (3.35), 211 (3.18) nm; ¹H NMR (CDCl₃, 500 MHz) and ¹³C NMR

(CDCl₃, 100 MHz), see Table 25; HRESIMS *m/z* 207.0647 [M + H]⁺ (calcd for C₁₁H₁₁O₄ 207.0652).

Computational Methods. Theoretical calculations of ECD spectra for compounds **5** and **6** were performed with the Gaussian 09 (Gaussian Inc., Pittsburgh, PA, USA) program package.¹⁶⁴ Geometry optimizations for both compounds were carried out using the PM3 semi-empirical force field calculations as implemented in the Spartan 08 program (Wavefunction Inc. Irvine, CA, USA).¹⁶⁵ A Monte Carlo search protocol¹⁶⁶ was carried out considering an energy cutoff of 5 kcal/mol. In each case, the minimum energy structures were filtered and checked for duplicity. Each conformer was geometrically optimized using hybrid DFT method B3LYP and basis set DGDZVP2 (B3LYP/DGDZVP2), and thermochemical parameters and the frequencies at 298 K and 1 atm. The self-consistent reaction field method (SCRF) with conductor-like continuum solvent model (COSMO) was employed to perform the ECD calculation of major conformers of compounds **5** and **6** in CH₃CN solution with the same basis set. The calculated excitation energy (in nm) and rotatory strength *R*, in dipole velocity (*R*_{vel}) and dipole length (*R*_{len}) forms, were simulated into an ECD curve by using the following Gaussian function:

$$\Delta\varepsilon(E) = \sum_{i=1}^n \Delta\varepsilon_i(E) = \sum_{i=1}^n \left(\frac{R_i E_i}{2.29 \times 10^{-39} \sqrt{\pi\sigma}} \exp \left[- \left(\frac{E - E_i}{\sigma} \right)^2 \right] \right)$$

where σ is the width of the band at 1/*e* height, and E_i and R_i are the excitation energies and rotatory strengths for transition *i*, respectively. $\sigma = 0.40$ eV and R_{vel} were used. All

quantum calculations were carried out on a Linux operating system in the KanBalam cluster from a Hewlett-Packard HP CP 4000, which includes 1368 AMD Opteron processors at 2.6 GHz and a RAM memory of 3 terabytes (KanBalam, Dirección General de Cómputo y de Tecnologías de Información y Comunicación, UNAM).

Antimicrobial Assay. Minimal inhibitory concentrations (MICs) of compounds **1-9** were measured as described previously.^{18,102,103} All measurements were made in duplicate. The positive controls were ampicillin, rifamycin, and amphotericin B.

Biofilm-Grown Cells Inhibition by a 96-Well Plate Assay. The inhibition of biofilm-grown cells of *S. aureus* strain ATCC 6358 was measured as described by Nett et al.¹⁶⁷ with the only change being the growth of the *S. aureus* strain in Mueller-Hinton broth at 37° C. The MIC was defined as the lowest concentration that resulted in 50% (IC₅₀) and 90% (IC₉₀) reduction in reduced XTT absorbance. Vancomycin was used as a positive control and showed an IC₉₀ of 0.5 µg/mL.

Supplementary Data

Table 26. CD and Optical Rotation Data, Experimental vs. Literature, of Compounds 1-4 and 7

compound	CD: Conc. solvent; λ_{\max} ($\Delta\epsilon$) nm		Optical rotation	
	Experimental	Literature	Experimental	Literature
1	1.7×10^{-5} M, CH ₃ CN 226 (-9.4); 207 (+17.5)	2.5×10^{-4} M, CH ₃ CN ^a 226 (-2.2); 207 (+5.2)	$[\alpha]_D^{25} = +300^\circ$ (c = 0.02, Chloroform)	$[\alpha]_D^{25} = +161^\circ$ (c = 0.19, Chloroform). ^a
2	1.7×10^{-5} M, CH ₃ CN 225 (-8.3); 205 (+20.2)	5.2×10^{-5} M, CH ₃ CN ^a 225 (-7.4); 207 (+12.3)	$[\alpha]_D^{25} = +229^\circ$ (c = 0.09, Chloroform)	$[\alpha]_D^{25} = +96^\circ$ (c = 0.11, Chloroform). ^a
3a	7.4×10^{-5} M, CH ₃ CN 267 (+21.4); 218 (-2.5)	4.1×10^{-5} M, CH ₃ CN ^b 260 (+2.1); 215 (-4.8)	$[\alpha]_D^{25} = +55^\circ$ (c = 0.07, Chloroform)	$[\alpha]_D^{25} = +61^\circ$ (c = 0.68, Chloroform). ^b
4	1.7×10^{-5} M, CH ₃ CN 267 (+23.0); 237 (+23.8); 212 (-21.2)	6.4×10^{-5} M, CH ₃ CN ^b 266 (+12.6); 213 (-10.0); 235 (+15.2)	$[\alpha]_D^{25} = +215^\circ$ (c = 0.02, Chloroform)	$[\alpha]_D^{25} = +143^\circ$ (c = 0.15, Chloroform). ^b
7	1.2×10^{-4} , CH ₃ CN 254 (+6.2); 215 (-46.8)	3.0×10^{-5} , CH ₃ CN ^a 258 (+2.7); 215 (-7.7)	$[\alpha]_D^{25} = -26^\circ$ (c = 0.09, Chloroform)	$[\alpha]_D^{25} = -27^\circ$ c = 0.20, Chloroform). ^a

^aTayone, W. C.; Honma, M.; Kanamaru, S.; Noguchi, S.; Tanaka, K.; Nehira, T.; Hashimoto, M. *J. Nat. Prod.* **2011**, *74*, 425-429.

^bTayone, W. C.; Kanamaru, S.; Honma, M.; Tanaka, K.; Nehira, T.; Hashimoto, M. *Biosci. Biotech. Bioch.* **2011**, *75*, 2390-2393.

Table 27. Relative Free Energies (ΔG_{rel})^a and Equilibrium Population (p)^b Values of the Conformers of 5a-5d

conformer	5a		conformer	5b	
	ΔG_{rel}	p (%)		ΔG_{rel}	p (%)
5a-1	0.0000	41.90	5b-1	0.0000	53.61
5a-2	0.1902	30.39	5b-2	0.6363	18.31
5a-3	0.2931	25.55	5b-3	0.9835	10.19
5a-4	1.7571	2.16	5b-4	1.1175	8.13
			5b-5	1.3668	5.34
			5b-6	1.7411	2.84
			5b-7	2.0879	1.58
conformer	5c		conformer	5d	
	ΔG_{rel}	p (%)		ΔG_{rel}	p (%)
5c-1	0.0000	90.30	5d-1	0.0000	49.95
5c-2	1.7079	5.05	5d-2	0.5309	20.39
5c-3	1.9940	3.12	5d-3	0.7430	14.25
5c-4	2.4188	1.52	5d-4	0.9891	9.41
			5d-5	1.2559	6.00

^aB3LYP B3LYP/DGDZVP2, in kcal/mol

^bPopulation percentages based on ΔG_{rel} , assuming Boltzmann statistics at T=298.15 K and 1 atm

Table 28. Relative Free Energies (ΔG_{rel})^a and Equilibrium Population (p)^b Values of the (*R*) and (*S*) Conformers of Compound 6

conformer	(R)-6		conformer	(S)-6	
	ΔG_{rel}	p (%)		ΔG_{rel}	p (%)
(R)-1	0.0000	52.75	(S)-1	0.0000	43.25
(R)-2	0.3242	30.52	(S)-2	0.4689	19.60
(R)-3	0.7324	15.32	(S)-3	0.4689	19.60
(R)-4	2.1486	0.14	(S)-4	0.7931	11.34
			(S)-5	1.2013	0.57
			(S)-6	2.6176	0.05

^aB3LYP B3LYP/DGDZVP2, in kcal/mol

^bPopulation percentages based on ΔG_{rel} , assuming Boltzmann statistics at T=298.15 K and 1 atm

Table 29. Antimicrobial Activities of Compounds 1-9

compound	Minimal inhibitory concentration ($\mu\text{g/mL}$)				
	<i>S. aureus</i>	<i>E. coli</i>	<i>M. smegmatis</i>	<i>S. cerevisiae</i>	<i>A. niger</i>
1	>108	108	108	>108	>108
2	>138	>138	>138	>138	>138
3	>190	>190	>190	>190	>190
4	33	>130	130	>138	>138
5	>108	>108	>108	>108	>108
6	>88	>88	>88	>88	>88
7	>153	>153	>153	>153	>153
8	>63	>63	>63	>63	>63
9	60	>60	>60	>60	>60
Ampicillin ^a	0.2	>250	>250	>250	>250
Rifamycin ^a	0.2	31	4	>250	>250
Amphotericin B ^a	0.2	>250	250	3.9	31

^aPositive controls.

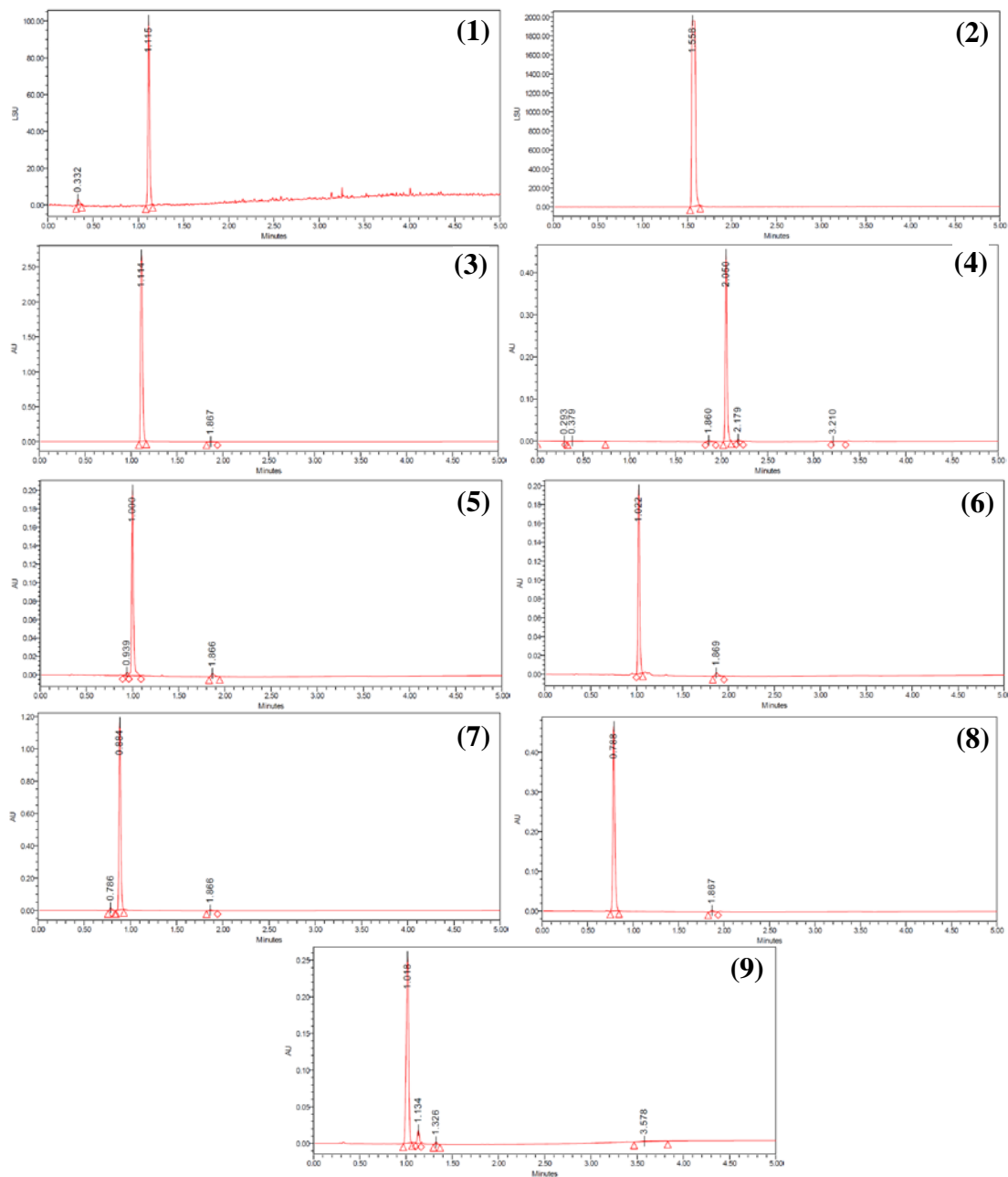


Figure 72. UPLC chromatograms of compounds **2-9** (λ 254 nm) and **1** (ELSD detection), demonstrating >95% purity for compounds **1-8** and >93% for compound **9**. All data were acquired via an Acquity UPLC system with a BEH C₁₈ (1.7 μ m 2.1 \times 50 mm) column and a CH₃CN/H₂O gradient that increased linearly from 20 to 100% CH₃CN over 4.5 min.

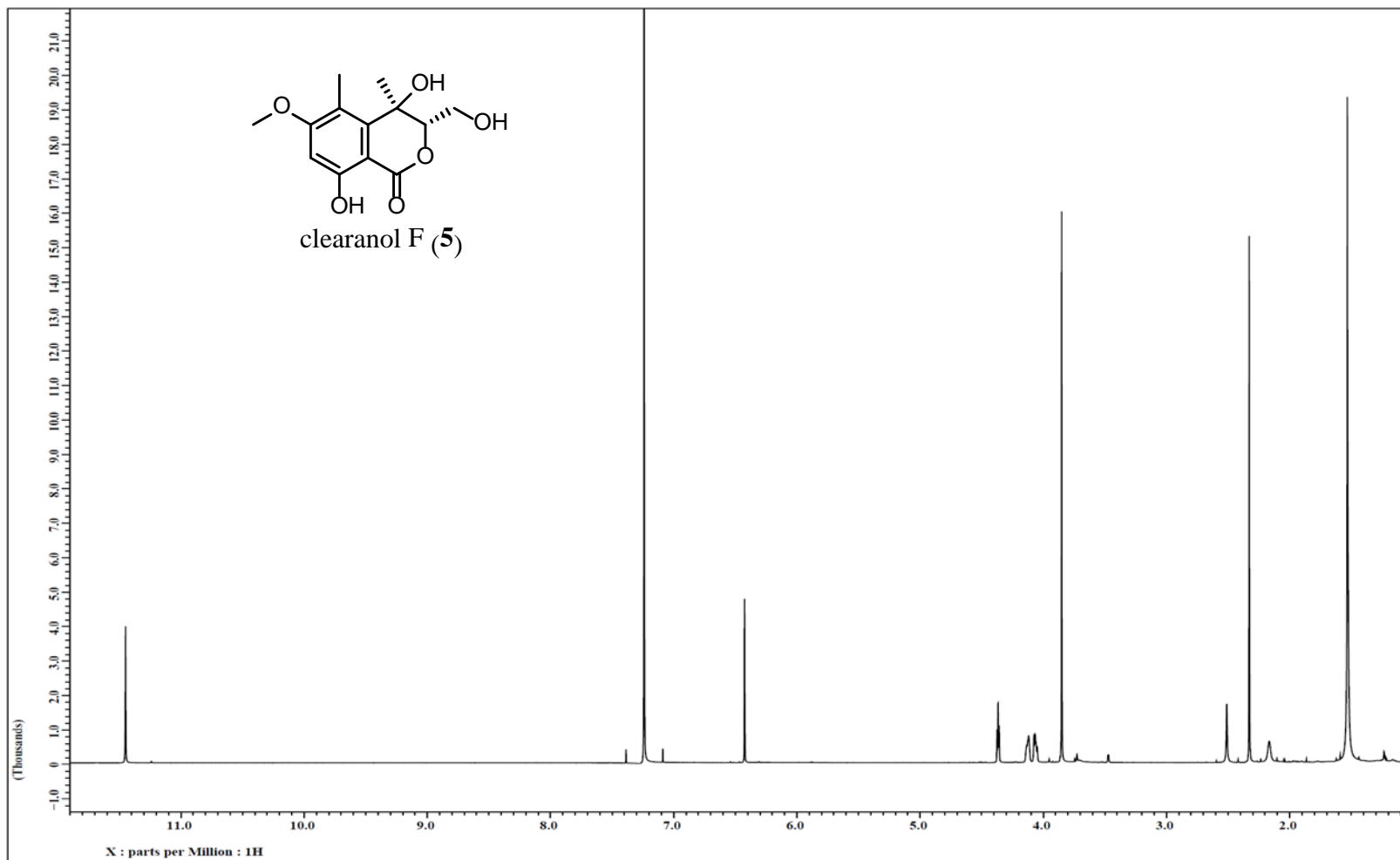


Figure 73. ^1H NMR spectrum of clearanol F (**5**) [700 MHz, CDCl_3].

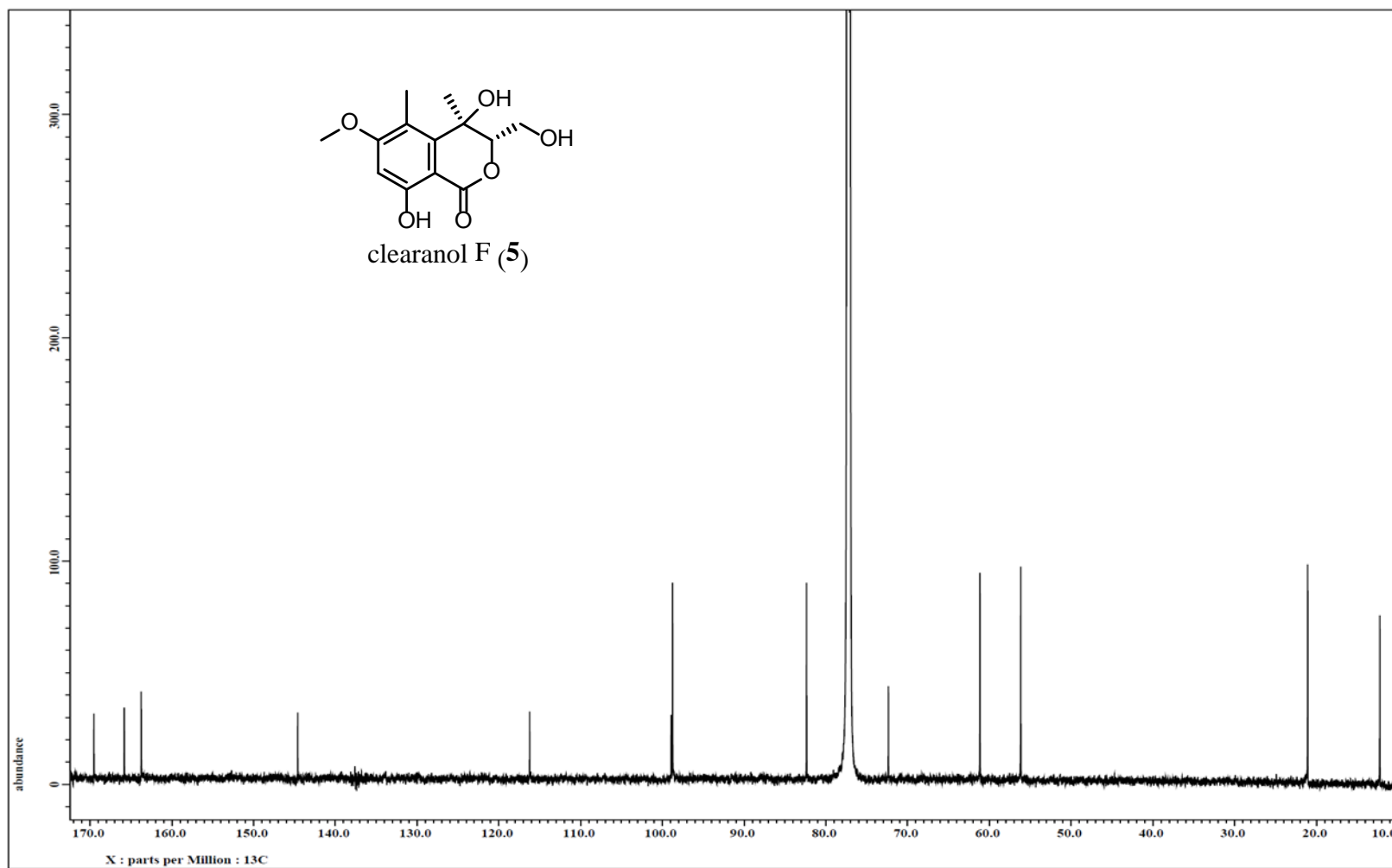


Figure 74. ^{13}C NMR spectrum of clearanol F (5) [175 MHz, CDCl_3].

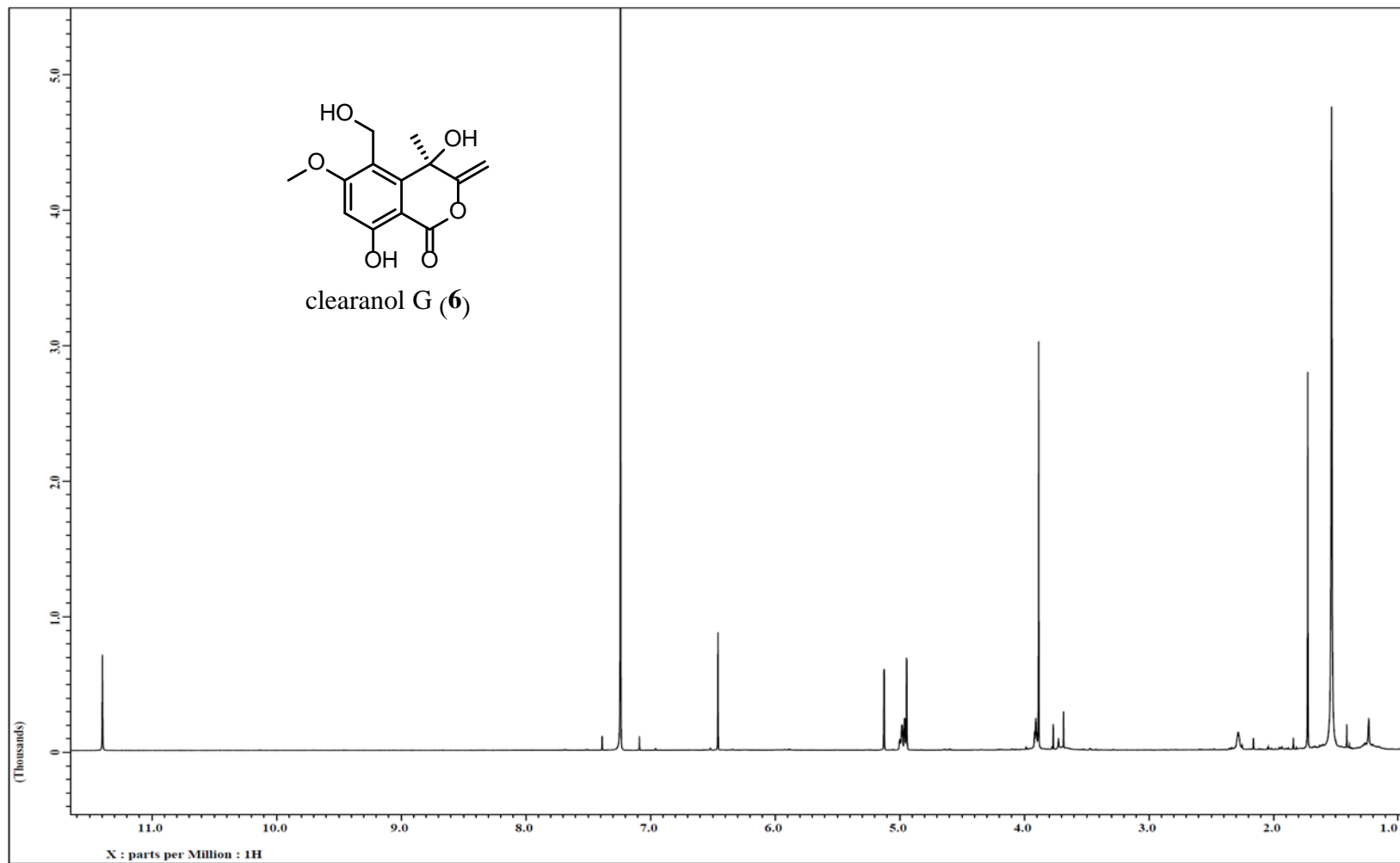


Figure 75. ^1H NMR spectrum of clearanol G (6) [700 MHz, CDCl_3].

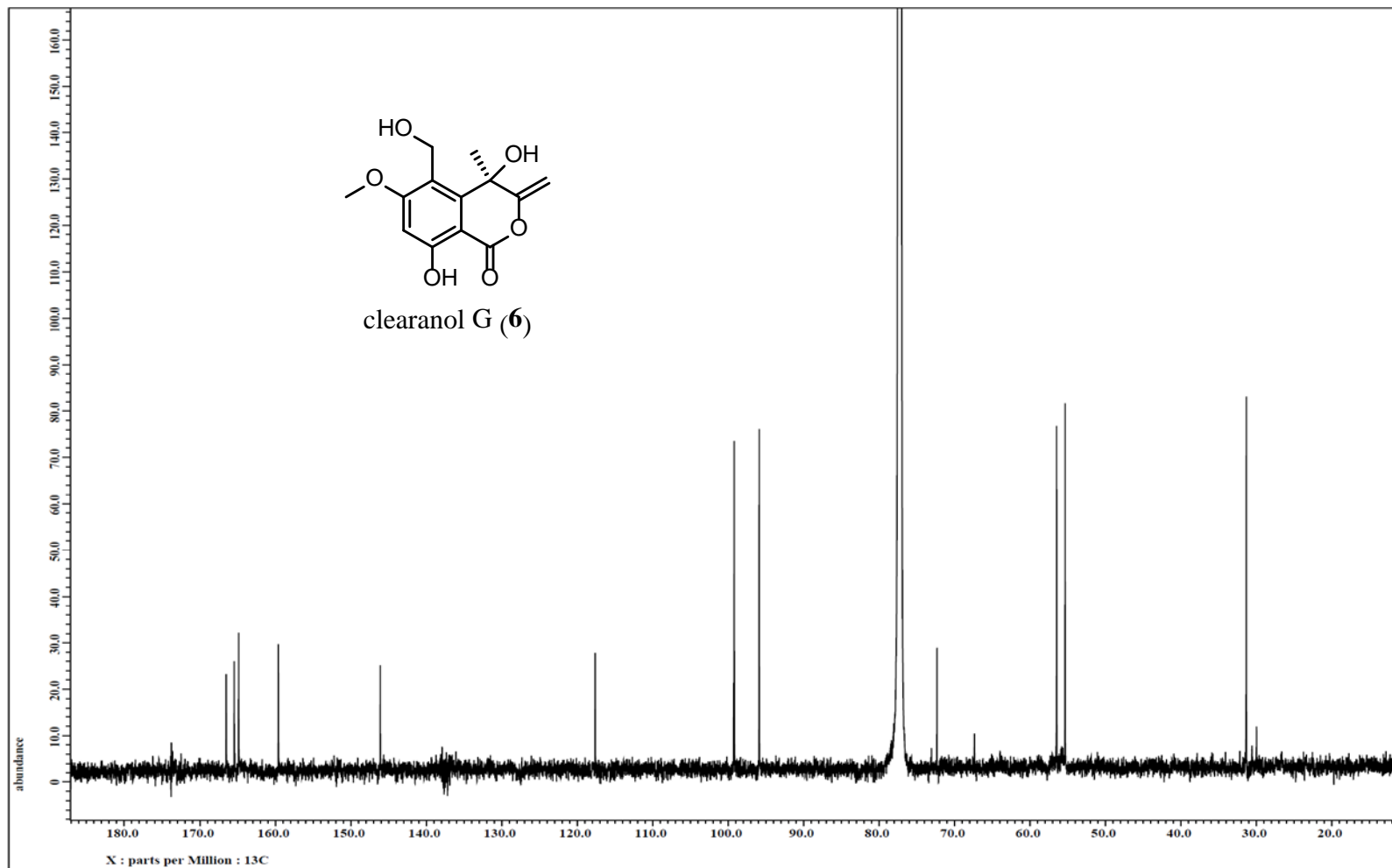


Figure 76. ^{13}C NMR spectrum of clearanol G (**6**) [175 MHz, CDCl_3].

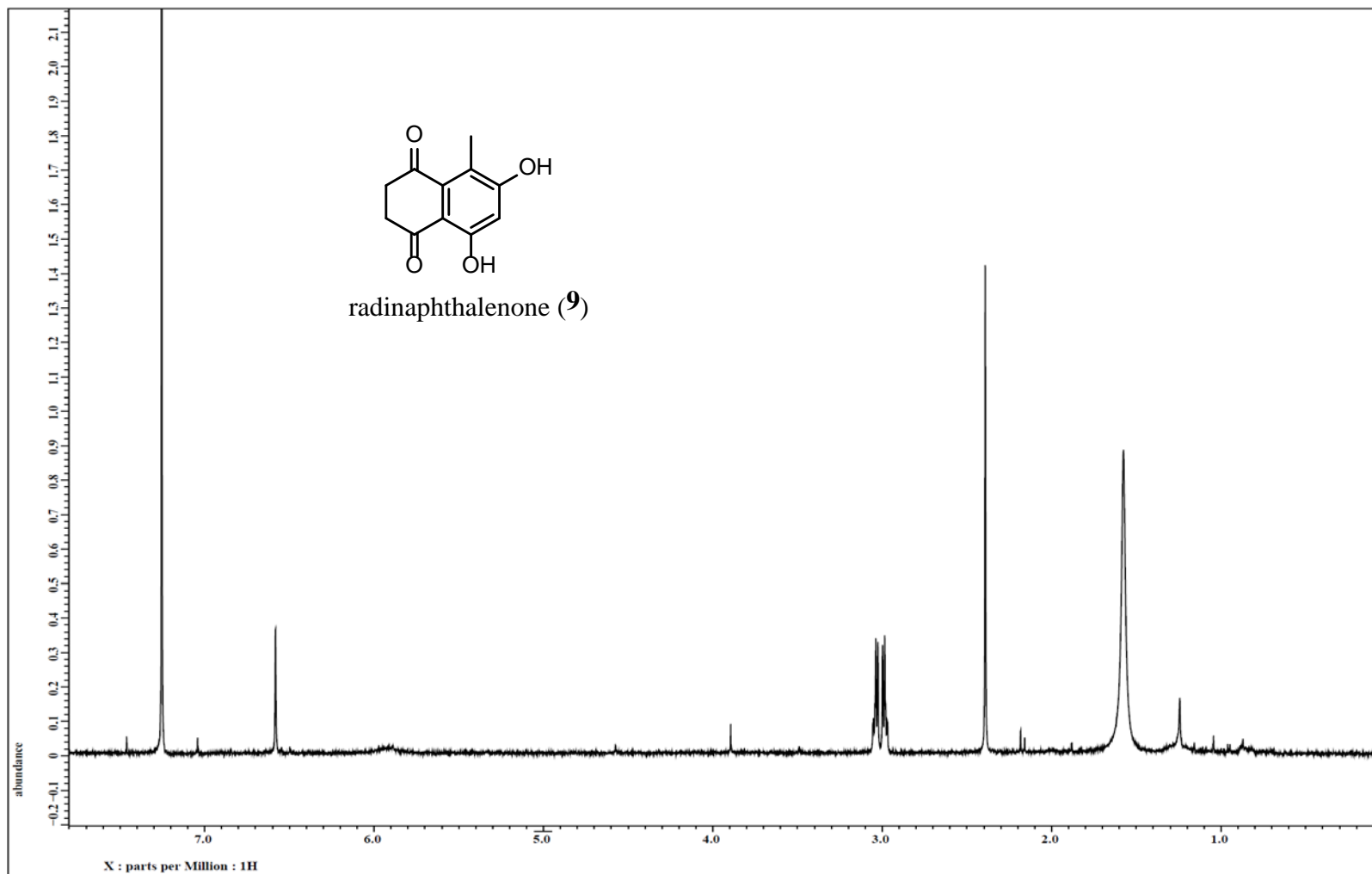


Figure 77. ¹H NMR spectrum of radinaphthalenone (9) [500 MHz, CDCl₃].

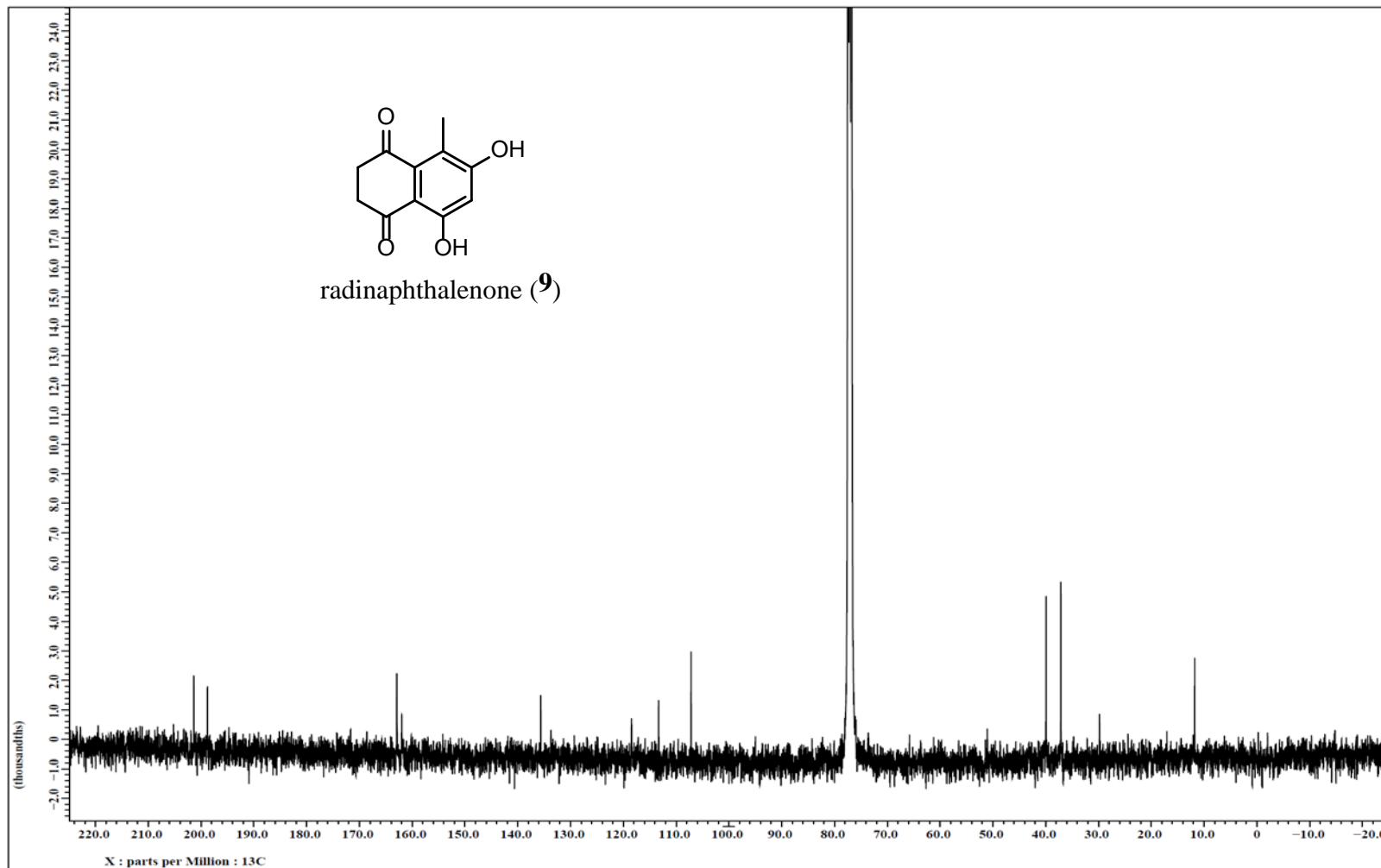


Figure 78. ^{13}C NMR Spectrum of radinaphthalenone (9) [100 MHz, CDCl_3].

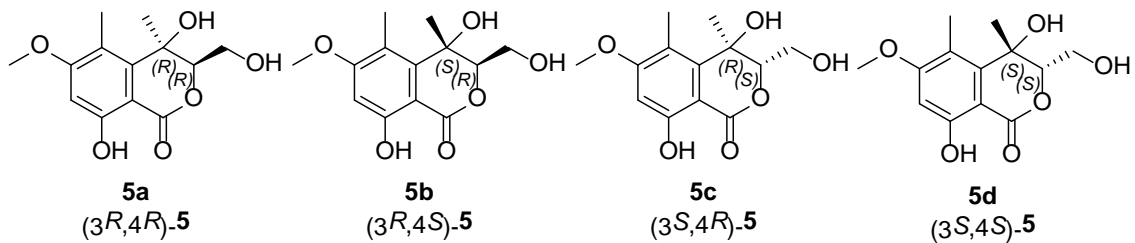
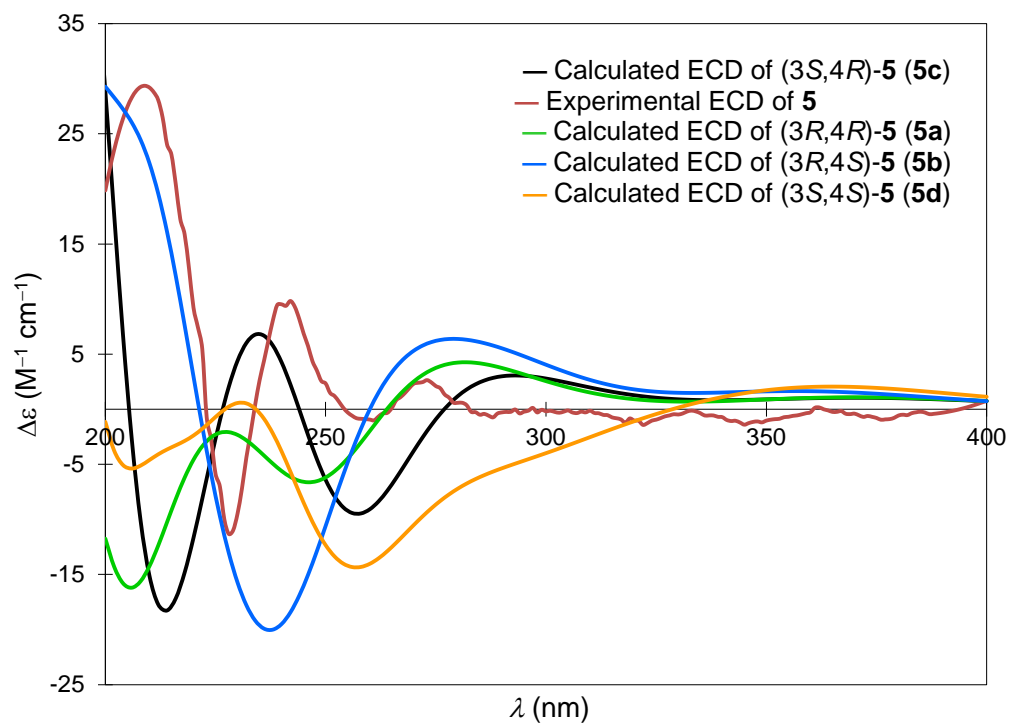


Figure 79. Experimental CD spectrum for **5** in CH_3CN compared with calculated CD spectra for compounds **5a-5d** at the B3LYP/DGDZVP2 Level.

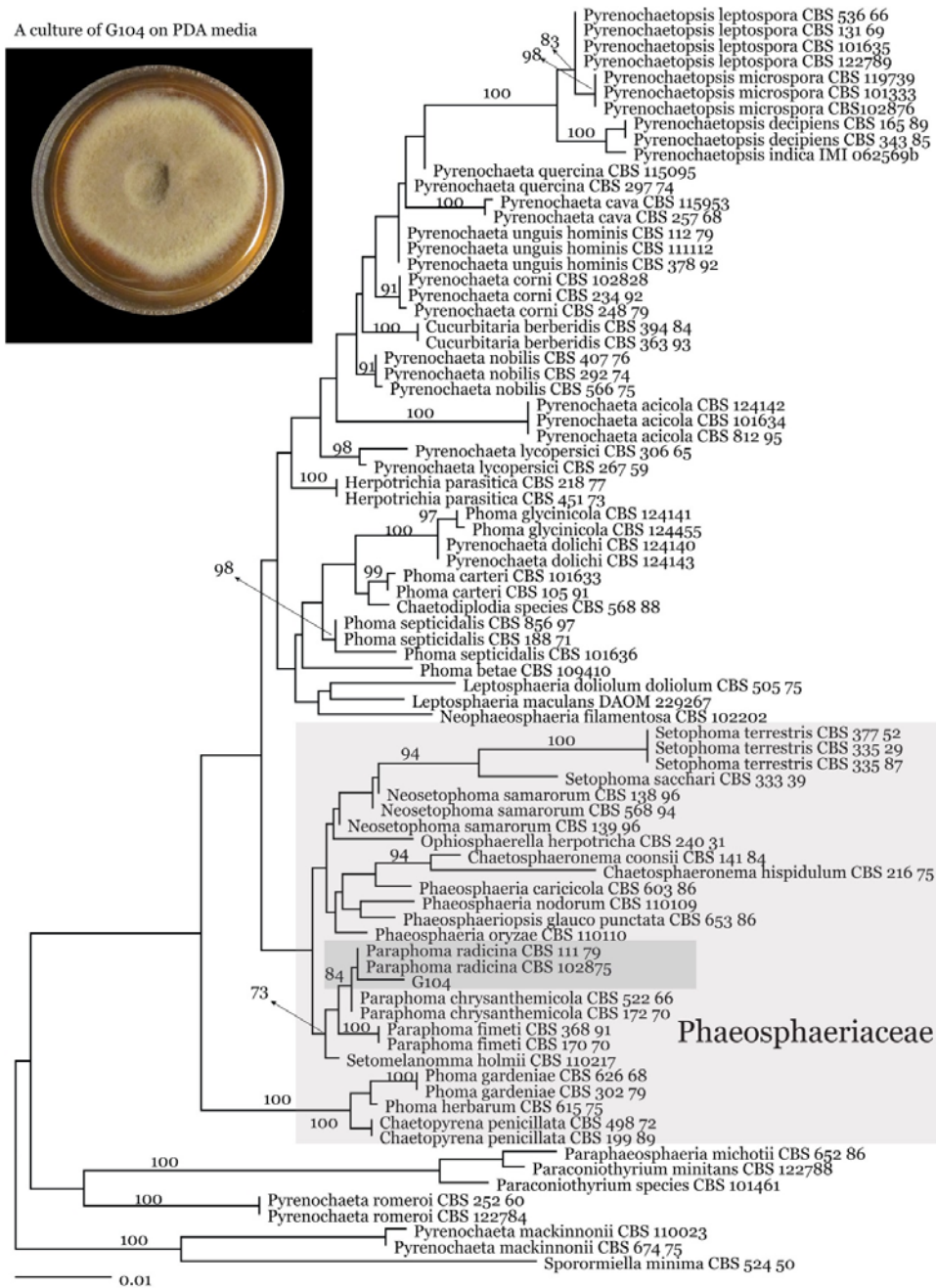


Figure 80. Phylogram of the most likely tree ($-\ln L = -7198.77$) from a RAxML analysis of 81 taxa (alignment downloaded from TreeBase (www.treebase.org) by Gruyter et al. *Mycologia* **2010**, *102*, 1066-1081). Partial LSU sequence (D1/D2 domains) of strain G104 was included in the ML analysis. Numbers above branches refer to RAxML bootstrap support values based on 1000 replicates. Strain G104 is highlighted and shows phylogenetic affinities with *P. radicina*.

CHAPTER VII

RESORCYLIC ACID LACTONES FROM A FRESHWATER *HALENOSPORA* SP.

Tamam El-Elimat, Huzefa A. Raja, Joseph O. Falkinham III, Cynthia S. Day, and Nicholas H. Oberlies. This chapter is intended for submission to *Journal of Natural Products* (2014).

Fourteen new resorcylic acid lactone analogues [greensporones A–N (**1-14**)], were isolated from an organic extract of a culture of a freshwater aquatic fungus *Halenospora* sp. The structures were elucidated using a set of spectroscopic and spectrometric techniques. The absolute configuration of one representative member of the compounds (**7**) was assigned using X-ray crystallography of an analogue that incorporated a heavy atom, while for compounds **8-11**, a modified Mosher's ester method was utilized. The relative configurations of compounds (**12-14**) were determined on the basis of NOE data. Compounds **12-14** were proposed as artifacts produced by intramolecular cycloetherification of ϵ -hydroxy- α,β -unsaturated ketone moieties of parent compounds during the extraction and purification processes. Compounds (**1-14**) were evaluated as TAK1-TAB1 inhibitors, and as antimicrobials against a panel of bacteria and fungi.

Fungi are one the highly diverse organisms that exist on earth, though they are not well investigated.¹⁶⁸ For example, of the 1.5 M to 5.1 M estimated species of fungi in the planet,^{8,23,169} less than 100,000 have been described in the literature.^{170,171} Interestingly,

fungi from freshwater habitats, specifically ascomycetes that inhabit and decompose submerged woody and herbaceous organic matter in lotic and lentic habitats, represent an even less well-studied area of mycology, resulting in slightly more than 3,000 described species to date.¹⁴⁷ Freshwater fungi also represent an understudied source of bioactive secondary metabolites. Only a few studies have explored the natural products of freshwater fungi, resulting in the identification of about 125 compounds or less than 1% of the 14,000 compounds that have been characterized from fungi.^{148,149} Hence, our group has launched investigations of freshwater fungi^{98,99,172} as potential sources of new scaffolds for drug design and development.

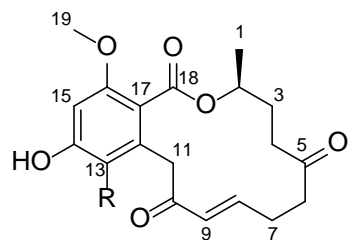
A freshwater fungus that was accessioned as G87 was sampled from submerged wood substrate in a stream on the campus of the University of North Carolina at Greensboro and was identified putatively as *Halenospora* sp., Helotiales, Leotiomycetes, Ascomycota. The organic extract exhibited promising toxicity in the brine shrimp test, and as a talented chemist, a series of fourteen new structurally related resorcylic acid lactones (RALs) were characterized [greensporones A–N (**1-14**)]. There has been growing interest in macrocycles in drug discovery due to their interesting biological activities and unique properties, including cell permeability and oral bioavailability.¹⁷³ Herein, we report the isolation, structure elucidation, and stereochemical assignment of compounds **1-14**. They were also evaluated as antimicrobials against a panel of bacteria and fungi. Moreover, as these polyketide derived metabolites were reported to be potent inhibitors of ATPases and kinases, including TAK1,^{141,142} they were examined as TAK1-TAB1 inhibitors, but found inactive.

Results and Discussion

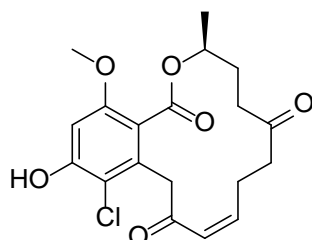
An organic extract [CHCl₃-MeOH (1:1)] of the G87 culture that was grown on rice was partitioned with 1:1 CH₃CN-MeOH and hexane. The resulting extract displayed promising toxicity in the brine shrimp test,^{49,174,175} 23% survival at 10 μg/mL, and hence was chosen for further investigations to explore its profile of secondary metabolites. The organic extract was fractionated using flash chromatography to afford five fractions. Of these, fractions 3 and 4 showed interesting HPLC profiles with PDA data indicating a series of structurally related compounds. Thus, these fractions were subjected to further purifications using preparative and semipreparative HPLC to yield fourteen compounds (**1-14**). The purity of the isolated compounds was measured by UPLC (Figure 86, Supporting Information).

Compound **1** (33.93 mg) was obtained as a colorless solid. The molecular formula was determined as C₁₉H₂₁O₆Cl by HRESIMS. The NMR, HRMS, and optical rotation data were similar to those for a recently reported RAL analogue, cryptosporiopsin A, described by Talontsi et al.¹⁷⁶ in 2012 from the culture of *Cryptosporiopsis* sp., an endophytic fungus from leaves and branches of *Zanthoxylum leprieurii* (Rutaceae). Although the planar structure between **1** and cryptosporiopsin A were identical, we have proposed a new name for **1** for two reasons. First, and as explained in more detail below, we have strong evidence that the absolute configuration for **1** at position 2 was *S*. In contrast, cryptosporiopsin A was drawn as *2R*; however, those authors did not discuss their reasoning for this conclusion, although it could be due to similarities they observed to ponchonin D.¹⁷⁶ Moreover, the trivial name proposed by those authors¹⁷⁶ was utilized

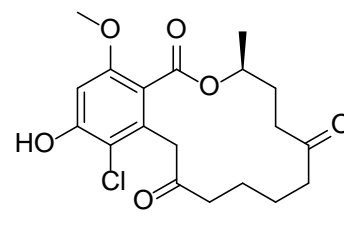
in 1969 for a structurally unrelated compound.^{20,21} As such, compound **1** was ascribed the new trivial name greensporone A.



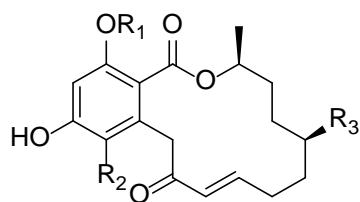
1: R = Cl
4: R = H



2



3



5: R₁ = CH₃ R₂ = H R₃ = H

6: R₁ = H R₂ = H R₃ = H

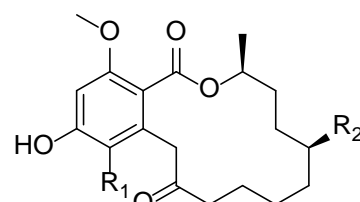
8: R₁ = CH₃ R₂ = Cl R₃ = OH

10: R₁ = CH₃ R₂ = H R₃ = OH

7: R₁ = H R₂ = H

11: R₁ = Cl R₂ = OH

9



5: R₁ = CH₃ R₂ = H R₃ = H

6: R₁ = H R₂ = H R₃ = H

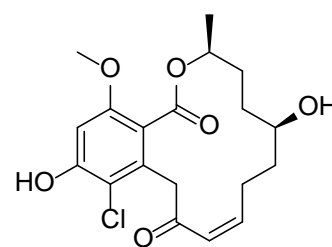
8: R₁ = CH₃ R₂ = Cl R₃ = OH

10: R₁ = CH₃ R₂ = H R₃ = OH

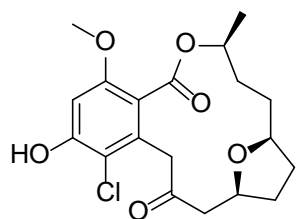
7: R₁ = H R₂ = H

11: R₁ = Cl R₂ = OH

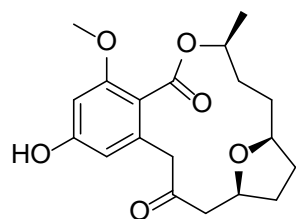
9



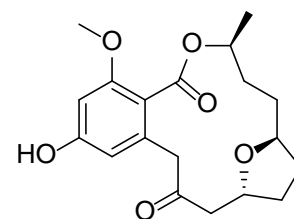
9



12



13



14

Figure 81. Structures of compounds **1-14**.

In addition to **1**, a series of structurally related RALs (**2-14**) that differ in the geometry and substitution pattern of the 14-membered macrocyclic lactone ring were isolated and structurally characterized by analyses of their HRMS and NMR data. Compound **2** (1.04 mg) was isolated as a colorless solid. The molecular formula was determined as C₁₉H₂₁O₆Cl, via HRESIMS along with ¹H, ¹³C, and edited-HSQC data (Tables 30 and 32; Figure 88, Supporting Information), establishing an index of hydrogen deficiency of 9. Analyses of the HRMS and NMR data suggested **2** as a RAL with structural similarity with **1**. For example, compound **2** showed two ketone carbonyls, δ_C 210.4 and 196.8 ppm for C-5 and C-10, respectively. The upfield shift of C-10 relative to C-5 indicated the conjugation of the C-10 ketone carbonyl with a double bond, resulting from an α,β -unsaturated ketone. Additional similarities included NMR signals characteristic of 6 aromatic carbons and one singlet aromatic proton, suggesting a pentasubstituted benzene ring, with two downfield shifted carbons (δ_C 153.3 and 156.6) indicating oxygenation as observed in **1**. Other substituents included a methoxy group, a methyl doublet ($J_{H3-1/H-2} = 6.3$ Hz), deshielded methylene protons ($J_{H-11a/H-11b} = 18.3$ Hz), and an ester group. ¹H-¹H COSY data identified two spin systems (H₃-1/H-2/H₂-3/H₂-4) and H₂-6/H₂-7/H-8/H-9) that were connected by the ketone carbonyl C-5, as supported by HMBC correlations (Figure 82). A key difference between compounds **1** and **2** was the geometry of C-8/C-9 double bond, being *Z* in **2** versus *E* in **1**, as evidenced by the coupling constants of the olefinic protons ($J_{H-8/H-9} = 11.5$ in **2** versus 16.0 Hz in **1**). All of the benzene ring and the macrocyclic lactone ring substituents were confirmed by HMBC

correlations (Figure 82). These data established the structure of **2**, being the *cis* analogue of **1**, and the trivial name greensporone B was ascribed.

Table 30. ^1H NMR Data (500 MHz) for 1-4 in CDCl_3 (Chemical Shifts in δ , Coupling Constants in Hz)

position	1	2	3	4
1	1.33, d (6.3)	1.30, d (6.3)	1.33, d (6.3)	1.36, d (6.3)
2	5.16, m	5.12, m	5.23, m	5.18, m
3	1.73, m	1.7, m	1.61, m	1.76, m
	1.97, m	1.89, m	2.14, m	2.01, m
4	2.42, dt (19.5, 6.3)	2.32, m	2.30, m	2.43, m
	2.57, m	2.56, m	2.62, m	2.67, m
6	2.47, m	2.36, m	2.25, m	2.47, m
	2.54, m	2.62, m	2.50, m	2.53, m
7	2.48, m	2.51, m	1.71, m	2.47, m
	2.54, m	3.85, m		2.56, m
8	6.88, ddd (16.0, 6.3, 2.9)	6.06, ddd (16.6, 11.5, 5.2)	1.51, m	6.79, m
			1.76, m	
9	6.06, d (16.0)	6.29, dd (11.5, 1.7)	2.41, ddd (16.0, 8.6, 2.9)	6.04, d (16.0)
			2.61, m	
11	3.84, d (16.0)	4.01, d (18.3)	3.90, d (18.3)	3.33, d (14.3)
	4.19, d (16.0)	4.11, d (18.3)	4.02, d (18.3)	4.31, d (14.3)
13				6.44, d (2.3)
15	6.58, s	6.58, s	6.56, s	6.31, d (2.3)
19	3.78, s	3.77, s	3.77, s	3.74, s
14-OH	6.02, br s	5.77, s	5.73, s	6.33, br s

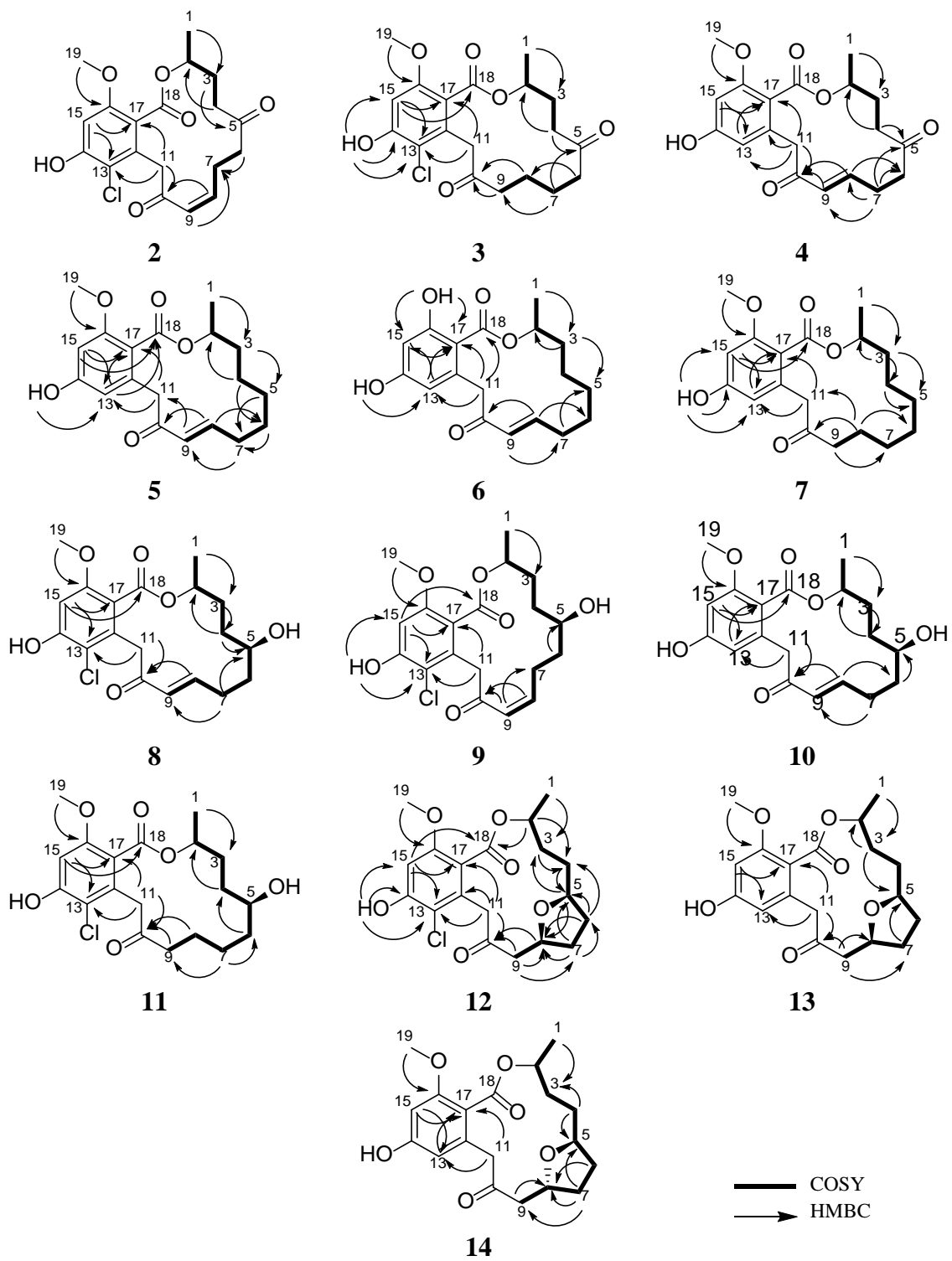


Figure 82. Key HMBC and COSY correlations of 2-14.

Compound **3** (1.15 mg), which was obtained as a colorless solid, had a molecular formula of $C_{19}H_{23}O_6Cl$ as evidenced by HRESIMS and analysis of 1H NMR, ^{13}C NMR and edited-HSQC data (Tables 30 and 32; Figure 89, Supporting Information). The HRMS and NMR data indicated **3** as a dihydro analogue of **1** as evidenced via a 2 amu difference in the HRMS data and by replacement of the H-8 and H-9 olefinic protons in **1** by four aliphatic protons (δ_H 1.51/1.76 and 2.41/2.61 for H₂-8 and H₂-9, respectively). Lack of conjugation of the C-8/C-9 double bond with the ketone carbonyl in **3** resulted in a downfield shift of C-10 in **3** (δ_C 206.3) relative to **1** (δ_C 194.4). Further analyses of NMR data, including 1H - 1H COSY and HMBC experiments (Figure 82) yielded the structure of **3**, which was ascribed the trivial name greensporone C.

Compound **4** (2.06 mg) was obtained as a colorless solid with a molecular formula of $C_{19}H_{22}O_6$ as evidenced by HRESIMS and analysis of 1H NMR, ^{13}C NMR and edited-HSQC data (Tables 30 and 32; Figure 90, Supporting Information). The HRMS and NMR data indicated **4** as a dechlorinated analogue of **1**, as evidenced by both the absence of the characteristic isotopic pattern of the chlorine in the HRMS data of **4**, and the appearance of an extra aromatic proton (δ_H 6.44) in the 1H NMR spectrum of **4** that based on coupling constant ($J_{H-13/H-15} = 2.3$ Hz) was *meta* coupled to H-15 (δ_H 6.31). Analyses of NMR spectra, including 1H - 1H COSY and HMBC data (Figure 82), yielded the structure of **4**, which was ascribed the trivial name greensporone D.

Compound **5** (22.66 mg) was also obtained as a colorless solid. The molecular formula was determined as $C_{19}H_{24}O_5$ via HRESIMS, establishing an index of hydrogen deficiency of 8. The NMR data suggested structural similarity with **4**. However, a key

difference was replacement of the C-5 ketone carbonyl in **4** (δ_C 209.9) by a methylene moiety ($\delta_C/\delta_H/\delta_H$ 25.6/1.31/1.39), which resulted in an extended ^1H - ^1H COSY spin system in **5** that spanned from H₃-1 to H-9. Further analyses of the NMR spectra, including HMBC data (Tables 31 and 32, Figure 82; Figure 91, Supporting Information) suggested the structure of **5**, which was given the trivial name greensporone E.

Compound **6** (1.81 mg), which was also obtained as a colorless solid, had a molecular formula of C₁₈H₂₂O₅ as determined by HRESIMS. The NMR data suggested structural similarity with **5** (Tables 31 and 32; Figure 92, Supporting Information). However, a key difference was replacement of the CH₃-19 (δ_C/δ_H 56.0/3.74) in **5** by a chelated phenolic proton (δ_H 11.76) in **6**, as supported by a 14 amu difference in the HRMS data. Analyses of the NMR spectra, including ^1H - ^1H COSY and HMBC data (Figure 82), established the structure of **6**, which was given the trivial name greensporone F.

Compound **7** (21.81 mg), which was isolated as a white solid, was identified as a dihydro derivative of **5**, as suggested by a 2 amu difference in the HRMS data. NMR data indicated replacement of the H-8 and H-9 olefinic protons in **5** by four aliphatic protons (δ_H 1.54/1.64 and 2.32/2.56 for H₂-8 and H₂-9, respectively) (Tables 31 and 32; Figure 93, Supporting Information). A downfield shift of C-10 in **7** (δ_C 211.1), relative to that of **5** (δ_C 199.5), was indicative of the lack of an α,β -unsaturated ketone carbonyl in **7**. These data, along with other NMR spectra, including ^1H - ^1H COSY and HMBC data (Figure 82), identified the structure of **7**, which was ascribed the trivial name greensporone G.

Table 31. ^1H NMR Data (500 MHz) for 5-8 in CDCl_3 (Chemical Shifts in δ , Coupling Constants in Hz)

position	5	6	7	8
1	1.32, d (6.3)	1.28, d (6.3)	1.30, d (6.3)	1.34, d (6.3)
2	5.15, m	5.13, m	5.23, m	5.08, m
3	1.58, m	1.50, m	1.60, m	1.74, m
	1.68, m	1.66, m		1.82, m
4	1.24, m	1.38, m	1.33 ^a , m	1.25, m
	1.51, m	1.50, m		1.75, m
5	1.31, m	1.45, m	1.21, m	3.55, m
	1.39, m		1.36, m	
6	1.56, m	1.68, m	1.34 ^a , m	1.61, m
				1.83, m
7	2.23, m	2.25, m	1.25, m	2.25, m
		2.35, m		
8	6.85, dt (16.0, 7.5)	7.06, dt (16.0, 7.5)	1.54, m	6.78, ddd (15.5, 9.2, 6.9)
9	6.10, d (16.0)	6.17, d (16.0)	2.32, m	6.08, d (15.5)
			2.56, m	
11	3.44, d (14.9)	3.92, d (17.2)	3.48, d (17.8)	3.85, d (17.2)
	4.34, d (14.9)	4.39, d (17.2)	4.29, d (17.8)	4.21, d (17.2)
13	6.47, d (2.3)	6.15, d (2.3)	6.17, d (2.3)	
15	6.31, d (2.3)	6.32, d (2.3)	6.19, d (2.3)	6.59, s
19	3.74, s		3.71, s	3.80, s
14-OH	7.89, br s	6.16, s	7.25, br s	5.86, s
16-OH		11.76, s		

^aSignals may be interchanged

Table 32. ^{13}C NMR Data (125 MHz) for 1-7 in CDCl_3 (Chemical Shifts in δ)

position	1	2	3	4	5	6	7
1	20.3	19.8	20.3	20.5	20.6	20.3	20.5
2	71.8	71.6	71.4	71.2	71.3	73.9	70.9
3	28.5	28.5	28.7	28.5	34.9	34.6	34.9
4	39.8	34.1	35.6	39.4	23.3	23.8	26.3 ^b
5	210.0	210.4	211.3	209.9	25.6	28.3	22.4
6	40.8	43.0	42.8	40.5	25.8	25.8	25.5 ^a
7	29.0	24.8	22.9	28.6	30.9	33.1	25.4
8	146.4	147.2	23.2	147.1	150.5	150.3	23.3
9	129.9	127.1	41.3	130.7	129.9	129.7	41.8
10	194.7	196.8	206.3	198.0	199.6	198.1	211.1
11	42.7	45.9	44.7	43.7	44.1	47.2	46.3
12	132.1	131.6	131.8	135.0	135.0	139.0	133.8
13	113.6	113.0	112.8	109.6	109.5	113.3	110.3
14	153.7	153.3	153.2	158.4	159.1	160.8	158.6
15	99.1	99.1	98.9	98.5	98.7	103.1	98.6
16	157.0	156.6	156.7	159.5	159.6	165.6	159.0
17	117.9	118.4	118.8	116.1	115.8	106.1	116.1
18	167.2	167.0	167.4	168.1	168.5	170.8	168.7
19	56.2	56.2	56.2	56.0	56.0	---	55.7

^aSignals may be interchanged

Compound **8** (2.40 mg) was obtained as a colorless solid with a molecular formula of $\text{C}_{19}\text{H}_{23}\text{O}_6\text{Cl}$ as determined via HRESIMS and analysis of ^1H NMR, ^{13}C NMR and edited-HSQC data (Tables 31 and 35; Figure 94, Supporting Information). The NMR data suggested structural similarity with **1**. However, a key difference was replacement of the C-5 ketone carbonyl (δ_{C} 210.0) in **1** by a carbinol carbon in **8** as evidenced from the NMR chemical shift values ($\delta_{\text{H}}/\delta_{\text{C}}$ 69.1/3.55) and a 2 amu difference in the HRMS data.

Further analyses of NMR spectra, including the extended ^1H - ^1H COSY spin system from H₃-1 to H-9 and HMBC data (Figure 82), established the structure of **8**, to which the trivial name greensporone H was ascribed.

Table 33. ^1H NMR Data (500 MHz) for 9-11 (Chemical Shifts in δ , Coupling Constants in Hz)

position	9 ^a	10 ^b	11 ^a
1	1.30, d (6.3)	1.21, d (5.7)	1.33, d (6.3)
2	5.13, m	4.91, m	5.24, m
3	1.75, m	1.51, m 1.76, m	1.69, m
4	1.11, m 1.66, m	1.06, m 1.52, m	1.24, m 1.61, m
5	3.48, m	3.35, m	3.70, m
6	1.61, m 1.77, m	1.41, m 1.68, m	1.47, m 1.56, m
7	2.12, m 3.48, m	2.15, m	1.37, m
8	6.08, ddd (16.0, 11.5, 4.6)	6.64, ddd (16.0, 8.0, 7.5)	1.53, m 1.75, m
9	6.30, dd (11.5, 1.7)	5.95, d (16.0)	2.29, ddd (13.8, 9.7, 3.4) 2.66, ddd (13.8, 8.6, 2.9)
11	4.03, d (18.3) 4.16, d (18.3)	3.36, d (16.0) 4.03, d (16.0)	3.88, d (18.3) 4.25, d (18.3)
13		6.25, d (2.3)	
15	6.58, s	6.35, d (2.3)	6.56, s
19	3.77, s	3.68, s	3.77, s
5-OH	1.2 br. s	4.48, br. s	3.76
14-OH	5.80, s	9.99, br. s	5.87, s
	^a In CDCl ₃		
	^b In DMSO		

Compound **9** (1.16 mg) was also isolated as a colorless solid. The molecular formula was determined as C₁₉H₂₃O₆Cl via HRESIMS, same as that of greensporone H (**8**). Analyses of the HRMS and NMR data suggested **9** as a geometric isomer of **8**, in reference to the C-8/C-9 double bond, having a *Z*-configuration in **9** versus an *E*-configuration in **8**, supported by the coupling constants of the olefinic protons ($J_{\text{H-8/H-9}} = 11.5$ Hz in **9** vs. 15.5 Hz in **8**) (Tables 33 and 35; Figure 95, Supporting Information). All other substituents, including the benzene ring and the macrocyclic lactone ring substituents, were confirmed by analyses of the ¹H-¹H COSY and HMBC data (Figure 82), establishing the structure of **9**, to which the trivial name greensporone I was ascribed.

Compound **10** (13.21 mg) was obtained as a white solid. HRESIMS and analysis of ¹H NMR, ¹³C NMR and edited-HSQC data suggested a molecular formula of C₁₉H₂₄O₆ (Tables 33 and 35; Figure 96, Supporting Information). The HRMS and NMR data designated **10** as a dechlorinated analogue of **8**, as evidenced by a 34 amu difference in the HRMS data and absence of the characteristic isotopic pattern of the chlorine. ¹H NMR data of **10** relative to **8** indicated an extra aromatic proton ($\delta_{\text{H}} 6.25$, $J = 2.3$ Hz), which was *meta* coupled to H-15 ($\delta_{\text{H}} 6.35$, $J = 2.3$ Hz). Further analyses of the NMR spectra including ¹H-¹H COSY and HMBC data (Figure 82), suggested the structure of **10**, which was ascribed the trivial name greensporone J.

Compound **11** (4.0 mg), which was isolated as a white solid, was identified as a dihydro derivative of **8** as evidenced by a 2 amu difference in the HRMS data. NMR data indicated replacement of the H-8 and H-9 olefinic protons in **8** by four aliphatic protons

(δ_{H} 1.53/1.75 and 2.29/2.66 for H₂-8 and H₂-9, respectively). A downfield shift of C-10 in **11** (δ_{C} 205.9) relative to that of **8** (δ_{C} 195.1) was indicative of the lack of conjugation of the C-8/C-9 double bond with the ketone carbonyl. These data along with other NMR data including ¹H-¹H COSY and HMBC experiments (Figure 82) identified the structure of **11**, which was ascribed the trivial name greensporone K.

Compound **8** underwent chemical changes in CDCl₃ solution resulted in the formation of compound **12**, which was obtained as a colorless solid. The molecular formula was determined as C₁₉H₂₃O₆Cl via HRESIMS along with ¹H, ¹³C, and edited-HSQC data (Tables 34 and 35; Figure 98, Supporting Information), establishing an index of hydrogen deficiency of 9. Analyses of the HRMS and NMR data suggested **2** as a RAL with structural similarity with **8**, sharing the same molecular formula. Key differences were the lack of the α,β -conjugated double bond in **12**, as evidenced by a downfield shift of the ketone carbonyl (δ_{C} 203.9) relative to **8** (δ_{C} 195.1), and the replacement of the C-8 and C-9 olefinic protons in **8** by three aliphatic protons in **12** ($\delta_{\text{C}}/\delta_{\text{H}}$ 76.3/4.32 and 46.6/2.53/2.81 for CH-8 and CH₂-9, respectively), suggesting oxygenation of C-8 in **12**. Another key difference was the downfield shift of C-5/H-5 in **12** ($\delta_{\text{C}}/\delta_{\text{H}}$ 79.3/3.79) relative to **8** ($\delta_{\text{C}}/\delta_{\text{H}}$ 69.1/3.55). Key HMBC correlations included H₂-6 to C-4 and C-8; H₂-7 to C-5, H₂-9 to C-7 and C-10; and H-8 to C-5 and C-10 (Figure 82). ¹H-¹H COSY identified one extended spin system H₃-1/H-2/H₂-3/H₂-4/H-5/H₂-6/H₂-7/H-8/H₂-9 (Figure 82). These data suggested a C-5 to C-8 tetrahydrofuran ring in **12** relative to **8**. The observed NOESY correlations between H-5/H-8 and H-2/H-5 indicated a *cis*-THF ring, thereby establishing the relative configuration at C-5 and C-8

(Figure 83). These data established the structure of **12**, to which the trivial name greensporone L was ascribed. We believe that **12** was produced by intramolecular cycloetherification of the ε -hydroxy- α,β -unsaturated ketone moiety in **8** (Figure 103, Supporting Information).

Table 34. ^1H NMR Data (500 MHz) for 12-14 (Chemical Shifts in δ , Coupling Constants in Hz)

position	12	13	14
1	1.32, d (6.2)	1.32, d (6.3)	1.32, d (6.9)
2	5.21, m	5.26, m	5.41, m
3	1.72, m	1.83, m	1.62, m
	1.90, m		2.33, m
4	1.38, m	1.51, m	1.48, m
	1.79, m	1.96, m	1.92, m
5	3.79, m	3.81, m	3.99, tdd (10.3, 4.6, 2.3)
6	1.55, m	1.50, m	1.30, m
	2.02, m		1.89, m
7	1.75, m	1.65, m	1.57, m
	1.91, m	1.94, m	2.10, m
8	4.33, m	4.14, m	4.27, qd (8.6, 2.9)
9	2.53, dd (13.5, 6.9)	2.55, dd (13.2, 8.0)	2.27, m
	2.81, dd (13.5, 4.6)	2.62, dd (13.2, 3.4)	2.49, dd (12.0, 8.6)
11	3.99, d (18.5)	3.90, d (17.2)	3.55, d (16.0)
	4.13, d (18.5)	3.99, d (17.2)	4.21, d (16.0)
13		6.25, d (2.3)	6.10, d (2.3)
15	6.59, s	6.34, d (2.3)	6.34, d (2.3)
19	3.77, s	3.77, s	3.78, s
14-OH	5.70, s	5.62, br. s	6.07, br. s

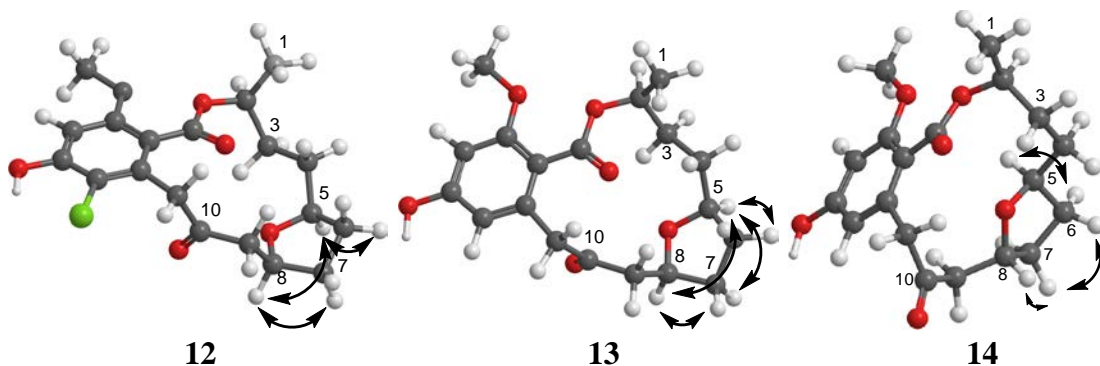


Figure 83. Key NOESY correlations of **12-14**.

Compound **13** (1.42 mg) was obtained as a white solid. HRESIMS and analysis of ^1H NMR, ^{13}C NMR and edited-HSQC data suggested a molecular formula of $\text{C}_{19}\text{H}_{24}\text{O}_6$ (Tables 34 and 35; Figure 99, Supporting Information). The HRMS and NMR data suggested **13** as a dechlorinated analogue of **12**, as evidenced by a 34 amu difference in the HRMS data of **13** and absence of the characteristic isotopic pattern of the chlorine atom. ^1H NMR data of **13** relative to **12** indicated an extra aromatic proton (δ_{H} 6.25) that was *meta* coupled to H-15 (δ_{H} 6.34) ($J_{\text{H-13/H-15}} = 2.3$ Hz). Further analyses of NMR data, including ^1H - ^1H COSY and HMBC data (Figure 82), suggested the structure of **13**, which was ascribed the trivial name greensporone M. Similar to **12**, NOESY correlations between H-5 and H-8 supported a *cis*-THF ring (Figure 83). As for **12**, compound **13** was likely an artifact produced by intramolecular cycloetherification of the ϵ -hydroxy- α,β -unsaturated ketone moiety in **10** during the extraction and purification processes. To test this hypothesis, an aliquot of **10** was suspended (not soluble) in CDCl_3 and a proton NMR spectrum was collected, a poor signal was obtained due to the insolubility issue. The NMR tube was left to stand at room temperature for few days, then another proton

NMR spectrum was collected. The NMR spectrum showed signals of good intensity that matched those of **13** (Figure 100, Supporting Information).

Table 35. ^{13}C NMR Data (175 MHz) for **12** and (125 MHz) for **8-11** and **13-14** in CDCl_3 (Chemical Shifts in δ)

position	8	9	10 ^a	11	12	13	14
1	20.1	19.9	20.1	20.3	21.5	20.9	18.3
2	71.3	71.0	69.3	70.8	73.4	72.7	72.3
3	31.0	31.0	30.2	30.7	33.8	33.0	30.1
4	29.4	29.1	29.2	29.8	34.7	31.3	30.0
5	69.1	69.0	66.1	68.7	79.3	79.5	77.2
6	35.0	36.7	34.6	36.1	31.6	33.5	33.5
7	28.8	24.3	28.2	23.2	29.8	30.5	32.2
8	147.7	148.3	148.2	23.7	76.3	76.1	76.5
9	128.1	127.1	128.4	41.7	46.6	47.9	47.2
10	195.1	196.7	195.9	205.9	203.9	207.7	210.1
11	44.2	45.7	44.6	44.3	48.6	49.0	48.6
12	132.6	131.7	135.6	131.8	132.1	134.2	134.3
13	113.4	112.9	109.7	113.4	113.1	109.2	108.1
14	153.7	153.2	159.8	153.4	153.3	157.7	158.0
15	99.2	100.0	98.5	99.0	99.1	98.3	98.3
16	157.6	156.6	159.2	157.0	157.0	159.0	158.8
17	118.2	118.5	114.1	118.2	119.2	117.3	118.0
18	167.1	167.6	167.3	167.7	166.9	167.7	167.8
19	56.3	56.1	55.9	56.1	56.4	56.0	56.0

^aIn DMSO

Compound **14** (1.80 mg) was obtained as a white solid. HRESIMS and analysis of ^1H NMR, ^{13}C NMR and edited-HSQC data suggested a molecular formula of $\text{C}_{19}\text{H}_{24}\text{O}_6$ (Tables 34 and 35; Figure 101, Supporting Information). The HRMS and NMR data

suggested structural similarity to **13**, both sharing the same molecular formula and the same planar structure, as evidenced from analyses of the 2D NMR data of **14**, including ^1H - ^1H COSY and HMBC spectra (Figure 82). However, a key difference was the absence of the H-5 to H-8 NOESY correlations in **14** relative to **13**. This observation was supported by NOESY correlations observed from H-8 to H-7b, H-7b to H-6a, and H-5 to H-6b, indicating that H-8, H-7b, and H-6a were on the same phase of the tetrahydrofuran ring (Figure 83). Hence, **14** and **13** differed in the spacial arrangement of the tetrahydrofuran ring, being *cis* in **13** versus *trans* in **14**. The trivial name greensporone N was ascribed to compound **14**.

The absolute configuration of the stereogenic center in **7** was established as *2S* by single-crystal X-ray diffraction analysis of the bromobenzoyl derivative (compound **15**, Figure 84, Figure 102, Supporting Information). The configuration of the C-2 asymmetric carbon in compounds **1-6** and **8-14** was proposed to be analogous to that of **7**; as described below, this supposition was supported by Mosher's esters in compounds **8-11**. The known greensporone A (**1**) [cryptosporiopsin A] was reported to have a *2R* configuration¹⁷⁶ by analogy to ponchonin D;¹⁷⁷ however, no direct measurements were made to confirm this. The RAL analogues identified in this study were structurally related to the well-known RAL monorden (*synonym* radicicol)^{178,179} and its analogues pochonins A-F¹⁷⁷ and K-P.¹⁸⁰ For monorden, single crystal X-ray diffraction via analysis of the anomalous scattering established the configuration of the CH₃ (C-2) as *R*.¹⁷⁹ However, optical rotation data comparison with monorden¹⁷⁷ and ^1H - ^1H coupling

constants and NOESY data analysis was used to assign the relative stereochemistry of pochonins.¹⁸⁰

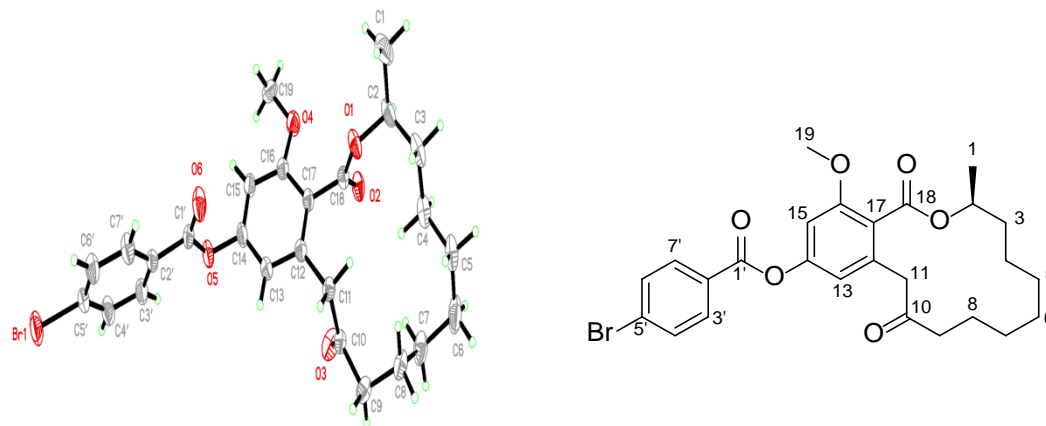


Figure 84. X-ray crystallographic structure of 14-(4-bromobenzoyl)greensporone G (**15**).

For compounds **8-11**, NOESY correlations were observed from H-2 to H-5, indicating that those pair of protons was on the same face of the macrocycle ring. The absolute configurations of **8-11** were assigned via a modified Mosher's ester method,⁶⁸ establishing the configurations as 2*S* and 5*S* (Figure 85). It is worth pointing out that due to the instability of compound **8** in solution, i.e. tendency to undergo intramolecular cycloetherification of the ϵ -hydroxy- α,β -unsaturated ketone moiety, the ¹H-NMR peaks corresponding to the (*S*)- and (*R*)-MTPA esters of **8** were of low intensity and we were unable to recognize the chemical shifts of other than H-2 and H-9.

Compounds (**1-14**) were evaluated as TAK1-TAB1 inhibitors using 5*Z*-7-oxozeaenol¹⁹ as a positive control and as antimicrobials against a panel of bacteria and fungi and were found inactive. Although inactive as TAK1-TAB1 inhibitors, the data

obtained extended our understanding of the structure activity relationship of the RAL family of compounds.

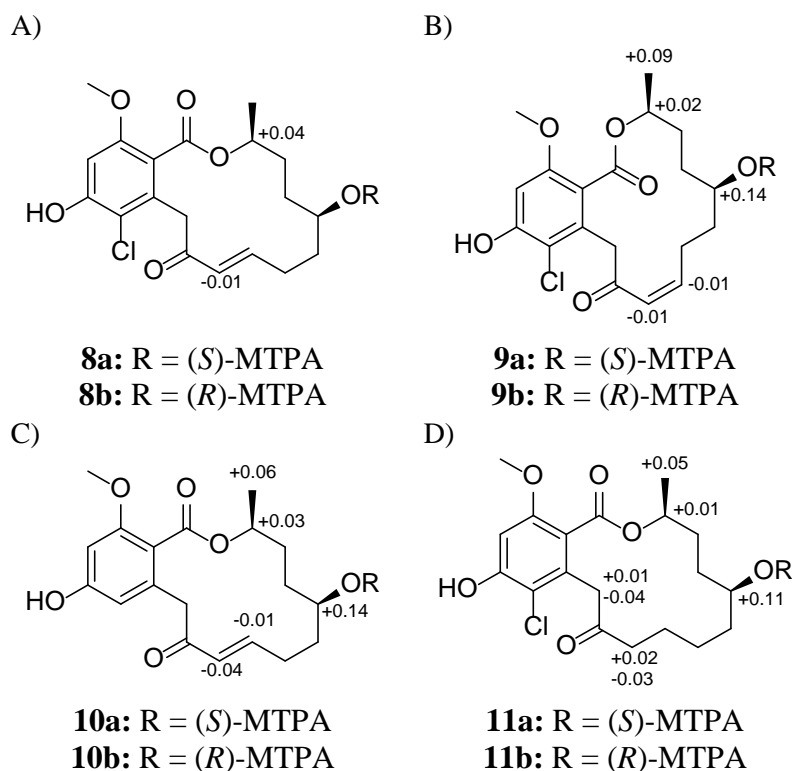


Figure 85. $\Delta\delta_{\text{H}}$ values [$\Delta\delta$ (in ppm) = $\delta_{\text{S}} - \delta_{\text{R}}$] obtained for (*S*)- and (*R*)-MTPA esters A) **8a** and **8b**, respectively of green sporone H (**8**), B) **9a** and **9b**, respectively of green sporone I (**9**), C) **10a** and **10b**, respectively of green sporone J (**10**), and D) **11a** and **11b**, respectively of green sporone K (**11**) in pyridine-*d*₅.

In conclusion, fourteen new RALs (**1-14**) were isolated and characterized from the freshwater fungus *Halenospora* sp. The absolute configuration of compound **7** was assigned using X-ray crystallography of an analogue that incorporated a heavy atom. NOE data were used to assign the relative configuration of compounds (**12-14**). While for compounds **8-11**, a modified Mosher's ester method was used. The current study proved

the importance of the freshwater fungi, a highly underexplored natural resource, as a rich source of new scaffolds for drug design and development.

Experimental Section

General Experimental Procedures. UV data were obtained using a Varian Cary 100 Bio UV-Vis spectrophotometer (Varian Inc., Walnut Creek, CA, USA). NMR data were collected using either a JEOL ECA-500 NMR spectrometer operating at 500 MHz for ^1H and 125 MHz for ^{13}C , (JEOL Ltd., Tokyo, Japan), or an Agilent 700 MHz NMR spectrometer (Agilent Technologies, Inc., Santa Clara, CA, USA), equipped with a cryoprobe, operating at 700 MHz for ^1H and 175 MHz for ^{13}C . Residual solvent signals were utilized for referencing. High resolution mass spectra (HRMS) were measured using a Thermo LTQ Orbitrap XL mass spectrometer equipped with an electrospray ionization source (Thermo Fisher Scientific, San Jose, CA, USA). A Waters Acquity UPLC system (Waters Corp., Milford, MA, USA) utilizing a Phenomenex Kinetex C_{18} column (1.3 μm ; 50 \times 2.1 mm) was used to evaluate the purity of the isolated compounds with data collected and analyzed using Empower 3 software. Phenomenex Gemini-NX C_{18} analytical (5 μm ; 250 \times 4.6 mm), preparative (5 μm ; 250 \times 21.2 mm), and semipreparative (5 μm ; 250 \times 10.0 mm) columns (all from Phenomenex, Torrance, CA, USA) were used on a Varian Prostar HPLC system equipped with ProStar 210 pumps and a Prostar 335 photodiode array detector (PDA), with data collected and analyzed using Galaxie Chromatography Workstation software (version 1.9.3.2, Varian Inc.). Flash chromatography was performed on a Teledyne ISCO CombiFlash Rf 200 using Silica Gold columns (both from Teledyne Isco, Lincoln, NE, USA) and monitored by UV and

evaporative light-scattering detectors. X-ray crystallography data were acquired using a Bruker APEX CCD diffractometer (MoK α radiation, graphite monochromator). All other reagents and solvents were obtained from Fisher Scientific and were used without further purification.

Fungal Strain Isolation and Identification. The fungal strain, G87, was isolated from a sample of submerged wood collected in July of 2011 from a freshwater stream at the campus of the University of North Carolina in Greensboro, North Carolina, USA (36°4' 16"N, 79°48' 28"W). A culture of strain G87 is preserved in the Department of Chemistry and Biochemistry culture collection at the University of North Carolina at Greensboro. The culture is stored on a potato dextrose agar slant with periodic transfer. Previously outlined collection methods and culturing conditions were followed.^{161,162} Molecular identification of strain G87 was carried out by sequencing the internal transcribed spacer regions 1 & 2 and 5.8S nrDNA (ITS)⁴⁵ along with the D1 and D2 regions of the 28S nuclear ribosomal large subunit rRNA gene (LSU).^{95,181} DNA extraction, PCR amplification, and sequencing were performed according to previously published procedures.^{63,81,97-99} A BLAST search in GenBank using the complete ITS rDNA sequence showed 98% sequence similarity of the strain G87 with several members of the Leotiomycetes, Ascomycota. In particular, strain G87 showed sequence homology with a number of sequences belonging to *Halenospora varia* (Anastasiou) E.B.G. Jones¹⁸² (GenBank KF156329; Identities = 474/483 (98%); Gaps = 0/483 (0%), *Halenospora varia*; GenBank AJ608987; Identities = 524/534 (98%); Gaps = 1/534 (0%), *Zalerion varium* (= *Halenospora varia*). *Zalerion varium* was originally placed in

the genus *Zalerion* (Lulworthiales, Ascomycota). However, based on ITS data, Bills and colleagues¹⁸³ found that *Z. varium* had phylogenetic affinities to the Leotiaceae, while the type species *Z. maritima* belonged to the Lulworthiales. Jones and colleagues¹⁸² subsequently transferred *Z. varium* to a new genus *Halenospora varia*, Leotiomyces, Ascomycota. Fungal strain G87 also showed 97-98% sequence similarity in ITS data to several other genera of aquatic fungi such as *Spirosphaera*, *Tricladium*, *Lambertella*, *Mycofalcella*. To better understand the phylogenetic affinities of G87 to these taxa in the Leotiomyces, a phylogenetic analysis using Maximum Likelihood was employed using combined ITS-LSU data for strain G87, along with sequences downloaded from top hits in the BLAST search using RAxML v. 7.0.4¹⁸⁴ run on the CIPRES Portal v. 2.0¹⁸⁵ with the default rapid hill-climbing algorithm and GTR model employing 1000 fast bootstrap searches. Clades with bootstrap values $\geq 70\%$ were considered significant and strongly supported.¹⁸⁶ Results of both BLAST and phylogenetic analysis suggested strain G87 to show affinities with *H. varia*, which resides in Clade 7 sensu Baschien and coworkers.¹⁸⁷ However, there was no significant support for G87 clustering with isolates of *H. varia* (Figure 104, Supporting Information). Based on these data, G87 is identified putatively as *Halenospora* aff. *varia*, Helotiales, Leotiomyces, Ascomycota. The combined ITS and LSU sequence will be deposited in the GenBank (accession no XXX).

Fermentation, Extraction and Isolation. A fresh culture of strain G87 was prepared in a slant and was inoculated into a 50 mL culture tube containing a seed liquid culture consisting of 2% MEA, potato dextrose agar (PDA, Difco), and YESD media. The culture tube was shaken at room temperature using a rotary shaker at 125 rpm until

the fungal strain showed good growth typically within 14 to 21 days. Afterwards, the seed culture was used to inoculate a 250 mL Erlenmeyer flask containing 30 mL of autoclaved rice medium, prepared using 10 g of rice and twice the volume of rice with H₂O. Fermentation was carried out by incubating the flask at 22 °C until showing good growth (approximately 14 days). Large scale cultures were prepared by the parallel processing of four such cultures in quadruplicates.

To each of the four small-scale solid fermentation cultures that constitute a large-scale culture of G87, 60 mL of 1:1 MeOH-CHCl₃ were added. The cultures were broken down into small pieces with a spatula and shaken using a rotary shaker overnight (~16 h) at ~125 rpm at room temperature. The samples were filtered with vacuum, and the remaining residues were washed with small volumes of 1:1 MeOH-CHCl₃. To the combined filtrates, 360 mL CHCl₃ and 360 mL H₂O were added; the mixture was stirred for 30 min and then transferred into a separatory funnel. The organic layer was evaporated to dryness under reduced pressure. The obtained organic extract was partitioned between 100 mL of 1:1 MeOH-CH₃CN and 100 mL of hexanes. The MeOH-CH₃CN layer was evaporated to dryness in vacuum. The defatted extract (~439 mg) was dissolved in a mixture of CHCl₃-MeOH, adsorbed onto Celite 545, and fractionated via flash chromatography using a gradient solvent system of hexane-CHCl₃-MeOH at a 30 mL/min flow rate and 61.0 column volumes over 34.1 min to afford five fractions. Fraction 3 (153.25 mg) was subjected to preparative HPLC using a gradient system of 40:60 to 60:40 of CH₃CN-H₂O (acidified with 0.1% formic acid) over 30 min at a flow rate of 21.24 mL/min to yield fifteen sub-fractions. Sub-fractions 4, 5, 7, 10, 12, and 13

yielded compounds **1** (19.65 mg), **2** (1.95 mg), **3** (1.28 mg), **5** (27.73 mg), **6** (2.95 mg), and **7** (30.24 mg), which eluted at ~9.8, 11.5, 13.5, 20.5, 22.7, and 23.5 min, respectively. Fraction 4 (99.72 mg) was subjected to preparative HPLC using a gradient system of 20:80 to 40:60 of CH₃CN-H₂O (acidified with 0.1% formic acid) over 40 min to 60:40 over 10 min at a flow rate of 21.24 mL/min to yield nineteen sub-fractions. Sub-fractions 3, 9, 11, 12 and 16 yielded compounds **10** (18.74 mg), **8** (5.17 mg), **11** (6.35 mg), **13** (1.42 mg) and **14** (1.80 mg), which eluted at 19.0, 25.0, 57.5, 28.5 and 37.3 min, respectively. Subfraction 10 (6.65 mg), which eluted at 26.0 min was subjected to further preparative HPLC purification using a gradient system of 50:50 to 60:40 of MeOH-H₂O (acidified with 0.1% formic acid) over 15 min at a flow rate of 21.24 mL/min to yield compounds **4** (2.06 mg) and **9** (1.16 mg), which eluted at ~8.3 and 9.7 min, respectively.

The isolated compounds, except for compounds **4**, **9**, and **12**, were further purified by preparative and semipreparative HPLC to generate material of high purity for biological evaluation using a mobile phase of MeOH-H₂O (acidified with 0.1% formic acid) at different gradient systems to yield compounds **1** (13.93 mg), **2** (1.04 mg), **3** (1.15 mg), **5** (22.66 mg), **6** (1.81 mg), **7** (21.81 mg), **8** (2.40 mg), **10** (13.21 mg), **11** (4.0 mg), **13** (2.55 mg), and **14** (2.78 mg).

Greensporone A (1): colorless solid; $[\alpha]_{\text{D}}^{20} = +5.0^{\circ}$ ($c = 0.20$, MeOH); $[\alpha]_{\text{D}}^{20} = -24.6^{\circ}$ ($c = 0.26$, Chloroform); UV (MeOH) λ_{max} (log ϵ) 293 (3.32), 233 (3.70) nm; ¹H NMR (CDCl₃, 500 MHz) and ¹³C NMR (CDCl₃, 125 MHz), see Tables 79 and 81; HRESIMS m/z 381.1090 [M + H]⁺ (calcd for C₁₉H₂₂O₆³⁵Cl 381.1099) and 383.1061 [M + H]⁺ (calcd for C₁₉H₂₂O₆³⁷Cl 383.1070).

Greensporone B (2): colorless solid; $[\alpha]_{\text{D}}^{20} = -37.5^{\circ}$ ($c = 0.10$, MeOH); UV (MeOH) λ_{max} (log ϵ) 292 (3.12), 225 (3.64) nm; ^1H NMR (CDCl_3 , 500 MHz) and ^{13}C NMR (CDCl_3 , 125 MHz), see Tables 30 and 32; HRESIMS m/z 381.1110 $[\text{M} + \text{H}]^+$ (calcd for $\text{C}_{19}\text{H}_{22}\text{O}_6^{35}\text{Cl}$ 381.1099) and 383.1059 $[\text{M} + \text{H}]^+$ (calcd for $\text{C}_{19}\text{H}_{22}\text{O}_6^{37}\text{Cl}$ 383.1070).

Greensporone C (3): colorless solid; $[\alpha]_{\text{D}}^{20} = +30.4^{\circ}$ ($c = 0.12$, MeOH); UV (MeOH) λ_{max} (log ϵ) 292 (3.25), 221 (3.62) nm; ^1H NMR (CDCl_3 , 500 MHz) and ^{13}C NMR (CDCl_3 , 125 MHz), see Tables 30 and 32; HRESIMS m/z 383.1267 $[\text{M} + \text{H}]^+$ (calcd for $\text{C}_{19}\text{H}_{24}\text{O}_6^{35}\text{Cl}$ 383.1256) and 385.12170 $[\text{M} + \text{H}]^+$ (calcd for $\text{C}_{19}\text{H}_{24}\text{O}_6^{37}\text{Cl}$ 385.1226).

Greensporone D (4): colorless solid; $[\alpha]_{\text{D}}^{20} = +55.7^{\circ}$ ($c = 0.10$, MeOH); UV (MeOH) λ_{max} (log ϵ) 287 (3.28), 234 (3.64) nm; ^1H NMR (CDCl_3 , 500 MHz) and ^{13}C NMR (CDCl_3 , 125 MHz), see Tables 30 and 32; HRESIMS m/z 347.1481 $[\text{M} + \text{H}]^+$ (calcd for $\text{C}_{19}\text{H}_{23}\text{O}_6$ 347.1489).

Greensporone E (5): colorless solid; $[\alpha]_{\text{D}}^{20} = +112.3^{\circ}$ ($c = 0.33$, MeOH); UV (MeOH) λ_{max} (log ϵ) 288 (3.32), 238 (3.65) nm; ^1H NMR (CDCl_3 , 500 MHz) and ^{13}C NMR (CDCl_3 , 125 MHz), see Tables 31 and 32; HRESIMS m/z 333.1711 $[\text{M} + \text{H}]^+$ (calcd for $\text{C}_{19}\text{H}_{25}\text{O}_5$ 333.1697).

Greensporone F (6): colorless solid; $[\alpha]_{\text{D}}^{20} = +29.8^{\circ}$ ($c = 0.09$, MeOH); UV (MeOH) λ_{max} (log ϵ) 302 (3.52), 263 (3.63), 237 (3.63) nm; ^1H NMR (CDCl_3 , 500 MHz)

and ^{13}C NMR (CDCl_3 , 125 MHz), see Tables 31 and 32; HRESIMS m/z 319.1553 $[\text{M} + \text{H}]^+$ (calcd for $\text{C}_{18}\text{H}_{23}\text{O}_5$ 319.1540).

Greensporone G (7): white solid; $[\alpha]_{\text{D}}^{20} = +79.5^\circ$ ($c = 0.29$, MeOH); UV (MeOH) λ_{max} ($\log \epsilon$) 286 (3.34), 252 (3.48), 224 (3.60) nm; ^1H NMR (CDCl_3 , 500 MHz) and ^{13}C NMR (CDCl_3 , 125 MHz), see Tables 31 and 32; HRESIMS m/z 335.1868 $[\text{M} + \text{H}]^+$ (calcd for $\text{C}_{19}\text{H}_{27}\text{O}_5$ 335.1853).

Greensporone H (8): colorless solid; $[\alpha]_{\text{D}}^{20} = -18.3^\circ$ ($c = 0.12$, MeOH); UV (MeOH) λ_{max} ($\log \epsilon$) 292 (3.34), 227 (3.61) nm; ^1H NMR (CDCl_3 , 500 MHz) and ^{13}C NMR (CDCl_3 , 125 MHz), see Tables 31 and 35; HRESIMS m/z 383.1273 $[\text{M} + \text{H}]^+$ (calcd for $\text{C}_{19}\text{H}_{24}\text{O}_6$ ^{35}Cl 383.1256) and 385.12195 $[\text{M} + \text{H}]^+$ (calcd for $\text{C}_{19}\text{H}_{24}\text{O}_6$ ^{37}Cl 383.1256).

Greensporone I (9): colorless solid; $[\alpha]_{\text{D}}^{20} = -31.9^\circ$ ($c = 0.12$, MeOH); UV (MeOH) λ_{max} ($\log \epsilon$) 292 (3.24), 230 (3.67) nm; ^1H NMR (CDCl_3 , 500 MHz) and ^{13}C NMR (CDCl_3 , 125 MHz), see Tables 33 and 35; HRESIMS m/z 383.1245 $[\text{M} + \text{H}]^+$ (calcd for $\text{C}_{19}\text{H}_{24}\text{O}_6$ ^{35}Cl 383.1256) and 385.1220 $[\text{M} + \text{H}]^+$ (calcd for $\text{C}_{19}\text{H}_{24}\text{O}_6$ ^{37}Cl 385.1226).

Greensporone J (10): white solid; $[\alpha]_{\text{D}}^{20} = +116.5^\circ$ ($c = 0.27$, MeOH); UV (MeOH) λ_{max} ($\log \epsilon$) 288 (3.33), 236 (3.64) nm; ^1H NMR (DMSO, 500 MHz) and ^{13}C NMR (DMSO, 125 MHz), see Tables 33 and 35; HRESIMS m/z 349.1657 $[\text{M} + \text{H}]^+$ (calcd for $\text{C}_{19}\text{H}_{25}\text{O}_6$ 349.1646).

Greensporone K (11): white solid; $[\alpha]_{\text{D}}^{20} = +26.0^{\circ}$ ($c = 0.20$, MeOH); UV (MeOH) λ_{max} (log ϵ) 292 (3.43), 226 (3.67) nm; ^1H NMR (CDCl_3 , 500 MHz) and ^{13}C NMR (CDCl_3 , 125 MHz), see Tables 33 and 35; HRESIMS m/z 385.1427 $[\text{M} + \text{H}]^+$ (calcd for $\text{C}_{19}\text{H}_{26}\text{O}_6^{35}\text{Cl}$ 385.1412) and 387.1374 $[\text{M} + \text{H}]^+$ (calcd for $\text{C}_{19}\text{H}_{26}\text{O}_6^{37}\text{Cl}$ 387.1383).

Greensporone L (12): colorless solid; $[\alpha]_{\text{D}}^{20} = +30.0^{\circ}$ ($c = 0.05$, MeOH); UV (MeOH) λ_{max} (log ϵ) 291 (3.34), 226 (3.60) nm; ^1H NMR (CDCl_3 , 700 MHz) and ^{13}C NMR (CDCl_3 , 175 MHz), see Tables 34 and 35; HRESIMS m/z 383.1268 $[\text{M} + \text{H}]^+$ (calcd for $\text{C}_{19}\text{H}_{24}\text{O}_6^{35}\text{Cl}$ 383.1256) and 385.1239 $[\text{M} + \text{H}]^+$ (calcd for $\text{C}_{19}\text{H}_{24}\text{O}_6^{37}\text{Cl}$ 385.1226).

Greensporone M (13): white solid; $[\alpha]_{\text{D}}^{20} = -30.7^{\circ}$ ($c = 0.11$, MeOH); UV (MeOH) λ_{max} (log ϵ) 286 (3.20), 248 (3.35), 224 (3.54) nm; ^1H NMR (CDCl_3 , 500 MHz) and ^{13}C NMR (CDCl_3 , 125 MHz), see Tables 34 and 35; HRESIMS m/z 349.1661 $[\text{M} + \text{H}]^+$ (calcd for $\text{C}_{19}\text{H}_{25}\text{O}_6$ 349.1646).

Greensporone N (14): white solid; $[\alpha]_{\text{D}}^{20} = +154.4^{\circ}$ ($c = 0.07$, MeOH); UV (MeOH) λ_{max} (log ϵ) 285 (3.17), 223 (3.55) nm; ^1H NMR (CDCl_3 , 500 MHz) and ^{13}C NMR (CDCl_3 , 125 MHz), see Tables 34 and 35; HRESIMS m/z 349.1661 $[\text{M} + \text{H}]^+$ (calcd for $\text{C}_{19}\text{H}_{25}\text{O}_6$ 349.1646).

14-(4-Bromobenzoyl)greensporone G (15): to a sample of compound **7** (7.7 mg, 1 eq.) dissolved in 1 mL anhydrous THF, 4-bromobenzoyl chloride (6.1 mg, 1.2 eq.) and DMAP (2.8 mg, 1 eq.) were added and the mixture was stirred at room temperature under

nitrogen. To enhance the solubility of the reagents, 0.3 mL anhydrous CH_2Cl_2 was added. The mixture was left stirring overnight and monitored for completion using TLC. The reaction mixture (16.8 mg) was purified via a reversed phase preparative HPLC using a Phenomenex Gemini-NX C_{18} (5 μm ; 250 \times 21.2 mm) column and a gradient system of 70:30 to 90:10 of $\text{CH}_3\text{CN}-\text{H}_2\text{O}$ (acidified with 0.1% formic acid) over 15 min at a flow rate of 21.24 mL/min to yield compound **15** (8.84 mg), which eluted at 17.3 min. ^1H NMR (CDCl_3 , 500 MHz) δ 8.02 (2H, d, $J = 8.6$), 7.65 (2H, d, $J = 8.6$), 6.74 (1H, d, $J = 2.3$), 6.67 (1H, d, $J = 2.3$), 5.27 (1H, m), 4.18 (1H, d, $J = 17.8$), 3.81 (3H, s), 3.61 (1H, d, $J = 17.8$), 2.55 (1H, ddd, $J = 13.2, 8.6, 4.6$), 2.33 (1H, ddd, $J = 13.2, 8.6, 4.6$), 1.71-1.51 (5H, m), 1.43-1.19 (7H, m), 1.34 (3H, d, $J = 6.3$) (Figure 102, Supporting Information). HRESIMS m/z 517.1205 $[\text{M} + \text{H}]^+$ (calcd for $\text{C}_{26}\text{H}_{30}^{79}\text{BrO}_6$ 517.1220) and 519.1185 $[\text{M} + \text{H}]^+$ (calcd for $\text{C}_{26}\text{H}_{30}^{81}\text{BrO}_6$ 519.1200).

Preparation of the (R)- and (S)-MTPA ester derivatives of greensporones H (8), I (9), J (10), and K (11): To 0.31, 0.20, 0.31, and 0.45 mg of compounds **8-11** were added 400 μL of pyridine- d_5 and transferred into an NMR tubes. To initiate the reactions, 20 μL of *S*-(+)- α -methoxy- α -(trifluoromethyl)phenylacetyl (MTPA) chloride were added into each NMR tube with careful shaking and then monitored immediately by ^1H NMR at the following time points 5, 10, and 15 min. The reactions completed within 5 min, yielding the mono (R)-MTPA ester derivatives (**8b**) of **8**, (**9b**) of **9**, (**10b**) of **10**, and (**11b**) of **11**. ^1H NMR data (500 MHz, pyridine- d_5) of **8b**: δ_{H} 6.13 (1H, m, H-2), 6.39 (1H, d, $J = 17.8$, H-9); of **9b**: 1.24 (3H, d, $J = 6.3$, H_3 -1), 5.13 (1H, m, H-2), 5.27 (1H, m, H-5), 6.13 (1H, td, $J = 12.0, 5.7$, H-8), and 6.42 (1H, d, $J = 12.0$, H-9); **10b**: 1.30 (3H,

d, $J = 6.3$, H₃-1), 5.22 (1H, m, H-2), 5.30 (1H, m, H-5), 6.97 (1H, dd, $J = 15.5, 7.5$, H-8), and 6.33 (1H, d, $J = 15.5$, H-9); **11b**: 1.28 (3H, d, $J = 6.3$, H₃-1), 5.36 (1H, m, H-2), 5.41 (1H, m, H-5), 2.37 (1H, m, H-9a), 2.79 (1H, m, H-9b), 4.19 (1H, d, $J = 18.9$, H-11a), and 4.39 (1H, $J = 18.9$, H-11b). In an analogous manner, 0.31, 0.20, 0.31, and 0.45 mg of compounds **8-11** dissolved in 400 μL pyridine-*d*₅ were reacted in NMR tubes with 20 μL (*R*)-(-)-*a*-MTPA chloride for 15 min, to afford the mono (*S*)-MTPA esters (**8a**, **9a**, **10a**, and **11a**). ¹H NMR data (500 MHz, pyridine-*d*₅) of **8a**: δ_{H} 6.17 (1H, m, H-2), 6.38 (1H, d, $J = 17.8$, H-9); of **9a**: 1.32 (3H, d, $J = 6.3$, H₃-1), 5.15 (1H, m, H-2), 5.41 (1H, m, H-5), 6.12 (1H, dd, $J = 12.0, 4.0$, H-8), and 6.41 (1H, d, $J = 12.0$, H-9); **10a**: 1.36 (3H, d, $J = 6.3$, H₃-1), 5.25 (1H, m, H-2), 5.44 (1H, m, H-5), 6.96 (1H, dd, $J = 15.5, 7.5$, H-8), and 6.29 (1H, d, $J = 15.5$, H-9); **11a**: 1.33 (3H, d, $J = 6.3$, H₃-1), 5.37 (1H, m, H-2), 5.52 (1H, m, H-5), 2.39 (1H, m, H-9a), 2.76 (1H, m, H-9b), 4.20 (1H, d, $J = 18.9$, H-11a), and 4.35 (1H, $J = 18.9$, H-11b).

X-ray Crystallography. Crystallographic data for compound **15** will be deposited with the Cambridge Crystallographic Data Centre, deposition number XXX. Compound's **15** crystals were grown in a mixture of ethyl acetate and hexane at room temperature. A clear colorless rectangular-parallelepiped-like specimen of C₂₆H₂₉BrO₆, approximate dimensions 0.120 mm \times 0.190 mm \times 0.520 mm, was used for the X-ray crystallographic analysis. The X-ray intensity data were measured on a Bruker APEX CCD system equipped with a graphite monochromator and a Mo K α sealed X-ray tube ($\lambda = 0.71073$ Å). The total exposure time was 18.57 h. The frames were integrated with the Bruker SAINT software package using a narrow-frame algorithm. The integration of the data

using a monoclinic unit cell yielded a total of 23715 reflections to a maximum θ angle of 30.20° (0.71 \AA resolution), of which 7231 were independent (average redundancy 3.270, completeness = 99.4%, $R_{\text{int}} = 3.10\%$) and 6524 (90.22%) were greater than $2\sigma(F^2)$. The final cell constants of $a = 22.9481(11) \text{ \AA}$, $b = 5.2631(3) \text{ \AA}$, $c = 21.5301(11) \text{ \AA}$, $\beta = 108.6660(10)^\circ$, volume = $2463.6(2) \text{ \AA}^3$, are based upon the refinement of the XYZ-centroids of 9887 reflections above $20 \sigma(I)$ with $7.114 < 2\theta < 61.72^\circ$. Data were corrected for absorption effects using the multi-scan method (SADABS). The ratio of minimum to maximum apparent transmission was 0.774. The calculated minimum and maximum transmission coefficients (based on crystal size) are 0.4710 and 0.8210. The structure was solved and refined using the Bruker SHELXTL Software Package, using the space group $C 1 2 1$, with $Z = 4$ for the formula unit, $C_{26}H_{29}BrO_6$. The final anisotropic full-matrix least-squares refinement on F^2 with 300 variables converged at $R1 = 3.69\%$, for the observed data and $wR2 = 9.56\%$ for all data. The goodness-of-fit was 1.033. The largest peak in the final difference electron density synthesis was $1.225 \text{ e}^-/\text{\AA}^3$ and the largest hole was $-0.811 \text{ e}^-/\text{\AA}^3$ with an RMS deviation of $0.057 \text{ e}^-/\text{\AA}^3$. On the basis of the final model, the calculated density was 1.395 g/cm^3 and $F(000)$, 1072 e^- . For absolute structure determination, Flack x determined using 2675 quotients $[(I^+)-(I^-)]/[(I^+)+(I^-)]$,¹⁸⁸ with absolute structure parameter of $-0.011(3)$. Crystal data, data collection and structure refinement details were summarized in Table 36, Supporting Information.

Antimicrobial Assay. Minimal inhibitory concentrations (MICs) of compounds (**1-11** and **13-14**) were measured against a panel of bacteria and fungi using methods that were described previously.^{18,102,103} All measurements were run in duplicate.

Tak1-TAB1 (Transforming growth factor- β activated kinase-1/TAK-1 binding protein 1) Inhibitor Assays. The assay was performed at BPS Bioscience Inc. 5Z-7-oxozeaenol¹⁹ was used as a positive control. Detailed experimental procedures are provided in the Supporting Information.

Supporting Information

Tak1-TAB1 (Transforming growth factor- β activated kinase-1/TAK-1 binding protein 1) Inhibitor Assays. The assay was performed using Kinase-Glo Plus luminescence kinase assay kit (Promega). It measures kinase activity by quantitating the amount of ATP remaining in solution following a kinase reaction. The luminescent signal from the assay is correlated with the amount of ATP present and is inversely correlated with the amount of kinase activity. Compounds (**1-14**) were diluted in 10% DMSO and 5 μ L of the dilution was added to a 50 μ L reaction so that the final concentration of DMSO is 1% in all of reactions. The compounds were preincubated with the enzyme in a reaction mixture for 10 min at room temperature. The enzymatic reactions were initiated by adding ATP (20 μ M at final) and conducted for 40 minutes at 30 °C. The 50 μ L reaction mixture contained 40 mM Tris, pH 7.4, 10 mM MgCl₂, 0.1 mg/mL BSA, 1 mM DTT, 0.2 mg/mL MBP substrate, 20 μ M ATP and Tak1-TAB1. After the enzymatic reaction, 50 μ L of Kinase-Glo Plus Luminescence kinase assay solution (Promega) was added to each reaction and the plate was incubated for 20 minutes at room temperature. Luminescence signal was measured using a BioTek *Synergy 2* microplate reader. Tak1-TAB1 activity assays were performed in duplicate at each concentration. The

luminescence data were analyzed using the computer software, Graphpad Prism. The difference between luminescence intensities in the absence of Tak1-TAB1 (Lu_t) and in the presence of Tak1-TAB1 (Lu_c) was defined as 100% activity ($Lu_t - Lu_c$). Using luminescence signal (Lu) in the presence of the compound, % activity was calculated as: % activity = $[(Lu_t - Lu)/(Lu_t - Lu_c)] \times 100\%$, where Lu = the luminescence intensity in the presence of the compound. The values of % activity versus a series of compound concentrations were then plotted using non-linear regression analysis of Sigmoidal dose-response curve generated with the equation $Y = B + (T - B) / (1 + 10^{((\text{LogEC}_{50} - X) \times \text{Hill Slope}))}$, where Y = percent activity, B = minimum percent activity, T = maximum percent activity, X = logarithm of compound and Hill Slope = slope factor or Hill coefficient. The IC_{50} value was determined by the concentration causing a half-maximal percent activity.

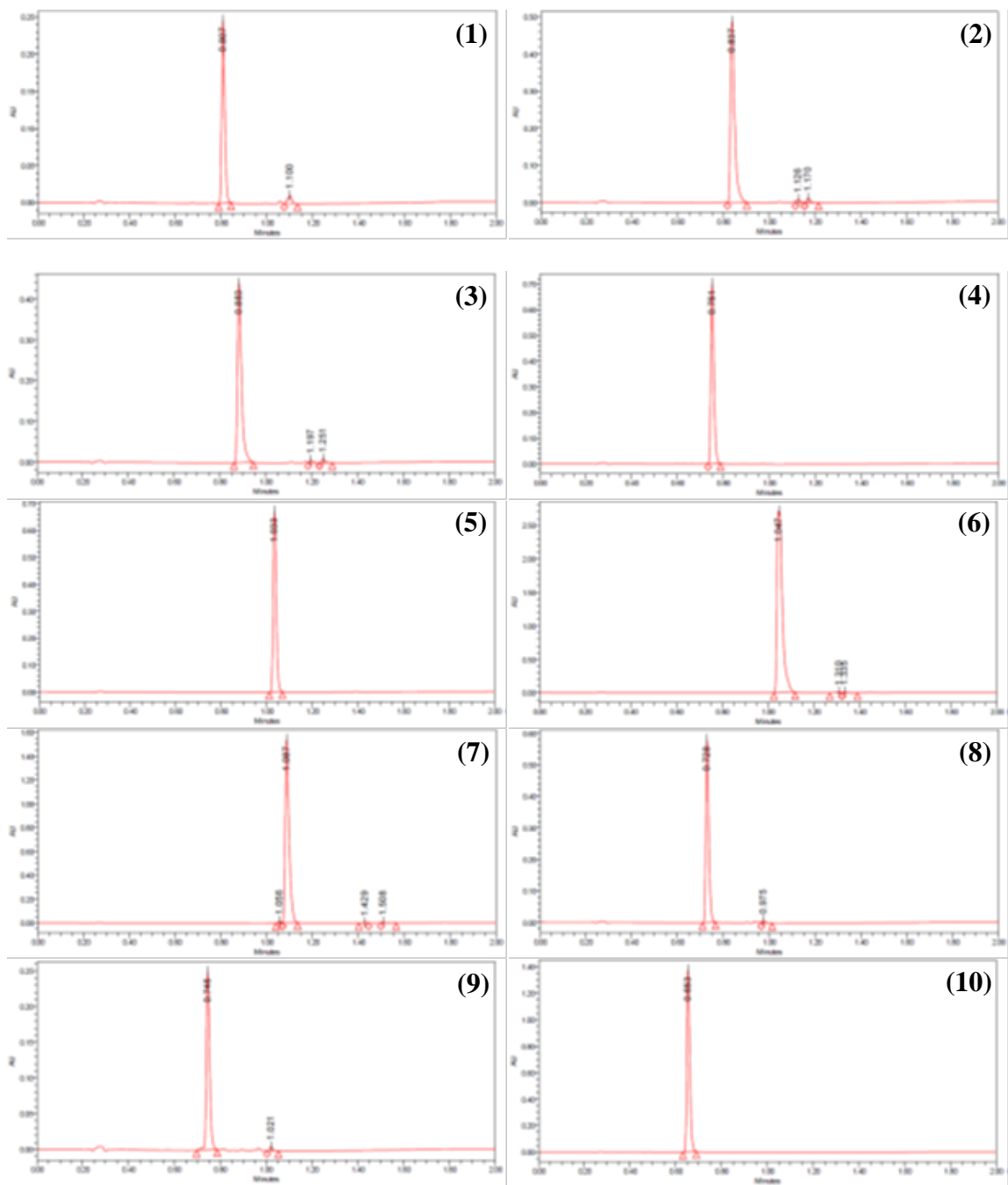


Figure 86. UPLC chromatograms of compounds **1-11** and **13-14** (λ 254 nm), demonstrating >96% purity for compounds **2-11** and **13-14** and >94% for compound **1**. All data were acquired via an Acquity UPLC system with a Phenomenex Kinetex C₁₈ (1.3 μ m; 50 \times 2.1 mm) column and a CH₃CN/H₂O gradient that increased linearly from 20 to 100% CH₃CN over 1.2 min.

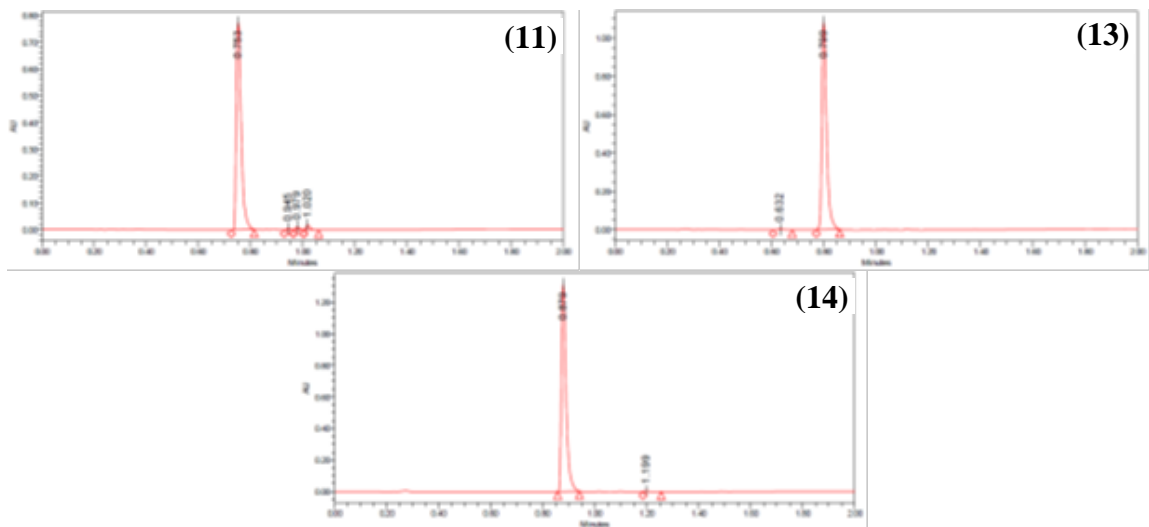


Figure 86 (continued). UPLC chromatograms of compounds **1-11** and **13-14** (λ 254 nm), demonstrating >96% purity for compounds **2-11** and **13-14** and >94% for compound **1**. All data were acquired via an Acquity UPLC system with a Phenomenex Kinetex C₁₈ (1.3 μ m; 50 \times 2.1 mm) column and a CH₃CN/H₂O gradient that increased linearly from 20 to 100% CH₃CN over 1.2 min.

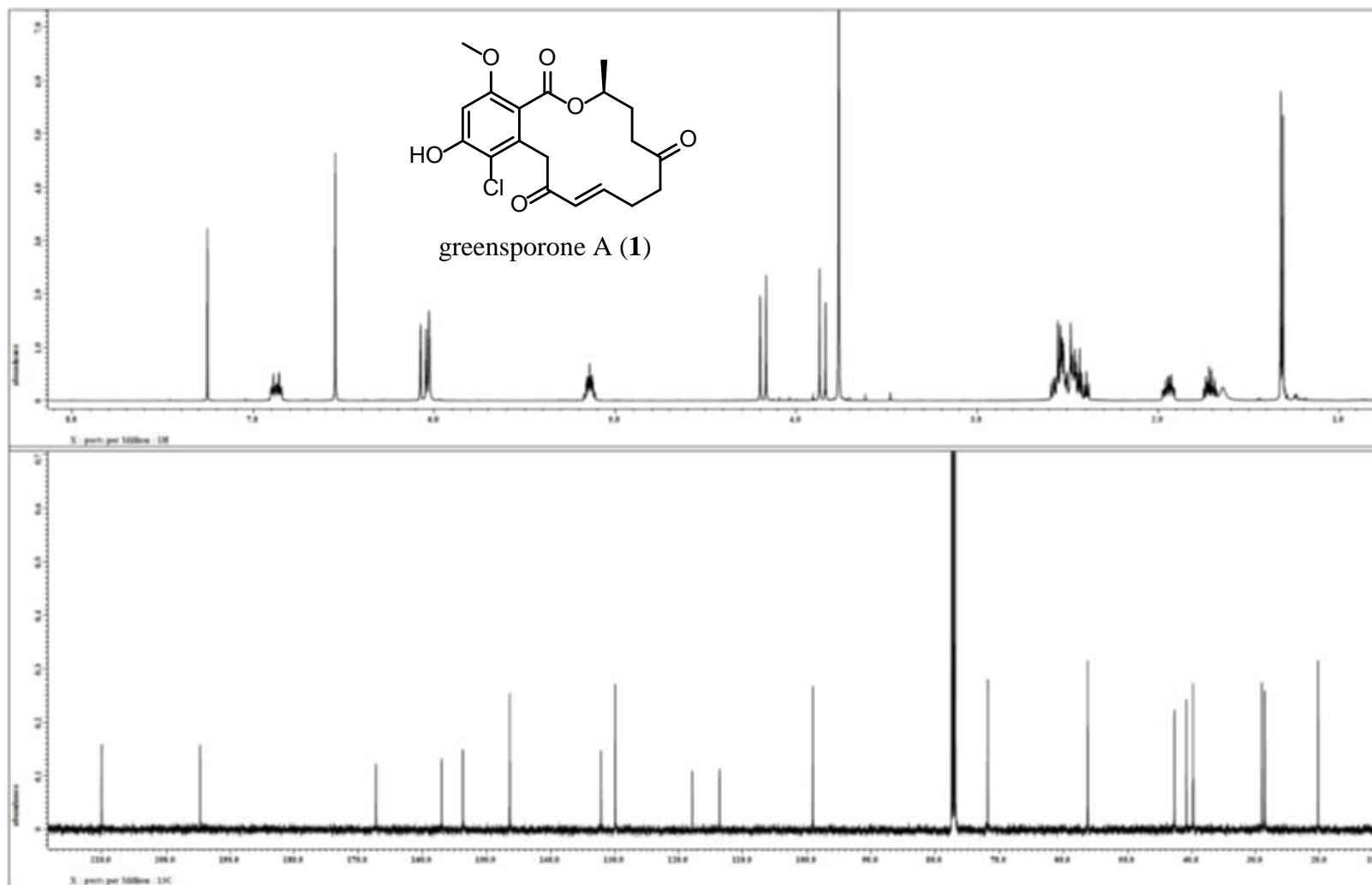


Figure 87. ^1H and ^{13}C NMR spectra of compound **1** [500 MHz for ^1H and 125 MHz for ^{13}C , CDCl_3].

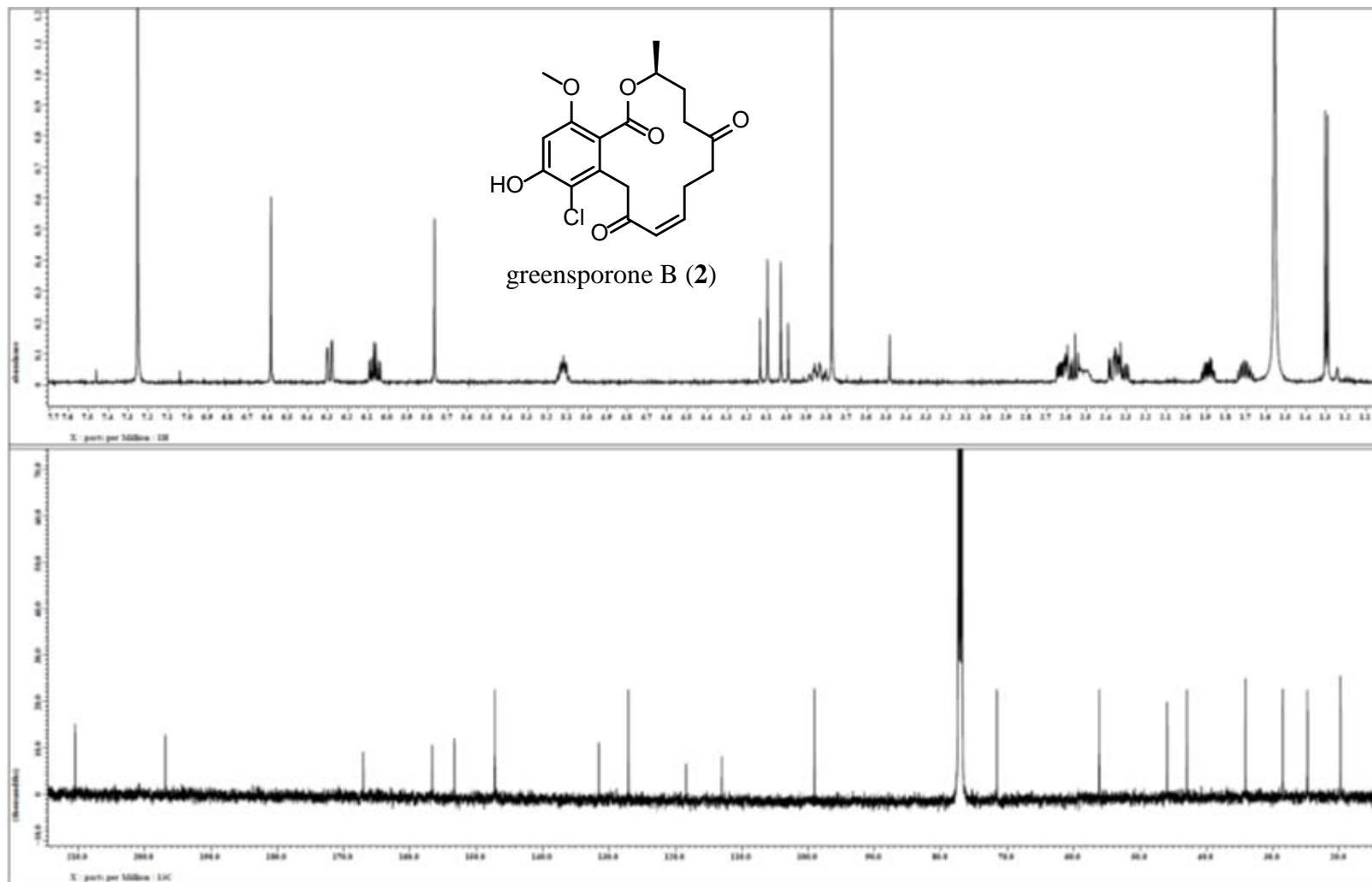


Figure 88. ^1H and ^{13}C NMR spectra of compound 2 [500 MHz for ^1H and 125 MHz for ^{13}C , CDCl_3].

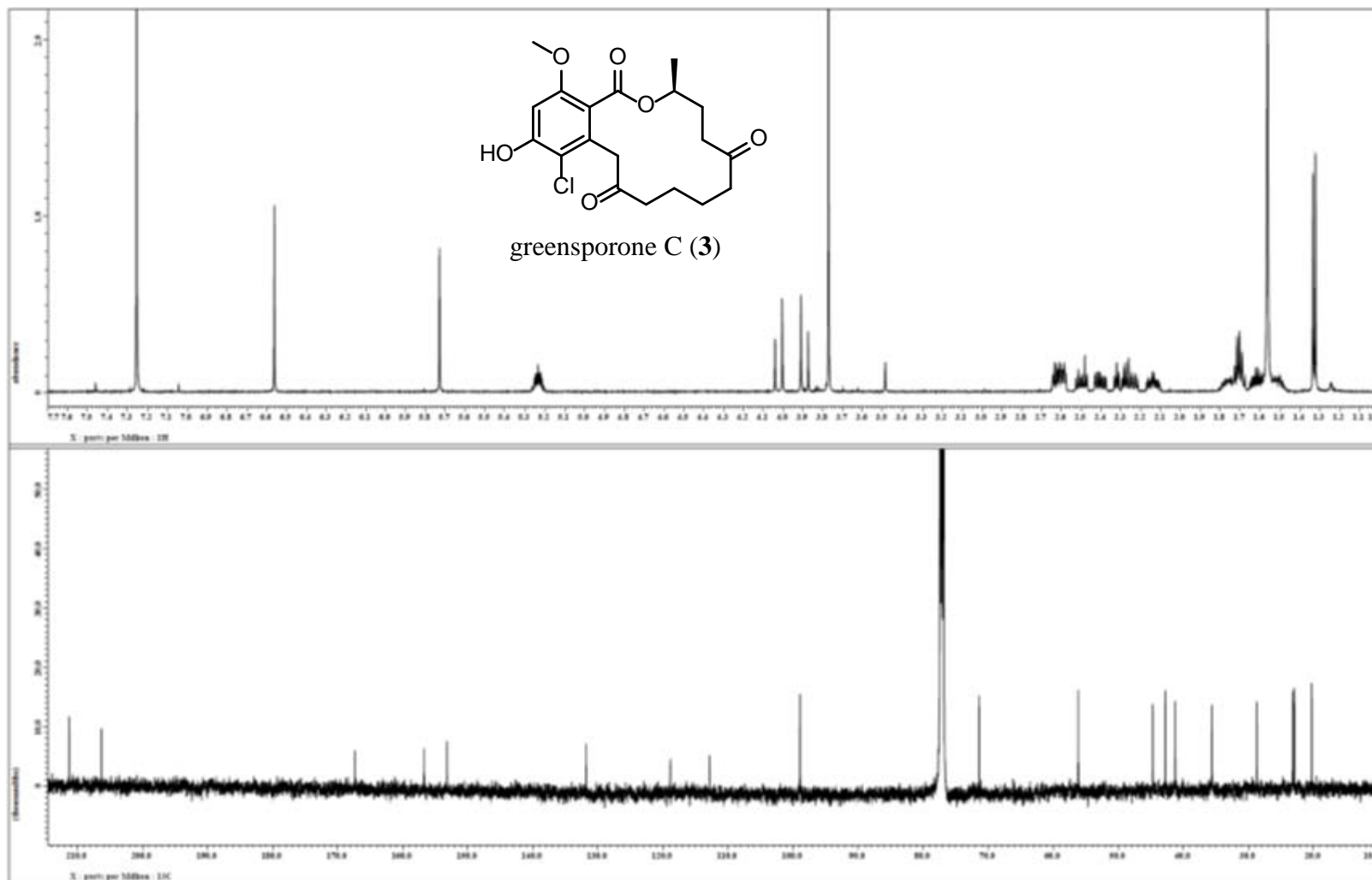


Figure 89. ^1H and ^{13}C NMR spectra of compound 3 [500 MHz for ^1H and 125 MHz for ^{13}C , CDCl_3].

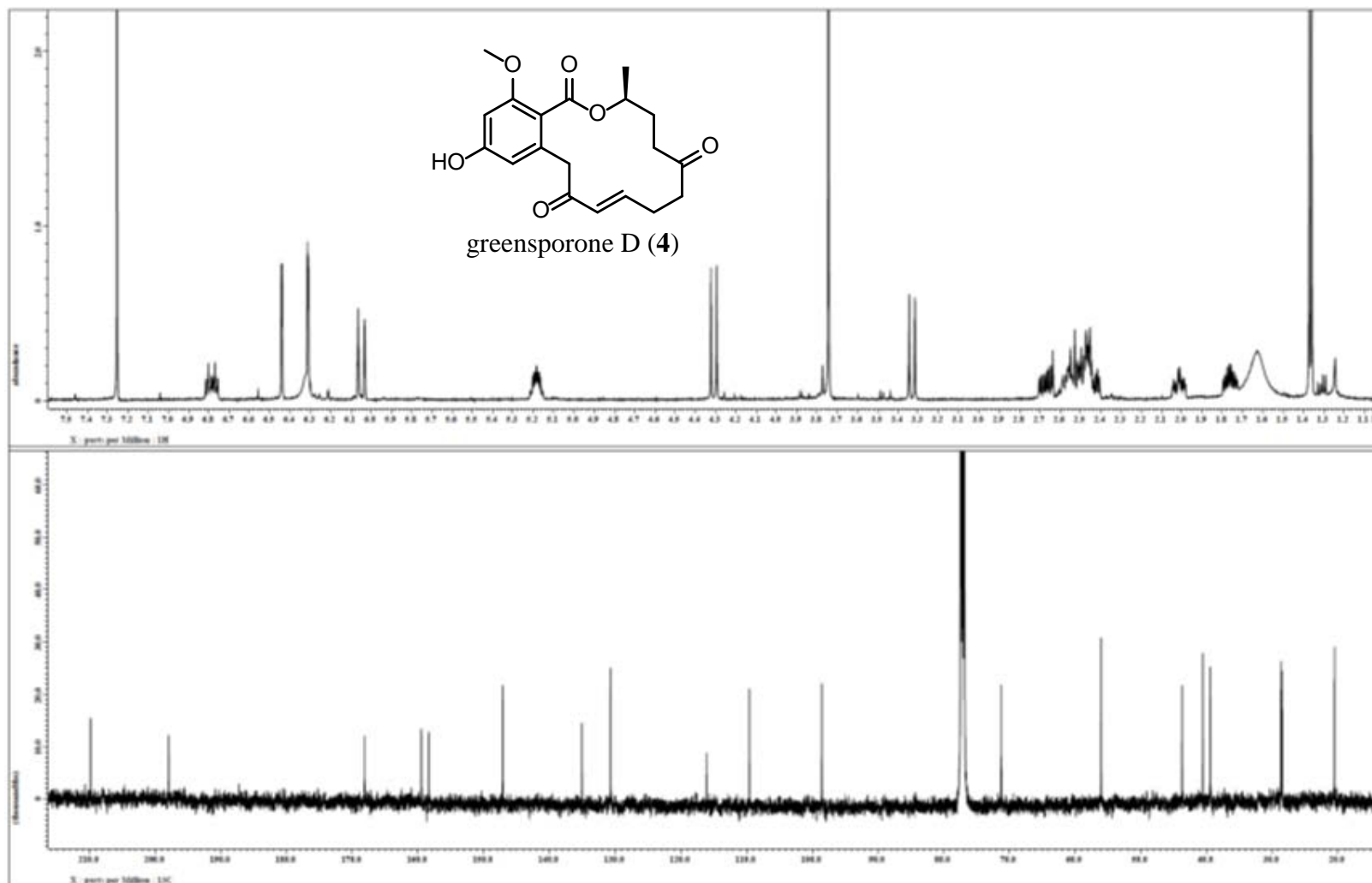


Figure 90. ^1H and ^{13}C NMR spectra of compound **4** [500 MHz for ^1H and 125 MHz for ^{13}C , CDCl_3].

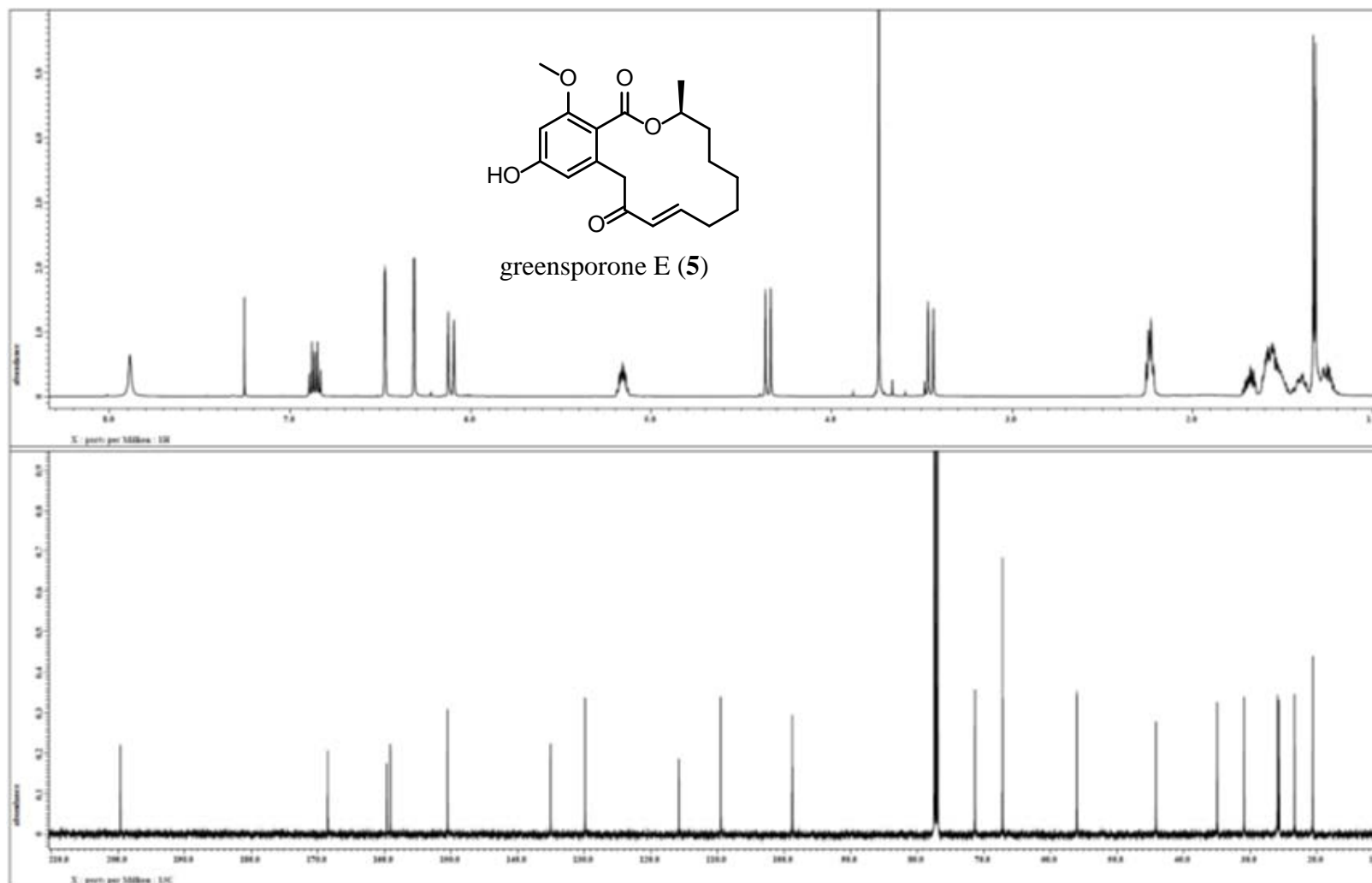


Figure 91. ^1H and ^{13}C NMR spectra of compound 5 [500 MHz for ^1H and 125 MHz for ^{13}C , CDCl_3].

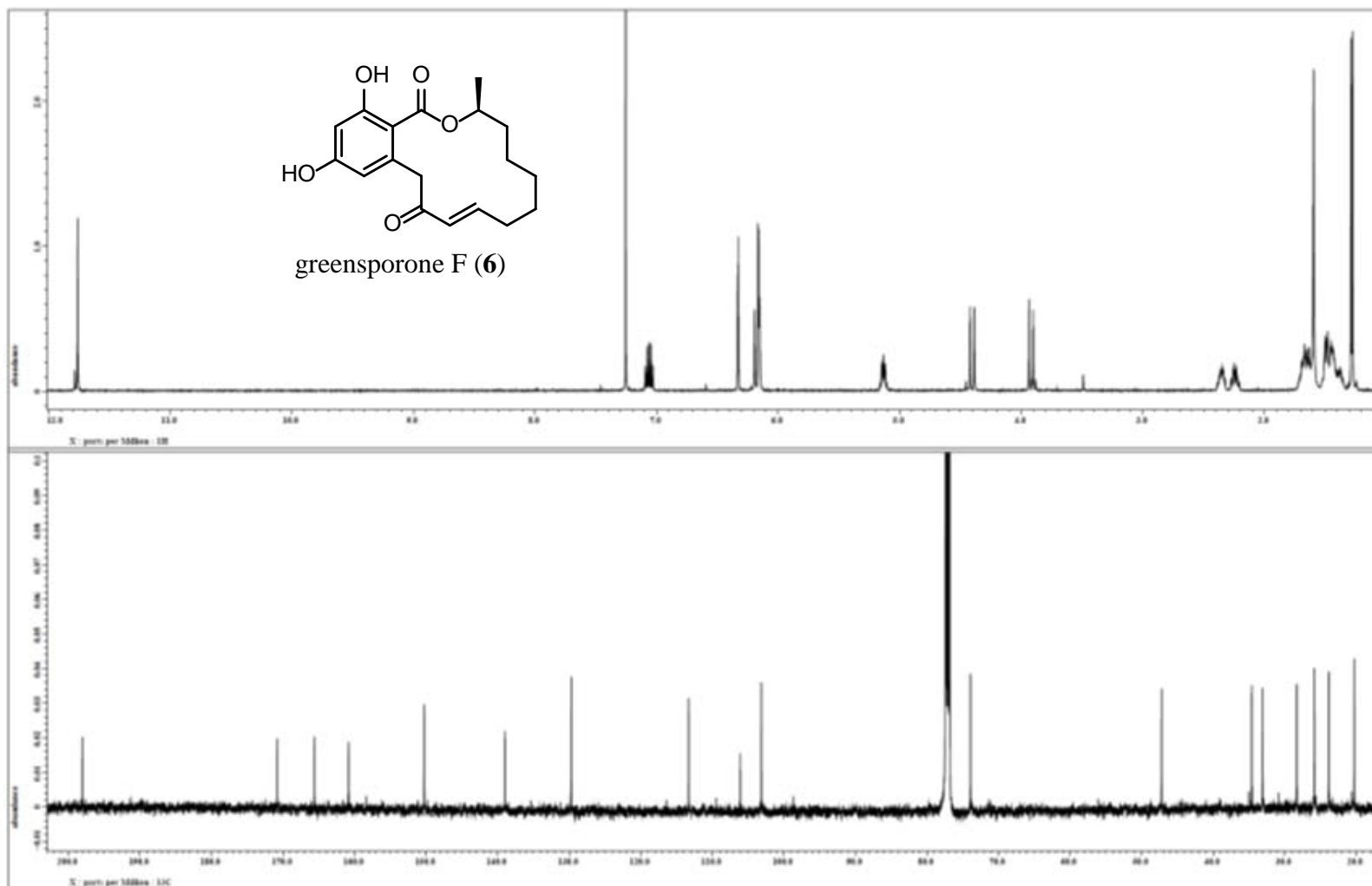


Figure 92. ^1H and ^{13}C NMR spectra of compound 6 [500 MHz for ^1H and 125 MHz for ^{13}C , CDCl_3].

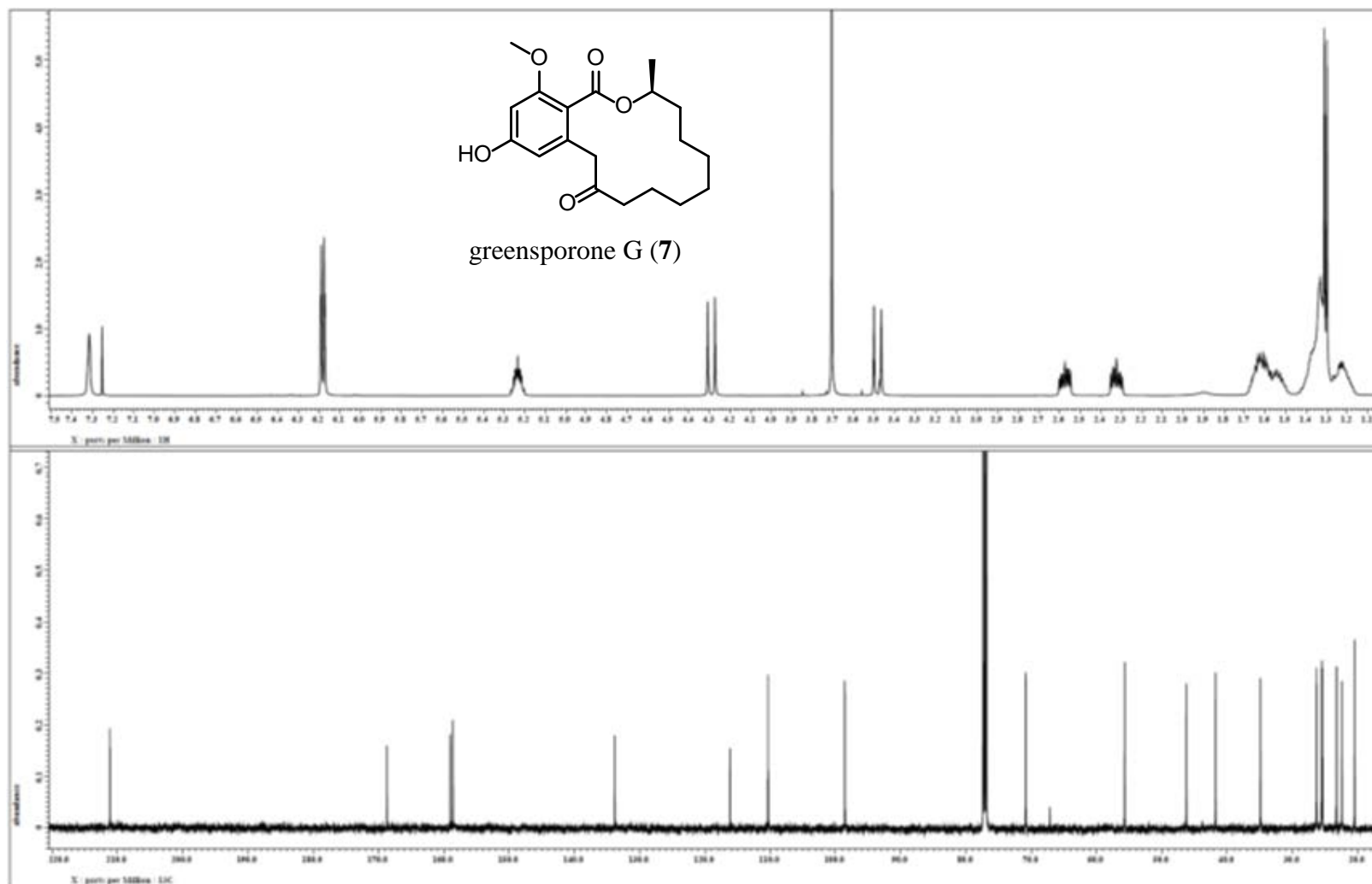


Figure 93. ^1H and ^{13}C NMR spectra of compound 7 [500 MHz for ^1H and 125 MHz for ^{13}C , CDCl_3].

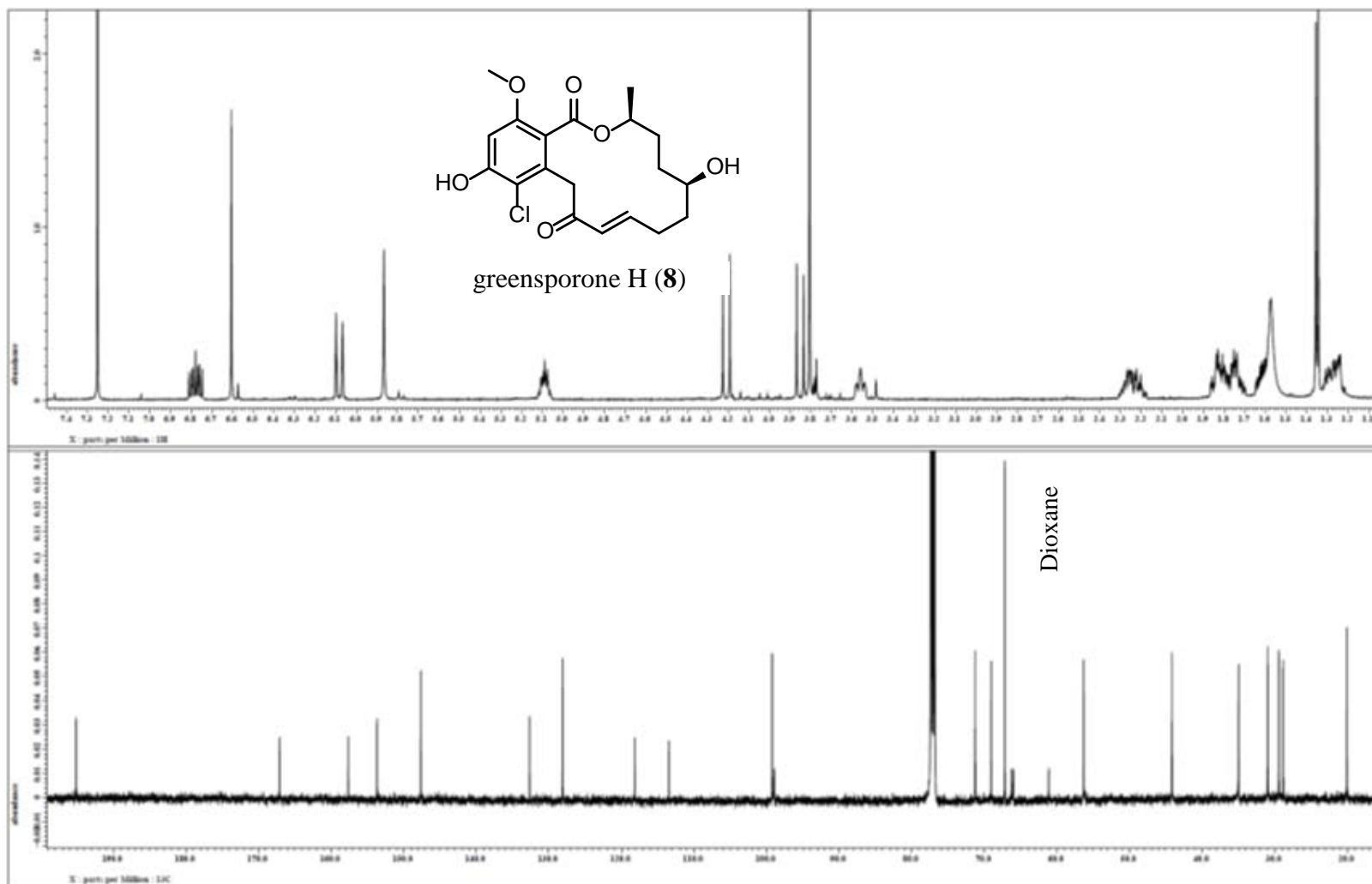


Figure 94. ^1H and ^{13}C NMR spectra of compound 8 [500 MHz for ^1H and 125 MHz for ^{13}C , CDCl_3].

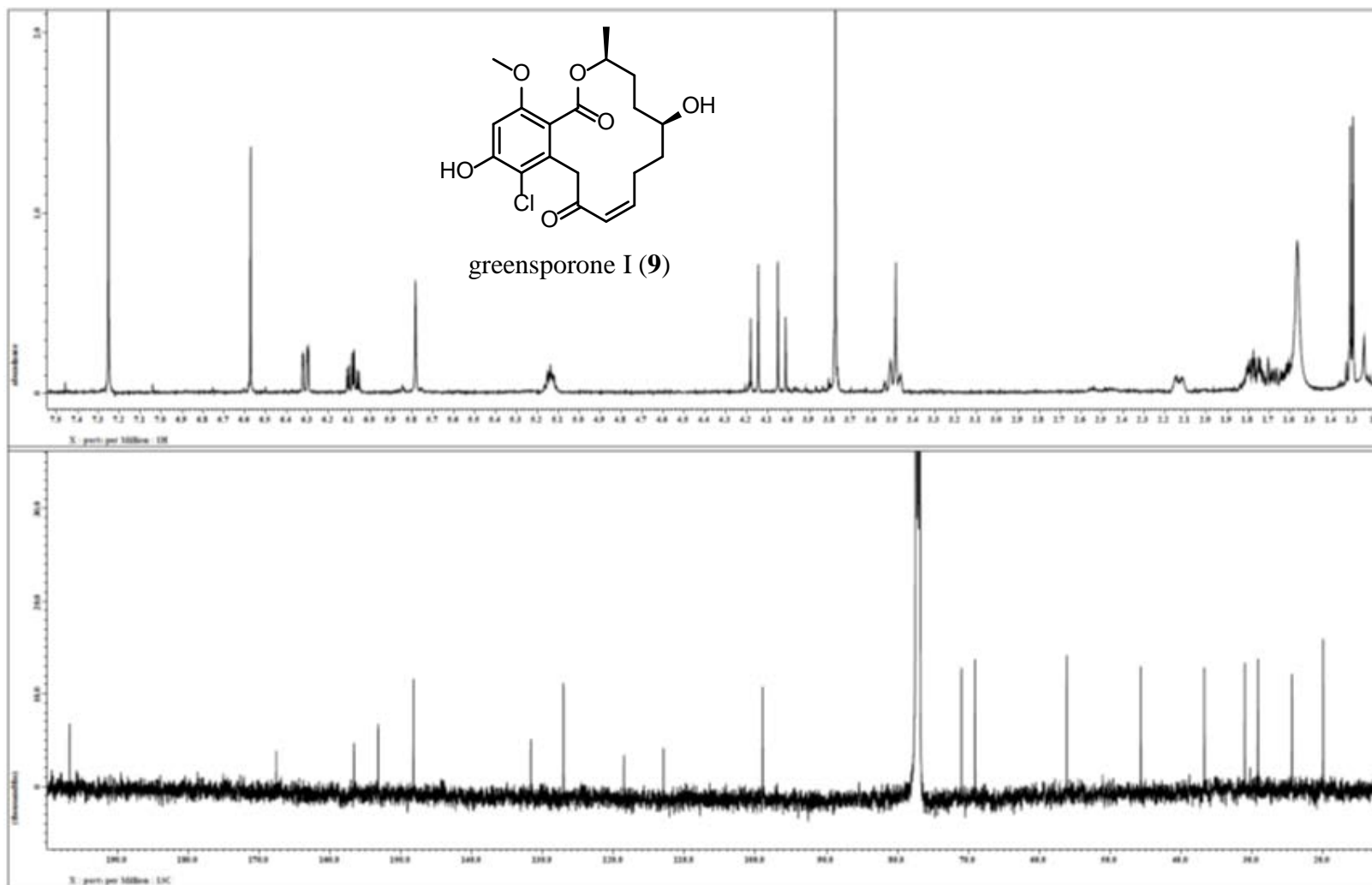


Figure 95. ^1H and ^{13}C NMR spectra of compound 9 [500 MHz for ^1H and 125 MHz for ^{13}C , CDCl_3].

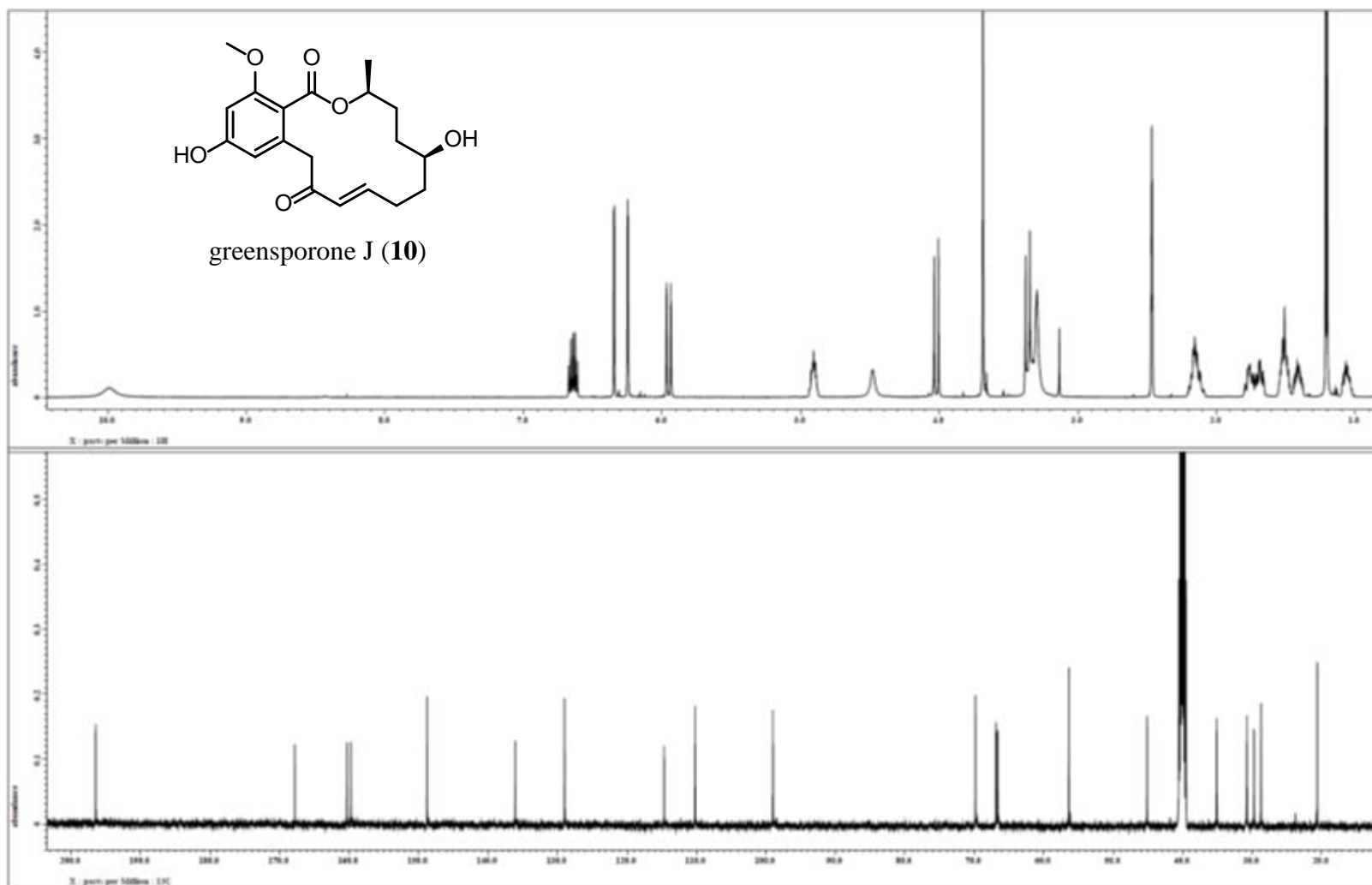


Figure 96. ^1H and ^{13}C NMR spectra of compound **10** [500 MHz for ^1H and 125 MHz for ^{13}C , DMSO].

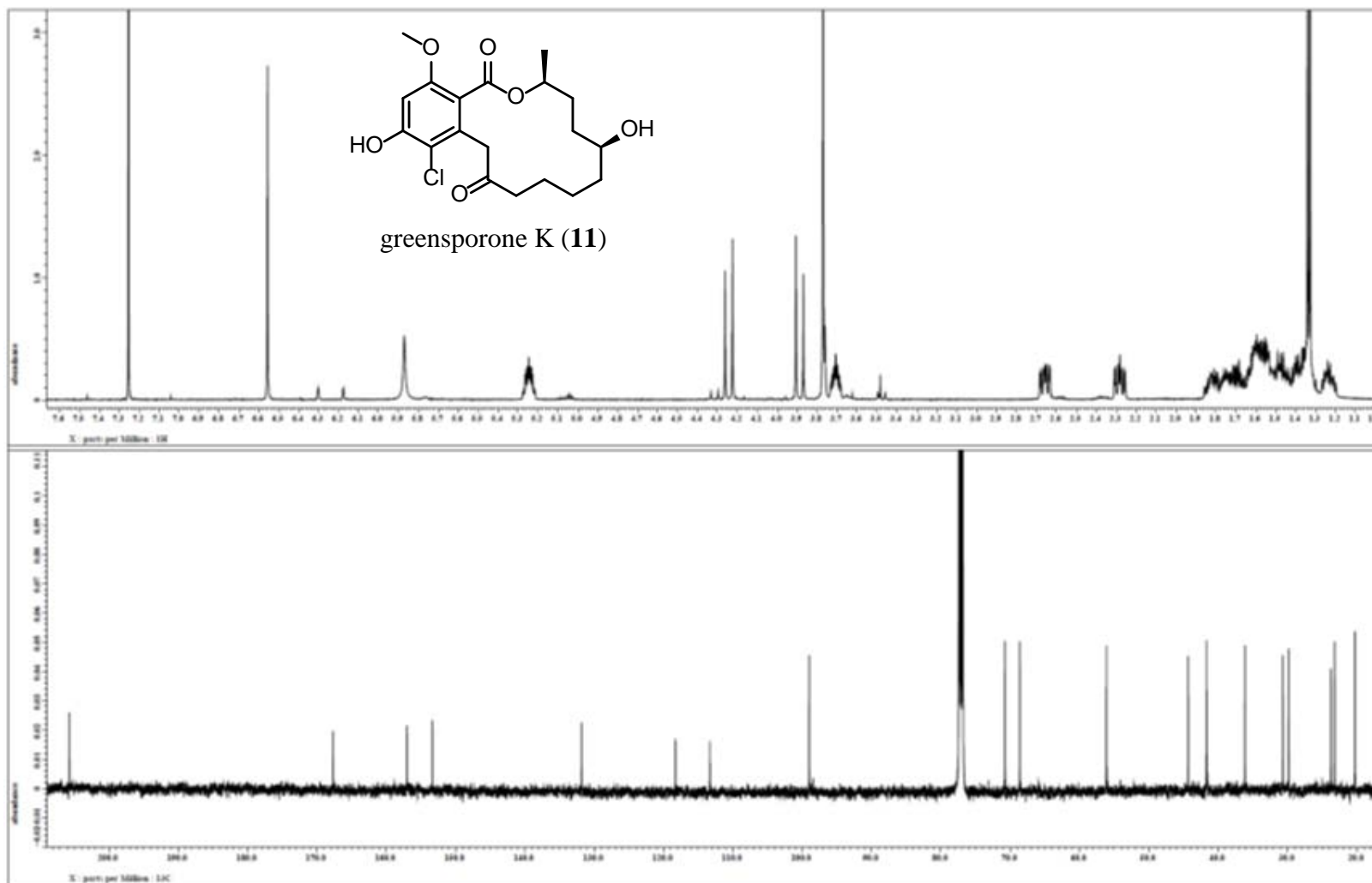


Figure 97. ^1H and ^{13}C NMR spectra of compound **11** [500 MHz for ^1H and 125 MHz for ^{13}C , CDCl_3].

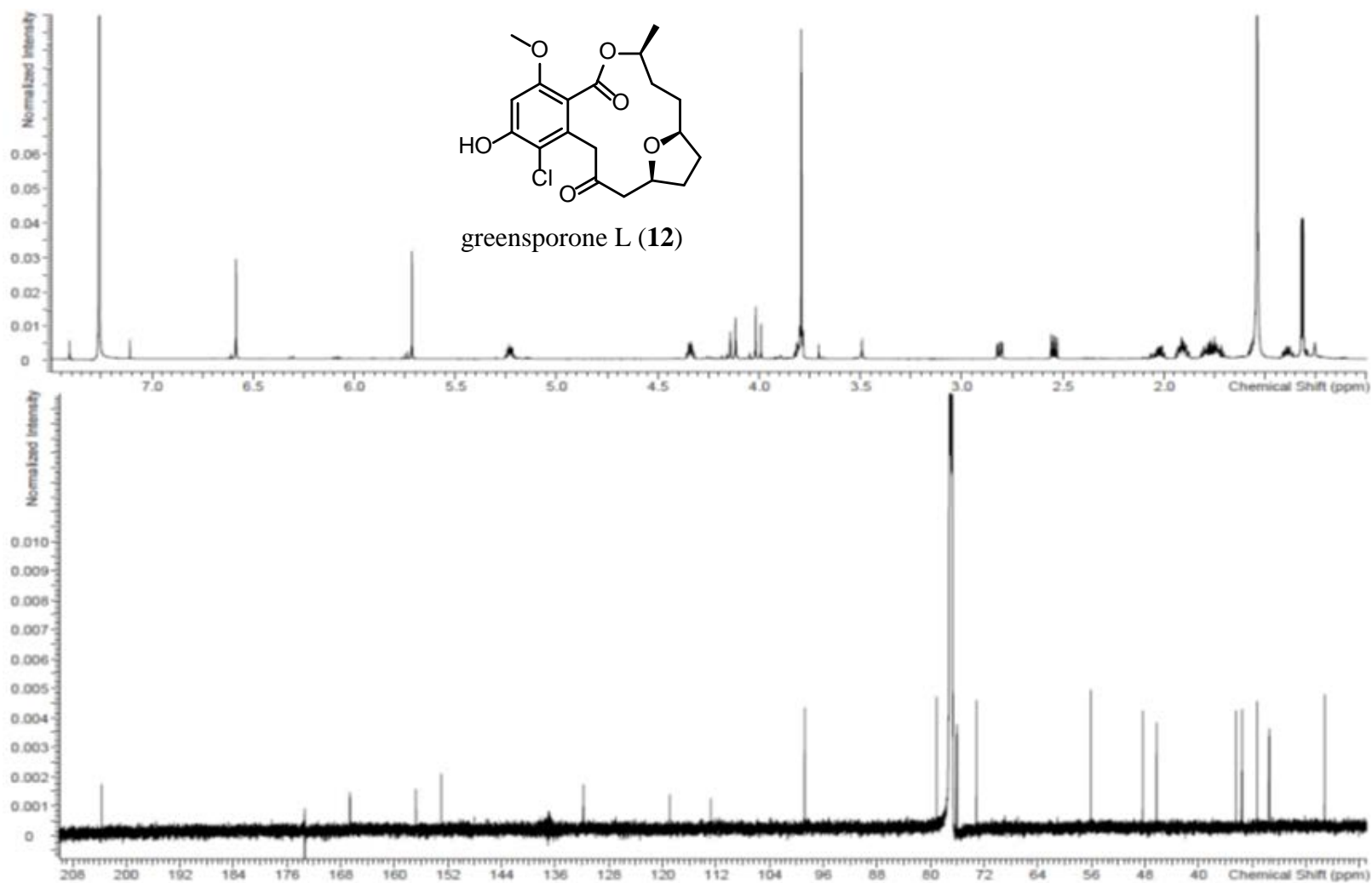


Figure 98. ^1H and ^{13}C NMR spectra of compound **12** [700 MHz for ^1H and 175 MHz for ^{13}C , CDCl_3].

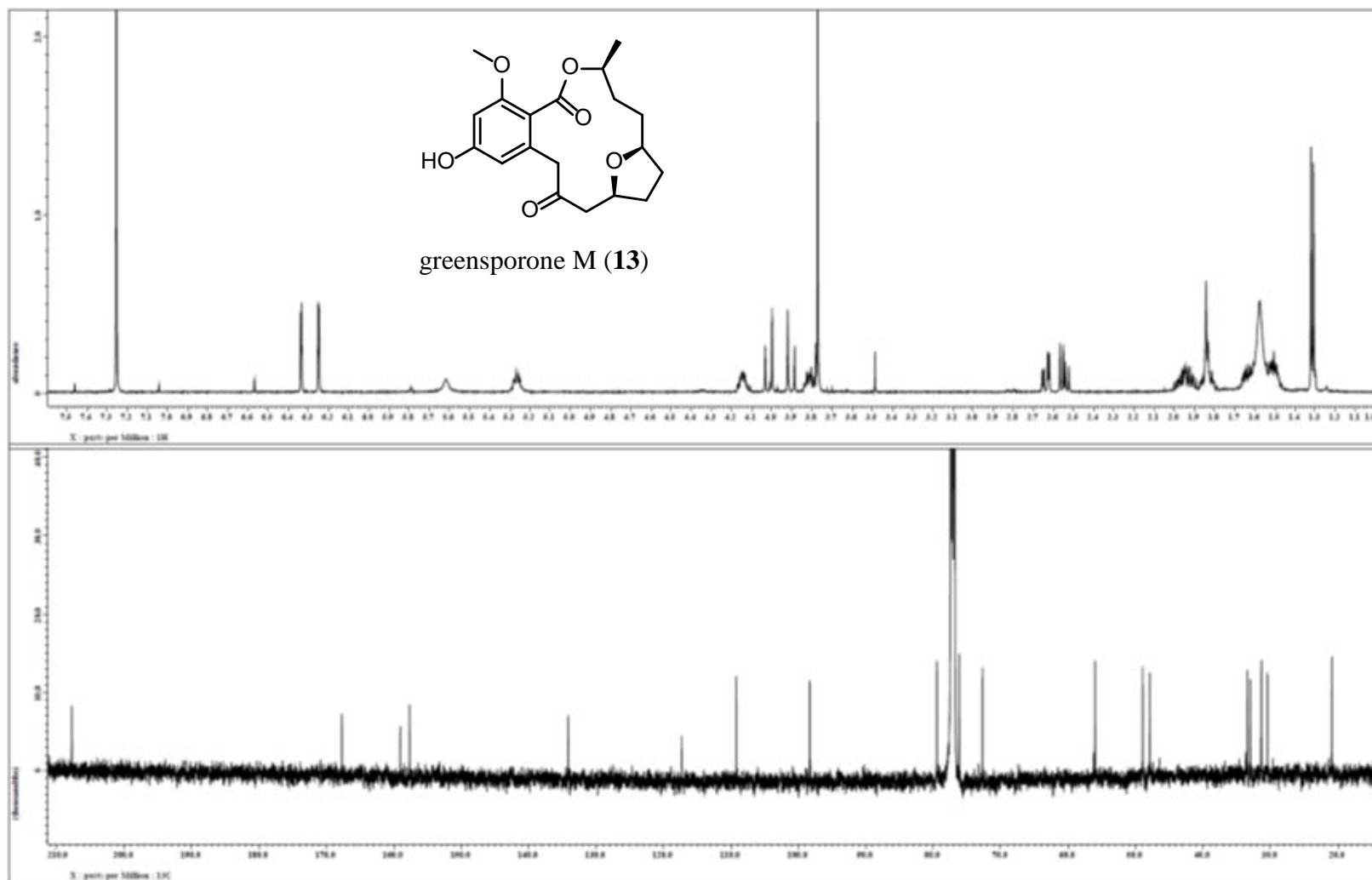


Figure 99. ^1H and ^{13}C NMR spectra of compound **13** [500 MHz for ^1H and 125 MHz for ^{13}C , CDCl_3].

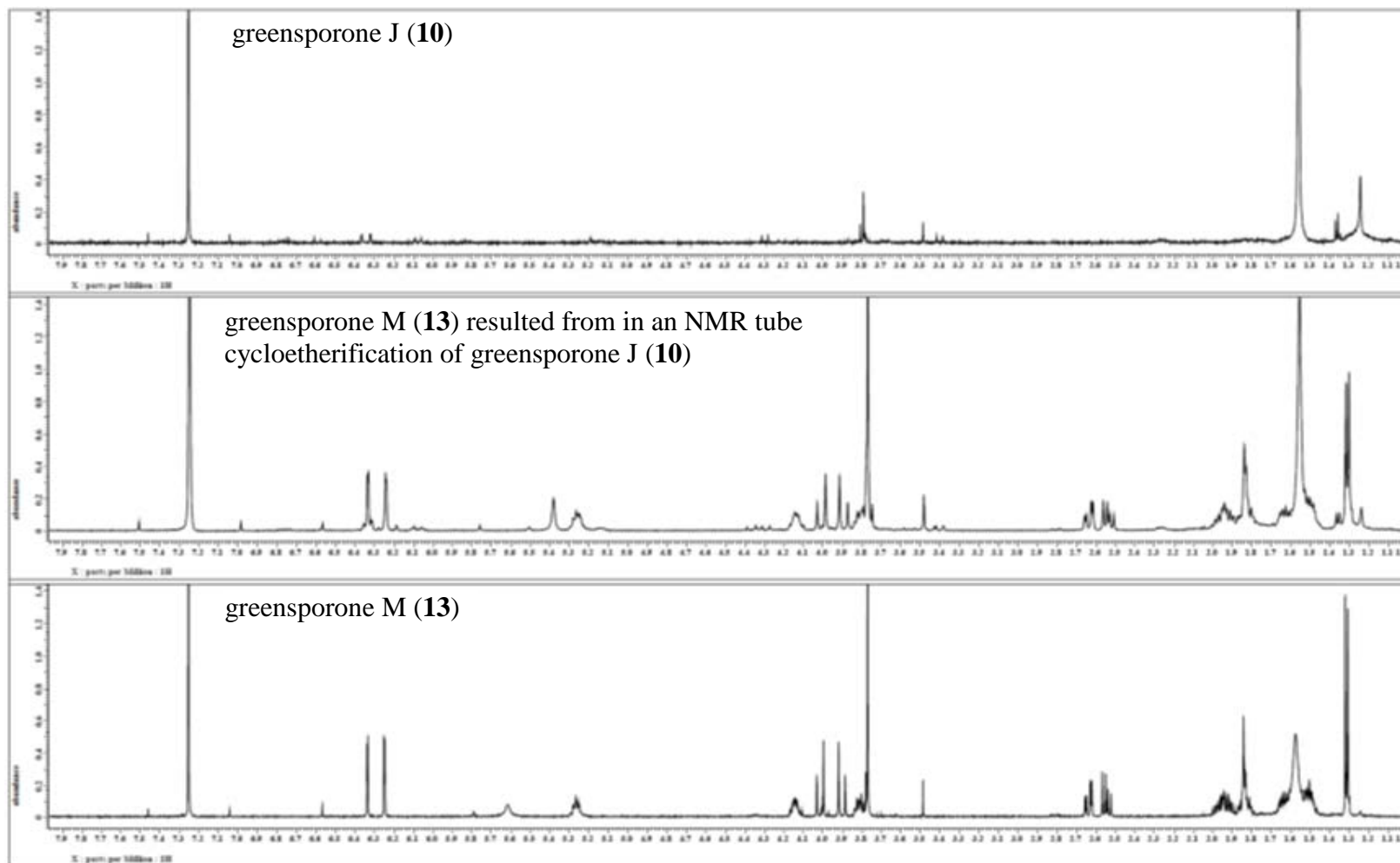


Figure 100. Stack plot of the ^1H NMR spectra of compound **10** (upper), compound **13** (lower) and the rearranged product of compound **10** (middle) [500 MHz, CDCl_3].

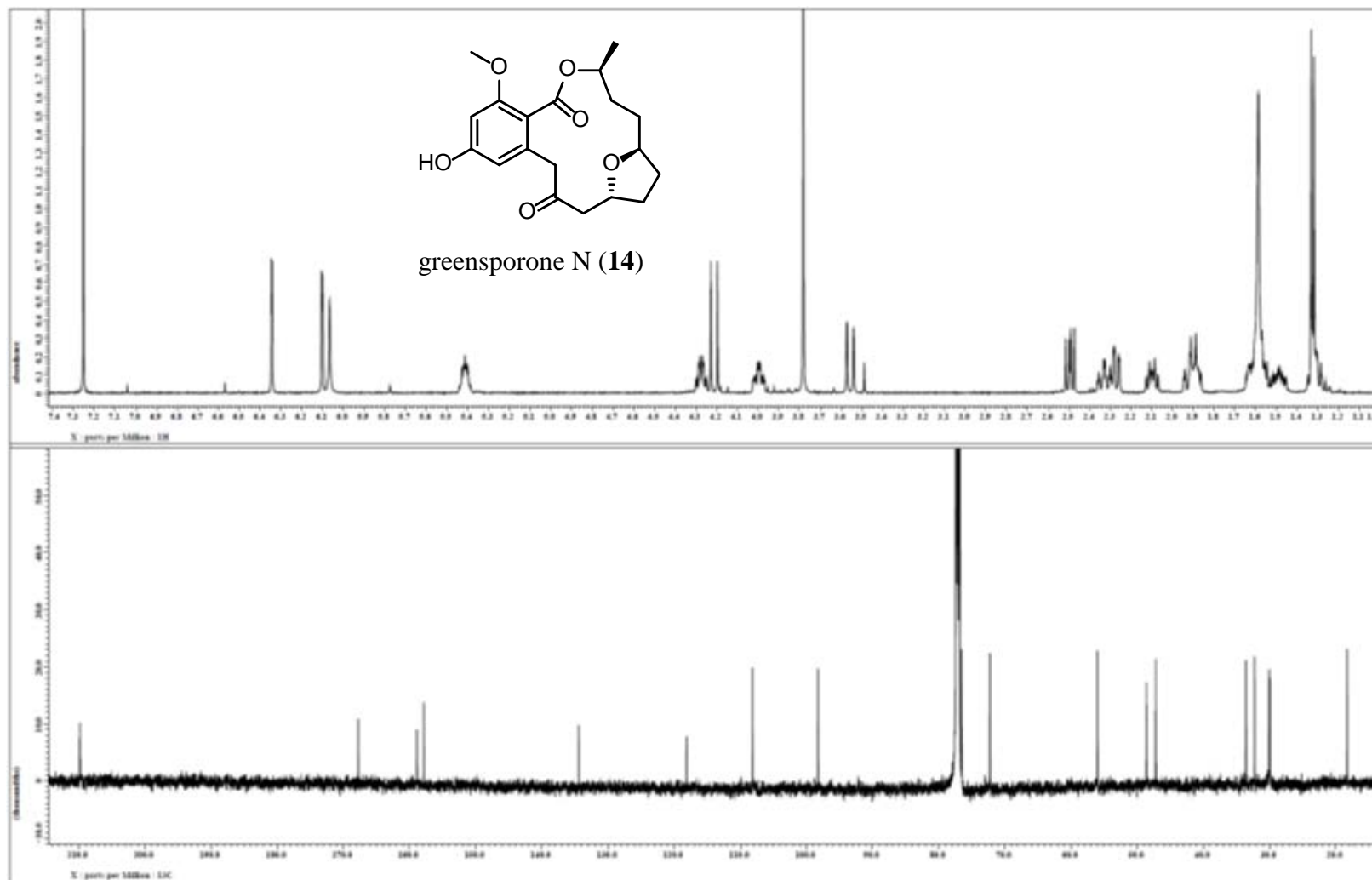


Figure 101. ^1H and ^{13}C NMR spectra of compound **14** [500 MHz for ^1H and 125 MHz for ^{13}C , CDCl_3].

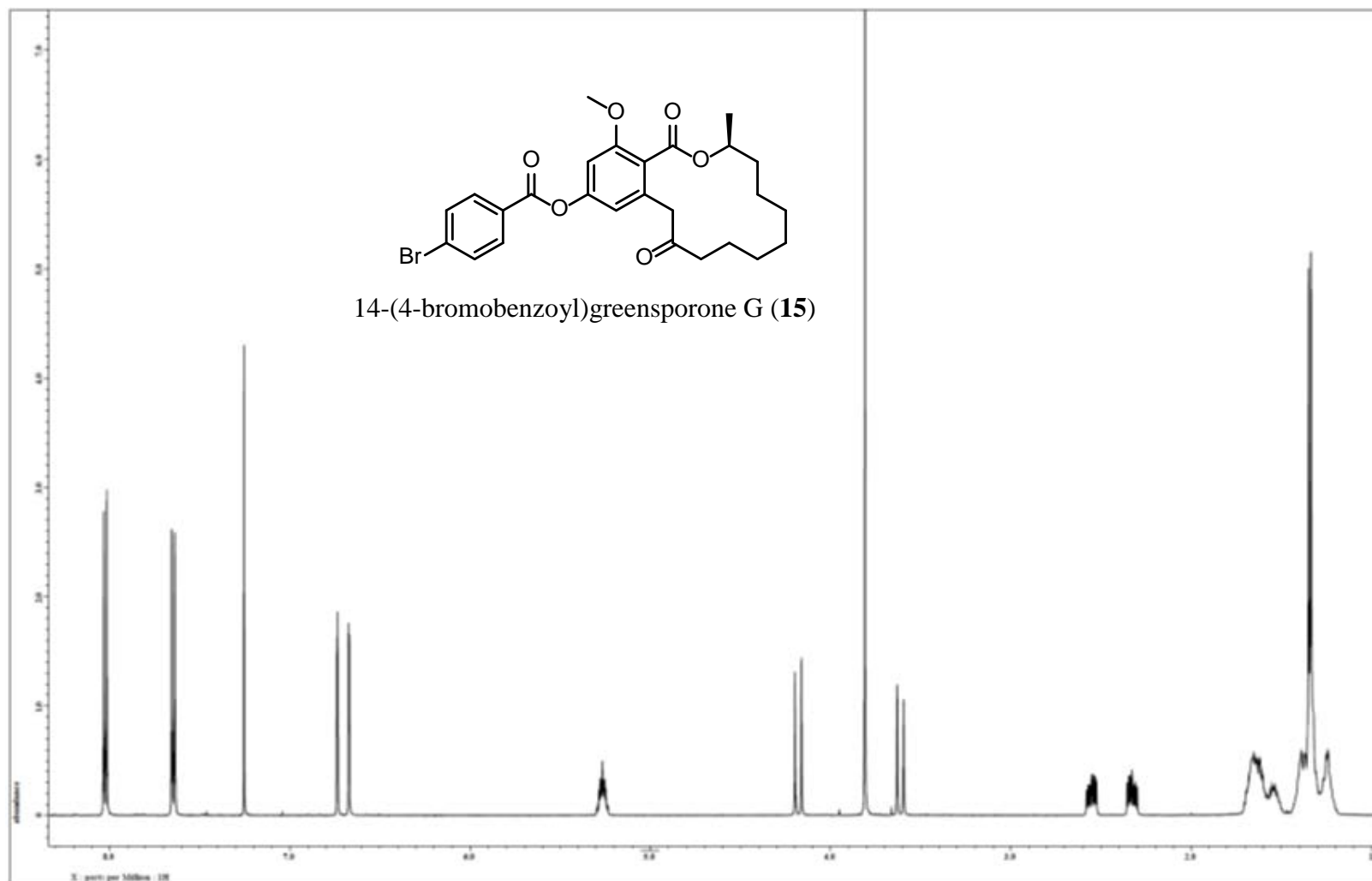


Figure 102. ¹H NMR spectrum of compound **15** [500 MHz, CDCl₃].

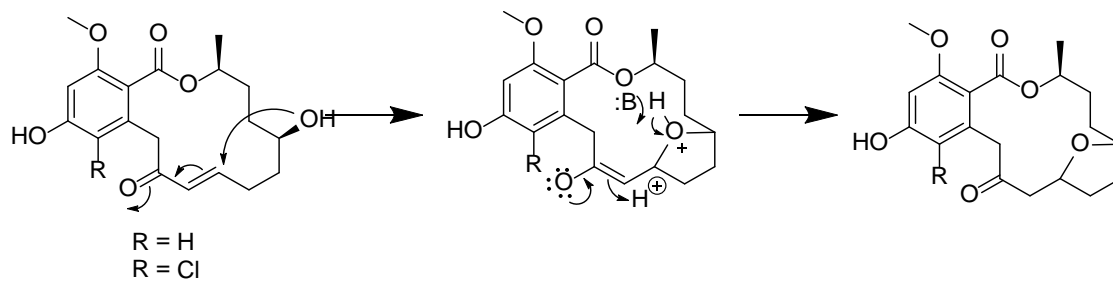


Figure 103. Proposed mechanism for the intramolecular cycloetherification of ϵ -hydroxy- α,β -unsaturated ketones.

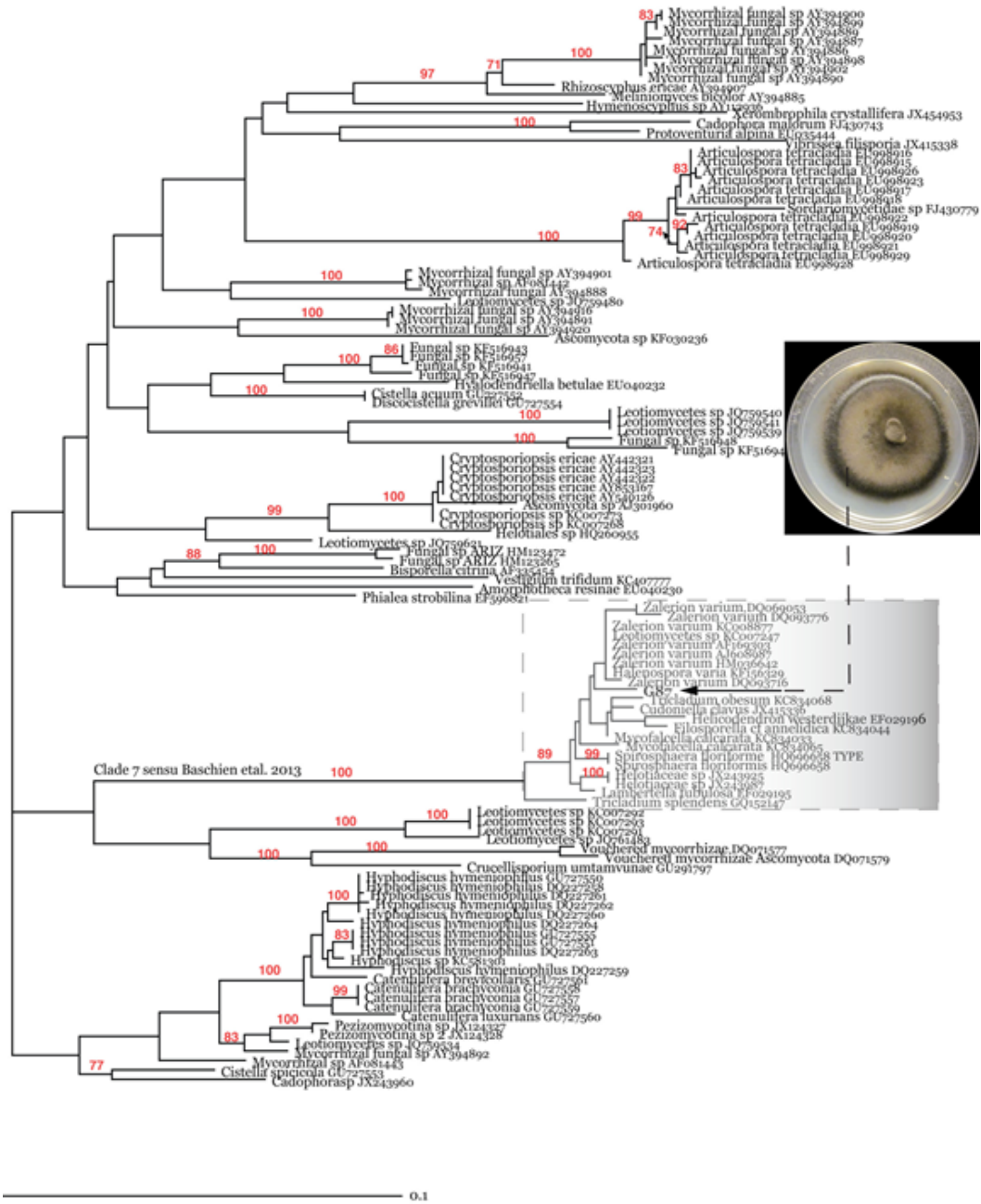


Figure 104. Phylogram of the most likely tree ($-\ln L = 10610.60$) from a RAxML analysis of 116 taxa based on combined ITS and D1/D2 regions of LSU nrDNA sequence data (1052 bp). Numbers refer to RAxML bootstrap support values $\geq 70\%$ based on 1000 replicates. Strain G87 is putatively identified as having phylogenetic affinities to *Halenospora varia* (Clade 7 sensu Baschien et al. 2013 highlighted). Bar indicates nucleotide substitution per site. A 3-week-old colony of G87 on PDA media is also shown.

Table 36. Crystal data, data collection, and refinement details of 15

Crystal data	
$C_{26}H_{29}BrO_6$	$F(000) = 1072$
$M_r = 517.40$	$D_x = 1.395 \text{ Mg m}^{-3}$
Monoclinic, $C2$	Mo $K\alpha$ radiation, $\lambda = 0.71073 \text{ \AA}$
$a = 22.9481 (11) \text{ \AA}$	Cell parameters from 9887 reflections
$b = 5.2631 (3) \text{ \AA}$	$\theta = 3.6\text{--}30.9^\circ$
$c = 21.5301 (11) \text{ \AA}$	$\mu = 1.71 \text{ mm}^{-1}$
$\beta = 108.6665 (6)^\circ$	$T = 193 \text{ K}$
$V = 2463.6 (2) \text{ \AA}^3$	Rectangular-parallelepiped, colourless
$Z = 4$	$0.52 \times 0.19 \times 0.12 \text{ mm}$
Data collection	
Bruker APEX CCD diffractometer	7231 independent reflections
Radiation source: sealed tube	6524 reflections with $I > 2\sigma(I)$
Graphite monochromator	$R_{\text{int}} = 0.031$
ϕ and ω scans	$\theta_{\text{max}} = 30.2^\circ$, $\theta_{\text{min}} = 3.6^\circ$
Absorption correction: multi-scan; Data were corrected for scaling and absorption effects using the multi-scan technique (<i>SADABS</i>). The ratio of minimum to maximum apparent transmission was 0.774. The calculated minimum and maximum transmission coefficients (based on crystal size) are 0.471 and 0.821.	$h = -32 \rightarrow 32$
$T_{\text{min}} = 0.577$, $T_{\text{max}} = 0.746$	$k = -7 \rightarrow 7$
23715 measured reflections	$l = -30 \rightarrow 30$
Refinement	
Refinement on F^2	Secondary atom site location: structure-invariant direct methods
Least-squares matrix: full	Hydrogen site location: inferred from neighbouring sites
$R[F^2 > 2\sigma(F^2)] = 0.037$	H-atom parameters constrained

Table 36 (Continued). Crystal data, data collection, and refinement details of 15

$wR(F^2) = 0.096$	$w = 1/[\sigma^2(F_o^2) + (0.0457P)^2 + 2.0649P]$ where $P = (F_o^2 + 2F_c^2)/3$
$S = 1.03$	$(\Delta/\sigma)_{\max} = 0.001$
7231 reflections	$\Delta_{\max} = 1.23 \text{ e } \text{\AA}^{-3}$
300 parameters	$\Delta_{\min} = -0.81 \text{ e } \text{\AA}^{-3}$
1 restraint	Absolute structure: Flack x determined using 2675 quotients $[(I+)-(I-)]/[(I+)+(I-)]$ (Parsons and Flack (2004), Acta Cryst. A60, s61).
Primary atom site location: structure- invariant direct methods	Absolute structure parameter: -0.011 (3)

CHAPTER VIII

FLAVONOLIGNANS FROM *ASPERGILLUS IIZUKAE*, A FUNGAL ENDOPHYTE OF MILK THISTLE (*SILYBUM MARIANUM*)

Tamam El-Elimat, Huzefa A. Raja, Tyler N. Graf, Stanley H. Faeth, Nadja B. Cech, and Nicholas H. Oberlies. *Journal of Natural Products* 2014, 77, 193-199.

Silybin A (**1**), silybin B (**2**), and isosilybin A (**3**), three of the seven flavonolignans that constitute silymarin, an extract of the fruits of milk thistle (*Silybum marianum*), were detected for the first time from a fungal endophyte, *Aspergillus iizukae*, isolated from the surface-sterilized leaves of *S. marianum*. The flavonolignans were identified using a UPLC-PDA-HRMS-MS/MS method by matching retention times, HRMS, and MS/MS data with authentic reference compounds. Attenuation of flavonolignan production was observed following successive sub-culturing of the original flavonolignan-producing culture, as is often the case with endophytes that produce plant-based secondary metabolites. However, production of **1** and **2** resumed when attenuated spores were harvested from cultures grown on a medium to which autoclaved leaves of *S. marianum* were added. The cycle of attenuation followed by resumed biosynthesis of these flavonolignans was replicated in triplicate.

Silybum marianum (L.) Gaertn. (Asteraceae), known commonly as milk thistle, has been used for centuries for treatment of liver disorders, including cirrhosis and chronic

hepatitis.¹⁸⁹⁻¹⁹⁵ Silymarin, the crude extract of the fruits (achenes), represents a mixture of at least seven flavonolignans [silybin A (**1**), silybin B (**2**), isosilybin A (**3**), isosilybin B (**4**), silychristin, isosilychristin, and silydianin] and the flavonoid taxifolin.¹⁹⁶ Silymarin has been the subject of intensive studies for its profound biological activities, particularly in the areas of cancer chemoprevention and hepatoprotection,¹⁹⁷⁻²⁰² and our group has been studying the chemistry of flavonolignans for more than ten years.²⁰³⁻²⁰⁷ Recently, studies were initiated on the chemical mycology of endophytic fungi in milk thistle by examining the chemical profiles of fungal endophytes and how these are influenced by the native substrate.

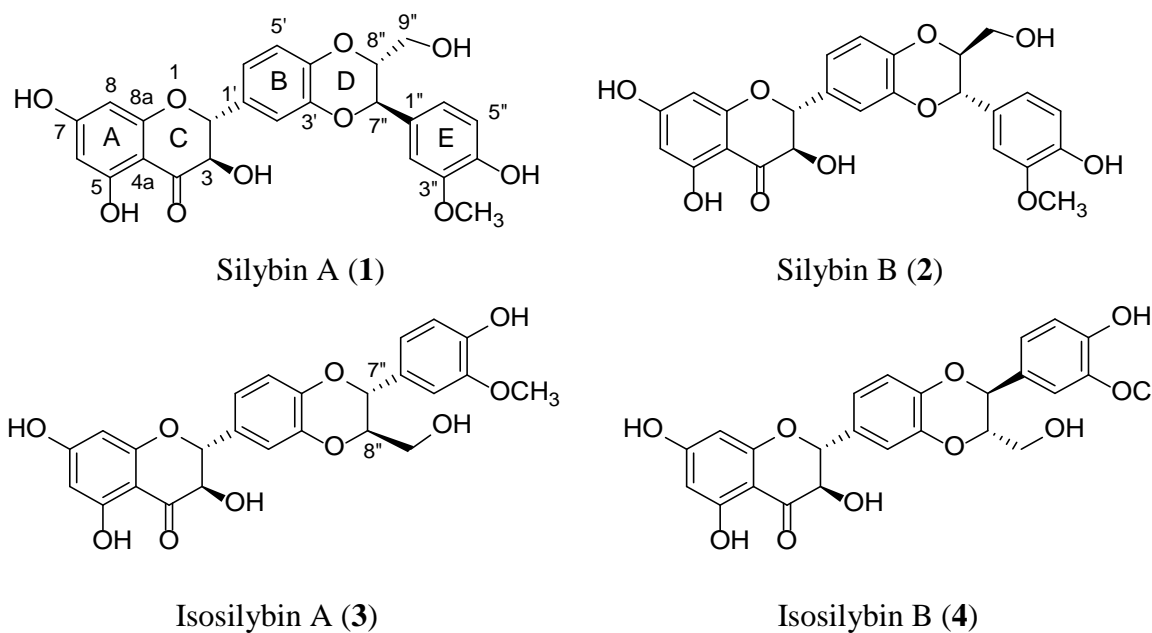


Figure 105. Structures of compounds **1-4**.

Fungal endophytes are a diverse group of primarily ascomycetous fungi, which are defined functionally by their asymptomatic occurrence within plants.^{208,209} They occur in

all major lineages of plants and in natural and anthropogenic communities ranging from the arctic region to the tropics.²¹⁰⁻²¹² The ecological roles and chemical interactions of endophytic fungi are currently under intense investigation, particularly in relation to their host plants.

The capability of certain endophytic fungi to produce compounds associated with plant secondary metabolites has gained prominence since the report of the anticancer agent taxol from *Taxomyces andreanae*, a fungal endophyte that was isolated from the inner bark of *Taxus brevifolia*.²¹³ Subsequently, several research groups have explored endophytic fungi for the production of associated plant secondary metabolites, and examples include the cytotoxic agents podophyllotoxin^{214,215} and deoxypodophyllotoxin,²¹⁶ camptothecin and related analogues,²¹⁷⁻²²² and vinblastine,²²³ the herbal antidepressant hypericin and its precursor emodin,^{224,225} and the insecticides azadirachtin A and B.²²⁶ Unfortunately, sustainable production of these and other compounds by fungal endophytes has proven difficult. Almost without exception, attenuation of production of the target compounds following sub-culturing of the endophytes occurs.²²⁷ The reasons for this attenuation could be attributed to factors that stem from loss of interactions with the host plant, coexisting endophytes (of fungal and/or bacterial origin), insects, and/or herbivores,^{228,229} resulting in the silencing of genes in axenic monocultures.²³⁰ Herein, reported for the first time is the production of two flavonolignans, silybin A (**1**) and silybin B (**2**), from an endophytic fungus that was isolated from the leaves of milk thistle. The fungus was identified as *Aspergillus iizukae*

Sugiyama (Eurotiomycetes, Ascomycota) using molecular and morphological characterization techniques.

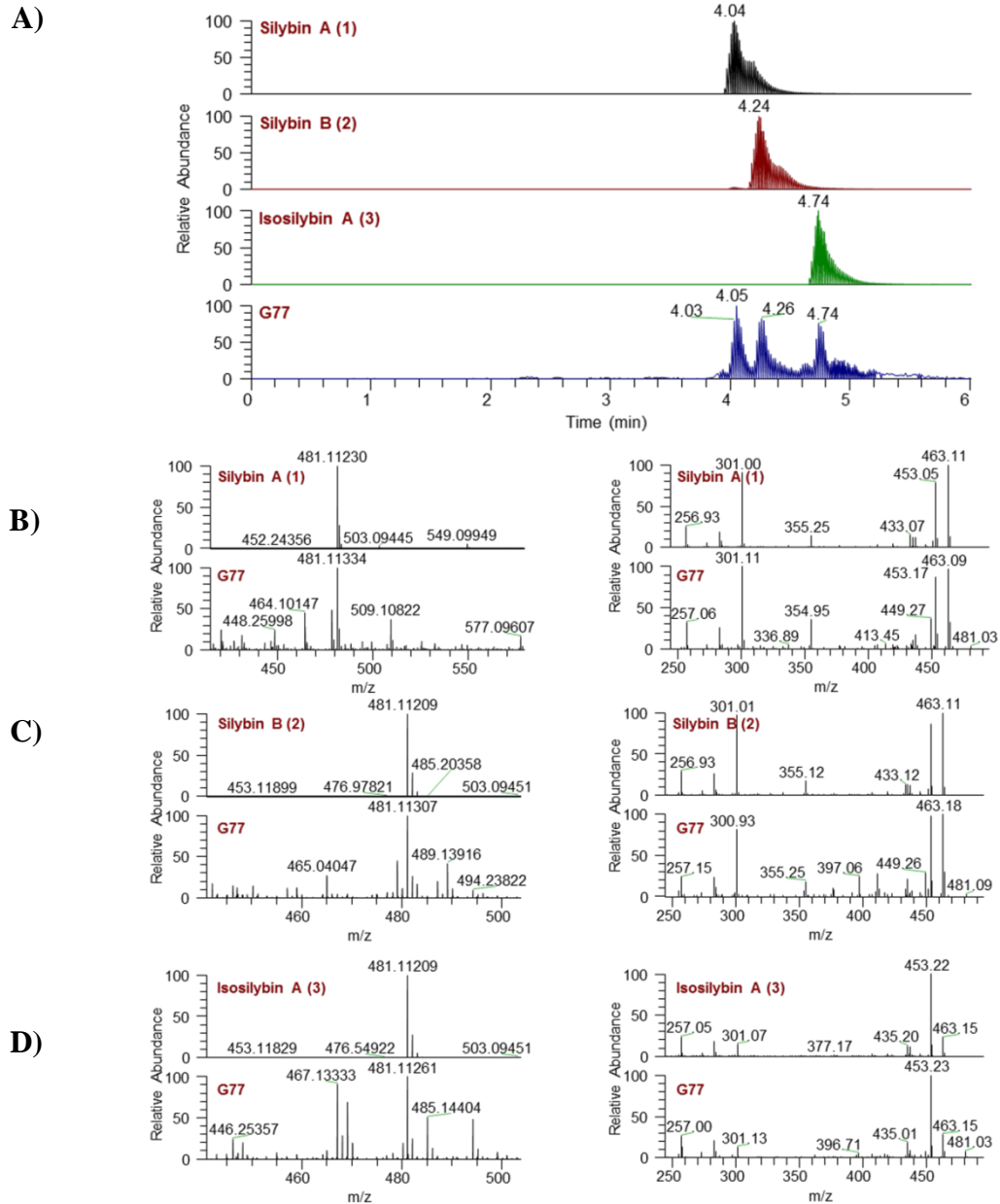


Figure 106. A) (-)-ESI SIC of reference standards compared to that of an extract of the fungus *A. izuzakae* (m/z : 481); (-)-ESI high-resolution mass spectra (left) and MS/MS CID fragmentation data (right) of B) silybin A (1), C) silybin B (2), and D) isosilybin A (3).

Following isolation of 21 unique fungal endophytes from leaves, stems, seeds, and roots of milk thistle, organic extracts of cultures grown on a solid medium were prepared and dereplicated against an in-house database of bioactive fungal secondary metabolites containing more than 180 compounds using a UPLC-PDA-HRMS-MS/MS method.⁸⁰ As a standard protocol, all cultures isolated in our laboratory were dereplicated before engaging in the scale-up or purification processes, so as to avoid the re-isolation of known compounds, particularly mycotoxins.^{80,231} Subsequently, the 21 fungal endophytes were examined for the production of flavonolignans. To do so, a database of authentic reference standards of the major silymarin constituents was constructed using the same dereplication strategy⁸⁰ by recording HRMS, MS/MS data, UV absorption maxima, and retention times utilizing the negative-ionization mode (Table 37, Supporting Information). The MS files of the extracts, which were acquired previously for dereplicating mycotoxins, were re-analyzed for the production of flavonolignans. Among the fungal endophyte isolates, only two cultures, coded G77 and G82, had detectable ions that matched, tentatively, with four flavonolignan standards (1-4) in terms of HRMS, MS/MS fragments and retention times. Interestingly, G77 was harvested from the leaves while G82 was harvested from the stems; however, they both were identified later as *A. iizukae*. The former culture produced a higher level of signals that matched that of the flavonolignans, and as such, was pursued further. Due to the close retention times, identical molecular ion peaks, and similar fragmentation patterns, the method⁸⁰ was unable to differentiate between either silybin A/silybin B or isosilybin A/isosilybin B. To discern between these pairs of diastereoisomers, a chromatographic method was

optimized to target flavonolignans, and this was utilized when re-acquiring the UPLC-PDA-HRMS-MS/MS data. Using this refined dereplication system (Table 37, Supporting Information), the compounds were identified as silybin A (**1**), silybin B (**2**), and isosilybin A (**3**) (Figure 106).

Upon successive sub-culturing of the original axenic flavonolignans-producing culture (*A. iizukae*), attenuation of the production of flavonolignans was observed. In an attempt to stimulate the fungus to biosynthesize these compounds, an experiment was designed by growing *A. iizukae* on potato dextrose agar (Difco) to which autoclaved milk thistle leaves were added (Figure 107). Following growth for one month, spores (asexual conidia) were transferred aseptically from the plate and were used either to inoculate the rice medium directly or to inoculate a liquid culture containing 2% soy peptone, 2% dextrose, and 1% yeast extract (YESD medium). After seven days, this liquid culture was used to inoculate the rice medium. In addition, an agar plug from a culture of *A. iizukae* that was grown on PDA medium without autoclaved milk thistle leaves was used to inoculate the rice medium directly. All three cultures were grown on rice for 21 days and then extracted and analyzed by UPLC-PDA-HRMS using the system optimized for flavonolignans. The flavonolignans, silybin A (**1**) and silybin B (**2**), were detected only in the solid medium that was inoculated directly by spores from *A. iizukae* grown on medium that included autoclaved milk thistle leaves. Upon sub-culturing of this flavonolignan-producing culture, the production of flavonolignans was attenuated again. However, flavonolignan production was re-stimulated by growing the attenuated culture on PDA medium with autoclaved milk thistle leaves and harvesting spores for inoculation

on rice medium (Figure 108). Importantly, the conidiophores were up to 1.5 mm long (Figure 109, Supporting Information).²³² Hence, it was easy to harvest a small amount of spores using the tip of a sterile bent sewing needle, which was attached to a 20 cm long needle holder, without touching the surface of the agar. Moreover, the flavonolignans were not detected in organic extracts of the milk thistle leaves used in this study.

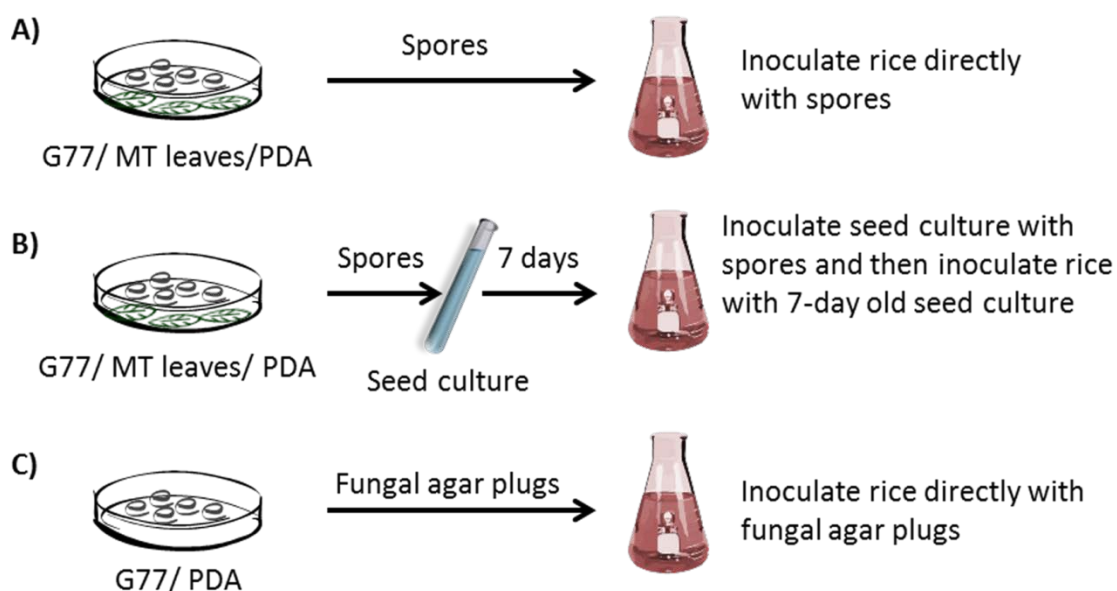


Figure 107. Experimental design for the fungus, *A. iizukae*, grown in potato dextrose agar culture with and without autoclaved milk thistle (*Silybum marianum*) leaves. Production of flavonolignans by the fungus, *A. iizukae*, was observed only in experiment A. G77 refers to the in-house code of the fungus *A. iizukae*, MT stands for milk thistle, and PDA for potato dextrose agar.

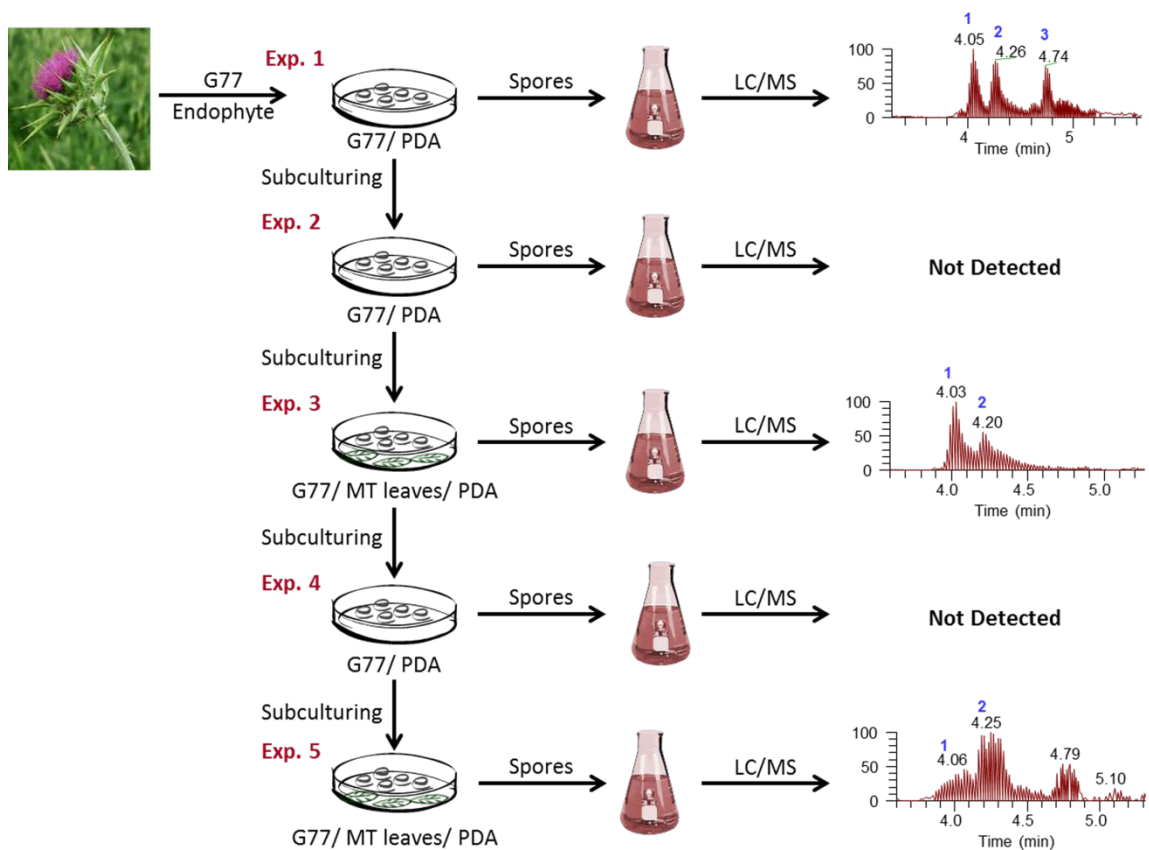


Figure 108. Flavonolignans production by *A. iizukae* upon sub-culturing. Abbreviations; G77: *A. iizukae*, MT: milk thistle, PDA: potato dextrose agar, 1: silybin A, 2: silybin B, and 3: isosilybin A.

The flavonolignan content of the various *A. iizukae* cultures was quantified using a calibration curve for an authentic sample of silybin B (2) (Figure 110, Supporting Information). The first *A. iizukae* isolate showed 0.22, 0.15, and 0.13 $\mu\text{g/g}$ extract of 1-3, respectively. The third *A. iizukae* culture showed 0.26 and 0.07 $\mu\text{g/g}$ extract of 1 and 2, respectively. The fifth *A. iizukae* culture showed 0.03 $\mu\text{g/g}$ extract for 1, while 2 was too low to be quantified. The limit of detection was estimated as 0.01 $\mu\text{g/g}$. Isosilybin A (3)

was detected only in the first *A. iizukae* culture, while none of the flavonolignans were detected in cultures 2 and 4 (Figure 108).

Neither artificial reconstitution of the interaction between a camptothecin attenuated fungal endophyte and its host plant,²³³ nor supplementing the fungal growth medium with host tissue extracts²²⁷ were successful in restoring the biosynthesis of camptothecin. However, in this flavonolignan example, the ability to stimulate biosynthesis of flavonolignan secondary metabolites by adding plant material to the axenic cultures may indicate stimulation of gene clusters ascribed to biosynthesis.

Obvious questions could be raised as to where the flavonolignans originated. The leaves that were amended to the cultures were ruled out for three reasons: there were no leaves in the medium when the flavonolignans were observed originally, compounds **1-4** were not detected in the leaves, and most importantly, the spores were removed from the Petri dishes without touching the agar medium before being transferred to the rice medium for growth. Also, contamination of both glassware and instrumentation were dismissed for at least three reasons: solvent blanks were injected between runs on the UPLC-PDA-HRMS-MS/MS system, the column on the UPLC was used exclusively for fungal samples, and the experiments between amended cultures (i.e. experiments 2 and 4 in Figure 108) did not show the production of flavonolignans. Further to this point, when the flavonolignans were observed originally, via a random screening of more than a score of fungal extracts, they were observed only in two samples. Later, it was determined that these isolates were identical via morphological and molecular methods. Finally, a misidentification of the flavonolignans was excluded, as the reference standards were

characterized thoroughly.^{203,205,234} Having eliminated all of those possibilities, we concluded that the leaves in the medium stimulated the biosynthesis of flavonolignans, such that these compounds could be observed upon growth of the fungus from spores on solid medium.

Discovery of endophytic fungi that can produce the same compounds of their associated host plants could be important from chemical and evolutionary perspectives. These may serve as a sustainable and alternative source for biologically active secondary metabolites that are produced by endangered or difficult-to-collect plant species. This has been attempted with a variety of metabolites.^{213,215,225} To date, the relative production levels in endophytic cultures have not been large enough to be considered viable. Future studies that explore adding substrates to culture media may improve this. From an evolutionary viewpoint, a horizontal transfer of genes encoding for secondary metabolites could have occurred between the host plant and its associated endophytic fungi.²³⁰ If so, then understanding how plant defenses against herbivores and pathogens evolved may need to also consider the impact of endophytic symbionts. Genomic studies of secondary metabolite gene clusters may provide additional information on how endophytic fungi are capable of producing plant-associated bioactive compounds and if there are cryptic gene clusters in fungal endophytes that are capable of yielding plant metabolic products. Such studies could yield fungal cultures that are amenable to genetic manipulation for the production of non-natural analogues of plant-based secondary metabolites.

Experimental Section

General Experimental Procedures. HRESIMS was performed on a Thermo LTQ Orbitrap XL mass spectrometer (ThermoFisher, San Jose, CA, USA) equipped with an electrospray ionization source in the negative ionization mode. Source conditions in the negative ionization mode were: 275 °C for capillary temperature, 3.5 kV for the source voltage, 42 V for capillary voltage, and 110 V for tube lens. Nitrogen was utilized for the sheath and auxiliary gases and set to 20 and 10 arb, respectively. Two scan events were carried out, full scan (100-2000) and ion trap MS/MS of the most intense ion from the parent mass list utilizing CID with normalized collision energy of 30. Thermo Scientific Xcalibur 2.1 software was used for instrument control and data analysis. UPLC was carried out on a Waters Acquity system [using a HSS T3 (2.1 × 100 mm, 1.8 μm) column (Waters Corp., Milford, MA, USA) equilibrated at 50 °C]. A mobile phase consisting of MeOH-H₂O (acidified with 0.1% formic acid) was used, starting with 30:70 then increasing linearly to 55% MeOH within 5 min, then returning to the starting conditions within 0.1 min, and holding for 0.9 min, for a total run time of 6 min and a flow rate of 0.6 mL/min. An Acquity UPLC photodiode array detector was used to acquire PDA spectra, which were collected from 201-499 nm with 3.6 nm resolution. Quantification of flavonolignans was performed using the same UPLC-MS method based on a linear calibration curve ($r^2 = 1.00$) of five concentrations (5, 10, 20, 40, and 80 μg/mL) of an authentic standard of silybin B (**2**) (Figure 109, Supporting Information).²⁰⁵

Isolation and Fermentation of Fungal Endophyte. A healthy, asymptomatic plant of *Silybum marianum* (milk thistle) was obtained from Horizon Herbs (lot # 6510), a

private farming company located in Williams, OR, USA, in August 2011. A voucher specimen of the plant material was deposited in the Herbarium of the University of North Carolina at Chapel Hill (NUC602014). The stems, leaves, roots, and seeds of the plant were cut into small pieces (approximately 2–5 mm in length) and washed in tap water. Subsequently, the segments were surface-sterilized by sequential immersion in 95% EtOH for 10 sec, NaClO (10–15% available chlorine, Sigma) for 2 min, and 70% EtOH for 2 min. The plant segments were transferred under aseptic conditions onto 2% malt extract agar (MEA, Difco; 20 g MEA, 1000 mL sterile distilled water with the antibiotics, streptomycin sulfate 250 mg/L and penicillin G 250 mg/L). To test the efficacy of the surface-sterilization procedure, and to confirm that emergent fungi were endophytic and not of epiphytic origin, individual surface-sterilized leaf, stem, root, and seed segments were spread and then removed on separate MEA plates with antibiotics; the absence of fungal growth on the nutrient medium confirmed the effectiveness of the sterilization procedure.²³⁵ Plates were sealed with Parafilm and incubated at room temperature until emergent fungal colonies were observed.

One of the endophytes from milk thistle leaves was accessioned as G77. The cultures of G77 were subsequently grown on 2% MEA, potato dextrose agar (PDA, Difco), and YESD media. After 14–21 days, spores of the fungus were used to inoculate 50 mL of a rice medium, prepared using 25 g of rice and twice the volume of rice with H₂O in a 250 mL Erlenmeyer flask. This inoculated medium was incubated at 22 °C until the culture showed good growth (approximately 14 days). A voucher culture of the G77 strain is

maintained in the Department of Chemistry and Biochemistry culture collection at the University of North Carolina at Greensboro.

Identification of the Fungal Strain. For molecular identification, DNA was extracted from fresh cultures of G77 grown on PDA amended with antibiotics (streptomycin sulfate 250 mg/L, penicillin G 250 mg/L, distilled water 1 L; antibiotics were added to the molten agar immediately after autoclaving). The nuclear internal transcribed spacers and intervening 5.8S gene, which together have been proposed as a barcoding marker for fungi,⁴⁵ along with the D1/D2 regions of the adjacent nuclear ribosomal large subunit,²³⁶ were amplified and sequenced following protocols published previously.⁶³ The consensus sequence of the ITS region was submitted for a BLAST search using the NCBI GenBank database to obtain species level information. The ITS sequence was then utilized in combination with the D1/D2 regions of the LSU for subsequent phylogenetic analysis. The top BLAST matches for G77 indicated similarities to sequences of *A. iizukae* (EF669597; Identities = 558/562 (99%), Gaps = 3/562 (0%)) and *A. iizukae* (EF669596; Identities = 558/ 562 (99%), Gaps = 3/562 (0%)). GenBank sequence EF669597 belongs to NRRL 3750, which is the type isolate of *A. iizukae*.²³⁷ The ITS sequence of G77 was also searched against the Fungal Barcoding database (<http://www.fungalbarcoding.org/>) using the pairwise sequence alignment. Results also suggested a 99% sequence similarity with an isolate of *A. iizukae* (DTO 065-G6). After the initial BLAST searches, top BLAST hits from the GenBank were downloaded and incorporated into a multiple sequence alignment of combined ITS and D1/D2 regions of LSU data using MUSCLE²³⁸ with default parameters in operation. MUSCLE was

implemented using the program Seaview v. 4.1.²³⁹ Maximum likelihood (ML) analyses were then performed using a RAxML v. 7.0.4^{240,241} run on the CIPRES Portal v. 2.0¹⁸⁵ with the default rapid hill-climbing algorithm and GTR model employing 1000 fast bootstrap searches. In addition, Bayesian analysis was also performed to assess support for tree topology using MrBayes.²⁴² The strain G77 was nested in a cluster with sequences of *A. iizukae* including the type isolate (NRRL 3750; EF669597) with moderate bootstrap support within the section Flavipedes (Figure 111, Supporting Information). Based on the results of the BLAST search and ML analysis, strain G77 was identified as *A. iizukae*. The combined ITS and partial LSU sequence for *A. iizukae* was deposited in GenBank (accession No. AB859956). *A. iizukae* Sugiyama was reported originally in soil from stratigraphic drilling core, Gymna Prefecture, Fujioka, Japan.²³² The endophytic strain isolated from milk thistle leaves was morphologically identical to the protologue.²³² The same analysis was conducted on G82, an isolate that was harvested from the stems of milk thistle; the taxonomy and phylogeny of G77 and G82 were identical.

Extraction. To each solid fermentation culture of *A. iizukae*, 60 mL of 1:1 MeOH-CHCl₃ were added. The culture was chopped with a spatula and shaken overnight (~16 h) at ~100 rpm at room temperature. The sample was filtered with vacuum, and the remaining residues were washed with 10 mL of 1:1 MeOH-CHCl₃. To the filtrate, 90 mL CHCl₃ and 150 mL H₂O were added; the mixture was stirred for 30 min and then transferred into a separatory funnel. The bottom layer was drawn off and evaporated to dryness. The dried organic extract was dissolved in 100 mL of 1:1 MeOH-CH₃CN and

100 mL of hexanes. The biphasic solution was transferred to a separatory funnel and shaken vigorously. The MeOH-CH₃CN layer was drawn off and evaporated to dryness under vacuum to yield 47.3, 301.7, and 575.9 mg of extract for the first, third, and fifth cultures, respectively. For UPLC-PDA-HRMS-MS/MS analysis, a sub-milligram aliquot of each extract was dissolved in equal volumes of MeOH and dioxane to obtain a final concentration of 2 mg/mL in a total volume of 150 μ L. To insure that flavonolignans were not carried over between successive injections, consecutive blanks of solvents were injected between samples during analysis on the UPLC-PDA-HRMS-MS/MS system.

Using the same protocols and solvent systems that were used for the fungal cultures, approximately 0.5 g of dry, finely ground milk thistle leaves were extracted and fractionated; this was repeated on three separate samples of leaves. An aliquot of each of the dried MeOH-CH₃CN extracts was analyzed for flavonolignans using the UPLC-PDA-HRMS-MS/MS method.

Supporting Information

Table 37. Chemical Formulas, Retention Times, UV Absorption Maxima, (-)-ESI HRMS, and (-)-ESI CID MS/MS of Silymarin constituents

compound	Chemical formula	Rt (min)		UV (nm)	ESI	
		Method I ^a	Method II ^b		[M-H] ⁻	MS/MS
Silybin A (1)	C ₂₅ H ₂₂ O ₁₀	3.42	4.04	230, 287	481.1128 (-2.5)	301.03, 453.12, 463.16, 257.07, 282.98, 454.15, 435.24, 437.34, 464.19, 451.25
Silybin B (2)	C ₂₅ H ₂₂ O ₁₀	3.46	4.24	230, 287	481.1127 (-2.7)	301.11, 463.19, 453.08, 257.05, 283.02, 433.11, 355.09, 435.28, 454.15, 464.26
Isosilybin A (3)	C ₂₅ H ₂₂ O ₁₀	3.58	4.74	230, 287	481.1130 (-2.2)	453.13, 257.01, 463.21, 454.19, 283.08, 437.14, 435.34, 300.90, 284.02, 229.01
Isosilybin B (4)	C ₂₅ H ₂₂ O ₁₀	3.60	4.89	232, 287	481.1125 (-3.2)	453.11, 257.05, 463.18, 283.02, 454.18, 301.01, 437.04, 435.20, 213.05, 215.14
Silydianin	C ₂₅ H ₂₂ O ₁₀	2.92	2.93	224, 289	481.1123 (-3.5)	453.16, 463.20, 454.26, 150.92, 168.84, 391.18, 178.97, 409.20, 437.18, 301.14
Silychristin	C ₂₅ H ₂₂ O ₁₀	2.85	2.54	230, 289	481.1130 (-2.2)	355.15, 463.11, 451.21, 337.08, 433.14, 325.16, 419.25, 453.17, 445.27, 435.13

Table 37 (Continued). Chemical Formulas, Retention Times, UV Absorption Maxima, (-)-ESI HRMS, and (-)-ESI CID MS/MS of Silymarin constituents

compound	Chemical formula	Rt (min)		UV (nm)	ESI	
		Method I ^a	Method II ^b		[M-H] ⁻	MS/MS
Isosilychristin	C ₂₅ H ₂₂ O ₁₀	2.85	2.30	230, 289	481.1126 (-2.9)	463.18, 445.19, 453.19, 437.11, 435.21, 178.94, 464.12, 311.10, 419.14, 433.24
Taxifolin	C ₁₅ H ₁₂ O ₇	2.09	1.59	228, 289	303.0501 (-3.0)	284.96, 176.98, 124.91, 275.14, 258.99, 178.99, 217.07, 241.03, 215.70, 174.98

^aUPLC was carried out using a BEH C₁₈ (2.1 × 50 mm, 1.7 μm) column equilibrated at 40 °C. A mobile phase consisting of CH₃CN-H₂O (acidified with 0.1% formic acid) was used, starting with 15:85 then increasing linearly to 100% CH₃CN within 8 min, holding for 1.5 min and then returning to the starting conditions within 0.5 min, for a total run time of 10 min and a flow rate of 0.3 mL/min.

^bUPLC was carried out using a HSS T3 (2.1 × 100 mm, 1.8 μm) column equilibrated at 50 °C. A mobile phase consisting of MeOH-H₂O (acidified with 0.1% formic acid) was used, starting with 30:70 then increasing linearly to 55% MeOH within 5 min, then returning to the starting conditions within 0.1 min, and holding for 0.9 min, for a total run time of 6 min and a flow rate of 0.6 mL/min.

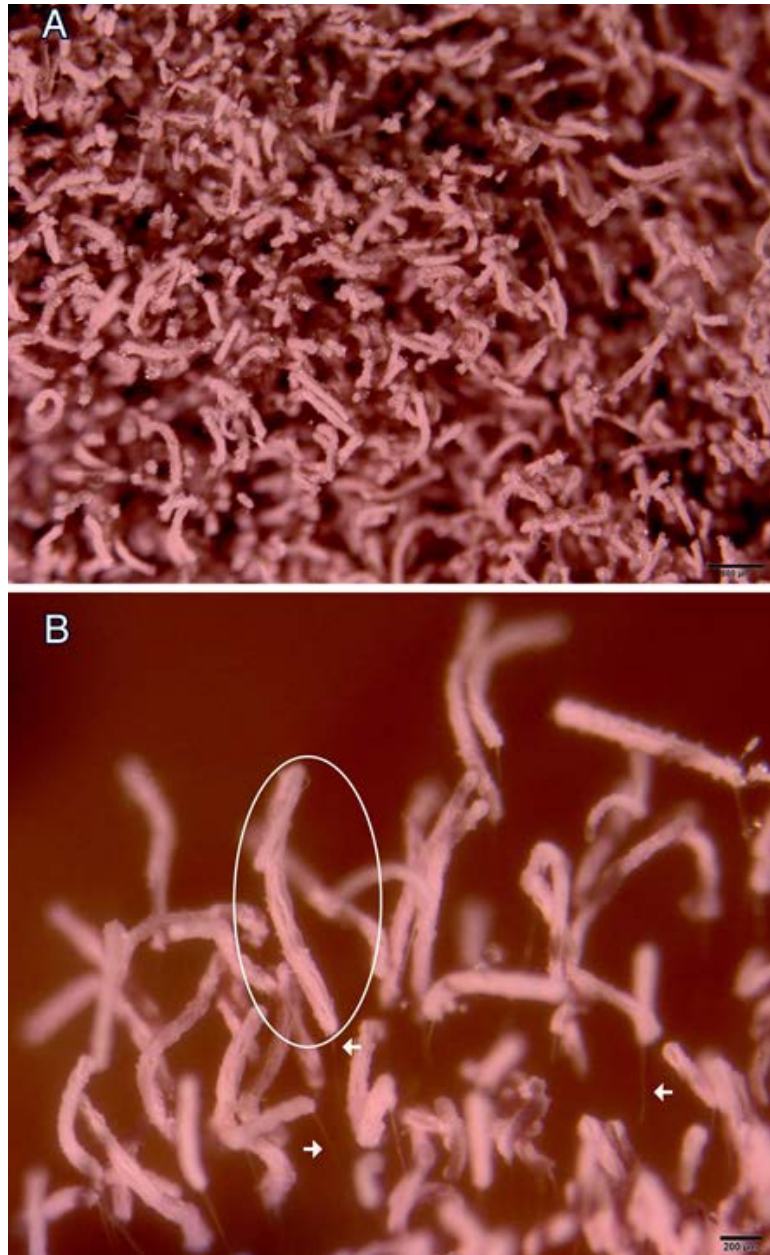


Figure 109. Stereomicrographs of *A. iizukae* culture on PDA media acquired using an Olympus SZX16 microscope equipped with an Olympus DP25 camera. In B, note the close up of columnar conidial heads (circled) and conidiophores (arrows). Bars: A = 500 μm . B = 200 μm . The conidial heads are where the conidia (i.e. spores) reside. In this fungus, the spores are formed well above (up to 1.5 mm) the surface of the agar in mature cultures. Hence, we were able to remove the spores with a bent sewing needle without touching the surface of the agar.

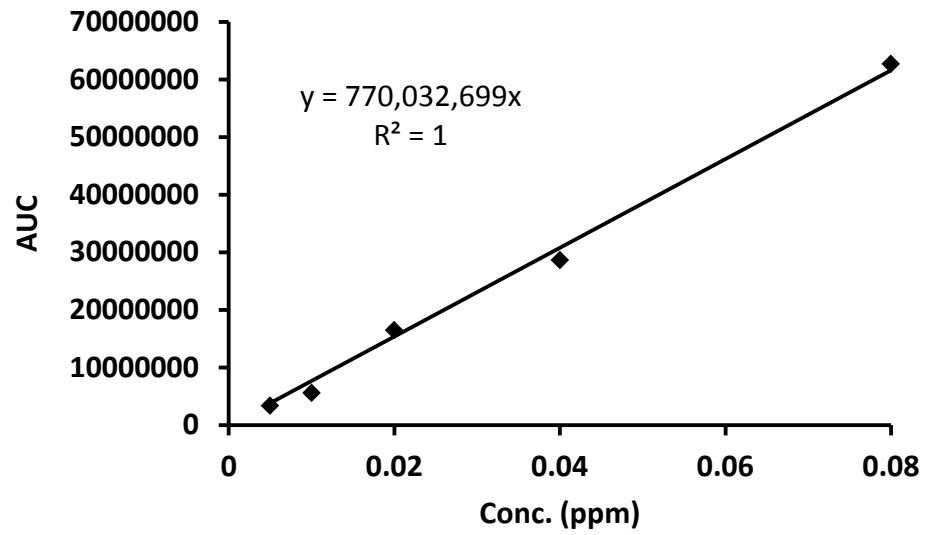


Figure 110. External calibration curve for silybin B measured by UPLC-ESIMS at five concentration levels (0.005, 0.01, 0.02, 0.04, and 0.08 $\mu\text{g}/\text{mL}$), each run in triplicate.

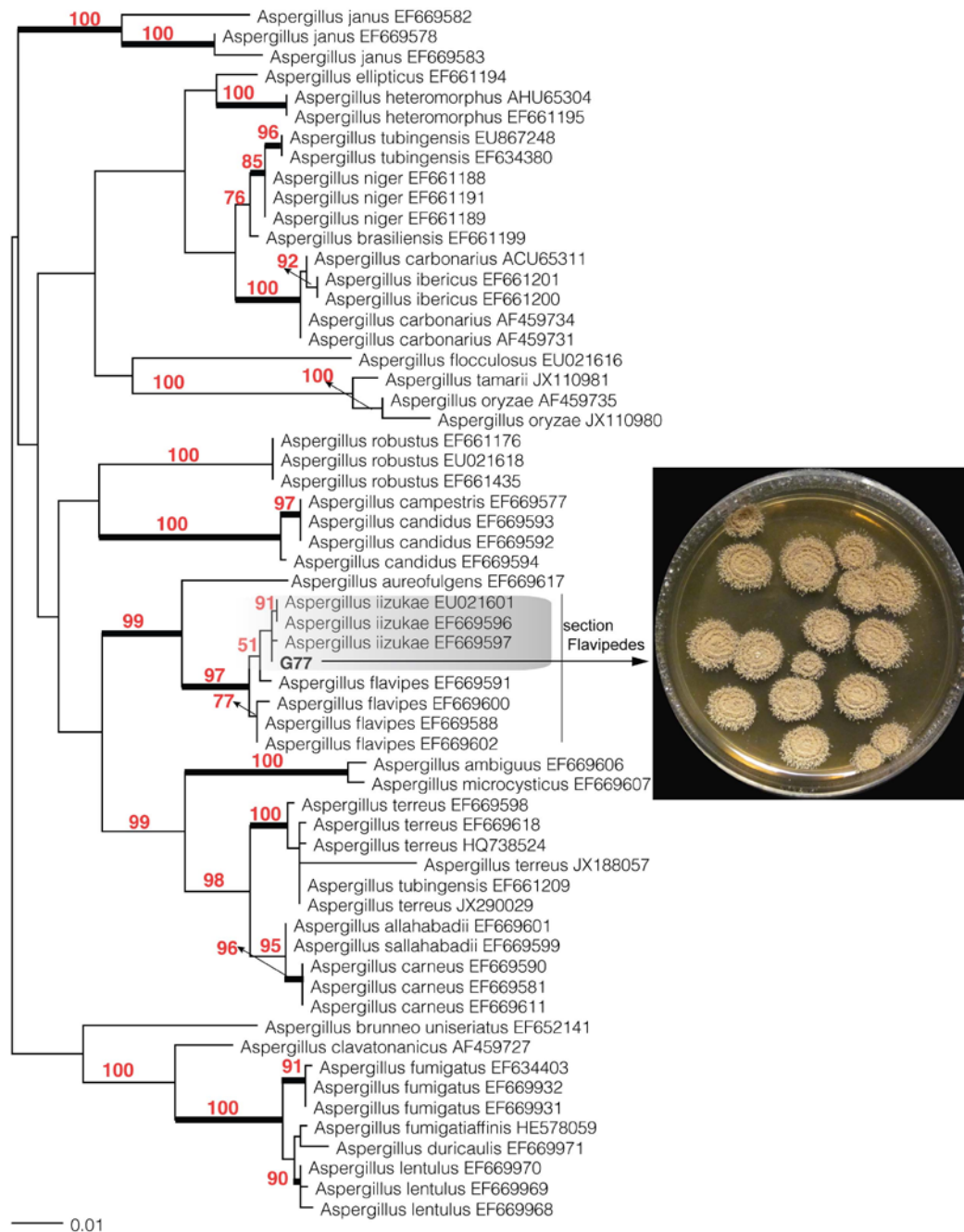


Figure 111. Phylogram of the most likely tree ($-\ln L = 4550.35$) from a RAxML analysis of 60 taxa based on complete ITS and partial region of the 28S large subunit nrDNA (1112 bp). Numbers refer to RAxML bootstrap support values based on 1000 replicates. Thickened branches indicate Bayesian probabilities $\geq 95\%$. G77 (highlighted in bold) is nested within the *A. iizukae* clade (highlighted in gray). The photograph shows *A. iizukae* growing on PDA (Difco) media.

CHAPTER IX
HIGH-RESOLUTION MS, MS/MS, AND UV DATABASE OF FUNGAL
SECONDARY METABOLITES AS A DEREPLICATION PROTOCOL FOR
BIOACTIVE NATURAL PRODUCTS

Tamam El-Elimat, Mario Figueroa, Brandie M. Ehrmann, Nadja B. Cech, Cedric J. Pearce, and Nicholas H. Oberlies. *Journal of Natural Products* 2013, 76, 1709-1716.

A major problem in the discovery of new biologically active compounds from natural products is the re-isolation of known compounds. Such re-isolations waste time and resources, distracting chemists from more promising leads. To address this problem, dereplication strategies are needed that enable crude extracts to be screened for the presence of known compounds before isolation efforts are initiated. In a project to identify anticancer drug leads from filamentous fungi, a significant dereplication challenge arises, as the taxonomy of the source materials are rarely known, and, thus, the literature cannot be probed to identify likely known compounds. An ultra-performance liquid chromatography-photodiode array-high-resolution tandem mass spectrometric (UPLC-PDA-HRMS-MS/MS) method was developed for dereplication of fungal secondary metabolites in crude culture extracts. A database was constructed by recording HRMS and MS/MS spectra of fungal metabolites, utilizing both positive- and negative-ionization modes. Additional details, such as UV-absorption maxima and retention times, were also recorded. Small-scale cultures that showed cytotoxic activities were

dereplicated before engaging in the scale-up or purification processes. Using these methods, approximately 50% of the cytotoxic extracts could be eliminated from further study after the confident identification of known compounds. The specific attributes of this dereplication methodology include a focus on bioactive secondary metabolites from fungi, the use of a 10-min chromatographic method, and the inclusion of both HRMS and MS/MS data.

Many natural product drug discovery programs utilize bioactivity-directed fractionation methodologies for the isolation of lead compounds from crude extracts, in which the bioassay results guide the purification processes.^{243,244} While countless studies demonstrate the utility of this approach in identifying new drug leads, with taxol and camptothecin possibly the most well-known examples,²⁴⁵⁻²⁴⁷ it is often criticized for resulting in the re-isolation and re-characterization of previously known compounds. This criticism of natural products research grows in significance annually, as over 246,000 compounds have been described from Nature, with approximately 4,000 new ones added each year.¹⁵¹ Thus, to expedite the discovery of new leads, and to avoid the re-isolation of previously known compounds, it is crucial to discriminate between known vs. new compounds as early as possible. This process, which is termed “dereplication”,²⁴⁸ enables the efficient use of human and financial resources,^{249,250} so that efforts can be focused on the discovery of structurally novel compounds.^{249,251}

Early dereplication strategies focused largely on botanical extracts. The ability to characterize a plant’s taxonomy (at least to the genus level) based on morphology can simplify the dereplication process, as it enables botanical extracts to be screened for

known chemical compounds specific to the taxa under investigation. Some examples include colchicinoids in *Colchicum* spp.,²⁵² acetogenins in plants of the Annonaceae,²⁵³ phenolics in the genus *Lippia*,²⁵⁴ steroidal alkaloids in *Buxus* spp.,²⁵⁵ and triterpenoids in the genus *Actaea*.²⁵⁶

In contrast, dereplication can be more complicated for organisms of unknown taxonomy.^{257,258} This is the case for our ongoing research aimed at identifying anticancer drug leads from non-sporulating filamentous fungi.^{11,17} Fungi are known to produce structurally diverse secondary metabolites that display a wide range of biological activities. Although fungi are relatively under-investigated,^{8,23} a major challenge with these organisms as a source of bioactive lead compounds is the production of mycotoxins, which can be observed across different fungal species. Examples of these include aflatoxins, ochratoxins, trichothecenes, citreoviridin, fumonisins, and various indole-derived tremorgenics.¹³ Indeed, a promising side application for the presently described dereplication procedure is the rapid identification of mycotoxins in foods, as mycotoxins continue to present safety challenges for the food supply.^{259,260} While molecular methods have accelerated the process,⁴⁵ assignment of fungal taxonomy can be a tedious procedure, and regardless, only about 100,000 of the estimated 1.5 to 5.1 million species of fungi have been ascribed a scientific name.^{8,23} Hence, the taxonomy of fungi being studied in natural products programs is often not known at all, or only determined after compounds have been isolated. Thus, there is a critical need for better strategies to dereplicate crude fungal extracts for the presence of known chemical entities, including mycotoxins and other biologically relevant compounds. In doing so,

resources for drug discovery can be devoted into those samples most likely to yield new chemical entities.¹⁷

Several dereplication methods have been reported in the literature for fungal secondary metabolites; however, all of these are hampered by at least one, if not several, limitations, including long run times (30 min or more), low-resolution mass measurements, and/or lack of confirmatory MS-MS data.^{257,261-264} A recent LC-UV/vis-MS-based dereplication strategy utilized UV spectra (acquired with a photodiode array detector) and ESI⁺/ESI time-of-flight MS for assignment of 719 microbial natural product and mycotoxin reference standards.²⁶² While effective, only 17% (29 compounds) of our database of cytotoxic fungal compounds overlapped with the standards used, as this earlier procedure did not have a focus on compounds with biological activity.²⁶² Moreover, a 30-min chromatographic method was utilized,²⁶² which may be too long for routine processing of scores of samples simultaneously, particularly for shared instruments. Finally, CID MS/MS data were not reported,²⁶² which serve to fingerprint and confirm the identity of dereplicated compounds. Thus, the goal of the present study was to harness the powerful resolution and short analysis time afforded by ultra-performance liquid chromatography (UPLC) coupled to the outstanding mass accuracy of an Orbitrap mass spectrometer to develop a rapid and effective method to dereplicate biologically active fungal extracts. In addition, MS/MS and UV (photodiode array) spectra were employed as an integral part of the strategy, so as to differentiate isobaric compounds often present in natural product extracts. Finally, given the likelihood of the co-elution of compounds in complex mixtures separated over short (<10

min) chromatographic run times, a data analysis strategy was incorporated (ACD/IntelliXtract), aimed at rapidly deconvoluting complex LC/MS chromatograms.

Results and Discussion

The foundation of the present UPLC-PDA-HRMS-MS/MS dereplication procedure was the construction of a database for the identification of more than 170 fungal secondary metabolites via recording chromatographic retention times, UV data, and full-scan (high-resolution) mass spectra and MS/MS spectra in both positive and negative electrospray ionization (ESI) modes. The chromatographic and tune methods were developed using a mixture of 36 compounds representing diverse structural classes that ranged from terpenoids to polyketides to depsipeptides. To test the developed method, a mixture of ten structurally diverse compounds was prepared and analyzed (Figures 114 and 115, Supporting Information). The resulting 10-min chromatographic method and associated high-resolution mass spectra could be used to discriminate between all the compounds in the database. Of these, only two resorcylic acid lactones, *7-epi-zeaenol* and *15-O-desmethyl-5Z-7-oxozeaenol*,¹⁹ did not ionize in the ESI⁺ mode, whereas 17 compounds, mostly trichothecenes,²³¹ did not ionize in the ESI⁻ mode (Table 38, Supporting Information). Also, the molecular ion peaks of aphidicolin and viridicatumtoxin were the only ones not detected in the positive-ion mode, due to the facile loss of H₂O; however, the molecular ion peak for the latter was observed in the negative-ion mode. All MS/MS fragmentation data were collected using collisionally induced dissociation (CID) with 30% collision energy, and the ten most intense

fragments for each compound were utilized in the database (Table 38, Supporting Information).

To initiate the dereplication process, small-scale cultures of fungi were grown on a solid medium and extracted using previously described protocols;^{19,22,62,63} the extracts were then evaluated for cytotoxicity against a panel of human cancer cell lines in culture, including MCF-7, H-460, and SF-268 cells.^{50,265} Samples deemed active were prepared for analysis by dissolving a sub-milligram aliquot of the bioactive crude extracts in equal volumes of MeOH and dioxane to obtain a final concentration of 2 mg/mL. The subsequent dereplication strategy utilized a three-step approach (Figure 112). First, UPLC-HRMS was used to acquire the TIC (total ion chromatogram) of the extract and hence measure the accurate masses of all ions detectable. This TIC was then uploaded into ACD MS Manager with add-in software Intellixtract, which cross-referenced the molecular ion peaks with the database that was constructed as a list of compound names, corresponding molecular weights, and retention times (Table 38, Supporting Information). These results were then confirmed manually using HRMS data, and the MS/MS and UV spectra were compared with the database to verify the identity of any hits. The use of the MS/MS data, retention times, and UV spectra confirmed the identity of the compounds in the extract; the only exception would be for the possible, albeit rare, case of isomers. Moreover, the ACD/IntelliXtract software, which has the capability to extract all chromatographic components in the LC/MS datasets, expedited the identification process, due to its capability of resolving overlapping and co-eluting components. Finally, using IntelliXtract, it was possible to reconstruct pure component

chromatograms for each chromatographic component and annotate spectral peaks with the mass of the protonated or deprotonated molecule.²⁶⁶

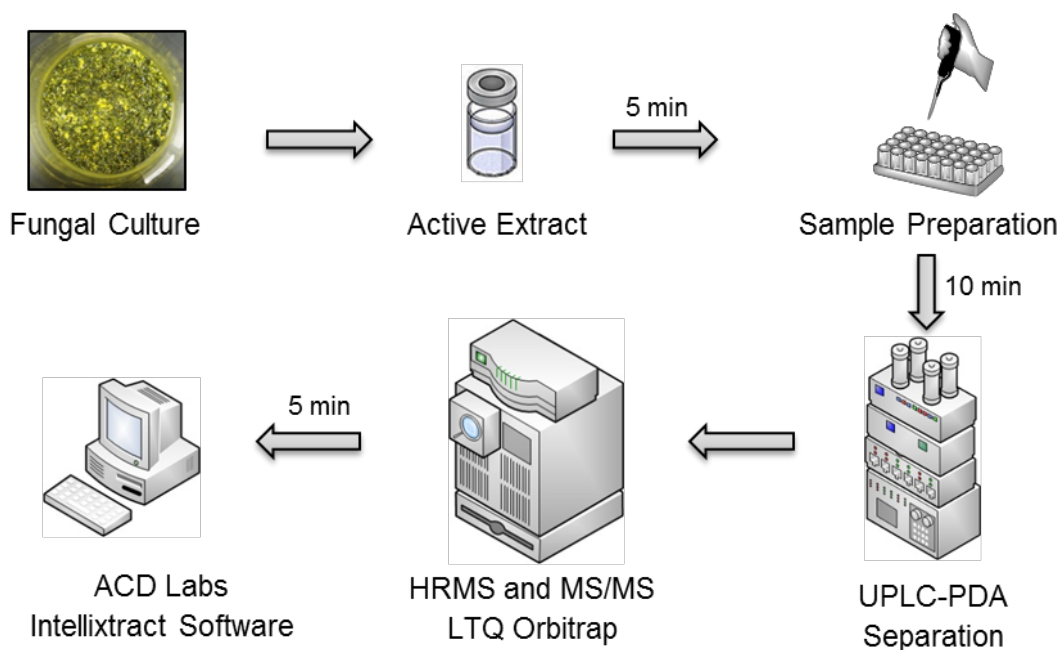


Figure 112. Schematic of the workflow for the proposed dereplication protocol. Aliquots of active fungal extracts were evaluated using an UPLC-PDA-HRESIMS-MS/MS method, the data were analyzed using ACD Labs Intellixtract software and compared with an in-house database, and extracts producing known compounds were excluded.

Using these procedures, 106 small-scale culture extracts were dereplicated. All of these displayed sufficiently potent cytotoxicity against a small cancer cell-line panel to warrant further investigation. However, based on the dereplication results, 55 samples were ruled out as containing known compounds. By doing so, resources were prioritized on samples most likely to yield new compounds. The three examples shown below

demonstrate the work flow of the dereplication methodology, illustrating its utility for a broad range of structural classes of bioactive natural products.

Dereplication of Verticillins (Epipolythiodioxopiperazine Alkaloids). An extract of the filamentous fungus MSX39480 displayed potent cytotoxic activity for the H460 cell line (94 and 88% inhibition of cell growth when tested at 20 and 2 $\mu\text{g/mL}$, respectively) and thus was subjected to the dereplication protocol. Seven epipolythiodioxopiperazine (ETP) alkaloids were dereplicated by matching retention times, HRMS, and MS/MS data, namely, 11'-deoxyverticillin (**1**), Sch 52900 (**2**), verticillin A (**3**), gliocladicillin A (**4**), gliocladicillin C (**5**), Sch 52901 (**6**), and verticillin H (**7**). To illustrate the value of the protocol, a compound eluting at 5.51 min with a m/z of 741.1285 was detected in the extract. The isotopic pattern of the molecular ion peak, in conjunction with intensity-ratio calculations, suggested the presence of four sulfur atoms. ACD/Intellixtract analysis of the UPLC-HRMS data identified this as compound **5**, a dimeric ETP alkaloid, and the accurate mass and retention time data matched that of a standard of **5** (Figures 114 and 115). As a confirmation, excellent agreement between the MS/MS spectra of the standard and unknown was achieved (Figure 114). The same methodology was used to verify the identity of compounds **1-4**, **6**, and **7** (Figure 115). Dimeric ETP alkaloids are bioactive secondary metabolites reported to have potent cytotoxic²⁶⁷⁻²⁷⁶ and antibacterial activities,²⁷⁷⁻²⁸² along with antiparasitic,²⁸³ nematocidal,²⁸⁴ antiviral,²⁸⁵ and immunosuppressive properties.²⁸⁶ Hence, this class of compounds has been well-studied, including previously in our laboratory,⁶² and, thus,

their rapid dereplication allowed us to focus on other leads with a greater potential to yield new substances.

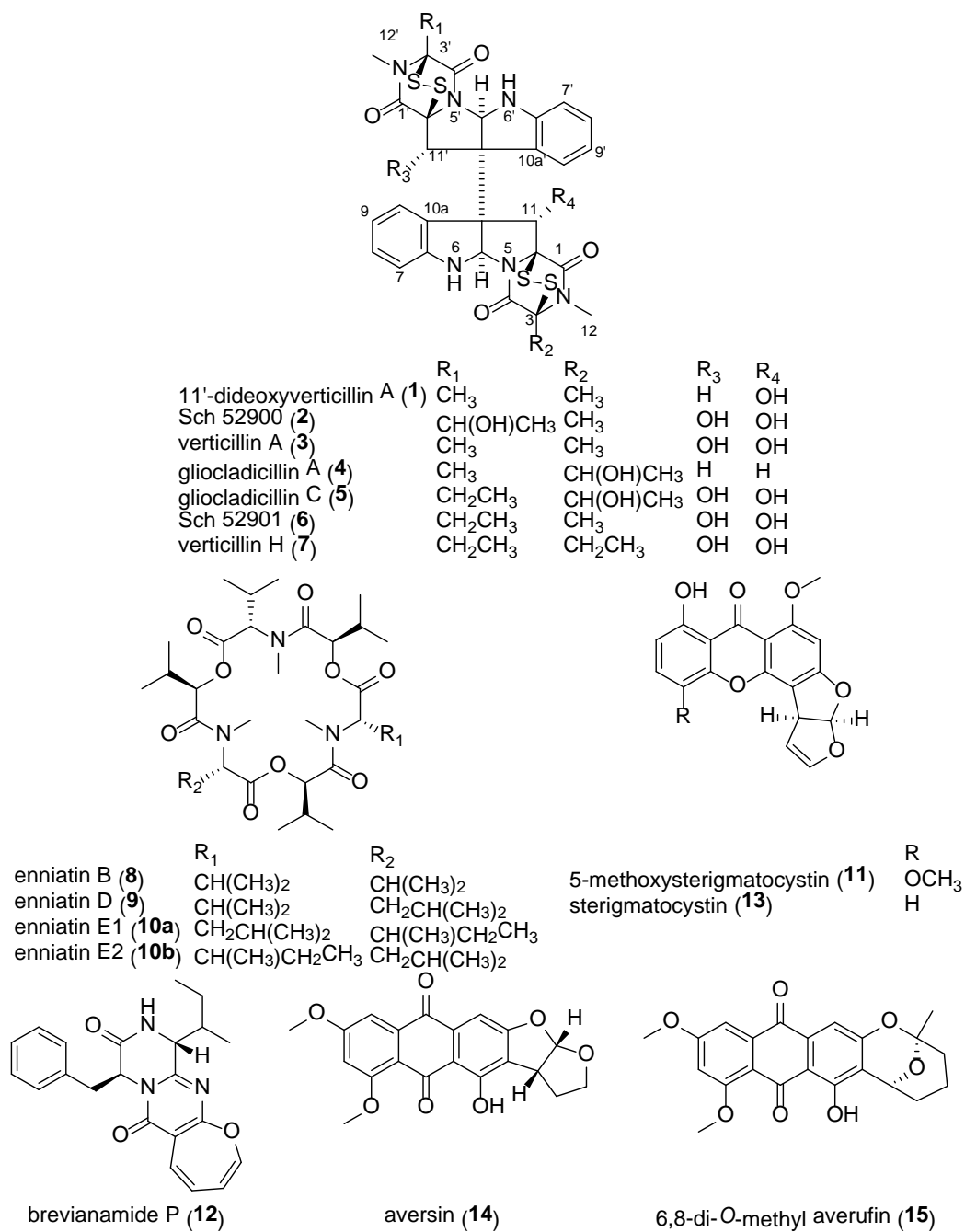


Figure 113. Structures of compounds 1-15.

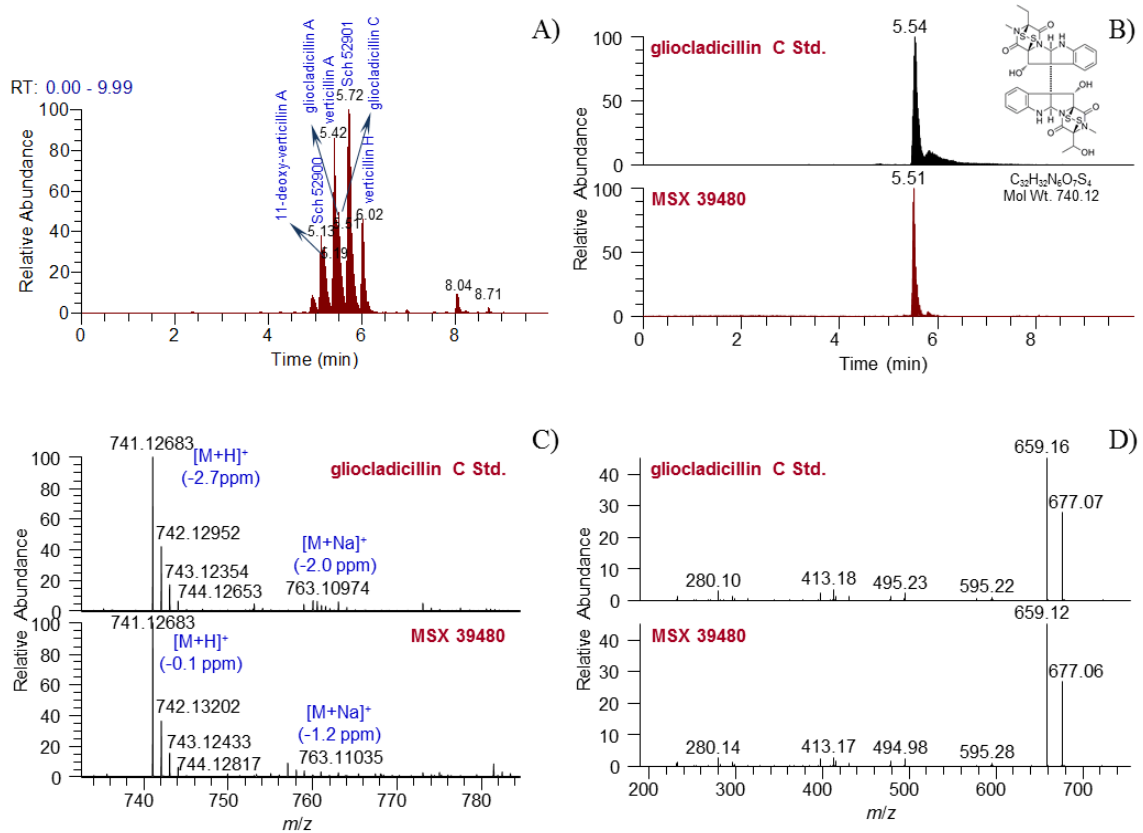


Figure 114. A. (+)-ESI SIC of crude MSX39480 extract (m/z : 681, 695, 697, 711, 725, 727, 741), B. Overlay chromatographic peaks of gliocladicillin C, C. (+)-HRESIMS of gliocladicillin C, and D. MS/MS CID fragmentation spectra of gliocladicillin C.

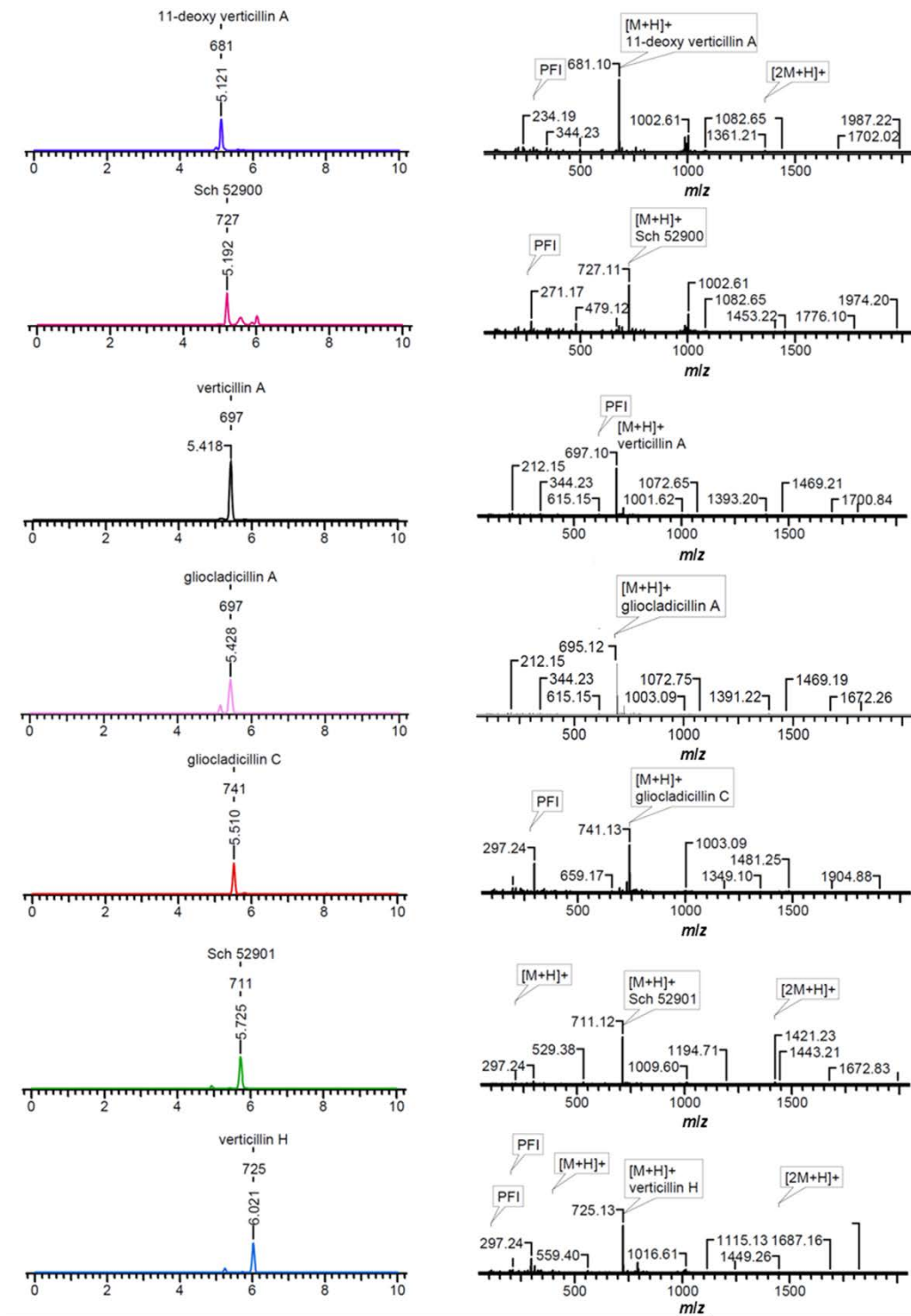


Figure 115. ACD/Intellixtract analysis of the TIC of an extract of MSX39480.

Dereplication of Enniatins. On the small scale, an extract of the fungus MSX44407 showed potent cytotoxicity (96 and 71% inhibition when tested against H460 cells at 20 and 2 $\mu\text{g/mL}$, respectively). The TIC of the crude extract revealed the presence of three major compounds eluting at 6.74, 7.01, and 7.25 min (Figure 116). ACD/Intellixtract analysis of the UPLC-HRMS data matched the second and third compounds to the cyclodepsipeptides, enniatins D (**9**) and the unresolved isomers, enniatins E1 (**10a**) and E2 (**10b**), respectively; HRMS and MS/MS data confirmed these assignments (Figure 116). While the mass spectrometric data of the first eluting compound did not match any substance in the database, the HRMS data yielded a molecular formula of $\text{C}_{33}\text{H}_{57}\text{N}_3\text{O}_9$ (m/z 640.4138 $[\text{M}+\text{H}]^+$, calcd for 640.4168). Searching the *Dictionary of Natural Products*¹⁵¹ using the molecular formula resulted in one lead, enniatin B (**8**). Although **8** was not in the database, given its structural similarity to compounds **9**, **10a**, and **10b**, the extract was assigned as not of further interest. Twenty-nine enniatins, which are cyclohexadepsipeptides, have been characterized in the literature, either as a single compounds or mixtures of unresolved isomers, and a recent review discusses their range of biological activities.⁸²

Dereplication of Aflatoxins. Another culture, MSX40080, showed potent cytotoxic activity when tested against H460 cells (95 and 76% growth inhibition when evaluated at 20 and 2 $\mu\text{g/mL}$, respectively). The TIC and PDA data of the crude extract suggested a series of structurally related compounds with distinctive UV absorption patterns. ACD/Intellixtract analysis of the UPLC-HRMS data lead to the identification of five compounds, 5-methoxysterigmatocystin (**11**), brevianamide P (**12**), sterigmatocystin (**13**),

aversin (**14**), and 6,8-di-*O*-methyl averufin (**15**). These assignments were confirmed by checking the HRMS and MS/MS spectra and UV absorption maxima with those in the database (Figures 117 and 118). Aflatoxins are regarded as nuisance mycotoxins with potent biological activity; hence their facile and rapid dereplication is important. These toxins have been investigated extensively due to their carcinogenic effects,²⁸⁷ particularly in contaminated grains.²⁸⁸

In conclusion, UPLC-PDA-HRMS-MS/MS methodology has been developed and implemented for the dereplication of cytotoxic secondary metabolites in crude extracts of fungal cultures. This methodology has several attributes that distinguish it from previous systems. First, the database, which includes full-scan high-resolution mass spectra and MS/MS spectra from both the positive- and negative-ionization modes coupled with UV-absorption maxima and retention times, is the first to be constructed based on cytotoxic fungal secondary metabolites. Furthermore, the use of UPLC enables a rapid (10 min) chromatographic method, the fastest utilized in a comprehensive natural product dereplication strategy. This in turn facilitates the rapid nature of the protocol, such that less than 25 min, including the time for sample preparation, is needed to acquire and interpret the data. Moreover, the use of HRMS and MS/MS data imparts a high degree of confidence in the structure of the dereplicated leads. Coupling these data with the use of the ACD/IntelliXtract, which extracts all chromatographic components in the LC-MS datasets and automatically assigns each as $[M+H]^+$ or $[M-H]^-$, expedites the identification process. In particular, the capability of the ACD/IntelliXtract to deconvolute overlapping and co-eluting components makes it possible to dereplicate trace compounds and enables

the application of a short (10-min) chromatographic run time. Finally, the method was designed as a qualitative tool, and as such, the sensitivity for individual compounds was not measured a priori, especially since sensitivity is compound specific. However, the coupling of the resolving power of the UPLC with the enhanced sensitivity of mass spectrometry enabled the detection of trace amounts of compounds in crude extracts. In using this protocol for over two years on hundreds of samples, compounds present in as low as 0.22 mg/g of extract were detected readily.

A promising side application of the dereplication methodology developed could be the detection and identification of mycotoxins in food commodities and agricultural products. Mycotoxins have attracted world-wide attention due to their profound negative economic consequences. It has been estimated that one quarter of the world's crops are contaminated with mycotoxins. Losses in the USA and Canada due to mycotoxins on the feed and livestock industries are of the order of \$5 billion annually.^{289,290} The protocol described could be utilized in any laboratory having a mass spectrometer coupled with a UPLC, using the same analytical column, thereby enabling the identification of a suite of mycotoxins, even without reference standards.

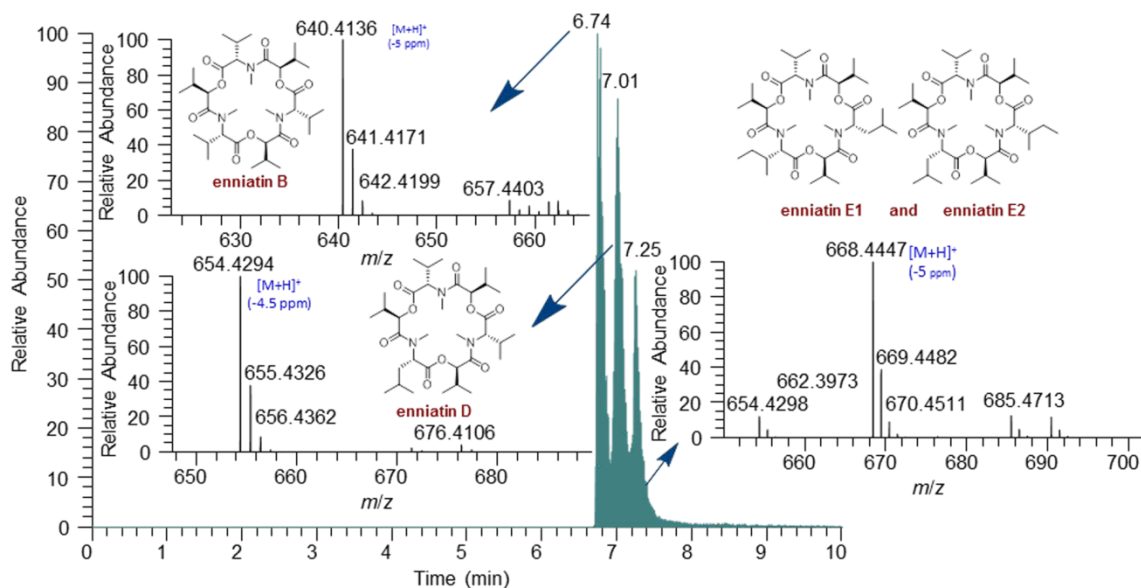


Figure 116. (+)-ESI SIC of the crude extract of MSX44407 (m/z : 668, 654, 640).

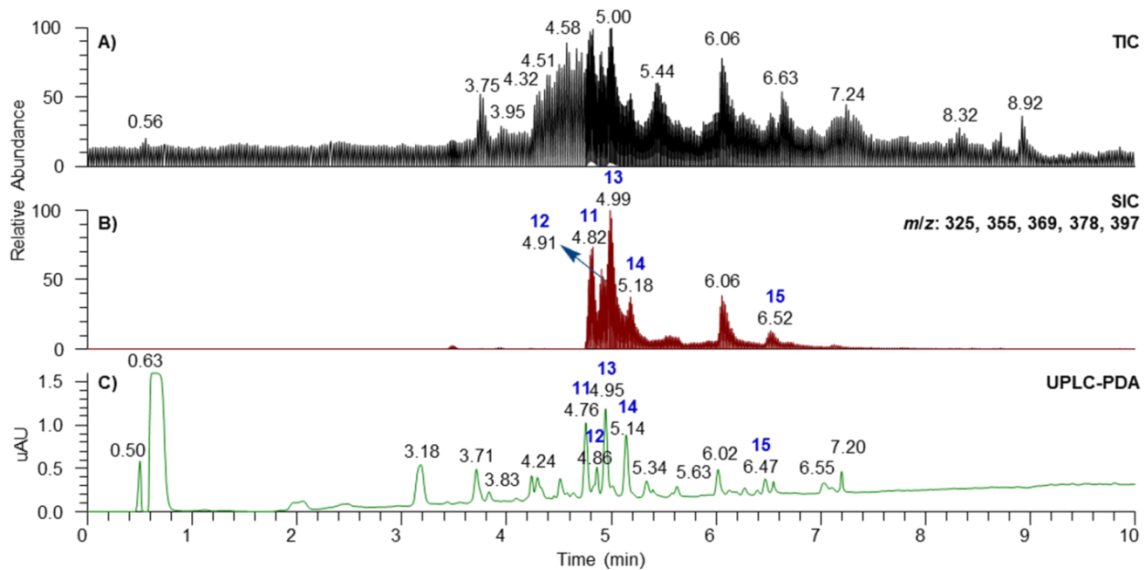


Figure 117. A. (+)-ESI TIC, B. SIC (m/z : 325, 355, 369, 378, and 397 for peaks 13, 11, 14, 12, and 15, respectively), and C. UPLC-PDA of the crude extract of MSX40080.

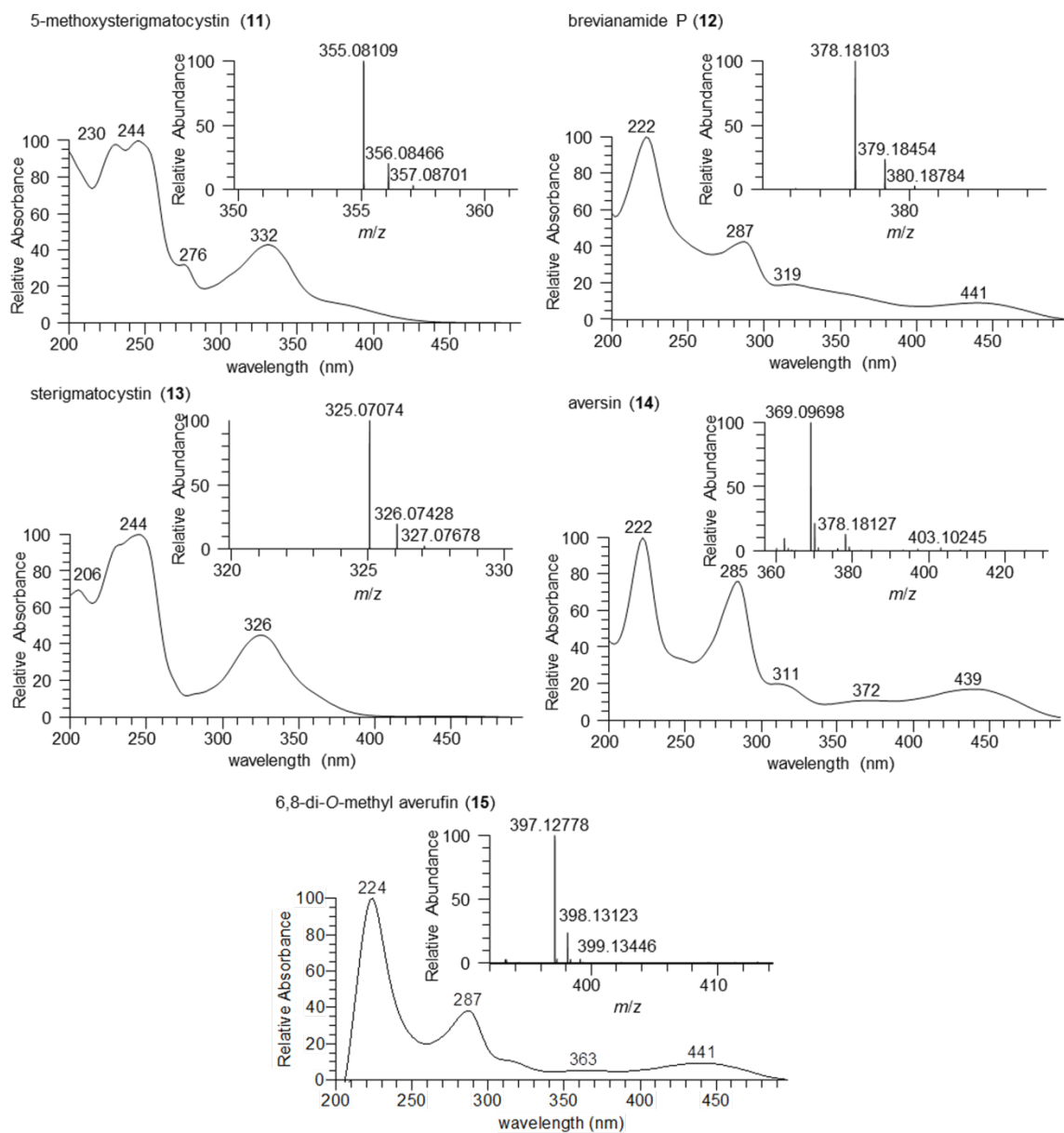


Figure 118. (+)-HRESIMS and PDA spectra of compounds **11-15**.

Experimental Section

General Experimental Procedures. HRESIMS was performed on a Thermo LTQ Orbitrap XL mass spectrometer (ThermoFisher, San Jose, CA) equipped with an electrospray ionization source. Source conditions in the positive-ionization mode were set at 275 °C for the capillary temperature, 4.5 kV for the source voltage, 20 V for capillary voltage, and 95 V for the tube lens. For the negative-ionization mode, the source conditions for temperature were 3.5 kV for the source voltage, 42 V for capillary voltage, and 110 V for the tube lens. Nitrogen was utilized for the sheath gas and set to 25 and 20 arb for the positive and negative modes, respectively. For the negative-ionization mode, nitrogen was also used as an auxiliary gas and set at 10 arb. In both modes, two scan events were carried out, full-scan (100-2000) and ion-trap MS/MS of the most intense ion from the parent mass list utilizing CID with a normalized collision energy of 30. External instrument calibration was performed using an LTQ ESI positive-ion calibration solution consisting of caffeine (20 µg/mL), MRFA (1 µg/mL) and Ultramark 1621 (0.001%) in an aqueous solution of CH₃CN (50%), MeOH (25%) and acetic acid (1%). For the ESI negative-ion calibration, sodium dodecyl sulfate (2.9 µg/mL) and sodium taurocholate (5.4 µg/mL) were added to the LTQ ESI calibration solution instead of caffeine and MRFA. Thermo Scientific Xcalibur 2.1 software was used for instrument control and data analysis. UPLC was carried out on a Waters Acquity system [using a BEH C₁₈ (2.1 × 50 mm, 1.7 µm) column (Waters Corp., Milford, MA, USA) equilibrated at 40 °C]. A mobile phase consisting of CH₃CN-H₂O (acidified with 0.1% formic acid) was used, starting with 15:85 then increasing linearly to 100% CH₃CN within 8 min, holding for

1.5 min and then returning to the starting conditions within 0.5 min. An Acquity UPLC photodiode array detector was used to acquire PDA spectra, which were collected from 200-500 nm with 4 nm resolution.

Reference Standards. Secondary metabolites were isolated and characterized from the Mycosynthetix Inc. library of filamentous fungi, as described previously.^{17,19-22,62,63,82,105,291}

Extraction Procedure. Small-scale cultures of fungi were grown on a solid, grain-based medium in 250 mL Erlenmeyer flasks, as described in detail previously.^{19,62,63} To each flask were added 60 mL of 1:1 MeOH-CHCl₃. The culture was chopped with a spatula and shaken overnight (~16 h; at ~100 rpm) at rt. Each sample was filtered using vacuum, and the remaining residues were washed with small volumes of 1:1 MeOH-CHCl₃. To the filtrate, 90 mL CHCl₃ and 150 mL H₂O were added; the mixture was stirred for 2 h, and then transferred into a separatory funnel. The bottom layer was drawn off into a round-bottomed flask and evaporated to dryness. The dried organic extract was re-constituted in 100 mL of 1:1 MeOH-CH₃CN and 100 mL of hexanes. The biphasic solution was stirred for 1 h and then transferred to a separatory funnel. The MeOH-CH₃CN layer was drawn off and evaporated to dryness under vacuum. This defatted material was then submitted for cytotoxic activity evaluation using a set of three cancer cell lines, as described previously.^{50,265} Extracts displaying potent cytotoxic activities (i.e., less than 20% survival when tested at 20 μg/mL) were dereplicated. A sub-milligram aliquot of the bioactive extracts was used for dereplication analysis by

dissolving the extract in equal volumes of MeOH and dioxane to obtain a final concentration of 2 mg/mL in a total volume of 150 μ L.

Data Analysis. Data from 172 fungal secondary metabolites are in the Supporting Information (Table 38), which lists the metabolites, molecular formula, retention time, UV-absorption maxima, high-resolution full-scan mass spectra, and MS-MS data (top ten most intense peaks), utilizing both the positive- and negative-ionization modes. ACD MS Manager with add-in software IntelliXtract, Advanced Chemistry Development, Inc. (Toronto, Canada), was used for the primary analysis of the LC-MS data.

Cytotoxicity Assay. The cytotoxicity measurements against the MCF-7⁴⁶ human breast carcinoma (Barbara A. Karmanos Cancer Center), NCI-H460⁴⁷ human large cell lung carcinoma (HTB-177, American Type Culture Collection (ATCC), and SF-268⁴⁸ human astrocytoma (NCI Developmental Therapeutics Program) cell lines were performed as described previously.^{50,265}

Supporting Information

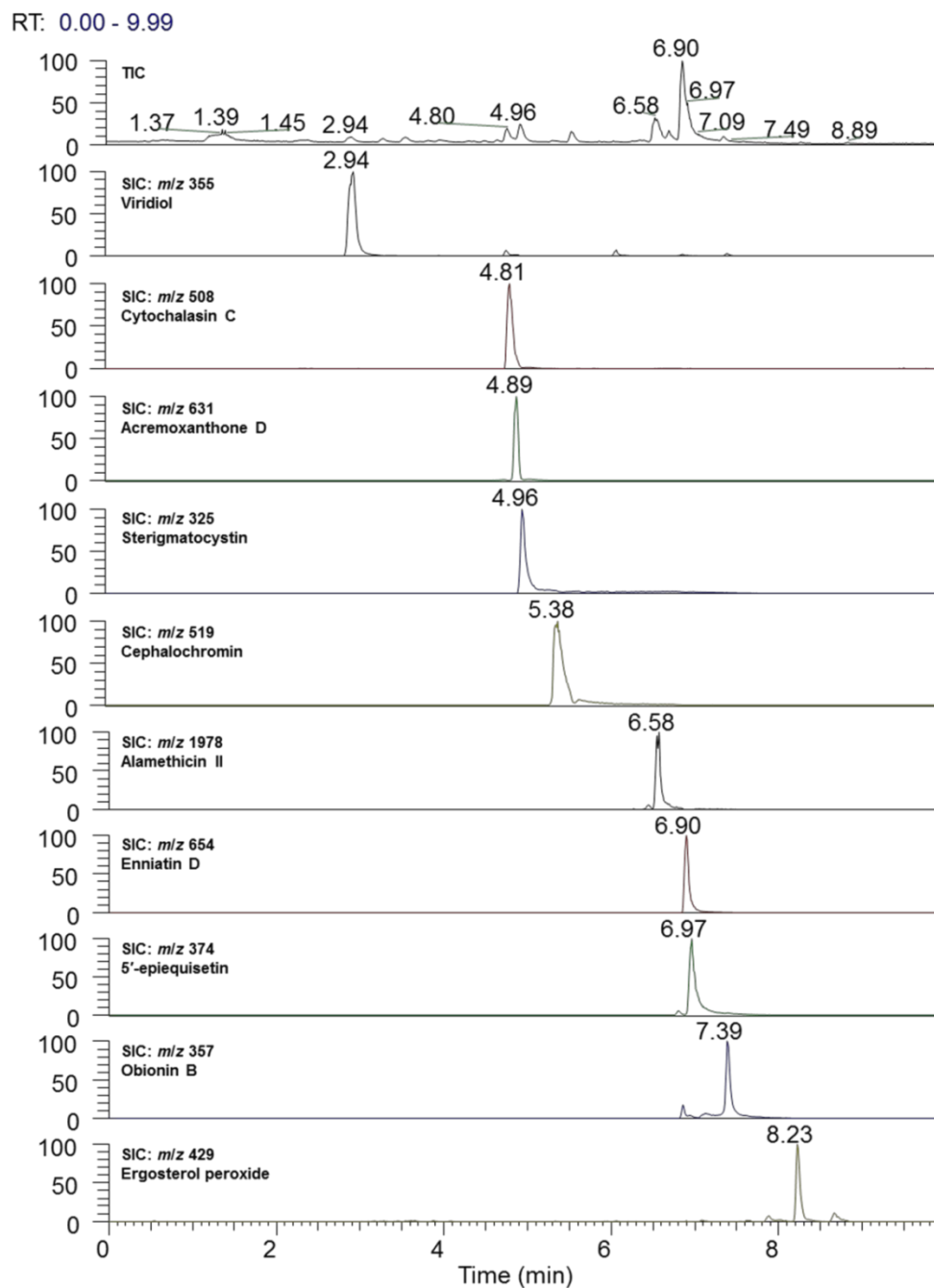
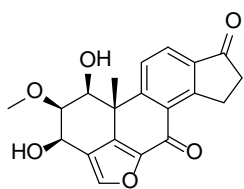
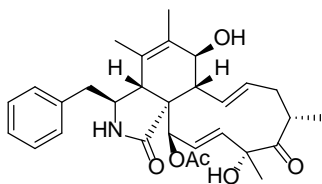


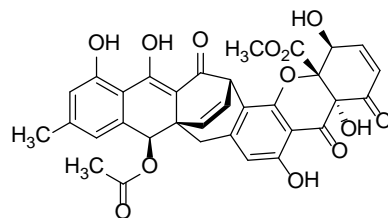
Figure 119. (+)-ESI TIC and SIC (m/z : 355, 508, 631, 325, 519, 1978, 654, 374, 357, and 429) of a mixture of ten standard compounds.



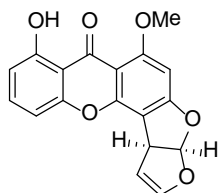
Viridiol



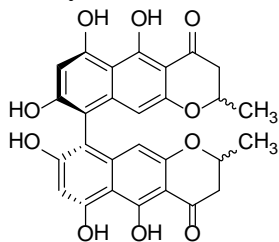
Cytochalasin C



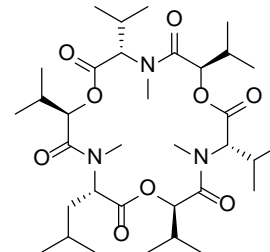
Acremoxanthone D



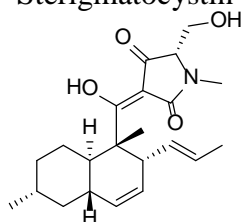
Sterigmatocystin



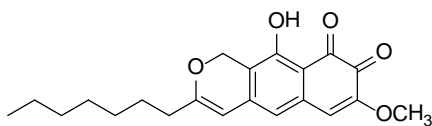
Cephalochromin



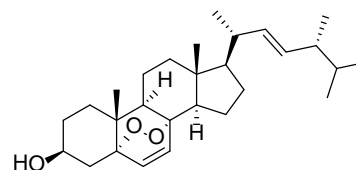
Enniatin D



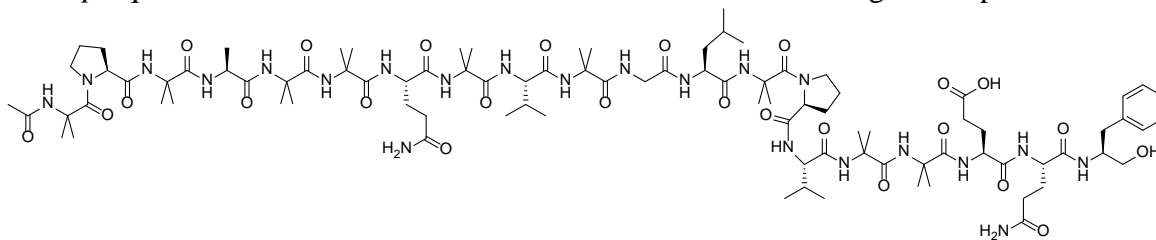
5'-epiequisetin



Obionin B



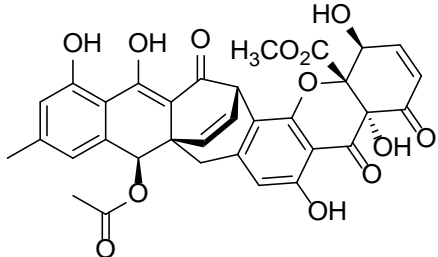
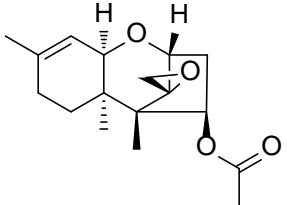
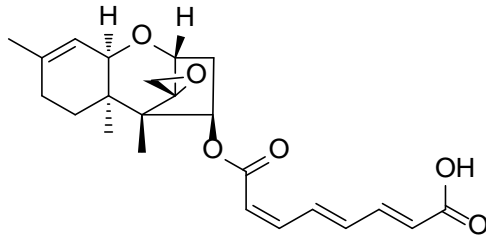
Ergosterol peroxide

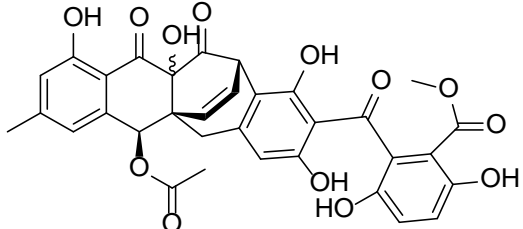
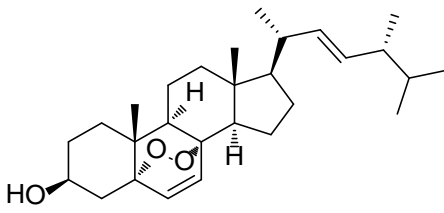
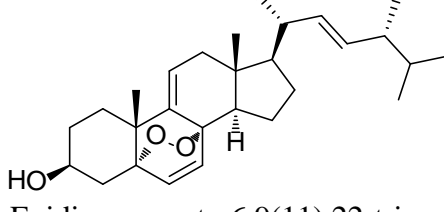
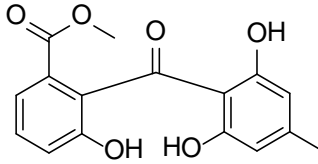


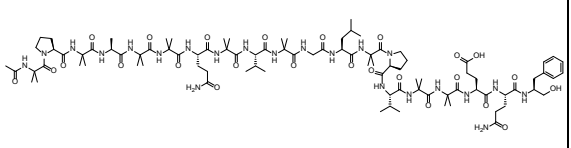
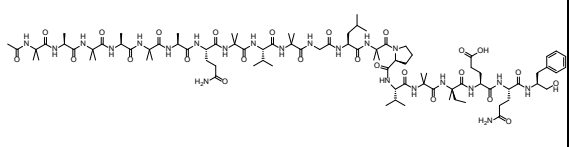
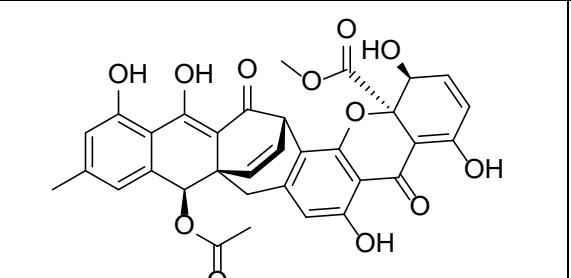
Alamethicin II

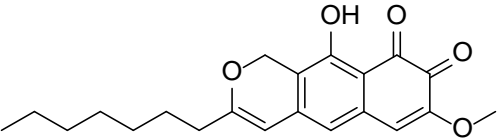
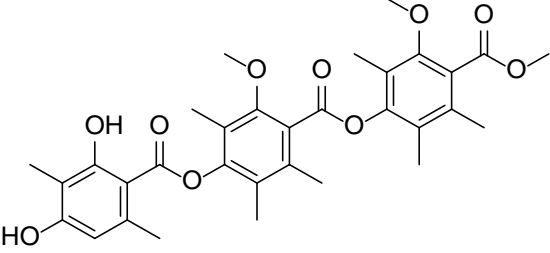
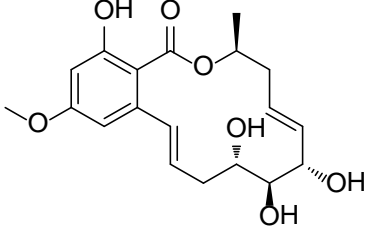
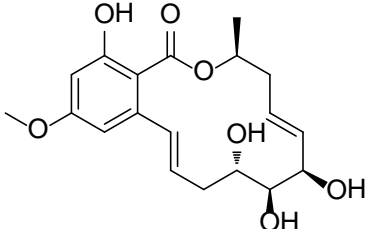
Figure 120. Structures of the ten compounds analyzed in figure 119.

Table 38. Chemical Structures, Chemical Formulas, Retention Times, UV Absorption Maxima, (+)/(-)-ESI HRMS, and (+)/(-)-ESI CID MS/MS of 172 Fungal Secondary Metabolites

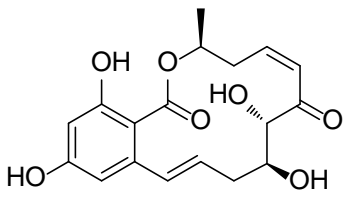
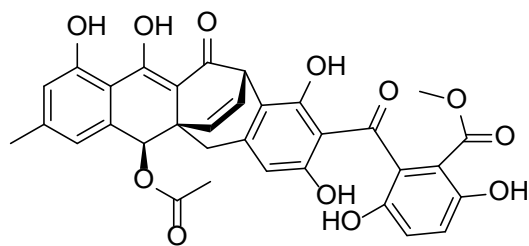
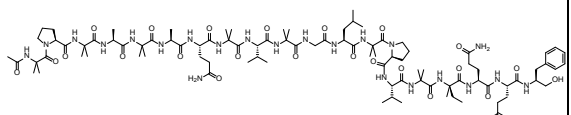
#	chemical structure and chemical formula	Rt (min)	UV (nm)	Positive ionization mode		Negative ionization mode	
				[M+H] ⁺	MS/MS	[M-H] ⁻	MS/MS
1.	 <p>Acremoxanthone D (C₃₃H₂₆O₁₃)</p>	4.91	228, 278, 289 363	631.1429 (-2.8)	543.18, 571.13 554.20, 525.21 553.16, 497.21 493.12, 509.20 477.12, 387.19	629.1292 (-1.4)	567.16, 507.17 445.15, 569.13 385.15, 492.13 493.18, 357.10 611.20, 463.10
2.	 <p>Trichodermin (C₁₇H₂₄O₄)</p>	4.57	213	293.1747 (0.0)	233.13, 215.12 187.04, 168.96 108.91, 275.05 197.08, 124.98 189.12, 205.09	ND	ND
3.	 <p>Harzianum A (C₂₃H₂₈O₆)</p>	4.25	306	401.1952 (-1.7)	215.18, 233.16 383.14, 187.06 151.00, 159.11 197.12, 132.97 145.06, 171.10	399.1813 (-0.1)	231.07, 248.76 213.25, 149.07 123.73, 337.35 249.58, 265.41 194.85, 369.14

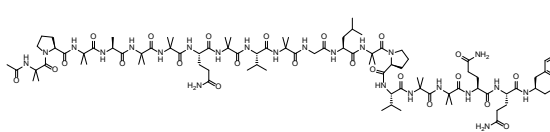
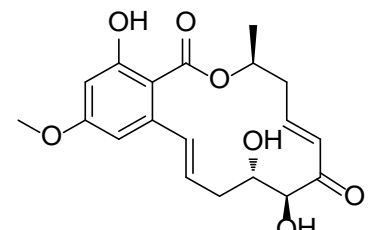
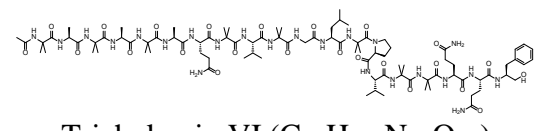
4.	 <p>Acremonidin C (C₃₃H₂₆O₁₃)</p>	5.20	226, 280, 345, 434	631.1426 (-3.1)	547.16, 459.14 487.15, 571.19 543.14, 447.17 387.13, 359.16 599.16, 553.21	629.1286 (-2.3)	597.18, 461.16 401.09, 383.09 357.18, 435.23 373.17, 553.26 493.17, 331.16
5.	 <p>Ergosterol peroxide (C₂₈H₄₄O₃)</p>	8.73	226	429.3365 (+0.5)	411.36, 393.33 287.17, 269.26 305.14, 191.09 267.17, 177.10 375.32, 341.39	ND	ND
6.	 <p>5,8-Epidioxyergosta-6,9(11),22-trien-3-ol (C₂₈H₄₂O₃)</p>	7.90	244	427.3110 (-1.6)	409.31, 285.15 303.19, 391.39 339.23, 381.39 267.18, 175.12 363.32, 147.09	ND	ND
7.	 <p>Moniliphenone (C₁₆H₁₄O₆)</p>	3.62	215, 283	303.0865 (+0.7)	179.00, 271.08 150.97, 146.89 179.98, 284.16 259.84, 285.15 302.19, 183.24	301.0720 (+0.7)	269.04, 283.19 148.96, 225.03 256.87, 150.76 122.96, 104.82 241.03, 211.02

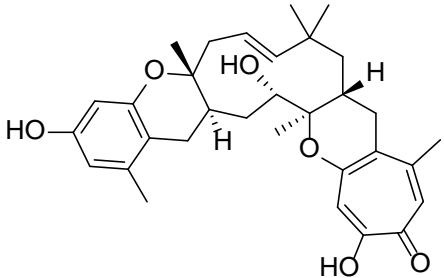
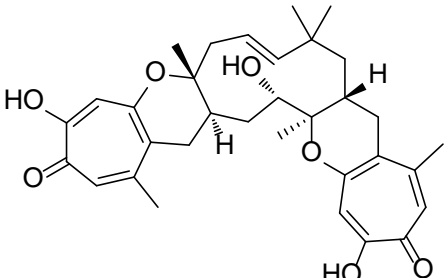
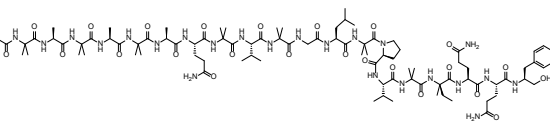
8.	 <p>Alamethicin II (C₉₃H₁₅₂N₂₂O₂₅)</p>	6.58	210	1978.133 (-2.0)	934.81 764.93 950.41 948.92 1203.09 1959.34 752.58 1205.46 1206.28 949.75	1976.117 (-2.6)	1849.16 1440.77 773.41 1568.03 1412.95 1327.86 1958.19 1667.01 1848.52 1425.92
9.	 <p>Longibranchin III (C₉₁H₁₅₀N₂₂O₂₅)</p>	6.16	209	1952.116 (-2.7)	1932.67 922.42 1177.72 919.79 823.55 1933.51 836.82 924.43 738.34 774.65	1950.104 (-1.6)	1932.22 787.52 1541.78 1513.92 1422.84 1667.16 1414.89 1523.87 1931.44 1511.01
10.	 <p>Acremoxanthone C (C₃₃H₂₆O₁₂)</p>	6.22	222, 272, 365	615.1481 (-2.7)	555.21, 495.18 467.20, 523.15 387.12, 195.05 527.18, 583.19 477.17, 505.21	613.1343 (-1.4)	581.13, 477.28 385.10, 551.17 445.07, 553.20 521.06, 491.09 537.21, 359.17

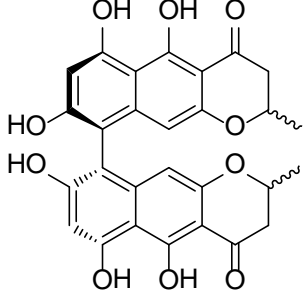
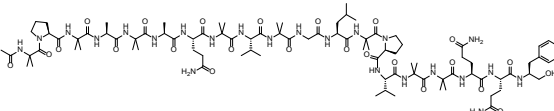
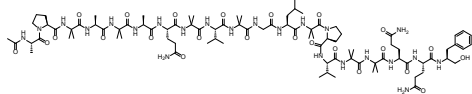
11.	 <p>Obionin B (C₂₁H₂₄O₅)</p>	7.47	241, 298, 465	357.1692 (-1.2)	339.25, 259.03 357.28, 311.18 329.20, 273.14 245.04, 342.19 258.09, 231.13	355.1558 (+2.0)	341.15, 340.38 355.17, 256.00 270.21, 257.10 327.22, 312.04 313.17, 354.50
12.	 <p>Thielavin Q (C₃₂H₃₆O₁₀)</p>	6.87	222, 274	581.2368 (-2.2)	548.65, 165.05 417.27, 357.02 193.01, 547.61 563.31, 562.36 581.57, 549.61	579.2232 (-0.6)	223.07, 414.86 162.98, 414.21 207.93, 176.05 165.05, 491.30 178.01, 535.83
13.	 <p>Zeaenol (C₁₉H₂₄O₇)</p>	3.72	237, 270, 311	365.1595 (0.0)	285.09, 311.28 329.25, 267.18 219.09, 293.15 237.06, 175.08 347.16, 243.17	363.1449 (0.0)	188.95, 207.04 162.92, 173.94 249.15, 191.02 235.07, 161.04 205.11, 187.08
14.	 <p>7-<i>epi</i>-Zeaenol (C₁₉H₂₄O₇)</p>	3.97	237, 270, 311	ND	ND	363.1442 (-1.9)	206.98, 89.07 163.04, 48.01 249.09, 73.98 191.15, 35.09 230.96, 04.98

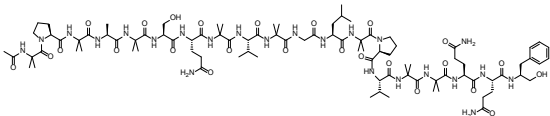
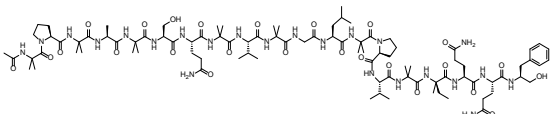
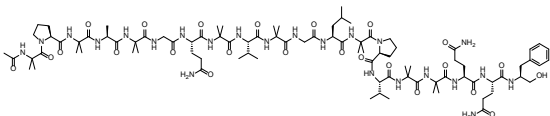
15.	<p>LL-Z1640-1 (C₁₉H₂₄O₇)</p>	4.26	232, 270, 311	365.1590 (-1.3)	347.18, 29.27 311.27, 37.00 219.00, 28.99 285.18, 75.00 251.11, 01.19	363.1450 (+0.2)	189.01, 45.07 235.02, 06.93 217.06, 74.00 261.05, 05.09 319.14, 01.29
16.	<p>Hypothemycin (C₁₉H₂₂O₈)</p>	3.93	230, 265, 306	379.1380 (-2.0)	253.04, 235.08 217.14, 329.13 347.13, 207.08 249.07, 303.07 311.17, 191.10	377.1247 (+1.4)	251.05, 359.05 207.06, 178.99 305.13, 341.19 205.06, 232.90 315.12, 193.00
17.	<p>5,6-Dihydro-9-deoxyzeaenol (C₁₉H₂₆O₆)</p>	4.71	228, 269, 309	351.1803 (+0.3)	333.16, 315.12 297.11, 289.22 271.16, 263.14 279.13, 245.22 231.19, 249.08	349.1657 (+0.1)	303.21, 285.20 302.24, 301.16 259.13, 332.16 329.15, 269.30 347.27, 235.12
18.	<p>5Z-7-Oxozeaenol (C₁₉H₂₂O₇)</p>	4.20	228, 272, 313	363.1435 (-0.9)	345.05, 327.19 237.01, 219.13 309.22, 283.17 319.12, 301.20 299.25, 281.09	361.1290 (-0.7)	235.01, 191.08 343.15, 189.04 217.06, 124.88 299.16, 317.14 273.13, 207.18

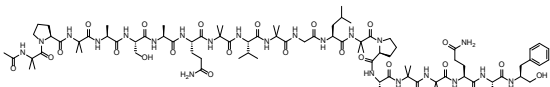
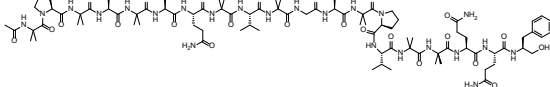
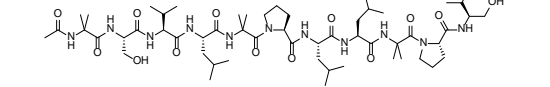
19.	 <p>15-<i>O</i>-Desmethyl-5<i>Z</i>-7-oxozeaenol (C₁₈H₂₀O₇)</p>	3.42	233, 274, 313	ND	ND	347.1129 (+1.1)	220.93, 202.99 176.98, 174.98 329.07, 284.99 303.18, 227.01 311.17, 243.03
20.	 <p>Acremonidin A (C₃₃H₂₆O₁₂)</p>	5.59	217, 278, 287, 359	615.1473 (-3.8)	421.19, 195.00 583.19, 333.16 361.23, 523.23 447.18, 555.24 387.23, 495.24	613.1337 (-2.4)	581.18, 445.17 595.27, 521.19 385.16, 477.24 537.13, 419.15 503.19, 563.37
21.	 <p>Atroviridin B (C₉₃H₁₅₃N₂₃O₂₄)</p>	6.31	211	1977.150 (-1.7)	1008.80 949.36 1009.60 1205.57 1747.43 1006.63 1332.12 771.44 812.59 1120.45	1975.135 (-1.8)	1848.16 1847.55 786.59 1509.94 1665.82 1830.44 1421.91 998.63 1310.65 1801.09

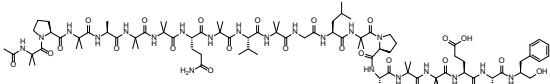
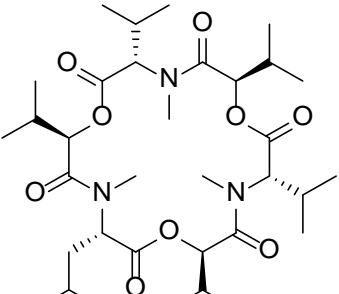
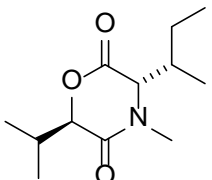
22.	 <p>Polysporin B (C₉₃H₁₅₃N₂₃O₂₄)</p>	6.46	210	1977.151 (-0.9)	949.10 949.91 750.45 823.92 765.90 1204.52 752.50 935.66 1848.75 773.11	1975.134 (-2.2)	1848.06 772.50 1848.80 1666.00 1830.22 1046.68 1212.17 1649.47 1956.35 1424.98
23.	 <p>5E-7-Oxozeaenol (C₁₉H₂₂O₇)</p>	4.02	228 270 311	363.1433 (-1.6)	345.18, 327.18 237.10, 219.09 309.12, 301.16 265.15, 283.19 233.11, 275.12	361.1293 (+0.1)	234.99, 191.09 189.04, 343.19 217.09, 125.03 317.24, 299.12 261.15, 273.08
24.	 <p>Trichokonin VI (C₉₀H₁₄₉N₂₃O₂₄)</p>	5.87	210	1937.119 (-1.7)	1657.07 726.46 922.29 756.39 1180.44 1178.94 1298.93 923.33 1586.79 1564.66	1935.102 (-2.5)	772.43 1917.19 1651.98 1495.80 1296.80 1808.14 1737.05 1407.86 1581.23 1161.67

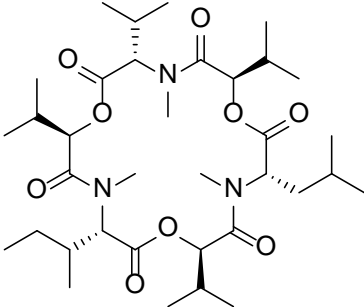
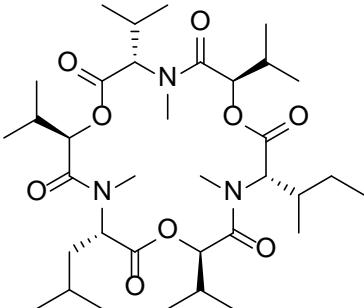
25.	 <p>Epolone A (C₃₂H₄₀O₆)</p>	6.42	206 220 254 363	521.2882 (-3.1)	367.26, 503.39 385.29, 201.19 337.26, 164.93 177.11, 245.16 203.07, 189.00	519.2751 (-0.2)	477.25, 383.31 478.36, 459.46 501.27, 164.01 479.56, 419.06 182.00, 351.47
26.	 <p>Pycnidione (C₃₃H₄₀O₇)</p>	5.95	220 , 254 , 363	549.2829 (-3.2)	531.39, 485.31 385.26, 513.41 367.20, 365.31 383.26, 201.02 397.42, 503.40	547.2694 (-1.2)	162.99, 505.35 383.28, 487.39 503.36, 529.28 463.32, 461.41 519.35, 469.32
27.	 <p>Trichokonin VII (C₉₁H₁₅₁N₂₃O₂₄)</p>	6.01	210	1951.134 (-1.8)	724.56 908.17 1461.13 1092.90 687.73 823.14 1844.45 1933.36 772.75 1906.27	1949.117 (-3.1)	786.56 1931.13 1665.97 1509.98 1822.11 1310.83 1751.15 1913.04 1161.58 1906.97

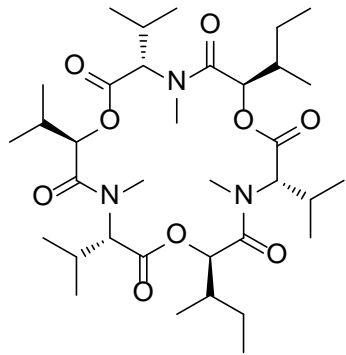
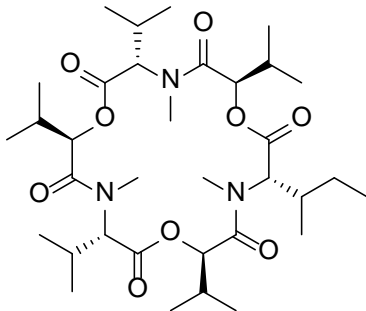
28.	 <p>Cephalochromin (C₂₈H₂₂O₁₀)</p>	5.45	230 270 293 328 417	519.1267 (-3.6)	260.09, 501.21 477.23, 459.17 519.24, 473.13 245.02, 476.34 218.04, 219.01	517.1138 (-0.4)	499.12, 517.14 473.29, 258.04 475.15, 457.23 449.17, 500.23 474.17, 431.27
29.	 <p>Alamethicin F50 (C₉₂H₁₅₁N₂₃O₂₄)</p>	6.15	217	1963.134 (-1.6)	949.25 1120.19 752.50 751.32 950.26 772.65 950.87 849.58 1012.56 1006.82	1961.119 (-1.9)	1834.13 772.55 1651.85 1943.13 1424.79 1495.89 1816.28 1900.07 1832.65 1835.08
30.	 <p>Atroviridin D (C₉₁H₁₄₉N₂₃O₂₄)</p>	5.27	217	1949.118 (-1.8)	720.23 1016.80 1090.70 1192.25 1551.42 580.30 739.55	1947.104 (-1.9)	772.49 1834.02 1929.20 1496.03 1652.13 1296.88 1173.65 1407.82 1581.10 651.41

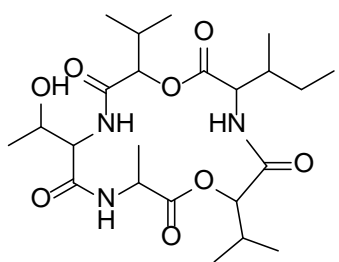
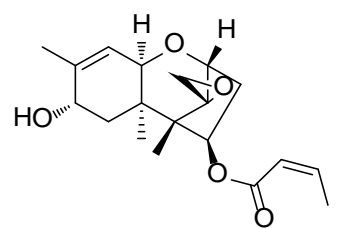
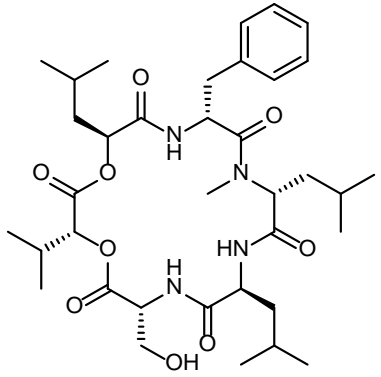
31.	 <p>Atroviridin E (C₉₂H₁₅₁N₂₃O₂₅)</p>	5.35	215	1979.130 (-1.3)	987.49 988.14 988.93 1009.45 1010.91 1010.27 1011.88 623.04 1001.74 1000.73	1977.113 (-2.4)	1032.40 1849.36 1685.33 1496.26 1903.04 1061.79 1800.68 1820.18 1795.63 1737.30
32.	 <p>Atroviridin F (C₉₃H₁₅₃N₂₃O₂₅)</p>	5.51	210	1993.148 (-0.2)	1002.30 1010.24 665.31 928.88 1710.32 1483.93 933.94 1174.82 1104.70 1276.67	1991.138 (+2.3)	1535.84 1919.80 1187.93 1115.79
33.	 <p>Atroviridin G (C₉₁H₁₄₉N₂₃O₂₄)</p>	5.55	217	1949.119 (-1.4)	920.33 1175.79 1018.75 1334.09 1635.51 1611.10 921.22 1573.14 795.61 972.47	1947.102 (-2.6)	1820.12 1819.52 1802.04 772.46 1482.02 1911.05 1322.50 1567.10 1296.50 1480.89

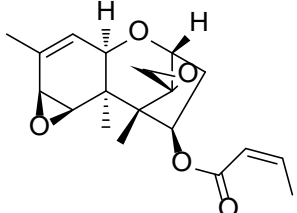
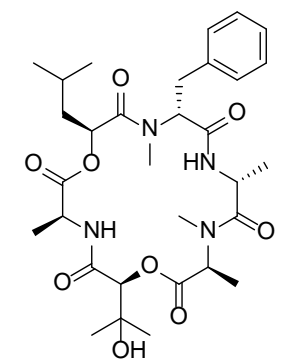
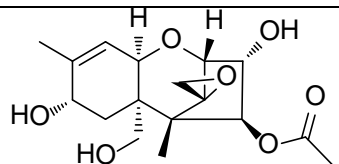
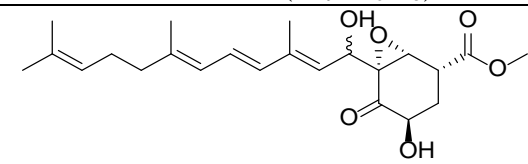
34.	 <p>Atroviridin H (C₉₁H₁₄₉N₂₃O₂₅)</p>	6.25	217	1965.121 (+2.2)	951.65 767.41 952.69 766.55 1207.64 866.30 867.39 1206.61 950.37 865.36	1963.105 (+1.3)	1835.18 773.56 1427.01 1944.18 1836.29 1399.03 1313.84 1408.86 1553.87 1834.49
35.	 <p>Atroviridin I (C₉₁H₁₄₉N₂₃O₂₄)</p>	5.98	217	1949.122 (-0.1)	923.37 921.46 751.22 754.46 948.45 1559.24 1009.45 936.56 752.66 1175.47	1947.104 (-1.9)	1820.18 772.63 1637.75 1393.90 637.41 754.55 1801.87 933.88 1802.49 1929.50
36.	 <p>Trichobrachin D-I (C₅₅H₉₇N₁₁O₁₃)</p>	6.04	220	1120.730 (-3.8)	920.58 512.31 609.43 921.58 1120.73 610.43 513.31 1121.73 922.58 201.16	1118.718 (-1.7)	1088.78 1100.73 1089.53 1046.47 1109.49 1047.08 1058.74 1071.04 1076.45 1101.51

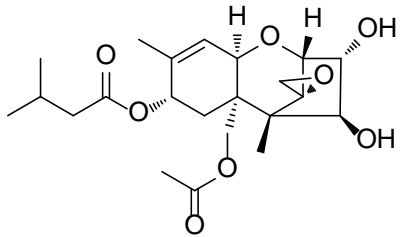
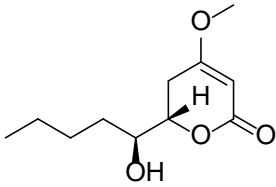
37.	 <p>Atroviridin J (C₉₄H₁₅₄N₂₂O₂₅)</p>	6.75	219	1992.150 (-1.4)	948.23 1203.45 764.30 863.19 770.48 1968.08 1972.89 877.11 962.47 756.66	1990.134 (-2.2)	1863.14 1454.96 787.52 1426.88 1582.04 1327.88 1862.52 1972.16 1681.03 1422.89
38.	 <p>Enniatin D (C₃₄H₅₉N₃O₉)</p>	6.95	211	654.4293 (-4.7)	196.06, 541.26 210.09, 214.04 441.23, 228.07 626.34, 427.29 328.30, 527.48	652.4167 (-1.8)	229.99, 457.46 439.15, 212.15 425.28, 244.21 226.20, 421.19 339.28, 407.34
39.	 <p>1,4-Perhydrooxazine-2,5-dione II (C₁₂H₂₁NO₃)</p>	7.44	211	228.1605 (4.7)	200.09, 99.99 114.03, 156.23 146.07, 210.27 175.29, 228.27 153.99, 159.93	226.1451 (+0.9)	182.10, 183.00 144.13, 184.05 164.03, 208.13 112.09, 154.11 128.03, 197.32

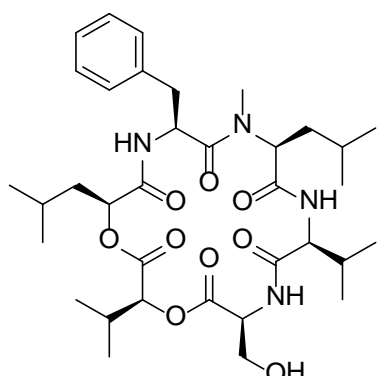
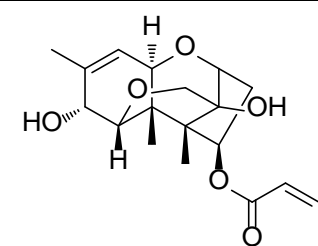
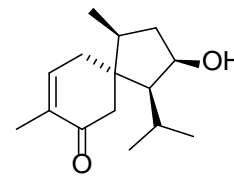
40.	 <p>Enniatin E1 (C₃₅H₆₁N₃O₉)</p>  <p>Enniatin E2 (C₃₅H₆₁N₃O₉)</p>	7.17	206	668.4459 (-3.2)	210.12, 228.10 541.36, 196.09 555.34, 214.04 441.25, 640.35 455.36, 328.22	666.4336 (+0.1)	226.18, 439.34 244.13, 230.13 212.03, 453.22 421.40, 435.44 333.04, 236.16
-----	--	------	-----	--------------------	--	--------------------	--

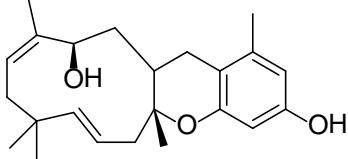
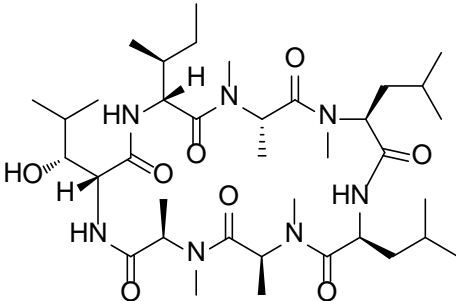
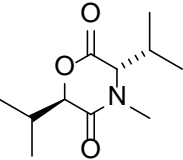
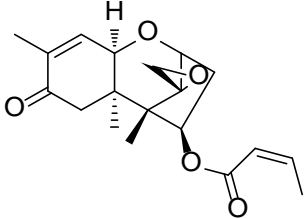
41.	 <p>Enniatin I (C₃₅H₆₁N₃O₉)</p>	7.22	211	668.4449 (-4.6)	210.13, 541.35 228.14, 196.12 214.11, 441.28 555.35, 640.41 455.29, 328.21	666.4335 (0.0)	226.18, 439.38 244.19, 453.45 212.18, 230.08 421.37, 435.23 339.44, 223.84
42.	 <p>Enniatin B1 (C₃₄H₅₉N₃O₉)</p>	7.01	211	654.4304 (-3.0)	210.08, 196.09 214.13, 541.45 527.39, 228.09 441.23, 626.45 427.28, 314.16	652.4178 (-0.1)	439.37, 212.01 230.03, 425.27 226.20, 244.12 421.39, 438.61 339.43, 407.27

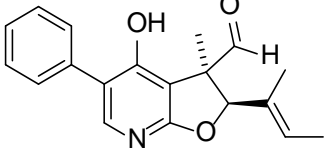
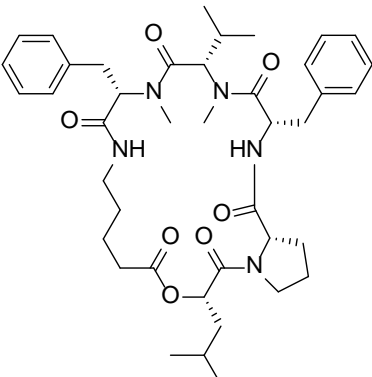
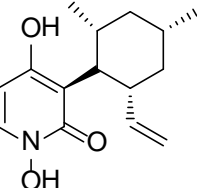
43.	 <p>Roseotoxin S (C₂₃H₃₉N₃O₈)</p>	4.12	220	486.2796 (-2.8)	468.34, 458.30 440.35, 385.19 287.18, 414.32 273.18, 357.16 333.26, 314.15	484.2664 (-0.2)	440.12, 245.06 289.21, 227.21 440.77, 270.86 466.34, 287.38 301.38, 269.18
44.	 <p>Trichothecinol B (C₁₉H₂₆O₅)</p>	4.03	206	335.1853 (+0.1)	231.06, 195.09 213.06, 249.08 185.05, 125.05 123.06, 201.17 317.21, 171.08	333.1710 (+1.0)	289.19, 286.96 303.30, 318.13 331.33, 226.95 253.36, 248.81 297.38, 265.09
45.	 <p>Trichodepsipeptide A (C₃₆H₅₆N₄O₉)</p>	6.41	224	689.4110 (-1.4)	671.41, 661.44 446.29, 576.35 489.44, 428.35 544.36, 421.38 449.20, 371.29	687.3984 (+1.3)	657.39, 518.22 656.73, 291.21 619.46, 611.42 601.38, 643.31 587.48, 307.35

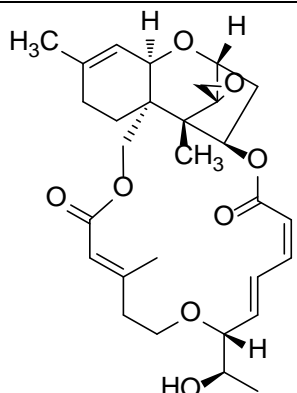
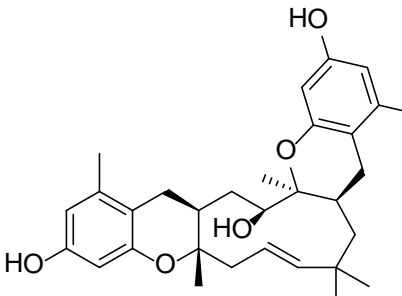
46.	 <p>Crotoicin (C₁₉H₂₄O₅)</p>	4.24	215	333.1699 (1.0)	247.10, 229.09 201.09, 173.09 211.06, 123.04 187.04, 183.12 159.01, 124.98	ND	ND
47.	 <p>Guangomide A (C₃₁H₄₆N₄O₉)</p>	5.49	217	619.3325 (-2.1)	362.18, 258.11 445.20, 601.30 344.19, 544.28 276.18, 516.27 473.38, 206.05	617.3184 (-1.4)	461.21, 448.27 274.17, 292.30 185.93, 430.24 204.10, 256.19 217.04, 403.07
48.	 <p>Neosolaniol (C₁₉H₂₆O₈)</p>	1.71	200	383.1703 (+0.6)	365.33, 355.37 382.51, 245.18 340.74, 335.32 305.14, 323.00 215.34, 383.33	ND	ND
49.	 <p>Trichothosporon A (C₂₂H₃₀O₇)</p>	3.24	226	407.2061 (-0.9)	389.17, 371.24 375.05, 353.20 233.21, 303.18 347.20, 247.22 357.14, 379.22	405.1924 (+1.2)	361.30, 373.03 387.01, 390.26 377.26, 262.47 346.04, 241.19 347.37, 316.90

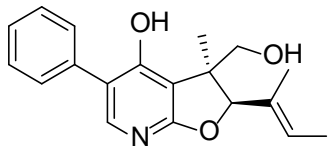
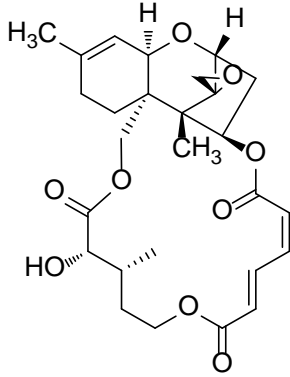
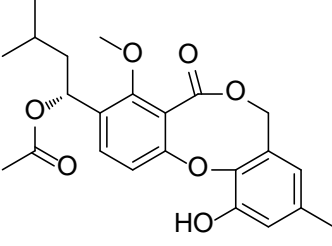
50.	 <p>HT-2 Toxin (C₂₂H₃₂O₈)</p>	3.90	222	425.2170 (+0.1)	263.05, 245.08 407.35, 408.29 325.29, 227.10 323.19, 199.17 305.19, 215.06	423.2022 (-0.5)	291.24, 355.16 387.15, 393.04 377.22, 278.55 267.20, 404.90 305.90, 395.79
51.	 <p>Pestalotin (C₁₁H₁₈O₄)</p>	3.20	237	215.1278 (0.0)	197.05, 153.11 183.13, 137.08 141.06, 171.06 165.13, 151.10 169.02, 139.09	213.1135 (+1.2)	169.08, 112.88 151.10, 197.79 181.05, 172.09 139.04, 153.00 185.97, 148.84
52.	01008-35-5*	3.65	254, 359	293.1391 (2.5)	275.14, 229.23 257.18, 261.22 191.13, 135.00 215.02, 247.22 233.27, 263.25	291.1246 (+2.7)	249.00, 205.06 163.00, 176.99 175.06, 204.03 231.97, 164.96 243.18, 273.11
53.	01008-34-4*	3.26	254, 359	293.1379 (-1.4)	275.22, 229.23 191.12, 135.04 257.16, 215.14 107.07, 175.10 177.15, 201.22	291.1241 (+1.1)	249.14, 205.08 162.97, 243.09 263.20, 151.01 135.03, 204.07 175.01, 176.87

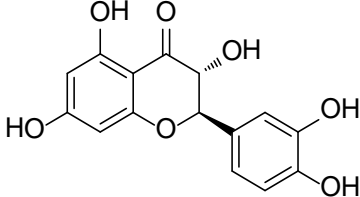
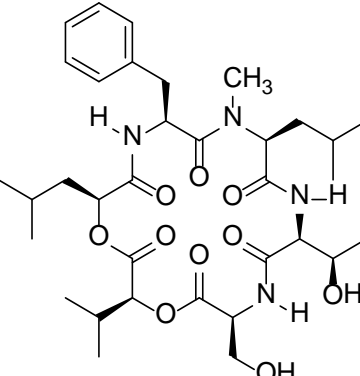
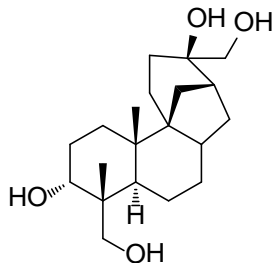
54.	 <p>Trichodepsipeptide B (C₃₅H₅₄N₄O₉)</p>	5.00	219	675.3963 (-0.1)	657.39, 647.44 432.29, 576.42 421.35, 414.29 449.29, 489.40 530.29, 674.45	673.3812 (-0.9)	643.36, 645.42 504.37, 291.09 655.23, 641.47 485.66, 486.27 559.42, 629.47
55.	 <p>Synthetic intermediate (C₁₉H₂₆O₆)</p>	2.87	211	351.1710 (-0.6)	247.10, 229.07 217.11, 211.08 201.16, 187.05 333.15, 265.09 173.08, 199.10	ND	ND
56.	 <p>2-Hydroxyacoronene (C₁₅H₂₄O₂)</p>	4.02	244	237.1846 (-1.5)	219.09, 201.06 147.04, 161.06 151.02, 191.04 163.05, 177.21 165.05, 135.04	235.1709 (+2.5)	217.18, 191.06 235.04, 207.30 192.00, 189.08 149.00, 150.86 175.01, 166.82

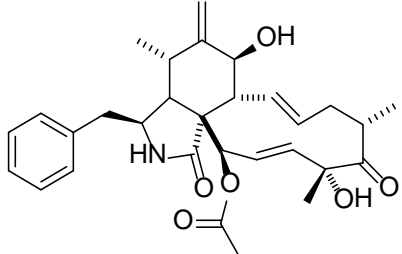
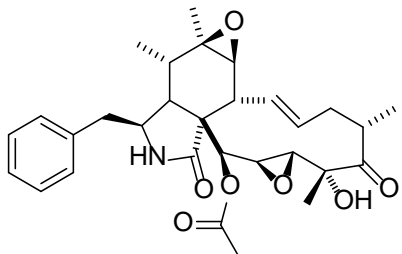
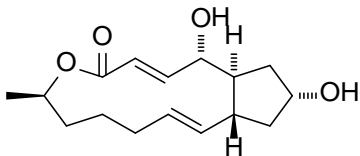
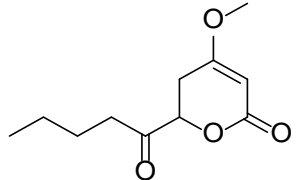
57.	 Pughinin A (C ₂₃ H ₃₂ O ₃)	5.15	226, 282	357.2422 (-0.6)	136.93, 215.13 339.28, 203.14 173.05, 159.12 297.19, 145.03 146.98, 191.10	355.2286 (+1.9)	355.20, 313.08 311.19, 134.90 341.18, 244.98 337.22, 327.19 285.84, 269.04
58.	 Ternatin (C ₃₇ H ₆₇ N ₇ O ₈)	5.72	215	738.5102 (-3.0)	411.34, 720.51 666.41, 326.20 295.23, 395.30 681.51, 635.46 413.20, 710.54	736.4969 (-1.3)	664.49, 511.46 455.35, 665.23 466.11, 493.43 355.50, 357.34 448.55, 466.71
59.	 1,4-Perhydrooxazine-2,5-dione I (C ₁₁ H ₁₉ NO ₃)	6.75	217	214.1435 (-1.4)	186.06, 85.96 157.97, 140.94 168.14, 172.04 179.17	212.1292 (+0.1)	167.98, 129.88 169.18, 194.16 111.79, 170.12 170.96, 197.96 150.12, 128.07
60.	 Trichothecin (C ₁₉ H ₂₄ O ₅)	4.60	226	333.1698 9 (+0.7)	211.08, 229.09 247.13, 201.08 186.98, 203.09 173.13, 175.10 158.95, 125.03	331.1553 3 (+0.7)	287.25, 263.06 269.34, 313.13 299.11, 271.15 285.14, 277.34 303.75, 258.90

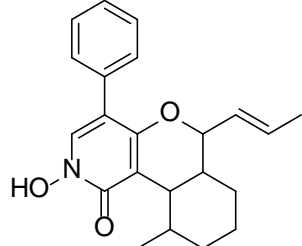
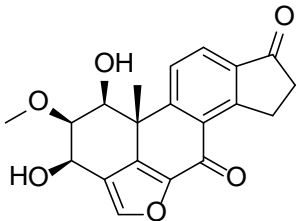
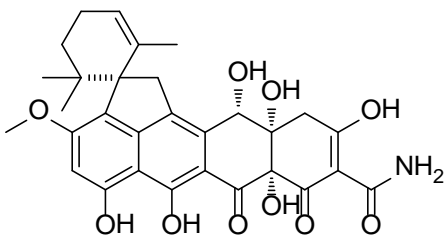
61.	 CJ-15,696 (C ₁₉ H ₁₉ NO ₃)	3.91	204, 233	310.1433 (-1.3)	292.17, 268.18 282.15, 200.07 238.11, 214.07 188.03, 254.11 242.15, 240.17	308.1288 (-1.3)	280.11, 308.18 293.12, 236.21 266.16, 262.17 250.12, 198.06 251.05, 281.17
62.	 T987A (C ₄₁ H ₅₇ N ₅ O ₇)	5.84	224	732.4310 (-2.7)	619.36, 591.43 704.43, 688.54 520.33, 581.48 458.29, 472.42 633.46, 575.54	730.4175 (-1.3)	631.41, 420.32 501.38, 520.38 402.20, 545.44 273.08, 259.14 547.39, 519.38
63.	01009-22-3P*	3.22	237	215.1282 (+1.9)	197.07, 153.09 183.10, 137.07 169.09, 151.06 165.14, 141.06 179.16, 119.11	213.1136 (+1.7)	169.06, 198.08 112.92, 150.93 180.97, 141.40 136.78, 82.97 212.89, 170.04
64.	 Pyridoxatin (C ₁₅ H ₂₁ NO ₃)	4.55	213, 289	264.1598 (+1.4)	139.93, 153.92 167.97, 182.03 180.03, 194.07 208.03, 196.07 166.04, 127.98	262.1443 (-2.2)	234.09, 218.10 243.98, 262.17 242.20, 200.19 124.98, 245.14 216.18, 175.14

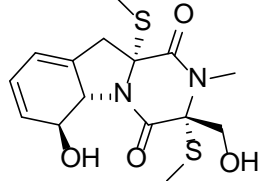
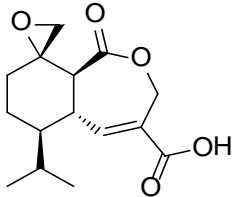
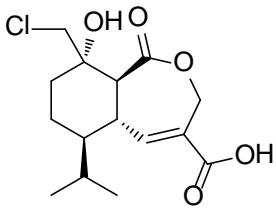
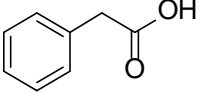
65.	01007-114-3*	6.01	219	338.2110 (-1.3)	216.04, 230.09 202.15, 189.95 258.17, 256.13 244.08, 282.14 268.25, 242.14	ND	ND
66.	 Roridin E (C ₂₉ H ₃₈ O ₈)	5.32	222, 263	515.2634 (-1.0)	361.21, 231.11 249.13, 497.35 331.25, 213.08 343.23, 185.02 203.11, 159.11	513.2496 (+0.3)	359.23, 402.67 469.45, 385.42 483.30, 451.41 201.13, 265.11 433.69, 429.01
67.	 Ramiferin (C ₃₁ H ₄₀ O ₅)	6.09	224, 282	493.2941 (-1.6)	339.19, 475.31 351.38, 369.33 215.24, 189.03 175.10, 203.20 227.13, 357.35	491.2798 (-1.0)	473.43, 445.27 447.38, 474.30 344.18, 491.15 326.24, 455.41 227.03, 421.59

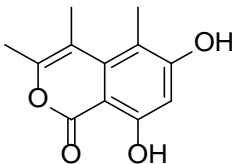
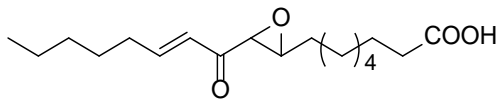
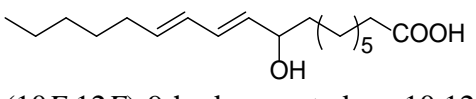
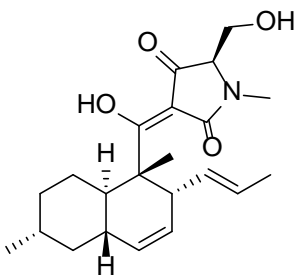
68.	 <p>CJ-16,169 (C₁₉H₂₁NO₃)</p>	4.19	206, 232	312.1593 (-0.5)	294.19, 282.25 200.07, 254.11 214.11, 188.05 240.15, 228.08 270.19, 268.17	310.1445 (-1.2)	280.15, 310.20 308.13, 281.23 252.11, 209.13 236.18, 198.05 262.07, 309.21
69.	 <p>Verrucarin A (C₂₇H₃₄O₉)</p>	4.49	226, 259	503.2267 (-1.7)	457.12, 373.16 249.10, 231.18 333.29, 390.90 213.09, 439.25 185.12, 195.14	501.2133 (+0.6)	253.17, 457.35 473.30, 371.34 225.08, 483.25 209.16, 353.19 335.13, 191.13
70.	 <p>Purpactin A (C₂₃H₂₆O₇)</p>	5.85	230, 282	415.1754 (+0.5)	NF	413.1606 (+0.1)	309.07, 353.15 294.28, 323.17 321.14, 134.88 278.15, 191.12 279.14, 293.21

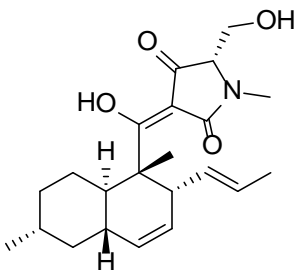
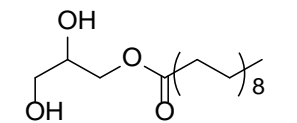
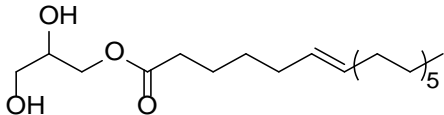
71.	 <p>Dihydroquercetin (C₁₅H₁₂O₇)</p>	2.12	228, 289	305.0660 (+1.2)	258.99, 287.01 152.93, 194.94 148.99, 231.02 179.07, 122.88 166.92, 161.07	303.0508 (-0.7)	285.08, 176.90 124.80, 275.06 258.99, 179.00 274.30, 241.09 217.05, 214.83
72.	 <p>Hirsutatin A (C₃₄H₅₂N₄O₁₀)</p>	5.50	217	677.3739 (-2.5)	659.37, 641.42 434.27, 649.49 514.28, 532.28 489.22, 416.30 421.33, 398.30	675.3612 (+0.2)	645.31, 506.34 505.25, 488.00 444.11, 470.23 291.25, 631.48 613.37, 601.44
73.	 <p>Aphidicolin (C₂₀H₃₄O₄)</p>	3.62	ND	321.2427 (+0.8) (M+H- H ₂ O)	222.08, 321.27 295.29, 169.08 339.37, 178.20 322.40, 120.98 269.28, 216.17	ND	ND

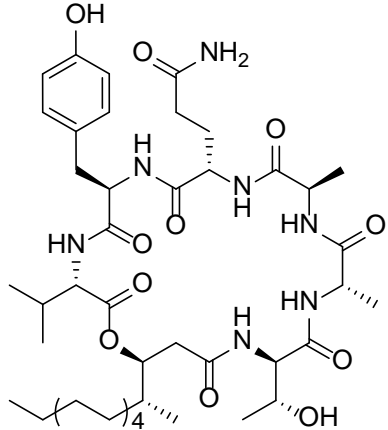
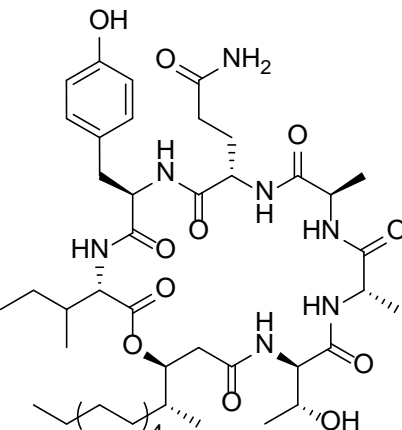
74.	 <p>Cytochalasin D; Zygosporin A (C₃₀H₃₇NO₆)</p>	4.33	220, 285	508.2689 (-1.0)	430.24, 490.15 448.25, 412.34 388.44, 406.32 370.27, 472.29 384.42, 402.38	506.2552 (+0.8)	348.33, 446.28 366.27, 488.15 428.23, 402.99 385.26, 464.40 462.34, 287.10
75.	 <p>19,20-epoxycytochalasin Q (C₃₀H₃₇NO₇)</p>	4.71	212	524.2629 (-2.7)	404.26, 428.29 446.28, 390.27 386.22, 464.39 368.17, 376.30 418.26, 358.34	522.2501 (+0.8)	462.37, 422.23 480.36, 504.20 444.28, 284.23 401.30, 266.10 404.21, 419.45
76.	 <p>Brefeldin A (C₁₆H₂₄O₄)</p>	3.71	228	281.1753 (+2.1)	245.08, 263.11 199.08, 217.16 227.13, 163.04 185.03, 132.98 189.04, 235.12	279.1605 (+1.1)	235.13, 261.12 161.23, 251.17 280.00, 252.07 96.85, 190.99 173.20, 138.84
77.	 <p>PC₃ (C₁₁H₁₆O₄)</p>	3.34 3.67	230	213.1126 (+2.3)	213.09, 110.88 167.04, 195.10 84.89, 138.93 152.98, 124.99 108.94, 106.94	211.0976 (+0.1)	167.13, 183.93 181.02, 211.08 137.13, 178.84 183.12, 96.85 112.93, 192.84

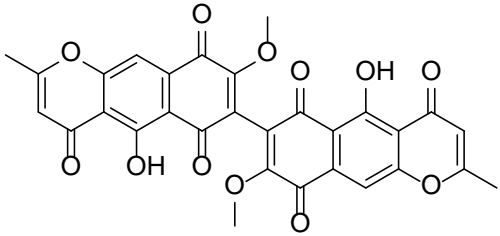
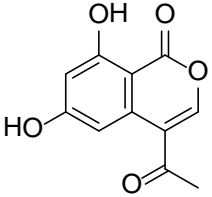
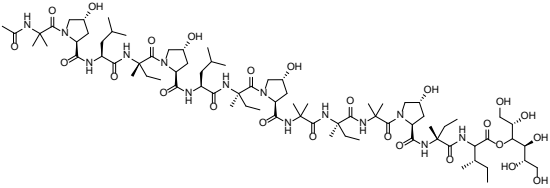
78.	 <p>Leporin B (C₂₂H₂₅NO₃)</p>	6.10	220, 241	352.1900 (-2.0)	216.01, 230.09 244.08, 296.17 270.11, 335.20 258.14, 282.13 272.11, 278.11	350.1762 (+0.1)	350.12, 115.88 306.22, 197.97 228.03, 332.30 201.00, 214.01 185.98, 322.16
79.	 <p>Viridiol (C₂₀H₁₈O₆)</p>	2.95	244, 319	355.1173 (-1.0)	281.05, 309.14 337.12, 249.08 277.13, 308.39 279.21, 305.17 253.15, 291.08	353.1034 (+1.0)	278.96, 325.17 335.16, 297.15 338.10, 279.87 294.41, 321.26 277.25, 309.15
80.	 <p>Viridicatumtoxin (C₃₀H₃₁NO₁₀)</p>	5.74	235, 383, 432	548.1908 (-1.3) M+H- H ₂ O	509.19, 548.23 510.21, 549.23 492.20, 380.23 493.22, 523.23 522.12, 530.21	564.1869 (-1.1)	502.31, 547.22 546.17, 520.27 529.22, 485.19 405.23, 459.32 503.27, 379.25

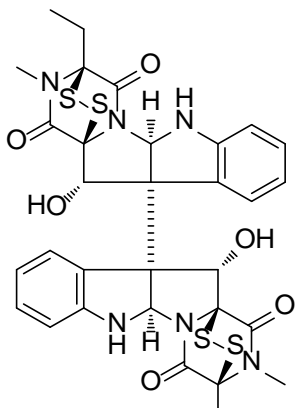
81.	 <p><i>Bisdethiobis(methylthio) gliotoxin</i> (C₁₅H₂₀N₂O₄S₂)</p>	3.33	215, 267	357.0940 (+0.7)	309.04, 243.12 291.01, 215.17 192.11, 233.19 261.20, 143.95 281.22, 278.11	355.0710 (+2.2)	277.11, 340.12 325.09, 307.04 327.11, 337.12 309.09, 354.96 278.08, 283.19
82.	 <p>Heptelidic acid (C₁₅H₂₀O₅)</p>	3.80	226	281.1390 (+2.2)	263.02, 245.02 217.05, 221.06 235.06, 203.06 189.04, 199.06 227.05, 171.10	279.1238 (+0.2)	205.23, 173.17 235.10, 191.11 217.03, 149.12 207.11, 189.16 176.94, 248.97
83.	 <p>Heptelidic acid chlorhydrin (C₁₅H₂₁ClO₅)</p>	3.88	232	317.1149 (-2.1) neutral	298.98, 253.10 281.02, 245.06 217.11, 263.07 239.10, 203.13 227.17, 235.20	315.1006 (+2.2)	279.14, 271.02 261.06, 234.92 191.16, 204.95 243.35, 217.04
84.	 <p>Phenylacetic acid (C₈H₈O₂)</p>	1.41	211	137.0597 (-0.4)	91.92, 136.93 90.86, 119.97 119.34, 115.92 118.29, 124.57	135.0453 (+0.8)	90.88, 134.93 107.99, 119.71 81.79, 92.88

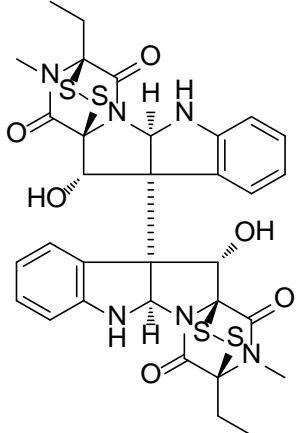
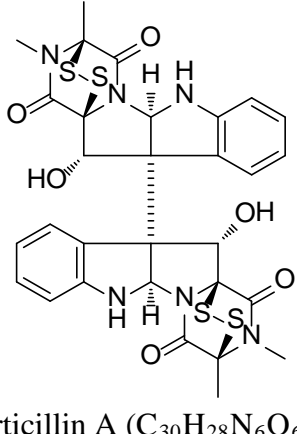
85.	 <p>Decarboxy-citrinone $C_{12}H_{12}O_4$</p>	4.37	246, 267, 339	221.0802 (-3.0)	174.99, 203.01 192.99, 220.98 164.99, 151.09 146.99, 122.99 137.01, 179.06	219.0660 (-1.2)	219.04, 204.02 174.97, 191.01 177.02, 201.05 148.94, 151.04 217.13, 189.02
86.	 <p>(<i>E</i>)-8-(3-(oct-2-enoyl)oxiran-2-yl)octanoic acid ($C_{18}H_{30}O_4$)</p>	5.52	232	311.2217 (+0.2)	293.25, 275.16 257.17, 265.17 110.93, 139.05 247.20, 163.05 177.02, 197.09	309.2066 (-1.6)	291.16, 281.22 273.12, 267.18 265.30, 263.25 247.29, 211.14 209.08, 193.03
87.	 <p>(<i>10E,12E</i>)-9-hydroxyoctadeca-10,12-dienoic acid ($C_{18}H_{32}O_3$)</p>	6.10	220	297.2422 (-0.9)	282.04, 279.19 283.06, 269.36 297.29, 280.24 251.18, 241.19 237.14, 261.21	295.2280 (+0.5)	182.98, 277.22 155.06, 251.27 138.92, 295.22 267.21, 233.17 137.05, 195.14
88.	 <p>Equisetin ($C_{22}H_{31}NO_4$)</p>	6.87	230, 295	374.2322 (-1.0)	356.22, 346.27 175.10, 170.04 200.03, 177.15 205.12, 184.02 143.98, 231.14	372.2169 (-0.2)	342.28, 298.18 324.22, 343.37 111.87, 123.85 314.20, 281.97 256.09, 371.94

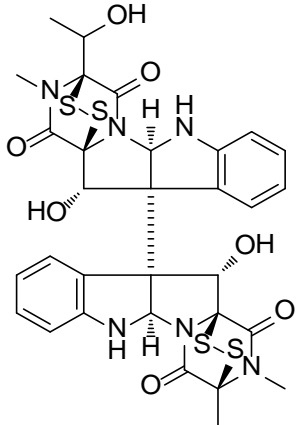
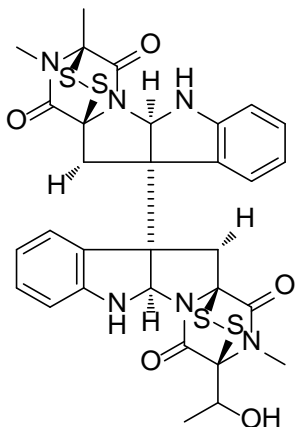
89.	 <p>5'-epiequisetin (C₂₂H₃₁NO₄)</p>	7.01	231, 296	374.2323 (-0.8)	356.24, 346.27 175.13, 170.01 200.02, 177.11 205.13, 184.02 143.96, 231.13	372.2173 (+1.0)	342.25, 298.29 324.29, 343.26 112.07, 124.01 241.15, 135.95 314.30, 230.14
90.	 <p>2,3-dihydroxypropyl stearate (C₂₁H₄₂O₄)</p>	8.55	ND	359.3154 (-0.6)	341.36, 267.16 313.39, 359.35 285.29, 342.06 274.89, 331.37 303.32, 255.14	ND	
91.	 <p>(<i>E</i>)-2,3-dihydroxypropyl octadec-6-enoate (C₂₁H₄₀O₄)</p>	7.98	226	357.2996 (-0.9)	339.32, 265.26 247.24, 283.17 135.08, 149.09 120.96, 163.08 151.09, 177.07	ND	

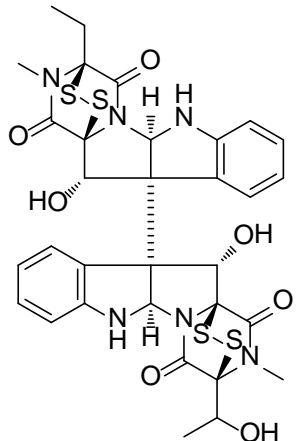
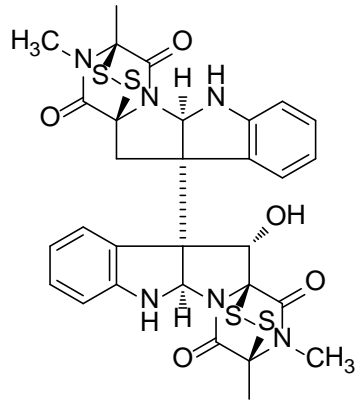
92.	 <p>Acuminatum C (C₄₄H₇₁N₇O₁₁)</p>	6.13	224, 276	874.5264 (-2.4)	856.60, 551.29 857.52, 775.52 534.39, 839.51 768.23, 434.17 757.46, 838.57	872.5120 (-2.2)	828.49, 854.69 588.47, 549.41 674.57, 606.53 632.45, 437.49 630.24, 829.34
93.	 <p>Acuminatum B (C₄₅H₇₃N₇O₁₁)</p>	6.42	224, 276	888.5410 (-3.5)	870.54, 565.30 871.56, 775.48 548.33, 853.61 434.17, 782.39 852.78, 757.65	886.5280 (-1.7)	842.49, 868.60 563.48, 602.36 646.45, 620.51 688.46, 664.48 437.28, 644.22

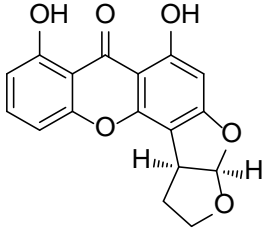
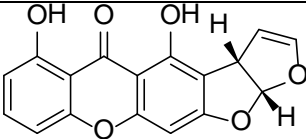
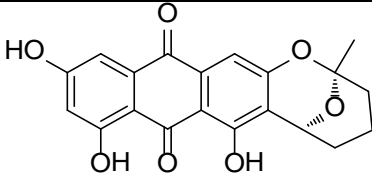
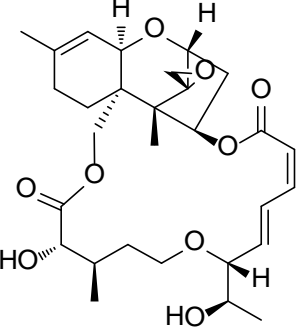
94.	 <p>Auropusarin (C₃₀H₁₈O₁₂)</p>	4.84	243, 269, 380	571.0860 (-1.9)	556.12, 511.15 539.15, 557.18 541.19, 512.17 540.13, 497.18 528.18, 524.11	569.0726 (0.0)	523.16, 538.08 537.29, 539.13 524.01, 554.02 509.19, 525.06 540.12, 569.14
95.	 <p>AGI-7 (C₁₁H₈O₅)</p>	3.04	230, 263, 326	221.0454 (+4.1)	178.98, 221.02 160.96, 203.04 136.92, 150.99 175.11, 165.08 193.06, 133.06	219.0297 (-1.1)	218.85, 216.95 177.01, 174.97 191.05, 130.95 146.90, 132.97 148.87, 172.92
96.	 <p>Clonostachin (C₇₈H₁₃₄N₁₄O₂₅)</p>	5.38	220	1667.973 (+0.5)	1612.73 763.39 1650.04 1583.62 1616.32 1671.57	1665.954 (-2.2)	1501.97 1538.92 1374.79 1483.88 1501.33 1049.60 1288.72 1356.65 1161.68 1502.62

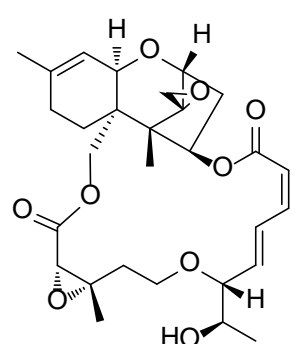
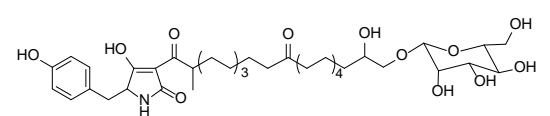
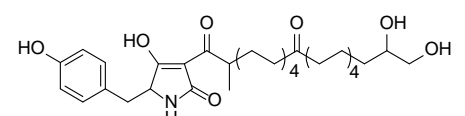
97.	01009-91-5*	5.41	219	1681.983 (-2.7)	847.22 846.48 854.06 848.06 845.84 1403.76 1077.69 1516.99 855.21 1419.15	1679.969 (-2.1)	1516.01 1515.00 1552.42 1370.88 1063.34 1553.23 1372.96 850.95 1388.48 1374.97
98.	 <p>Sch 52901 (C₃₁H₃₀N₆O₆S₄)</p>	5.75	209, 300	711.1161 (-3.0)	629.17, 647.13 646.52, 383.22 397.25, 465.13 233.16, 479.12 565.21, 232.11	709.1040 (+0.4)	645.00, 610.97 579.24, 613.26 643.15, 554.17 508.90, 577.26 461.20, 463.31

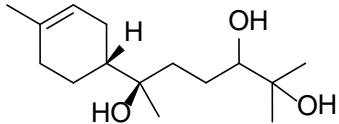
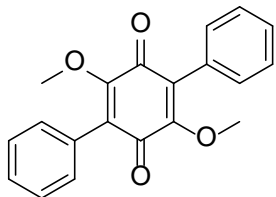
99.	 <p>Verticillin H (C₃₂H₃₂N₆O₆S₄)</p>	6.02	211, 302	725.1321 (-2.5)	643.09, 661.02 397.26, 415.10 479.22, 579.36 233.05, 232.12 298.20, 478.50	723.1199 (+0.8)	659.17, 658.53 657.04, 625.13 477.09, 411.16 593.07, 595.43 526.08, 568.45
100.	 <p>Verticillin A (C₃₀H₂₈N₆O₆S₄)</p>	5.45	217, 298	697.1016 (-1.5)	615.16, 633.01 383.18, 465.23 233.09, 401.22 632.28, 551.25 284.13, 232.11	695.0877 (-0.5)	631.12, 597.10 565.19, 599.19 660.91, 495.01 463.07, 598.58 629.20, 446.96

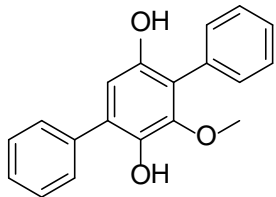
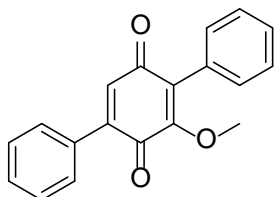
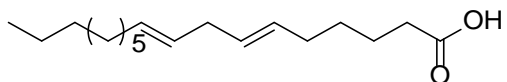
101.	 <p>Sch 52900 (C₃₁H₃₀N₆O₇S₄)</p>	5.19	213, 300	727.1112 (-2.3)	645.10, 663.10 413.23, 266.14 383.22, 495.16 662.42, 465.08 296.16, 233.14	725.0981 (-0.6)	661.01, 583.16 597.09, 647.07 661.98, 627.14 643.08, 595.24 617.16, 659.21
102.	 <p>Gliocladicillin A (C₃₁H₃₀N₆O₅S₄)</p>	5.41	206, 298	695.1216 (-2.5)	629.09, 631.15 479.00, 630.31 397.18, 280.08 268.17, 233.13 613.17, 384.25	693.1082 (-0.8)	629.06, 595.23 627.06, 563.30 461.24, 446.95 561.35, 381.23 597.05, 395.14

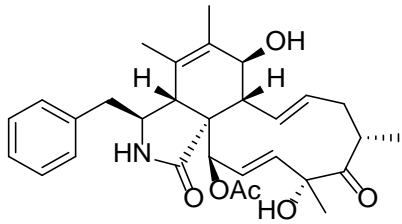
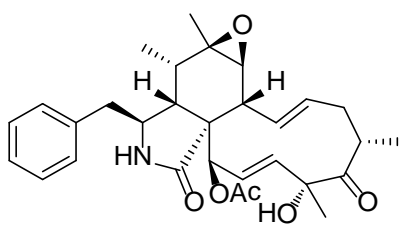
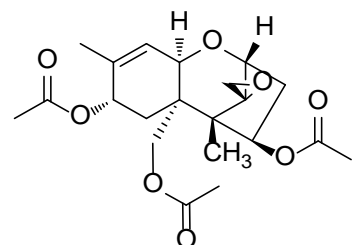
103.	 <p>Gliocladicillin C ($C_{32}H_{32}N_6O_7S_4$)</p>	5.54	207 298	741.1268 (-2.7)	659.16, 677.04 413.26, 280.16 495.12, 676.40 397.31, 296.16 479.00, 233.06	739.1128 (-2.0)	675.09, 597.19 611.07, 643.21 657.26, 660.95 567.21, 631.23 675.94, 565.26
104.	 <p>11-Deoxyverticillin A ($C_{30}H_{28}N_6O_5S_4$)</p>	5.12	215, 298	681.1060 (-2.5)	615.11, 465.02 617.22, 383.22 616.30, 233.12 268.15, 266.10 384.23, 385.23	679.0933 (+0.2)	615.00, 581.10 613.06, 547.10 446.93, 381.31 549.33, 583.11 644.81, 587.84

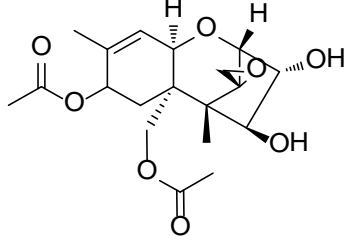
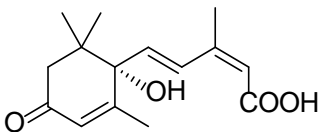
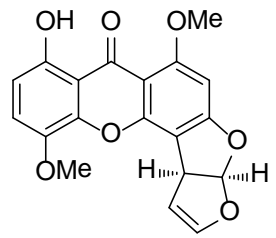
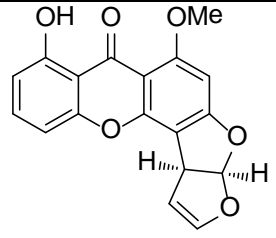
105.	 <p>De-O-methyldihydrosterigmatocystin (C₁₇H₁₂O₆)</p>	5.92	230, 248, 333	313.0610 (-2.2)	285.11, 313.09 257.04, 286.19 295.12, 243.11 284.25, 202.99 269.09, 258.10	311.0563 (+0.7)	311.04, 282.99 312.16, 283.99 255.04, 242.89 281.13, 182.99 293.00, 255.99
106.	 <p>Sterigmatin (C₁₇H₁₀O₆)</p>	6.22	224, 250, 322	311.0551 (+0.3)	283.10, 255.19 269.07, 284.12 293.25, 265.07 311.18, 241.14 267.13, 292.57	309.0396 (-2.8)	309.19, 264.94 281.12, 282.02 240.83, 96.92 248.11, 280.47 266.22, 262.77
107.	 <p>Averufin (C₂₀H₁₆O₇)</p>	6.35	222, 267, 293, 321, 450	369.0960 (-2.3)	351.11, 311.09 299.12, 327.09 285.09, 309.11 333.12, 273.03 323.12, 369.12	367.0820 (-1.0)	367.05, 284.08 295.14, 285.15 368.25, 297.13 282.98, 310.08 296.05, 308.97
108.	 <p>Roridin A (C₂₉H₄₀O₉)</p>	4.46	224, 263	533.2731 9 (-2.5)	249.09, 231.12 333.22, 403.01 385.10, 213.17 185.06, 195.03 203.15, 247.10	531.2609 3 (+1.8)	401.39, 513.39 487.27, 371.34 469.34, 365.20 357.21, 501.45 237.16, 265.19

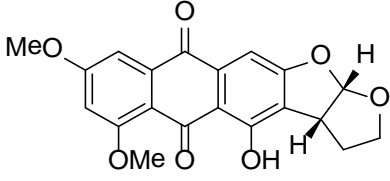
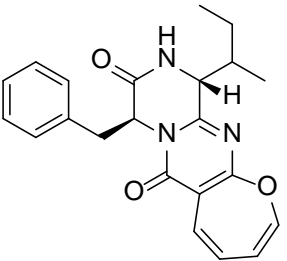
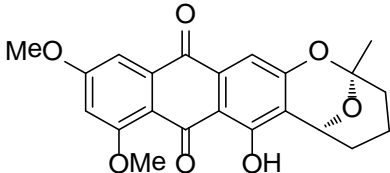
109.	 <p>Roridin D (C₂₉H₃₈O₉)</p>	4.81	224, 259	531.2576 (-2.3)	249.10, 231.21 485.27, 403.03 185.11, 213.12 347.20, 203.13 195.18, 331.22	529.2455 (+2.2)	263.12, 485.19 511.27, 501.29 235.14, 441.26 374.94 163.04 237.13, 219.17
110.	 <p>Virgineone (C₄₀H₆₃NO₁₂)</p>	5.41	222, 280	750.4418 (-0.6)	588.47, 570.44 732.39, 552.64 678.38, 612.61 714.36, 552.04 540.43, 696.54	748.4251 (-3.5)	642.41, 686.41 643.53, 480.41 586.45, 687.58 524.39, 436.45 654.46, 506.58
111.	 <p>Virgineone aglycone (C₃₄H₅₃NO₇)</p>	6.10	224, 280	588.3879 (-2.6)	570.49, 552.40 206.11, 534.43 540.50, 337.39 464.45, 400.34 440.50, 365.43	586.3731 (-3.2)	480.44, 481.53 524.51, 436.42 492.60, 542.61 204.02, 406.33 418.22, 525.65
112.	01009-74-3*	5.91	226, 293, 374		586.43, 568.38 730.27, 550.52 676.40, 694.46 587.13, 365.34 538.43, 712.76		584.35, 585.45 746.57, 540.39 566.52, 626.47 522.53, 702.54 703.57, 541.48

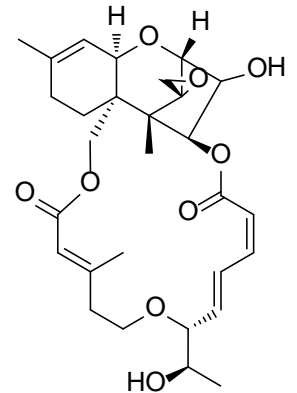
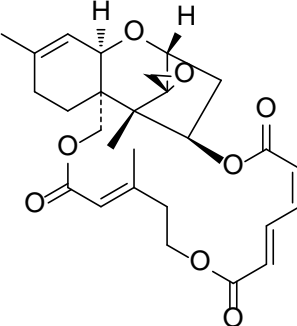
113.	 <p>5,6-dihydroxybisabolol (C₁₅H₂₈O₃)</p>	3.73	220, 281	257.2118 (+2.7)	221.12, 239.09 203.11, 127.02 118.97, 133.05 108.98, 147.03 149.07, 240.04	255.1968 (+1.1)	211.18, 237.25 159.01, 136.96 227.97, 81.03 212.60, 201.22 219.13, 208.92
114.	01007-150-1*	5.24	232, 257, 293, 372	287.0918 (+1.4)	269.12, 272.07 254.07, 259.15 287.16, 257.09 258.13, 226.08 267.11, 270.00	285.0774 (+1.8)	255.15, 284.98 270.11, 240.97 257.04, 225.02 239.92, 270.98 196.83, 242.03
115.	01007-150-3 (01008-93-2)*	6.39	228, 259, 287, 380	257.0811 (+1.1)	257.09, 242.02 214.11, 243.05 258.11, 225.04 226.14, 227.13 213.25, 215.06	ND	ND
116.	01007-150-4*	6.77	232, 254, 289, 369	271.0963 (-0.8)	256.08, 271.10 239.04, 228.10 257.10, 241.11 240.07, 272.22 227.25, 212.95	ND	ND
117.	 <p>Betulinan A (C₂₀H₁₆O₄)</p>	5.52	224, 265, 324	321.1121 (0.0)	289.26, 306.11 293.15, 274.21 258.08, 271.11 290.17, 261.22 259.18, 233.11	319.0985 (+2.7)	304.00, 291.10 276.01, 319.20 287.20, 289.18 247.08, 292.07 277.13, 231.27

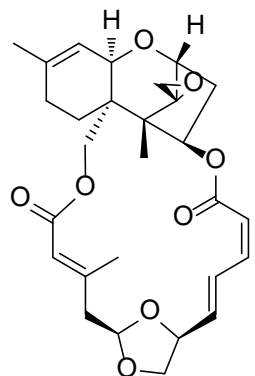
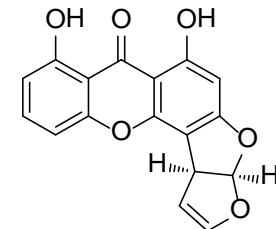
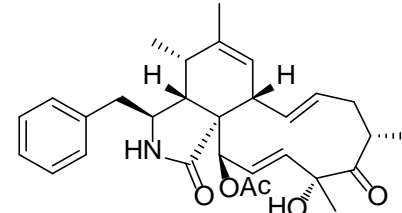
118.	 BTH-II0204-207:A (C ₁₉ H ₁₆ O ₃)	4.87	224, 259, 311	293.1172 (-0.2)	261.16, 278.08 277.13, 275.16 292.20, 233.18 262.12, 243.12 259.20, 232.11	291.1033 (+2.1)	276.05, 263.00 291.00, 173.00 275.09, 219.09 247.18, 273.11 264.07, 249.12
119.	 Betulinan C (C ₁₉ H ₁₄ O ₃)	5.64	226, 259, 337	291.1018 (+0.6)	276.06, 259.08 260.10, 231.11 273.09, 213.08 263.08, 258.09 245.16, 291.16	289.0881 (+3.8)	289.07, 261.03 275.06, 260.11 288.20, 245.03 271.15, 287.09 262.00, 259.09
120.	01008-147-2*	3.56	220	239.1278 (+0.1)	221.04, 195.16 154.93, 183.07 203.06, 132.98 137.01, 193.14 164.96, 177.12	237.1134 (+0.5)	181.06, 237.22 219.15, 123.06 174.97, 152.93 146.84, 146.04 137.01, 192.98
121.	 6,9-Octadecadienoic acid (C ₁₈ H ₃₂ O ₂)	7.25		281.2476 (+0.2)	263.21, 264.23 246.28, 245.18 148.84, 151.06 120.97, 135.15 221.24, 163.15	ND	ND

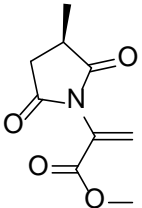
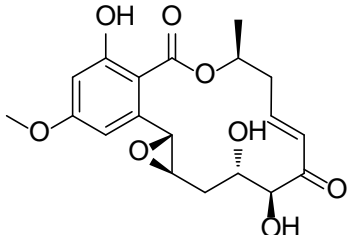
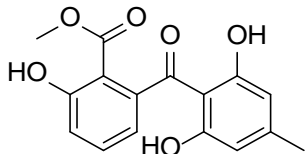
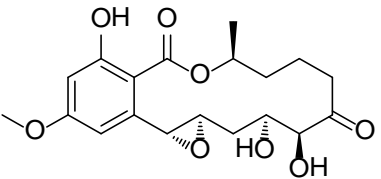
122.	 <p>Cytochalasin C (C₃₀H₃₇NO₆)</p>	4.83	219, 283	508.2684 (-1.9)	430.32, 490.16 448.38, 412.30 388.37, 406.40 472.20, 402.26 466.27, 370.55	506.2543 (-1.1)	446.26, 488.23 241.16, 428.18 460.29, 464.51 418.24, 436.11 403.32, 291.21
123.	 <p>Cytochalasin Q_{HYP} (C₃₀H₃₇NO₆)</p>	5.00	213, 285	508.2683 (-2.1)	490.20, 430.31 448.26, 412.26 402.36, 388.40 406.31, 394.32 384.27, 374.42	506.2544 (-0.8)	446.28, 464.46 488.25, 428.27 463.70, 385.33 388.33, 436.35 354.36, 418.37
124.	 <p>8-Acetoxyneosolaniol (C₂₁H₂₈O₉)</p>	3.28	226	425.1804 (-0.5)	305.18, 215.13 245.03, 263.05 173.12, 365.33 199.07, 191.08 227.17, 169.12	ND	ND

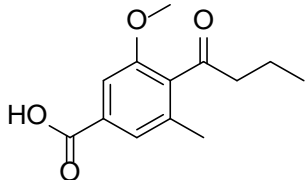
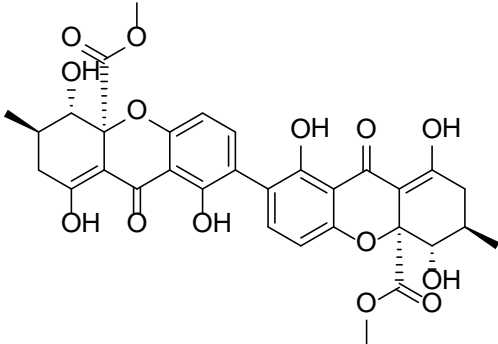
125.	 <p>Ioneosolaniol (C₁₉H₂₆O₈)</p>	2.42	219	383.1696 (-1.3)	263.11, 323.10 245.14, 305.09 365.11, 227.08 199.07, 287.15 215.07, 217.11	ND	ND
126.	 <p>Abscisic acid (C₁₅H₂₀O₄)</p>	3.16	222, 263	265.1437 (+1.1)	247.07, 229.09 219.14, 209.10 201.16, 205.09 187.18, 163.07 203.11, 185.15	263.1287 (-0.6)	152.92, 219.08 204.05, 201.09 110.91, 161.04 245.06, 186.10 138.14, 137.38
127.	 <p>5-Methoxysterigmatocystin (C₁₉H₁₄O₇)</p>	4.84	230, 244, 274, 330	355.0812 (0.0)	340.09, 327.16 325.07, 341.19 355.17, 312.12 311.19, 326.09 328.18, 297.10	353.0663 (-1.2)	338.04, 325.12 257.01, 307.33 308.88, 353.36 285.03, 339.18 262.81, 269.23
128.	 <p>Sterigmatocystin (C₁₈H₁₂O₆)</p>	5.03	232, 244, 326	325.0707 (+0.1)	310.11, 297.13 325.10, 311.13 282.12, 281.08 293.10, 296.09 298.15, 283.12	323.0559 (-0.5)	323.18, 308.18 294.99, 323.96 276.69, 305.33 280.00, 252.45 309.09, 278.90

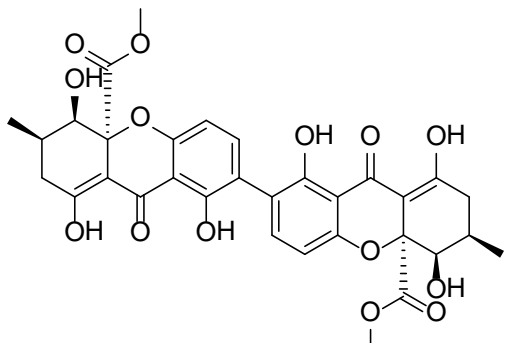
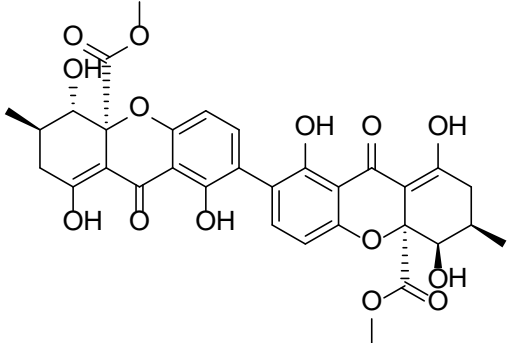
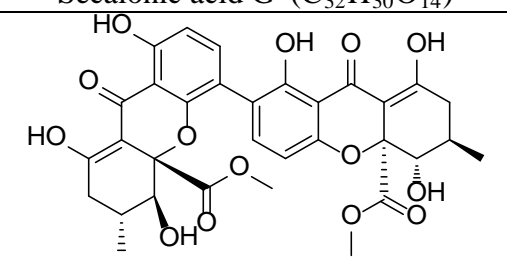
129.	 <p>Aversin (C₂₀H₁₆O₇)</p>	5.21	222, 285, 315, 441	369.0966 (-0.7)	351.16, 341.13 339.15, 340.17 313.13, 352.18 323.19, 369.13 327.14, 354.13	367.0823 (-0.1)	337.10, 339.15 338.08, 352.05 353.22, 349.14 292.85, 323.30 367.09, 329.15
130.	 <p>Brevianamide P (C₂₂H₂₃N₃O₃)</p>	4.92	224, 287, 443	378.1806 (-1.7)	231.11, 361.21 322.18, 321.15 360.22, 287.19 350.28, 243.16 248.11, 230.11	376.1663 (-1.1)	285.07, 284.07 319.09, 229.11 256.19, 188.01 160.86, 227.98 244.21, 333.16
131.	 <p>6,8-Di-O-Methyl averufin (C₂₂H₂₀O₇)</p>	6.55	224, 287, 443	397.1277 (-1.2)	339.17, 379.18 313.13, 327.14 355.17, 337.07 361.25, 301.22 351.22, 380.22	395.1139 (+0.6)	311.92, 297.02 395.27, 377.22 313.05, 327.12 323.12, 309.09 337.02, 291.47

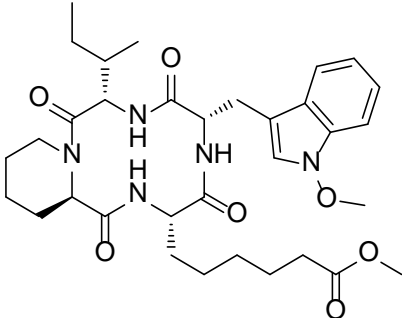
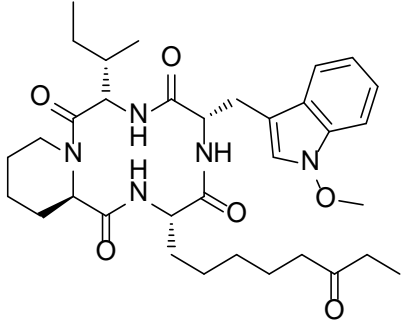
132.	 <p>Roridin L (C₂₉H₃₈O₉)</p>	4.37	222, 259	531.2578 (-2.0)	377.25, 513.22 359.34, 401.21 247.10, 229.15 265.19, 383.30 395.21, 495.36	529.2442 (-0.2)	375.26, 485.37 401.04, 247.14 417.35, 511.32 451.09, 265.12 499.05, 233.32
133.	 <p>Verrucarin J, Muconomycin B (C₂₇H₃₂O₈)</p>	5.53	222, 261	485.2161 (-1.8)	343.25, 231.12 373.25, 213.20 249.17, 185.05 201.07, 187.11 203.13, 159.01	483.2027 (+0.5)	389.21, 439.15 173.09, 465.21 235.05, 395.32 160.81, 373.07 211.28, 254.99

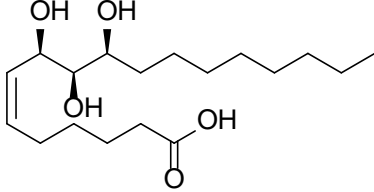
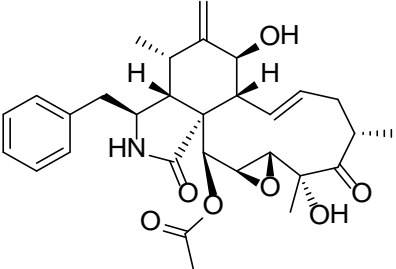
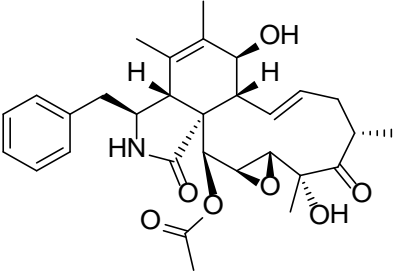
134.	 <p>Roridin H; Verrucarin H (C₂₉H₃₆O₈)</p>	6.07	224, 259	513.2472 (-2.2)	231.12, 359.22 249.15, 213.20 201.12, 495.19 182.76, 203.18 185.10, 331.23	ND	ND
135.	 <p>De-<i>O</i>-methylsterigmatocystin (C₁₇H₁₀O₆)</p>	6.03	228, 248, 333	311.0551 (+0.1)	283.07, 311.11 282.10, 284.20 269.01, 255.03 241.04, 200.97 264.02, 312.15	309.0407 (+0.7)	309.14, 265.07 281.18, 240.94 266.10, 263.12 96.88, 290.17 156.71, 172.94
136.	 <p>Zygosporin G (C₃₀H₃₇NO₅)</p>	5.93	217, 276	492.2736 (-1.8)	474.18, 414.34 396.30, 432.33 267.19, 249.30 372.32, 386.41 322.32, 390.41	490.2610 (+2.3)	444.37, 472.40 462.36, 446.30 315.53, 307.06 428.46, 460.32 399.45, 193.24

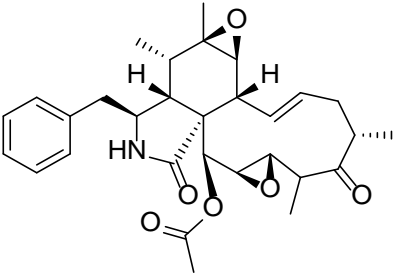
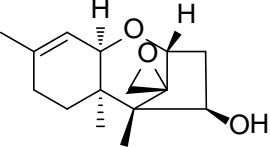
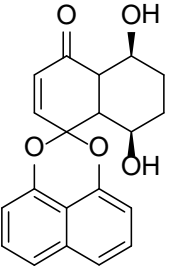
137.	 <p>Versimide (C₉H₁₁NO₄)</p>	1.65	214	198.0760 (-0.3)	165.95, 198.10 96.98, 82.96 80.90, 95.01 68.91, 92.98 106.95, 121.02	ND	ND
138.	 <p>Aigialomycin A (C₁₉H₂₂O₈)</p>	3.77	232, 263, 304	379.1379 (-2.2)	253.00, 235.00 343.25, 361.09 325.15, 231.00 265.00, 206.98 249.05, 126.98	377.1235 (-1.7)	251.01, 359.09 207.03, 305.07 341.21, 178.98 233.12, 315.16 205.06, 263.06
139.	 <p>Nidulalin B (C₁₆H₁₄O₆)</p>	3.60	222, 276	303.0859 (-1.3)	192.95, 271.13 178.99, 136.86 167.09, 179.59 193.75, 286.30 88.99, 109.03	301.0709 (-3.0)	268.99, 283.08 134.84, 225.04 257.20, 241.05 91.00, 108.87 165.03, 269.74
140.	 <p>Dihydrohypothemycin (C₁₉H₂₄O₈)</p>	4.01	219, 265, 304	381.1534 (-2.7)	363.12, 345.18 327.12, 303.13 253.00, 265.09 309.24, 249.15 285.11, 235.02	379.1393 (-1.6)	178.94, 307.11 233.05, 361.05 277.12, 163.98 180.96, 343.13 205.03, 335.13

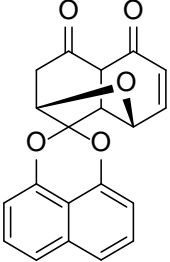
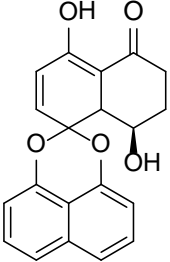
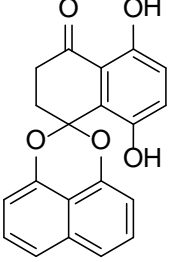
141.	01020-76-1*	4.16	222, 272, 350	321.0961 (-2.3)	261.04, 303.11 289.09, 219.00 247.06, 271.11 192.95, 149.02 275.17, 136.98	319.0819 (-1.3)	275.18, 243.22 287.23, 257.09 205.13, 300.92 162.74, 219.88 215.03, 220.99
142.	 Pyrenochaetic acid C (C ₁₃ H ₁₆ O ₄)	4.40	217, 250, 304	237.1185 (-1.2)	219.08, 175.09 194.05, 195.10 236.06, 200.99 192.95, 161.95 160.01, 177.05	235.0974 0 (-0.8)	191.00, 176.06 235.09, 163.18 120.96, 191.60 177.23, 207.15 179.11, 68.98
143.	 Secalonic acid A (C ₃₂ H ₃₀ O ₁₄)	5.26	222, 263, 337	639.1688 (-2.8)	561.27, 589.16 579.27, 621.25 501.27, 571.27 455.21, 543.17 603.28, 511.28	637.1545 (-2.8)	577.30, 619.24 543.19, 417.23 605.23, 559.11 587.15, 541.34 593.29, 499.24

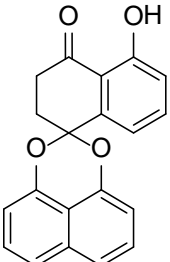
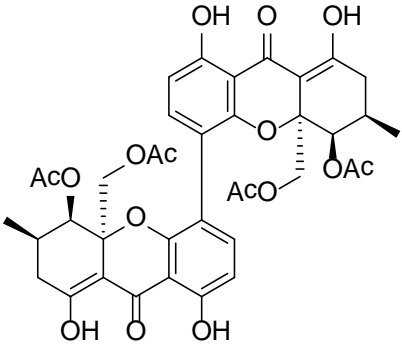
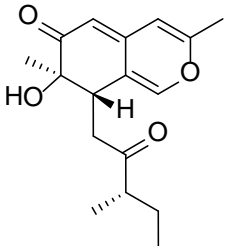
144.	 <p>Secalonic acid E (C₃₂H₃₀O₁₄)</p>	5.50	220, 265, 337	639.1691 (-2.7)	561.24, 589.26 579.26, 621.20 455.31, 571.26 501.19, 603.25 543.35, 607.30	637.1538 (-3.1)	593.25, 543.30 605.30, 619.19 549.29, 577.20 561.22, 499.29 575.37, 587.15
145.	 <p>Secalonic acid G (C₃₂H₃₀O₁₄)</p>	5.39	220, 259, 337	639.1693 (-2.5)	561.28, 589.23 579.24, 621.23 571.22, 455.32 501.28, 543.20 603.35, 511.28	637.1542 (-3.3)	577.20, 593.13 543.19, 619.21 605.25, 561.31 499.29, 587.18 533.24, 525.23
146.	 <p>Penicillixanthone A (C₃₂H₃₀O₁₄)</p>	5.90	220, 262, 335	639.1694 (-2.2)	621.23, 589.24 579.26, 561.24 571.32, 603.37 501.40, 543.14 589.94, 455.33	637.1542 (-3.2)	605.18, 577.26 619.12, 593.22 543.15, 561.36 587.20, 557.20 551.21, 525.24

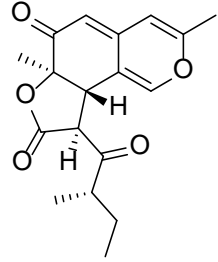
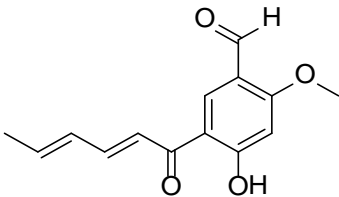
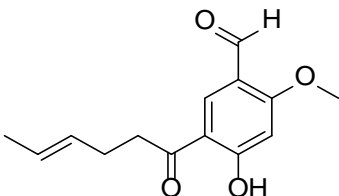
147.	01020-138-1*	5.29	220, 259, 335	639.1691 (-2.8)	561.23, 589.24 579.27, 571.24 501.21, 455.22 621.23, 565.29 547.35, 193.01	637.1541 (-3.4)	593.19, 561.21 543.33, 549.29 517.20, 365.25 577.19, 605.35 533.21, 575.22
148.	 <p>New Natural Product, reported by synthesis (C₃₃H₄₇N₅O₇)</p>	5.29	222, 289	626.3533 (-2.4)	466.26, 594.46 595.36, 513.32 598.38, 422.31 483.37, 296.13 596.38, 297.22	624.3387 (-2.6)	464.24, 594.42 465.41, 592.44 477.23, 254.21 562.46, 225.21 595.04, 340.21
149.	 <p>Apicidin (C₃₄H₄₉N₅O₆)</p>	5.44	222, 287	624.3737 (-2.9)	464.24, 592.44 593.37, 511.36 294.20, 596.46 420.28, 481.33 467.17, 594.47	622.3593 (-2.8)	462.32, 592.46 463.44, 475.22 590.57, 223.01 252.07, 336.32 310.22, 183.04

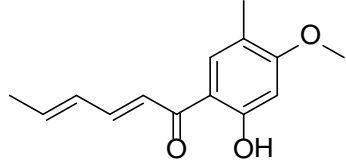
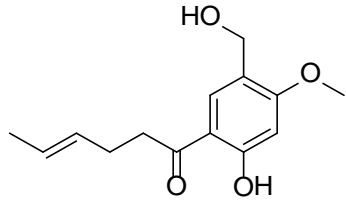
150.	 <p>(8<i>R</i>*,9<i>R</i>*,10<i>S</i>*,6<i>Z</i>)- trihydroxyoctadec-6-enoic acid (Oxylipin) (C₁₈H₃₄O₅)</p>	4.32	220	331.2476 (-0.8)	313.39, 285.40 289.27, 331.25 316.26, 302.98 295.33, 281.01 275.39, 206.99	329.2322 (-3.5)	311.34, 211.15 199.04, 293.17 168.92, 181.11 275.24, 192.98 227.16, 197.11
151.	 <p>19,20-Epoxychochalsin D (C₃₀H₃₇NO₇)</p>	4.03	217	524.2637 (-1.2)	428.30, 446.23 464.30, 404.28 386.33, 390.29 410.32, 400.32 368.28, 239.12	522.2488 (-1.7)	480.38, 504.22 462.32, 444.23 268.27, 422.25 324.37, 404.32 348.24, 266.16
152.	 <p>19,20-Epoxychochalsin C (C₃₀H₃₇NO₇)</p>	4.54	215	524.2634 (-1.6)	428.30, 446.30 386.29, 464.25 404.26, 390.32 400.34, 418.30 410.25, 281.14	522.2490 (-1.4)	404.24, 462.32 480.42, 362.32 504.24, 402.28 401.22, 444.17 464.29, 360.29

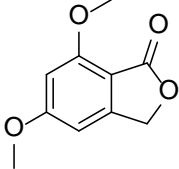
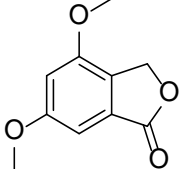
153.	 <p>18-Deoxy-19,20-epoxycytochalasin Q (C₃₀H₃₇NO₆)</p>	5.18	211	508.2683 (-2.1)	430.29, 412.35 402.31, 448.33 265.17, 267.14 384.31, 346.18 374.38, 372.29	506.2542 (-1.1)	460.19, 446.19 428.34, 464.37 478.00, 308.28 307.25, 318.08 423.13, 436.18
154.	 <p>Trichodermol (C₁₅H₂₂O₃)</p>	3.22	230	251.1642 (+0.1)	233.12, 215.07 187.20, 205.14 197.13, 108.95 136.92, 158.98 95.03, 173.13	ND	ND
155.	 <p>Decaspirone C (C₂₀H₁₈O₅)</p>	4.45	230, 298, 326	339.1223 (-1.3)	321.14, 285.07 303.15, 159.00 143.95, 159.98 144.97, 253.07 130.91, 321.77	337.1076 (-1.7)	319.04, 293.17 159.10, 275.04 291.20, 234.95 251.17, 337.01 263.02, 158.02

156.	 <p>Palmarumycin CP3 (C₂₀H₁₄O₅)</p>	5.07	226, 298, 326	335.0913 (-0.4)	307.14, 289.14 174.98, 161.01 279.15, 158.95 175.99, 317.08 147.05, 160.01	333.0760 (-2.6)	158.94, 289.03 305.06, 315.18 271.08, 303.16 157.92, 261.16 287.08, 146.96
157.	 <p>Palmarumycin CP4 (C₂₀H₁₆O₅)</p>	5.36	224, 298, 326	337.1068 (-0.6)	319.17, 158.98 301.14, 160.00 130.97, 253.11 161.09, 291.12 174.96, 277.25	335.0920 (-1.5)	158.91, 251.16 291.13, 157.87 307.14, 317.08 273.05, 250.06 233.04, 289.05
158.	 <p>Palmarumycin CP₁₇ (C₂₀H₁₄O₅)</p>	5.80	228, 298, 365	335.0910 (-1.1)	303.15, 158.94 285.10, 174.94 161.03, 176.00 317.07, 143.97 160.05, 275.12	333.0764 (-1.4)	159.06, 265.15 315.24, 289.01 158.42, 333.13 189.95, 312.96 178.00, 286.94

159.	 <p>Palmarumycin CP₂ (C₂₀H₁₄O₄)</p>	5.03	222, 331	319.0960 (-1.6)	159.93, 301.14 158.96, 160.96 174.92, 302.12 130.99, 273.08 145.01, 132.92	317.0814 (-1.6)	158.89, 174.96 299.12, 316.98 298.30, 172.97 159.95, 173.99 273.18, 316.09
160.	 <p>Phomoxanthone A (C₃₈H₃₈O₁₆)</p>	6.56	220, 254, 333	751.2224 (-1.2)	673.16, 691.17 631.35, 733.04 613.31, 571.20 511.24, 553.30 732.32, 678.34	749.2068 (-2.6)	689.19, 629.24 569.26, 671.24 509.38, 611.31 647.28, 731.25 629.85, 587.18
161.	 <p>Chermesinone A (C₁₇H₂₂O₄)</p>	4.15	222, 354	291.1585 (-2.2)	189.22, 245.17 273.20, 231.24 201.20, 145.13 255.17, 161.19 174.20, 175.21	ND	ND

162.	 <p>Chermesinone B (C₁₈H₂₀O₅)</p>	4.50	222, 354	317.1379 (-1.3)	233.08, 215.08 187.07, 159.08 245.13, 273.12 205.14, 189.11 281.14, 188.12	315.1230 (-2.5)	273.15, 229.01 271.13, 253.06 189.00, 210.98 231.11, 187.08 243.15, 225.08
163.	 <p>5'-formyl-2'-hydroxyl-4'-methoxy-(<i>E,E</i>)-sorbophenone (C₁₄H₁₄O₄)</p>	5.33	225, 266, 311, 343	247.0960 (-2.0)	178.95, 197.03 190.97, 218.97 229.03, 201.06 150.93, 190.00 164.98, 177.07	245.0815 (-1.6)	227.09, 230.05 211.96, 183.95 150.02, 245.06 163.93, 213.00 202.07, 200.90
164.	 <p>5'-Formyl-2'-hydroxy-4'-methoxy-(<i>E</i>)-4-hexenophenone (C₁₄H₁₆O₄)</p>	5.48	253, 282, 322	249.1119 (-0.9)	178.88, 231.02 221.11, 152.94 206.95, 164.93 203.07, 193.08 176.97, 175.05	247.0971 (-2.2)	163.81, 247.07 177.88, 217.12 188.97, 231.00 149.94, 177.14 202.98, 232.04

165.	 <p>1-(2'-hydroxy-4'-methoxy-5'-methylphenyl)-2,4-<i>E,E</i>-hexadien-1-one (C₁₄H₁₆O₃)</p>	6.16	234, 310, 357	233.1171 (-0.5)	214.99, 164.97 205.05, 191.09 151.01, 187.01 176.99, 204.12 201.12, 233.09	231.1025 (-0.7)	215.97, 197.94 213.00, 203.15 231.08, 175.01 150.00, 137.03 201.02, 184.94
166.	01021-11-2*	5.48	243, 277, 314	279.1230 (+1.1)	247.02, 208.94 235.08, 183.06 229.12, 150.91 261.17, 217.01 204.96, 193.11	277.1077 (-1.5)	277.14, 193.92 192.84, 247.06 219.06, 179.85 261.02, 262.21 206.98, 163.95
167.	 <p>1-(2'-hydroxy-4'-methoxy-5'-hydroxymethylphenyl)-<i>E</i>-4-hexen-1-one (C₁₄H₁₈O₄)</p>	4.64	233, 275, 319	251.1277 (-0.5)	180.97, 233.16 215.09, 221.09 158.96, 186.99 136.99, 205.08 177.06, 203.02	249.1131 (-0.6)	231.05, 216.06 248.95, 135.05 213.04, 176.99 188.11, 217.09 233.03, 201.01
168.	01021-2-7*	4.44	230, 311, 350	249.1126 (+0.1)	231.05, 180.93 219.15, 207.08 203.00, 200.95 204.08, 213.07 191.07, 174.97	247.0974 (-0.8)	163.96, 232.01 247.19, 199.03 229.11, 178.03 214.03, 217.06 200.94, 230.92

169.	01021-12-1*	4.43	223, 250, 314, 335	263.0913 (-0.3)	245.05, 195.04 204.07, 177.02 187.00, 191.12 188.95, 219.11 217.00, 175.99	261.0765 (-1.3)	188.99, 217.02 187.98, 199.06 171.06, 187.31 173.02, 202.11 246.08, 168.89
170.	 5,7-dimethoxy-1(3 <i>H</i>)-isobenzofuranone 5,7-Dimethoxyphthalide (C ₁₀ H ₁₀ O ₄)	2.50	217, 258, 291	195.0647 (-2.6)	194.99, 134.90 149.03, 139.02 165.01, 162.99 145.00, 119.01 120.91, 90.90	193.0501 (-2.6)	177.88, 192.84 148.96, 149.89 162.91, 146.91 165.01, 133.78 175.02, 134.88
171.	 4,6-Dimethoxy-1(3 <i>H</i>)-isobenzofuranone 4,6-Dimethoxyphthalide (C ₁₀ H ₁₀ O ₄)	3.53	197, 222, 250, 308	195.0647 (-2.6)	194.99, 134.89 148.92, 162.92 144.87, 118.93 177.01, 166.97 150.99, 138.96	193.0501 (-2.9)	148.93, 193.01 146.85, 177.95 167.00, 121.07 133.91, 134.93 165.19, 174.90
172.	01021-127-2*	6.40	193, 219, 232, 276, 326	235.1322 (-2.8)	165.06, 235.04 217.04, 151.01 193.06, 189.03 191.11, 179.09 174.96, 177.03	233.1176 (-3.0)	233.01, 189.14 149.96, 218.20 136.96, 178.03 174.85, 217.47 203.20, 164.07

ND: Not Detected

*New compound, not published yet

CHAPTER X

CHEMICAL DIVERSITY OF METABOLITES FROM FUNGI, CYANOBACTERIA, AND PLANTS RELATIVE TO FDA-APPROVED ANTICANCER AGENTS

Tamam El-Elimat, Xiaoli Zhang, David Jarjoura, Franklin J. Moy, Jimmy Orjala, A. Douglas Kinghorn, Cedric J. Pearce, and Nicholas H. Oberlies. *ACS Medicinal Chemistry Letters* 2012, 3, 645-649.

A collaborative project has been undertaken to explore filamentous fungi, cyanobacteria, and tropical plants for anticancer drug leads. Through principal component analysis, the chemical space covered by compounds isolated from these three sources over the last four years was compared to each other and to the chemical space of selected FDA-approved anticancer drugs. Using literature precedence, nine molecular descriptors were examined: molecular weight, number of chiral centers, number of rotatable bonds, number of acceptor atoms for H-bonds (N,O,F), number of donor atoms for H-bonds (N and O), topological polar surface area using N,O polar contributions, Moriguchi octanol-water partition coefficient, number of nitrogen atoms, and number of oxygen atoms. Four principal components explained 87% of the variation found among 343 bioactive natural products and 96 FDA-approved anticancer drugs. Across the four dimensions, fungal, cyanobacterial and plant isolates occupied both similar and distinct areas of chemical space that collectively aligned well with FDA-approved anticancer

agents. Thus, examining three separate resources for anticancer drug leads yields compounds that probe chemical space in a complementary fashion.

In a multidisciplinary project to identify anticancer leads from diverse natural product sources, 343 distinct compounds have been characterized from aquatic cyanobacteria, filamentous fungi, and tropical plants; over 33% of these represent new chemical entities, and many of the known compounds have not been evaluated as anticancer leads previously.^{11,292} The compounds were isolated based on bioactivity in one or more anticancer-related in vitro assays, and the structural variety of the resulting leads was broad, ranging from peptides to polyketides to terpenoids and myriad combinations thereof.^{19-22,105,293-296} One of our goals was to measure how this chemical diversity compared to that of FDA-approved anticancer agents.

In assessing the chemical diversity of a set of compounds, most approaches rely upon computational analyses of structural and physicochemical parameters, also known as molecular descriptors.²⁹⁷⁻³⁰⁰ Typically, these molecular descriptors include topological descriptors, physical property descriptors, atom and bond counts, surface area descriptors, and charge descriptors.³⁰¹ Each compound can therefore be defined in a chemical reference space of the n -dimensions of interrelated molecular descriptor variables.³⁰¹ A standard approach for reducing the dimensionality of the descriptors, while maintaining almost all of the variation among the compounds, is principal components analysis (PCA).³⁰¹⁻³⁰³ Although the multivariate statistical methods behind PCA and rotations to

simple structure involve complex algorithms, bivariate plots of the components often impart meaning that tend to be missed by bivariate plots of the original variables.

PCA has been used to compare molecular properties of different classes of compounds, particularly in relation to libraries of natural products (Table 40, Supplementary Information). Feher and Schmidt²⁹⁷ utilized ten molecular descriptors and PCA to examine three different compound libraries: natural products, molecules from combinatorial synthesis, and drug molecules. For this, the Chapman and Hall *Dictionary of Drugs* was used as a source of drug molecules ($n = 10,968$); the combinatorial database was assembled from the following databases: Maybridge HTS database, the ChemBridge EXPRESS-Pick database, the ComGenex collection, the ChemDiv International Diversity Collection, the ChemDiv CombiLab Probe Libraries, and the SPECS screening compounds database [out of the 670,536 combinatorial compounds, a random selection of 2% was used ($n = 13,506$)]; the natural compounds ($n = 3,287$) were assembled from the following sources: the BioSPECS natural products database, the ChemDiv natural products database, and the Interbioscreen IBS2001N and HTS-NC databases.²⁹⁷ Singh et al.³⁰⁰ presented a multiple criteria approach for the comparative analysis of combinatorial libraries, drugs, natural products, and molecular libraries small molecule repository using six molecular descriptors.³⁰⁰ A set of 20 natural products and 20 synthetic drugs (half of them being the top selling drugs of 2004) were compared for structural diversity by Tan³⁰⁴ using PCA with nine molecular descriptors. A similar study of the top 200 selling drugs of 2006 relative to Merck's sample collection, 595 natural products, using nine molecular descriptors was carried out by Singh and Culberson.²⁹⁹ As catalogued in Table

40, even though the sample sets varied, there was some overlap between the molecular descriptors utilized in all four studies.

To examine the chemical space covered by secondary metabolites we isolated in pursuit of anticancer leads (105 from filamentous fungi, 75 from cyanobacteria, and 163 from tropical plants) and FDA-approved anticancer agents (96), nine molecular descriptors were selected (Table 40): molecular weight (MW), number of chiral centers (nCC), number of rotatable bonds (nRBN), number of acceptor atoms for H-bonds [N,O,F; nH_{Acc}], number of donor atoms for H-bonds [N and O; nH_{Don}], topological polar surface area using N,O polar contributions [TPSA(NO)], Moriguchi octanol-water partition coefficient (MLOGP), number of nitrogen atoms (nN), and number of oxygen atoms (nO). Four of these descriptors (MW, nH_{Don}, nH_{Acc}, and MLOGP) were used in formulating the “rule of five”.³⁰⁵ The topological polar surface area is an important parameter when assessing the solubility, permeability, and transport of a compound.³⁰⁶ Chirality is a key characteristic of natural products, often reflected in their stereospecificity and affinity toward chiral biological targets.²⁹⁹ For better binding with receptors, rigid structures are preferable over flexible ligands, as binding is thermodynamically preferred and accompanied by lower entropy and hence stronger binding;^{299,307} calculating the number of rotatable bonds is an indicator of the rigidity of structures. Finally, oxygen and nitrogen atoms are important for the specific binding of ligands to receptors.²⁹⁷ In total, we used nine molecular descriptors and the same set utilized by Tan³⁰⁴ (Table 40).

Very high correlations were observed between the eight molecular descriptors and MW. This is most apparent from the correlation coefficients in row 1 of Table 41 (all except two were close to $r = 0.9$, see Supporting Information). This was not surprising, as the high correlations were a consequence of the eight other descriptors being highly dependent on the size of the compounds, and thus, their variation can be most simply explained by their MW. Therefore, to understand how the compounds differ from each other by more than the simple measure of MW, the eight other descriptors for each compound were transformed to relative measures by dividing each by a compound's MW. For example, dividing nN by MW provides a size independent measure of nitrogen abundance in a compound. After standardization, the correlations in Table 42 (Supporting Information) revealed that all the measures remain somewhat correlated with each other; however, these correlations were no longer as dependent on MW. As MW was included as one of the variables in the PCA, it remains represented in the decomposition of variation of the compounds.

Results of the PCA (Table 39) revealed that the first, second, third, and fourth principal components explained 44%, 17%, 13%, and 13% of the total compound variance across all nine measures, respectively, and accounted for 87% of the variance in total. The loadings in Table 39 were obtained by varimax rotation³⁰⁸ in an attempt to achieve simpler structure, but the results differed little from the un-rotated solution, which was the simple PCA solution. Factor one explained almost half of the variance and was dominated by loadings of TPSA(NO), nH_{Acc}, MLOGP (negative), nO, and nH_{Don}, which reflects the relatively higher correlations among these variables (with MLOGP

negatively correlated). Since TPSA(NO), nH_{Acc}, nO, and nH_{Don} are reflective of the polarity of a compound and they dominate this factor, it appears that these compounds vary most with regard to polarity (after standardization by MW). As MLOGP is a measure of molecular hydrophobicity, it was reasonable for it to be negatively correlated with the polarity descriptors. Factor two was dominated by the abundance of nitrogen atoms, and to some degree, was relative to the abundance of oxygen atoms, as seen by the negative loading there. Essentially, the FDA-approved anticancer drugs have a higher abundance of nitrogen than the natural product isolates. Factor three was dominated by nRBN and was negatively correlated with nCC. Finally, factor four was dominated by MW, but it was somewhat associated with nCC, even after normalization. This suggested an intriguing postulate, in that chiral centers may impart a greater degree of drug-like properties, especially when considering the nCC in compounds like taxol²⁴⁵ and the recently approved eribulin [Halaven],³⁰⁹ which are 11 and 19, respectively.

Plots of the principal components impart a visual representation of the data. Since component 1 explained 44% of the variance, it was held constant, and Figures 121-123 (Supporting Information) compare component 1 to components 2, 3, and 4, respectively. In Figure 121D there is much overlap, but some drugs seem to have higher values on both components 1 and 2. Also plant sources tend to have lower values on component 2 (Figure 121C), which was dominated by the abundance of nitrogen as noted above. Figure 122 again shows much overlap, with plant sources (and some fungi), showing higher values for component 3 (Figure 122A and 122C). Component 3 was dominated by nRBN, and was somewhat inversely relative to nCC. Figure 123 shows much overlap in

MW, but some of the fungal secondary metabolites had relatively high MWs, and the means for both cyanobacteria and fungi were higher than for drugs and tropical plants.

Table 39. Loadings for the First Four Principal Components for PCA Analysis of Fungal Secondary Metabolites (n = 105), Cyanobacteria (n = 75), Tropical Plants (n = 163) and Anticancer Drugs (n = 96)

principal component	PCLOA 01	PCLOA 02	PCLOA 03	PCLOA 04
Eigenvalue	3.69	1.62	1.27	1.25
cumulative Eigenvalue (%)	44	61	74	87
MW	0.20	0.13	0.19	0.88
nRBN	-0.02	-0.08	0.89	0.25
nN	0.28	0.91	0.01	0.05
nO	0.80	-0.59	0.02	-0.02
nH _{Don}	0.65	0.49	0.08	0.10
nH _{Acc}	0.94	0.14	0.06	0.04
TPSA(NO)	0.95	0.24	0.05	0.01
MLOGP	-0.85	-0.14	0.11	-0.33
nCC	-0.10	-0.29	-0.64	0.54

By inspecting the PCA plots, there were anticancer drugs residing outside the overlapping area with the isolated compounds; perhaps these drugs possess key structural features that should be considered in the natural product isolation studies. Accordingly, these non-overlapping drugs were identified from each plot, and it was found that they were mainly the same across all plots. The drugs were allopurinol, leucovorin calcium, aminolevulinic acid, fluorouracil, hydroxyurea, dacarbazine, cytarabine, azacitidine, decitabine, amifostine, fludarabine phosphate, temozolomide, nelarabine, and zoledronic

acid (Figure 124). Structurally, all these drugs are abundant in nitrogen and most are nucleoside-based drugs. Mechanistically, although they are listed among the FDA-approved anticancer drugs, not all are used specifically as cancer chemotherapeutic agents, with some being employed adjunctively with other anticancer drugs.³¹⁰ Hence, the above reasons could at least, in part, explain why the compounds from the three investigated natural resources failed to cover the chemical space occupied by those drugs. Moreover, as noted by a reviewer of this manuscript, there are likely some technical biases embedded in the data, as many synthetic compounds favor the inclusion of *N* atoms while natural product isolates tend to favor inclusion of *O* atoms; such biases may evolve to be irrelevant in the future.

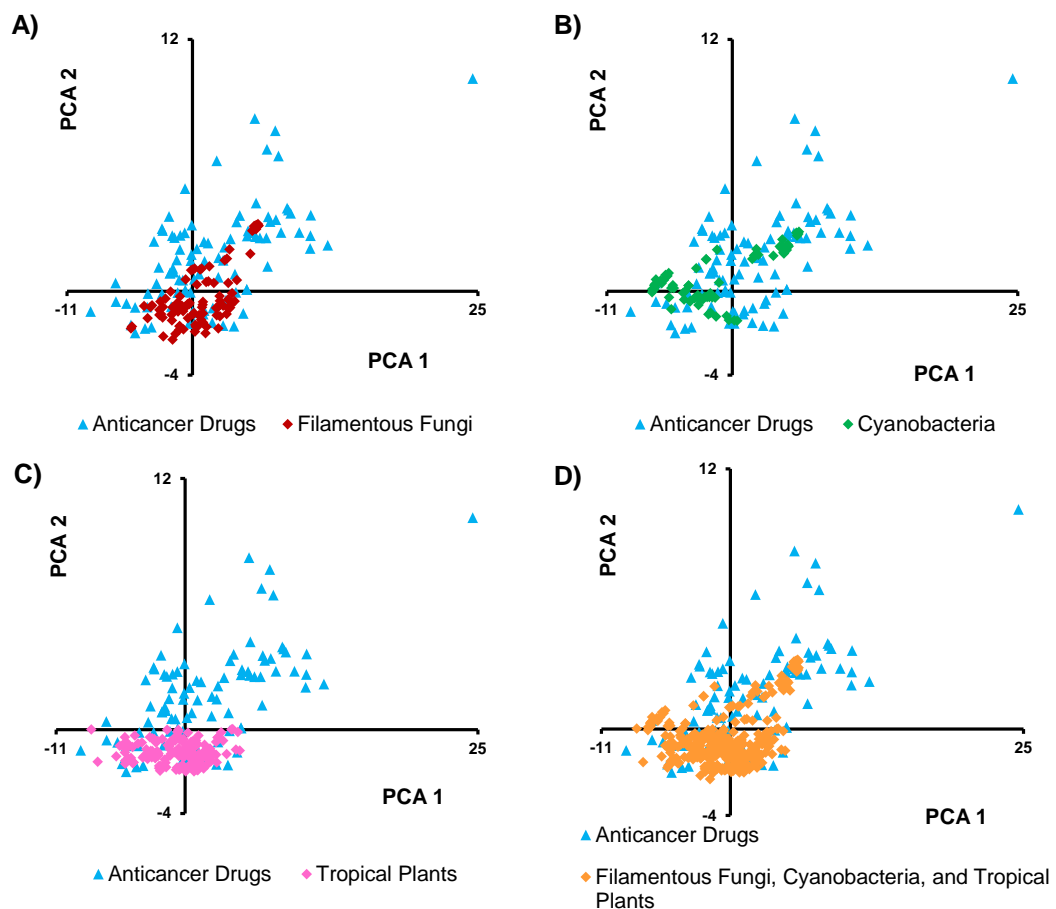


Figure 121. Plots of the first two principal components of the isolated secondary metabolites from A) filamentous fungi ($n = 105$), B) cyanobacteria ($n = 75$), and C) tropical plants ($n = 163$) relative to anticancer agents ($n = 96$). Plot D combines the data from all three natural product sources ($n = 343$) vs. anticancer agents ($n = 96$).

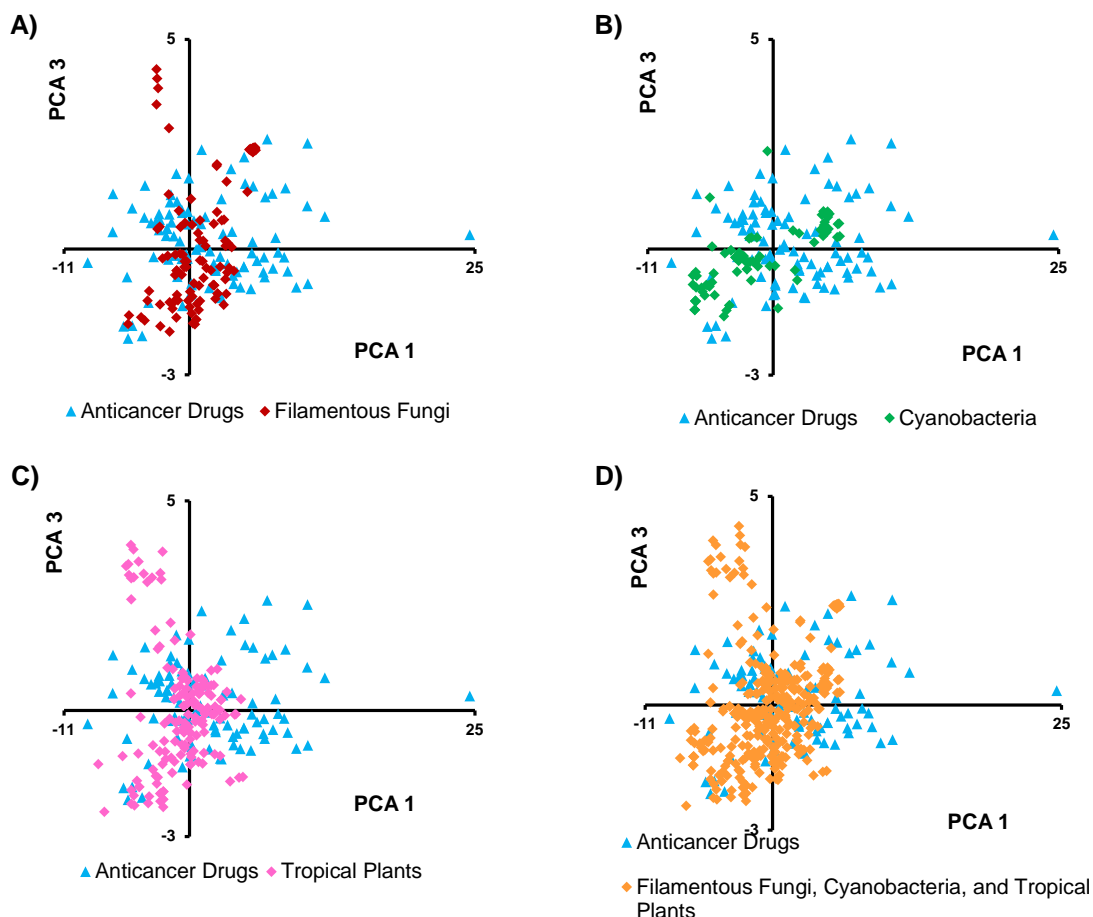


Figure 122. Plot of the first and third principal components of the isolated secondary metabolites from filamentous fungi (n = 105), cyanobacteria (n = 75), tropical plants (n = 163) and anticancer drugs (n = 96).

Analyzing the different plots clearly shows that anticancer drugs tended to cover a larger chemical space than the three analyzed sets of compounds, although with high overlap among them. This could be explained, at least in part, by the fact that the anticancer drugs included both natural and synthetic compounds. Of the 96 FDA-approved drugs studied, 59% were either natural products or compounds derived and/or inspired from natural products, in agreement with Newman and Cragg.⁵ However, the

sum conclusion was that the isolates from fungi, cyanobacteria and tropical plants represented somewhat different areas of chemical space, and thus, the collective strategy of probing these three natural resources for anticancer drug leads individually should be complementary.

Supporting Information

Experimental Procedures. The natural products utilized in this study were isolated in pursuit of anticancer leads. The recent literature may be examined for examples of descriptions of the isolation and structure elucidation of compounds from filamentous fungi, cyanobacteria, and tropical plants by our collaborative team. The FDA-approved anticancer agents were selected from two complementary sources: those posted on the website of the Developmental Therapeutic Program NCI/NIH and the recently approved anticancer drugs from the orange book on the FDA website. All molecular descriptors, except number of chiral centers, were calculated using Dragon software for molecular descriptor calculation (version 6.0 – 2010; Talete srl, Milano, Italy). The number of chiral centers was tabulated by inspection. SAS was used for principal component analysis varimax rotation of the 9 variable correlation matrix (Proc Princomp and Factor). Components score were obtained after variance standardization.

Table 40. Molecular Descriptors Utilized in the Current Study Compared to Related PCA Studies in the Literature ^{297,299,300,304}

molecular descriptors	Feher and Schmidt ²⁹ ₇	Singh et al. ³⁰⁰	Tan ³⁰ ₄	Singh and Culberson ²⁹ ₉	Current study
molecular weight (MW)	---	×	×	×	×
number of chiral centers (nCC)	×	---	×	×	×
number of rotatable bonds (NRBN)	×	×	×	×	×
number of solvated acceptor atoms for H-bonds (N,O,F) [N _{Acc,solv}]	×	×	×	×	×
number of solvated donor atoms for H-bonds (N and O) [N _{Don,solv}]	×	×	×	---	×
topological polar surface area [TPSA(NO)]	---	×	×	×	×
octanol/water partition coefficient	---	×	×	×	×
number of nitrogen atoms (nN)	---	---	×	×	×
number of oxygen atoms (nO)	---	---	×	×	×
number of C-N bonds (nCN)	×	---	---	---	---
number of C-O bonds (nCO)	×	---	---	---	---
number of C-halogen bonds (nCX)	×	---	---	---	---
number of C-S bonds (nCS)	×	---	---	---	---
ratio of aromatic atoms to ring atoms	×	---	---	---	---
ring fusion degree	×	---	---	---	---
normalized bond flexibility	---	---	---	×	---

Table 41. Pearson Correlation Coefficients for Raw Data

correlation coefficient	MW	nRBN	nN	nO	nH _{Don}	nH _{Acc}	TPSA	MLOGP	nCC
MW	1.0000	0.8713	0.8185	0.8878	0.9001	0.9466	0.9459	-0.6667	0.6500
nRBN	0.8713	1.0000	0.8174	0.7533	0.8493	0.8681	0.8702	-0.6292	0.4024
nN	0.8185	0.8174	1.0000	0.6271	0.8768	0.8777	0.8795	-0.7712	0.3450
nO	0.8878	0.7533	0.6271	1.0000	0.8061	0.9202	0.9097	-0.7564	0.6632
nH _{Don}	0.9001	0.8493	0.8768	0.8061	1.0000	0.9258	0.9607	-0.7850	0.4993
nH _{Acc}	0.9466	0.8681	0.8777	0.9202	0.9258	1.0000	0.9906	-0.8427	0.5682
TPSA	0.9459	0.8702	0.8795	0.9097	0.9607	0.9906	1.0000	-0.8373	0.5591
MLOGP	-0.6667	-0.6292	-0.7712	-0.7564	-0.7850	-0.8427	-0.8373	1.0000	-0.3916
nCC	0.6500	0.4024	0.3450	0.6632	0.4993	0.5682	0.5591	-0.3916	1.0000

Table 42. Pearson Correlation Coefficients for Molecular Weight Standardized Data

correlation coefficient	MW	nRBN	nN	nO	nH _{Don}	nH _{Acc}	TPSA	MLOGP	nCC
MW	1.0000	0.2423	0.1755	0.0879	0.2571	0.2449	0.2201	-0.4706	0.1445
nRBN	0.2423	1.0000	-0.0071	0.0249	0.0669	0.0604	0.0296	0.0694	-0.2509
nN	0.1755	-0.0071	1.0000	-0.3057	0.4915	0.4680	0.4842	-0.3778	-0.2184
nO	0.0879	0.0249	-0.3057	1.0000	0.2136	0.6711	0.6170	-0.5665	0.0529
nH _{Don}	0.2571	0.0669	0.4915	0.2136	1.0000	0.5692	0.7763	-0.5713	-0.1417
nH _{Acc}	0.2449	0.0604	0.4680	0.6711	0.5692	1.0000	0.9172	-0.8048	-0.1255
TPSA	0.2201	0.0296	0.4842	0.6170	0.7763	0.9172	1.0000	-0.7766	-0.1471
MLOGP	-0.4706	0.0694	-0.3778	-0.5665	-0.5713	-0.8048	-0.7766	1.0000	-0.0515
nCC	0.1445	-0.2509	-0.2184	0.0529	-0.1417	-0.1255	-0.1471	-0.0515	1.0000

Table 43. Summary Statistics of Different Properties Among Secondary Metabolites from Filamentous Fungi ($n = 105$), Cyanobacteria ($n = 75$), Tropical plants ($n = 163$) and Anticancer Drugs ($n = 96$)

source	Variables	Raw data		After MW standardization	
		Mean	Std. Dev.	Mean	Std. Dev.
Anticancer Drugs ($n = 96$)	MW	412.76	248.04	1.000	0.000
	RBN	5.31	5.12	0.012	0.008
	nN	3.02	2.79	0.009	0.008
	nO	4.92	4.73	0.011	0.007
	nHDon	3.09	3.46	0.008	0.008
	nHAcc	8.00	5.69	0.020	0.009
	TPSA	113.88	89.62	0.295	0.164
	MLOGP	1.12	2.24	0.003	0.007
	CC	3.30	4.87	0.006	0.007
Cyanobacteria ($n = 75$)	MW	628.78	338.39	1.000	0.000
	RBN	7.77	7.35	0.011	0.007
	nN	3.79	4.44	0.005	0.004
	nO	6.01	6.10	0.007	0.005
	nHDon	5.12	5.27	0.007	0.004
	nHAcc	9.12	10.49	0.011	0.008
	TPSA	150.41	152.65	0.193	0.106
	MLOGP	2.30	3.55	0.006	0.006
	CC	6.28	4.31	0.010	0.004
Filamentous Fungi ($n = 105$)	MW	660.36	555.30	1.000	0.000
	RBN	12.14	17.60	0.014	0.012
	nN	4.19	7.72	0.003	0.004
	nO	8.98	6.87	0.014	0.004
	nHDon	5.74	8.11	0.007	0.004
	nHAcc	13.17	14.29	0.018	0.004
	TPSA	196.95	218.11	0.263	0.073
	MLOGP	0.53	3.65	0.004	0.005
	CC	5.69	3.92	0.010	0.006

Table 43 (Continued). Summary Statistics of Different Properties Among Secondary Metabolites from Filamentous Fungi ($n = 105$), Cyanobacteria ($n = 75$), Tropical plants ($n = 163$) and Anticancer Drugs ($n = 96$)

source	Variables	Raw data		After MW standardization	
		Mean	Std. Dev.	Mean	Std. Dev.
Tropical Plants ($n = 163$)	MW	450.42	152.31	1.000	0.000
	RBN	5.90	4.25	0.014	0.011
	nN	0.06	0.27	0.000	0.001
	nO	6.57	3.68	0.014	0.005
	nHDon	2.37	2.10	0.005	0.003
	nHAcc	6.60	3.65	0.014	0.005
	TPSA	100.87	52.82	0.220	0.064
	MLOGP	2.70	1.84	0.007	0.004
CC	4.58	5.46	0.009	0.008	

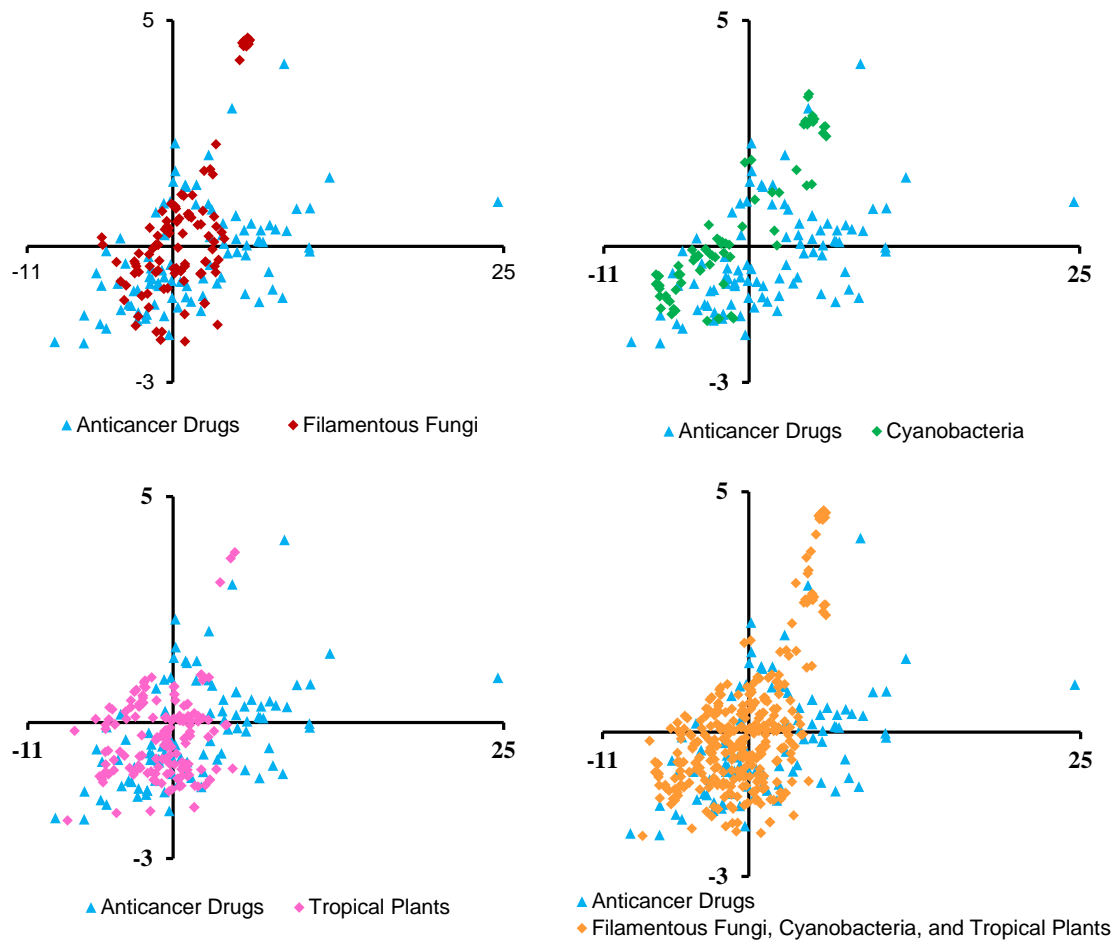


Figure 123. Plot of the first and fourth principal components of the isolated secondary metabolites from filamentous fungi ($n = 105$), cyanobacteria ($n = 75$), tropical plants ($n = 163$) and anticancer drugs ($n = 96$).

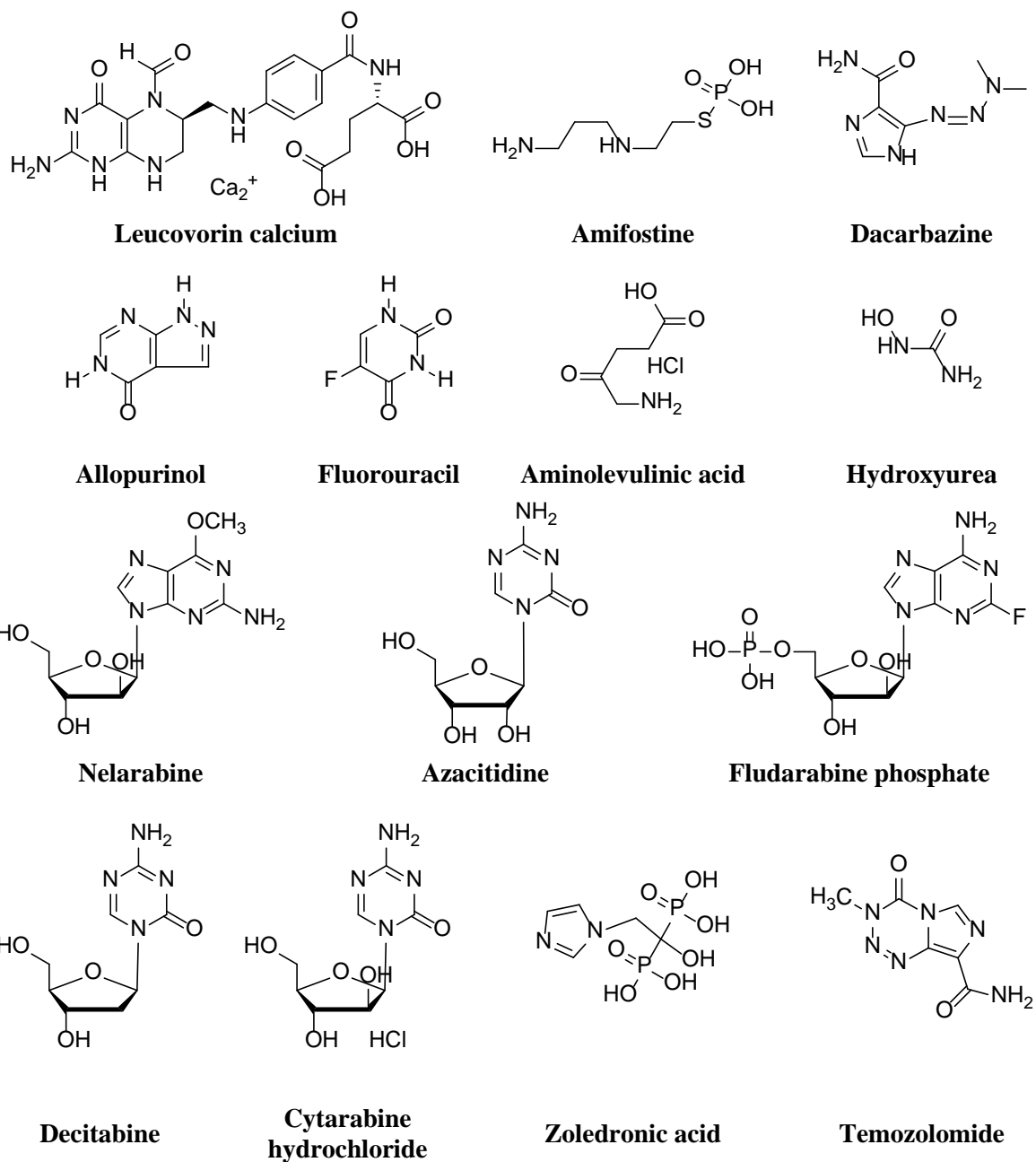


Figure 124. Chemical structures of the anticancer drugs that were not overlapping in the chemical space with the investigated compounds in the PCA plots in Figures 121, 122, and 123.

REFERENCES

- (1) Braun, C. A.; Anderson, C. M. *Pathophysiology: A Clinical Approach*; Second ed.; Lippincott Williams & Wilkins: Baltimore, 2011.
- (2) American Cancer Society. *Cancer Facts & Figures 2013*; American Cancer Society: Atlanta, 2013.
- (3) Jemal, A.; Bray, F.; Center, M. M.; Ferlay, J.; Ward, E.; Forman, D. *Ca-Cancer J. Clin.* **2011**, *61*, 69-90.
- (4) Pratt, W. B.; Ruddon, R. W.; Ensminger, W. D.; Maybaum, J. *The Anticancer Drugs*; Second ed.; Oxford University Press, Inc.: New York, 1994; p 360.
- (5) Newman, D. J.; Cragg, G. M. *J. Nat. Prod.* **2012**, *75*, 311-335.
- (6) Oberlies, N. H.; Kroll, D. J. *J. Nat. Prod.* **2004**, *67*, 129-135.
- (7) Harvey, A. L. *Drug Discovery Today* **2008**, *13*, 894-901.
- (8) Blackwell, M. *Am. J. Bot.* **2011**, *98*, 426-438.
- (9) Fleming, A. *Penicillin, its practical application*; Butterworth & Co., Ltd: London, 1946; p 380.
- (10) Vagelos, P. *Science* **1991**, *252*, 1080-4.
- (11) Orjala, J.; Oberlies, N. H.; Pearce, C. J.; Swanson, S. M.; Kinghorn, A. D. In *Bioactive Compounds from Natural Sources. Natural Products as Lead Compounds in Drug Discovery*; 2nd ed., Tringali, C., Ed.; Taylor & Francis: London, UK, 2012; pp 37-63.

- (12) Hawksworth, D. L. *Biodivers. Conserv.* **2012**, *21*, 2425-2433.
- (13) Gloer, J. B. In *Environmental and Microbial Relationships*; Kubicek, C. P.; Druzhinina, I. S., Eds.; Springer: Berlin-Heidelberg, 2007; Vol. 4, pp 257-283.
- (14) Strader, C. R.; Pearce, C. J.; Oberlies, N. H. *J. Nat. Prod.* **2011**, *74*, 900-907.
- (15) Hanada, M.; Sugawara, K.; Kaneta, K.; Toda, S.; Nishiyama, Y.; Tomita, K.; Yamamoto, H.; Konishi, M.; Oki, T. *J. Antibiot.* **1992**, *45*, 1746-1752.
- (16) U.S. Department of Health and Human Services U.S. Food and Drug Administration: FDA approves Kyprolis for some patients with multiple myeloma. <http://www.fda.gov/NewsEvents/Newsroom/PressAnnouncements/ucm312920.htm>
- (17) El-Elimat, T.; Zhang, X.; Jarjoura, D.; Moy, F. J.; Orjala, J.; Kinghorn, A. D.; Pearce, C. J.; Oberlies, N. H. *ACS Med. Chem. Lett.* **2012**, *3*, 645-649.
- (18) Ayers, S.; Ehrmann, B. M.; Adcock, A. F.; Kroll, D. J.; Carcache de Blanco, E. J.; Shen, Q.; Swanson, S. M.; Falkinham, J. O., 3rd; Wani, M. C.; Mitchell, S. M.; Pearce, C. J.; Oberlies, N. H. *J. Pept. Sci.* **2012**, *18*, 500-510.
- (19) Ayers, S.; Graf, T. N.; Adcock, A. F.; Kroll, D. J.; Matthew, S.; Carcache de Blanco, E. J.; Shen, Q.; Swanson, S. M.; Wani, M. C.; Pearce, C. J.; Oberlies, N. H. *J. Nat. Prod.* **2011**, *74*, 1126-1131.
- (20) Ayers, S.; Graf, T. N.; Adcock, A. F.; Kroll, D. J.; Shen, Q.; Swanson, S. M.; Matthew, S.; Carcache de Blanco, E. J.; Wani, M. C.; Darveaux, B. A.; Pearce, C. J.; Oberlies, N. H. *J. Antibiot.* **2012**, *65*, 3-8.

- (21) Ayers, S.; Graf, T. N.; Adcock, A. F.; Kroll, D. J.; Shen, Q.; Swanson, S. M.; Wani, M. C.; Darveaux, B. A.; Pearce, C. J.; Oberlies, N. H. *Tetrahedron Lett.* **2011**, *52*, 5128-5230.
- (22) Sy-Cordero, A. A.; Graf, T. N.; Adcock, A. F.; Kroll, D. J.; Shen, Q.; Swanson, S. M.; Wani, M. C.; Pearce, C. J.; Oberlies, N. H. *J. Nat. Prod.* **2011**, *74*, 2137-2142.
- (23) Hawksworth, D. L. *Mycol. Res.* **1991**, *95*, 641-655.
- (24) Lee, I.-K.; Yun, B.-S.; Cho, S.-M.; Kim, W.-G.; Kim, J.-P.; Ryoo, I.-J.; Koshino, H.; Yoo, I.-D. *J. Nat. Prod.* **1996**, *59*, 1090-1092.
- (25) Biggins, J. B.; Liu, X.; Feng, Z.; Brady, S. F. *J. Am. Chem. Soc.* **2011**, *133*, 1638-1641.
- (26) Sawayama, Y.; Tsujimoto, T.; Sugino, K.; Nishikawa, T.; Isobe, M.; Kawagishi, H. *Bioscience, Biotechnology, and Biochemistry* **2006**, *70*, 2998-3003.
- (27) Zhang, C.; Ondeyka, J. G.; Herath, K. B.; Guan, Z.; Collado, J.; Pelaez, F.; Leavitt, P. S.; Gurnett, A.; Nare, B.; Liberator, P.; Singh, S. B. *J. Nat. Prod.* **2006**, *69*, 710-712.
- (28) Nakagawa, F.; Enokita, R.; Naito, A.; Iijima, Y.; Yamazaki, M. *J. Antibiot.* **1984**, *37*, 6-9.
- (29) Claveau, D.; Chen, S. L.; O'Keefe, S.; Zaller, D. M.; Styhler, A.; Liu, S.; Huang, Z.; Nicholson, D. W.; Mancini, J. A. *J. Pharmacol. Exp. Ther.* **2004**, *310*, 752-760.
- (30) Press, N. J.; Banner, K. H. *Prog. Med. Chem.* **2009**, *47*, 37-74.

- (31) Goldhoff, P.; Warrington, N. M.; Limbrick, D. D., Jr.; Hope, A.; Woerner, B. M.; Jackson, E.; Perry, A.; Piwnica-Worms, D.; Rubin, J. B. *Clin. Cancer Res.* **2008**, *14*, 7717-7725.
- (32) Farias, C. B.; Lima, R. C.; Lima, L. O.; Flores, D. G.; Meurer, L.; Brunetto, A. L.; Schwartsmann, G.; Roesler, R. *Oncology* **2008**, *75*, 27-31.
- (33) Jeon, Y. H.; Heo, Y. S.; Kim, C. M.; Hyun, Y. L.; Lee, T. G.; Ro, S.; Cho, J. M. *Cell. Mol. Life Sci.* **2005**, *62*, 1198-1220.
- (34) U.S. Department of Health and Human Services U.S. Food and Drug Administration. Approval Package For: Application Number: 022522orig1s000. 2011. http://www.accessdata.fda.gov/drugsatfda_docs/nda/2011/022522Orig1s000Approv.pdf (accessed June 2, 2012),
- (35) Savai, R.; Pullamsetti, S. S.; Banat, G.-A.; Weissmann, N.; Ghofrani, H. A.; Grimminger, F.; Schermuly, R. T. *Expert Opin. Invest. Drugs* **2010**, *19*, 117-131.
- (36) Sengupta, R.; Sun, T.; Warrington, N. M.; Rubin, J. B. *Trends Pharmacol. Sci.* **2011**, *32*, 337-344.
- (37) Wang, P.; Wu, P.; Ohleth, K. M.; Egan, R. W.; Billah, M. M. *Mol. Pharmacol.* **1999**, *56*, 170-174.
- (38) Houslay, M. D.; Schafer, P.; Zhang, K. Y. J. *Drug Discovery Today* **2005**, *10*, 1503-1519.
- (39) Kumar, D.; Patel, G.; Vijayakrishnan, L.; Dastidar, S. G.; Ray, A. *Chem. Biol. Drug Des.* **2011**, *79*, 810-818.

- (40) Kranz, M.; Wall, M.; Evans, B.; Miah, A.; Ballantine, S.; Delves, C.; Dombroski, B.; Gross, J.; Schneck, J.; Villa, J. P.; Neu, M.; Somers, D. O. *Bioorg. Med. Chem.* **2009**, *17*, 5336-5341.
- (41) Mpamhanga, C. P.; Chen, B.; McLay, I. M.; Ormsby, D. L.; Lindvall, M. K. *J. Chem. Inf. Model.* **2005**, *45*, 1061-1074.
- (42) Dym, O.; Xenarios, I.; Ke, H.; Colicelli, J. *Mol. Pharmacol.* **2002**, *61*, 20-25.
- (43) *Glide*, version 5.6; Schrodinger, LLC: New York, NY, 2011.
- (44) Friesner, R. A.; Murphy, R. B.; Repasky, M. P.; Frye, L. L.; Greenwood, J. R.; Halgren, T. A.; Sanschagrin, P. C.; Mainz, D. T. *J. Med. Chem.* **2006**, *49*, 6177-6196.
- (45) Schoch, C. L.; Seifert, K. A.; Huhndorf, S.; Robert, V.; Spouge, J. L.; Levesque, C. A.; Chen, W.; Fungal Barcoding Consortium. *Proc. Natl. Acad. Sci. U.S.A.* **2012**, *109*, 6241-6246.
- (46) Soule, H. D.; Vazquez, J.; Long, A.; Albert, S.; Brennan, M. *J. Natl. Cancer Inst.* **1973**, *51*, 1409-1416.
- (47) Carney, D. N.; Gazdar, A. F.; Bunn, P. A., Jr.; Guccion, J. G. *Stem Cells* **1982**, *1*, 149-164.
- (48) Rosenblum, M. L.; Gerosa, M. A.; Wilson, C. B.; Barger, G. R.; Pertuiset, B. F.; de Tribolet, N.; Dougherty, D. V. *J. Neurosurg.* **1983**, *58*, 170-176.
- (49) Alali, F. Q.; El-Elimat, T.; Li, C.; Qandil, A.; Alkofahi, A.; Tawaha, K.; Burgess, J. P.; Nakanishi, Y.; Kroll, D. J.; Navarro, H. A.; Falkinham, J. O.; Wani, M. C.; Oberlies, N. H. *J. Nat. Prod.* **2005**, *68*, 173-178.

- (50) Li, C.; Lee, D.; Graf, T. N.; Phifer, S. S.; Nakanishi, Y.; Riswan, S.; Setyowati, F. M.; Saribi, A. M.; Soejarto, D. D.; Farnsworth, N. R.; Falkinham, J. O., 3rd; Kroll, D. J.; Kinghorn, A. D.; Wani, M. C.; Oberlies, N. H. *J. Nat. Prod.* **2009**, *72*, 1949-1953.
- (51) Xu, R. X.; Rocque, W. J.; Lambert, M. H.; Vanderwall, D. E.; Luther, M. A.; Nolte, R. T. *J. Mol. Biol.* **2004**, *337*, 355-365.
- (52) *Schrödinger Suite 2010 Protein Preparation Wizard*, Epic version 2.1, Impact version 5.6, Prime version 2.2; Schrödinger, LLC: New York, NY, 2010.
- (53) Gardes, M.; Bruns, T. D. *Mol. Ecol.* **1993**, *2*, 113-118.
- (54) White, T. J.; Bruns, T.; Lee, S.; Taylor, J. In *PCR Protocols. A Guide to Methods and Applications*; Innis, M. A.; Gelfand, D. H.; Sninsky, J. J.; White, T. J., Eds.; Academic Press: San Diego, CA, 1990; pp 315-322.
- (55) Rehner, S. A.; Samuels, G. J. *Can. J. Bot.* **1995**, *73*, 816-823.
- (56) Vilgalys, R.; Hester, M. *J. Bacteriol.* **1990**, *172*, 4238-4246.
- (57) Benson, D. A.; Karsch-Mizrachi, I.; Clark, K.; Lipman, D. J.; Ostell, J.; Sayers, E. W. *Nucleic Acids Res.* **2012**, *40*, D48-D53.
- (58) Altschul, S. F.; Gish, W.; Miller, W.; Myers, E. W.; Lipman, D. J. *J. Mol. Biol.* **1990**, *215*, 403-410.
- (59) Begerow, D.; Nilsson, H.; Unterseher, M.; Maier, W. *Appl. Microbiol. Biotechnol.* **2010**, *87*, 99-108.
- (60) Nilsson, R. H.; Kristiansson, E.; Ryberg, M.; Hallenberg, N.; Larsson, K. H. *Evol. Bioinf. Online* **2008**, *4*, 193-201.
- (61) Schmitt, I.; Barker, F. K. *Nat. Prod. Rep.* **2009**, *26*, 1585-1602.

- (62) Figueroa, M.; Graf, T. N.; Ayers, S.; Adcock, A. F.; Kroll, D. J.; Yang, J.; Swanson, S. M.; Munoz-Acuna, U.; Carcache de Blanco, E. J.; Agrawal, R.; Wani, M. C.; Darveaux, B. A.; Pearce, C. J.; Oberlies, N. H. *J. Antibiot.* **2012**, *65*, 559-564.
- (63) El-Elimat, T.; Figueroa, M.; Raja, H. A.; Graf, T. N.; Adcock, A. F.; Kroll, D. J.; Day, C. S.; Wani, M. C.; Pearce, C. J.; Oberlies, N. H. *J. Nat. Prod.* **2013**, *76*, 382-387.
- (64) Nozawa, O.; Okazaki, T.; Sakai, N.; Komurasaki, T.; Hanada, K.; Morimoto, S.; Chen, Z. X.; He, B. M.; Mizoue, K. *J. Antibiot.* **1995**, *48*, 113-8.
- (65) Gao, X. L.; Nakadai, M.; Snider, B. B. *Org. Lett.* **2003**, *5*, 451-454.
- (66) Gao, X.; Snider, B. B. *J. Org. Chem.* **2004**, *69*, 5517-27.
- (67) *trans*-Dihydrowaol A (**2**): colorless oil; $[\alpha]_D^{26} = -56^\circ$ ($c = 0.1$, MeOH); ^1H NMR (CDCl_3 , 500 MHz) and ^{13}C NMR (CDCl_3 , 125 MHz) (see Supplementary Data); HRESIMS m/z 239.1278 $[\text{M}+\text{H}]^+$ (calcd for $\text{C}_{13}\text{H}_{19}\text{O}_4$ 239.1278).
- (68) Hoye, T. R.; Jeffrey, C. S.; Shao, F. *Nat. Protoc.* **2007**, *2*, 2451-2458.
- (69) Preparation of the (*R*)- and (*S*)-MTPA ester derivatives of *trans*-dihydrowaol A (**2**): To 0.75 mg of compound **2** was added 400 μL of pyridine- d_5 and transferred into an NMR tube. To initiate the reaction, 10 μL of *S*-(+)- α -methoxy- α -(trifluoromethyl)phenylacetyl (MTPA) chloride was added into the NMR tube with careful shaking and then monitored immediately by ^1H NMR at the following time points 0, 15, 30, and 60 min. The reaction was found to be complete within 30 min, yielding the mono (*R*)-MTPA ester derivative (**2b**) of **2**. ^1H NMR data of **2b** (500 MHz, pyridine- d_5): 5.93 (1H, m, H-2'), 5.89 (1H, m, H-1'), 5.69 (1H, m, H-2''), 5.60 (1H, m, H-1''), 5.53 (1H, bq, $J = 2.3$, H-3), 4.81 (1H, dd, $J = 8.6, 8.0$, H-7), 4.48 (1H, d, $J = 5.7$, H-2), 3.94

(1H, dd, $J = 9.2, 8.6$, H-7a), 2.69 (1H, m, H-4a), 2.67 (1H, m, H-4 β), 2.29 (1H, m, H-4 α), 1.63 (3H, d, $J = 6.9$, H₃-3'), and 1.55 (3H, d, $J = 6.3$, H₃-3''). In an analogous manner, 0.75 mg of compound **2** dissolved in 400 μ L pyridine-*d*₅ was reacted in a second NMR tube with 10 μ L (*R*)-(-)- α -MTPA chloride for 30 min, to afford the mono (*S*)-MTPA ester (**2a**). ¹H NMR data of **2a** (500 MHz, pyridine-*d*₅): δ_{H} 5.88 (1H, m, H-2'), 5.77 (1H, m, H-1'), 5.70 (1H, m, H-2''), 5.60 (1H, m, H-1''), 5.56 (1H, bq, $J = 3.4$, H-3), 4.89 (1H, dd, $J = 8.6, 8.0$, H-7), 4.15 (1H, d, $J = 6.9$, H-2), 3.85 (1H, m, H-7a), 2.84 (1H, m, H-4a), 2.77 (1H, m, H-4 β), 2.37 (1H, m, H-4 α), 1.53 (3H, d, $J = 6.3$, H₃-3'), and 1.50 (3H, d, $J = 6.3$, H₃-3'').

(70) *cis*-Dihydrowaol A (**3**): colorless oil; $[\alpha]_{\text{D}}^{26} = -32^{\circ}$ ($c = 0.1$, MeOH); ¹H NMR (CDCl₃, 500 MHz) and ¹³C NMR (CDCl₃, 125 MHz) (see Supplementary Data); HRESIMS m/z 239.1280 [M+H]⁺ (calcd for C₁₃H₁₉O₄ 239.1278).

(71) Kim, H.; Zinkus, J.; Swanson, S.; Orjala, J. *Planta Med.* **2012**, *78*, PI83.

(72) Oh, H.; Swenson, D. C.; Gloer, J. B.; Shearer, C. A. *Tetrahedron Lett.* **2001**, *42*, 975-977.

(73) Hayashi, K.; Takizawa, M.; Noguchi, K., Japanese Patent 10,287,679, 1998; *Chem. Abstr.* **1999**, *130*, 3122e.

(74) Krohn, K.; Hussain, H.; Florke, U.; Schulz, B.; Draeger, S.; Pescitelli, G.; Salvadori, P.; Antus, S.; Kurtan, T. *Chirality* **2007**, *19*, 464-470.

(75) Kock, I.; Krohn, K.; Egold, H.; Draeger, S.; Schulz, B.; Rheinheimer, J. *Eur. J. Org. Chem.* **2007**, *2007*, 2186-2190.

- (76) Qin, S.; Krohn, K.; Flörke, U.; Schulz, B.; Draeger, S.; Pescitelli, G.; Salvadori, P.; Antus, S.; Kurtán, T. *Eur. J. Org. Chem.* **2009**, 2009, 3279-3284.
- (77) Krohn, K.; Biele, C.; Drogies, K.-H.; Steingröver, K.; Aust, H.-J.; Draeger, S.; Schulz, B. *Eur. J. Org. Chem.* **2002**, 2002, 2331-2336.
- (78) Grafenhan, T.; Schroers, H. J.; Nirenberg, H. I.; Seifert, K. A. *Stud. Mycol.* **2011**, 79-113.
- (79) Raja, H.; Schoch, C. L.; Hustad, V.; Shearer, C.; Miller, A. *MycoKeys* **2011**, 1, 63-94.
- (80) El-Elimat, T.; Figueroa, M.; Ehrmann, B. M.; Cech, N. B.; Pearce, C. J.; Oberlies, N. H. *J. Nat. Prod.* **2013**, 76, 1709-1716.
- (81) El-Elimat, T.; Figueroa, M.; Raja, H. A.; Adcock, A. F.; Kroll, D. J.; Swanson, S. M.; Wani, M. C.; Pearce, C. J.; Oberlies, N. H. *Tetrahedron Lett.* **2013**, 54, 4300-4302.
- (82) Sy-Cordero, A. A.; Pearce, C. J.; Oberlies, N. H. *J. Antibiot.* **2012**, 65, 541-549.
- (83) Hertlein, E.; Beckwith, K. A.; Lozanski, G.; Chen, T. L.; Towns, W. H.; Johnson, A. J.; Lehman, A.; Ruppert, A. S.; Bolon, B.; Andritsos, L.; Lozanski, A.; Rassenti, L.; Zhao, W.; Jarvinen, T. M.; Senter, L.; Croce, C. M.; Symer, D. E.; de la Chapelle, A.; Heerema, N. A.; Byrd, J. C. *Plos One* **2013**, 8, e76607.
- (84) Harned, A. M.; Volp, K. A. *Nat. Prod. Rep.* **2011**, 28, 1790-1810.
- (85) Geigert, J.; Stermitz, F. R.; A., S. H. *Tetrahedron* **1973**, 29, 2343-2345.
- (86) Reátegui, R. F.; Wicklow, D. T.; Gloer, J. B. *J. Nat. Prod.* **2006**, 69, 113-117.
- (87) Optiz, L.; Hänsel, R. *Arch. Pharm.* **1971**, 304, 228-230.

- (88) Yoshikawa, K.; Kokudo, N.; Hashimoto, T.; Yamamoto, K.; Inose, T.; Kimura, T. *Biol. Pharm. Bull.* **2010**, *33*, 1355-1359.
- (89) Nakano, Y.; Takashima, T. *Mokuzai Gakkaishi* **1975**, *21*, 577-580.
- (90) dos Santos, E. D.; Beatriz, A.; de Lima, D. P.; Marques, M. R.; Leite, C. B. *Quim. Nova* **2009**, *32*, 1856-1859.
- (91) Evidente, A.; Superchi, S.; Cimmino, A.; Mazzeo, G.; Mugnai, L.; Rubiales, D.; Andolfi, A.; Villegas-Fernandez, A. M. *Eur. J. Org. Chem.* **2011**, 5564-5570.
- (92) Stermitz, F. R.; Adamovics, J. A.; Geigert, J. *Tetrahedron* **1975**, *31*, 1593-1595.
- (93) Ichihashi, K.; Osawa, T.; Toyokuni, S.; Uchida, K. *J. Biol. Chem.* **2001**, *276*, 23903-23913.
- (94) Wang, M.; McIntee, E. J.; Cheng, G.; Shi, Y.; Villalta, P. W.; Hecht, S. S. *Chem. Res. Toxicol.* **2001**, *14*, 423-430.
- (95) Liu, K. L.; Porrás-Alfaro, A.; Kuske, C. R.; Eichorst, S. A.; Xie, G. *Appl. Environ. Microbiol.* **2012**, *78*, 1523-1533.
- (96) Eberhardt, U. In *DNA Barcodes*; Kress, W. J.; Erickson, D. L., Eds.; Humana Press: New York, NY, USA, 2012; Vol. 858, pp 183-205.
- (97) Figueroa, M.; Raja, H.; Falkinham, J. O.; Adcock, A. F.; Kroll, D. J.; Wani, M. C.; Pearce, C. J.; Oberlies, N. H. *J. Nat. Prod.* **2013**, *76*, 1007-1015.
- (98) Raja, H. A.; Oberlies, N. H.; El-Elimat, T.; Miller, A. N.; Zelski, S. E.; Shearer, C. A. *Mycoscience* **2013**, *54*, 353-361.
- (99) Raja, H. A.; Oberlies, N. H.; Figueroa, M.; Tanaka, K.; Hirayama, K.; Hashimoto, A.; Miller, A. N.; Zelski, S. E.; Shearer, C. A. *Mycologia* **2013**, *105*, 959-976.

- (100) Rae, J.; Creighton, C.; Meck, J.; Haddad, B.; Johnson, M. *Breast Cancer Res. Treat.* **2007**, *104*, 13-19.
- (101) Leibovitz, A.; Stinson, J. C.; McCombs, W. B.; McCoy, C. E.; Mazur, K. C.; Mabry, N. D. *Cancer Res.* **1976**, *36*, 4562-4569.
- (102) Falkinham, J. O.; Macri, R. V.; Maisuria, B. B.; Actis, M. L.; Sugandhi, E. W.; Williams, A. A.; Snyder, A. V.; Jackson, F. R.; Poppe, M. A.; Chen, L.; Ganesh, K.; Gandour, R. D. *Tuberculosis* **2012**, *92*, 173-181.
- (103) Williams, A. A.; Sugandhi, E. W.; Macri, R. V.; Falkinham, J. O.; Gandour, R. D. *J. Antimicrob. Chemother.* **2007**, *59*, 451-458.
- (104) Lin, Z. J.; Falkinham, J. O.; Tawfik, K. A.; Jeffs, P.; Bray, B.; Dubay, G.; Cox, J. E.; Schmidt, E. W. *J. Nat. Prod.* **2012**, *75*, 1518-1523.
- (105) Ayers, S.; Ehrmann, B. M.; Adcock, A. F.; Kroll, D. J.; Wani, M. C.; Pearce, C. J.; Oberlies, N. H. *Tetrahedron Lett.* **2011**, *52*, 5733-5735.
- (106) Bräse, S.; Encinas, A.; Keck, J.; Nising, C. F. *Chem. Rev.* **2009**, *109*, 3903-3990.
- (107) Masters, K.-S.; Bräse, S. *Chem. Rev.* **2012**, *112*, 3717-3776.
- (108) Franck, B. In *The Biosynthesis of Mycotoxins: A study in Secondary Metabolism*; Steyn, P., Ed.; Academic Press: New York, 1980; pp 157-191.
- (109) Stoll, A.; Renz, J.; Brack, A. *Helv. Chim. Acta* **1952**, *35*, 2022-2034.
- (110) Kurobane, I.; Iwahashi, S.; Fukuda, A. *Drugs Exp. Clin. Res.* **1987**, *13*, 339-344.
- (111) Liao, G.; Zhou, J.; Wang, H.; Mao, Z.; Xiao, W.; Wang, H.; She, Z.; Zhu, Y. *Oncol. Rep.* **2010**, *23*, 387-395.

- (112) McPhee, F.; Caldera, P. S.; Bemis, G. W.; McDonagh, A. F.; Kuntz, I. D.; Craik, C. S. *Biochem. J.* **1996**, *320* (Pt 2), 681-686.
- (113) Eglinton, G.; King, F. E.; Lloyd, G.; Loder, J. W.; Marshall, J. R.; Robertson, A.; Whalley, W. B. *J. Chem. Soc.* **1958**, 1833-1842.
- (114) Zhang, W.; Krohn, K.; Ullah, Z.; Florke, U.; Pescitelli, G.; Di Bari, L.; Antus, S.; Kurtan, T.; Rheinheimer, J.; Draeger, S.; Schulz, B. *Chem-Eur J* **2008**, *14*, 4913-4923.
- (115) Bräse, S.; Gläser, F.; Kramer, C. S. In *The Chemistry of Mycotoxins*; Bräse, S.; Gläser, F.; Kramer, C.; Lindner, S.; Linsenmeier, A. M.; Masters, K. S.; Meister, A. C.; Ruff, B. M.; Zhong, S., Eds.; Springer: Vienna, 2013; pp 91-108.
- (116) Andersen, R.; Buchi, G.; Kobbe, B.; Demain, A. L. *J. Org. Chem.* **1977**, *42*, 352-353.
- (117) Steyn, P. S. *Tetrahedron* **1970**, *26*, 51-57.
- (118) Kurobane, I.; Vining, L. C.; McInnes, A. G. *J. Antibiot.* **1979**, *32*, 1256-1266.
- (119) Franck, B.; Gottschalk, E.-M.; Ohnsorge, U.; Hüper, F. *Chem. Ber.* **1966**, *99*, 3842-3862.
- (120) Howard, C. C.; Johnstone, R. A. W.; Entwistle, I. D. *J. Chem. Soc., Chem. Commun.* **1973**, 464-464.
- (121) Kurobane, I.; Vining, L. C.; McInnes, A. G. *Tetrahedron Lett.* **1978**, *19*, 4633-4636.
- (122) Bringmann, G.; Bruhn, T.; Maksimenka, K.; Hemberger, Y. *Eur. J. Org. Chem.* **2009**, *2009*, 2717-2727.
- (123) Stephens, P. J.; Harada, N. *Chirality* **2010**, *22*, 229-233.

- (124) Stephens, P. J.; Pan, J.-J.; Devlin, F. J.; Urbanová, M.; Hájíček, J. *J. Org. Chem.* **2007**, *72*, 2508-2524.
- (125) Acuña, U. M. o.; Figueroa, M.; Kavalier, A.; Jancovski, N.; Basile, M. J.; Kennelly, E. J. *J. Nat. Prod.* **2010**, *73*, 1775-1779.
- (126) Jiang, T.; Tian, L.; Guo, A. H.; Fu, H. Z.; Pei, Y. H.; Lin, W. H. *Acta Pharm. Sin.* **2002**, *37*, 271-274.
- (127) Kurobane, I.; Vining, L. C.; Mcinnes, A. G. Secalonic acids. 4,424,373, 1984.
- (128) Guo, Z. Y.; She, Z. G.; Shao, C. L.; Wen, L.; Liu, F.; Zheng, Z. H.; Lin, Y. C. *Magn. Reson. Chem.* **2007**, *45*, 777-780.
- (129) Arunpanichlert, J.; Rukachaisirikul, V.; Tadpetch, K.; Phongpaichit, S.; Hutadilok-Towatana, N.; Supaphon, O.; Sakayaroj, J. *Phytochem. Lett.* **2012**, *5*, 604-608.
- (130) Bose, N. K.; Chaudhury, D. N. *J. Indian Chem. Soc.* **1966**, *43*, 411-415.
- (131) Isaka, M.; Suyarnsestakorn, C.; Tanticharoen, M.; Kongsaree, P.; Thebtaranonth, Y. *J. Org. Chem.* **2002**, *67*, 1561-1566.
- (132) Agatsuma, T.; Takahashi, A.; Kabuto, C.; Nozoe, S. *Chem. Pharm. Bull.* **1993**, *41*, 373-375.
- (133) Sato, H.; Konoma, K.; Sakamura, S. *Agric. Biol. Chem.* **1981**, *45*, 1675-1679.
- (134) Kawahara, N.; Sekita, S.; Satake, M.; Udagawa, S.; Kawai, K. *Chem. Pharm. Bull.* **1994**, *42*, 1720-1723.
- (135) Pretsch, E.; Bühlmann, P.; Affolter, C. *Structure Determination of Organic Compounds: Tables of Spectral Data*; Springer: 2000.

- (136) Fusetani, N.; Sugawara, T.; Matsunaga, S.; Hirota, H. *J. Org. Chem.* **1991**, *56*, 4971-4974.
- (137) Gao, G.; Qi, S.; Zhang, S.; Yin, H.; Xiao, Z.; Li, M.; Li, Q. *Pharmazie* **2008**, *63*, 542-544.
- (138) Jiang, H.-L.; Luo, X.-H.; Wang, X.-Z.; Yang, J.-L.; Yao, X.-J.; Crews, P.; Valeriote, F. A.; Wu, Q.-X. *Fitoterapia* **2012**, *83*, 1275-1280.
- (139) Zhai, A.; Zhu, X.; Wang, X.; Chen, R.; Wang, H. *Eur. J. Pharmacol.* **2013**, *713*, 58-67.
- (140) Zhai, A.; Zhang, Y.; Zhu, X.; Liang, J.; Wang, X.; Lin, Y.; Chen, R. *Neurochem. Int.* **2011**, *58*, 85-91.
- (141) Serba, C.; Winssinger, N. *Eur. J. Org. Chem.* **2013**, *2013*, 4195-4214.
- (142) Wu, J. Q.; Powell, F.; Larsen, N. A.; Lai, Z. W.; Byth, K. F.; Read, J.; Gu, R. F.; Roth, M.; Toader, D.; Saeh, J. C.; Chen, H. W. *ACS Chem. Biol.* **2013**, *8*, 643-650.
- (143) Harada, M.; Yano, S.; Watanabe, H.; Yamazaki, M.; Miyaki, K. *Chem. Pharm. Bull.* **1974**, *22*, 1600-1606.
- (144) Bao, J.; Sun, Y. L.; Zhang, X. Y.; Han, Z.; Gao, H. C.; He, F.; Qian, P. Y.; Qi, S. *H. J. Antibiot.* **2013**, *66*, 219-223.
- (145) Franck, B. *Angew. Chem., Int. Ed. Engl.* **1969**, *8*, 251-260.
- (146) Franck, B.; Gottschalk, E. M. *Angew. Chem., Int. Ed. Engl.* **1964**, *3*, 441-441.
- (147) Shearer, C. A.; Descals, E.; Kohlmeyer, B.; Kohlmeyer, J.; Marvanova, L.; Padgett, D.; Porter, D.; Raja, H. A.; Schmit, J. P.; Thorton, H. A.; Voglymayr, H. *Biodivers. Conserv.* **2007**, *16*, 49-67.

- (148) Hernández-Carlos, B.; Gamboa-Angulo, M. *Phytochem. Rev.* **2011**, *10*, 261-286.
- (149) Dong, J. Y.; Shen, K. Z.; Sun, R. *Mycosystema* **2011**, *30*, 206-217.
- (150) Grant, G. M.; Gross, E. R. *Oceanography, a view of earth*; 7th ed.; Prentice Hall: Upper Saddle River, New Jersey, 1996; p 472.
- (151) *Dictionary of Natural Products Online 21.2*; Taylor & Francis Group: London, 2013.
- (152) Tayone, W. C.; Honma, M.; Kanamaru, S.; Noguchi, S.; Tanaka, K.; Nehira, T.; Hashimoto, M. *J. Nat. Prod.* **2011**, *74*, 425-429.
- (153) Gereá, A. L.; Branscum, K. M.; King, J. B.; You, J. L.; Powell, D. R.; Miller, A. N.; Spear, J. R.; Cichewicz, R. H. *Tetrahedron Lett.* **2012**, *53*, 4202-4205.
- (154) Tayone, W. C.; Kanamaru, S.; Honma, M.; Tanaka, K.; Nehira, T.; Hashimoto, M. *Biosci. Biotechnol. Biochem.* **2011**, *75*, 2390-2393.
- (155) Chinworrungsee, M.; Kittakoop, P.; Isaka, M.; Chanphen, R.; Tanticharoen, M.; Thebtaranonth, Y. *J. Chem. Soc., Perkin Trans. 1* **2002**, 2473-2476.
- (156) Schuffler, A.; Liermann, J. C.; Opatz, T.; Anke, T. *Chembiochem* **2011**, *12*, 148-154.
- (157) Gan, M.; Liu, Y.; Bai, Y.; Guan, Y.; Li, L.; Gao, R.; He, W.; You, X.; Li, Y.; Yu, L.; Xiao, C. *J. Nat. Prod.* **2013**, *76*, 1535-1540.
- (158) Figueroa, M.; Gonzalez, M. D.; Rodriguez-Sotres, R.; Sosa-Peinado, A.; Gonzalez-Andrade, M.; Cerda-Garcia-Rojas, C. M.; Mata, R. *Bioorg. Med. Chem.* **2009**, *17*, 2167-2174.
- (159) Morganjones, G.; White, J. F. *Mycotaxon* **1983**, *18*, 57-65.

- (160) Park, S. Y.; Yang, S. H.; Choi, S. K.; Kim, J. G.; Park, S. H. *Korean J. Microbiol. Biotechnol.* **2007**, *35*, 1-10.
- (161) Shearer, C. A.; Langsam, D. M.; Longcore, J. E. In *Measuring and Monitoring Biological Diversity: Standard Methods for Fungi*; Mueller, G. M.; Bills, G. F.; Foster, M. S., Eds.; Smithsonian Institution Press: Washington, D.C., 2004; pp 513-531.
- (162) Raja, H.; Schmit, J.; Shearer, C. *Biodivers. Conserv.* **2009**, *18*, 419-455.
- (163) de Gruyter, J.; Woudenberg, J. H. C.; Aveskamp, M. M.; Verkley, G. J. M.; Groenewald, J. Z.; Crous, P. W. *Mycologia* **2010**, *102*, 1066-1081.
- (164) Frisch, M. J. T., G. W.; Schlegel, H. B.; Scuseria, G. E.; Robb, M. A.; Cheeseman, J. R.; Zakrzewski, V. G.; Montgomery, J. A., Jr.; Vreven, T.; Kudin, K. N.; Burant, J. C.; Millam, J. M.; Iyengar, S. S.; Tomasi, J.; Barone, V.; Mennucci, B.; Cossi, M.; Scalmani, G.; Rega, N.; Petersson, G. A.; Nakatsuji, H.; Hada, M.; Ehara, M.; Toyota, K. F., R.; Hasegawa, J.; Ishida, M. N., T.; Honda, Y.; Kitao, O.; Nakai, H.; Klene, M.; Li, X.; Knox, J. E.; Hratchian, H. P.; Cross, J. B.; Adamo, C.; Jaramillo, J.; Gomperts, R.; Stratmann, R. E.; Yazyev, O.; Austin, A. J.; Cammi, R.; Pomelli, C.; Ochterski, J. W.; Ayala, P. Y.; Morokuma, K.; Voth, G. A.; Salvador, P.; Dannenberg, J. J.; Zakrzewski, V. G.; Dapprich, S.; Daniels, A. D.; Strain, M. C.; Farkas, O.; Malick, D. K.; Rabuck, A. D.; Raghavachari, K.; Foresman, J. B.; Ortiz, J. V.; Cui, Q.; Baboul, A. G.; Clifford, S.; Cioslowski, J.; Stefanov, B. B.; Liu, G.; Liashenko, A.; Piskorz, P.; Komaromi, I.; Martin, R. L.; Fox, D. J.; Keith, T.; Al-Laham, M. A.; Peng, C. Y.; Nanayakkara, A.; Challacombe, M.; Gill, P. M. W.; Johnson, B.; Chen, W.; Wong, M.

W.; Gonzalez, C.; Pople, J. A. *Gaussian 03, ReVision B.02*; Gaussian Inc.: Pittsburgh, PA, 2003.

(165) Kong, J.; White, C. A.; Krylov, A. I.; Sherrill, D.; Adamson, R. D.; Furlani, T. R.; Lee, M. S.; Lee, A. M.; Gwaltney, S. R.; Adams, T. R.; Ochsenfeld, C.; Gilbert, A. T. B.; Kedziora, G. S.; Rassolov, V. A.; Maurice, D. R.; Nair, N.; Shao, Y. H.; Besley, N. A.; Maslen, P. E.; Dombroski, J. P.; Daschel, H.; Zhang, W. M.; Korambath, P. P.; Baker, J.; Byrd, E. F. C.; Van Voorhis, T.; Oumi, M.; Hirata, S.; Hsu, C. P.; Ishikawa, N.; Florian, J.; Warshel, A.; Johnson, B. G.; Gill, P. M. W.; Head-Gordon, M.; Pople, J. A. *J Comput Chem* **2000**, *21*, 1532-1548.

(166) Chang, G.; Guida, W. C.; Still, W. C. *J. Am. Chem. Soc.* **1989**, *111*, 4379-4386.

(167) Nett, J. E.; Cain, M. T.; Crawford, K.; Andes, D. R. *J. Clin. Microbiol.* **2011**, *49*, 1426-1433.

(168) Primack, R. B. *Essentials of Conservation Biology*; 5th ed.; Sinauer Associates, Inc.: Sunderland, MA, 2010; p 601.

(169) Hawksworth, D. L.; Rossman, A. Y. *Phytopathology* **1997**, *87*, 888-91.

(170) Kirk, P. M.; Cannon, P. F.; Minter, D. W.; Staplers, J. A. *Dictionary of the Fungi*; 10th ed.; CABI: Europe-UK, 2008; p 784.

(171) Scheffers, B. R.; Joppa, L. N.; Pimm, S. L.; Laurance, W. F. *Trends in Ecology & Evolution* **2012**, *27*, 501-510.

(172) El-Elimat, T.; Raja, H. A.; Figueroa, M.; Falkinham III, J. O.; Oberlies, N. H. *Phytochemistry* **2014**, *Submitted*.

(173) Giordanetto, F.; Kihlberg, J. *J. Med. Chem.* **2013**, *57*, 278-295.

- (174) Meyer, B. N.; Ferrigni, N. R.; Putnam, J. E.; Jacobsen, L. B.; Nichols, D. E.; McLaughlin, J. L. *Planta Med.* **1982**, *45*, 31-34.
- (175) McLaughlin, J. L.; Rogers, L. L. *Drug Inf. J.* **1998**, *32*, 513-524.
- (176) Talontsi, F. M.; Facey, P.; Tatong, M. D. K.; Islam, M. T.; Frauendorf, H.; Draeger, S.; von Tiedemann, A.; Laatsch, H. *Phytochemistry* **2012**, *83*, 87-94.
- (177) Hellwig, V.; Mayer-Bartschmid, A.; Muller, H.; Greif, G.; Kleymann, G.; Zitzmann, W.; Tichy, H. V.; Stadler, M. *J. Nat. Prod.* **2003**, *66*, 829-837.
- (178) Mirrington, R. N.; Ritchie, E.; Shoppee, C. W.; Taylor, W. C.; Sternhell, S. *Tetrahedron Lett.* **1964**, *5*, 365-370.
- (179) Cutler, H. G.; Arrendale, R. F.; Springer, J. P.; Cole, P. D.; Roberts, R. G.; Hanlin, R. T. *Agric. Biol. Chem.* **1987**, *51*, 3331-3338.
- (180) Shinonaga, H.; Kawamura, Y.; Ikeda, A.; Aoki, M.; Sakai, N.; Fujimoto, N.; Kawashima, A. *Tetrahedron* **2009**, *65*, 3446-3453.
- (181) Porrás-Alfaro, A.; Liu, K. L.; Kuske, C. R.; Xie, G. *Appl. Environ. Microbiol.* **2014**, *80*, 829-840.
- (182) Jones, E. B. G.; Sakayaroj, J.; Suetrong, S.; Somrithipol, S.; Pang, K. L. *Fungal Divers.* **2009**, *35*, 1-187.
- (183) Bills, G. F.; Platas, G.; Pelaez, F.; Masurekar, P. *Mycol. Res.* **1999**, *103*, 179-192.
- (184) Stamatakis, A.; Hoover, P.; Rougemont, J. *Syst. Biol.* **2008**, *57*, 758-771.
- (185) Miller, M. A.; Pfeiffer, W.; Schwartz, T. In *Creating the CIPRES Science Gateway for Inference of Large Phylogenetic Trees; Proceedings of the Gateway*

Computing Environments Workshop (GCE), New Orleans, LA, November 14, 2010; pp 1-8.

(186) Hillis, D. M.; Bull, J. J. *Syst. Biol.* **1993**, *42*, 182-192.

(187) Baschien, C.; Tsui, C. K. M.; Gulis, V.; Szewzyk, U.; Marvanova, L. *Fungal Biol.* **2013**, *117*, 660-672.

(188) Parsons, S.; Flack, H. *Acta Crystallogr., Sect. A: Found. Crystallogr.* **2004**, *60*, s61.

(189) Polyak, S. J.; Oberlies, N. H.; Pecheur, E. I.; Dahari, H.; Ferenci, P.; Pawlotsky, J. *M. Antiviral Ther.* **2013**, *18*, 141-7.

(190) Abenavoli, L.; Capasso, R.; Milic, N.; Capasso, F. *Phytother. Res.* **2010**, *24*, 1423-1432.

(191) Deep, G.; Agarwal, R. *Cancer Metastasis Rev.* **2010**, *29*, 447-463.

(192) Ramasamy, K.; Agarwal, R. *Cancer Lett.* **2008**, *269*, 352-362.

(193) Agarwal, R.; Agarwal, C.; Ichikawa, H.; Singh, R. P.; Aggarwal, B. B. *Anticancer Res.* **2006**, *26*, 4457-4498.

(194) Comelli, M. C.; Mengs, U.; Schneider, C.; Prosdocimi, M. *Integr. Cancer Ther.* **2007**, *6*, 120-129.

(195) Gazak, R.; Walterova, D.; Kren, V. *Curr. Med. Chem.* **2007**, *14*, 315-338.

(196) Kroll, D. J.; Shaw, H. S.; Oberlies, N. H. *Integr. Cancer Ther.* **2007**, *6*, 110-119.

(197) Davis-Searles, P. R.; Nakanishi, Y.; Kim, N. C.; Graf, T. N.; Oberlies, N. H.; Wani, M. C.; Wall, M. E.; Agarwal, R.; Kroll, D. J. *Cancer Res.* **2005**, *65*, 4448-4457.

- (198) Deep, G.; Oberlies, N. H.; Kroll, D. J.; Agarwal, R. *Carcinogenesis* **2007**, *28*, 1533-1542.
- (199) Deep, G.; Gangar, S. C.; Oberlies, N. H.; Kroll, D. J.; Agarwal, R. *Mol. Carcinog.* **2010**, *49*, 902-912.
- (200) Deep, G.; Gangar, S. C.; Rajamanickam, S.; Raina, K.; Gu, M.; Agarwal, C.; Oberlies, N. H.; Agarwal, R. *Plos One* **2012**, *7*.
- (201) Polyak, S. J.; Morishima, C.; Lohmann, V.; Pal, S.; Lee, D. Y. W.; Liu, Y. Z.; Graf, T. N.; Oberlies, N. H. *Proc. Natl. Acad. Sci. U.S.A.* **2010**, *107*, 5995-5999.
- (202) Wagoner, J.; Morishima, C.; Graf, T. N.; Oberlies, N. H.; Teissier, E.; Pecheur, E. I.; Tavis, J. E.; Polyak, S. J. *Plos One* **2011**, *6*.
- (203) Napolitano, J. G.; Lankin, D. C.; Graf, T. N.; Friesen, J. B.; Chen, S.-N.; McAlpine, J. B.; Oberlies, N. H.; Pauli, G. F. *J. Org. Chem.* **2013**, *78*, 2827-2839.
- (204) Sy-Cordero, A. A.; Graf, T. N.; Runyon, S. P.; Wani, M. C.; Kroll, D. J.; Agarwal, R.; Brantley, S. J.; Paine, M. F.; Polyak, S. J.; Oberlies, N. H. *Bioorg. Med. Chem.* **2013**, *21*, 742-747.
- (205) Graf, T. N.; Wani, M. C.; Agarwal, R.; Kroll, D.; Oberlies, N. H. *Planta Med.* **2007**, *73*, 1495-1501.
- (206) Althagafy, H. S.; Meza-Avina, M. E.; Oberlies, N. H.; Croatt, M. P. *J. Org. Chem.* **2013**, *78*, 7594-7600.
- (207) Althagafy, H. S.; Graf, T. N.; Sy-Cordero, A. A.; Gufford, B. T.; Paine, M. F.; Wagoner, J.; Polyak, S. J.; Croatt, M. P.; Oberlies, N. H. *Bioorg. Med. Chem.* **2013**, *21*, 3919-3926.

- (208) Carroll, G. *Ecology* **1988**, *69*, 2-9.
- (209) Stone, J. K.; Polishook, J. D.; White, J. F., Jr. In *Biodiversity of Fungi: Inventory and Monitoring Methods*; Mueller, G. M.; Bills, G. F.; Foster, M. S., Eds.; Elsevier Academic Press: Burlington, MA, USA, 2004; pp 241-270.
- (210) Petrini, O. In *Microbial Ecology of Leaves*; Andrews, J. H.; Hirano, S. S., Eds.; Springer-Verlag: New York, 1991; pp 179-197.
- (211) Stone, J. K.; Bacon, C. W.; White, J.F. Jr. In *Microbial Endophytes*; Bacon, C. W.; White, J.F. Jr., Eds.; Marcel Dekker: New York, 2000; pp 3-29.
- (212) Arnold, A. E. *Fungal Biol. Rev.* **2007**, *21*, 51-66.
- (213) Stierle, A.; Strobel, G.; Stierle, D. *Science* **1993**, *260*, 214-216.
- (214) Eyberger, A. L.; Dondapati, R.; Porter, J. R. *J. Nat. Prod.* **2006**, *69*, 1121-1124.
- (215) Puri, S. C.; Nazir, A.; Chawla, R.; Arora, R.; Riyaz-ul-Hasan, S.; Amna, T.; Ahmed, B.; Verma, V.; Singh, S.; Sagar, R.; Sharma, A.; Kumar, R.; Sharma, R. K.; Qazi, G. N. *J. Biotechnol.* **2006**, *122*, 494-510.
- (216) Kusari, S.; Lamshoft, M.; Spiteller, M. *J. Appl. Microbiol.* **2009**, *107*, 1019-1030.
- (217) Shweta, S.; Gurumurthy, B. R.; Ravikanth, G.; Ramanan, U. S.; Shivanna, M. B. *Phytomedicine* **2013**, *20*, 337-342.
- (218) Puri, S. C.; Verma, V.; Amna, T.; Qazi, G. N.; Spiteller, M. *J. Nat. Prod.* **2005**, *68*, 1717-1719.
- (219) Rehman, S.; Shawl, A. S.; Kour, A.; Andrabi, R.; Sudan, P.; Sultan, P.; Verma, V.; Qazi, G. N. *Appl. Biochem. Microbiol.* **2008**, *44*, 203-209.

- (220) Rehman, S.; Shawl, A. S.; Kour, A.; Sultan, P.; Ahmad, K.; Khajuria, R.; Qazi, G. *N. Nat. Prod. Res.* **2009**, *23*, 1050-1057.
- (221) Shweta, S.; Zuehlke, S.; Ramesha, B. T.; Priti, V.; Kumar, P. M.; Ravikanth, G.; Spiteller, M.; Vasudeva, R.; Shaanker, R. U. *Phytochemistry* **2010**, *71*, 117-122.
- (222) Kusari, S.; Zuhlke, S.; Spiteller, M. *J. Nat. Prod.* **2009**, *72*, 2-7.
- (223) Guo, B.; Li, H.; Zhang, L. *J. Yunnan Univ.* **1998**, *20*, 214-215.
- (224) Kusari, S.; Zuhlke, S.; Kosuth, J.; Cellarova, E.; Spiteller, M. *J. Nat. Prod.* **2009**, *72*, 1825-1835.
- (225) Kusari, S.; Lamshoft, M.; Zuhlke, S.; Spiteller, M. *J. Nat. Prod.* **2008**, *71*, 159-162.
- (226) Kusari, S.; Verma, V. C.; Lamshoeft, M.; Spiteller, M. *World J. Microbiol. Biotechnol.* **2012**, *28*, 1287-1294.
- (227) Gurudatt, P. S.; Priti, V.; Shweta, S.; Ramesha, B. T.; Ravikanth, G.; Vasudeva, R.; Amna, T.; Deepika, S.; Ganeshaiyah, K. N.; Shaanker, R. U.; Puri, S.; Qazi, N. *Curr. Sci.* **2010**, *98*, 1006-1010.
- (228) Kusari, S.; Hertweck, C.; Spiteller, M. *Chem. Biol.* **2012**, *19*, 792-798.
- (229) Kusari, S.; Pandey, S. P.; Spiteller, M. *Phytochemistry* **2013**, *91*, 81-87.
- (230) Sachin, N.; Manjunatha, B. L.; Kumara, P. M.; Ravikanth, G.; Shweta, S.; Suryanarayanan, T. S.; Ganeshaiyah, K. N.; Shaanker, R. U. *Curr. Sci.* **2013**, *104*, 178-182.
- (231) Sy-Cordero, A. A.; Graf, T. N.; Wani, M. C.; Kroll, D. J.; Pearce, C. J.; Oberlies, N. H. *J. Antibiot.* **2010**, *63*, 539-544.

- (232) Sugiyama, J. *J. Fac. Sci., Univ. Tokyo, Sect. 3* **1967**, 9 Parts 10 and 11, 374-405.
- (233) Kusari, S.; Zuhlke, S.; Spiteller, M. *J. Nat. Prod.* **2011**, 74, 764-775.
- (234) Sy-Cordero, A. A.; Day, C. S.; Oberlies, N. H. *J. Nat. Prod.* **2012**, 75, 1879-1881.
- (235) Schulz, B.; Wanke, U.; Draeger, S.; Aust, H. J. *Mycol. Res.* **1993**, 97, 1447-1450.
- (236) Guadet, J.; Julien, J.; Lafay, J. F.; Brygoo, Y. *Mol. Biol. Evol.* **1989**, 6, 227-242.
- (237) Peterson, S. W. *Mycologia* **2008**, 100, 205-226.
- (238) Edgar, R. C. *Nucleic Acids Res.* **2004**, 32, 1792-1797.
- (239) Gouy, M.; Guindon, S.; Gascuel, O. *Mol. Biol. Evol.* **2010**, 27, 221-224.
- (240) Stamatakis, A.; Aberer, A. J.; Goll, C.; Smith, S. A.; Berger, S. A.; Izquierdo-Carrasco, F. *Bioinformatics* **2012**, 28, 2064-2066.
- (241) Stamatakis, A. *Bioinformatics* **2006**, 22, 2688-2690.
- (242) Huelsenbeck, J. P.; Ronquist, F. In *Statistical Methods in Molecular Evolution*; Nielsen, R., Ed.; Springer: New York, NY, USA, 2005; pp 183-232.
- (243) Ghisalberty, E. L. In *Detection, Isolation and Structural Determination*; Colegate, S. M.; Molyneux, R. J., Eds.; CRC Press Inc.: Boca Raton, FL, 1993; pp 9-57.
- (244) Kingston, D. G. I. In *The Practice of Medicinal Chemistry*; Meyer, P., Ed.; London, 1996; pp 101-116.
- (245) Wani, M. C.; Taylor, H. L.; Wall, M. E.; Coggon, P.; McPhail, A. T. *J. Am. Chem. Soc.* **1971**, 93, 2325-2327.
- (246) Wall, M. E.; Wani, M. C.; Cook, C. E.; Palmer, K. H.; McPhail, A. T.; Sim, G. A. *J. Am. Chem. Soc.* **1966**, 88, 3888-3890.
- (247) Oberlies, N. H.; Kroll, D. J. *J. Nat. Prod.* **2004**, 67, 129-135.

- (248) Blunt, J.; Munro, M.; Upjohn, M. In Fattorusso, E.; Gerwick, W. H.; Taglialatela-Scafati, O., Eds.; Springer: Dordrecht, The Netherlands, 2012; pp 389-421.
- (249) Hostettmann, K.; Wolfender, J. L.; Terreaux, C. *Pharm. Biol.* **2001**, *39 Suppl. 1*, 18-32.
- (250) Wolfender, J. L.; Ndjoko, K.; Hostettmann, K. *J. Chromatogr. A* **2003**, *1000*, 437-455.
- (251) Wolfender, J.-L.; Queiroz, E. F.; Hostettmann, K. *Exp. Opin. Drug Discov.* **2006**, *1*, 237-260.
- (252) Alali, F. Q.; Gharaibeh, A.; Ghawanmeh, A.; Tawaha, K.; Oberlies, N. H. *Phytochem. Anal.* **2008**, *19*, 385-394.
- (253) Le Ven, J.; Schmitz-Afonso, I.; Lewin, G.; Lapr evote, O.; Brunelle, A.; Touboul, D.; Champy, P. *J. Mass Spectrom.* **2012**, *47*, 1500-1509.
- (254) Funari, C. S.; Eugster, P. J.; Martel, S.; Carrupt, P.-A.; Wolfender, J.-L.; Silva, D. H. S. *J. Chromatogr. A* **2012**, *1259*, 167-178.
- (255) Musharraf, S. G.; Goher, M.; Shahnaz, S.; Choudhary, M. I.; Atta-ur-Rahman. *Rapid Commun. Mass Spectrom.* **2013**, *27*, 169-178.
- (256) Qiu, F.; Imai, A.; McAlpine, J. B.; Lankin, D. C.; Burton, I.; Karakach, T.; Farnsworth, N. R.; Chen, S. N.; Pauli, G. F. *J. Nat. Prod.* **2012**, *75*, 432-443.
- (257) Lang, G.; Mayhudin, N. A.; Mitova, M. I.; Sun, L.; van der Sar, S.; Blunt, J. W.; Cole, A. L. J.; Ellis, G.; Laatsch, H.; Munro, M. H. G. *J. Nat. Prod.* **2008**, *71*, 1595-1599.
- (258) Mitova, M. I.; Murphy, A. C.; Lang, G.; Blunt, J. W.; Cole, A. L. J.; Ellis, G.; Munro, M. H. G. *J. Nat. Prod.* **2008**, *71*, 1600-1603.

- (259) Murphy, P. A.; Hendrich, S.; Landgren, C.; Bryant, C. M. *J. Food Sci.* **2006**, *71*, R51-R65.
- (260) Kabak, B.; Dobson, A. D.; Var, I. *Crit. Rev. Food Sci. Nutr.* **2006**, *46*, 593-619.
- (261) Nielsen, K. F.; Smedsgaard, J. *J. Chromatogr. A* **2003**, *1002*, 111-136.
- (262) Nielsen, K. F.; Månsson, M.; Rank, C.; Frisvad, J. C.; Larsen, T. O. *J. Nat. Prod.* **2011**, *74*, 2338-2348.
- (263) Fredenhagen, A.; Derrien, C.; Gassmann, E. *J. Nat. Prod.* **2005**, *68*, 385-391.
- (264) Larsen, T. O.; Smedsgaard, J.; Nielsen, K. F.; Hansen, M. E.; Frisvad, J. C. *Nat. Prod. Rep.* **2005**, *22*, 672-695.
- (265) Alali, F. Q.; El-Elimat, T.; Li, C.; Qandil, A.; Alkofahi, A.; Tawaha, K.; Burgess, J. P.; Nakanishi, Y.; Kroll, D. J.; Navarro, H. A.; Falkinham, J. O., 3rd; Wani, M. C.; Oberlies, N. H. *J. Nat. Prod.* **2005**, *68*, 173-178.
- (266) Balogh, M. P. *LCGC North America* **2006**, *24*, 762-769.
- (267) Chen, Y.; Guo, H.; Du, Z.; Liu, X. Z.; Che, Y.; Ye, X. *Cell Proliferation* **2009**, *42*, 838-847.
- (268) Isham, C. R.; Tibodeau, J. D.; Jin, W.; Xu, R.; Timm, M. M.; Bible, K. C. *Blood* **2007**, *109*, 2579-2588.
- (269) Zhang, Y. X.; Chen, Y.; Guo, X. N.; Zhang, X. W.; Zhao, W. M.; Zhong, L.; Zhou, J.; Xi, Y.; Lin, L. P.; Ding, J. *Anti-Cancer Drugs* **2005**, *16*, 515-524.
- (270) Takahashi, C.; Numata, A.; Matsumura, E.; Minoura, K.; Eto, H.; Shingu, T.; Ito, T.; Hasegawa, T. *J. Antibiot.* **1994**, *47*, 1242-1249.

- (271) Takahashi, C.; Numata, A.; Ito, Y.; Matsumura, E.; Araki, H.; Iwaki, H.; Kushida, K. *J. Chem. Soc., Perkin Trans. 1* **1994**, 1859-1864.
- (272) Takahashi, C.; Minoura, K.; Yamada, T.; Numata, A.; Kushida, K.; Shingu, T.; Hagishita, S.; Nakai, H.; Sato, T.; Harada, H. *Tetrahedron* **1995**, *51*, 3483-3498.
- (273) Chen, Y.; Zhang, Y.-X.; Li, M.-H.; Zhao, W.-M.; Shi, Y.-H.; Miao, Z.-H.; Zhang, X.-W.; Lin, L.-P.; Ding, J. *Biochem. Biophys. Res. Commun.* **2005**, *329*, 1334-1342.
- (274) Saito, T.; Suzuki, Y.; Koyama, S.; Natori, S.; Iitaka, Y.; Kinoshita, T. *Chem. Pharm. Bull.* **1998**, *36*, 1942-1956.
- (275) Son, B. W.; Jensen, P. R.; Kauffman, C. A.; Fenical, W. *Nat. Prod. Lett.* **1999**, *13*, 213-222.
- (276) Feng, Y.; Blunt, J. W.; Cole, A. L.; Munro, M. H. G. *J. Nat. Prod.* **2004**, *67*, 2090-2092.
- (277) Zheng, C. J.; Park, S. H.; Koshino, H.; Kim, Y. H.; Kim, W. G. *J. Antibiot.* **2007**, *60*, 61-64.
- (278) Zheng, C. J.; Kim, C. J.; Bae, K. S.; Kim, Y. H.; Kim, W. G. *J. Nat. Prod.* **2006**, *69*, 1816-1819.
- (279) Bertinetti, B. V.; Rodriguez, M. A.; Godeas, A. M.; Cabrera, G. M. *J. Antibiot.* **2010**, *63*, 681-683.
- (280) Argoudelis, A. D. *J. Antibiot.* **1972**, *25*, 171-178.
- (281) Joshi, B. K.; Gloer, J. B.; Wicklow, D. T. *J. Nat. Prod.* **1999**, *62*, 730-733.
- (282) Minato, H.; Matsumoto, M.; Katayama, T. *J. Chem. Soc. D* **1971**, 44-45.

- (283) Watts, K. R.; Ratnam, J.; Ang, K. H.; Tenney, K.; Compton, J. E.; McKerrow, J.; Crews, P. *Bioorg. Med. Chem.* **2010**, *18*, 2566-2574.
- (284) Dong, J. Y.; He, H. P.; Shen, Y. M.; Zhang, K. Q. *J. Nat. Prod.* **2005**, *68*, 1510-1513.
- (285) Ovenden, S. P.; Sberna, G.; Tait, R. M.; Wildman, H. G.; Patel, R.; Li, B.; Steffy, K.; Nguyen, N.; Meurer-Grimes, B. M. *J. Nat. Prod.* **2004**, *67*, 2093-2095.
- (286) Erkel, G.; Gehrt, A.; Anke, T.; Sterner, O. *Z. Naturforsch., C* **2002**, *57*, 759-767.
- (287) Heathcote, J. G.; Hibbert, J. R. *Aflatoxins: Chemical and Biological Aspects*; Elsevier Scientific Publishing. Co.: Amsterdam, 1978.
- (288) Rodrigues, I.; Naehrer, K. *Toxins (Basel)* **2012**, *4*, 663-675.
- (289) Bennett, J. W.; Klich, M. *Clin. Microbiol. Rev.* **2003**, *16*, 497-516.
- (290) Anonymous. *Manual on the Application of the HACCP System in Mycotoxin Prevention and Control*; Food and Agriculture Organization of the United Nations: Rome, 2001.
- (291) Ayers, S.; Ehrmann, B. M.; Adcock, A. F.; Kroll, D. J.; Carcache de Blanco, E. J.; Shen, Q.; Swanson, S. M.; Falkinham, J. O.; Wani, M. C.; Mitchell, S. M.; Pearce, C. J.; Oberlies, N. H. *J. Pept. Sci.* **2012**, *18*, 500-510.
- (292) Kinghorn, A. D.; Carcache de Blanco, E. J.; Chai, H. B.; Orjala, J.; Farnsworth, N. R.; Soejarto, D. D.; Oberlies, N. H.; Wani, M. C.; Kroll, D. J.; Pearce, C. J.; Swanson, S. M.; Kramer, R. A.; Rose, W. C.; Fairchild, C. R.; Vite, G. D.; Emanuel, S.; Jarjoura, D.; Cope, F. O. *Pure Appl. Chem.* **2009**, *81*, 1051-1063.

- (293) Kim, H.; Kronic, A.; Lantvit, D.; Shen, Q.; Kroll, D. J.; Swanson, S. M.; Orjala, J. *Tetrahedron* **2012**, *68*, 3205-3209.
- (294) Zi, J.; Lantvit, D. D.; Swanson, S. M.; Orjala, J. *Phytochemistry* **2012**, *74*, 173-177.
- (295) Pan, L.; Yong, Y.; Deng, Y.; Lantvit, D. D.; Ninh, T. N.; Chai, H.; Carcache de Blanco, E. J.; Soejarto, D. D.; Swanson, S. M.; Kinghorn, A. D. *J. Nat. Prod.* **2012**, *75*, 444-452.
- (296) Deng, Y.; Chin, Y. W.; Chai, H. B.; de Blanco, E. C.; Kardono, L. B.; Riswan, S.; Soejarto, D. D.; Farnsworth, N. R.; Kinghorn, A. D. *Phytochem Lett* **2011**, *4*, 213-217.
- (297) Feher, M.; Schmidt, J. M. *J. Chem. Inf. Comput. Sci.* **2003**, *43*, 218-227.
- (298) Lee, M. L.; Schneider, G. *J. Comb. Chem.* **2001**, *3*, 284-289.
- (299) Singh, S. B.; Culberson, J. C. In *Natural Product Chemistry for Drug Discovery*; Buss, A. D.; Butler, M. S., Eds.; The Royal Society of Chemistry: Cambridge, UK, 2010; pp 28-43.
- (300) Singh, N.; Guha, R.; Giulianotti, M. A.; Pinilla, C.; Houghten, R. A.; Medina-Franco, J. L. *J. Chem. Inf. Model.* **2009**, *49*, 1010-1024.
- (301) Xue, L.; Stahura, F. L.; Bajorath, J. *Methods Mol. Biol.* **2004**, *275*, 279-290.
- (302) Harman, H. H. *Modern Factor Analysis*; 3rd ed.; University of Chicago Press: Chicago, 1976; p 508.
- (303) *Proc Factor and Proc Princomp Procedure, SAS/STAT Users Guide*, 9.2; SAS Institute Inc: Cary, NC, 2002.
- (304) Tan, D. S. *Nat. Chem. Biol.* **2005**, *1*, 74-84.

- (305) Lipinski, C. A.; Lombardo, F.; Dominy, B. W.; Feeney, P. J. *Adv. Drug Delivery Rev.* **2001**, *46*, 3-26.
- (306) Ertl, P.; Rohde, B.; Selzer, P. *J. Med. Chem.* **2000**, *43*, 3714-3717.
- (307) Klebe, G.; Bohm, H. J. *J. Recept. Signal Transduction Res.* **1997**, *17*, 459-73.
- (308) Crawford, C.; Ferguson, G. *Psychometrika* **1970**, *35*, 321-332.
- (309) Towle, M. J.; Salvato, K. A.; Budrow, J.; Wels, B. F.; Kuznetsov, G.; Aalfs, K. K.; Welsh, S.; Zheng, W.; Seletsky, B. M.; Palme, M. H.; Habgood, G. J.; Singer, L. A.; DiPietro, L. V.; Wang, Y.; Chen, J. J.; Quincy, D. A.; Davis, A.; Yoshimatsu, K.; Kishi, Y.; Yu, M. J.; Littlefield, B. A. *Cancer Res.* **2001**, *61*, 1013-1021.
- (310) NCI Drug Dictionary. <http://www.cancer.gov> (11/2011),